



Carlos Miguel Rocha Abreu

Developments in Reversible Deactivation Radical Polymerization: New Ecofriendly Catalytic Systems and Vinyl Chloride (co)Polymerization Methods

PhD Thesis in Chemical Engineering, supervised by Professor Doctor Jorge Fernando Jordão Coelho, Professor Doctor Arménio Coimbra Serra and Professor Doctor Krzysztof Matyjaszewski, submitted to the Department of Chemical Engineering, Faculty of Science and Technology, University of Coimbra

Agosto, 2017



UNIVERSIDADE DE COIMBRA

Carlos Miguel Rocha Abreu

**Developments in Reversible Deactivation
Radical Polymerization:
New Ecofriendly Catalytic Systems and
Vinyl Chloride (co)Polymerization Methods**

Thesis submitted to the Faculty of Sciences and Technology of the University of
Coimbra, to obtain the Degree of Doctor in Chemical Engineering.

Coimbra

2017



UNIVERSIDADE DE COIMBRA

Carlos Miguel Rocha Abreu

**Developments in Reversible Deactivation
Radical Polymerization:
New Ecofriendly Catalytic Systems and
Vinyl Chloride (co)Polymerization Methods**

Thesis submitted to the Faculty of Sciences and Technology of the University of Coimbra,
to obtain the Degree of Doctor in Chemical Engineering.

Advisors:

Prof. Dr. Jorge Fernando Jordão Coelho

Prof. Dr. Arménio Coimbra Serra

Prof. Dr. Krzysztof Matyjaszewski

Host institutions:

University of Coimbra

Carnegie Mellon University

Financing:

Portuguese Foundation for Science and Technology (FCT)

Doctoral degree grant: SFRH/BD/88528/2012

Coimbra

2017



UNIVERSIDADE DE COIMBRA

Financial support:



À minha mãe (in memoriam),

Acknowledgments

O meu Muito Obrigado a todos aqueles que de modo directo ou indirecto contribuíram para o sucesso deste trabalho.

Ao Professor Jorge Coelho, meu orientador científico. Agradeço por ter acreditado e confiado em mim desde o início, me ter motivado e concedido as melhores oportunidades ao longo dos últimos anos. Agradeço também toda a ajuda prestada, todo o conhecimento transmitido e o facto de me ter proporcionado uma incrível experiência em Pittsburgh (Estados Unidos da América). Sem dúvida que contribuiu imenso para o meu desenvolvimento.

Ao Professor Arménio Serra, pela confiança demonstrada, pela sua disponibilidade e por todas as discussões, conselhos e sugestões ao longo do trabalho.

To Professor Krzysztof Matyjaszewski I want to express my deepest gratitude for welcoming in his laboratory at Carnegie Mellon University and for the helpful discussions, comments and advices. I'm grateful for such wonderful opportunity. I would also like to extend my great appreciation to his wife for having me at home during my stay at Pittsburgh. I've found a home far from home with you both.

A todos os membros do Polymer Synthesis and Characterization (Polysyc), em especial ao pessoal do laboratório B37, pelo bom ambiente de trabalho criado e pelas discussões de resultados durante o nosso duro processo de desenvolvimento de novos sistemas de RDRP.

To the group members of the Matyjaszewski Polymer Group, it was a pleasure to meet you all and have the chance to work with you. Thank you for the good advices, support, friendship and fun we shared during my stay.

Ao Departamento de Engenharia Química e a todos os seus funcionários, pelas condições proporcionadas.

À Fundação para a Ciência e Tecnologia (FCT), pelo financiamento deste trabalho.

Acknowledgments

E, por fim, mas não menos importante, a toda a minha família e todos os meus amigos, a minha eterna gratidão pelo esforço, pelo incentivo e por terem apoiado sempre todas as minhas decisões.

Abstract

The aim of this work was the study and development of new ecofriendly catalytic systems for reversible deactivation radical polymerization (RDRP). It was also a goal the development of new vinyl chloride (VC) (co)polymerizations systems using RDRP methods.

Atom transfer radical polymerization (ATRP) is among the most efficient, versatile and robust RDRP techniques. The new generation of catalytic systems for RDRP of vinyl monomers should be non-toxic, inexpensive and provide fast polymerizations in environmentally friendly media. In this context, in the present work Food and Drug Administration (FDA) approved inorganic sulfites such as sodium dithionite ($\text{Na}_2\text{S}_2\text{O}_4$), sodium metabisulfite ($\text{Na}_2\text{S}_2\text{O}_5$), and sodium bisulfite (NaHSO_3) were found as a new class of very efficient reducing agents and supplemental activators (SARA) for ATRP. In combination with catalytic amounts of $\text{Cu(II)Br}_2/\text{Me}_6\text{TREN}$ (Me_6TREN : tris[2-(dimethylamino)ethyl]amine) in dimethyl sulfoxide (DMSO) at ambient temperature (30 °C), poly(methyl acrylate) (PMA) with controlled molecular weight, low dispersity ($D < 1.05$), and well-defined chain-end functionality, was synthesized as a proof-of-concept. In addition, an unusual synergistic effect between an ionic liquid, 1-butyl-3-methylimidazolium hexafluorophosphate (BMIM-PF_6), and DMSO mixtures was found for this ecofriendly SARA ATRP.

The novel developed inorganic sulfites catalyzed ATRP was also successfully extended to the (co)polymerization of activated vinyl monomers, such as methyl acrylate (MA), *n*-butyl acrylate (*n*-BA), methyl methacrylate (MMA) and 2-(dimethylamino)ethyl methacrylate (DMAEMA), in ecofriendly solvents (alcohols and alcohol/water mixtures) at ambient temperature. In this system, the use of inorganic sulfites and ecofriendly solvents (alcohol-water mixtures are inexpensive and have low boiling points) is a remarkable advantage for the possibility of scaling-up of the ATRP method.

The aqueous SARA ATRP using inorganic sulfites was successfully developed for the first time. This study methodically investigated the different parameters of SARA ATRP for the synthesis of well-defined water-soluble polymers (*e.g.*, poly[oligo(ethylene oxide)

methyl ether acrylate] (POEOA)) in aqueous media catalyzed by Cu(II)Br₂/tris(2-pyridylmethyl)amine (TPMA) (<30 ppm) using a slow feeding of inorganic sulfites at room temperature. The developed system was also extended to the synthesis of block copolymers using a “one-pot” method. As proof-of-concept, under biologically relevant conditions, the aqueous SARA ATRP using inorganic sulfites was successfully applied to synthesize a well-defined bovine serum albumin protein-polymer (BSA-[P(OEOA₄₈₀)₃₀]) hybrid.

The development of efficient RDRP methods for control of nonactivated vinyl monomers (*e.g.*, vinyl acetate, *N*-vinylpyrrolidone and vinyl chloride) remains an important challenge. Poly(vinyl chloride) (PVC) is one of the most widely consumed polymers worldwide due to its general versatility and low cost. Conventional free radical polymerization (FRP) of VC is the only available industrial process to produce the polymer in large scale. The several intrinsic limitations of FRP triggered interest in synthesizing this polymer by RDRP methods. Until 2012, the most successful RDRP of VC had been achieved by single electron transfer degenerative chain transfer living radical polymerization (SET-DTLRP) or Metal Catalyzed RDRP (termed SET-LRP).

In this context, in the present work reversible addition-fragmentation chain transfer (RAFT) polymerization of VC was developed. The success of the RAFT polymerization process (control over the molecular weight, the molecular weight distribution and the molecular architecture of the resulting polymers) is strongly related to the appropriate selection of the RAFT agent (usually termed CTA). Cyanomethyl methyl(phenyl)carbamodithioate (CMPCD) was shown to be an efficient RAFT agent. The results demonstrated that a careful selection of the reaction conditions (initiator type and concentration, solvent type and concentration, temperature) is critical for achieving PVC products with controlled features (the lowest dispersity ever reported for PVC obtained by any RDRP method, $\mathcal{D} \sim 1.4$). Structural analysis, via ¹H-NMR and MALDI-TOF-MS, revealed that the PVC chains contained well preserved functional groups and no structural defects. Moreover, the “living” nature of the PVC that was synthesized via RAFT polymerization method was confirmed by successful chain extension and PVC-based block copolymerization experiments.

The work continued with the synthesis of PVC by nitroxide-mediated polymerization (NMP) using the SG1-based BlocBuilder alkoxyamine at low temperature (30 and 42 °C). With a judicious selection of the polymerization conditions (dichloromethane (DCM) as solvent using 1/1 monomer-to-solvent ratio), first order kinetics and linear evolutions of the molecular weight with VC conversion were obtained with decreasing D down to 1.6-1.4. The structural characterizations ($^1\text{H-NMR}$ and $^{31}\text{P-NMR}$) of the resulting PVC suggested the existence of very small content of structural defects and the high preservation of the chain-end functional groups (~91% SG1 chain-end functionality). PVC-SG1 macroinitiators were successfully used in chain extension experiments using VC, MMA and mixture of monomers (90% of MMA and 10% of styrene (S)) and confirmed the “livingness” of the PVC-SG1 macroinitiators, giving access to different PVC-based block copolymers.

Even though water is the ideal solvent in terms of nontoxicity, very few examples of monomers/polymers are water-soluble. Therefore, alternative green organic solvents are highly desirable. Thus, considering the very promising results that were obtained in previous parts of this work, cyclopentyl methyl ether (CPME) was successfully introduced as green solvent in RAFT polymerization, not only of VC but also of vinyl acetate (VAc) (using CMPCD as CTA), S and MA (using 2-(dodecylthiocarbonothioylthio)-2-methylpropionic acid (DDMAT) as CTA), and NMP of VC and S (using the SG1-based BlocBuilder alkoxyamine). The structures of the obtained RAFT-polymers and NMP-polymers were proved by $^1\text{H-NMR}$, $^{31}\text{P-NMR}$ and MALDI-TOF-MS. The “living” nature of the polymers was confirmed carrying out successful chain extension and block copolymerization experiments. The results proved that CPME is an excellent green substitute to avoid the use of toxic solvents (*e.g.*, tetrahydrofuran (THF), DMSO, DCM and dimethylformamide (DMF)) in two of the most popular RDRP methods (RAFT and NMP).

Resumo

O principal objectivo deste trabalho consistiu no estudo e desenvolvimento de novos sistemas catalíticos mais ecológicos para a polimerização via radical por desactivação reversível (RDRP). Este trabalho teve também como objectivo o desenvolvimento de novos sistemas de (co)polimerização de cloreto de vinilo (VC) recorrendo aos métodos RDRP.

A polimerização via radical por transferência de átomo (ATRP) é a mais eficiente, versátil e robusta entre as técnicas de RDRP. Os sistemas catalíticos da última geração para RDRP de monómeros vinílicos devem ser não-tóxicos, económicos, e com rápidas polimerizações em condições “amigas” do meio ambiente. Neste contexto e no âmbito deste trabalho de doutoramento, foram utilizados sulfitos inorgânicos aprovados pelo *Food and Drug Administration* (FDA) tais como: ditionito de sódio ($\text{Na}_2\text{S}_2\text{O}_4$), metabissulfito de sódio ($\text{Na}_2\text{S}_2\text{O}_5$), e bissulfito de sódio (NaHSO_3), como uma nova classe de agentes redutores e activadores suplementares (SARA) muito eficientes para ATRP. Como prova de conceito, estes sulfitos em combinação com pequenas quantidades de $\text{Cu(II)Br}_2/\text{Me}_6\text{TREN}$ (Me_6TREN : tris[2-(dimetilamino)etil]amina) em dimetilsulfóxido (DMSO) à temperatura ambiente (30 °C), foram utilizados para sintetizar poli(acrilato de metilo) (PMA) com peso molecular controlado, baixo valor de dispersividade ($D < 1.05$), e funcionalidade bem definida do terminal de cadeia. Para além disso, foi também descoberto para este SARA ATRP proposto, um surpreendente efeito sinérgico em misturas de um líquido iónico, hexafluorofosfato de 1-butyl-3-metilimidazólio (BMIM- PF_6), e DMSO.

O novo sistema ATRP catalisado por sulfitos inorgânicos foi também expandido com sucesso, utilizando solventes mais ecológicos (álcoois e misturas de álcool/água) para a (co)polimerização de monómeros vinílicos activados, tais como: acrilato de metilo (MA), acrilato de *n*-butilo (*n*-BA), metacrilato de metilo (MMA) e 2-(dimetilamino) metacrilato de etilo (DMAEMA) à temperatura ambiente. Neste sistema, o uso de sulfitos inorgânicos e solventes mais ecológicos (misturas de álcool/água são económicas e possuem baixos pontos de ebulição) é uma notável vantagem para a possibilidade de industrialização do método de ATRP.

Também no âmbito deste trabalho de doutoramento foi desenvolvido pela primeira vez SARA ATRP exclusivamente em água utilizando sulfitos inorgânicos. Neste estudo foi metodicamente investigado os diferentes parâmetros de SARA ATRP em meio aquoso à temperatura ambiente para a síntese de polímeros bem definidos solúveis em água (por exemplo, poli(acrilato de eter oligo(etileno óxido) metilo (POEOA)), catalisado por Cu(II)Br_2 /tris(2-piridilmetil)amina (TPMA) (<30 ppm) sendo adicionado lenta e continuamente à mistura reaccional um sulfito em solução aquosa. O sistema desenvolvido também foi expandido para a síntese de copolímeros de bloco através de uma estratégia “*one-pot*”. Como prova de conceito, este SARA ATRP em água utilizando sulfitos inorgânicos foi aplicado com sucesso, sob condições biologicamente relevantes, para a síntese de um híbrido de proteína albumina do soro bovino–polímero (BSA-[P(OEOA₄₈₀)₃₀]).

O desenvolvimento de métodos RDRP eficientes para o controlo de polimerização de monómeros vinílicos não-activados (por exemplo, acetato de vinilo, *N*-vinilpirrolidona e cloreto de vinilo) continua a ser um grande desafio. Devido à sua versatilidade e baixo custo, o poli(cloreto de vinilo) (PVC) é um dos polímeros mais consumidos em todo o mundo. A polimerização convencional via radical livre (FRP) é o único processo industrial disponível para produzir PVC em grande escala. As várias limitações intrínsecas de FRP desencadearam o interesse em sintetizar este polímero por métodos RDRP. Até 2012, os métodos RDRP de VC mais bem-sucedidos foram conseguidos por meio de polimerização via radical viva por transferência de cadeia degenerativa e transferência de electrão (SET-DTLRP) ou RDRP catalisada por metais (chamado SET-LRP).

Neste contexto, no presente trabalho foi desenvolvida a polimerização via radical por transferência de cadeia reversível por adição-fragmentação (RAFT) de VC. O sucesso da polimerização RAFT (controlo do peso molecular, distribuição do peso molecular e arquitectura molecular dos polímeros resultantes) está fortemente relacionado com a selecção apropriada do agente RAFT (geralmente denominado CTA). Assim, o cianometil metil(fenil)carbamoditioato (CMPCD) mostrou ser um agente RAFT muito eficiente. Os resultados demonstraram que uma selecção cuidadosa das condições de reacção (tipo de iniciador e sua concentração, tipo de solvente e sua concentração, e

temperatura) são fundamentais para a obtenção de produtos de PVC com características controladas (o menor valor de dispersividade alguma vez obtido para o PVC por qualquer método RDRP, $\bar{D} \sim 1.4$). A análise estrutural, via $^1\text{H-NMR}$ e MALDI-TOF-MS, revelou que as cadeias de PVC continham os grupos funcionais e não apresentavam defeitos estruturais. Além disso, a natureza "viva" do PVC, que foi sintetizado através deste método de polimerização RAFT, foi confirmada através de experiências de extensão de cadeia e de copolimerização em bloco de base PVC bem-sucedidas.

Na subsequente etapa do trabalho foi apresentada a síntese de PVC por meio de polimerização via radical mediada por nitróxidos (NMP) a baixa temperatura (entre 30 e 42 °C), utilizando uma alcóxiamina base SG1, *BlocBuilder*. Com uma selecção criteriosa das condições de polimerização (diclorometano (DCM) como solvente e utilizando uma relação monómero/solvente de 1/1) foram obtidas cinéticas de primeira ordem, evoluções lineares do peso molecular com a conversão de VC e diminuição dos valores de \bar{D} (de 1.6 até 1.4) ao longo da polimerização. As caracterizações estruturais realizadas ($^1\text{H-NMR}$ and $^{31}\text{P-NMR}$) do PVC resultante sugeriram a existência de uma quantidade muito pequena de defeitos estruturais e uma elevada preservação dos grupos funcionais nos terminais de cadeia (~ 91% de funcionalidade SG1). Os macroiniciadores de PVC-SG1 foram utilizados com sucesso em experiências de extensão de cadeia usando VC, metacrilato de metilo (MMA) e mistura de monómeros (90% de MMA e 10% de estireno: S) que confirmaram a sua natureza "viva", dando acesso a diferentes tipos de copolímeros de bloco de base PVC.

Apesar de a água ser o solvente ideal em termos de não-toxicidade, muito poucos exemplos de monómeros/polímeros são solúveis em água. Portanto, é altamente desejável o uso de solventes orgânicos "verdes" alternativos. Assim, considerando os resultados muito promissores que foram obtidos em partes anteriores deste trabalho, o éter ciclopentil metilo (CPME) foi introduzido como solvente verde com bastante sucesso na polimerização RAFT, não apenas de VC, mas também de acetato de vinilo (VAc) (usando CMPCD como CTA), S e MA (utilizando ácido 2-(dodeciltiocarbonotioiltio)-2-metilpropiónico (DDMAT) como CTA); e NMP de VC e S (utilizando a alcóxiamina base SG1, *BlocBuilder*). As estruturas dos polímeros obtidos por RAFT e NMP foram comprovadas por $^1\text{H-NMR}$, $^{31}\text{P-NMR}$ e MALDI-TOF-MS. A natureza "viva" dos

polímeros foi também confirmada através de experiências de extensão de cadeia e de copolimerização em bloco bem-sucedidas. Os resultados provaram que o CPME é um excelente substituto “verde” que evita o uso de solventes tóxicos (por exemplo, tetraidrofurano (THF), DMSO, DCM e dimetilformamida (DMF)) em dois dos métodos RDRP mais populares (RAFT e NMP).

List of Publications

Articles published from the research work presented in this thesis:

Abreu, C. M. R., Mendonça, P. V., Serra, A. C., Popov, A. V., Matyjaszewski, K., Guliashvili, T., and Coelho, J. F. J., *Inorganic Sulfites: Efficient Reducing Agents and Supplemental Activators for Atom Transfer Radical Polymerization*. ACS Macro Letters, **2012**, *1*, 1308-1311 (Chapter 2).

Mendes, J. P., Branco, F., **Abreu, C. M. R.**, Mendonça, P. V., Popov, A. V., Guliashvili, T., Serra, A. C., and Coelho, J. F. J., *Synergistic Effect of 1-Butyl-3-methylimidazolium Hexafluorophosphate and DMSO in the SARA ATRP at Room Temperature Affording Very Fast Reactions and Polymers with Very Low Dispersity*. ACS Macro Letters, **2014**, *3*, 544-547 (Chapter 2).

Abreu, C. M. R., Serra, A. C., Popov, A. V., Matyjaszewski, K., Guliashvili, T., and Coelho, J. F. J., *Ambient Temperature Rapid SARA ATRP of Acrylates and Methacrylates in Alcohol-Water Solutions Mediated by a Mixed Sulfite/Cu(II)Br₂ Catalytic System*. Polymer Chemistry, **2013**, *4*, 5629-5636 (Chapter 3).

Abreu, C. M. R., Fu, L., Carmali, S., Serra, A. C., Matyjaszewski, K., and Coelho, J. F. J., *Aqueous SARA ATRP Using Inorganic Sulfites*. Polymer Chemistry, **2017**, *8*, 375-387 (Chapter 4).

Abreu, C. M. R., Mendonça, P. V., Serra, A. C., Coelho, J. F. J., Popov, A. V., Gryn'ova, G., Coote, M. L., and Guliashvili, T., *Reversible Addition-Fragmentation Chain Transfer Polymerization of Vinyl Chloride*. Macromolecules, **2012**, *45*, 2200-2208 (Chapter 5).

Abreu, C. M. R., Mendonça, P. V., Serra, A. C., Noble, B. B., Guliashvili, T., Nicolas, J., Coote, M. L., and Coelho, J. F. J., *Nitroxide-Mediated Polymerization of Vinyl Chloride at Low Temperature: Kinetic and Computational Studies*. Macromolecules, **2016**, *49*, 490-498 (Chapter 6).

Abreu, C. M. R., Maximiano, P., Guliashvili, T., Nicolas, J., Serra, A. C., and Coelho, J. F. J., *Cyclopentyl methyl ether as a green solvent for reversible-addition fragmentation chain transfer and nitroxide-mediated polymerizations*. RSC Advances, **2016**, 6, 7495-7503 (Chapter 7).

Articles in preparation from the research work presented in this thesis:

Abreu, C. M. R., Fonseca A. C., Rocha, N. M. P., Guthrie, J. T., Serra, A. C., Coelho, J. F. J., *Poly(Vinyl Chloride):Current Status and Future Perspectives via Reversible Deactivation Radical Polymerization Method* (Chapter 1).

Articles published from the collaboration in other projects during the PhD program:

Abreu, C. M. R., Mendonça, P. V., Serra, A. C., Coelho, J. F. J., Popov, A. V., and Guliashvili, T., *Accelerated Ambient-Temperature ATRP of Methyl Acrylate in Alcohol-Water Solutions with a Mixed Transition-Metal Catalyst System*. Macromolecular Chemistry and Physics, **2012**, 213, 1677-1687.

Mendes, J. P., Branco, F., **Abreu, C. M. R.**, Mendonça, P. V., Serra, A. C., Popov, A. V., Guliashvili, T., and Coelho, J. F. J., *Sulfolane: an Efficient and Universal Solvent for Copper-Mediated Atom Transfer Radical (co)Polymerization of Acrylates, Methacrylates, Styrene, and Vinyl Chloride*. ACS Macro Letters, **2014**, 3, 858-861.

Maximiano, P., Mendes, J. P., Mendonca, P. V., **Abreu, C. M. R.**, Guliashvili, T., Serra, A. C., and Coelho, J. F. J., *Cyclopentyl methyl ether: A new green co-solvent for supplemental activator and reducing agent atom transfer radical polymerization*. Journal of Polymer Science Part a-Polymer Chemistry, **2015**, 53, 2722-2729.

Mendes, J. P., Mendonca, P. V., Maximiano, P., **Abreu, C. M. R.**, Guliashvili, T., Serra, A. C., and Coelho, J. F. J., *Getting faster: low temperature copper-mediated SARA ATRP*

of methacrylates, acrylates, styrene and vinyl chloride in polar media using sulfolane/water mixtures. Rsc Advances, **2016**, 6, 9598-9603.

Kopeć, M., Yuan, R., Gottlieb, E., **Abreu, C. M. R.**, Song, Y., Wang, Z., Coelho, J. F. J., Matyjaszewski, K., and Kowalewski, T., *Polyacrylonitrile-*b*-poly(butyl acrylate) Block Copolymers as Precursors to Mesoporous Nitrogen-Doped Carbons: Synthesis and Nanostructure.* Macromolecules, **2017**, 50, 2759-2767.

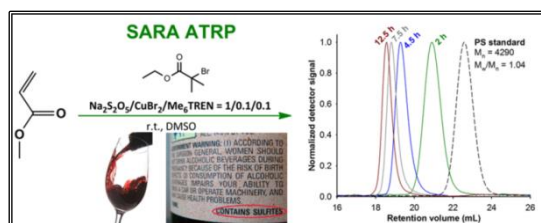
Thesis Outline

The main goals of this PhD project were the development of new ecofriendly catalytic systems for reversible deactivation radical polymerization (RDRP), and the development of new vinyl chloride (VC) (co)polymerizations systems using RDRP methods. Concerning the goals described, this PhD dissertation is organized in eight chapters:



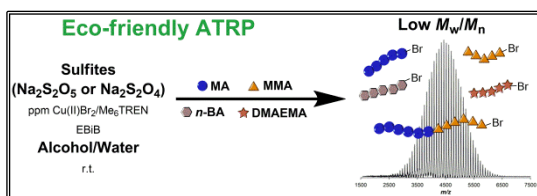
Chapter 1 provides a literature review covering both the reversible deactivation radical polymerization (RDRP) field, and the RDRP methods available for the synthesis of PVC-based materials.

The first part of the experimental work (**Chapters 2 to 4**) is dedicated to the study and development of new ecofriendly catalytic system for atom transfer radical polymerization (ATRP).



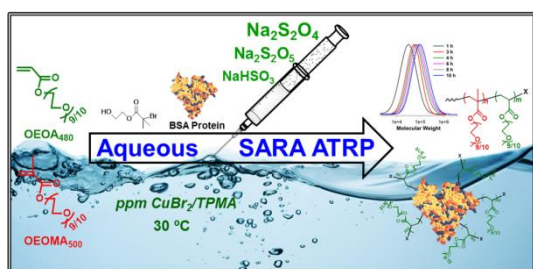
Chapter 2 introduces Food and Drug Administration (FDA) approved inorganic sulfites such as sodium dithionite ($\text{Na}_2\text{S}_2\text{O}_4$), sodium metabisulfite ($\text{Na}_2\text{S}_2\text{O}_5$), and sodium bisulfite (NaHSO_3) as a new class of very

efficient reducing agents and supplemental activators (SARA) for ATRP. It also presents an unusual synergistic effect between an ionic liquid, 1-butyl-3-methylimidazolium hexafluorophosphate (BMIM-PF_6), and DMSO mixtures for this ecofriendly SARA ATRP.



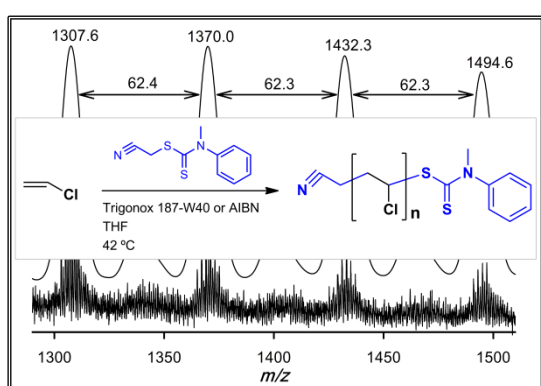
Chapter 3 expands the novel developed inorganic sulfites catalyzed ATRP to the (co)polymerization of activated vinyl monomers, such as methyl acrylate (MA), *n*-

butyl acrylate (*n*-BA), methyl methacrylate (MMA) and 2-(dimethylamino)ethyl methacrylate (DMAEMA), in ecofriendly solvents (alcohols and alcohol-water mixtures) at ambient temperature.

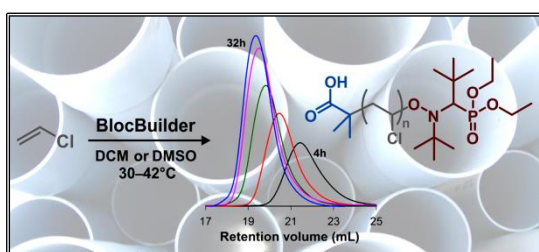


Chapter 4 presents the aqueous SARA ATRP using inorganic sulfites. As proof-of-concept, the developed method was extended to the synthesis of a well-defined bovine serum albumin protein-polymer (BSA-[P(OEOA₄₈₀)₃₀]) hybrid, under biologically relevant conditions.

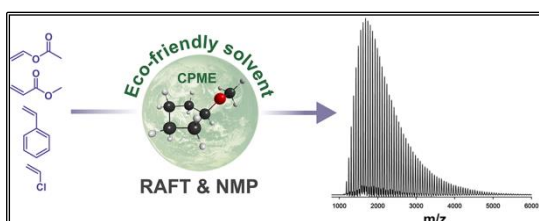
The second part of the experimental work (**Chapters 5 to 7**) is dedicated to the study and development new vinyl chloride (VC) (co)polymerizations systems using RDRP methods.



Chapter 5 introduces reversible addition-fragmentation chain transfer (RAFT) (co)polymerization of VC. The content of this chapter is of significant importance as it could open the door to various macromolecular architectures comprising PVC segments using RAFT and all its benefits compared to other RDRP methods.



Chapter 6 presents the novel SG1-mediated (co)polymerization of VC initiated by the BlocBuilder alkoxyamine at low temperatures via nitroxide-mediated polymerization (NMP). This study establishes a new route to afford a wide range of new complex macrostructures based on PVC segments.



Chapter 7 reports the introduction of cyclopentyl methyl ether (CPME) as green solvent for NMP and RAFT polymerizations. The content of this chapter proves that CPME is an excellent green substitute to avoid the use of toxic solvents in two of the most popular RDRP methods.



Chapter 8 presents the most relevant conclusions from this PhD research and some final remarks, along with further recommendations for future work.

List of Acronyms

AGET	Activators generated by electron transfer
ARGET	Activators regenerated by electron transfer
AscA	Ascorbic acid
ATRA	Atom transfer radical addition
ATRP	Atom transfer radical polymerization
<i>n</i> BA	<i>n</i> -Butyl acrylate
<i>t</i> BA	<i>tert</i> -Butyl acrylate
BMIM-PF ₆	1-Butyl-3-methylimidazolium hexafluorophosphate
bpy	2,2'-Bipyridine
4f-BiB	Pentaerythritol tetrakis(2-bromoisobutyrate)
6f-BiB	Dipentaerythritol hexakis(2-bromoisobutyrate)
BSA	Bovine serum albumin
<i>dn/dc</i>	Refractive Index Increment
CLRP	Controlled/living radical polymerization
CPME	Cyclopentyl methyl ether
DCM	Dichloromethane
DHB	2,5-Dihydroxybenzoic acid
DMAEMA	2-(Dimethylamino)ethyl methacrylate
DMF	Dimethylformamide

List of Acronyms

DMSO	Dimethyl sulfoxide
DP	Degree of polymerization
DT	Degenerative chain transfer
DV	Differential viscometer
eATRP	Electrochemically mediated atom transfer radical polymerization
EBiB	Ethyl α -bromoisobutyrate
EtOH	Ethanol
FDA	Food and Drug Administration
FRP	Free radical polymerization
FTIR-ATR	Fourier transform infrared attenuated total reflection
HABA	2-(4-Hydroxyphenylazo)benzoic acid
HBiB	2-hydroxyethyl α -bromoisobutyrate
HPLC	High performance liquid chromatography
ICAR	Initiators for continuous activator regeneration
IL	Ionic liquid
IUPAC	International Union of Pure and Applied Chemistry
IPA	Isopropanol
LALLS	Low-angle laser-light scattering
LRP	Living radical polymerization
MALDI-TOF	Matrix assisted laser desorption/ionization time-of-flight mass

MA	Methyl acrylate
MMA	Methyl methacrylate
Me6TREN	Tris[2-(dimethylamino)ethyl]amine)
NIPAAm	<i>N</i> -isopropylacrylamide
NMP	Nitroxide mediated polymerization
NMR	Nuclear magnetic resonance
OEOA	Oligo(ethylene oxide) methyl ether acrylate
OEOMA	Oligo(ethylene oxide) methyl ether methacrylate
OSET	Outer sphere electron transfer process
PRE	Persistent radical effect
PBA	Poly(butyl acrylate)
PDMAEMA	Poly(2-(dimethylamino)ethyl methacrylate)
PMA	Poly(methyl acrylate)
PMMA	Poly(methyl methacrylate)
PVAc	Poly(vinyl acetate)
PVC	Poly(vinyl chloride)
PMDETA	<i>N,N,N',N'',N'''</i> -Pentamethyldiethylenetriamine
POEOA	Poly(ethylene glycol) methyl ether acrylate
POEOMA	Poly(ethylene glycol) methyl ether methacrylate
ppm	Parts per million

List of Acronyms

PS	Polystyrene
PTFE	Polytetrafluoroethylene
RALLS	Right-angle laser-light scattering
RAFT	Reversible addition-fragmentation chain transfer
RDRP	Reversible deactivation radical polymerization
RI	Refractive index
SARA	Supplemental activator and reducing agent
SET	Single-electron transfer
SEC	Size exclusion chromatography
SFRP	Stable free radical polymerization
Sty	Styrene
UV-Vis	Ultraviolet-visible
VAc	Vinyl acetate
VC	Vinyl chloride
TEMPO	2,2,6,6-Tetramethylpiperidinyl-1-oxy
THF	Tetrahydrofuran
TMS	Tetramethylsilane
TPMA	Tris(pyridin-2-ylmethyl)amine
TREN	Tris(2-aminoethyl)amine

Nomenclature

D	Dispersity
$M_{n,NMR}$	Number-average molecular weight determined by NMR spectroscopy
$M_{n,SEC}$	Number-average molecular weight determined by SEC
$M_{n,th}$	Theoretical number-average molecular weight
M_w	Weight-average molecular weight
$k_{p,app}$	Apparent rate constant of propagation
k_a	Activation rate constant
k_d	Deactivation rate constant
k_{disp}	Disproportionation rate constant
k_{comp}	Comproportionation rate constant
K_{ATRP}	ATRP equilibrium constant
T	Temperature

Contents

Acknowledgments _____	VII
Abstract _____	IX
Resumo _____	XIII
List of Publications _____	XVII
Thesis Outline _____	XXI
List of Acronyms _____	XXV
Nomenclature _____	XXIX
Contents _____	XXXI
List of Figures _____	XXXVII
List of Schemes _____	XLIX
List of Tables _____	LI
Motivation, Targets and Research Significance _____	LIII
Chapter 1. Literature Review _____	1
1.1. Free Radical Polymerization (FRP) _____	3
1.1.1. Addressing FRP Limitations _____	5
1.2. Reversible Deactivation Radical Polymerization (RDRP) _____	7
1.2.1. Generic Description, Advantages and Limitations on RDRP _____	7
1.2.2. Generic Description of the Main RDRP Techniques _____	11
1.2.3. Nitroxide-Mediated Polymerization (NMP) _____	14

1.2.4. Organometallic Mediated Radical Polymerization (OMRP) _____	16
1.2.5. Atom Transfer Radical Polymerization (ATRP) _____	20
1.2.6. Reversible Addition-Fragmentation Chain Transfer Polymerization (RAFT) _____	24
1.2.7. Iodine/Reverse Iodine Transfer Polymerization (ITP/RITP) _____	26
1.3. Polymerization of Vinyl Chloride _____	27
1.3.1. Properties and Applications of PVC _____	28
1.3.2. Limitations of the PVC Industrial Products that are based on FRP ____	30
1.4. RDRP Methods for VC Polymerization _____	39
1.4.1. Early RDRP Techniques for VC Polymerization _____	41
1.4.2. SET-DTLRP of VC _____	42
1.4.3. SFRP/NMP of VC _____	49
1.4.4. Metal Catalyzed RDRP of VC _____	50
1.4.5. SARA ATRP of VC _____	52
1.4.6. CMRP of VC _____	53
1.4.7. Summary of the RDRP Methods Studied for the VC Polymerization _	54
Chapter 2. Inorganic Sulfites: Efficient Reducing Agents and Supplemental Activators for Atom Transfer Radical Polymerization _____	89
2.1. Abstract _____	91
2.2. Introduction _____	91
2.3. Experimental Section _____	93
2.3.1. Materials _____	93
2.3.2. Techniques _____	94
2.3.3. Procedures _____	95
2.4. Results and Discussion _____	98
2.4.1. SARA ATRP using Inorganic Sulfites _____	98
2.4.2. Model Experiments to Elucidate the SARA ATRP Mechanism _____	100
2.4.3. Variation of Targeted Degree of Polymerization and Monomer _____	104
2.4.4. Solvent Mixtures of BMIM-PF ₆ and DMSO in the SARA ATRP Using Inorganic Sulfites _____	105
2.4.5. Analysis of the PMA Structure _____	110

2.4.6. Evaluation of the PMA Livingness _____	113
2.5. Conclusions _____	114
2.6. References _____	114
Chapter 3. Ambient Temperature Rapid SARA ATRP in Ecofriendly Solvents Mediated by Inorganic Sulfite/Cu(II)Br₂ Catalytic System _____	121
3.1. Abstract _____	123
3.2. Introduction _____	123
3.3. Experimental Section _____	125
3.3.1. Materials _____	125
3.3.2. Techniques _____	126
3.3.3. Procedures _____	127
3.4. Results and Discussion _____	129
3.4.1. SARA ATRP using Inorganic Sulfites in Alcohol-Water Mixtures ____	129
3.4.2. Effect of Water Content (Solvent Mixture) on the Polymerization ____	131
3.4.3. Variation of Targeted Degree of Polymerization _____	133
3.4.4. Preparation of Functional Star-Shaped PMA _____	134
3.4.5. Extension to the Polymerization of Other Monomers _____	137
3.4.6. Analysis of the PMA Structure _____	140
3.4.7. Evaluation of the PMA Livingness _____	143
3.5. Conclusions _____	144
3.6. References _____	144
Chapter 4. Aqueous Supplemental Activator and Reducing Agent Atom Transfer Radical Polymerization Using Inorganic Sulfites _____	151
4.1. Abstract _____	155
4.2. Introduction _____	155
4.3. Experimental Section _____	157
4.3.1. Materials _____	157
4.3.2. Techniques _____	158
4.3.3. Procedures _____	159
4.4. Results and Discussion _____	160

4.4.1. Aqueous SARA ATRP Using Inorganic Sulfites _____	160
4.4.2. Effect of the Feeding Rate of Sulfite (FRS) on the Polymerization ____	162
4.4.3. Model Experiments to Elucidate the SARA ATRP Mechanism _____	166
4.4.4. Effect of the Ligand (L) and its Concentration on the Polymerization _	171
4.4.5. Effect of an Added Salt and its Concentration on the Polymerization _	172
4.4.6. Effect of Sulfite (or SARA Agent) Used on the Polymerization _____	176
4.4.7. Variation of Cu Concentration, Targeted DP and Monomer _____	177
4.4.8. Start/Stop Polymerizations _____	180
4.4.9. Chain Extension Experiments _____	181
4.4.10. Synthesis of a Protein–Polymer Hybrid _____	182
4.5. Conclusions _____	186
4.6. References _____	186

Chapter 5. Reversible Addition-Fragmentation Chain Transfer

(co)Polymerization of Vinyl Chloride _____	193
5.1. Abstract _____	195
5.2. Introduction _____	195
5.3. Experimental Section _____	196
5.3.1. Materials _____	196
5.3.2. Techniques _____	197
5.3.3. Procedures _____	198
5.3.4. Computational Procedures _____	200
5.4. Results and Discussion _____	200
5.4.1. RAFT Polymerizations of VC under Different Conditions _____	200
5.4.2. Kinetic Study and Mechanistic Aspects of RAFT Polymerization of VC _____	203
5.4.3. Analysis of the PVC Structure _____	206
5.4.4. Evaluation of the PVC Livingness _____	210
5.5. Conclusions _____	211
5.6. References _____	212

Chapter 6. Nitroxide-Mediated (co)Polymerization of Vinyl Chloride at Low Temperature	217
6.1. Abstract	219
6.2. Introduction	219
6.3. Experimental Section	221
6.3.1. Materials	221
6.3.2. Techniques	222
6.3.3. Procedures	223
6.3.4. Computational Procedures	225
6.4. Results and Discussion	225
6.4.1. Influence of the Solvent	225
6.4.2. Influence of the Monomer Concentration	228
6.4.3. Influence of Polymerization Temperature	228
6.4.4. Variation of Targeted Degree of Polymerization	229
6.4.5. Analysis of the PVC Structure	231
6.4.6. Evaluation of the PVC Livingness	233
6.5. Conclusions	235
6.6. References	235
Chapter 7. Cyclopentyl Methyl Ether as a Green Solvent for Reversible-Addition Fragmentation Chain Transfer and Nitroxide-Mediated Polymerizations	243
7.1. Abstract	245
7.2. Introduction	245
7.3. Experimental Section	246
7.3.1. Materials	246
7.3.2. Techniques	247
7.3.3. Procedures	248
7.4. Results and Discussion	252
7.4.1. RAFT Polymerization in CPME	252
7.4.2. Structural Analysis of the RAFT-Derived Polymers	256
7.4.3. Evaluation of the RAFT-Derived Polymer Livingness	259

7.4.4. NMP in CPME _____	260
7.4.5. Structural Analysis of the NMP-Derived Polymers _____	263
7.4.6. Evaluation of the NMP-Derived Polymer Livingness _____	264
7.5. Conclusions _____	265
7.6. References _____	266
Chapter 8. Conclusions & Future Work _____	273
8.1. Overall Conclusions _____	275
8.2. Recommendations for Future Work _____	277
Appendices _____	279
Appendix A: Supporting Information for Chapter 2 _____	A1
Appendix B: Supporting Information for Chapter 3 _____	B1
Appendix C: Supporting Information for Chapter 4 _____	C1
Appendix D: Supporting Information for Chapter 5 _____	D1
Appendix E: Supporting Information for Chapter 6 _____	E1

List of Figures

- Figure 1.1.** Controlled molecular structures attained by RDRP methods. _____ 8
- Figure 1.2.** GPC traces of the macroinitiator before (right curve) and after the chain extension experiment or the block copolymerization (left curve). _____ 10
- Figure 1.3.** Structures of nitroxide and alkoxyamine derivatives commonly used in NMP. _____ 15
- Figure 1.4.** Structures of organometallic complexes commonly used in OMRP. _____ 18
- Figure 1.5.** Milestones in PVC History from 1835 to 2000. _____ 28
- Figure 1.6.** Milestones in RDRP methods for VC polymerization. _____ 40
- Figure 1.7.** Diversity of PVC structures obtained by SET-DTLRP. _____ 45
- Figure 1.8.** Stress-strain curves of PVC-*b*-PBA-*b*-PVC block copolymers with different compositions (left), and a PVC-*b*-PBA-*b*-PVC block copolymer and some flexible PVC made with DOP. _____ 47
- Figure 1.9.** Diversity of PVC-based block copolymer structures obtained by SET-DTLRP. _____ 48
- Figure 1.10.** GPC traces of the (a) PVC-Br macroinitiator (black line), and the PMA-*b*-PVC-*b*-PMA (blue line) and PS-*b*-PVC-*b*-PS block copolymers (red line); (b) PVC-Br macroinitiator (right curve), and the PMA-*b*-PVC-*b*-PMA block copolymer (left curve) prepared by “one-pot” SARA ATRP chain extension. _____ 52
- Figure 2.1.** Kinetic plots of MA conversion and $\ln[M]_0/[M]$ vs. time (a, c and e) and plot of number average molecular weights ($M_{n, \text{GPC}}$) and \mathcal{D} (M_w/M_n) vs. theoretical number-average molecular weights ($M_{n, \text{th}}$) (b, d and f) for ATRP of MA in the presence of $\text{CuBr}_2/\text{Me}_6\text{TREN}$ with different reducing agents (RA = $\text{Na}_2\text{S}_2\text{O}_4$ (a and b), $\text{Na}_2\text{S}_2\text{O}_5$ (c and d) and NaHSO_3 (e and f). Conditions: $[\text{MA}]_0/[\text{EBiB}]_0/[\text{RA}]_0/[\text{CuBr}_2]_0/[\text{Me}_6\text{TREN}]_0 = 222/1/1/0.1/0.1$ at 30 °C in DMSO; $[\text{MA}]_0/[\text{DMSO}] = 2/1$ (v/v). _____ 99
- Figure 2.2.** Kinetic plots of monomer conversion and $\ln[M]_0/[M]$ vs. time (a and c) and plot of $M_{n, \text{GPC}}$ and \mathcal{D} (M_w/M_n) vs. $M_{n, \text{th}}$ (b and d) for SARA ATRP of MA catalyzed with mixed catalyst system $\text{Na}_2\text{S}_2\text{O}_4/\text{CuBr}_2/\text{Me}_6\text{TREN}$ for different $[\text{Na}_2\text{S}_2\text{O}_4]_0/[\text{CuBr}_2]_0$: 0.5/0.1 (a and b) and 2/0.1 (c and d). Conditions: $[\text{MA}]_0/[\text{EBiB}]_0/[\text{Na}_2\text{S}_2\text{O}_4]_0/[\text{CuBr}_2]_0/[\text{Me}_6\text{TREN}]_0 = 222/1/(0.5 \text{ or } 2)/0.1/0.1$ at 30 °C in DMSO; $[\text{MA}]_0/[\text{DMSO}] = 2/1$ (v/v). _____ 100

Figure 2.3. Kinetic plots of monomer conversion and $\ln[M]_0/[M]$ vs. time (a and c) and plot of $M_{n,GPC}$ and $\mathcal{D} (M_w/M_n)$ vs. $M_{n,th}$ (b and d) for $[MA]_0/[Na_2S_2O_4]_0 = 222/1$ (a and b) and $[MA]_0/[EBiB]_0/[Na_2S_2O_4]_0 = 222/1/1$ (c and d) at 30 °C in DMSO; $[MA]_0/[DMSO] = 2/1$ (v/v). _____ 101

Figure 2.4. The UV-vis spectra of reduction of $Cu(II)Br_2/Me_6TREN$ by $Na_2S_2O_4$ in DMSO recorded at different reaction times (30 °C), $[Na_2S_2O_4]_0/[CuBr_2]_0/[Me_6TREN]_0 = 0.1/0.01/0.01$ mmol/mL. _____ 102

Figure 2.5. Kinetic plots of monomer conversion and $\ln[M]_0/[M]$ vs. time (a and c) and plot of $M_{n,GPC}$ and $\mathcal{D} (M_w/M_n)$ vs. $M_{n,th}$ (b and d) for SARA ATRP of MA catalyzed with mixed catalyst system $Na_2S_2O_4/CuBr_2/Me_6TREN$ for different DP's: 70 (a and b) and 1100 (c and d). Conditions: $[MA]_0/[EBiB]_0/[Na_2S_2O_4]_0/[CuBr_2]_0/[Me_6TREN]_0 = (70 \text{ or } 1100)/1/1/0.1/0.1$ at 30 °C in DMSO; $[MA]_0/[DMSO] = 2/1$ (v/v). _____ 104

Figure 2.6. Kinetic plots of conversion and $\ln[M]_0/[M]$ vs. time (a and c) and plots of $M_{n,GPC}$ and $\mathcal{D} (M_w/M_n)$ vs. $M_{n,th}$ (b and d) for the SARA ATRP of MA catalyzed by $Na_2S_2O_4/CuBr_2/Me_6TREN$ in (a and b) $BMIM-PF_6/DMSO = 5/95$ (v/v) and (c and d) $BMIM-PF_6/DMSO = 50/50$ (v/v). Conditions: $[MA]_0/[solvent] = 2/1$ (v/v); $[MA]_0/[EBiB]_0/[Na_2S_2O_4]_0/[CuBr_2]_0/[Me_6TREN]_0 = 222/1/1/0.1/0.1$ (molar); $T = 30$ °C. 106

Figure 2.7. k_p^{app} values of the SARA ATRP of MA catalyzed by $Na_2S_2O_4/CuBr_2/Me_6TREN$ in $BMIM-PF_6/DMSO$ mixtures, for different contents of $BMIM-PF_6$ in the reaction mixture. Conditions: $[MA]_0/[solvent] = 2/1$ (v/v); $[MA]_0/[EBiB]_0/[Na_2S_2O_4]_0/[CuBr_2]_0/[Me_6TREN]_0 = 222/1/1/0.1/0.1$ (molar); $T = 30$ °C. 106

Figure 2.8. a) UV-Vis spectra in different $BMIM-PF_6/DMSO$ mixtures with Reichardt's dye 30 (50 μM); b) Experimental $E_T(30)$ value in different $BMIM-PF_6/DMSO$ mixtures (the dashed line represents the predicted $E_T(30)$). _____ 107

Figure 2.9. Viscosity values in different $BMIM-PF_6/DMSO$ mixtures. _____ 110

Figure 2.10. The 1H NMR spectrum of PMA-Br ($M_{n,GPC} = 4100$; $\mathcal{D} = 1.05$; $M_{n,NMR} = 3727$; active chain-end functionality = 90 %). The PMA is atactic: $[dr] = [dm] = 0.5$. The solvent is $CDCl_3$. _____ 111

Figure 2.11. MALDI-TOF-MS in the linear mode (using HABA as matrix) of PMA-Br ($M_{n,GPC} = 4100$; $\mathcal{D} = 1.05$) from m/z 500 to 7500. _____ 112

Figure 2.12. Enlargement of the MALDI-TOF-MS from m/z 3450 to 3950 of PMA-Br ($M_{n,GPC} = 4100$; $\bar{D} = 1.05$). _____ 112

Figure 2.13. GPC traces of the PMA before (right curve) and after the chain extension (left curve) experiment. _____ 113

Figure 3.1. Kinetic plots of conversion and $\ln[M]_0/[M]$ vs. time (a, c, e) and plots of $M_{n,GPC}$ and $\bar{D} (M_w/M_n)$ vs. $M_{n,th}$ (b, d, f) for SARA ATRP of MA catalyzed in the presence of $\text{Cu(II)Br}_2/\text{Me}_6\text{TREN}$ with different reducing agents [$\text{Na}_2\text{S}_2\text{O}_4$ (a, b, e, f) and $\text{Na}_2\text{S}_2\text{O}_5$ (c, d)] in different alcohol-water [90/10 (v/v)] mixtures [EtOH-H₂O (a, b, c, d) and MeOH-H₂O (e, f)] at 30 °C. Conditions: $[\text{MA}]_0/[\text{solvent}] = 2/1$ (v/v); $[\text{MA}]_0/[\text{EBiB}]_0/[\text{Na}_2\text{S}_2\text{O}_4 \text{ or } \text{Na}_2\text{S}_2\text{O}_5]_0/[\text{Cu(II)Br}_2]_0/[\text{Me}_6\text{TREN}]_0 = 222/1/1/0.1/0.1$. ____ 130

Figure 3.2. Kinetic plots of conversion and $\ln[M]_0/[M]$ vs. time (a, c, e) and plot of $M_{n,GPC}$ and $\bar{D} (M_w/M_n)$ vs. $M_{n,th}$ (b, d, f) for SARA ATRP of MA catalyzed with $\text{Na}_2\text{S}_2\text{O}_4$ in the presence of $\text{Cu(II)Br}_2/\text{Me}_6\text{TREN}$ at 30 °C in EtOH-H₂O mixtures with different contents of water. Conditions: $[\text{MA}]_0/[\text{EBiB}]_0/[\text{Na}_2\text{S}_2\text{O}_4]_0/[\text{Cu(II)Br}_2]_0/[\text{Me}_6\text{TREN}]_0 = 222/1/1/0.1/0.1$; $[\text{MA}]_0/[\text{solvent}] = 2/1$ (v/v). _____ 132

Figure 3.3. Kinetic plots of conversion and $\ln[M]_0/[M]$ vs. time (a and c) and plot of $M_{n,GPC}$ and $\bar{D} (M_w/M_n)$ vs. $M_{n,th}$ (b and d) for SARA ATRP of MA catalyzed with $\text{Na}_2\text{S}_2\text{O}_4$ in the presence of $\text{Cu(II)Br}_2/\text{Me}_6\text{TREN}$ at 30 °C in EtOH-H₂O (v/v) = 90/10. Conditions: $[\text{MA}]_0/[\text{solvent}] = 2/1$ (v/v); $[\text{MA}]_0/[\text{EBiB}]_0/[\text{Na}_2\text{S}_2\text{O}_4]_0/[\text{Cu(II)Br}_2]_0/[\text{Me}_6\text{TREN}]_0 = \text{DP}/1/1/0.1/0.1$, for DP = 60 (a and b) and DP = 1100 (c and d). _____ 133

Figure 3.4. Kinetic plots of conversion and $\ln[M]_0/[M]$ vs. time (a and c) and plot of $M_{n,GPC}$ and $\bar{D} (M_w/M_n)$ vs. $M_{n,th}$ (b and d) for SARA ATRP of MA catalyzed with $\text{Na}_2\text{S}_2\text{O}_4$ in the presence of $\text{Cu(II)Br}_2/\text{Me}_6\text{TREN}$ at 30 °C in EtOH-H₂O (v/v) = 90/10. Conditions: $[\text{MA}]_0/[\text{solvent}] = 2/1$ (v/v); $[\text{MA}]_0/[\text{EBiB}]_0/[\text{Na}_2\text{S}_2\text{O}_4]_0/[\text{Cu(II)Br}_2]_0/[\text{Me}_6\text{TREN}]_0 = \text{DP}/1/1/0.1/0.1$, for DP = 60 (a and b) and DP = 1100 (c and d). _____ 135

Figure 3.5. Kinetic plots of conversion and $\ln[M]_0/[M]$ vs. time (a, c, e) and plot of $M_{n,GPC}$ and $\bar{D} (M_w/M_n)$ vs. $M_{n,th}$ (b, d, f) for SARA ATRP of *n*-BA (a, b), MMA (c, d) and DMAEMA (e, f) catalyzed with $\text{Na}_2\text{S}_2\text{O}_4$ in the presence of $\text{Cu(II)Br}_2/\text{Me}_6\text{TREN}$ at 30 °C in EtOH-H₂O (v/v) = 90/10. Conditions: $[\text{MA}]_0/[\text{solvent}] = 2/1$ (v/v); $[\text{Mon.}]_0/[\text{EBiB}]_0/[\text{Na}_2\text{S}_2\text{O}_4]_0/[\text{Cu(II)Br}_2]_0/[\text{Me}_6\text{TREN}]_0 = 222/1/1/0.1/0.1$. _____ 138

Figure 3.6. The ^1H NMR spectrum of PMA-Br obtained at high conversion ($M_{n,\text{GPC}} = 4400$; $\mathcal{D} = 1.04$; $M_{n,\text{NMR}} = 4410$; active chain-end functionality = 99 %). The PMA is atactic: $[\text{dr}] = [\text{dm}] = 0.5$. The solvent is CDCl_3 . _____ 140

Figure 3.7. MALDI-TOF-MS (a) in the linear mode (using DHB as matrix) of PMA-Br ($M_{n,\text{GPC}} = 4400$, $\mathcal{D} = 1.04$); (b) Enlargement of the MALDI-TOF-MS from m/z 4150 to 47500 of PMA-Br. _____ 141

Figure 3.8. The ^1H NMR spectrum of four arm star PMA- Br_4 obtained at high conversion ($M_{n,\text{GPC}} = 37200$; $\mathcal{D} = 1.05$; $M_{n,\text{NMR}} = 43085$; active chain-end functionality = 99 %). The PMA is atactic: $[\text{dr}] = [\text{dm}] = 0.5$. The solvent is CDCl_3 . _____ 142

Figure 3.9. GPC traces of the PMA-Br macroinitiator before (right curve), after the chain extension experiment and PMA-*b*-PMMA block copolymer (left curves). _____ 143

Figure 4.1. (a) Kinetic plots of conversion and $\ln[M]_0/[M]$ vs. time; (b) plot of number-average molecular weights ($M_{n,\text{GPC}}$) and \mathcal{D} (M_w/M_n) vs. conversion for aqueous SARA ATRP of OEOA₄₈₀ at 30 °C; and (c) GPC traces vs. time. Conditions: $[\text{OEOA}_{480}]_0/[\text{HEBiB}]_0/[\text{Na}_2\text{S}_2\text{O}_4]_0/[\text{Cu(II)Br}_2]_0/[\text{TPMA}]_0 = 250/1/1/0.05/0.4$; $[\text{NaCl}]_0 = 100$ mM; $[\text{OEOA}_{480}]_0/[\text{Water}] = 1/3$. _____ 161

Figure 4.2. (a, d and g) Kinetic plots of conversion and $\ln[M]_0/[M]$ vs. time; (b, e and h) plot of $M_{n,\text{GPC}}$ and \mathcal{D} (M_w/M_n) vs. conversion for aqueous SARA ATRP of OEOA₄₈₀ at 30 °C; and (c, f and i) GPC traces vs. time. Conditions: $[\text{OEOA}_{480}]_0/[\text{HEBiB}]_0/[\text{Cu(II)Br}_2]_0/[\text{TPMA}]_0 = 250/1/0.05/0.4$; $\text{FR}(\text{Na}_2\text{S}_2\text{O}_4) = 8$ (a, b and c), 64 (d, e and f) and 128 (g, h and i) nmol/min; $[\text{NaCl}]_0 = 100$ mM; $[\text{OEOA}_{480}]_0/[\text{Water}] = 1/3$. _____ 163

Figure 4.3. k_p^{app} values of the SARA ATRP of OEOA₄₈₀ catalyzed by $\text{CuBr}_2/\text{TPMA}$ in water at 30 °C vs. $\text{FR}(\text{Na}_2\text{S}_2\text{O}_4)^{1/2}$. Conditions: $[\text{OEOA}_{480}]_0/[\text{HEBiB}]_0/[\text{Cu(II)Br}_2]_0/[\text{TPMA}]_0 = 250/1/0.05/0.4$; $[\text{OEOA}_{480}]_0/[\text{Water}] = 1/3$. _____ 164

Figure 4.4. (a) Kinetic plots of conversion and $\ln[M]_0/[M]$ vs. time; (b) plot of $M_{n,\text{GPC}}$ and \mathcal{D} (M_w/M_n) vs. conversion for aqueous SARA ATRP of OEOA₄₈₀ at 30 °C; and (c) GPC traces vs. time. Conditions: $[\text{OEOA}_{480}]_0/[\text{HEBiB}]_0/[\text{Cu(II)Br}_2]_0/[\text{TPMA}]_0 = 250/1/0.05/0.4$; $\text{FR}(\text{Na}_2\text{S}_2\text{O}_4) = 64$ nmol/min (until 4.5h) and $\text{FR}(\text{Na}_2\text{S}_2\text{O}_4) = 8$ nmol/min (until 32h); $[\text{NaCl}]_0 = 100$ mM; $[\text{OEOA}_{480}]_0/[\text{Water}] = 1/3$. _____ 164

Figure 4.5. (a) Kinetic plots of conversion and $\ln[M]_0/[M]$ vs. time; (b) plot of $M_{n,GPC}$ and $\bar{D} (M_w/M_n)$ vs. conversion for aqueous SARA ATRP of OEOA₄₈₀ at 30 °C; and (c) GPC traces vs. time. Conditions: $[OEOA_{480}]_0/[HEBiB]_0/[Cu(II)Br_2]_0/[TPMA]_0 = 250/1/0/0$; $FR(Na_2S_2O_4) = 64$ nmol/min; $[NaCl]_0 = 100$ mM; $[OEOA_{480}]_0/[Water] = 1/3$. 166

Figure 4.6. (a) Kinetic plots of conversion and $\ln[M]_0/[M]$ vs. time; (b) plot of $M_{n,GPC}$ and $\bar{D} (M_w/M_n)$ vs. conversion for aqueous SARA ATRP of OEOA₄₈₀ at 30 °C; and (c) GPC traces vs. time. Conditions: $[OEOA_{480}]_0/[HEBiB]_0/[Cu(II)Br_2]_0/[TPMA]_0 = 250/0/0/0$; $FR(Na_2S_2O_4) = 64$ nmol/min; $[NaCl]_0 = 100$ mM; $[OEOA_{480}]_0/[Water] = 1/3$. 167

Figure 4.7. Determination of the supplemental activator apparent rate constant for HEBiB in water at 30 °C feeding $Na_2S_2O_4$. Conditions: $[HEBiB]_0 = 20$ mM; $FR(Na_2S_2O_4) = 64$ nmol/min. _____ 167

Figure 4.8. UV–vis spectra of reduction of $Cu(II)Br_2/TPMA$ by $Na_2S_2O_4$ in water at 30 °C; $[CuBr_2]_0/[TPMA]_0/[Na_2S_2O_4]_0/[NaBr]_0 = 2.5/20/2.5/50$ mM. _____ 168

Figure 4.9. Determination of reduction rate of $[Cu(II)Br_2]_0/[TPMA]_0$ in water at 30 °C feeding $Na_2S_2O_4$. Conditions: $[Cu(II)Br_2]_0/[TPMA]_0/[NaCl]_0 = 10/80/100$ mM; $FR(Na_2S_2O_4) = 64$ nmol/min. _____ 169

Figure 4.10. (a) Kinetic plots of conversion and $\ln[M]_0/[M]$ vs. time; (b) plot of $M_{n,GPC}$ and $\bar{D} (M_w/M_n)$ vs. conversion for aqueous SARA ATRP of OEOA₄₈₀ at 30 °C; and (c) GPC traces vs. time. Conditions: $[OEOA_{480}]_0/[HEBiB]_0/[Cu(II)Br_2]_0/[TPMA]_0 = 250/1/0.05/0.1$; $FR(Na_2S_2O_4) = 64$ nmol/min; $[NaCl]_0 = 100$ mM; $[OEOA_{480}]_0/[Water] = 1/3$. _____ 171

Figure 4.11. (a) Kinetic plots of conversion and $\ln[M]_0/[M]$ vs. time; (b) plot of $M_{n,GPC}$ and $\bar{D} (M_w/M_n)$ vs. conversion for aqueous SARA ATRP of OEOA₄₈₀ at 30 °C; and (c) GPC traces vs. time. Conditions: $[OEOA_{480}]_0/[HEBiB]_0/[Cu(II)Br_2]_0/[Me_6TREN]_0 = 250/1/0.05/0.4$; $FR(Na_2S_2O_4) = 64$ nmol/min; $[NaCl]_0 = 100$ mM; $[OEOA_{480}]_0/[Water] = 1/3$. _____ 172

Figure 4.12. (a, d, g and j) Kinetic plots of conversion and $\ln[M]_0/[M]$ vs. time; (b, e, h and k) plot of $M_{n,GPC}$ and $\bar{D} (M_w/M_n)$ vs. conversion for aqueous SARA ATRP of OEOA₄₈₀ at 30 °C; and (c, f, i and l) GPC traces vs. time. Conditions: $[OEOA_{480}]_0/[HEBiB]_0/[Cu(II)Br_2]_0/[TPMA]_0 = 250/1/0.05/0.4$; $FR(Na_2S_2O_4) = 64$ nmol/min; $[OEOA_{480}]_0/[Water] = 1/3$; (a, b and c) $[TEACl]_0 = 100$ mM, (d, e and f) $[NaBr]_0 = 100$ mM, (g, h and i) $[NaCl]_0 = 10$ mM, and (j, k and l) $[Salt]_0 = 0$ mM. _____ 173

Figure 4.13. (a) Kinetic plots of conversion and $\ln[M]_0/[M]$ vs. time; (b) plot of $M_{n, \text{GPC}}$ and \bar{D} (M_w/M_n) vs. conversion for aqueous SARA ATRP of OE OA₄₈₀ at 30 °C; and (c) GPC traces vs. time. Conditions: $[\text{OE OA}_{480}]_0/[\text{HEBiB}]_0/[\text{Cu(II)Br}_2]_0/[\text{TPMA}]_0 = 250/1/0.05/0.4$; $[\text{OE OA}_{480}]_0/[\text{Water}] = 1/3$; $\text{FR}(\text{Na}_2\text{S}_2\text{O}_5) = 64$ nmol/min; $[\text{NaCl}]_0 = 100$ mM. _____ 176

Figure 4.14. (a) Kinetic plots of conversion and $\ln[M]_0/[M]$ vs. time; (b) plot of $M_{n, \text{GPC}}$ and \bar{D} (M_w/M_n) vs. conversion for aqueous SARA ATRP of OE OA₄₈₀ at 30 °C; and (c) GPC traces vs. time. Conditions: $[\text{OE OA}_{480}]_0/[\text{HEBiB}]_0/[\text{Cu(II)Br}_2]_0/[\text{TPMA}]_0 = 250/1/0.05/0.4$; $[\text{OE OA}_{480}]_0/[\text{Water}] = 1/3$; $\text{FR}(\text{NaHSO}_3) = 64$ nmol/min; $[\text{NaCl}]_0 = 100$ mM. _____ 176

Figure 4.15. (a and d) Kinetic plots of conversion and $\ln[M]_0/[M]$ vs. time; (b and e) plot of $M_{n, \text{GPC}}$ and \bar{D} (M_w/M_n) vs. conversion for aqueous SARA ATRP of OE OA₄₈₀ at 30 °C; and (c and f) GPC traces vs. time. Conditions: (a, b and c) $[\text{OE OA}_{480}]_0/[\text{HEBiB}]_0/[\text{Cu(II)Br}_2]_0/[\text{TPMA}]_0 = 1000/1/0.05/0.4$; (d, e and f) $[\text{OE OA}_{480}]_0/[\text{HEBiB}]_0/[\text{Cu(II)Br}_2]_0/[\text{TPMA}]_0 = 1000/1/0.01/0.08$; $[\text{OE OA}_{480}]_0/[\text{Water}] = 1/3$; $\text{FR}(\text{Na}_2\text{S}_2\text{O}_4) = 16$ nmol/min; $[\text{NaCl}]_0 = 100$ mM. _____ 178

Figure 4.16. (a) Kinetic plots of conversion and $\ln[M]_0/[M]$ vs. time; (b) plot of $M_{n, \text{GPC}}$ and \bar{D} (M_w/M_n) vs. conversion for aqueous SARA ATRP of OE OA₄₈₀ at 30 °C; and (c) GPC traces vs. time. Conditions: $[\text{OE OA}_{480}]_0/[\text{HEBiB}]_0/[\text{Cu(II)Br}_2]_0/[\text{TPMA}]_0 = 50/1/0.05/0.4$; $[\text{OE OA}_{480}]_0/[\text{Water}] = 1/3$; $\text{FR}(\text{Na}_2\text{S}_2\text{O}_4) = 64$ nmol/min; $[\text{NaCl}]_0 = 100$ mM. _____ 178

Figure 4.17. (a) Kinetic plots of conversion and $\ln[M]_0/[M]$ vs. time; (b) plot of $M_{n, \text{GPC}}$ and \bar{D} (M_w/M_n) vs. conversion for aqueous SARA ATRP of OE OMA₅₀₀ at 30 °C; and (c) GPC traces vs. time. Conditions: $[\text{OE OMA}_{500}]_0/[\text{HEBiB}]_0/[\text{Cu(II)Br}_2]_0/[\text{TPMA}]_0 = 50/1/0.05/0.4$; $[\text{OE OMA}_{500}]_0/[\text{Water}] = 1/3$; $\text{FR}(\text{Na}_2\text{S}_2\text{O}_4) = 64$ nmol/min; $[\text{NaCl}]_0 = 100$ mM. _____ 180

Figure 4.18. (a) Kinetic plots of conversion and $\ln[M]_0/[M]$ vs. time; (b) plot of $M_{n, \text{GPC}}$ and \bar{D} (M_w/M_n) vs. conversion for aqueous SARA ATRP of OE OA₄₈₀ at 30 °C; and (c) GPC traces vs. time. Conditions: $[\text{OE OA}_{480}]_0/[\text{HEBiB}]_0/[\text{Cu(II)Br}_2]_0/[\text{TPMA}]_0 = 250/1/0.05/0.1$; $\text{FR}(\text{Na}_2\text{S}_2\text{O}_4) = 64$ nmol/min; $[\text{NaCl}]_0 = 100$ mM; $[\text{OE OA}_{480}]_0/[\text{Water}] = 1/3$. _____ 181

Figure 4.19. (a) Kinetic plots of conversion and $\ln[M]_0/[M]$ vs. time; (b) plot of $M_{n, \text{GPC}}$ and \mathcal{D} (M_w/M_n) vs. conversion for aqueous SARA ATRP of OEOA₄₈₀ at 30 °C; and (c) GPC traces vs. time. Conditions: $[\text{OEOA}_{480}]_0/[\text{HEBiB}]_0/[\text{Cu(II)Br}_2]_0/[\text{TPMA}]_0 = 250/1/0.05/0.1$; $\text{FR}(\text{Na}_2\text{S}_2\text{O}_4) = 64 \text{ nmol/min}$; $[\text{NaCl}]_0 = 100 \text{ mM}$; $[\text{OEOA}_{480}]_0/[\text{Water}] = 1/3$. _____ 182

Figure 4.20. (a) Kinetic plots of conversion and $\ln[M]_0/[M]$ vs. time; (b) plot of $M_{n, \text{GPC}}$ and \mathcal{D} (M_w/M_n) vs. conversion for aqueous SARA ATRP of OEOA₄₈₀ at 30 °C; and (c) GPC traces vs. time. Conditions: $[\text{OEOA}_{480}]_0/[\text{BSA-O-[iBBr]}_{30}]_0/[\text{Cu(II)Br}_2]_0/[\text{TPMA}]_0 = 250/1/0.05/0.4$; $[\text{OEOA}_{480}]_0/[\text{PBS}] = 1/6$; $\text{FR}(\text{Na}_2\text{S}_2\text{O}_4) = 16 \text{ nmol/min}$. _____ 183

Figure 4.21. SDS-PAGE of native BSA (66 kDa), BSA-O-[iBBr]₃₀ (75 kDa), various concentrations of BSA-[P(OEOA₄₈₀)₃₀ hybrids, and protein markers. _____ 184

Figure 4.22. Dynamic light scattering distribution of BSA-O-[iBBr]₃₀ before polymerization (blue line) and BSA-[P(OEOA₄₈₀)₃₀ nanoparticles; Conditions: $[\text{OEOA}_{480}]_0/[\text{BSA-O-[iBBr]}_{30}]_0/[\text{Cu(II)Br}_2]_0/[\text{TPMA}]_0 = 250/1/0.05/0.4$; $[\text{OEOA}_{480}]_0/[\text{Water}] = 1/6$; $\text{FR}(\text{Na}_2\text{S}_2\text{O}_4) = 16 \text{ nmol/min}$. _____ 184

Figure 5.1. Structures of a) cyanomethyl methyl(phenyl)carbamdithioate (CMPCD), b) Trigonox 187-W40 (diisobutryl peroxide or DIBPO) and c) 2,2'-azobisisobutyronitrile (AIBN). _____ 196

Figure 5.2. RAFT polymerization of VC in THF at 42 °C mediated by CMPCD using Trigonox 187-W40 as conventional initiator. (a) Conversion and $\ln[M]_0/[M]$ vs. time. (b) M_n^{GPC} and M_w/M_n vs. M_n^{th} . Reaction conditions: $[\text{VC}]_0/[\text{CMPCD}]_0/[\text{Trigonox}]_0 = 100/1/0.2$; $[\text{VC}]_0/[\text{THF}] = 1/1$ (v/v). _____ 204

Figure 5.3. RAFT polymerization of VC in THF at 42 °C mediated by CMPCD using Trigonox 187-W40 as conventional initiator. (a) Conversion and $\ln[M]_0/[M]$ vs. time. (b) M_n^{GPC} and M_w/M_n vs. M_n^{th} . Reaction conditions: $[\text{VC}]_0/[\text{CMPCD}]_0/[\text{Trigonox}]_0 = 250/1/0.2$; $[\text{VC}]_0/[\text{THF}] = 1/1$ (v/v). _____ 204

Figure 5.4. RAFT polymerization of VC in THF at 42 °C mediated by CMPCD using AIBN as conventional initiator. (a) Conversion and $\ln[M]_0/[M]$ vs. time. (b) M_n^{GPC} and M_w/M_n vs. M_n^{th} . Reaction conditions: $[\text{VC}]_0/[\text{CMPCD}]_0/[\text{AIBN}]_0 = 250/1/0.2$; $[\text{VC}]_0/[\text{THF}] = 1/1$ (v/v). _____ 205

Figure 5.5. MALDI-TOF-MS in the linear mode of RAFT-PVC (Table 5.1, entry 8: $M_n^{\text{GPC}} = 3000 \text{ g/mol}$, $\mathcal{D} = 1.50$) mediated by CMPCD. _____ 207

- Figure 5.6.** Enlargement of the MALDI-TOF-MS from m/z 1300 to 1500 of RAFT-PVC (Table 5.1, entry 8: $M_n^{\text{GPC}} = 3000$ g/mol, $\mathcal{D} = 1.50$) mediated by CMPCD in the (i) linear and (ii) reflectron mode. _____ 208
- Figure 5.7.** (i) Enlargement of the MALDI-TOF-MS in the reflectron mode of Figure 5.6 from m/z 1300 to 1320 and (ii) theoretical isotope distribution of the m/z 1300-1320 region ($\text{DP} = 17$, $\text{C}_{44}\text{H}_{61}\text{Cl}_{17}\text{N}_2\text{S}_2\text{Na}$) using *Isotope Distribution Calculator* software. ____ 208
- Figure 5.8.** ^1H NMR spectra of Trigonox 187-W40 initiator (top), CMPCD RAFT agent (middle) and RAFT-PVC obtained (Table 5.1, entry 8: $M_n^{\text{GPC}} = 3000$ g/mol, $\mathcal{D} = 1.50$) in d_8 -THF. _____ 209
- Figure 5.9.** GPC traces of the PVC-CTA macroCTA before (black curve), after the chain extension experiment (green curve) and PVC-*b*-PVAc block copolymer (blue curve). _____ 210
- Figure 5.10.** The ^1H NMR spectrum of the PVC-*b*-PVAc diblock copolymer ($M_n^{\text{GPC}} = 16600$; $\mathcal{D} = 1.64$) in THF- d_8 . _____ 211
- Figure 6.1.** NMP of VC in DCM at 42 °C initiated by the SG1-based BlocBuilder alkoxyamine. (a) Conversion and $\ln[M]_0/[M]$ vs. time. (b) Number-average molecular weight (M_n^{SEC}) and dispersity (M_w/M_n) vs. theoretical number-average molecular weight (M_n^{th}). (c) Evolution of the SEC traces during the polymerization. Reaction conditions: $[\text{VC}]_0/[\text{BlocBuilder}]_0 = 250/1$; $[\text{VC}]_0/[\text{solvent}] = 1/1$ (v/v). _____ 227
- Figure 6.2.** NMP of VC in DCM at 42 °C initiated by the SG1-based BlocBuilder alkoxyamine. (a) Conversion and $\ln[M]_0/[M]$ vs. time. (b) M_n^{SEC} and M_w/M_n vs. M_n^{th} . (c) Evolution of the SEC traces during the polymerization. Reaction conditions: $[\text{VC}]_0/[\text{BlocBuilder}]_0 = 100/1$; $[\text{VC}]_0/[\text{solvent}] = 1/1$ (v/v). _____ 230
- Figure 6.3.** ^1H NMR spectra in d_8 -THF of (a) the BlocBuilder alkoxyamine and (b) the purified PVC ($M_n^{\text{SEC}} = 6000$; $\mathcal{D} = 1.60$) obtained in Table 6.4, entry 1. _____ 231
- Figure 6.4.** Enlargements of ^1H NMR spectra in d_8 -THF of the purified PVC ($M_n^{\text{SEC}} = 6000$; $\mathcal{D} = 1.60$) obtained in Table 6.4, entry 1 and a purified PVC ($M_n^{\text{SEC}} = 29.3 \times 10^3$; $\mathcal{D} = 1.76$) obtained by FRP using the same conditions. _____ 232
- Figure 6.5.** ^{31}P NMR spectrum in d_8 -THF of the purified PVC ($M_n^{\text{SEC}} = 6000$; $\mathcal{D} = 1.60$) obtained in Table 6.4, entry 1. _____ 233

Figure 6.6. SEC chromatograms of the PVC-SG1 macroinitiator (conv. = 49%, M_n^{th} = 4300, M_n^{SEC} = 6000, \mathcal{D} = 1.60) (black line), and the extended PVC-*b*-PVC (conv. = 44%, M_n^{th} = 26500, M_n^{SEC} = 20600, \mathcal{D} = 1.59) (blue line) after “one-pot” chain extension in DCM. _____ 234

Figure 6.7. SEC chromatograms of the PVC-SG1 macroinitiator (conv. = 66%, M_n^{th} = 5000, M_n^{SEC} = 6600, \mathcal{D} = 1.56) (black line), the PVC-*b*-PMMA diblock copolymer (conv._{MMA} = 45.5%, M_n^{th} = 52100, M_n^{SEC} = 44700, \mathcal{D} = 1.89) (red line) by NMP in DMSO, and PVC-*b*-P(MMA-*co*-S) (conv._{MMA} = 34.5%, conv._S = 36.8%, M_n^{th} = 44800, M_n^{SEC} = 36400, \mathcal{D} = 1.78) (blue line) block copolymer by NMP in DMF at 100 °C for 54 and 44h, respectively. _____ 234

Figure 7.1. RAFT polymerization of MA in CPME at 60 °C mediated by DDMAT using AIBN as conventional initiator. (a) Conversion and $\ln[M]_0/[M]$ vs. time. (b) Number-average molecular weight (M_n^{SEC}) and dispersity (M_w/M_n) vs. theoretical number-average molecular weight (M_n^{th}). Reaction conditions: $[MA]_0/[DDMAT]_0/[AIBN]_0 = 222/1/0.5$; $[MA]_0/[CPME] = 2/1$ (v/v). _____ 252

Figure 7.2. RAFT polymerization of S in CPME at 60 °C mediated by DDMAT using AIBN as conventional initiator. (a) Conversion vs. time and $\ln[M]_0/[M]$ vs. time. (b) M_n^{SEC} and M_w/M_n vs. M_n^{th} . Reaction conditions: $[S]_0/[DDMAT]_0/[AIBN]_0 = 222/1/0.5$; $[S]_0/[CPME] = 2/1$ (v/v). _____ 253

Figure 7.3. RAFT polymerization of VC in CPME at 42 °C mediated by CMPCD using Trigonox as conventional initiator. (a) Conversion and $\ln[M]_0/[M]$ vs. time. (b) M_n^{SEC} and M_w/M_n vs. M_n^{th} . Reaction conditions: $[VC]_0/[CMPCD]_0/[Trigonox]_0 = 250/1/0.2$; $[VC]_0/[CPME] = 1/1$ (v/v). _____ 254

Figure 7.4. (a) MALDI-TOF-MS in the linear mode (using HABA as matrix) of PVC-CTA (M_n^{SEC} = 4200, \mathcal{D} = 1.54) obtained in Table 7.1, entry 5; (b) Enlargement of the MALDI-TOF-MS from m/z 1500 to 1900 of PVC-CTA. _____ 257

Figure 7.5. The ^1H NMR spectrum in THF- d_8 of PVC-CTA (M_n^{SEC} = 4200; \mathcal{D} = 1.54) obtained in Table 7.1, entry 5. _____ 258

Figure 7.6. The ^1H NMR spectrum in THF- d_8 of PVAc-CTA (M_n^{SEC} = 9000; \mathcal{D} = 1.18) obtained in Table 7.1, entry 3. _____ 258

Figure 7.7. (a) SEC traces of the PVC-CTA (conv_{VC} = 59%, M_n^{th} = 4500, M_n^{SEC} = 4200, \mathcal{D} = 1.54) macro-CTA (right curve), and the “one-pot” extended PVC (conv_{VC} = 42%,

$M_n^{\text{th}} = 23800$, $M_n^{\text{SEC}} = 17300$, $\mathcal{D} = 1.53$) (left curve). (b) SEC traces of the PVAc-CTA ($\text{conv}_{\text{VAc}} = 99\%$, $M_n^{\text{th}} = 8700$, $M_n^{\text{SEC}} = 9000$, $\mathcal{D} = 1.18$) macro-CTA (right curve), and the PVAc-*b*-PVC ($\text{conv}_{\text{VC}} = 51\%$, $M_n^{\text{th}} = 41100$, $M_n^{\text{SEC}} = 30200$, $\mathcal{D} = 1.59$) block copolymer (left curve). _____ 259

Figure 7.8. The ^1H NMR spectrum of the PVAc-*b*-PVC diblock copolymer ($M_n^{\text{SEC}} = 30200$; $\mathcal{D} = 1.59$) in THF- d_8 . _____ 260

Figure 7.9. NMP of S in CPME at 80 °C initiated by SG1-based BlocBuilder alkoxyamine. (a) Conversion and $\ln[M]_0/[M]$ vs. time. (b) M_n^{SEC} and M_w/M_n vs. M_n^{th} . Reaction conditions: $[S]_0/[\text{BlocBuilder}]_0 = 222/1$; $[S]_0/[\text{CPME}] = 2/1$ (v/v). _____ 261

Figure 7.10. NMP of VC in CPME at 42 °C initiated by SG1-based BlocBuilder alkoxyamine. (a) Conversion and $\ln[M]_0/[M]$ vs. time. (b) M_n^{SEC} and M_w/M_n vs. M_n^{th} . Reaction conditions: $[\text{VC}]_0/[\text{BlocBuilder}]_0 = 250/1$; $[\text{VC}]_0/[\text{CPME}] = 1/1$ (v/v). _____ 262

Figure 7.11. The ^1H NMR spectrum in d_8 -THF of a purified PVC ($M_n^{\text{SEC}} = 4300$; $\mathcal{D} = 1.55$) obtained in Table 7.2, entry 4. _____ 264

Figure 7.12. ^{31}P NMR spectrum in d_8 -THF of the purified PVC ($M_n^{\text{SEC}} = 4300$; $\mathcal{D} = 1.55$) obtained in Table 7.2, entry 4. _____ 264

Figure 7.13. SEC chromatograms of the PVC-SG1 macroinitiator ($\text{conv}_{\text{VC}} = 52.2\%$, $M_n^{\text{th}} = 3800$, $M_n^{\text{SEC}} = 4300$, $\mathcal{D} = 1.55$) (black line) and the PVC-*b*-PVC diblock copolymer ($\text{conv}_{\text{VC}} = 47.2\%$, $M_n^{\text{th}} = 29800$, $M_n^{\text{SEC}} = 23600$, $\mathcal{D} = 1.61$) (blue line) after “one-pot” chain extension in CPME. _____ 265

Figure A.1. (a, c and e) Kinetic plots of conversion and $\ln[M]_0/[M]$ vs. time and (b, d and f) plots of $M_{n,\text{GPC}}$ and \mathcal{D} (M_w/M_n) vs. $M_{n,\text{th}}$ for the SARA ATRP of MA catalyzed by $\text{Na}_2\text{S}_2\text{O}_4/\text{CuBr}_2/\text{Me}_6\text{TREN}$ in (a and b) BMIM-PF₆/DMSO = 95/5, (c and e) BMIM-PF₆/DMSO = 75/25 and (e and f) BMIM-PF₆/DMSO = 25/75. Conditions: $[\text{MA}]_0/[\text{solvent}] = 2/1$ (v/v); $[\text{MA}]_0/[\text{EBiB}]_0/[\text{Na}_2\text{S}_2\text{O}_4]_0/[\text{CuBr}_2]_0/[\text{Me}_6\text{TREN}]_0 = 222/1/1/0.1/0.1$ (molar); T = 30 °C. _____ A1

Figure A.2. Kinetic plots of conversion and $\ln[M]_0/[M]$ vs. time (a) and plots of $M_{n,\text{GPC}}$ and \mathcal{D} (M_w/M_n) vs. $M_{n,\text{th}}$ (b) for the SARA ATRP of MA catalyzed by $\text{Na}_2\text{S}_2\text{O}_4/\text{TBA-PF}_6/\text{CuBr}_2/\text{Me}_6\text{TREN}$ in DMSO. Conditions: $[\text{MA}]_0/[\text{solvent}] = 2/1$ (v/v); $[\text{MA}]_0/[\text{EBiB}]_0/[\text{Na}_2\text{S}_2\text{O}_4]_0/[\text{TBAPF}_6]_0/[\text{CuBr}_2]_0/[\text{Me}_6\text{TREN}]_0 = 222/1/1/3/0.1/0.1$ (molar); T = 30 °C. _____ A2

Figure A.3. UV-Vis spectra of reduction of $\text{CuBr}_2/\text{Me}_6\text{TREN}$ by $\text{Na}_2\text{S}_2\text{O}_4$ in (a) pure DMSO, (b) BMIM-PF₆/DMSO (25/75) and (c) BMIM-PF₆/DMSO (50/50) at 30 °C. ____ A3

Figure A.4. ^1H NMR spectrum, in CDCl_3 , of PMA-Br obtained by SARA ATRP of MA catalyzed by $\text{Na}_2\text{S}_2\text{O}_4/\text{CuBr}_2/\text{Me}_6\text{TREN}$, in $\text{BMIM-PF}_6/\text{DMSO} = 50/50$ (v/v) at high conversion ($M_{n,\text{GPC}} = 6900$, $\mathcal{D} = 1.05$, $M_{n,\text{NMR}} = 6600$; active chain-end functionality = 92%). Conditions: $[\text{MA}]_0/[\text{solvent}] = 2/1$ (v/v); $[\text{MA}]_0/[\text{EBiB}]_0/[\text{Na}_2\text{S}_2\text{O}_4]_0/[\text{CuBr}_2]_0/[\text{Me}_6\text{TREN}]_0 = 222/1/1/0.1/0.1$ (molar); $T = 30$ °C. The PMA is atactic: $[\text{dr}] = [\text{dm}] = 0.5$. _____ A4

Figure A.5. MALDI-TOF-MS in the linear mode (using HABA as matrix) of PMA-Br ($M_{n,\text{GPC}} = 6.9 \times 10^3$, $\mathcal{D} = 1.05$) obtained by SARA ATRP of MA catalyzed by $\text{Na}_2\text{S}_2\text{O}_4/\text{CuBr}_2/\text{Me}_6\text{TREN}$, in $\text{BMIM-PF}_6/\text{DMSO} = 50/50$ (v/v). Conditions: $[\text{MA}]_0/[\text{solvent}] = 2/1$ (v/v); $[\text{MA}]_0/[\text{EBiB}]_0/[\text{Na}_2\text{S}_2\text{O}_4]_0/[\text{CuBr}_2]_0/[\text{Me}_6\text{TREN}]_0 = 222/1/1/0.1/0.1$ (molar); $T = 30$ °C. _____ A4

Figure A.6. Enlargement of the MALDI-TOF-MS from m/z 6450 to 7050 of PMA-Br ($M_{n,\text{GPC}} = 6.9 \times 10^3$, $\mathcal{D} = 1.05$) obtained by SARA ATRP of MA catalyzed by $\text{Na}_2\text{S}_2\text{O}_4/\text{CuBr}_2/\text{Me}_6\text{TREN}$, in $\text{BMIM-PF}_6/\text{DMSO} = 50/50$ (v/v). Conditions: $[\text{MA}]_0/[\text{solvent}] = 2/1$ (v/v); $[\text{MA}]_0/[\text{EBiB}]_0/[\text{Na}_2\text{S}_2\text{O}_4]_0/[\text{CuBr}_2]_0/[\text{Me}_6\text{TREN}]_0 = 222/1/1/0.1/0.1$ (molar); $T = 30$ °C. _____ A5

Figure A.7. GPC traces of the PMA before (right curve) and after the chain extension (left curve) experiment. _____ A5

Figure B.1. (Kinetic plot of conversion and $\ln[\text{M}]_0/[\text{M}]$ vs. time (a) and plot of $M_{n,\text{GPC}}$ and \mathcal{D} (M_w/M_n) vs. $M_{n,\text{th}}$ (b) for ATRP of MMA catalyzed with $\text{Na}_2\text{S}_2\text{O}_4$ in the presence of $\text{Cu(II)Br}_2/\text{Me}_6\text{TREN}$ at 30 °C in DMSO. Conditions: $[\text{MMA}]_0/[\text{DMSO}] = 2/1$ (v/v); $[\text{MMA}]_0/[\text{EBiB}]_0/[\text{Na}_2\text{S}_2\text{O}_4]_0/[\text{Cu(II)Br}_2]_0/[\text{Me}_6\text{TREN}]_0 = 222/1/1/0.1/0.1$. _____ B1

Figure C.1. (a and d) Kinetic plots of conversion and $\ln[\text{M}]_0/[\text{M}]$ vs. time; (b and e) plot of $M_{n,\text{GPC}}$ and \mathcal{D} (M_w/M_n) vs. conversion for aqueous SARA ATRP of OEOA_{480} at 30 °C; and (c and f) GPC traces vs. time. Conditions: $[\text{OEOA}_{480}]_0/[\text{HEBiB}]_0/[\text{Cu(II)Br}_2]_0/[\text{TPMA}]_0 = 250/1/0.05/0.4$; $\text{FR}(\text{Na}_2\text{S}_2\text{O}_4) = 16$ (a, b and c) and 32 (d, e and f) nmol/min; $[\text{NaCl}]_0 = 100$ mM; $[\text{OEOA}_{480}]_0/[\text{Water}] = 1/3$. _____ C1

Figure D.1. MALDI-TOF-MS in the linear mode (using α -cyano-4-hydroxycinnamic acid (CHCA) as matrix) of RAFT-PVC ($M_n^{\text{GPC}} = 3300$; $\mathcal{D} = 1.48$) mediated by CMPCD. D1

Figure D.2. (i) Enlargement of the MALDI-TOF-MS in the reflectron mode from m/z 925 to 945 and (ii) theoretical isotope distribution of the m/z 925-945 region ($\text{DP} = 11$, $\text{C}_{32}\text{H}_{43}\text{Cl}_{11}\text{N}_2\text{S}_2\text{Na}$) using *Isotope Distribution Calculator* software. _____ D1

Figure E.1. NMP of VC in DCM at 42 °C initiated by the SG1-based BlocBuilder alkoxyamine. Number-average molecular weight (M_n^{SEC}) vs. conversion for different target DP_n values: (a) 250 and (b) 100. Reaction conditions: $[VC]_0/[BlocBuilder]_0 = DP_n/1$; $[VC]_0/[solvent] = 1/1$ (v/v). _____ E1

Figure E.2. ^1H NMR spectrum in d_8 -THF of the PVC-*b*-PMMA diblock copolymer ($\text{conv.}_{\text{MMA}} = 45.5\%$, $M_n^{\text{th}} = 52100$, $M_n^{\text{SEC}} = 44700$, $\mathcal{D} = 1.89$) obtained by NMP in DMSO. Reaction conditions: $[MMA]_0/[PVC\text{-}SG1]_0 = 1000/1$; $[MMA]_0/[DMSO] = 1/1$ (v/v). _____ E1

Figure E.3. ^1H NMR spectrum in d_8 -THF of the PVC-*b*-P(MMA-*co*-S) block copolymer ($\text{conv.}_{\text{MMA}} = 34.5\%$, $\text{conv.}_S = 36.8\%$, $M_n^{\text{th}} = 44800$, $M_n^{\text{SEC}} = 36400$, $\mathcal{D} = 1.78$) obtained by NMP in DMF. Reaction conditions: $[MMA]_0/[S]_0/[PVC\text{-}SG1]_0 = 1000/100/1$; $[MMA + S]_0/[DMF] = 1/1$ (v/v). _____ E2

Figure E.4. Possible dehydrochlorinated PVC-SG1 structures, with relative stabilities of the alkenes. BDFEs of the marked bond and relative alkene stability calculated at 40 °C are given in kJ mol^{-1} . _____ E10

List of Schemes

Scheme 1.1. General mechanism of the FRP. _____	4
Scheme 1.2. Equilibrium between active and dormant species. _____	6
Scheme 1.3. RDRP mechanisms. _____	12
Scheme 1.4. General mechanism of ATRP. _____	20
Scheme 1.5. Schematic representation of the different ATRP variation techniques. _____	22
Scheme 1.6. Detailed mechanism of copper-catalyzed SET-LRP and ATRP. _____	23
Scheme 1.7. General mechanism of RAFT polymerization. _____	25
Scheme 1.8. General mechanism of ITP. _____	26
Scheme 1.9. Zipper dehydrochlorination reaction. _____	32
Scheme 1.10. Mechanisms involved in the formation of allylic chloride structures. _____	33
Scheme 1.11. Auxiliary mechanism for chain transfer to the monomer during VC polymerization, where P [•] is the head-to-tail macroradical. _____	35
Scheme 1.12. Mechanisms involved in the formation of long-branch points. _____	36
Scheme 1.13. Mechanisms involved in the formation of 2,4-dichloro- <i>n</i> -butyl-branches. _____	36
Scheme 1.14. General mechanism proposed for SET-DTLRP of VC in water. _____	43
Scheme 1.15. PVC structure obtained by proposed SET-LRP initiated with CHBr ₃ . _____	50
Scheme 1.16. Synthesis of PVC- <i>b</i> -PVAc block copolymers from PVAc-Co(acac) ₂ macroinitiator. _____	54
Scheme 2.1. General mechanism of (a) ARGET ATRP and (b) ICAR ATRP. _____	92
Scheme 3.1. General mechanism of copper catalyzed ATRP. _____	124
Scheme 4.1. Aqueous SARA ATRP of OEOA ₄₈₀ and OEOMA ₅₀₀ by Feeding Inorganic Sulfites. _____	157
Scheme 5.1. Mechanism of the RAFT Polymerization of VC Mediated by CMPCD and Initiated by Trigonox 187-W40. _____	206
Scheme 6.1. General Scheme and Conditions for the NMP of VC Initiated by the SG1-based BlocBuilder Alkoxyamine. _____	221

Scheme D.1. Equilibrium constants (**bold**; L mol⁻¹) and corresponding Gibbs free energies (*italics*; kJ mol⁻¹) of addition (*a* and *c*) and chain transfer (*b*) reactions in THF at 42 °C, calculated using three-layer ONIOM approximation for electronic energies and UAKS-PCM/B3LYP/6-31G(d) method for solvation free energies. _____ D4

List of Tables

Table 1.1. Resume of the RDRP methods developed for the VC (co)polymerization. ___	55
Table 2.1. SARA ATRP of MA in the Presence of CuBr ₂ /Me ₆ TREN and Na ₂ S ₂ O ₄ at 30 °C in DMSO (33 vol% DMSO). _____	103
Table 2.2. Kinetic Data for the SARA ATRP of MA in BMIM-PF ₆ /DMSO Mixtures. ___	108
Table 3.1. SARA ATRP of MA in the Presence of Inorganic Sulfites (Na ₂ S ₂ O ₄ or Na ₂ S ₂ O ₅) and Cu(II)Br ₂ /Me ₆ TREN at 30 °C in Different Alcohol-Water Mixtures (33 vol % Solvent). _____	136
Table 3.2. SARA ATRP of Acrylates, Methacrylates and Copolymers in the Presence of Na ₂ S ₂ O ₄ and Cu(II)Br ₂ /Me ₆ TREN at 30 °C (33 vol % Solvent). [Monomer] ₀ /[EBiB] ₀ /[Na ₂ S ₂ O ₄] ₀ /[Cu(II)Br ₂] ₀ /[Me ₆ TREN] ₀ = 222/1/1/0.1/0.1. _____	139
Table 4.1. Aqueous SARA ATRP of OEOA ₄₈₀ with Varied Feeding Rate of Na ₂ S ₂ O ₄ (FR _S). _____	165
Table 4.2. Aqueous SARA ATRP using Inorganic Sulfites. _____	170
Table 4.3. Aqueous SARA ATRP of OEOA ₄₈₀ with Varied Ligands (L) and L/Cu Ratios. _____	175
Table 4.4. Aqueous SARA ATRP of OEOA ₄₈₀ with Varied Salts and Salt Concentrations. _____	175
Table 4.5. Aqueous SARA ATRP of OEOA ₄₈₀ with Various Sulfites. _____	179
Table 4.6. Aqueous SARA ATRP of OEOA ₄₈₀ and OEOMA ₅₀₀ with Varied Cu Concentrations and DP. _____	179
Table 4.7. Aqueous SARA ATRP of OEOA ₄₈₀ with Start/Stop Cycles. _____	181
Table 4.8. “One-Pot” Chain Extension Experiments from P(OEOA ₄₈₀) and P(OEOMA ₅₀₀). _____	185
Table 4.9. SARA ATRP of OEOA ₄₈₀ in PBS Initiated by BSA-O-[iBBr] ₃₀ . _____	185
Table 5.1. RAFT Polymerizations of VC with CMPCD as a RAFT Agent under Different Conditions. _____	201
Table 6.1. Conversion and Macromolecular Characteristics Obtained for the NMP of VC Using Different Solvents at 42 °C after 24 h. _____	226

Table 6.2. Conversion and Macromolecular Characteristics Obtained for the NMP of VC in DCM at 42 °C after 24 h. _____	228
Table 6.3. Conversion and Macromolecular Characteristics Obtained for the NMP of VC in DCM at Different Temperatures after 24 h. _____	229
Table 6.4. Conversion and Macromolecular Characteristics Obtained for the NMP of VC in DCM at 42 °C for Different Targeted DP_n values ($[VC]_0/[BlocBuilder]_0$). _____	230
Table 7.1. Kinetic Parameters Obtained for RAFT Polymerizations in CPME with Different Monomers. Conditions: Reaction Temperature = 42 °C; $[Monomer]_0/[Solvent] = 2/1$ (v/v). _____	255
Table 7.2. NMP of VC Initiated by the BlocBuilder Alkoxyamine at 42 °C, using CPME as a Solvent under Different Experimental Conditions. _____	263
Table D.1. Gas and solution-phase energetics at 315.15 K of reactions in Scheme D.1. _	D5
Table D.2. Contributions to the 0 K enthalpies of species in the model calculations. ____	D5
Table D.3. Contributions to the gas and solution-phase free energies of species in this study at 315.15 K. _____	D6
Table E.1. SG1-mediated NMP of MMA, STY and VC at 40 °C. _____	E6
Table E.2. SG1-mediated NMP of MMA, STY and VC at 100 °C. _____	E7
Table E.3. Radical Stabilization Energies (RSE), Bond Dissociation Free-Energies (BDFE) and K for SG1-Mediated NMP of VC, S and MMA. _____	E9

Motivations, Targets and Research Significance

Over the last decades, the scientific community has been focused in the strong need for polymers with controlled architectures, chain-end functionalities and narrow molecular weight distributions. Reversible deactivation radical polymerization (RDRP) methods offer control over structure that is similar to ionic living polymerizations, but with all the advantages associated with radical based polymerizations. Atom transfer radical polymerization (ATRP) is among the most efficient, versatile and robust RDRP techniques. However, sometimes the inevitable use of metal catalysts and harmful organic solvents to afford homogenous reaction conditions, which can contaminate the final product, are some of the limitations of this method. In this context, this project aimed the development of new ATRP systems for vinyl monomers using non-toxic and inexpensive compounds that could provide fast polymerizations in environmentally friendly media. At the same time, it was expected that the goals set for these novel catalytic systems could expand of the range of applications, as well as enhance the possibility of future industrial implementation.

Despite all the achievements, RDRP of nonactivated monomers (*e.g.*, vinyl acetate, *N*-vinylpyrrolidone and vinyl chloride) remains enormously challenging of the scientific community. Poly(vinyl chloride) (PVC) is one of the highest volume polymers (~39.3 million tons in 2013) and can only be prepared on an industrial scale by free-radical polymerization (FRP). The several intrinsic limitations of FRP triggered interest in synthesizing this polymer by RDRP methods. However, several features of vinyl chloride (VC) make its control by RDRP techniques particularly challenging, such as: a very high reactivity, an unusually high chain transfer constant to the monomer, and the non-solubility of PVC in its monomer as well as in most common organic solvents. Some attempts to produce PVC by RDRP methods have been reported, namely by single electron transfer degenerative chain transfer living radical polymerization (SET-DTLRP) or Metal Catalyzed RDRP. However, the study of other RDRP techniques facilitates a deeper understanding of VC polymerization and broadening the number of PVC-based macromolecular structures could have valuable synthetic utility. In this context, this project also aimed the development of new VC (co)polymerizations systems using RDRP

methods. The development of effective RDRP methods for nonactivated monomers, as VC, is also of outmost importance for a deeper mechanistic understanding of these processes.

Chapter 1

Literature Review



Part of this chapter, regarding the VC polymerization, was submitted for publication:

Abreu, C. M. R., Fonseca A. C., Rocha, N. M. P., Guthrie, J. T., Serra, A. C., Coelho, J. F. J., *Poly(Vinyl Chloride):Current Status and Future Perspectives via Reversible Deactivation Radical Polymerization Methods.*

1.1. Free Radical Polymerization (FRP)

Free radical polymerization (FRP) procedures are responsible for the production of about 50% of the synthetic polymers that are currently in use.¹ This popularity is based on several important points, such as: the ease of control in industrial operations; the tolerance to impurities and monomer functionality; the tolerance of the process to protic compounds such as water (extremely important due to environmental and economic aspects);^{1,2} the non-requirement of stringent purification of reagents; the possibility of being able to carry out the polymerization under different technological processes (such as solution, suspension, emulsion and bulk),^{1,3,4} each giving good reproducibility of the products' properties.⁴ In terms of the process developments and optimizations, various studies have been carried out trying to increase the productivity.² Options have included developing new initiators (or cocktails),⁵ employing larger reactors² and using mathematical approaches that are based on the modelling and control strategies.⁶⁻¹⁰

Five different polymerization process variations can be used in the commercial manufacture of polymeric products. There are polymerization via suspension, emulsion, mass (or bulk), micro-suspension and solution.^{2,11,12} These processes are relatively different, from the macroscopic standpoint, using different reactors and producing polymer grains having different appearance, morphology and properties. At the molecular level, the mechanisms involved during the reaction and processes are similar. Scheme 1.1 identifies the elementary reactions that are related to the FRP.^{6,9,10,13}

Generally, the FRP polymerization is mainly composed of four major reactions. These are initiation, propagation, chain transfer and termination.^{3,4,14} The initiation reaction is usually defined by two processes. Firstly (Scheme 1.1, reaction 1.1), the conventional initiator is decomposed, leading to the formation of species known as radicals (radical generation). Subsequently, (Scheme 1.1, reaction 1.2) a monomer unit is added to the growing radical (formation of the monoadduct). In propagation, (Scheme 1.1, reaction 1.3), a first-order kinetic step, with respect to a growing radical concentration, is followed. A succession of rapid propagation steps occurs with high regioselectivity, to form growing radical centers. The reactions depicted as 1.4, 1.5 and 1.6 (Scheme 1.1) represent the options for chain transfer reactions (to monomer(s), to polymer(s), to

solvent(s) or to additive(s)) that could arise during this process. In the final stage of polymerization, (Scheme 1.1, reactions 1.7 and 1.8), a bimolecular reaction occurs, mainly involving propagating radical chains, by combination or disproportionation, resulting polymer dead-chain ends. Reaction of propagating radical chains with radical fragments from the initial initiator decomposition is also possible (Scheme 1.1, reaction 1.9).

	Reaction	Rate expression	
Initiation	$I \longrightarrow 2 R^\bullet$	$k_d [I]$	(1.1)
	$R^\bullet + M \longrightarrow P_1^\bullet$	$k_i [R^\bullet] [M]$	(1.2)
Propagation	$P_n^\bullet + M \longrightarrow P_{n+1}^\bullet$	$k_p [P_n^\bullet] [M]$	(1.3)
Transfer to monomer	$P_n^\bullet + M \longrightarrow P_n + M^\bullet$	$k_{tr,M} [P_n^\bullet] [M]$	(1.4)
Transfer to polymer	$P_n^\bullet + P_y \longrightarrow P_n + P_y^\bullet$	$k_{tr,P} [P_n^\bullet] [P_y]$	(1.5)
Transfer to solvent	$P_n^\bullet + S \longrightarrow P_n + S^\bullet$	$k_{tr,S} [P_n^\bullet] [S]$	(1.6)
Termination	$P_n^\bullet + P_m^\bullet \longrightarrow P_{n+m}$	$k_{tc} [P_n^\bullet] [P_m^\bullet]$	(1.7)
	$P_n^\bullet + P_m^\bullet \longrightarrow P_n + P_m$	$k_{td} [P_n^\bullet] [P_m^\bullet]$	(1.8)
	$P_n^\bullet + R^\bullet \longrightarrow P_n R$	$k_{ti} [P_n^\bullet] [R^\bullet]$	(1.9)

Scheme 1.1. General mechanism of the FRP.^{6,9}

The possibility of controlling the final structure of the polymer, and its molecular weight, as well as implementing macromolecular engineering¹⁵ strategies with this technology, to improve the polymer properties, is not feasible using this process. This is because of the short time between each monomer addition and the existence of termination reactions.¹⁴ Therefore, polymers that have been produced by FRP generally present broad molecular weight distributions, typically $\mathcal{D} > 2$. Also, the addition of another monomer into the reaction, for the preparation of block copolymers, with controlled compositions, becomes impossible.^{16,17}

1.1.1. Addressing FRP Limitations

In FRP, the initiation and propagation steps are inevitably accompanied by termination and side chain reactions, which negate the provision of extensive control over the molecular weight, the molecular weight distribution and the polymer structure. Also, there are strong limitations that are associated with the preparation of block copolymers, in which are combined several features/properties within the same structure, because of the great reactivity of the propagating radicals. The controlled synthesis of polymers by radical-based methods was long considered to be unachievable because two radicals always terminate very quickly.¹⁸ Indeed, the synthesis of well-controlled structures has been limited for decades to the realm of living ionic polymerizations.

According to the pioneering work of Szwarc,¹⁹ “*living polymers are polymers that retain their ability to propagate for a long time and grow to desired maximum size while their degree of termination and chain transfer is still negligible*”. This definition recognizes that the aforementioned undesired reactions are impossible to avoid in absolute terms, but can be reduced to an insignificant number, that will not have impact on the final product. Due to their intrinsic nature, living ionic polymerizations present several limitations involving the chemical incompatibility of the propagating centers (anionic or cationic) with a wide range of monomer functionalities,²⁰ the need for extremely pure compounds (monomers and solvents), the need for the complete absence of water or protic impurities and the need for very stringent control of the reactions conditions. These features have posed serious restrictions to the synthesis of a large number of polymers that possess well-defined structures and/or to the use of conditions that can be implemented on an industrial scale.

The concept of merging the features of a living process with those of a radical based process opens up a myriad of opportunities regarding the universal syntheses of the (co)polymers having well-defined structures, under mild reaction conditions. In theory, this polymerization system should be able to reduce dramatically the occurrence of termination reactions and side reactions. The possibility of avoiding both irreversible radical terminations was considered to be non-feasible for decades, since these reactions occur under diffusion-controlled rates.²¹ From a theoretical perspective, a radical

terminated chains will be minor (~1-10%). The chains that are not active at a certain moment (being in their dormant state) are fully capable of being reinitiated or functionalized.

In FRP, at any time, only ppm amounts of growing radicals with around 1s of life time are present in the system. This concentration results from the balance of the rate of initiation and the rate of termination. Under these conditions, almost all of the polymer chains are essentially dead. Contrarily, in RDRP methods, at any time, there are very small numbers of terminated chains (1-10%). This is because polymers that are growing chains, with a radical nature, are few in number and most of the polymer chains are in a dormant state ready to be activated. If the initiation is fast enough, a concurrent growth of all of the chains occurs.²²

1.2. Reversible Deactivation Radical Polymerization (RDRP)

1.2.1. Generic Description, Advantages and Limitations on RDRP

Since their discovery, living polymerizations have been studied and developed through thousands of contributions from many scientists. Several types of living polymerizations have been studied and proposed: anionic systems,²⁰ cationic systems,^{23,24} ring-opening systems,²⁵⁻²⁸ coordination-insertion^{29,30} and radical systems.^{16,17,22,31-36} The desire to prepare new, well-defined structures (blocks, stars, comb-like, networks, end-functionalized and other materials without traditional problems) (Figure 1.1) motivated the study of living polymerization options. On this matter, RDRP techniques have received remarkable attention. The number of publications on RDRP has increased dramatically¹⁷ within the scientific community. This interest is due to the fact that RDRP techniques provide flexibility and the mild experimental conditions that are similar to those of FRP, while allowing one to achieve precise control over the polymer structures, as would be expected from an ionic polymerization.^{37,38} The RDRP strategy, from the theoretical standpoint, allows the synthesis of living polymers under a radical mechanism, with all of the associated advantages of the radical processes. In addition, the possibility

of implementing such techniques in aqueous environment (very interesting from environmental and economic standpoints) was predicted from the beginning of the development of RDRP.^{37,39,40} The high tolerance of growing radicals to different functional groups that allows the straightforward synthesis of (co)polymers with minimum requisites. In addition, contrarily to step-growth polymerization, very high molecular weight polymers can be easily attained without requiring long polymerization times, or perfect stoichiometric balances between the monomers used. Besides homogeneous conditions, as bulk and solution, the radical based process can also be easily application in heterogeneous media (*e.g.*, suspension, emulsion, etc.) using water as the continuous phase.³⁷ This particular feature is decisive from the economic and environmental standpoints when industrial applications are envisaged.

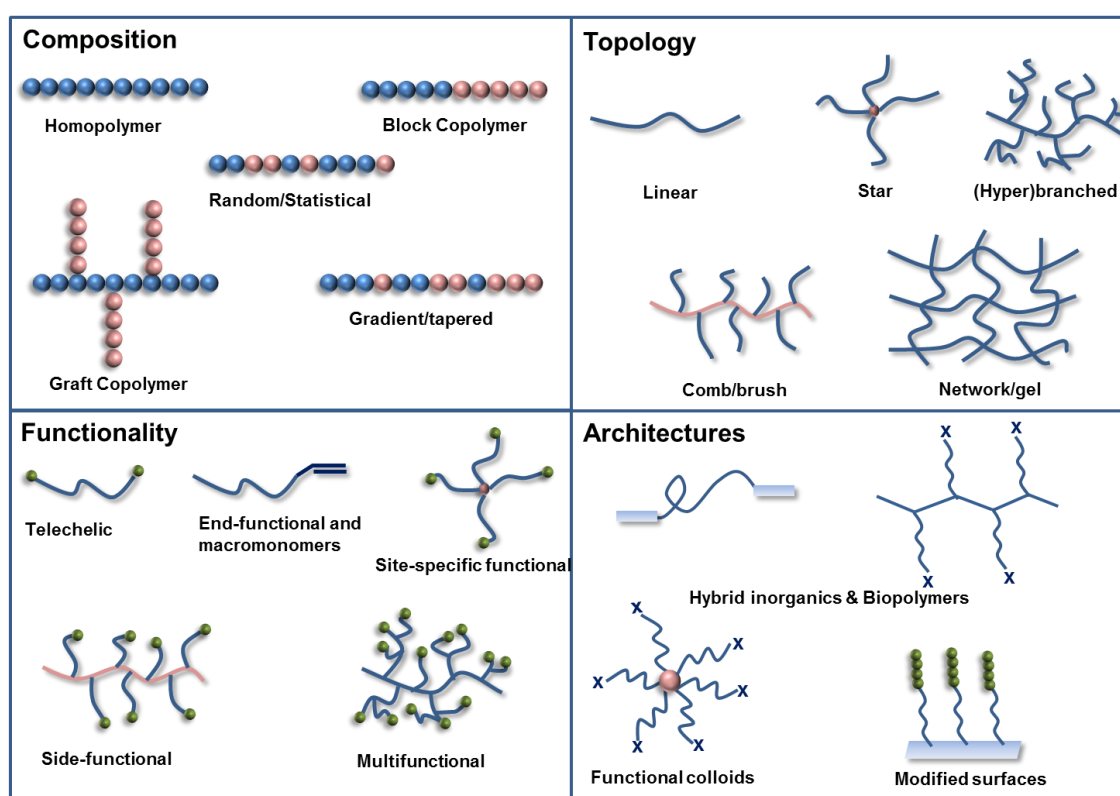


Figure 1.1. Controlled molecular structures attained by RDRP methods.^{15,40-42}

The post-polymerization modifications of polymeric structures and the control of their chemical functionalities have enabled the creation of countless new materials, with targeted properties for specific applications.⁴² High performance materials that have been

produced by RDRP can be applied in a wide range of commercial products, such as surfactants, lubricants, dispersants, coatings, paints, adhesives, thermoplastic elastomers, biomaterials, membranes, drug delivery agents and electronic materials, among others.^{16,37,43}

The dynamic equilibrium that exists between growing radicals and dormant species (that have no activity), based on the fast reversible activation/deactivation of the growing radicals (keeping the concentration very low during the polymerization), is the basis of to all RDRP techniques.^{17,43} The main similarity between FRP and RDRP is the radical nature of the chain growth process leading to similar chemoselectivities, regioselectivities and stereoselectivities.³⁸ The main difference is the nature of the steady state concentration of radicals. In FRP processes, this results from ratio of the rate of the initiation and the rate of termination whereas, for RDRP, it is the balance between the activation process and the deactivation process. Although the propagation step is similar in both cases, with addition of monomer units to the growing radicals, the lifetime is completely different in RDRP (ranging 0.1-1 ms and are reversibly deactivated) whereas in FRP is ~ 1 s. This decrease in the lifetime of the active radicals leads to a reduction of about 90% of the probability of the existing termination reactions. Additionally, in RDRP the number of polymer chains that are growing is much greater than in FRP. Also the rate of termination and the rate of chain transfer to monomer per chain are much less in RDRP, making their effects negligible.^{38,43} Thus, it is to be expected that the polymer molecular weight would increase linearly with the conversion. Also, the polymers that are obtained using RDRP methods possess active chain-ends that can be reinitiated by further monomer addition (living character) or further functionalized.

The more appropriate ways of determining the living character of the polymer growth include following the polymerization kinetics, by determining the evolution of the molecular weight distribution and monitoring the functionalities with conversion.^{38,40}

Although it is a typical feature of a RDRP process, the linearity between $\ln[M]_0/[M]$ versus time does not guarantee the living character of the system, because the only requirement for such behavior is the constant number of growing radicals and these may not all have a living nature. The kinetic data should be always correlated with the results

of other evaluations, because of the necessity to ensure the presence of active chain-ends, which can be confirmed by nuclear magnetic resonance (NMR), matrix-assisted laser desorption ionization time-of-flight mass spectrometry (MALDI-TOF-MS), electrospray ionization (ESI) mass spectroscopy,^{44,45} or by carrying out a reinitiation experiment (from the macroinitiator, where the complete movement of the macroinitiator towards a high molecular weight value should be clearly visible) (Figure 1.2).^{38,40}

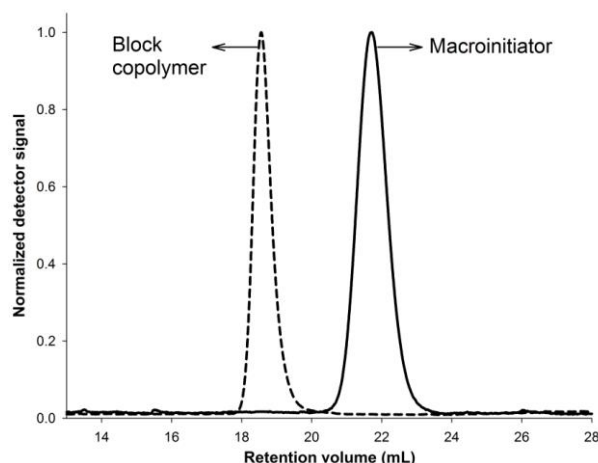


Figure 1.2. GPC traces of the macroinitiator before (right curve) and after the chain extension experiment or the block copolymerization (left curve).⁴⁶

Although considerable opportunities are presented by the use of RDRP area, there are still some limitations that need to be overcome for the full implementation of RDRP technologies at an industrial level. The problems that are common to the different RDRP techniques include the existence of a residual content of control agents in the final polymer product (problems concerning color, odor, stability, and environmental legislative conformity), the process complexity and the cost, when compared to conventional radical polymerizations.³⁹ Taking these into account, new challenges and new potential areas will be investigated in the immediate and medium term future. These include: the need to control the extent of heterogeneity of the polymers in order to optimize and fine tune the properties of the products rather than letting them be spontaneously generated; the need to decrease the process costs for commercial products; the development of new materials containing functional groups for orthogonal chemistry (in contrast to ionic and coordination polymerization, RDRP techniques are tolerant of

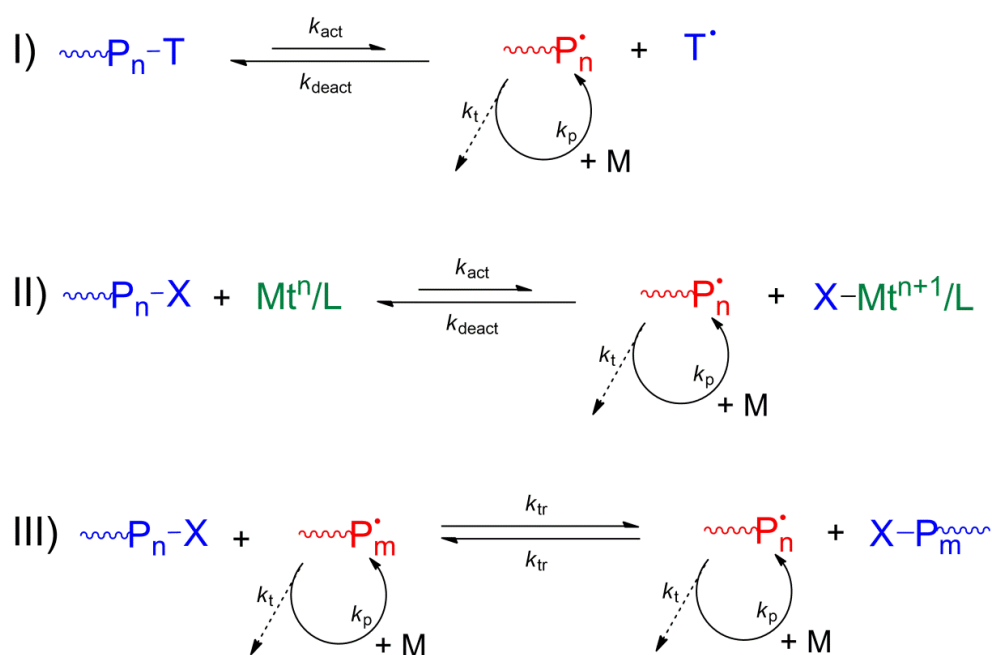
many functionalities); the synthesis of polymers for energy provision and environmental improvement areas; and the use of computational modeling and simulation studies (analysis of complex kinetic multi-reaction systems and the prediction of properties of polymers with novel architectures).¹⁷

1.2.2. Generic Description of the Main RDRP Techniques

The synthesis of new polymers with precise control of molecular weight, molecular weight distribution, morphology, topology and tacticity opens a tremendous opportunity to access materials with unique structural and functional features.^{15,41,42} All methods rely on the reversible generation of carbon-centered radicals (activation) from dormant species. The functional groups used varied for the different RDRP methods and as well as the activation/deactivation mechanism. These differences turn each method unique in terms of compounds required and mechanism involved, which are decisive when selecting the most suitable method to attain specific macromolecules.^{17,41,43}

Different approaches are available to mediate the previously mentioned dynamic equilibrium between active species and dormant species, which keeps the concentration of radicals very low during the polymerization. These strategies can be divided in three different mechanisms that differ by the nature of the deactivation process (Scheme 1.3).^{17,37,41,47}

One process is based on reversible deactivation by coupling or reversible termination (RT) mechanism that relies on the persistent radical effect (PRE) also called *spin trap* (Scheme 1.3-I). This effect was identified by Fischer,⁴⁸ and describes the formation of a product (R-T) that results from the reaction of a transient radical (R^{\bullet}) and a persistent radical (T^{\bullet}). At the early stage of reaction, due to self-termination of a tiny amount of transient radicals (R^{\bullet}), the persistent radicals accumulate in the system, and will promote the formation of the cross-coupling product (R-T). The RT involves the homolytic cleavage of the dormant species (P_n-T) resulting a propagating radical chain (P_n^{\bullet}) and a persistent free radical (T^{\bullet}). This specie should not react with itself or start the polymerization.^{32,47}



Scheme 1.3. RDRP mechanisms.^{17,37,41,47}

Examples of persistent radicals are nitroxides as used in nitroxide-mediated polymerizations (NMP),³⁶ metal complexes like in organometallic mediated radical polymerization (OMRP).⁴⁷ Because all growing chains required a trapping agent these methods use stoichiometric amounts mediating species. The ratio $k_{\text{deact}}/k_{\text{act}}$ is strongly dependent on the reactions conditions, namely initiator, solvent, monomer, additives and temperature.^{36,47}

Another approach is based on the reversible deactivation by atom transfer (Scheme 1.3-II). This process is governed also by PRE, being the activation of the dormant species done by redox-active transition metal catalyst in combination with an alkyl halide. The active radicals are formed by homolytic cleavage of the C-X bond of the dormant species catalyzed by a lower oxidation-state transition-metal complex. The generated macroradical reacts with a higher-oxidation-state transition-metal complex forming dormant species and regenerating the activator. Despite this process also rely on PRE as RT, because the dormant species are formed due to the halogen atoms transferred by the metal catalyst, substoichiometric amounts of metal complex are enough to control the polymerization. This particular feature is extremely important aiming to achieve

technologies that allow the synthesis of complex macromolecules that have residual contamination of metals.^{17,41,43,49} Atom transfer radical polymerization (ATRP) is the most representative technique of this process and has been reported using a wide variety of transition metal complexes.²²

The third system, the so-called degenerative transfer radical methods (Scheme 1.3-III) that involve an atom exchange (*e.g.* iodine transfer polymerization – ITP),⁵⁰ a group transfer (*e.g.* cobalt-mediated radical polymerization – CMRP systems for vinyl acetate polymerizations)⁵¹ or addition-fragmentation process (*e.g.* reversible addition-fragmentation chain transfer –RAFT,³⁵ and macromolecular architecture design by interchange of xanthates – MADIX).⁵² This process is based on a thermodynamically neutral bimolecular exchange between of growing radicals and dormant species. The methods that are based on a DT equilibrium mechanism do not obey to a PRE effect and follow a conventional radical polymerization. They follow a steady state that is established by balancing the initiation rate and the termination rate.^{17,41,43} The reaction proceeds via slow initiation and fast termination with a steady state of growing radicals but, as a regular RDRP system, control over the molecular weight and the polymer structure can be achieved. This is because the constant rate of chain transfer between the active radicals and dormant species is significantly greater than that of the propagation.^{17,41} In fact, the concentration of chain transfer agent (CTA) is much greater than that of the radical initiator(s). Consequently, the CTA is the responsible for the formation of the dormant species. The quality of the control that is achieved in the degenerative processes is strongly dependent on the CTA structure and its suitability for use with the monomer that is being polymerized.^{35,53}

One interesting characteristic of these methods concerns their resemblance in terms of polymerization kinetics to FRP systems because the rate of polymerization does not depend on the concentration of the transfer agent. Indeed, the rate of polymerization depends on the square root of the concentration of the radical initiator. In these systems the rate of activation/deactivation should be much faster propagation to achieve narrow molecular weight distribution. Conventional free radical initiators are used to generate the required active species that will start the polymerization via various stimulus (thermolysis, photolysis and redox processes).^{35,54}

In the next sections the main concepts and fundamentals of the most studied RDRP methods will be presented. Therefore, it will be presented the most relevant information about each method, namely the roots, important achievements and main mechanistic considerations. The proper selection of the RDRP technique requires the balance of different aspects involving the polymerization. The adaptability of the controlling agents and reactivity of the monomer are among the most important ones.

1.2.3. Nitroxide-Mediated Polymerization (NMP)

Nitroxide-mediated polymerization (NMP) is based on based the RT mechanism between the growing radicals and stable radical (T^{\bullet}) that acts as a controlling agent to form the dormant species. The latter can be activated back to growing radicals by the thermal homolytic cleavage. This stable radical plays the role of a persistent radical deactivator, in way that is analogous to the higher valence state metal/ligand complex in ATRP. The established activation/deactivation equilibrium ($K=k_{\text{deact}}/k_{\text{act}}$) as well as the PRE mediates the control over the polymerization. Contrarily to other RDRP methods, in NMP neither catalyst (*e.g.* ATRP) nor bimolecular exchange (*e.g.* RAFT) is required, being the process controlled exclusively by the temperature.

In 1993, Georges et al. reported the NMP of styrene⁵⁵ in the presence of benzoyl peroxide and the mediating stable free radical TEMPO (2,2,6,6-tetramethylpiperidinyl-1-oxy) at 120 °C. This study is considered the first example of a successful RDRP using a nitroxide-based system. The ratio $[\text{nitroxide}]_0/[\text{initiator}]_0$ is extremely important to allow an excess of the free nitroxide that drives the equilibrium toward dormant species. For a long time, conventional free radical initiators were employed to start NMP. However, this strategy had associated some unavoidable problems aiming to obtain perfect well-defined polymers. Indeed, it is almost impossible to control the efficiency of primary radicals produced by thermal decompositions. This fact is associated to two different reasons: the loss of formed radicals due to cage effect; and also the structure of the resulting radicals because they can undergo rearrangements or fragmentation.¹ An elegant alternative⁵⁶⁻⁵⁸ involves the use of an alkoxyamine, which is not more than a single initiator molecule whose decomposition results into both initiating radical and nitroxide.⁵⁶⁻⁵⁸

To expand the range of polymerizable monomers, lower the polymerization temperatures and reduce the reaction times, many nitroxides and alkoxyamine derivatives have been synthesized and successfully used controlled polymerizations (Figure 1.3). The different structures allowed establishing important relationships between the structure of these mediating agents and the control features of the polymerization. It is known for example that the stability of the nitroxide is deeply affected by the nature of the substituting group bonded to the nitrogen atom, which will have impact on reactivity of the nitroxide as well as possible side reactions. For example, usually nitroxides that have H-atom in the α -position to the N atom are unstable and will disproportionate forming a hydroxylamine and a nitron.⁵⁹⁻⁶¹ However, bicyclic nitroxides that bear a H atom in the same position are relatively stable.⁶²

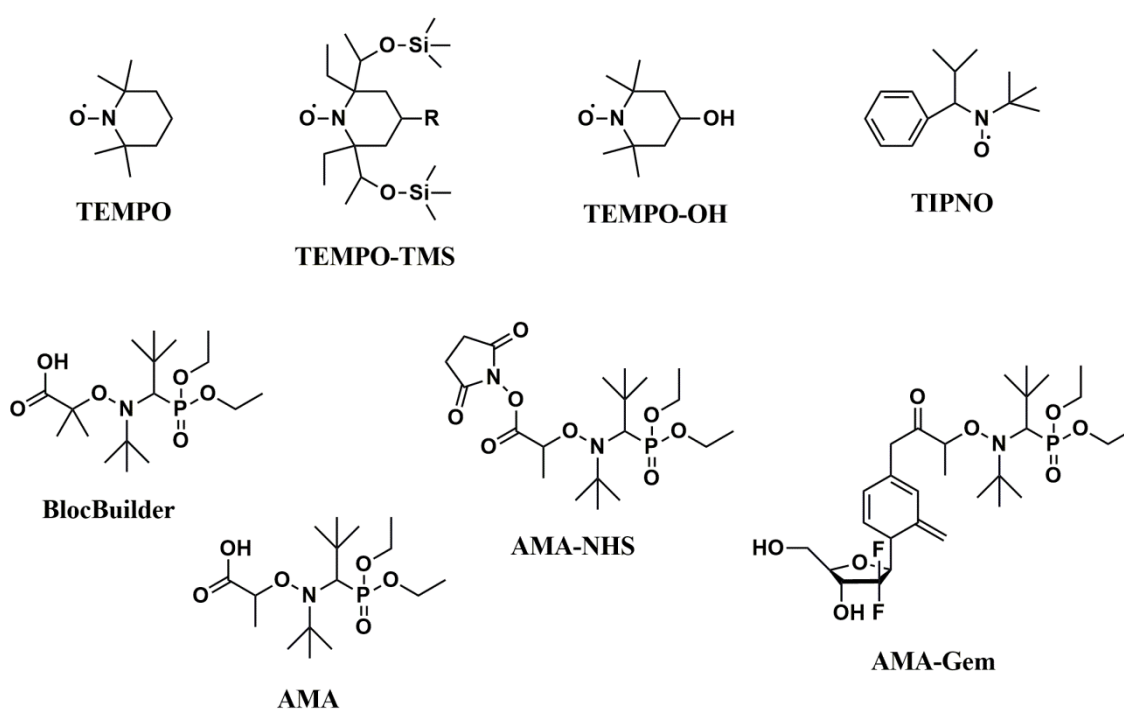


Figure 1.3. Structures of nitroxide and alkoxyamine derivatives commonly used in NMP.^{36,63}

The range of monomers that can be polymerized using NMP is extremely vast,³⁶ namely: acrylates, meth(acrylate)s,^{64,65} styrenics,⁶⁶⁻⁶⁸ vinylpyridines,⁶⁹⁻⁷¹ acrylamides,^{72,73} dienes,^{74,75} and non-activated monomers.^{76,77}

One very interesting alternative to the common use of nitroxides and alkoxyamines is the so-called *in-situ* NMP.^{31,78} In this approach, the controlling agents are produced *in situ* in the polymerization medium using easily accessible precursors; some of them are currently available in the market. Among the reported precursors, nitrones, nitroso compounds, hydroxylamines, amines, sodium nitrite, and nitric oxide, nitrones are the most popular.⁷⁹ This methodology needs a pre-reaction step at a lower temperature before the start of polymerization.⁸⁰ The *in situ* NMP approach has been successfully implemented at moderate temperatures.⁸¹⁻⁸³ Nevertheless, some of the precursors like nitroso based compounds are toxic and thermally unstable. A better understanding of the structures of nitroxides and alkoxyamines formed *in situ* during the pre-activation step will be essential to create more efficient processes.

1.2.4. Organometallic Mediated Radical Polymerization (OMRP)

Organometallic mediated radical polymerization (OMRP) is based on the fast and reversible homolytic cleavage of a metal-carbon bond. One of the main advantages of this system is associated to the possible adjustment of the metal-carbon bond strength by a proper selection of metal center and design center.⁴⁷ It is interesting to note that depending on the particular metal/ligand combination, initiation strategy and monomer used, the OMRP can proceed either RT or DT, or eventually both mechanisms.^{47,84,85} In RT, the transition metal acts as a reversible spin trap, and the polymerization can be started using a conventional free radical initiator with a redox-active metal complex, or employing a complex that contains already a metal-carbon bond. In this process the established equilibrium should favor the formation of deactivated polymer chains through the formation of dormant metal-carbon bonds.⁸⁴ This condition is mandatory to maintain a low concentration of active radicals, and by that means control the polymerization avoiding the termination and side breaking reactions.^{47,84} A low metal-carbon bond dissociation will lead to a high radical concentration, which could favor side reactions.⁸⁶ Also, high metal-carbon bond dissociation will inhibit the polymerization. As mentioned OMRP can also occur through a DT process.^{32,47} This mechanism is predominant when the

amount of active radicals formed exceeds the amount of metal. The metallic species transfers one polymer chain for another one in concerted manner.^{32,47,84}

One side reaction that should be considered in OMRP is the catalytic chain transfer (CCT), which results from the intermolecular transfer of a hydride between the propagating radical and the metal complex.^{32,47,85} This unwanted reaction generates new propagating radical chains that are responsible for the appearance of short chains and olefin-terminated oligomers. The mechanism involved is understood as conventional hydrogen transfer, however the possibility of a bond formation followed by β -H elimination cannot be ruled out. The livingness of the synthesized polymers depends on keeping very low the CCT reactions occurrence.^{47,85} The tendency of the monomers to undergo CCT is closely related to their structure. Monomers having hydrogen atoms prone to abstraction (*e.g.* α -methyl styrene and methacrylates) are CCT active, while other monomers like acrylates and acrylonitrile are much less prone to CCT.^{32,85}

OMRP was initially developed using cobalt complexes, but nowadays is possible to find large variety of metal complexes that have been successfully used (Figure 1.4).⁴⁷ Depending on the organometallic species employed to control the polymerization, different acronyms have been used: a generic designation of organometallic radical polymerization (OMRP),^{87,88} cobalt mediated polymerization (CMRP),^{32,89} organotellurium-mediated radical polymerization (TERP),^{90,91} organostibine mediated radical polymerization (SBRP),⁹² and organobismuthine mediated radical polymerization (BIRP).^{34,93}

The first example of OMRP was reported in by Wayland 1992 using rhodium based catalyst.⁹⁴ Different metal have successfully used in OMRP, namely rhodium, cobalt, molybdenum, osmium iron, titanium, chromium and vanadium.⁴⁷ Among those, organocobalt complexes have received a lot of attention to achieve carbon-centered radicals due easy cleavage of Co-C bonds under relatively mild reaction conditions.³² Wayland⁹⁵ and Harwood⁹⁶ have reported almost simultaneously the first use of cobalt complexes to control the polymerization of acrylic monomers. These systems based on porphyrins⁹⁵ and cobaloximes⁹⁶ with isopropylidinato cobalozime (RCo(dmg)2(py) were used for the polymerization of ethyl acrylate in chloroform. The cobalt porphyrin

complexes have been explored for catalytic chain transfer polymerization. In 2004, it was reported an innovative strategy to generate Co(III) *in situ* 2,2-azo-bis-4-(4-methoxy-2,4-dimethyl valeronitrile) (V70) for the polymerization of methyl acrylate.⁹⁷

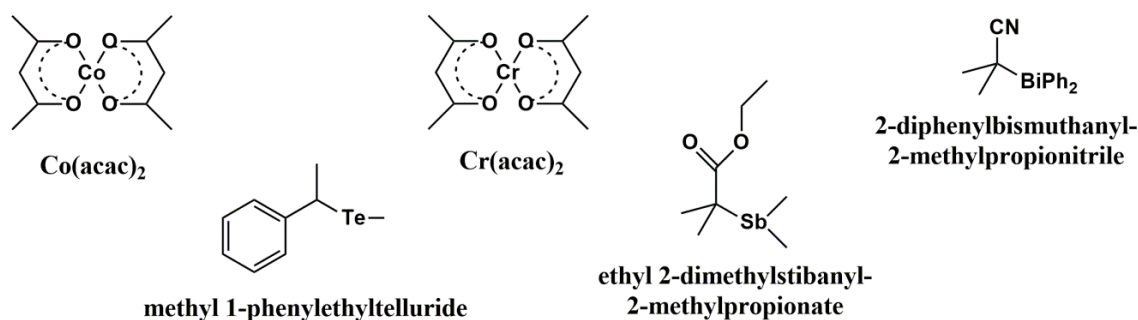


Figure 1.4. Structures of organometallic complexes commonly used in OMRP.⁴⁷

Another important landmark in this area was done in 2005 by Jérôme that, using commercial available $\text{Co}(\text{acac})_2$ and V-70, reported the efficient bulk polymerization of vinyl acetate.⁹⁸ This result was particularly relevant knowing the non-activated nature of this monomer, which brings difficulties in terms of monomer activation and the control over the equilibrium between dormant species and extremely reactive radicals. This CMRP system was successfully extended to heterogeneous reaction medium, such as suspension⁹⁹ and miniemulsion.¹⁰⁰ Later studies, have shown that polymerization of vinyl acetate using the system $\text{Co}(\text{acac})_2/\text{V70}$ is mediated by a degenerative transfer process in absence of Lewis bases, but in the presence of electron donors (*e.g.* water) proceeds through reversible termination. Indeed, the presence of the electron donor blocks the coordination site on the cobalt center that is required for the normal associative radical exchange process during the degenerative transfer mechanism.^{51,101} The $\text{Co}(\text{acac})_2$ system was successfully used for the polymerization of monomers including N-vinyl-2-pyrrolidone,^{102,103} acrylonitrile (AN),¹⁰⁴ butyl acrylate,¹⁰⁵ vinyl pivalate,¹⁰⁶ and vinyl chloride.^{107,108} More recently, CMRP has also extended in the precision synthesis of poly(ionic liquid)s (PILs) in aqueous media.¹⁰⁹

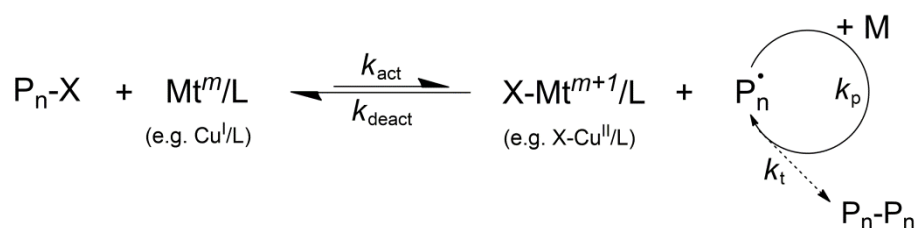
Concerning the industrial implementation OMRP has two main issues associated, the costs related to the metal complex (and its removal) and the limited range of monomers that can be used.⁴⁷

Organotellurium,^{90,91,110} organostibine^{92,111} and organobismuthine-mediated RDRP⁹³ (TERP, SBRP and BIRP, respectively) are relatively new methods. In 1999, Yamago discovered that the reversible radical generation using organotellurium compounds via carbon-tellurium bond thermolysis and photolysis.¹¹² In further contributions these organotellurium compounds were used as mediate controlled polymerizations.^{90,91,113} Years later, the same group introduced the use of organostibines¹¹¹ and organobismuthines⁹³ to promote the controlled polymerization of conjugated and nonconjugated vinyl monomers. In these systems the nature of the heteroatoms is determinant on the stability and reactivity of mediating compound and their efficiency in the polymerization control. One important advantage of these controlling agents concerns in their easy synthesis in large scale. In contrast, some required to be stored under nitrogen atmosphere which limits their application at the industrial scale due to limitations associated to handling and manipulation. On this matter, organotellurium compounds are the most resistant to oxidation. Nevertheless, the development of a new generation of oxygen-resistant compounds is eagerly needed. The polymerization conditions have observed important advances over the years. Mechanistically, these methods proceed through reversible termination and degenerative chain transfer, being the latter always predominant in TERP.

Initially, the formation of carbon centered radicals from the mixture organotellurim and monomer was achieved thermally using reaction temperatures above 80°C.⁹¹ Milder temperatures were attained with the addition of conventional radical initiators.¹¹⁴ In a further improvement, the C-Te direct photolysis allowed to reduce dramatically the polymerization temperature,¹¹⁰ allowing the reaction to occur even at 0°C. These methods have been used to synthesize a variety of monomer families, namely styrenics,¹¹⁵ acrylates,¹¹⁰ methacrylates,^{91,113} acrylamides,¹¹⁶ and some non-activated monomers.^{90,113} Under the scope of this Thesis, one particular feature that should be stressed, is the possibility of synthesize non-activated monomers using these techniques. The mechanistic details involving each of the aforementioned methods can be found in two reviews devoted to this topic.^{34,117}

1.2.5. Atom Transfer Radical Polymerization (ATRP)

Atom transfer radical polymerization (ATRP)^{22,118} is probably the most used method for preparing a wide range of polymers with tailor-made characteristics.¹¹⁹⁻¹²⁶ ATRP is based on the creation of a fast transition metal complex-mediated equilibrium between dormant species (macroinitiators P_n-X , where X represents a halogen or pseudohalogen) and active species (macroradical, P_n^\bullet). The dormant species are activated by a lower oxidation state transition metal complex Mt^n/L , where Mt^n represents the transition metal species in oxidation state n and L is a ligand. The transition metal complex acts as an activator to form growing radicals (P_n^\bullet) intermittently, and is deactivated by transition metal complexes at a higher oxidation state, which coordinates the halide species, $X-Mt^{n+1}/L$. The reverse reaction (k_{deact}) occurs when the deactivator reacts with the propagating radical to re-form the dormant species and the activator (Scheme 1.4).^{46,127-130} The reactivity of complexes can be finely tuned through the judicious selection of metal and ligand.



Scheme 1.4. General mechanism of ATRP.^{128,130}

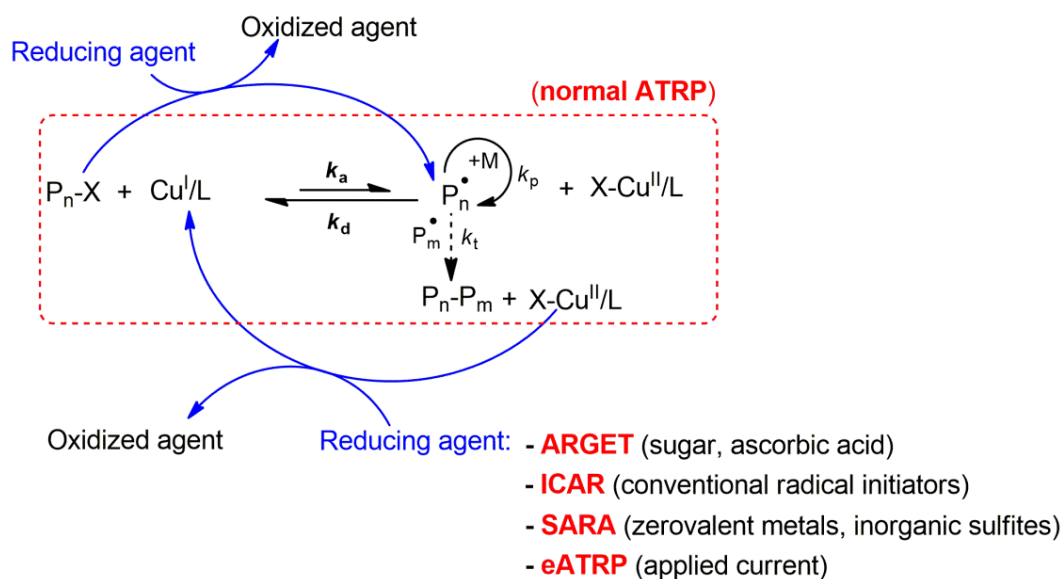
In the original ATRP technique, developed by the Matyjaszewski and Sawamoto research groups in 1995,^{40,118,125,131} the large amounts of redox-active ATRP catalysts limited the industrial implementation of this process, due to the excessive cost of the catalytic systems and the need to remove the residual metals from the polymer matrix after the polymerization. Another limitation of ATRP that has been reported by Matyjaszewski is that the technique could not be used to polymerize non-conjugated monomers, such as VC.¹³² Over the years, ATRP has been the most extensively studied and applied RDRP technique^{17,22,41} for the polymerization of different families of monomers, such as acrylonitrile, (meth)acrylates, styrenics and water soluble monomers, due to its versatility and the easy access of the required reagents.^{22,40,41} The major disadvantages that have

been associated with the method are the need for residual catalyst removal and the need for the protection of acidic monomers during the polymerization.⁴¹

Aiming at achieving faster, more efficient and greener procedures, without the loss of the control over the polymerization and loss of control over chain-end functionality, a new generation of ATRP methods was developed. These include activators that are regenerated by electron transfer (ARGET),¹³³⁻¹³⁶ initiators for continuous activator regeneration (ICAR),^{137,138} supplementary activators and reducing agents (SARA) ATRP,^{46,129,130,139-142} electrochemically mediated ATRP (*e*ATRP),¹⁴³⁻¹⁴⁵ and photochemically mediated ATRP (Scheme 1.5).¹⁴⁶⁻¹⁴⁸ Recently, some metal free ATRP approaches have been reported.¹⁴⁹⁻¹⁵¹ The development of these ATRP variations allowed the reduction in the amounts of transition metal complexes (typically copper complexed with nitrogen-based ligands) used as the redox active ATRP, catalysts from >10000 ppm to less than 100 ppm in the presence of various reducing agents (including zerovalent metals,^{127,129,130} organotin complexes,^{134,135} ascorbic acid,¹³⁴ and glucose).¹³⁴ Indeed, these reducing agents allow a continuous *in situ* regeneration of the activator species (low oxidation state transition metal complexes).

As shown in Schemes 1.4 and 1.5, the copper-based catalyst complexes are responsible for a dynamic equilibrium between very small amounts of propagating radicals and alkyl halides, as dormant species. ATRP is accompanied by an unavoidable radical – radical termination process, resulting in the buildup of a small excess of X-Cu(II)/L deactivator - persistent radical effect (PRE).¹⁵²

Part of the work presented in this Thesis aimed to contribute to the development of new ecofriendly ATRP systems as well as for the expansion of the technique to different monomer families. In this context, Food and Drug Administration (FDA) approved inorganic sulfites have been used and will be presented as a new class of efficient SARA agents for ATRP (**Chapters 2 to 4**).^{46,128,153,154}

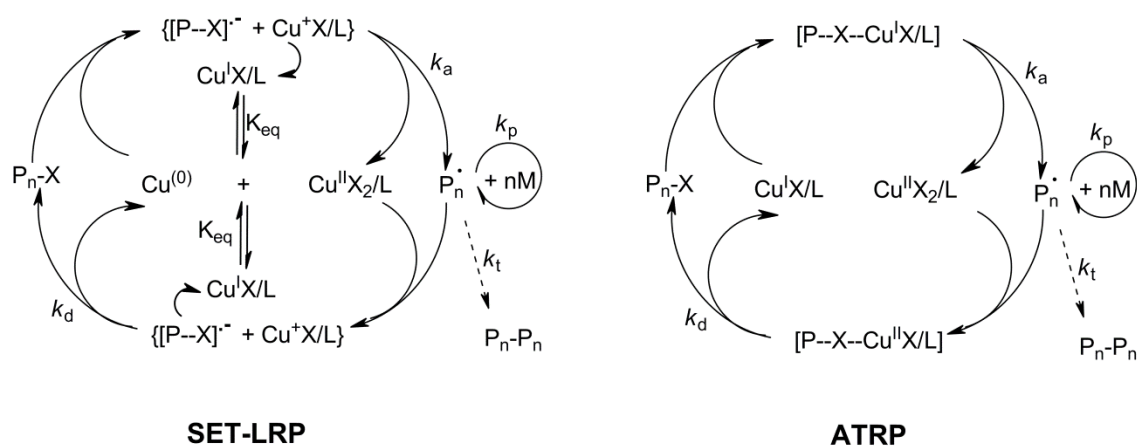


Scheme 1.5. Schematic representation of the different ATRP variation techniques.

The field of RDRP, because it involves the use of transition metal mediated catalysts has been the subject of intense debate, regarding the operating mechanism. Two different perspectives have been and are being debated to describe the mechanism that controls the polymerization (Scheme 1.6). In the original publication,¹⁵⁵ the authors coined the term for the method as ATRP, because of similarities with the well-known atom transfer radical addition (ATRA) reaction.^{49,156-159} From the mechanistic standpoint, an halogen atom transfer from the alkyl halide to the Cu(I) complex can be described by either an outer-sphere electron transfer (OSET) process or an inner-sphere electron transfer (ISET) process.¹⁶⁰

In ATRP methods, the irreversible termination reactions and the side reactions are considerably suppressed due to the PRE, following the mechanism described above. The activation is based on an inner-sphere (bonded) electron transfer (ISET) process between the initiator (R-X) and the transition-metal catalyst in a lower state of oxidation. The ISET from the transition-metal complex to the dormant species, and the homolytic cleavage of the C-X (X=Cl, Br) bond occurs in a concerted manner. By contrast, in the seminal Single-Electron Transfer Living Radical Polymerization (SET-LRP) paper from Percec's group¹⁶¹ it was proposed that activation of the dormant species (RX) occurs exclusively by "nascent" Cu(0) species, through an outer-sphere (nonbonded) electron-

transfer (OSET) process (Scheme 1.6). Also, it was postulated that the activation of dormant species under SET-LRP conditions involves the formation of radical-anion intermediates. These are considered to emanate from an alkyl halide initiator, whose stepwise decomposition occurs through the “heterolytic” cleavage of the C-X (X=halogen) bond. In SET-LRP, it has also been proposed that the complex $\text{Cu}^{\text{I}}\text{X}/\text{L}$ (L=chelating nitrogen-based ligand), generated *in situ*, disproportionates “spontaneously” into $\text{Cu}(0)$ and $\text{Cu}^{\text{II}}\text{X}_2/\text{L}$ species (regeneration of the activator and generation of the deactivator respectively, Scheme 1.6), thus assuming that the SET-LRP process is not based on the persistent radical effect (accumulation of excess deactivator species through the bimolecular termination of propagating radicals).



Scheme 1.6. Detailed mechanism of copper-catalyzed SET-LRP and ATRP.

Over the years, the research groups of Matyjaszewski¹⁶²⁻¹⁶⁶ and Percec¹⁶⁷⁻¹⁷⁰ have published numerous contributions, each supporting their opposite visions regarding the real activator of this process. The development of a clear understanding of the mechanism is crucial to the development of more efficient catalytic systems and to the extension of this method to other monomer families. Most of the studies that have been published have been carried out using “ideal” conditions, model compounds and/or computational simulations. In 2012,¹³⁹ the first report of the determination of the $[\text{Cu}(\text{I})\text{Br}]/[\text{L}]$ and the extent of $\text{Cu}(\text{I})\text{Br}/\text{L}$ disproportionation during the polymerization was presented. The results suggested that $\text{Cu}(0)$ acts as a supplemental activator and as a reducing agent of $\text{Cu}(\text{II})\text{Br}_2/\text{L}$ to $\text{Cu}(\text{I})\text{Br}/\text{L}$, confirming the ATRP concept. Very recently, Matyjaszewski’s

group published a mini-review entitled “SARA-ATRP or SET-LRP. End of controversy?”,¹⁷¹ presenting much experimental and theoretical data that clearly supports the ATRP theory.

The ATRP methods using Cu(0) as SARA agent have been applied with success to a broad range of functional monomers, both conjugated monomers and non-conjugated monomers, using homogeneous conditions and heterogeneous conditions, promoting fast reactions with very low occurrence of termination reactions, enabling the preparation of very high molecular weight polymers, at room temperature or below.¹⁶¹ The polymers obtained exhibited a predictable molecular weight evolution and distribution, had perfect retention of chain functionality and showed no detectable structural defects.^{161,172}

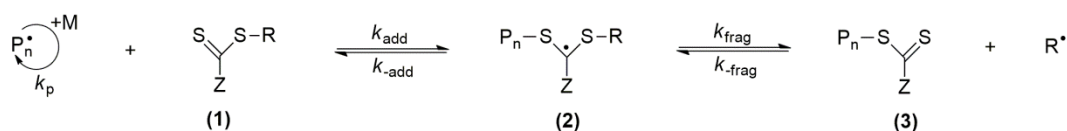
1.2.6. Reversible Addition-Fragmentation Chain Transfer Polymerization (RAFT)

Reversible addition-fragmentation chain transfer (RAFT) polymerizations involve a fast degenerative exchange between various dithio-based compounds, serving as dormant species and radicals that must be continuously supplied to the system.^{53,173} These are regulated by a reversibly degenerative transfer of a leaving group (R) between a growing polymer chain and a CTA, via addition-fragmentation. Conventional radical initiators, e.g. azobisisobutyronitrile (AIBN), are typically used to form the primary growing radical chains that can then react with the CTA in the initiation step.^{17,35,40}

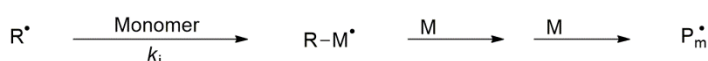
As shown in Scheme 1.7, the mechanism of RAFT polymerizations involves a series of reversible addition-fragmentation steps.^{33,35,173,174} The adduct radical **2**, which fragments to a polymeric thiocarbonylthio compound **3** and a new radical R^{\bullet} , is obtained by adding a propagating radical P_n^{\bullet} to the RAFT agent compound **1** (Scheme 1.7-a). The polymerization is reinitiated by the radical R^{\bullet} and gives a new propagating radical P_m^{\bullet} . Successive addition-fragmentation steps set up an equilibrium between the propagating radicals P_n^{\bullet} and P_m^{\bullet} and the dormant polymeric thiocarbonylthio compounds **3** and **5** via the intermediate radical **4** (Scheme 1.7-b). A narrower molecular weight distribution (low values of dispersity - \bar{D}) is obtained by the equilibrium of the growing chains. The

majority of the polymer chains are end-functionalized throughout to the end of the polymerization, by a thiocarbonylthio group (dormant chains).^{53,54,173,175}

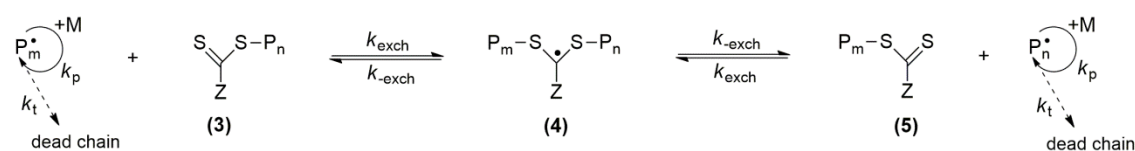
(a) Reversible chain transfer / propagation:



Reinitiation:



(b) Chain equilibration / propagation:



Scheme 1.7. General mechanism of RAFT polymerization.^{33,35,173,174}

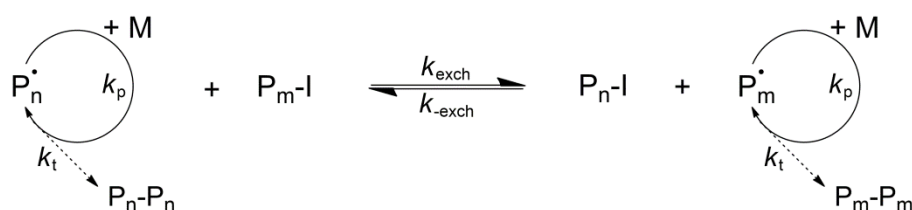
The success of the RAFT polymerization (the control over the polymers' molecular weight, molecular weight distribution and molecular architecture) is strongly related to the appropriate selection of the RAFT agent (or CTA).^{41,54} The general CTA requirements are that the leaving group (R) must possess a good capacity for homolytic cleavage from the CTA and must be able to be reinitiated in the radical form.¹⁷⁶ The CTA must be quickly consumed.³⁷ Also, the rate constant of exchange (k_{exch}) must be greater than the rate constant of propagation (k_p).⁴¹ Chain transfer agents as dithioesters, dithiocarbamates, trithiocarbonates, and xanthates (thiocarbonylthio compounds) have been used to control the polymerization.^{40,41,54} Such selection depends on the suitability for use with a specific monomer. When using xanthates as the CTA, the process is often termed “macromolecular design via the interchange of xanthates” (MADIX).^{52,54}

The RAFT process is one of the more successful RDRP techniques because it enables the polymerization of a broad range of monomers using relatively mild conditions.^{17,37} However, it also presents disadvantages, such as the significant retardation in the polymerization of low molecular weight polymers, in the complexity of the synthesis of

some RAFT agents, in the high cost of the commercially available RAFT agents and because of a gel effect that is observed at high monomer conversion.⁴⁰

1.2.7. Iodine/Reverse Iodine Transfer Polymerization (ITP/RITP)

The iodine transfer polymerization (ITP) technique, developed in the late 1970s by Tatemoto *et al.*,¹⁷⁷ is a DT polymerization requiring alkyl iodides as the transfer agents to mediate the dynamic equilibrium.^{37,50} As shown in Scheme 1.8, the iodine atom is exchanged between a polymeric radical and a dormant chain, without the formation of an intermediate radical.^{50,178} The ITP systems usually have poor control, leading to \mathcal{D} values that are above 1.3). This effect has mainly been attributed to a rate constant of exchange (k_{exch}) that is three times lower than that of other DT systems.⁴¹ Styrene and certain fluoro-monomers were the first reported examples of monomers being polymerized by ITP.^{50,179} Kamigaito *et al.* have employed ITP to control the tacticity of poly(vinyl acetate) using a fluoroalcohol solvent¹⁸⁰ and also using manganese mediated photoinduced polymerization process.^{181,182} Nowadays, different monomers can be polymerized, including acrylates, alpha-fluoro acrylates, styrenics and vinylidene halides.^{178,183}



Scheme 1.8. General mechanism of ITP.^{17,50}

The ITP of monomers involving tertiary propagating radicals (such as methacrylates) was not successful because such polymerization would require the use of alkyl iodides with a better leaving group (such compounds are inherently even more unstable).⁵⁰ To overcome these limitations, Lacroix-Desmazes and co-workers^{183,184} developed and patented a new process that was based on using molecular iodine (I_2) as a control agent, which they termed reverse iodine transfer polymerization (RITP). In this procedure, free radicals

(yielded by a conventional initiator) react with I_2 to generate, *in situ*, the reversible chain transfer agent. In this step, the monomer conversion during this period is essentially negligible. For this reason, this period has been termed the “inhibition period”. After this step, the polymerization proceeds to establish the DT equilibrium.^{50,183} The simplicity and the availability of organoiodine dormant species are the two main advantages of ITP/RITP that justify its frequent use.

1.3. Polymerization of Vinyl Chloride

Vinyl chloride (VC) monomer [CAS number 75-01-4] is an organo-chloro compound with the formula $H_2C=CHCl$. Its Q - and e - values (0.44 and 0.2 respectively) indicate the low reactivity of the VC monomer and very high reactivity of the corresponding radical. VC is classified as a non-conjugated, weak-electron-withdrawing vinyl monomer.¹⁸⁵ Among the commonly used monomers, the free radical polymerization of VC presents one of the larger values of chain transfer (C) to monomer. For example at 60 °C, the values are $1.0 \times 10^{-3} < C_{VC} < 1.6 \times 10^{-3}$. These values are two orders of magnitude larger than that of methyl methacrylate (MMA) and styrene (S), $7.0 \times 10^{-6} < C_{MMA} < 2.5 \times 10^{-5}$ and $3.0 \times 10^{-5} < C_S < 6.0 \times 10^{-5}$.^{185,186} Additionally, the rate constants of propagation (k_p) and termination (k_t) are two orders of magnitude larger than those of MMA and S.^{185,187} Therefore, conventional free radical polymerization inevitably leads to anomalous structures and severe consequences for the thermal stability of the resulting PVC.¹⁸⁸

VC was first produced in 1835 by Liebig and Regnault.¹⁸⁹ The molecule was obtained by treating 1,2-dichloroethane with a solution of potassium hydroxide in ethanol. In 1872, Braumann accidentally produced a white solid, from VC monomer that was left under sunlight, resulting in the creation of PVC for the first time.¹⁹⁰ It was not until decades later that this product would be turned into one of the more consumed polymers in history. However, for many years the use of PVC in commercial products failed because of difficulties in processing. In 1926, Semon and Stahl discovered that the use of organic phosphates and phthalates (used nowadays as plasticizers) could provide a PVC product with enhanced flexibility.¹⁹¹

PVC is the basis of one of the larger markets for polymers. Its annual production exceeds 32 million tons.¹⁹² Endo,¹⁹³ Saeki and Emura,² Starnes,¹⁹⁴ Braun,¹⁹⁵ Leadbitter¹⁹⁶ and Mersiowsky¹⁹⁷ have published special issues devoted to describing the major milestones in PVC manufacturing history, the development of the macromolecular chemistry in PVC synthesis, the technical progress of PVC production and issues related to PVC recycling and sustainability.

Figure 1.5 presents a summary of the major milestones in PVC history, from 1835 to 2000. This review concerns research developments that have been achieved in the preparation of PVC materials created using the RDRP of VC, after 2000.

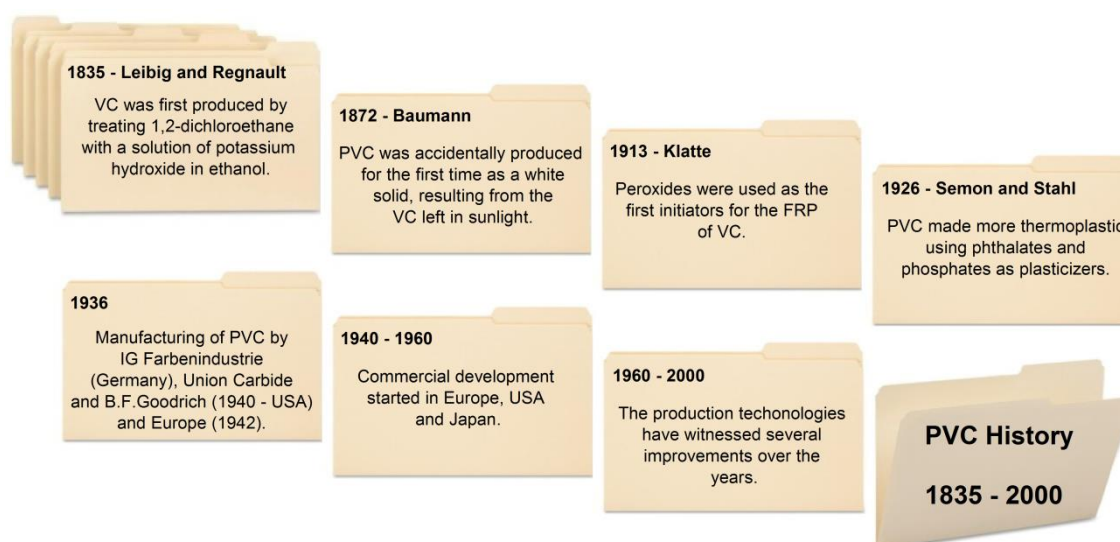


Figure 1.5. Milestones in PVC History from 1835 to 2000.

1.3.1. Properties and Applications of PVC

Packaging, healthcare devices, toys, electrical wire insulation, clothes, furniture, interior decoration, building materials, automotive industry products, pipes, window frames, bottles, and credit cards represent some of the materials that are used in the extensive spectrum of PVC applications.^{198,199} The relatively low price (ratio of price vs quality) and its wide versatility are the major reasons for the enormous commercial success of PVC.⁶

PVC is typically obtained as a white solid powder. After processing it becomes a material that is rigid, light, chemically inert, relatively harmless and resistant to fire.^{200,201} A particular feature that distinguishes PVC from other polymers that derive from vinyl monomers is the fact that in the VC molecule more than a half of its atomic mass is due to the chlorine atom. For this reason, the price is not so dependent on hydrocarbon-based feed-stocks when compared to other monomers such as styrene, since chlorine is typically obtained a waste product of the chlor-alkali (caustic soda) industry.^{201,202} The chloro content also provides PVC with excellent combustion resistance, having an ignition temperature as high as 455 °C.^{201,202} The hardness and the stiffness of PVC are due to the presence of the chlorine atoms. These cause an increase in the inter chain attraction. The C-Cl dipole of PVC causes PVC to be more polar than are other widely consumed polymers, such as the poly(ethylene) (PE), poly(propylene) (PP) or poly(styrene) (PS). PVC has a very few solubility options. The solubility parameter is about 19.4 MPa^{1/2}.²⁰³ Thus, only a few solvents (such as cyclohexanone and tetrahydrofuran) are able to dissolve this polymer.^{203,204} The α -hydrogen atom of PVC is responsible for much of the interaction ability, making it possible to form hydrogen bonds between PVC and other polymers and copolymers of different nature, particularly with those that have basic groups such as amide groups and carbonyl groups.²⁰⁵

One of the more serious issues in the PVC industry is the need for the use of plasticizers for flexible applications and the unavoidable migration of these compounds.^{206,207} There are many materials that are suitable plasticizers for PVC. These generally require solubility parameters that are similar to that of PVC, with a high molecular weight and molecular size to dissolve PVC at room temperature. These compounds are incorporated by mixing at elevated temperatures to give mixtures that later are stable at room temperature. The European Union introduced restrictions in the use of some plasticizers in critical applications such as children toys, packaging and medical devices.²⁰⁸ The loss of plasticizers can result in a serious contamination of the materials/surfaces that are in contact with PVC, as well as the deterioration of its mechanical properties.²⁰⁹ This problem was the main reason for the need to develop new flexible PVC materials, containing non-extractable compounds.²¹⁰⁻²¹⁵ Even though there have been various discussions concerning the recognized, considerable VC toxicity, the demand for

halogen-free materials, the use of plasticizer free polymers and the use of toxic metal-free components for stabilization, the worldwide production of PVC continues to grow at a rate of more than 4% a year.¹⁹²

1.3.2. Limitations of the PVC Industrial Products that are based on FRP

The FRP of vinyl monomers does not allow the preparation of well-defined polymers (controlled molecular weight, polydispersity, end functionality, composition and macromolecular architecture), due to the lack of control of polymer chain growth.^{1,16,17}

These characteristics are more pronounced in the polymerization of VC, since VC has one of the larger values of chain transfer constant to the monomer.^{185,186} Thus, PVC products that have been obtained by FRP present unwanted structures, known as structural defects, which are responsible for some of the more important technological problems that are faced in the PVC-use-based industries.¹⁹³ The global consumption of PVC represents a complex paradox, considering that this polymer is a material with lesser thermal stability compared to the thermal stability of its major competitors.¹⁹⁴ The poor thermal stability of PVC is characterized by the loss of HCl, resulting from the mechanism of dehydrochlorination and by the subsequent appearance of coloration and changes in application properties. The recognized commercial success of PVC is associated with the discovery of the suitable compounds (stabilizers and additives) that allow the processing of PVC, and give options for improving the properties of PVC to satisfy the market requirements.²¹⁶ The inferior thermal stability of the PVC is influenced by the fact that, at its melt state temperature, severe decomposition occurs, making polymer processing impossible without the use of additives.²¹⁷

The major limitations and problems that are associated with PVC synthesis and manufacture on an industrial scale are considered and developed in the following sections. The points of issue include the uncontrolled molecular weight of PVC product, the presence of structural defects and the “additive” compounds that are used in the PVC polymer/binder/substrate formulations. The living character that can be provided by RDRP methods offers an efficient strategy by which such limitations can be overcome.

Uncontrolled Molecular Weight

One of the more important disadvantages of FRP technology relates to the poor control of the molecular weight of the products.^{16,17} One of the major features of VC polymerization, in comparison with many other monomers, is the fact that the molecular weight is completely controlled by the polymerization temperature.^{4,218,219} On increasing the temperature, the chain transfer reaction to the monomer becomes more important, preventing the chain from growing, which decreases the final molecular weight.⁴ This kind of control has implications in terms of the thermal stability of the product since the use high temperatures also results in various structural defects. Therefore, the lower molecular weight PVC grades have a significantly lower thermal stability.^{205,220} This limitation precludes the preparation of PVC materials possessing either an ultra-high molecular weight or a very low molecular weight.^{221,222} Achieving the former specification would be extremely interesting due to the possibility of preparing PVC materials with superior mechanical properties. Achieving the latter option would be attractive to the preparation of PVC-based polymers with a decreased melt flow index, enabling easier processing to be realized.^{12,218,223}

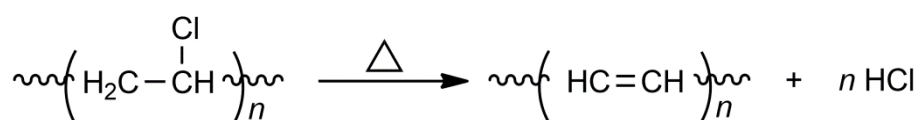
The PVC industries have tried to address such problems using strategies that have been shown not to be efficient. Since the polymerization temperature controls the final molecular weight of the PVC, for high molecular weight polymers, a low polymerization temperature should be used.^{221,224} This option results in an increase in the reaction times. Previous studies have demonstrated that PVC that has been prepared by FRP has a maximum molecular weight ($M_{n,SEC}$) of 92000, even at 21 °C, due to the occurrence of chain transfer reactions.^{221,224} Although attempts have been made to overcome this problem by the use of technologies that “link” the polymer growing chain (*e.g.* crosslinking agents added at low concentrations during the course of the polymerization),^{225,226} the resulting lack of increase in the molecular weight that could be obtained did not justify the production cost of the resulting product, at least for standard applications.

At greater reaction temperatures, for example 75 °C, a lower molecular weight is obtained by FRP, this being 28200 ($D = 2.14$).^{221,222,224} Another strategy involves the use of chain

transfer agents. However, the thermal stability of the obtained polymer is quite poor.²²² Such strategies have other important limitations when applied at the industrial level, since they involve the addition of expensive compounds, increasing greatly the price of the final material.^{188,222}

Structural Defects

It has long been recognized, that PVC contains anomalous structural defects that are responsible for the low thermal stability of this polymer.²²⁷ These unwanted defects comprise the major sites for the start of the well-known zipper dehydrochlorination reactions (Scheme 1.9) that generate conjugated polyene sequences (highly colored) and lead eventually to the destruction of many of the polymer's useful properties.^{194,227} Due to the technological relevance and scientific importance of PVC, the identification and quantification of these structural defects have been of great interest to PVC researchers and technologists for more than 60 years. Several strategies have been followed as possible routes to the reduction of both the number of the defects and to reducing their effects on thermal stability.

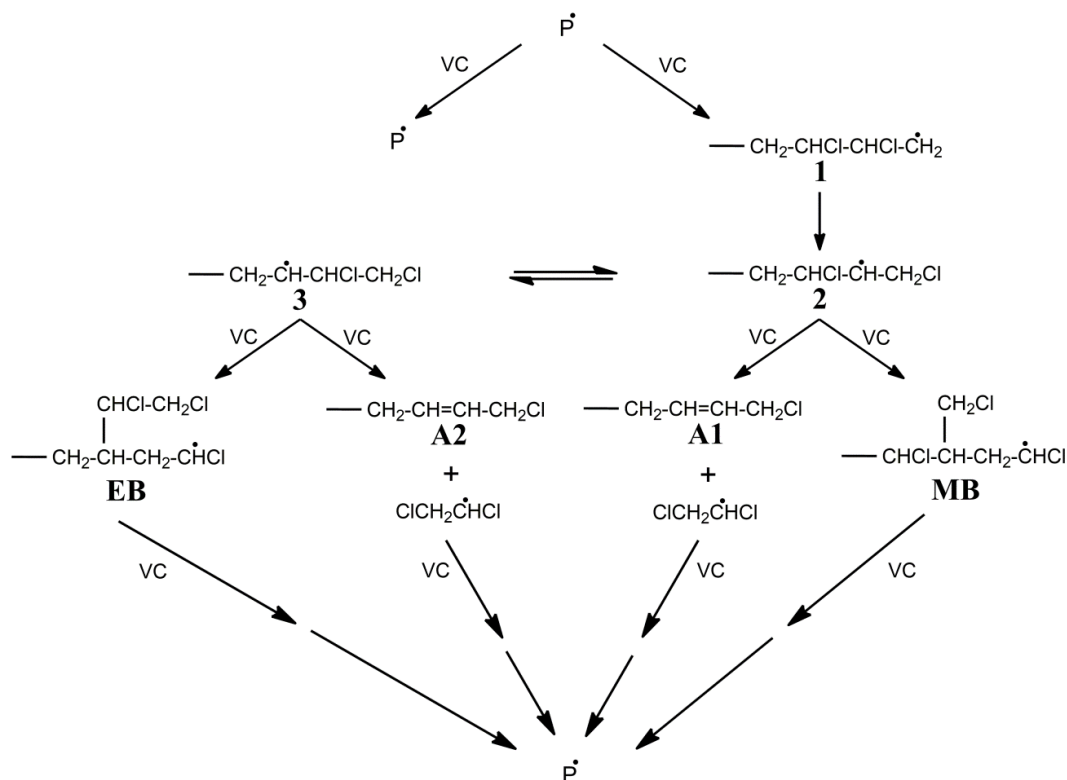


Scheme 1.9. Zipper dehydrochlorination reaction.^{194,227,228}

There are several reasons for the occurrence of these structural defects. These include the presence of allylic centers and the presence of tertiary halogen atoms.²²⁹⁻²³² The kinds of structure, $\sim\text{CO}(\text{CH}=\text{CH})_n\text{CHCl}\sim$ ($n \geq 1$), resulting from incidental air oxidation,²³³ and the *GTTG* conformation of isotactic triads, derived from ordinary monomer units, are two that are of relevance.²³⁴ However, according to Starnes,¹⁹⁴ these are described as being of minor importance. In fact, it has been suggested that the main species responsible for the dehydrochlorination processes²²⁸ that are formed during the polymerization, are those arising from allylic chloride and tertiary chloride structural defects (Scheme 1.10). This conclusion is shared by other specialists in this field.²²⁹⁻²³² The mechanism used to explain the formation of structural defects, as presented in this review, is based on the

findings published by Starnes²³⁵⁻²⁴⁸ and subsequently reviewed in three further publications.^{194,227,249}

In 1993, Starnes *et al.*²³⁸ proposed a mechanism that involves the formation of allylic chloride structures (Scheme 1.10). These structures result from a head-to-head placement of the monomer, which occurs infrequently, instead of the regular head-to-tail addition.² According to this mechanism, ethyl-branch (**EB**) and methyl-branch (**MB**) segments are produced, as well as chloroallylic end groups (**A1** and **A2**).^{238,249} The sum of the **MB** and the **EB** loadings in the polymers prepared, per monomer unit, represents a characteristic value that is dependent on the temperature and independent of the monomer pressure. At each temperature, the “concentration” of **EB** increases at the expense of the **MB** “concentration” when the monomer concentration is lowered. The observations that relate to the chemistry occurring after head-to-head monomer addition are considered in Scheme 1.10.^{194,238}



Scheme 1.10. Mechanisms involved in the formation of allylic chloride structures.^{194,227,238,249}

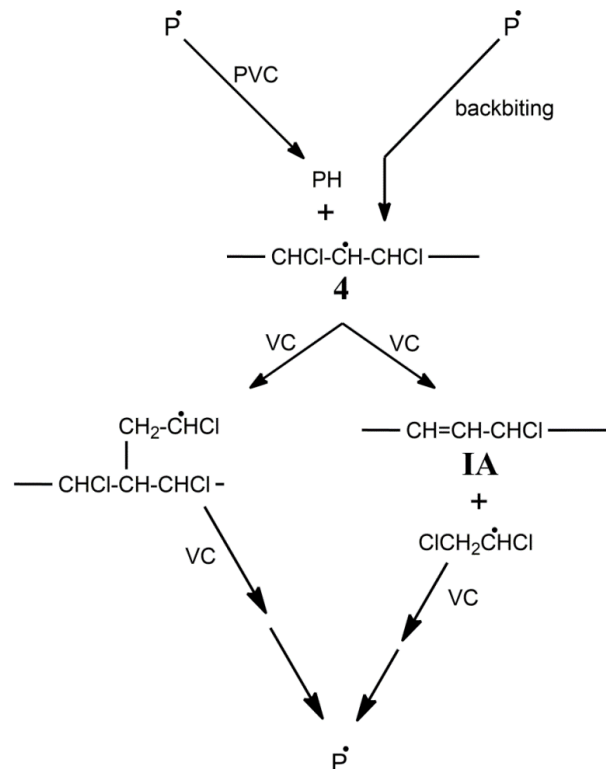
Scheme 1.10 shows that after the head-to-head addition, radical **1** suffers a rearrangement by a 1,2-shift of the chloro substituent to create **2**. This conversion is so rapid that head-to-head structures, resulting from the addition of **1** to the monomer, have never been found in PVC.^{238,249} Another 1,2-Cl shift converts **2** into the doubly rearranged radical **3**. The **MB** and **EB** segments result from the normal addition of monomer to types **2** and **3** radicals, respectively. The abstraction of the chlorine atom by VC from radicals **2** and **3** occurs in a single step (in both cases) and results in chain transfer to the VC monomer during polymerization, forming chloroallylic end groups (**A1** and **A2**) and 1,2-dichloroethyl radicals ($\text{ClCH}_2\text{C}^*\text{HCl}$), whose addition to the monomer continues the radical chain propagation steps. This transfer of the chlorine atom, which is kinetically of first-order with respect to the VC concentration, does not involve unimolecular β -scission to give a chlorine atom that then is scavenged by VC forming $\text{ClCH}_2\text{C}^*\text{HCl}$ radicals. Based on kinetic data, it has been proven that the rate constant for transfer to the monomer, following a head-to-head emplacement ($C_{\text{M,HH}}$), is a true constant whose value is independent of the concentration of the VC.^{194,227,238,249}

As previously explained, for the VC polymerization, the M_n value is completely dependent on the polymerization temperature because of chain transfer reactions to the monomer.^{218,219,221,222,224} However, independently of the constant $C_{\text{M,HH}}$, the instantaneous M_n decreases considerably with decreasing monomer concentration.^{194,250} This could be considered to be contradictory. Starnes *et al.* in 1996,²⁵¹ invoked the concurrent operation of a second mechanism for transfer to monomer which was termed an "auxiliary transfer process" (Scheme 1.11). This mechanism shows type **4** radicals to be formed from the head-to-tail polymerized VC (P^*) units by intermolecular or intramolecular H atom abstraction (backbiting).^{194,249,251} The polymeric radical **4** may add to the monomer and initiate the growing process of a long-branch known as a tertiary branch.²⁵⁰ However, the removal of a β -chlorine atom from these radicals by the monomer, in a single step, gives the unstable internal chloroallylic structure (**IA**) and a Cl^* radical that may start a new polymer chain, an approach that has more relevance from a thermal stability standpoint. The relative importance of this auxiliary mechanism increases with decreasing concentrations of VC, since H atom abstraction by P^* competes directly with the main propagation reaction of monomer addition.^{194,249,251}

Contrary to the chain transfer constant $C_{M,HH}$, the auxiliary transfer constant ($C_{M,aux}$) is not actually a constant, since it is inversely dependent on the concentration of VC.^{194,227,251} Thus, the overall transfer constant ($C_{M,total}$) can be given by:

$$C_{M,total} = C_{M,HH} + C_{M,aux} \quad (1.10)$$

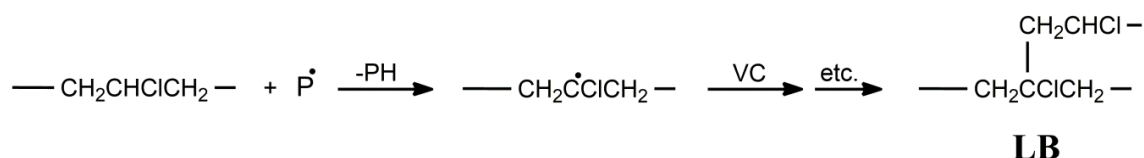
Thus quantification can be achieved by determining the total number of double bonds by ^1H NMR.^{194,227,251} Starnes *et al.*²⁵¹ have determined $C_{M,total}$ for reactions at different temperatures. They obtained very different values, for example, 2.7×10^{-3} (at 82 °C), 1.5×10^{-3} (at 56 °C) and 0.6×10^{-3} (at 32 °C). The polymerization conditions control the formation of structural defects to a great extent. A decrease in the reaction temperature (decrease in $C_{M,HH}$ and in $C_{M,aux}$), along with the use of the VC in excess (decrease $C_{M,aux}$), can produce a significant decrease in $C_{M,total}$.^{194,235,251}



Scheme 1.11. Auxiliary mechanism for chain transfer to the monomer during VC polymerization, where P^\bullet is the head-to-tail macroradical.^{194,227,235,249,251}

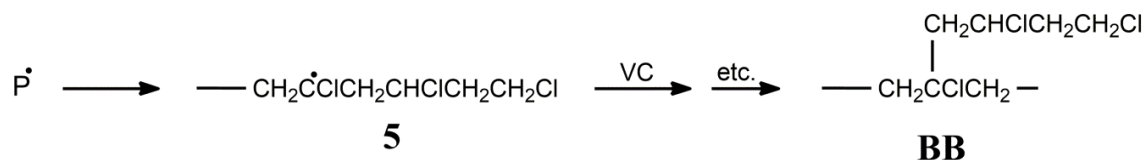
As previously indicated, in addition to the allylic chloride structures, the tertiary chloro-based structural defects are also responsible for the dehydrochlorination process and

consequently, for the low thermal stability of PVC. The existence of tertiary chloro structures in PVC was identified many years ago.^{194,245} There are two categories of these structures, long-branch points (**LB**) and 2,4-dichloro-*n*-butyl-branch points (**BB**). The first appears at low concentration in commercial products and results from the occurrence of chain transfer to the polymer, via the mechanism depicted in Scheme 1.12.^{194,227,244}



Scheme 1.12. Mechanisms involved in the formation of long-branch points.^{194,227,244}

BB structures are formed when the backbiting in P^\bullet occurs in a 1,5 process (*i.e.*, from the carbon atom that is fifth from the end of the growing chain), giving radical **5** and the subsequent addition of VC to this radical (Scheme 1.13).^{194,244,249} For polymerization temperatures ranging from 42 to 82 °C, as in a normal suspension process, it has been found that the **BB** frequency in occurrence ranges between 1.0 and 2.4 per thousand monomer units.^{194,244}



Scheme 1.13. Mechanisms involved in the formation of 2,4-dichloro-*n*-butyl-branches.^{194,227,244}

The occurrence of reactions that lead to the formation of tertiary chloride structures is almost insignificant for temperatures that are below 42 °C.^{227,244} In addition, the “concentration” of these structures becomes much more relevant after reaching the critical conversion.^{194,252}

Compounding Formulations

Synthesized PVC is a colorless rigid material with very limited thermal stability and with the propensity to adhere to metallic surfaces when heated.²¹⁷ This PVC can be converted

into a softer material by compounding it with plasticizers, particularly phthalate esters such as di-(2-ethylhexyl) phthalate (DEHP).¹⁹⁹ Thus, to tailor the properties of PVC, it is necessary to add other compounds, which provide a basis for increasing the range of properties of the final product.^{253,254} A typical PVC formulation contains the following materials: PVC, heat stabilizers, plasticizers, lubricants, fillers, pigments, polymer impact modifiers and processing aids.²⁵⁵

There are different grades of PVC and these have different properties. The high molecular weight PVC (Fikentscher *K* value > 70) is recommended for the manufacture of various flexible products achieved by extrusion, injection molding and calendaring, where good mechanical properties, as well as high flexibility, are required.^{2,217,222} The lower molecular weight product (*K* value < 60) is recommended for the manufacture of rigid products such as injection molded articles, calendared and extruded sheeting and blow-molded products.^{2,217,222}

Heat stabilizers are responsible for the increase in the thermal stability of PVC, achieved by retarding or eliminating the degradation routes during processing.²¹⁶ These compounds are intended to neutralize the resulting hydrogen chloride and avoid further degradation. Typically, they are complex compound mixtures based on the sulfates of lead, zinc, calcium, barium and cadmium.²⁵⁶ In the selection of the stabilizers, one should consider several factors, such as the PVC grade used, synergistic effects with other compounds that are included in the formulation, the cost of the stabilizer(s) *versus* the final value of the product, the optical properties of the final material and aspects related to toxicity, environmental impact and any effects on lubrication and printing.^{203,225}

The plasticizer compounds have a solubility parameter that is similar to that of PVC. These, when added to the PVC formulation, cause an increase in its flexibility and workability. This effect is brought about by an increase in the free volume and, as a consequence, a decrease in the glass transition temperature (T_g).^{217,257,258} The most widely used PVC plasticizers are phthalate esters, particularly DEHP (50% of worldwide phthalate production), which usually represents up to 40–50% of the total weight.¹⁹⁹ Although DEHP is recognized as the most suitable additive for the plasticization and processability of PVC, several studies have detailed its high toxicity.²⁰⁶ This feature is

also shared by other plasticizers. The migration of plasticizers from the PVC matrix is one of the more serious problems that are encountered in packaging technology, especially for products such as in food and pharmaceuticals applications. This migration occurs because the plasticizers are not chemically bound to PVC and, thus, with time, can be released into the surrounding environment.^{199,206,209} Several alternatives have been considered such as the chemical or the physical treatment of flexible PVC to reduce this plasticizer migration,¹⁹⁹ although none of proposed solutions showed the desired success. However, RDRP methods have opened the possibility of preparing flexible materials based on PVC without using currently available plasticizers.^{213,223,259}

Additives that are selected to prevent the sticking of PVC to processing equipment are termed lubricants. These can be external species if they avoid the adhesion of the PVC polymer to the metal surfaces of the equipment by forming a barrier between the PVC polymer and the metal surfaces, or internal if they are intended to improve the flow of the melt. Such action requires that there is reasonable compatibility between the metal surface and the PVC product.^{203,216,254,258}

Fillers, including pigments are compounds that are used to decrease the cost of the final product by the direct substitution of polymer and/or to provide coloration of the resultant product. Fillers are typically mineral in their nature (*e.g.*, calcium carbonate) and can lead to significant changes in the mechanical properties of the product.^{217,225} Pigments are chosen on the basis of their compatibility with the polymer matrix and their stability, during processing and in service.

Polymer impact modifiers and processing aids are used to improve the mechanical properties and the finish properties of the final product. The latter are mainly used in rigid PVC applications, because of the high melt viscosity of the formulation which leads to significant difficulties during processing. The more commonly used examples include ethylene-vinyl acetate (EVA) and acrylonitrile-butadiene-styrene (ABS) families of copolymers.^{203,225}

There has been much effort towards overcoming the major problems of the FRP of VC. Such problems include the inability to control the macromolecular structures and the thermal stability of PVC. Generally, these have failed. The assumption, after decades of

research, that FRP mechanisms always have termination reactions led to the quest for methods that would allow one to control the polymer structure at a molecular level as well as control the architecture, topology, composition and molecular weight, using feasible reaction conditions. As discussed in the Section 1.2 (RDRP), the solution to this issue was the development of a system that was based on a radical mechanism that could reproduce the living concept of exchange between dormant radicals and active radicals, thus limiting the concentration of active radicals.

1.4. RDRP Methods for VC Polymerization

Controlling the radical polymerization of VC has been a long-term challenge because of the great reactivity of the propagating radical and the great extent of chain transfer to the monomer.¹⁸⁵⁻¹⁸⁷ Also, the RDRP of VC was considered to be unfeasible due to the considerably stability of the possible 1,1-dichloro alkane dormant species.^{132,260} Different attempts to produce PVC using the metallocene-mediated polymerization of VC had no success.²⁶¹⁻²⁶³ Important advances in the development of RDRP techniques have provided a basis for overcoming this problem. As shown in Figure 1.6, the first RDRP technique applied to VC that was presented to the polymer research community was the Single-Electron Transfer Degenerative Chain Transfer Living Radical Polymerization (SET-DTLRP), which was essentially developed between the years 2001 and 2006 by Percec and co-workers.^{187,213-215,264-275} This has been the most studied method, giving the largest number of articles published on the RDRP of VC. Also, Braun and co-workers published their work on the NMP of VC in 2003.²⁷⁶ At that time, considering the lower potential of the SFRP/NMP proposed when compared to SET-DTLRP, this method was only poorly developed, resulting in only two publications for VC polymerization.^{276,277} In 2006, Percec and co-workers were able to side-step the iodine DT process of the SET-DTLRP and develop Single-Electron Transfer Living Radical Polymerization (SET-LRP) that was successfully applied to the controlled polymerization of VC.^{161,278,279} Detrembleur and co-workers presented the cobalt-mediated radical polymerization (CMRP) of VC in 2012.^{107,108} During the course of this PhD project and with my collaboration, the SARA ATRP of VC using sulfolane,²⁸⁰ sulfone/water mixtures,²⁸¹ CPME/DMSO mixtures²⁸²

and sulfolane/1-butyl-3-methylimidazolium hexafluorophosphate (BMIM-PF₆) (75/25 (v/v))²⁸³ as solvents have been proposed.

In the scope of this thesis project, the first RAFT polymerization of VC was proposed (**Chapter 5**).²⁸⁴ The results have been extremely promising with respect to the development of this technique to VC polymerization. For this reason, it was proposed the use of cyclopentyl methyl ether (CPME) as a green solvent for RAFT (co)polymerization of VC (**Chapter 7**).²⁸⁵ In **Chapter 6**, a new NMP of VC using the SG1-based BlocBuilder alkoxyamine at low temperature was proposed.²⁸⁶ Such as in RAFT, CPME was also used as a green solvent for the NMP of VC (**Chapter 7**).²⁸⁵

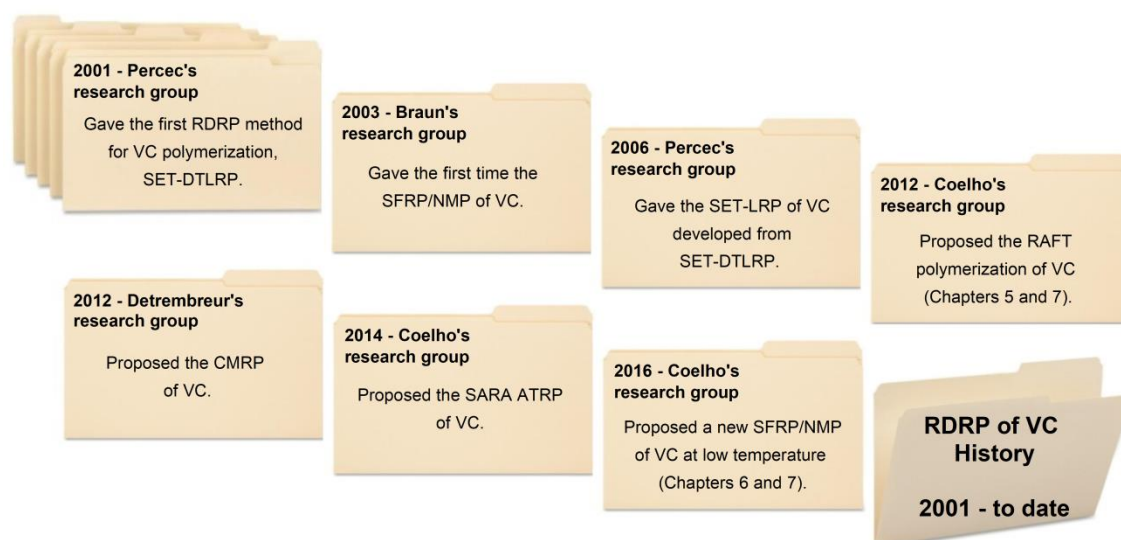


Figure 1.6. Milestones in RDRP methods for VC polymerization.

In the following sections, details of the RDRP techniques (SET-DTLRP, the first SFRP/NMP, Metal-catalyzed RDRP: SET-LRP and SARA ATRP, and CMRP) are presented that have been applied to VC polymerization, except the RDRP techniques that were developed under the slope of this thesis (RAFT – **Chapter 5** and **7**, and the new NMP – **Chapter 6** and **7**).

1.4.1. Early RDRP Techniques for VC Polymerization

Problems associated with the handling of VC and the predicted difficulties in the RDRP of VC may explain why relatively few research groups have studied its polymerization through RDRP methods.¹⁷² Following several developments, reported between 1995 and 2001 by Percec and co-workers²⁸⁷⁻²⁹⁶, based on the RDRP principles, the first publication that was entirely devoted to the RDRP of VC was published in 2001.¹⁸⁷

Following the path defined previously, the RDRP of VC was initially carried out using a metal-catalyzed, LRP approach. A large variety of catalysts, initiators, ligands, additives, solvents, temperatures and reaction times conditions was used. The most promising systems were based on iodine-containing initiators and copper in the zero oxidation state I-CH₂-Ph-CH₂-I/Cu(0)/bpy, in *o*-dichlorobenzene, at 130 °C. However, low conversions (< 40%) were achieved.¹⁸⁷ A plausible mechanism was invoked to explain the chain transfer reactions that occurred in the presence of the metal catalyst. The low conversion obtained for this system was most probably related to the high temperature that was used which, at the beginning of the reaction, would contribute to the cleavage of C-I bonds by a thermolysis mechanism, leading only to VC dimerizations.^{172,187,266}

In 2002, a short communication²⁶⁶ was published, showing a remarkable progression towards the possibility of establishing a RDRP route to VC. According to the authors, the major breakthroughs that were reported were the clear definition of the role of the Cu(0) in the metal catalyzed RDRP, the presentation of the iodine DT process simultaneously with a SET mechanism and the use of aqueous media and low polymerization temperatures. Such conditions are critical to the further implementation of this strategy on an industrial scale. This polymerization system was able to reach conversions that were above 80% at 25 °C, after 24 hours. Further work was published as an extension of the previous communication.²⁶⁵ This showed the possibility of preparing PVC that was free from structural defects and had a controlled molecular weight, and a relatively narrow dispersity ($\bar{D} \sim 1.5$). There was also evidence for the presence of active chain ends ($\sim\text{CHClI}$) and greater syndiotacticity. A mechanism based on competitive activation by a SET that was mediated by Cu(0) and iodine DT process was provided.²⁶⁵

1.4.2. SET-DTLRP of VC

The possibility of carrying out the Cu(0) metal catalyzed LRP of VC in aqueous media, at room temperature makes this polymerization route more environmentally attractive than those conducted in organic media.^{265,266} The replacement of Cu(0) by a non-transition metal catalyst, such as Na₂S₂O₄, turns the process even more environmentally appealing, eliminating the existence of any metallic impurities in the polymer obtained.¹⁷²

The replacement of Cu(0) by non-transition metal catalysts was firstly achieved by Percec and co-workers in 2004.²⁶⁴ This success was based on previous works on the metal catalyzed LRP of VC.^{265,266} This approach was coined, for the first time, SET-DTLRP.²⁶⁴ This process is mediated mainly by a combination of a competitive SET mechanism and a DT mechanism. The iodine dormant chains ends, (CHI₃, ~CHI₂ and ~CHClI) could be activated via a SET mediated process, or via DT mediated by growing radicals.

This polymerization (Scheme 1.14) is initiated with iodoform (CHI₃) and catalyzed by sodium dithionite (Na₂S₂O₄), in the presence of a buffer (NaHCO₃). Using CHI₃, the polymerization results in a propagating radical that grows in two directions and produces a polymer having two active chloriodomethyl chain ends. In water, the S₂O₄²⁻ ion dissociates into SO₂^{•-} that mediates the initiation and reactivation steps, via a SET mechanism. The exchange between dormant species and active propagating species also includes the exchange of DT to dormant species. Additionally, the SO₂ released from SO₂^{•-} during the SET process can add reversibly to PVC radicals and can provide additional transient dormant ~SO₂[•] radicals.²⁶⁴

This method, performed at temperatures from 25 to 35 °C, produced a telechelic PVC product with a predictable molecular weight evolution, ($M_{n,SEC} = 2000-55000$) and narrower dispersity than that obtained from FRP methods (\mathcal{D} in the range 1.6 - 1.9), containing two active ~CH₂-CHClI chain ends. The living nature of this PVC was demonstrated by a reinitiation experiment. The telechelic PVC, which was obtained by SET-DTLRP, was free of structural defects and presented greater thermal stability and syndiotacticity²⁶⁵ than the PVC produced under similar conditions by a FRP process. Moreover, it was determined that the highest temperature at which it was possible to

industrially available reactors and suspension agents, making this process very attractive from the technological point of view.²⁶⁴

Attempts to accelerate the SET-DTLRP of VC with the aid of various electron transfer cocatalysts (ETC) such as 1,1'-dialkyl-4,4'-bipyridinium dihalides or alkyl viologens (such as, methyl viologen (MV^{2+}) and octyl viologen (OV^{2+})),^{267,271} or using a phase-transfer catalyst (PTC) (such as cetyltrimethylammonium bromide [$nC_{16}H_{33}(CH_3)_3N^+Br^-$, CetMe₃NBr] or tetrabutylammonium iodide [$(nC_4H_9)_4N^+I^-$, Bu₄NI]),²⁷¹ and the use of thiourea dioxide [$(NH_2)_2C=SO_2$] as catalyst, have been reported.

The SET-DTLRP of VC that was initiated with CHI_3 results in a telechelic PVC, having similar chain ends $[I(CICHCH_2)_mCHI(CH_2CHCl)_nI]$. CHI_3 behaves as a bifunctional initiator and allows the synthesis of PVC macroinitiators for use in further ABA block copolymerizations. However, with methylene iodide (CH_2I_2), as a monofunctional initiator, one obtains a unique telechelic PVC with asymmetric functional chain ends $[ICH_2(CH_2CHCl)_{n-1}CH_2CHClI]$ that may be used for the synthesis of PVC macroinitiators for AB block copolymerization.²⁷⁰ It is noteworthy that these asymmetric functional chain ends have dissimilar reactivities and can therefore be independently functionalized using different chemistries. Bifunctional initiators, such as bis(2-iodopropionyloxy)ethane (BIPE), 2,5-diiodohexanedioate (DMDIH), and bis(2-methoxyethyl) 2,5-diiodohexanedioate (BMEDIH) have been used to create α,ω -di(iodo)PVC having two identical chain ends. Also the tetrafunctional initiator, pentaerythritol tetrakis(2-iodopropionate) (4IPr), has been used to yield the first four-arm star PVC that contains four identical active chain ends (Figure 1.7).²⁹⁹ The same initiator was further used to yield a four-armed-star poly(butyl acrylate) (PBA) macroinitiator and consequently a four-armed-star block-copolymer $[PVC-b-PBA-CH(CH_3)-CO-O-CH_2]_4C$.³⁰⁰ Other studies have been carried out such as the functionalization of the active chain ended α,ω -di(iodo)PVC, obtained by SET-DTLRP with 2-allyloxyethanol ($CH_2=CHCH_2OCH_2CH_2OH$).²⁷² The resulting product was the first example of a telechelic α,ω -di(hydroxy)PVC.

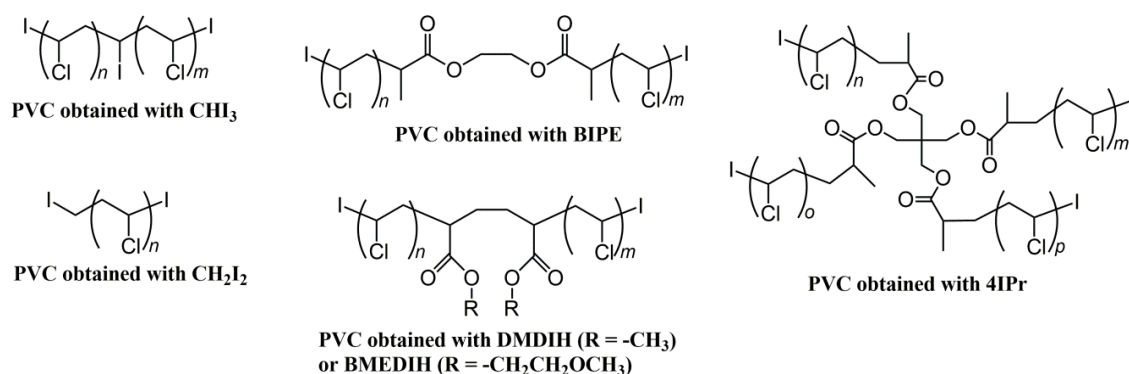


Figure 1.7. Diversity of PVC structures obtained by SET-DTLRP.^{264,270,299}

PVC-based block copolymers

The more important market avenues for PVC are based on flexible applications.³⁰¹ Nowadays, to achieve a material that is suitable for such applications, the PVC needs to be mixed with external plasticizers.²¹⁷ However, this strategy brought significant problems for the PVC industry in recent past relate to the use of plasticizers and their unavoidable migration.²⁰⁶ Because of this, the European Union has introduced restrictions in the use of plasticizers in applications such as packaging, children's toys, and medical devices.²⁰⁸ The potential contamination of the environment and the deterioration of mechanical properties²⁰⁹ are two of the major problems to be considered. To overcome such problems, the use of low-migration polymeric plasticizers^{199,302} has been proposed as well as blending with other polymers.³⁰¹ However, both solutions gave far from satisfactory results. It is well known that poly(alkyl acrylates) are very useful in the polymer-based industries because, by varying the alkyl substituent group, one can develop a wide range of mechanical properties and thermal properties.^{281,303,304} For instance, poly(*n*-butyl acrylate) (PBA), with its low glass transition temperature and extensive durability, has an enormous range of applications, as in adhesives, coatings, textiles, providing soft polymeric segments leading to thermoplastic elastomers.^{213,305}

Based on this context, the use of SET-DTLRP mediated by $\text{Na}_2\text{S}_2\text{O}_4/\text{NaHCO}_3$ initiated with CHI_3 in water, has been applied to the polymerization of a variety of acrylate monomers such as ethyl acrylate (EA),³⁰⁶ *n*-butyl acrylate (BA),^{303,305} *i*-butyl acrylate (*i*BA),³⁰³ *t*-butyl acrylate (*t*BA),^{303,307} lauryl acrylate (LA),³⁰⁸ 2-ethylhexyl acrylate

(2EHA),³⁰⁷ 2-methoxy ethyl acrylate (MEA),³⁰⁹ hydroxypropyl acrylate (HPA)^{210,211,310,311} and isobornyl acrylate (IA).²¹² These polyacrylate macroinitiators were further used for the synthesis of block copolymers based on acrylates and PVC, with RDRP features. These block copolymers provide a basis for tuning the properties of PVC, leading to PVC-based materials having different morphologies, with enhanced resistance to different chemical environments and with tailor-made mechanical properties.²¹⁴

PVC-*b*-PBA-*b*-PVC^{213,223,259} and PVC-*b*-P2EHA-*b*-PVC²¹⁴ block copolymers were presented as the first block copolymers that were based on combinations of thermoplastic PVC and elastomeric polyacrylates. These ABA block copolymers present glass transition temperatures (T_g) that range between the original value for the PVC homopolymer ($T_{g,PVC} \sim 85$ °C) and for polyacrylates ($T_{g,P2EHA} \sim -65$ °C and $T_{g,PBA} \sim -43$ °C), being relatively close to the theoretical value calculated from the Fox equation [$1/T_g = W_1/T_1 + W_2/T_2$].^{213,214} The influence of the composition of PVC-*b*-PBA-*b*-PVC block copolymers on the thermal properties and the mechanical performance of final products was studied.²²³ As shown in Figure 1.8, it is possible to prepare materials with mechanical properties that go from being rigid and hard materials to elastomers. A comparison of the mechanical performance of these flexible block copolymers, prepared by SET-DTLRP, with that of the commercial flexible PVC, prepared with dioctyl phthalate (DOP) (Figure 1.8) has been reported.²⁵⁹ This technology represents an important industrial advance, leading to the preparation of flexible compounds that are based on PVC that is free of conventional plasticizers.

In 2009, our research group reported the first synthesis of an amphiphilic PVC-based block copolymer, namely PVC-*b*-poly(hydroxypropyl acrylate) (PHPA)-*b*-PVC, created via a RDRP process.²¹⁰ The synthesis of this block copolymer was carried out in a 6.5L pilot reactor, using the SET-DTRLRP method.²⁵⁹ The synthesis of PVC-*b*-PHPA-*b*-PVC was included as part of a study that was aimed at creating new PVC molecular structures, on the basis of the SET-DTLRP mechanism, to be used as coupling agents in PVC-wood flour composites.^{210,311}

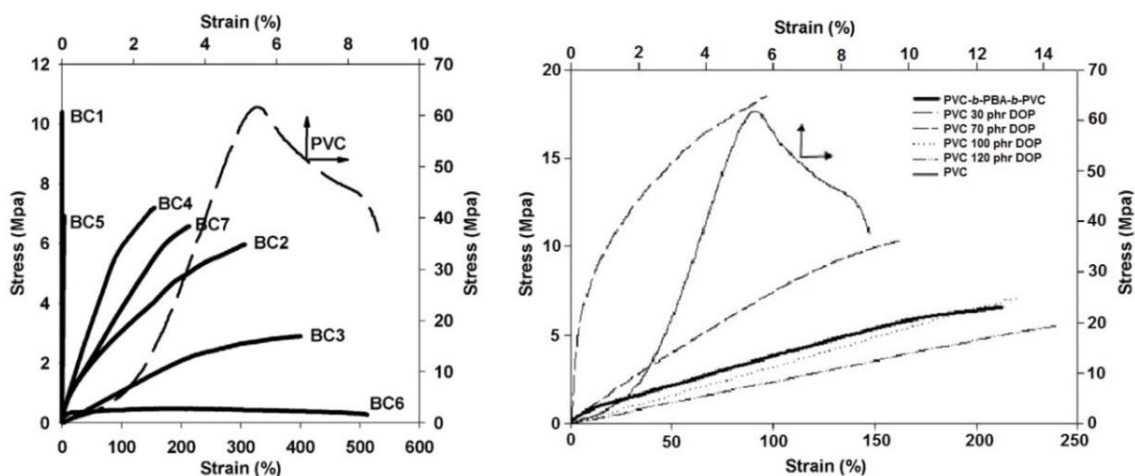


Figure 1.8. Stress-strain curves of PVC-*b*-PBA-*b*-PVC block copolymers with different compositions (left), and a PVC-*b*-PBA-*b*-PVC block copolymer and some flexible PVC made with DOP.^{223,259}

Before the development of SET-DTLRP, conventional FRP was only able to produce PVC having a maximum M_n value of about 113000. SET-DTLRP that is mediated by $\text{Na}_2\text{S}_2\text{O}_4/\text{NaHCO}_3$ allows one to prepare ultrahigh molecular weight PVC products ($M_{n,\text{SEC}} \sim 200000$; $D \sim 1.70$).²⁶⁸ The PVC obtained by SET-DTLRP has a T_g (~ 93 °C) that is greater than that of commercial PVC. Additionally the product is free from structural defects. An even greater T_g value (~ 100 - 133 °C) has been obtained with PVC-*b*-poly(isobornyl acrylate) (PIA)-*b*-PVC block copolymers.²¹² PIA is an amorphous polymer with excellent optical transparency, giving stability on aging, due to its insensitivity to normal UV radiation induced degradation.

All of the PVC-based copolymers that have been described so far are a type of “ABA” block copolymer, with PVC as the A block, since they have been obtained from α,ω -di(iodo)polyacrylate macroinitiators. The use of CuCl/bpy-catalyzed SET-DTLRP provided the first general approach to the synthesis of ABA block copolymers with PVC as the B block (Figure 1.9).²⁷⁵ Cu(0)/TREN catalyzed SET-DTLRP provided the α,ω -di(iodo)PVC macroinitiators²⁶⁴ that were subsequently used in the CuCl/bpy-catalyzed polymerization of MMA in diphenyl ether (Ph_2O), at 90 °C. This approach yielded PMMA-*b*-PVC-*b*-PMMA block copolymers (Figure 1.9) with $M_{n,\text{SEC}}$ up to 95000 having excellent control of the molecular weight distribution ($D \sim 1.21$). Other catalytic systems

were tested, yielding the same block copolymers. Catalyst systems such as $\text{CuCl}/\text{Me}_6\text{TREN}$, in dimethyl sulfoxide (DMSO) at $90\text{ }^\circ\text{C}$,²⁷⁴ and $\text{Cu}(0)/\text{Me}_6\text{TREN}$ in DMSO at $25\text{ }^\circ\text{C}$ have been used.²⁷³ In addition, a variety of conditions have been developed. These include catalysts [CuCl , CuI , Cu_2O , and $\text{Cu}(0)$], ligands [bipyridine, Me_6TREN , poly(ethyleneimine) (PEI) and hexamethyl triethylenetetramine (HMTETA)], initiators [CH_3CHClI , CH_2I_2 , CHI_3 , and $\text{F}(\text{CF}_2)_8\text{I}$], solvents [diphenyl ether, toluene, tetrahydrofuran (THF), DMSO, dimethylformamide (DMF), ethylene carbonate, dimethylacetamide (DMAC) and cyclohexanone], and temperatures from 0 to $90\text{ }^\circ\text{C}$. These were used in studies of the synthesis of $\text{PMMA-}b\text{-PVC-}b\text{-PMMA}$ block copolymers.³¹² The synthesis of the block copolymer $\text{PMA-}b\text{-PVC-}b\text{-PMA}$, catalyzed by $\text{Cu}(0)/\text{Me}_6\text{TREN}$, in DMSO, at $25\text{ }^\circ\text{C}$ has also been reported.²¹⁵

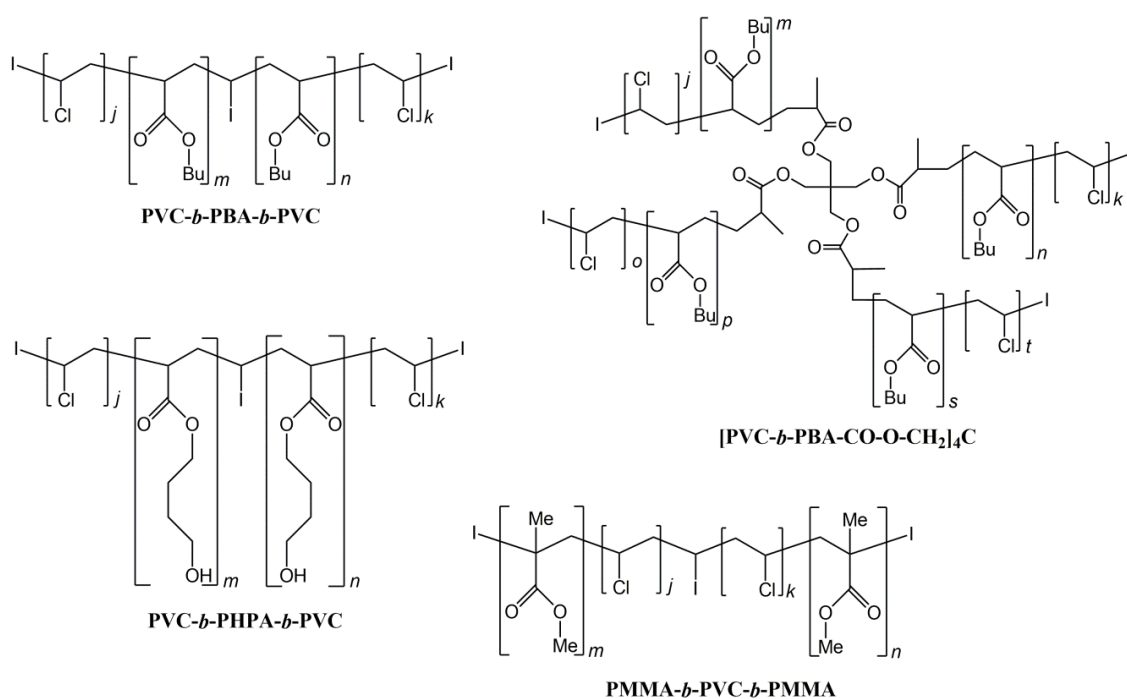


Figure 1.9. Diversity of PVC-based block copolymer structures obtained by SET-DTLRP.^{210,213,275,300}

1.4.3. SFRP/NMP of VC

As mentioned previously, Braun and co-workers investigated the first NMP of VC.^{276,277} The synthesis of PVC that was obtained by TEMPO-mediated SFRP and some of its derivatives was carried out at temperatures that were greater than 70 °C.²⁷⁶ No kinetic data were reported that could support the RDRP of VC by SFRP/NMP. The resulting PVC had a $D > 2.0$ and no improvements in the thermal stability were reported, relative to that of the commercial FRP product.^{276,277} These results are typical of those obtained when very high temperatures are used (the maximum temperature for the RDRP of VC is about 42 °C).²⁶⁴ The authors were able to use the PVC as a macroinitiator for the block copolymerization of activated monomers at temperatures that were greater than 100 °C. The synthesis of a PVC/PS copolymer and that of a flexible copolymer PVC/Poly(butadiene) with T_g values of approximately 22 °C were the most significant result.^{276,277}

Considering the high temperatures that were required for the cleavage of the terminal C-nitroxide bond in the SFRP/NMP route^{31,39} and that the maximum temperature for the polymerization of VC under RDRP conditions is about 42 °C,²⁶⁴ the living nature of PVC materials that were obtained by SFRP/NMP would have been very difficult to prove. Also, the relatively high polymerization temperatures may lead to the degradation of PVC segments via dehydrochlorination reactions.

Over the years, the development of the SFRP/NMP has provided a basis for a decrease in the required high polymerization temperature.^{39,43,313} Thus, in the scope of this work, a new NMP of VC using the SG1-based BlocBuilder alkoxyamine at low temperature ranging from 30 to 42 °C was proposed (**Chapter 6**).²⁸⁶ The results have been extremely promising with respect to the development of this technique to VC polymerization. For this reason, the use of cyclopentyl methyl ether (CPME) was also studied as a green solvent for NMP of VC (**Chapter 7**).²⁸⁵

[CHBr₃]₀/[TREN]₀ ratio and of the amount of DMSO used in the reaction.²⁷⁹ The ratio of [CHBr₃]₀/[TREN]₀ determines the ratio of [TREN]₀ to mass of Cu(0) powder or the surface area of Cu(0) wire. The more efficient conditions for the Cu(0) wire-catalyzed SET-LRP of VC were determined, providing a method that could ease the removal of the catalyst from the PVC-based product and its recycling, and the acquisition of a white PVC that does not require any further purification. In addition, in each use of the Cu(0) wire catalyst, only ~ 4 mg were consumed, indicating that the catalyst can be reused many times without significant changes to the mass or surface area of the catalyst.²⁷⁹ These findings make this mechanism very promising if one intends to implement production on an industrial scale, although there are some obstacles to be overcome. These include the need to use DMSO (high boiling point) as a solvent and the use of expensive compounds as ligands.

Considering the potential that has been already demonstrated by proposed SET-LRP¹⁷² and the lack of extensive research into the use of the technique for VC polymerization (with only three publications so far),^{161,278,279} there is still some room for optimization of the reaction conditions, to achieve a better control over the polymerization reaction, that will inevitably lead to lower dispersity values. Moreover, as exploited for the SET-DTLRP mechanism, the synthesis of more complex structures that are based on the telechelic PVC obtained, such as block copolymers with linear and star topologies, still remains an unexplored area of research.

Until recently (2012), the only RDRP techniques that have been applied to VC polymerization were SET-DTLRP,^{188,210-215,221-223,259,264-266,268,269,271,272,275,298,321} NMP^{276,277} and SET-LRP.^{161,278,279} Since their development, several studies involving homopolymerization, copolymerization, functionalization and scaling-up have been reported. Despite these advances, there is a need to adapt other RDRP techniques to the polymerization of VC and other monomers as a route to broadening the scope of monomers that are compatible with block copolymer synthesis.

1.4.5. SARA ATRP of VC

During the course of this PhD work and with my collaboration, the use of sulfolane as an efficient solvent for the SARA ATRP of acrylates, methacrylates, styrene and VC has been proposed, being applied ppm amounts of soluble copper catalyst.²⁸⁰ Besides giving control over the homopolymerization of several families of the monomers mentioned, as proof-of-concept, block copolymers of PS-*b*-PVC-*b*-PS (Figure 1.10(a)) with controlled structure were prepared for the first time using a RDRP technique. Also, block copolymers of the type PMA-*b*-PVC-*b*-PMA, Figure 1.10(b), were created using a straightforward method that involved venting off the VC from the reactor (a gas at room temperature) after the synthesis of α,ω -di(bromo)PVC and the addition of MA. The effective results were achieved because of the dipolar aprotic solvent that was used.²⁸⁰

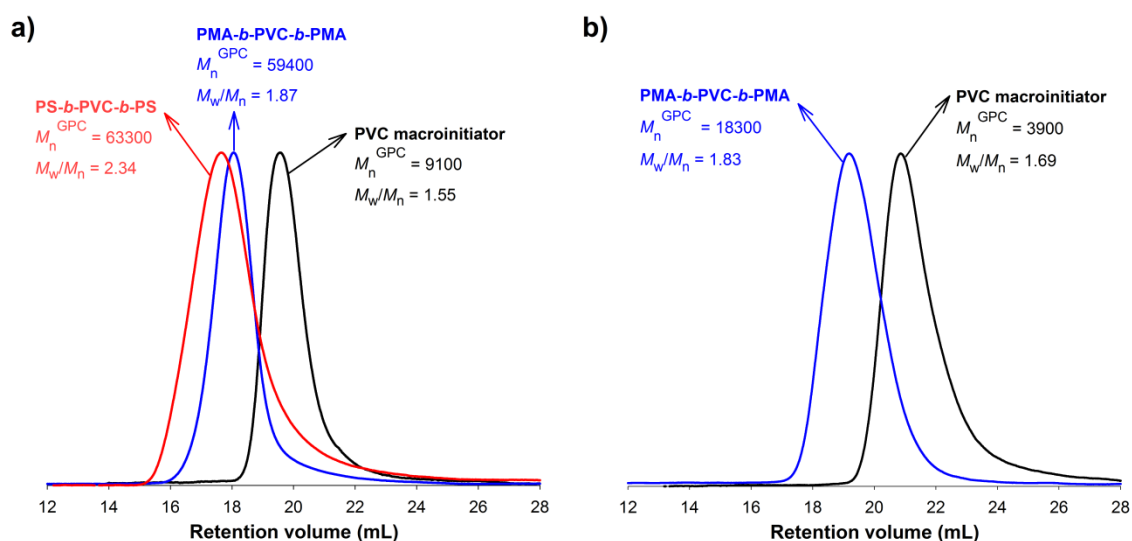


Figure 1.10. GPC traces of the (a) PVC-Br macroinitiator (black line), and the PMA-*b*-PVC-*b*-PMA (blue line) and PS-*b*-PVC-*b*-PS block copolymers (red line); (b) PVC-Br macroinitiator (right curve), and the PMA-*b*-PVC-*b*-PMA block copolymer (left curve) prepared by “one-pot” SARA ATRP chain extension.²⁸⁰

Using sulfolane/water (90/10 (v/v)) mixtures faster (co)polymerizations of VC were obtained.²⁸¹ The polymerization conditions used can be considered very attractive for a future industrial implementation of the technique. In the same vein, solvent mixtures of CPME/DMSO (70/30 (v/v))²⁸² and sulfolane/1-butyl-3-methylimidazolium hexafluorophosphate (BMIM-PF₆) (75/25 (v/v))²⁸³ were successfully used for the SARA

ATRP of VC catalyzed by Cu(0)/CuBr₂ at 42 °C. The use of synthesized α,ω -di(bromo)PVC macroinitiators, with their low \bar{D} (1.57), allowed the preparation of PMA-*b*-PVC-*b*-PMA block copolymers.²⁸¹⁻²⁸³

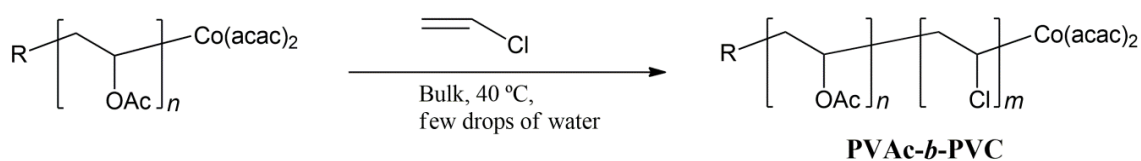
1.4.6. CMRP of VC

In the CMRP system, the deactivating species, which allow the creation of a dynamic equilibrium between the small amounts of propagating radicals and the dormant species, is a cobalt complex.^{32,47,85,322} This system belongs to the OMRP.³²

Detrembleur and co-workers have reported the CMRP of VC in the presence of bis(acetylacetonato)cobalt(II) (Co(acac)₂) as a controlling agent.^{107,108} In the first work,¹⁰⁷ an alkyl-Co(III) compound was used (synthesized from conventional initiator V-70 and Co(acac)₂), or a simpler V-70/Co(acac)₂ binary system as initiators, in a bulk polymerization of VC and in the statistical copolymerization of VC-VAc. At 40 °C, the VC conversion was extremely low (< 10%). Co(acac)₂ appeared a better controlling agent for the PVAc radicals than for those of PVC.¹⁰⁷ The authors have found that Co(acac)₂ traps the PVAc radicals more efficiently than PVC radicals. This observation suggests that C-Co bond is stronger at the polymer chain end for PVAc than for PVC. The presented kinetic data were very limiting in support of the RDRP of VC. Moreover, ¹H-NMR analysis indicated that the level of structural defects of the PVC synthesized by CMRP was similar to that obtained for PVC prepared by FRP at the same temperature. The resulting PVC and PVC-*co*-PVAc showed \bar{D} values that were greater than 2.0.

The synthesis of PVAc-*b*-PVC block copolymers from a PVAc-Co(acac)₂ macroinitiator (Scheme 1.16) has been reported.¹⁰⁸ In this work, a controlled structured PVAc macroinitiator was obtained, ($\bar{D} = 1.16$). However, for its reinitiation in the presence of VC, the monomer conversions were again very low, high \bar{D} were obtained. The low conversions were assumed to result from the accumulation of Co(acac)₂, which shifts the equilibrium dormant/active species to the dormant ones. Interestingly, it was found that the addition of water consumes part of the excess of Co(acac)₂ that accumulates in the early stages of the polymerization, and increases the conversion. Another strategy to

increase conversion deals with consumption of the deactivation by the slow decomposition of a free radical initiator. The authors recognized that contamination of the copolymers by some homopolymer of PVC could be present.¹⁰⁸ In addition to the results provided by ¹H NMR analyses, the formation of block copolymer structures was supported by its self-assembly into PVAc-*b*-PVC core-shell micelles in methanol, as indicated by dynamic light scattering (DLS) measurements and atomic force microscopy (AFM) analyses.



Scheme 1.16. Synthesis of PVC-*b*-PVAc block copolymers from PVAc-Co(acac)₂ macroinitiator.¹⁰⁸

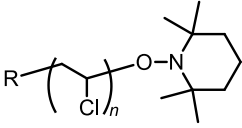
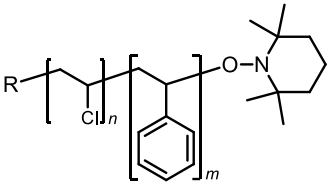
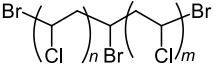
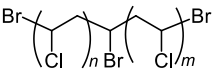
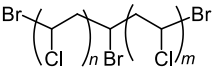
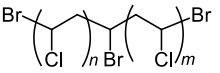
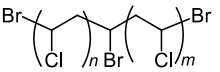
1.4.7. Summary of the RDRP Methods Studied for the VC Polymerization

Table 1.1 resumes the different RDRP methods that have been studied for VC polymerization, including the main reaction conditions, range of molecular weights, dispersity as well as structures synthesized.

Table 1.1. Resume of the RDRP methods developed for the VC (co)polymerization.

Method	Control agent/ Macroinitiator	Catalytic system	Solvent	Temp. (° C)	$M_n \times 10^{-3}$	\bar{D}	Polymer structure	References
SET-DTLRP	CHI ₃	Na ₂ S ₂ O ₄ / NaHCO ₃	Water (suspension)	25 - 42	2 - 115	1.6 - 1.9		221,222,224,264,267, 269,298,321
	CHI ₃	Cu(0)/TREN	Water (suspension)	25	2 - 15	1.5 - 2.0		265
	CHI ₃	CuCl/Me ₆ TREN	DMSO	90	2 - 15	1.5 - 2.0		273,274
	CH ₂ I ₂	Na ₂ S ₂ O ₄ / NaHCO ₃	Water (suspension)	25 - 35	2 - 25	1.5 - 2.0		270
	BIPE	Na ₂ S ₂ O ₄ / NaHCO ₃	Water (suspension)	25 - 35	2 - 65	1.6 - 1.7		299
	4IPr	Na ₂ S ₂ O ₄ / NaHCO ₃	Water (suspension)	25 - 35	4 - 15	1.7 - 2.0		299

I-PBA-I	$\text{Na}_2\text{S}_2\text{O}_4/\text{NaHCO}_3$	Water (suspension)	25 - 42	10 - 210	1.6 - 1.7		213,223,259,305
I-PHPA-I	$\text{Na}_2\text{S}_2\text{O}_4/\text{NaHCO}_3$	Water (suspension)	25 - 42	10 - 80	1.6 - 2.2		211,323,324
PBA-I ₄	$\text{Na}_2\text{S}_2\text{O}_4/\text{NaHCO}_3$	Water (suspension)	25 - 35	15 - 150	1.6 - 2.6		300
I-PVC-I	$\text{Cu}(0)/\text{Me}_6\text{TREN}$	DMSO	25	15 - 155	1.4 - 1.6		215,273

SFRP/NMP	TEMPO	Initiator/TEMPO	Water (suspension)	70 - 90	18 - 31	2.0 – 2.4		276,277
	PVC-TEMPO	Initiator/TEMPO	Water (suspension)	100	> 30	> 2.0		277
SET-LRP	CHBr ₃	Cu(0)/TREN	DMSO	25	5 - 40	1.4 - 1.7		161,279
	CHBr ₃	Cu(0)/Cu ^{II} Br ₂ /TREN	DMSO	25	3 - 60	1.4 - 1.7		278
SARA ATRP	CHBr ₃	Cu(0)/TREN	Sulfolane	30 - 42	3 - 20	1.4 - 1.6		280,281
	CHBr ₃	Cu(0)/Cu ^{II} Br ₂ /TREN	CPME/DMSO	42	3 - 20	1.5 - 1.6		282
	CHBr ₃	Cu(0)/TREN	Sulfolane/ BMIM-PF ₆	42	3 - 23	1.8 - 1.9		283

	Br-PVC-Br	Cu(0)/TREN	Sulfolane CPME/DMSO	30 - 42	6 - 60	1.5 - 1.7		280-282
	Br-PVC-Br	Cu(0)/TREN	Sulfolane	60	9 - 65	1.6 - 2.0		280
CMRP	Co(acac) ₂	V-70/Co(acac) ₂	(in bulk)	40 - 80	13 - 65	2.0 - 2.3		107
	PVAc-Co(acac) ₂	V-70/Co(acac) ₂	(in bulk)	40	20 - 70	1.9 - 2.4		108

1.5. References

1. Moad, G. and Solomon, D. H., *The chemistry of free radical polymerization*, **1995**, Oxford: Elsevier.
2. Saeki, Y. and Emura, T., *Technical progresses for PVC production*. Progress in Polymer Science, **2002**, 27, 2055-2131.
3. O'Driscoll, K. F., *Free Radical Polymerization Kinetics - Revisited*. Pure & Applied Chemistry, **1981**, 53, 617-626.
4. Ugelstad, J., Mork, P. C., and Hansen, F. K., *Kinetics and Mechanism of Vinyl Chloride Polymerization*. Pure & Applied Chemistry, **1981**, 53, 323-363.
5. Pinto, J. P. and Giudici, R., *Optimization of a cocktail of initiators for suspension polymerization of vinyl chloride in batch reactors*. Chemical Engineering Science, **2001**, 56, 1021-1028.
6. Kiparissides, C., Daskalakis, G., Achilias, D. S., and Sidiropoulou, E., *Dynamic Simulation of Industrial Poly(vinyl chloride) Batch Suspension Polymerization Reactors*. Industrial & Engineering Chemistry Research, **1997**, 36, 1253-1267.
7. Silva, D. C. M., *Controlo Predictivo Não-Linear de Processos Químicos - Aplicação a Sistemas de Polimerização Descontínuos*, **2006**, University of Coimbra: Coimbra.
8. Miura, N., Imaeda, M., Hashimoto, K., Wood, R. K., Hattori, H., and Onishi, M., *Auto-tuning PID controlled based on generalized minimum variance control for a PVC reactor*. Journal of Chemical Engineering of Japan, **1998**, 31, 626-632.
9. Kiparissides, C., *Polymerization Reactor Modeling: A Review of Recent Developments and Future Directions*. Chemical Engineering Science, **1996**, 51, 1637-1639.
10. Xie, T. Y., Hamielec, P. E., Wood, P. E., and Woods, D. R., *Experimental investigation of vinyl chloride polymerization at high conversion: mechanism, kinetics and modelling*. Polymer, **1991**, 32, 537-557.
11. Bao, Y. Z. and Brooks, B. W., *Particle Features of Poly(vinyl chloride) Resins Prepared by a New Heterogeneous Polymerization Process*. Journal of Applied Polymer Science, **2003**, 90, 954-958.
12. Smallwood, P. V., *The formation of grains of suspension poly(vinyl chloride)*. Polymer, **1986**, 27, 1609-1618.
13. Hamielec, A. E., Gomez-Vaillard, R., and Marten, F. L., *Diffusion-Controlled Free Radical Polymerization. Effect on Polymerization Rate and Molecular Properties of Polyvinyl Chloride*. Journal of Macromolecular Science - Chemistry, **1982**, A17, 1005-1020.

14. Yamada, B. and Zetterlund, P. B., *General Chemistry of Radical Polymerization*, in *Handbook of Radical Polymerization*, K. Matyjaszewski and T.P. Davis, Editors. **2002**, Wiley Blackwell: New Jersey. p. 117-186.
15. Matyjaszewski, K. and Tsarevsky, N. V., *Macromolecular Engineering by Atom Transfer Radical Polymerization*. *Journal of the American Chemical Society*, **2014**, *136*, 6513-6533.
16. Moad, G., Rizzardo, E., and Thang, S. H., *Toward Living Radical Polymerization*. *Accounts of Chemical Research*, **2008**, *41*, 1133-1142.
17. Matyjaszewski, K., *Controlled Radical Polymerization: State of the Art in 2008*, in *Controlled/Living Radical Polymerization: Progress in ATRP***2009**, American Chemical Society: Washington DC. p. 3-13.
18. Goto, A. and Fukuda, T., *Kinetics of living radical polymerization*. *Progress in Polymer Science*, **2004**, *29*, 329-385.
19. Szwarc, M., "Living" Polymers. *Nature*, **1956**, *178*, 1168.
20. Hsieh, H. L. and Quirk, R. P., *Anionic Polymerization: Principles and practical applications*, **1996**, New York: Marcel Dekker, Inc.
21. Matyjaszewski, K. and Davis, T. P., *General Concepts and History of Living Radical Polymerization*, in *Handbook of Radical Polymerization***2002**, Wiley Blackwell: New Jersey. p. 361-406.
22. Matyjaszewski, K., *Atom Transfer Radical Polymerization (ATRP): Current Status and Future Perspectives*. *Macromolecules*, **2012**, *45*, 4015-4039.
23. Matyjaszewski, K. and Sawamoto, M., *Controlled/Living carbocationic polymerization*, in *Cationic polymerizations mechanisms synthesis and applications*, K. Matyjaszewski, Editor **1996**, Marcel Dekker, Inc.: New York. p. 265-380.
24. Sawamoto, M., *Controlled polymer synthesis by cationic polymerization*, in *Cationic polymerizations mechanisms synthesis and applications*, K. Matyjaszewski, Editor **1996**, Marcel Dekker: New York. p. 381-436.
25. Schrock, R. R., *Living ring-opening metathesis polymerization catalyzed by well-characterized transition-metal alkylidene complexes* *Accounts of Chemical Research*, **1990**, *23*, 158-165.
26. Grubbs, R. H. and Tumas, W., *Polymer synthesis and organotransition metal chemistry*. *Science*, **1989**, *243*, 907-915.
27. Brunelle, D. J., ed. *Ring-opening polymerization: mechanisms, catalysis, structure, utility*. **1993**, Carl Hanser Verlag: Munich.
28. Bielawski, C. W. and Grubbs, R. H., *Living ring-opening metathesis polymerization*. *Progress in Polymer Science*, **2007**, *32*, 1-29.

29. Nakamura, A., Anselment, T. M. J., Claverie, J., Goodall, B., Jordan, R. F., Mecking, S., Rieger, B., Sen, A., van Leeuwen, P. W. N. M., and Nozaki, K., *Ortho-Phosphinobenzenesulfonate: A Superb Ligand for Palladium-Catalyzed Coordination–Insertion Copolymerization of Polar Vinyl Monomers*. *Accounts of Chemical Research*, **2013**, *46*, 1438-1449.
30. Nakamura, A., Ito, S., and Nozaki, K., *Coordination–Insertion Copolymerization of Fundamental Polar Monomers*. *Chemical Reviews*, **2009**, *109*, 5215-5244.
31. Sciannamea, V., Jerome, R., and Detrembleur, C., *In-Situ Nitroxide-Mediated Radical Polymerization (NMP) Processes: Their Understanding and Optimization*. *Chemical Reviews*, **2008**, *108*, 1104-1126.
32. Debuigne, A., Poli, R., Jérôme, C., Jérôme, R., and Detrembleur, C., *Overview of cobalt-mediated radical polymerization: Roots, state of the art and future prospects*. *Progress in Polymer Science*, **2009**, *34*, 211-239.
33. Moad, G., Rizzardo, E., and Thang, S. H., *Living Radical Polymerization by the RAFT Process – A Second Update*. *Australian Journal of Chemistry*, **2009**, *62*, 1402-1472.
34. Yamago, S., *Precision Polymer Synthesis by Degenerative Transfer Controlled/Living Radical Polymerization Using Organotellurium, Organostibine, and Organobismuthine Chain-Transfer Agents*. *Chemical Reviews*, **2009**, *109*, 5051-5068.
35. Moad, G., Rizzardo, E., and Thang, S. H., *Living Radical Polymerization by the RAFT Process – A Third Update*. *Australian Journal of Chemistry*, **2012**, *65*, 985-1076.
36. Nicolas, J., Guillaneuf, Y., Lefay, C., Bertin, D., Gimes, D., and Charleux, B., *Nitroxide-mediated polymerization*. *Progress in Polymer Science*, **2013**, *38*, 63-235.
37. Cunningham, M. F., *Controlled/living radical polymerization in aqueous dispersed systems*. *Progress in Polymer Science*, **2008**, *33*, 365-398.
38. Matyjaszewski, K., ed. *Controlled/living radical polymerization progress in ATRP, NMP and RAFT*. **2000**, American Chemical Society: Washington DC.
39. Destarac, M., *Controlled Radical Polymerization: Industrial Stakes, Obstacles and Achievements*. *Macromolecular Reaction Engineering*, **2010**, *4*, 165-179.
40. Qiu, J., Charleux, B., and Matyjaszewski, K., *Controlled/living radical polymerization in aqueous media: homogeneous and heterogeneous systems*. *Progress in Polymer Science*, **2001**, *26*, 2083-2134.
41. Braunecker, W. A. and Matyjaszewski, K., *Controlled/living radical polymerization: Features, developments, and perspectives*. *Progress in Polymer Science*, **2007**, *32*, 93-146.

42. Matyjaszewski, K. and Tsarevsky, N. V., *Nanostructured functional materials prepared by atom transfer radical polymerization*. *Nature Chemistry*, **2009**, *1*, 276-288.
43. Zetterlund, P. B., Kagawa, Y., and Okubo, M., *Controlled/Living Radical Polymerization in Dispersed Systems*. *Chemical Reviews*, **2008**, *108*, 3747-3794.
44. Ah Toy, A., Vana, P., Davis, T. P., and Barner-Kowollik, C., *Reversible Addition Fragmentation Chain Transfer (RAFT) Polymerization of Methyl Acrylate: Detailed Structural Investigation via Coupled Size Exclusion Chromatography–Electrospray Ionization Mass Spectrometry (SEC–ESI-MS)*. *Macromolecules*, **2004**, *37*, 744-751.
45. Barner-Kowollik, C., Davis, T. P., and Stenzel, M. H., *Probing mechanistic features of conventional, catalytic and living free radical polymerizations using soft ionization mass spectrometric techniques*. *Polymer*, **2004**, *45*, 7791-7805.
46. Abreu, C. M. R., Mendonça, P. V., Serra, A. C., Popov, A. V., Matyjaszewski, K., Guliashvili, T., and Coelho, J. F. J., *Inorganic Sulfites: Efficient Reducing Agents and Supplemental Activators for Atom Transfer Radical Polymerization*. *ACS Macro Letters*, **2012**, *1*, 1308-1311.
47. Allan, L. E. N., Perry, M. R., and Shaver, M. P., *Organometallic mediated radical polymerization*. *Progress in Polymer Science*, **2012**, *37*, 127-156.
48. Fischer, H., *Unusual selectivities of radical reactions by internal suppression of fast modes*. *Journal of the American Chemical Society*, **1986**, *108*, 3925-3927.
49. Pintauer, T. and Matyjaszewski, K., *Atom transfer radical addition and polymerization reactions catalyzed by ppm amounts of copper complexes*. *Chemical Society Reviews*, **2008**, *37*, 1087-1097.
50. David, G., Boyer, C., Tonnar, J., Ameduri, B., Lacroix-Desmazes, P., and Boutevin, B., *Use of Iodocompounds in Radical Polymerization*. *Chemical Reviews*, **2006**, *106*, 3936-3962.
51. Maria, S., Kaneyoshi, H., Matyjaszewski, K., and Poli, R., *Effect of Electron Donors on the Radical Polymerization of Vinyl Acetate Mediated by [Co(acac)₂]: Degenerative Transfer versus Reversible Homolytic Cleavage of an Organocobalt(III) Complex*. *Chemistry – A European Journal*, **2007**, *13*, 2480-2492.
52. Perrier, S. and Takolpuckdee, P., *Macromolecular design via reversible addition–fragmentation chain transfer (RAFT)/xanthates (MADIX) polymerization*. *Journal of Polymer Science Part A: Polymer Chemistry*, **2005**, *43*, 5347-5393.
53. Chiefari, J., Chong, Y. K., Ercole, F., Krstina, J., Jeffery, J., Le, T. P. T., Mayadunne, R. T. A., Meijs, G. F., Moad, C. L., Moas, G., Rizzardo, E., and Thang, S. H., *Living Free-Radical Polymerization by Reversible Addition-Fragmentation Chain Transfer: The RAFT Process*. *Macromolecules*, **1998**, *31*, 5559-5562.

54. Boyer, C., Bulmus, V., Davis, T. P., Ladmiral, V., Liu, J. Q., and Perrier, S., *Bioapplications of RAFT Polymerization*. Chemical Reviews, **2009**, *109*, 5402-5436.
55. Georges, M. K., Veregin, R. P. N., Kazmaier, P. M., and Hamer, G. K., *Narrow Molecular Weight Resins by a Free-Radical Polymerization Process*. Macromolecules, **1993**, *26*, 2987-2988.
56. Solomon, D. H., Rizzardo, E., and Cacioli, P., *Polymerization process and polymers produced thereby*. **1986**, US 4,581,429.
57. Hawker, C. J., *Molecular Weight Control by a "Living" Free-Radical Polymerization Process*. Journal of the American Chemical Society, **1994**, *116*, 11185-11186.
58. Hawker, C. J., Barclay, G. G., Orellana, A., Dao, J., and Devonport, W., *Initiating Systems for Nitroxide-Mediated "Living" Free Radical Polymerizations: Synthesis and Evaluation*. Macromolecules, **1996**, *29*, 5245-5254.
59. Ingold, K. U., Adamic, K., Bowman, D. F., and Gillan, T., *Kinetic applications of electron paramagnetic resonance spectroscopy. I. Self-reactions of diethyl nitroxide radicals*. Journal of the American Chemical Society, **1971**, *93*, 902-908.
60. Bowman, D. F., Gillan, T., and Ingold, K. U., *Kinetic applications of electron paramagnetic resonance spectroscopy. III. Self-reactions of dialkyl nitroxide radicals*. Journal of the American Chemical Society, **1971**, *93*, 6555-6561.
61. Bowman, D. F., Brokenshire, J. L., Gillan, T., and Ingold, K. U., *Kinetic applications of electron paramagnetic resonance spectroscopy. II. Self-reactions of N-alkyl nitroxides and N-phenyl nitroxide*. Journal of the American Chemical Society, **1971**, *93*, 6551-6555.
62. Dupeyre, R.-M. and Rassa, A., *Nitroxides. XIX. Norpseudopelletierine-N-oxyl, a New, Stable, Unhindered Free Radical*. Journal of the American Chemical Society, **1966**, *88*, 3180-3181.
63. Georges, M. K., Lukkarila, J. L., and Szkurhan, A. R., *TEMPO-Mediated n-Butyl Acrylate Polymerizations*. Macromolecules, **2004**, *37*, 1297-1303.
64. Guillaneuf, Y., Gimes, D., Marque, S. R. A., Astolfi, P., Greci, L., Tordo, P., and Bertin, D., *First Effective Nitroxide-Mediated Polymerization of Methyl Methacrylate*. Macromolecules, **2007**, *40*, 3108-3114.
65. Delaittre, G., Dire, C., Rieger, J., Putaux, J.-L., and Charleux, B., *Formation of polymer vesicles by simultaneous chain growth and self-assembly of amphiphilic block copolymers*. Chemical Communications, **2009**, 2887-2889.
66. Catala, J. M., Bubel, F., and Hammouch, S. O., *Living Radical Polymerization: Kinetic Results*. Macromolecules, **1995**, *28*, 8441-8443.

67. Butz, S., Hillermann, J., Schmidt-Naake, G., Kressler, J., Thomann, R., Heck, B., and Stühn, B., *Synthesis and microphase separation of diblock copolymers of styrene and p-chlorostyrene prepared by using N-oxyl capped macroinitiators*. *Acta Polymerica*, **1998**, *49*, 693-699.
68. Bultz, E. and Bender, T. P., *NMP of Chloromethylstyrene with Minimized PDI: The Role of the Initiator/Nitroxide System and the Meta Isomer*. *Macromolecules*, **2011**, *44*, 3666-3669.
69. Bohrisch, J., Wendler, U., and Jaeger, W., *Controlled radical polymerization of 4-vinylpyridine*. *Macromolecular Rapid Communications*, **1997**, *18*, 975-982.
70. Chalari, I., Pispas, S., and Hadjichristidis, N., *Controlled free-radical polymerization of 2-vinylpyridine in the presence of nitroxides*. *Journal of Polymer Science Part A: Polymer Chemistry*, **2001**, *39*, 2889-2895.
71. Ding, X. Z., Fischer, A., Yang, S., Wu, P., Brembilla, A., and Lochon, P., *Solvent effects on TEMPO-mediated radical polymerizations: behaviour of 3-vinylpyridine in a protic solvent*. *European Polymer Journal*, **2001**, *37*, 1561-1569.
72. Grassl, B., Clisson, G., Khoukh, A., and Billon, L., *Nitroxide-mediated radical polymerization of acrylamide in water solution*. *European Polymer Journal*, **2008**, *44*, 50-58.
73. Harth, E., Bosman, A., Benoit, D., Helms, B., Fréchet, J. M. J., and Hawker, C. J., *A practical approach to the living polymerization of functionalized monomers: application to block copolymers and 3-dimensional macromolecular architectures*. *Macromolecular Symposia*, **2001**, *174*, 85-92.
74. Keoshkerian, B., Georges, M., Quinlan, M., Veregin, R., and Goodbrand, B., *Polyacrylates and Polydienes to High Conversion by a Stable Free Radical Polymerization Process: Use of Reducing Agents*. *Macromolecules*, **1998**, *31*, 7559-7561.
75. Pradel, J.-L., Ameduri, B., and Boutevin, B., *Use of controlled radical polymerization of butadiene with AIBN and TEMPO for the determination of the NMR characteristics of hydroxymethyl groups*. *Macromolecular Chemistry and Physics*, **1999**, *200*, 2304-2308.
76. Lutz, J. F., Lacroix-Desmazes, P., Boutevin, B., Le Mercier, C., Gimes, D., Bertin, D., and Tordo, P., *Comparative study of a series of nitroxides and alkoxyamines in controlled/"living" radical polymerization*. *Abstracts of Papers of the American Chemical Society*, **2002**, *224*, U446-U446.
77. Yoshida, E., *Nitroxide-mediated photo-living radical polymerization of vinyl acetate*. *Colloid and Polymer Science*, **2009**, *288*, 73.
78. Elena, V. K. and Dmitry, F. G., *Nitroxide radicals formed in situ as polymer chain growth regulators*. *Russian Chemical Reviews*, **2009**, *78*, 535.

79. Nesvadba, P., Kramer, A., Steinmann, A., and Stauffer, W., *Polymerizable compositions containing alkoxyamine compounds derived from nitroso or nitrono compounds*. **1999**.
80. Grishin, D. F., Semenycheva, L. L., Pavlovskaya, M. V., and Sokolov, K. V., *Features of Radical Polymerization of Vinyl Chloride in the Presence of Nitroxyl Radicals*. Russian Journal of Applied Chemistry, **2001**, 74, 1594-1599.
81. Detrembleur, C., Teyssié, P., and Jérôme, R., *Control of the Radical Polymerization of tert-Butyl Methacrylate in Water by a Novel Combination of Sodium Nitrite and Iron(II) Sulfate*. Macromolecules, **2002**, 35, 1611-1621.
82. Detrembleur, C., Sciannamea, V., Koulic, C., Claes, M., Hoebeke, M., and Jérôme, R., *Controlled Nitroxide-Mediated Radical Polymerization of Styrene, Styrene/Acrylonitrile Mixtures, and Dienes Using a Nitrono*. Macromolecules, **2002**, 35, 7214-7223.
83. Detrembleur, C., Jerome, C., De Winter, J., Gerbaux, P., Clement, J.-L., Guillaneuf, Y., and Gimes, D., *Nitroxide mediated polymerization of methacrylates at moderate temperature*. Polymer Chemistry, **2014**, 5, 335-340.
84. Poli, R., *Radical Coordination Chemistry and Its Relevance to Metal-Mediated Radical Polymerization*. European Journal of Inorganic Chemistry, **2011**, 2011, 1513-1530.
85. Poli, R., *New Phenomena in Organometallic-Mediated Radical Polymerization (OMRP) and Perspectives for Control of Less Active Monomers*. Chemistry – A European Journal, **2015**, 21, 6988-7001.
86. Poli, R., *Relationship between One-Electron Transition-Metal Reactivity and Radical Polymerization Processes*. Angewandte Chemie International Edition, **2006**, 45, 5058-5070.
87. Demarteau, J., Kermagoret, A., German, I., Cordella, D., Robeyns, K., De Winter, J., Gerbaux, P., Jerome, C., Debuigne, A., and Detrembleur, C., *Halomethylcobalt(bis-acetylacetonate) for the controlled synthesis of functional polymers*. Chemical Communications, **2015**, 51, 14334-14337.
88. Kermagoret, A., Debuigne, A., Jérôme, C., and Detrembleur, C., *Precision design of ethylene- and polar-monomer-based copolymers by organometallic-mediated radical polymerization*. Nat Chem, **2014**, 6, 179-187.
89. Debuigne, A., Jérôme, C., and Detrembleur, C., *Isoprene-Assisted Radical Coupling of (Co)polymers Prepared by Cobalt-Mediated Radical Polymerization*. Angewandte Chemie International Edition, **2009**, 48, 1422-1424.
90. Yamago, S., Iida, K., and Yoshida, J.-i., *Tailored Synthesis of Structurally Defined Polymers by Organotellurium-Mediated Living Radical Polymerization (TERP): Synthesis of Poly(meth)acrylate Derivatives and Their Di- and Triblock Copolymers*. Journal of the American Chemical Society, **2002**, 124, 13666-13667.

91. Yamago, S., Iida, K., and Yoshida, J.-i., *Organotellurium Compounds as Novel Initiators for Controlled/Living Radical Polymerizations. Synthesis of Functionalized Polystyrenes and End-Group Modifications*. Journal of the American Chemical Society, **2002**, *124*, 2874-2875.
92. Yamago, S., Yamada, T., Togai, M., Ukai, Y., Kayahara, E., and Pan, N., *Synthesis of Structurally Well-Defined Telechelic Polymers by Organostibine-Mediated Living Radical Polymerization: In Situ Generation of Functionalized Chain-Transfer Agents and Selective ω -End-Group Transformations*. Chemistry – A European Journal, **2009**, *15*, 1018-1029.
93. Yamago, S., Kayahara, E., Kotani, M., Ray, B., Kwak, Y., Goto, A., and Fukuda, T., *Highly Controlled Living Radical Polymerization through Dual Activation of Organobismuthines*. Angewandte Chemie International Edition, **2007**, *46*, 1304-1306.
94. Wayland, B. B., Poszmik, G., and Fryd, M., *Metalloradical reactions of rhodium(II) porphyrins with acrylates: reduction, coupling, and photopromoted polymerization*. Organometallics, **1992**, *11*, 3534-3542.
95. Wayland, B. B., Poszmik, G., Mukerjee, S. L., and Fryd, M., *Living Radical Polymerization of Acrylates by Organocobalt Porphyrin Complexes*. Journal of the American Chemical Society, **1994**, *116*, 7943-7944.
96. Arvanitopoulos, L. D., Greuel, M. P., and Harwood, H. J., *Living Free-Radical Polymerization using Aeryl Cobaloximes as Photoinitiators*. Abstracts of Papers of the American Chemical Society, **1994**, *208*, 402-POLY.
97. Lu, Z., Fryd, M., and Wayland, B. B., *New Life for Living Radical Polymerization Mediated by Cobalt(II) Metalloradicals*. Macromolecules, **2004**, *37*, 2686-2687.
98. Debuigne, A., Caille, J.-R., and Jérôme, R., *Highly Efficient Cobalt-Mediated Radical Polymerization of Vinyl Acetate*. Angewandte Chemie International Edition, **2005**, *44*, 1101-1104.
99. Debuigne, A., Caille, J.-R., Detrembleur, C., and Jérôme, R., *Effective Cobalt Mediation of the Radical Polymerization of Vinyl Acetate in Suspension*. Angewandte Chemie International Edition, **2005**, *44*, 3439-3442.
100. Detrembleur, C., Debuigne, A., Bryaskova, R., Charleux, B., and Jérôme, R., *Cobalt-Mediated Radical Polymerization of Vinyl Acetate in Miniemulsion: Very Fast Formation of Stable Poly(vinyl acetate) Latexes at Low Temperature*. Macromolecular Rapid Communications, **2006**, *27*, 37-41.
101. Debuigne, A., Champouret, Y., Jérôme, R., Poli, R., and Detrembleur, C., *Mechanistic Insights into the Cobalt-Mediated Radical Polymerization (CMRP) of Vinyl Acetate with Cobalt(III) Adducts as Initiators*. Chemistry – A European Journal, **2008**, *14*, 4046-4059.
102. Jeon, H. J., You, Y. C., and Youk, J. H., *Synthesis and characterization of amphiphilic poly(N-vinyl pyrrolidone)-b-poly(ϵ -caprolactone) copolymers by a*

- combination of cobalt-mediated radical polymerization and ring-opening polymerization.* Journal of Polymer Science Part A: Polymer Chemistry, **2009**, *47*, 3078-3085.
103. Debuigne, A., Morin, A. N., Kermagoret, A., Piette, Y., Detrembleur, C., Jérôme, C., and Poli, R., *Key Role of Intramolecular Metal Chelation and Hydrogen Bonding in the Cobalt-Mediated Radical Polymerization of N-Vinyl Amides.* Chemistry – A European Journal, **2012**, *18*, 12834-12844.
104. Debuigne, A., Michaux, C., Jérôme, C., Jérôme, R., Poli, R., and Detrembleur, C., *Cobalt-Mediated Radical Polymerization of Acrylonitrile: Kinetics Investigations and DFT Calculations.* Chemistry – A European Journal, **2008**, *14*, 7623-7637.
105. Hurtgen, M., Debuigne, A., Jérôme, C., and Detrembleur, C., *Solving the Problem of Bis(acetylacetonato)cobalt(II)-Mediated Radical Polymerization (CMRP) of Acrylic Esters.* Macromolecules, **2010**, *43*, 886-894.
106. Bunck, D. N., Sorenson, G. P., and Mahanthappa, M. K., *Cobalt-mediated radical polymerization routes to poly(vinyl ester) block copolymers.* Journal of Polymer Science Part A: Polymer Chemistry, **2011**, *49*, 242-249.
107. Piette, Y., Debuigne, A., Jerome, C., Bodart, V., Poli, R., and Detrembleur, C., *Cobalt-mediated radical (co)polymerization of vinyl chloride and vinyl acetate.* Polymer Chemistry, **2012**, *3*, 2880-2891.
108. Piette, Y., Debuigne, A., Bodart, V., Willet, N., Duwez, A.-S., Jerome, C., and Detrembleur, C., *Synthesis of poly(vinyl acetate)-b-poly(vinyl chloride) block copolymers by Cobalt-Mediated Radical Polymerization (CMRP).* Polymer Chemistry, **2013**, *4*, 1685-1693.
109. Cordella, D., Kermagoret, A., Debuigne, A., Riva, R., German, I., Isik, M., Jérôme, C., Mecerreyes, D., Taton, D., and Detrembleur, C., *Direct Route to Well-Defined Poly(ionic liquid)s by Controlled Radical Polymerization in Water.* ACS Macro Letters, **2014**, *3*, 1276-1280.
110. Yamago, S., Ukai, Y., Matsumoto, A., and Nakamura, Y., *Organotellurium-Mediated Controlled/Living Radical Polymerization Initiated by Direct C–Te Bond Photolysis.* Journal of the American Chemical Society, **2009**, *131*, 2100-2101.
111. Yamago, S., Ray, B., Iida, K., Yoshida, J.-i., Tada, T., Yoshizawa, K., Kwak, Y., Goto, A., and Fukuda, T., *Highly Versatile Organostibine Mediators for Living Radical Polymerization.* Journal of the American Chemical Society, **2004**, *126*, 13908-13909.
112. Yamago, S., Miyazoe, H., and Yoshida, J., *Reversible generation of glycosyl radicals from telluroglycosides under photochemical and thermal conditions.* Tetrahedron Letters, **1999**, *40*, 2339-2342.

113. Yamago, S., Iida, K., Nakajima, M., and Yoshida, J.-i., *Practical Protocols for Organotellurium-Mediated Living Radical Polymerization by in Situ Generated Initiators from AIBN and Ditellurides*. *Macromolecules*, **2003**, *36*, 3793-3796.
114. Goto, A., Kwak, Y., Fukuda, T., Yamago, S., Iida, K., Nakajima, M., and Yoshida, J.-i., *Mechanism-Based Invention of High-Speed Living Radical Polymerization Using Organotellurium Compounds and Azo-Initiators*. *Journal of the American Chemical Society*, **2003**, *125*, 8720-8721.
115. Kwak, Y. W., Goto, A., Fukuda, T., Yamago, S., and Ray, B., *Mechanism and kinetics of organostibine-mediated living radical polymerization of styrene*. *Zeitschrift Fur Physikalische Chemie-International Journal of Research in Physical Chemistry & Chemical Physics*, **2005**, *219*, 283-293.
116. Yusa, S.-i., Yamago, S., Sugahara, M., Morikawa, S., Yamamoto, T., and Morishima, Y., *Thermo-Responsive Diblock Copolymers of Poly(N-isopropylacrylamide) and Poly(N-vinyl-2-pyrrolidone) Synthesized via Organotellurium-Mediated Controlled Radical Polymerization (TERP)*. *Macromolecules*, **2007**, *40*, 5907-5915.
117. Jones, J. S. and Gabbai, F. P., *Coordination and Redox Non-innocent Behavior of Hybrid Ligands Containing Tellurium*. *Chemistry Letters*, **2016**, *45*, 376-384.
118. Wang, J.-S. and Matyjaszewski, K., *Controlled/"Living" Radical Polymerization. Atom Transfer Radical Polymerization in the Presence of Transition-Metal Complexes*. *Journal of American Chemical Society*, **1995**, *117*, 5614-5615.
119. Lee, H.-i., Pietrasik, J., Sheiko, S. S., and Matyjaszewski, K., *Stimuli-responsive molecular brushes*. *Progress in Polymer Science*, **2010**, *35*, 24-44.
120. Siegwart, D. J., Oh, J. K., and Matyjaszewski, K., *ATRP in the design of functional materials for biomedical applications*. *Progress in Polymer Science*, **2012**, *37*, 18-37.
121. Golas, P. L. and Matyjaszewski, K., *Marrying click chemistry with polymerization: expanding the scope of polymeric materials*. *Chemical Society Reviews*, **2010**, *39*, 1338-1354.
122. Gao, H. and Matyjaszewski, K., *Synthesis of functional polymers with controlled architecture by CRP of monomers in the presence of cross-linkers: From stars to gels*. *Progress in Polymer Science*, **2009**, *34*, 317-350.
123. Sheiko, S. S., Sumerlin, B. S., and Matyjaszewski, K., *Cylindrical molecular brushes: Synthesis, characterization, and properties*. *Progress in Polymer Science*, **2008**, *33*, 759-785.
124. Davis, K. A. and Matyjaszewski, K., *Statistical, gradient, block, and graft copolymers by controlled/living radical polymerizations*. *Advances in Polymer Science*, **2002**, *159*, 1-166.

125. Kamigaito, M., Ando, T., and Sawamoto, M., *Metal-Catalyzed Living Radical Polymerization*. Chemical Reviews, **2001**, *101*, 3689-3745.
126. Ouchi, M., Terashima, T., and Sawamoto, M., *Transition Metal-Catalyzed Living Radical Polymerization: Toward Perfection in Catalysis and Precision Polymer Synthesis*. Chemical Reviews, **2009**, *109*, 4963-5050.
127. Rocha, N., Mendonça, P. V., Mendes, J. P., Simões, P. N., Popov, A. V., Guliashvili, T., Serra, A. C., and Coelho, J. F. J., *Facile Synthesis of Well-Defined Telechelic Alkyne-Terminated Polystyrene in Polar Media Using ATRP With Mixed Fe/Cu Transition Metal Catalyst*. Macromolecular Chemistry and Physics, **2013**, *214*, 76-84.
128. Abreu, C. M. R., Serra, A. C., Popov, A., Matyjaszewski, K., Guliashvili, T., and Coelho, J. F. J., *Ambient temperature rapid SARA ATRP of acrylates and methacrylates in alcohol/water solutions mediated by mixed sulfites/Cu(II)Br₂ catalytic system*. Polymer Chemistry, **2013**.
129. Abreu, C. M. R., Mendonça, P. V., Serra, A. C., Coelho, J. F. J., Popov, A. V., and Guliashvili, T., *Accelerated Ambient-Temperature ATRP of Methyl Acrylate in Alcohol–Water Solutions with a Mixed Transition-Metal Catalyst System*. Macromolecular Chemistry and Physics, **2012**, *213*, 1677-1687.
130. Cordeiro, R. A., Rocha, N., Mendes, J. P., Matyjaszewski, K., Guliashvili, T., Serra, A. C., and Coelho, J. F. J., *Synthesis of well-defined poly(2-(dimethylamino)ethyl methacrylate) under mild conditions and its co-polymers with cholesterol and PEG using Fe(0)/Cu(ii) based SARA ATRP*. Polymer Chemistry, **2013**, *4*, 3088-3097.
131. Kato, M., Kamigaito, M., Sawamoto, M., and Higashimura, T., *Polymerization of Methyl Methacrylate with the Carbon Tetrachloride/Dichlorotris-(triphenylphosphine)ruthenium(II)/Methylaluminum Bis(2,6-di-tert-butylphenoxide) Initiating System: Possibility of Living Radical Polymerization*. Macromolecules, **1995**, *28*, 1721-1723.
132. Queffelec, J., Gaynor, S. G., and Matyjaszewski, K., *Optimization of Atom Transfer Radical Polymerization Using Cu(I)/Tris(2-(dimethylamino)ethyl)amine as a Catalyst*. Macromolecules, **2000**, *33*, 8629-8639.
133. Kwak, Y., Magenau, A. J. D., and Matyjaszewski, K., *ARGET ATRP of Methyl Acrylate with Inexpensive Ligands and ppm Concentrations of Catalyst*. Macromolecules, **2011**, *44*, 811-819.
134. Jakubowski, W. and Matyjaszewski, K., *Activators Regenerated by Electron Transfer for Atom-Transfer Radical Polymerization of (Meth)acrylates and Related Block Copolymers*. Angewandte Chemie International Edition, **2006**, *45*, 4482-4486.

135. Jakubowski, W., Min, K., and Matyjaszewski, K., *Activators Regenerated by Electron Transfer for Atom Transfer Radical Polymerization of Styrene*. *Macromolecules*, **2005**, *39*, 39-45.
136. Gnanou, Y. and Hizal, G., *Effect of phenol and derivatives on atom transfer radical polymerization in the presence of air*. *Journal of Polymer Science Part A: Polymer Chemistry*, **2004**, *42*, 351-359.
137. Matyjaszewski, K., Jakubowski, W., Min, K., Tang, W., Huang, J., Braunecker, W. A., and Tsarevsky, N. V., *Diminishing catalyst concentration in atom transfer radical polymerization with reducing agents*. *Proceedings of the National Academy of Sciences*, **2006**, *103*, 15309-15314.
138. Konkolewicz, D., Magenau, A. J. D., Averick, S. E., Simakova, A., He, H., and Matyjaszewski, K., *ICAR ATRP with ppm Cu Catalyst in Water*. *Macromolecules*, **2012**, *45*, 4461-4468.
139. Guliashvili, T., Mendonça, P. V., Serra, A. C., Popov, A. V., and Coelho, J. F. J., *Copper-Mediated Controlled/"Living" Radical Polymerization in Polar Solvents: Insights into Some Relevant Mechanistic Aspects*. *Chemistry-a European Journal*, **2012**, *18*, 4607-4612.
140. Mendonça, P. V., Serra, A. C., Coelho, J. F. J., Popov, A. V., and Guliashvili, T., *Ambient temperature rapid ATRP of methyl acrylate, methyl methacrylate and styrene in polar solvents with mixed transition metal catalyst system*. *European Polymer Journal*, **2011**, *47*, 1460-1466.
141. Góis, J. R., Rocha, N., Popov, A. V., Guliashvili, T., Matyjaszewski, K., Serra, A. C., and Coelho, J. F. J., *Synthesis of well-defined functionalized poly(2-(diisopropylamino)ethyl methacrylate) using ATRP with sodium dithionite as a SARA agent*. *Polymer Chemistry*, **2014**, *5*, 3919-3928.
142. Góis, J. R., Konkolewicz, D., Popov, A., Guliashvili, T., Matyjaszewski, K., Serra, A. C., and Coelho, J., *Improvement of the Control over SARA ATRP of 2-(Diisopropylamino)ethyl Methacrylate by Slow and Continuous Addition of Sodium Dithionite*. *Polymer Chemistry*, **2014**, *5*, 4617-4626.
143. Li, B., Yu, B., Huck, W. T. S., Zhou, F., and Liu, W., *Electrochemically Induced Surface-Initiated Atom-Transfer Radical Polymerization*. *Angewandte Chemie International Edition*, **2012**, *51*, 5092-5095.
144. Magenau, A. J. D., Strandwitz, N. C., Gennaro, A., and Matyjaszewski, K., *Electrochemically Mediated Atom Transfer Radical Polymerization*. *Science*, **2011**, *332*, 81-84.
145. Bortolamei, N., Isse, A. A., Magenau, A. J. D., Gennaro, A., and Matyjaszewski, K., *Controlled Aqueous Atom Transfer Radical Polymerization with Electrochemical Generation of the Active Catalyst*. *Angewandte Chemie International Edition*, **2011**, *50*, 11391-11394.

146. Mosnáček, J. and Ilčíková, M., *Photochemically Mediated Atom Transfer Radical Polymerization of Methyl Methacrylate Using ppm Amounts of Catalyst*. *Macromolecules*, **2012**, *45*, 5859-5865.
147. Konkolewicz, D., Schröder, K., Buback, J., Bernhard, S., and Matyjaszewski, K., *Visible Light and Sunlight Photoinduced ATRP with ppm of Cu Catalyst*. *ACS Macro Letters*, **2012**, *1*, 1219-1223.
148. Fors, B. P. and Hawker, C. J., *Control of a Living Radical Polymerization of Methacrylates by Light*. *Angewandte Chemie International Edition*, **2012**, *51*, 8850-8853.
149. Treat, N. J., Sprafke, H., Kramer, J. W., Clark, P. G., Barton, B. E., Read de Alaniz, J., Fors, B. P., and Hawker, C. J., *Metal-free atom transfer radical polymerization*. *Journal of the American Chemical Society*, **2014**, *136*, 16096-16101.
150. Pan, X., Lamson, M., Yan, J., and Matyjaszewski, K., *Photoinduced metal-free atom transfer radical polymerization of acrylonitrile*. *ACS Macro Letters*, **2015**, *4*, 192-196.
151. Liu, X., Zhang, L., Cheng, Z., and Zhu, X., *Metal-free photoinduced electron transfer-atom transfer radical polymerization (PET-ATRP) via a visible light organic photocatalyst*. *Polymer Chemistry*, **2016**, *7*, 689-700.
152. Fischer, H., *The Persistent Radical Effect: A Principle for Selective Radical Reactions and Living Radical Polymerizations*. *Chemical Reviews*, **2001**, *101*, 3581-3610.
153. Mendes, J. P., Branco, F., Abreu, C. M. R., Mendonça, P. V., Popov, A. V., Guliashvili, T., Serra, A. C., and Coelho, J. F. J., *Synergistic Effect of 1-Butyl-3-methylimidazolium Hexafluorophosphate and DMSO in the SARA ATRP at Room Temperature Affording Very Fast Reactions and Polymers with Very Low Dispersity*. *ACS Macro Letters*, **2014**, *3*, 544-547.
154. Abreu, C. M. R., Fu, L., Carmali, S., Serra, A. C., Matyjaszewski, K., and Coelho, J. F. J., *Aqueous SARA ATRP using inorganic sulfites*. *Polymer Chemistry*, **2017**, *8*, 375-387.
155. Matyjaszewski, K., Gaynor, S., and Wang, J.-S., *Controlled Radical Polymerizations: The Use of Alkyl Iodides in Degenerative Transfer*. *Macromolecules*, **1995**, *28*, 2093-2095.
156. Minisci, F., *Free-radical additions to olefins in the presence of redox systems*. *Accounts of Chemical Research*, **1975**, *8*, 165-171.
157. Severin, K., *Ruthenium Catalysts for the Kharasch Reaction*. *Current Organic Chemistry*, **2006**, *10*, 217-224.

158. Eckenhoff, W. T. and Pintauer, T., *Copper Catalyzed Atom Transfer Radical Addition (ATRA) and Cyclization (ATRC) Reactions in the Presence of Reducing Agents*. *Catalysis Reviews*, **2010**, 52, 1-59.
159. Pintauer, T., *Catalyst Regeneration in Transition-Metal-Mediated Atom-Transfer Radical Addition (ATRA) and Cyclization (ATRC) Reactions*. *European Journal of Inorganic Chemistry*, **2010**, 2010, 2449-2460.
160. Lin, C. Y., Coote, M. L., Gennaro, A., and Matyjaszewski, K., *Ab initio evaluation of the thermodynamic and electrochemical properties of alkyl halides and radicals and their mechanistic implications for atom transfer radical polymerization*. *Journal of the American Chemical Society*, **2008**, 130, 12762-74.
161. Percec, V., Guliashvili, T., Ladislaw, J. S., Wistrand, A., Stjerndahl, A., Sienkowska, M. J., Monteiro, M. J., and Sahoo, S., *Ultrafast synthesis of ultrahigh molar mass polymers by metal-catalyzed living radical polymerization of acrylates, methacrylates, and vinyl chloride mediated by SET at 25 degrees C*. *Journal of the American Chemical Society*, **2006**, 128, 14156-14165.
162. Braunecker, W. A., Tsarevsky, N. V., Gennaro, A., and Matyjaszewski, K., *Thermodynamic Components of the Atom Transfer Radical Polymerization Equilibrium: Quantifying Solvent Effects*. *Macromolecules*, **2009**, 42, 6348-6360.
163. Konkolewicz, D., Krys, P., Góis, J. R., Mendonça, P. V., Zhong, M., Wang, Y., Gennaro, A., Isse, A. A., Fantin, M., and Matyjaszewski, K., *Aqueous RDRP in the Presence of Cu⁰: The Exceptional Activity of CuI Confirms the SARA ATRP Mechanism*. *Macromolecules*, **2014**, 47, 560-570.
164. Konkolewicz, D., Wang, Y., Zhong, M., Krys, P., Isse, A. A., Gennaro, A., and Matyjaszewski, K., *Reversible-Deactivation Radical Polymerization in the Presence of Metallic Copper. A Critical Assessment of the SARA ATRP and SET-LRP Mechanisms*. *Macromolecules*, **2013**, 46, 8749-8772.
165. Wang, Y., Zhong, M., Zhu, W., Peng, C.-H., Zhang, Y., Konkolewicz, D., Bortolamei, N., Isse, A. A., Gennaro, A., and Matyjaszewski, K., *Reversible-Deactivation Radical Polymerization in the Presence of Metallic Copper. Comproportionation–Disproportionation Equilibria and Kinetics*. *Macromolecules*, **2013**, 46, 3793-3802.
166. Peng, C.-H., Zhong, M., Wang, Y., Kwak, Y., Zhang, Y., Zhu, W., Tonge, M., Buback, J., Park, S., Krys, P., Konkolewicz, D., Gennaro, A., and Matyjaszewski, K., *Reversible-Deactivation Radical Polymerization in the Presence of Metallic Copper. Activation of Alkyl Halides by Cu⁰*. *Macromolecules*, **2013**, 46, 3803-3815.
167. Nguyen, N. H., Levere, M. E., Kulis, J., Monteiro, M. J., and Percec, V., *Analysis of the Cu(0)-Catalyzed Polymerization of Methyl Acrylate in Disproportionating and Nondisproportionating Solvents*. *Macromolecules*, **2012**, 45, 4606-4622.

-
168. Levere, M. E., Nguyen, N. H., and Percec, V., *No Reduction of CuBr₂ during Cu(0)-Catalyzed Living Radical Polymerization of Methyl Acrylate in DMSO at 25 °C*. *Macromolecules*, **2012**, *45*, 8267-8274.
169. Nguyen, N. H. and Percec, V., *Disproportionating versus nondisproportionating solvent effect in the SET-LRP of methyl acrylate during catalysis with nonactivated and activated cu(0) wire*. *Journal of Polymer Science Part A: Polymer Chemistry*, **2011**, *49*, 4227-4240.
170. Rosen, B. M. and Percec, V., *A density functional theory computational study of the role of ligand on the stability of CuI and CuII species associated with ATRP and SET-LRP*. *Journal of Polymer Science Part A: Polymer Chemistry*, **2007**, *45*, 4950-4964.
171. Konkolewicz, D., Wang, Y., Krys, P., Zhong, M., Isse, A. A., Gennaro, A., and Matyjaszewski, K., *SARA ATRP or SET-LRP. End of controversy?* *Polymer Chemistry*, **2014**, *5*, 4396-4417.
172. Rosen, B. M. and Percec, V., *Single-Electron Transfer and Single-Electron Transfer Degenerative Chain Transfer Living Radical Polymerization*. *Chemical Reviews*, **2009**, *109*, 5069-5119.
173. Moad, G., Rizzardo, E., and Thang, S. H., *Living Radical Polymerization by the RAFT Process*. *Australian Journal of Chemistry*, **2005**, *58*, 379-410.
174. Moad, G., Rizzardo, E., and Thang, S. H., *Living Radical Polymerization by the RAFT Process—A First Update*. *Australian Journal of Chemistry*, **2006**, *59*, 669-692.
175. Rizzardo, E., Chiefari, J., Mayadunne Roshan, T. A., Moad, G., and Thang San, H., *Synthesis of Defined Polymers by Reversible Addition-Fragmentation Chain Transfer: The RAFT Process*, in *Controlled/Living Radical Polymerization* **2000**, American Chemical Society: Washington DC. p. 278-296.
176. Drache, M. and Schmidt-Naake, G., *Initialization of RAFT Agents with Different Leaving Groups – Determination of the Transfer Coefficients*. *Macromolecular Symposia*, **2008**, *271*, 129-136.
177. Tatemoto, M., *Development of "Iodine Transfer Polymerization" and Its Applications to Telechelically Reactive Polymers*. *Kobunshi Ronbunshu*, **1992**, *49*, 765-783.
178. Tasdelen, M. A., Kahveci, M. U., and Yagci, Y., *Telechelic polymers by living and controlled/living polymerization methods*. *Progress in Polymer Science*, **2011**, *36*, 455-567.
179. Goto, A., Ohno, K., and Fukuda, T., *Mechanism and Kinetics of Iodide-Mediated Polymerization of Styrene*. *Macromolecules*, **1998**, *31*, 2809-2814.
180. Koumura, K., Satoh, K., Kamigaito, M., and Okamoto, Y., *Iodine Transfer Radical Polymerization of Vinyl Acetate in Fluoroalcohols for Simultaneous*

- Control of Molecular Weight, Stereospecificity, and Regiospecificity.* *Macromolecules*, **2006**, 39, 4054-4061.
181. Koumura, K., Satoh, K., and Kamigaito, M., *Manganese-Based Controlled/Living Radical Polymerization of Vinyl Acetate, Methyl Acrylate, and Styrene: Highly Active, Versatile, and Photoresponsive Systems.* *Macromolecules*, **2008**, 41, 7359-7367.
182. Koumura, K., Satoh, K., and Kamigaito, M., *Mn₂(CO)₁₀-induced controlled/living radical copolymerization of vinyl acetate and methyl acrylate: Spontaneous formation of block copolymers consisting of gradient and homopolymer segments.* *Journal of Polymer Science Part A: Polymer Chemistry*, **2009**, 47, 1343-1353.
183. Lacroix-Desmazes, P., Tonnar, J., and Boutevin, B., *Reverse Iodine Transfer Polymerization (RITP) in Emulsion.* *Macromolecular Symposia*, **2007**, 248, 150-157.
184. Tonnar, J., Lacroix-Desmazes, P., and Boutevin, B., *Living Radical ab Initio Emulsion Polymerization of n-Butyl Acrylate by Reverse Iodine Transfer Polymerization (RITP): Use of Persulfate as Both Initiator and Oxidant.* *Macromolecules*, **2007**, 40, 6076-6081.
185. Odian, G., *Principles of polymerization*, **1991**, New York: Wiley.
186. Brandrup, J. and Immergut, E. H., *Polymer Handbook*, **1989**, New York: Wiley.
187. Asandei, A. D. and Percec, V., *From metal-catalyzed radical telomerization to metal catalyzed radical polymerization of vinyl chloride: Toward living radical polymerization of vinyl chloride.* *Journal of Polymer Science Part A Polymer Chemistry*, **2001**, 39, 3392-3418.
188. Coelho, J. F. J., *New Technologies for Homopolymerization and Copolymerization of Vinyl Chloride*, **2006**, University of Coimbra.
189. Regnault, H. V., *Ueber die Zusammensetzung des Chlorkohlenwasserstoffs (Oel des ölbildenden Gases).* *Liebigs Annalen*, **1835**, 14, 22-38.
190. Braumann, E., *Ueber einige Vinylverbindungen.* *Liebigs Ann*, **1872**, 163, 308-322.
191. Semon, W. L. and Stahl, G. A., *History of polymer science engineering.* 2nd ed, **1989**, New York: John Wiley & Sons. 295.
192. *Research and Markets: Polyvinyl Chloride (PVC) Global Supply Dynamics to 2020 - China Emerges as the Leader in Global Production.* 2011 [cited 2014 July 23]; Available from: <http://www.reuters.com/article/2011/01/10/idUS131266+10-Jan-2011+BW20110110>.
193. Endo, K., *Synthesis and structure of poly(vinyl chloride).* *Progress in Polymer Science*, **2002**, 27, 2021-2054.

194. Starnes, W. H., *Structural and mechanistic aspects of the thermal degradation of poly(vinyl chloride)*. Prog. Polym. Sci., **2002**, 27, 2133-2170.
195. Braun, D., *Recycling of PVC*. Progress in Polymer Science, **2002**, 27, 2171-2195.
196. Leadbitter, J., *PVC and sustainability*. Progress in Polymer Science, **2002**, 27, 2197-2226.
197. Mersiowsky, I., *Long-term fate of PVC products and their additives in landfills*. Progress in Polymer Science, **2002**, 27, 2227-2277.
198. Moulay, S., *Chemical modification of poly(vinyl chloride)—Still on the run*. Progress in Polymer Science, **2010**, 35, 303-331.
199. Chiellini, F., Ferri, M., Morelli, A., Dipaola, L., and Latini, G., *Perspectives on alternatives to phthalate plasticized poly(vinyl chloride) in medical devices applications*. Progress in Polymer Science, **2013**, 38, 1067-1088.
200. Semon, W. L. and Stahl, G. A., *History of Vinyl Chloride Polymers*. Journal of Macromolecular Science-Chemistry, **1981**, A15, 1263-1278.
201. *PVC Forum South East Europe*. 2010 [cited 2014 July 23]; Available from: <http://www.seepvcforum.com>.
202. *How is PVC made?* 2014 [cited 2014 July 23]; Available from: <http://www.pvc.org>.
203. Brydson, J. A., *Plastics Materials*. 7th ed, **1999**, Oxford: Butterworth Heinemann.
204. Small, P. A., *Some Factors Affecting the Solubility of Polymers*. Journal of Applied Chemistry, **1953**, 3, 71-80.
205. Vogl, O., Kwei, T. K., and Qin, M., *Head to Head Polymers.42. Head to Head Poly(vinyl halide) Blends: Thermal and Degradation Behaviour*. Journal of Macromolecular Science - Pure and Applied Chemistry, **1997**, A34, 1747-1769.
206. Tickner, J. A., Schettler, T., Guidotti, T., McCally, M., and Rossi, M., *Health risks posed by use of Di-2-ethylhexyl phthalate (DEHP) in PVC medical devices: A critical review*. American Journal of Industrial Medicine, **2001**, 39, 100-111.
207. Belhaneche-Bensemra, N., Zeddou, C., and Ouahmed, S., *Study of Migration of Additives from Plasticized PVC*. Macromolecular Symposia, **2002**, 180, 191-201.
208. Wang, Q. and Storm, B. K., *Migration of Additives from Poly(vinyl chloride) (PVC) Tubes into Aqueous Media*. Macromol. Symp., **2005**, 225, 191-203.
209. Papaspyrides, C. D. and Tingas, S. G., *Effect of thermal annealing on plasticizer migration in poly(vinyl chloride)/dioctyl phthalate system*. Journal of Applied Polymer Science, **2001**, 79, 1780-1786.
210. Rocha, N., Coelho, J. F. J., Fonseca, A. C., Kazlauciusas, A., Gil, M. H., Gonçalves, P. M., and Guthrie, J. T., *Poly(vinyl Chloride) and Wood Flour Press*

- Mould Composites: New Bonding Strategies*. Journal of Applied Polymer Science, **2009**, *113*, 2727-2738.
211. Rocha, N., Gamelas, J. A. F., Gonçalves, P. M., Gil, M. H., and Guthrie, J. T., *Influence of physical-chemical interactions on the thermal stability and surface properties of poly(vinyl chloride)-b-poly(hydroxypropyl acrylate)-b-poly(vinyl chloride) block copolymers*. European Polymer Journal, **2009**, *45*, 3389-3398.
212. Coelho, J. F. J., Mendonça, P. V., Popov, A. V., Percec, V., Gonçalves, P. M., and Gil, M. H., *Synthesis of High Glass Transition Temperature Copolymers Based on Poly(vinyl chloride) via Single Electron Transfer-Degenerative Chain Transfer Mediated Living Radical Polymerization (SET-DTLRP) of Vinyl Chloride in Water*. Journal of Polymer Science Part a-Polymer Chemistry, **2009**, *47*, 7021-7031.
213. Coelho, J. F. J., Silva, A. M. F., Popov, A. V., Percec, V., Abreu, M. V., Gonçalves, P. M., and Gil, M. H., *Synthesis of poly(vinyl chloride)-b-poly(n-butyl acrylate)-b-poly(vinyl chloride) by the competitive single-electron-transfer/degenerative-chain-transfer-mediated living radical polymerization in water*. Journal of Polymer Science Part a-Polymer Chemistry, **2006**, *44*, 3001-3008.
214. Percec, V., Popov, A. V., Ramirez-Castillo, E., and Hinojosa-Falcon, L. A., *Synthesis of poly(vinyl chloride)-b-poly(2-ethylhexyl acrylate)-b-poly(vinyl chloride) by the competitive single-electron-transfer/degenerative-chain-transfer mediated living radical polymerization of vinyl chloride initiated from alpha,omega-di(iodo)poly(2-ethylhexyl acrylate) and catalyzed with sodium dithionite in water*. Journal of Polymer Science Part a-Polymer Chemistry, **2005**, *43*, 2276-2280.
215. Percec, V., Guliashvili, T., and Popov, A. V., *Ultrafast synthesis of poly(methyl acrylate) and poly(methyl acrylate)-b-poly(vinyl chloride)-b-poly(methyl acrylate) by the Cu(0)/tris(2-dimethylaminoethyl)amine-catalyzed living radical polymerization and block copolymerization of methyl acrylate initiated with 1,1-chloroiodoethane and alpha,omega-di(iodo)poly(vinyl chloride) in dimethyl sulfoxide*. Journal of Polymer Science Part a-Polymer Chemistry, **2005**, *43*, 1948-1954.
216. Jennings, T. and Starnes, W., *PVC Stabilizers and Lubricants*, in *PVC Handbook*, C.E. Wilkes, et al., Editors. **2005**, Hanser Gardner Publications, Inc.: EUA. p. 95-166.
217. Alsopp, M. W. and Vianello, G., *Poly(vinyl chloride)*, in *Encyclopedia of Polymer Science & Technology: Plastics, Resins, Rubbers, Fibres*, H.F. Mark, Editor **2003**, John Wiley & Sons: New Jersey, EUA. p. 437-476.
218. Nass, L. I. and Heiberger, C. A., *Encyclopedia of PVC: Compounding Processes, Product Design, and Specifications*, **1992**, New York: Marcel Dekker, Inc.

-
219. Mark, H. F., Bikales, N. M., Overberger, C. G., and Menges, G., *Encyclopedia of Polymer Science and Engineering*. Vol. 17, **1989**, New York: Wiley Interscience.
220. Kamal, I. M., Adam, G. A., and Getta, H. K., *The effect of molecular weight on the thermal stability of poly(vinyl chloride)*. *Thermochimica Acta*, **1983**, 62, 355-359.
221. Coelho, J. F. J., Fonseca, A. C., Gonçalves, P. M., Popov, A. V., and Gil, M. H., *Scaling-up of poly(vinyl chloride) prepared by single electron transfer-degenerative chain transfer mediated living radical polymerization in water media—II: High molecular weight-ultra stable PVC*. *Chemical Engineering Science*, **2012**, 69, 122-128.
222. Coelho, J. F. J., Fonseca, A. C., Góis, J. R., Gonçalves, P. M., Popov, A. V., and Gil, M. H., *Scaling-up of poly(vinyl chloride) prepared by single electron transfer degenerative chain transfer mediated living radical polymerization in water media: 1) Low molecular weight. Kinetic analysis*. *Chemical Engineering Journal*, **2011**, 169, 399-413.
223. Coelho, J. F. J., Carreira, M., Popov, A. V., Gonçalves, P. M., and Gil, M. H., *Thermal and mechanical characterization of poly(vinyl chloride)-b-poly(butyl acrylate)-b-poly(vinyl chloride) obtained by single electron transfer - degenerative chain transfer living radical polymerization in water*. *European Polymer Journal*, **2006**, 42, 2313-2319.
224. Coelho, J. F. J., Gonçalves, P. M., Miranda, D., and Gil, M. H., *Characterization of suspension poly(vinyl chloride) resins and narrow polystyrene standards by size exclusion chromatography with multiple detectors: Online right angle laser-light scattering and differential viscometric detectors*. *European Polymer Journal*, **2006**, 42, 751-763.
225. Burgess, R. H., ed. *Manufacture and Processing of PVC*. *Manufacture and Processing of PVC*, ed. R.H. Burgess, **1982**, Applied Science Publishers: London. Chapter 1.
226. Monsanto, *British Patent 954983*. British Patent 954983, **1964**.
227. Starnes, W. H., Jr., *Structural defects in poly(vinyl chloride)*. *J. Polym. Sci., Part A: Polym. Chem.*, **2005**, 43, 2451-2467.
228. Starnes, W. H., Jr. and Ge, X., *Mechanism of autocatalysis in the thermal dehydrochlorination of poly(vinyl chloride)*. *Macromolecules*, **2004**, 37, 352-359.
229. Iván, B., *Thermal stability, degradation, and stabilization mechanisms of poly(vinyl chloride)*. *Advances in Chemistry Series*, **1996**, 249, 19-32.
230. Troitskii, B. B. and Troitskaya, L. S., *Some aspects of the thermal degradation of poly(vinyl chloride)* *International Journal of Polymeric Materials*, **1998**, 41, 285-324.

231. Yassin, A. A. and Sabaa, M. D., *Degradation and Stabilization of Poly(Vinyl Chloride)*. Journal of Macromolecular Science - Reviews in Macromolecular Chemistry & Physics, **1990**, C30, 491-588.
232. Iván, B., T., K., and Tüdös, F., *Degradation and stabilization of poly(vinyl chloride)*, in *Degradation and stabilization of polymers*, H.H.G. Jellinek and H. Kachi, Editors. **1989**, Elsevier: New York.
233. Minsker, K. S., *Characteristic effects in degradation and stabilization of halogen-containing polymers*. International Journal of Polymeric Materials, **1994**, 24, 235-251.
234. Millán, J. L., Martínez, G., Gómez-Elvira, J. M., Guarrotxena, N., and Tiemblo, P., *Influence of tacticity on the thermal degradation of PVC: 8. A comprehensive study of the local isotactic GTTG- conformation dependence of the mechanism of initiation*. Polymer, **1996**, 37, 219-230.
235. Starnes, W. H., Jr., Zaikov, V. G., Chung, H. T., Wojciechowski, B. J., Tran, H. V., Saylor, K., and Benedikt, G. M., *Intramolecular Hydrogen Transfers in Vinyl Chloride Polymerization: Routes to Doubly Branched Structures and Internal Double Bonds*. Macromolecules, **1998**, 31, 1508-1517.
236. Benedikt, G. M., Cozens, R. J., Goodall, B. L., Rhodes, L. F., Bell, M. N., Kemball, A. C., and Starnes, W. H. J., *New Structural and Mechanistic Chemistry in Polymerizations of Vinyl Chloride Initiated by Di-tert- alkylmagnesiums*. Macromolecules, **1997**, 30, 10-21.
237. Starnes, W. H. J., Wojciechowski, B. J., Chung, H., Benedikt, G. M., Park, G. S., and Saremi, A. H., *Dichlorobutyl Branch Formation and the Question of Diffusion-Controlled Propagation in the Polymerization of Vinyl Chloride*. Macromolecules, **1995**, 28, 945-949.
238. Starnes, W. H. J. and Wojciechowski, B. J., *Mechanism and microstructure in the free-radical polymerization of vinyl-chloride head-to-head addition revisited*. Makromolekulare Chemie-Macromolecular Symposia, **1993**, 70, 1-11.
239. Starnes, W. H. J., Chung, H., Wojciechowski, B. J., Skillicorn, D. E., and Benedikt, G. M., *Exclusive Formation of the Thermally Labile Structures in Poly(vinyl chloride) Via Hydrogen Abstraction by Macroradicals*. Polymer Preprints American Chemical Society, Division of Polymer Chemistry, **1993**, 34, 114-115.
240. Starnes, W. H. J., Wojciechowski, B. J., Velazquez, A., and Benedikt, G. M., *Molecular Microstructure of Ethyl Branch Segments in Poly(vinyl chloride)*. Macromolecules, **1992**, 25, 3638-3641.
241. Starnes, W. H. J., Villacorta, G. M., Schilling, F. C., Plitz, I. M., Park, G. S., and Saremi, A. H., *Residual Primary Halogen in Reductively Dehalogenated Poly(vinyl chloride)*. Macromolecules, **1985**, 18, 1780-1786.

-
242. Starnes, W. H. J., Plitz, I. M., Hische, D. C., Freed, D. J., Schilling, C., and Schilling, M. L., *Stabilization of Poly(vinyl chloride) by Thiols. A Mechanistic Study*. *Macromolecules*, **1985**, *11*, 373-382.
243. Starnes, W. H. J., Plitz, I. M., Schilling, C., Villacorta, G. M., Park, G. S., and Saremi, A. H., *Poly(vinyl Chloride) Structural Segments Derived from Azobis(isobutyronitrile)*. *Macromolecules*, **1984**, *17*, 2507-2512.
244. Starnes, W. H. J., Schilling, F. C., Plitz, I. M., Cais, R. E., Freed, D. J., Hartless, R. L., and Bovey, F. A., *Branches Structures in Poly(vinyl chloride) and the Mechanism of Chain Transfer to Monomer during Vinyl Chloride Polymerization*. *Macromolecules*, **1983**, *16*, 790-807.
245. Starnes, W. H. J., Schilling, F. C., Plitz, I. M., Cais, R. E., and Bovey, F. A., *Detailed Microstructure and Concentration of Chlorinated n-Butyl Branches in Poly(vinyl chloride)*. *Polymer Bulletin*, **1981**, *4*, 555-562.
246. Starnes, W. H. J. and Edelson, D., *Mechanistic Aspects of the Behaviour of Molybdenum(VI) Oxide as a Fire-Retardant Additive for Poly(vinyl chloride). An Interpretive Review*. *Macromolecules*, **1979**, *12*, 797-802.
247. Graedel, T. E., Franey, J. F., Starnes, W. H. J., Hische, D. C., and Warren, P. C., *The Interaction of Hydrogen Sulfide with Lead- and Barium-Cadmium-Zinc-Stabilized Poly(vinyl Chloride)*. *Journal of Applied Polymer Science*, **1979**, *23*, 1769-1779.
248. Starnes, W. H. J., Hartless, R. L., Schilling, C., and Bovey, F. A., *Reductive Dehalogenation with Tri(n-Butyl)Tin Hydride: A Powerful New Technique For Use In Poly(Vinyl Chloride) Microstructure Investigations*. *Polymer Preprints American Chemical Society, Division of Polymer Chemistry*, **1977**, *18*, 499-504.
249. Starnes Jr, W. H., *Overview and assessment of recent research on the structural defects in poly(vinyl chloride)*. *Polymer Degradation and Stability*, **2012**, *97*, 1815-1821.
250. Hjertberg, T. and Sörvik, E. M., *Formation of Anomalous Structures in PVC and Their Influence on Thermal Stability. 2. Branch structures and tertiary chloride*. *Polymer*, **1983**, *24*, 673-683.
251. Starnes, W. H. J., Chung, H., Wojciechowski, B. J., Skillicorn, D. E., and Benedikt, G. M., *Auxiliary mechanism for transfer to monomer during vinyl chloride polymerization - Implications for thermal stability of poly(vinyl chloride)*. *Polymer Durability Advances in Chemistry Series*, **1996**, *249*, 3-18.
252. Xie, T. Y., Hamielec, P. E., Rogstedt, M., and Hjertberg, T., *Experimental investigation of vinyl chloride polymerization at high conversion: polymer microstructure and thermal stability and their relationship to polymerization conditions*. *Polymer*, **1994**, *35*, 1526-1534.
253. Summers, J. W., *A Review of Vinyl Technology*. *Journal of Vinyl Additive and Technology*, **1997**, *3*, 130-139.

254. Summers, J. W., *Lubrication mechanism of poly(vinyl chloride) compounds: Changes upon PVC fusion (gelation)*. *Journal of Vinyl & Additive Technology*, **2005**, *11*, 57-62.
255. Summers, J. W., *Vinyl Chloride Polymers*, in *Kirk-Othmer Encyclopedia of Chemical Technology* **2000**, Wiley Blackwell: New Jersey.
256. Mesch, K. A., *Heat Stabilizers*, in *Kirk-Othmer Encyclopedia of Chemical Technology* **2000**, John Wiley & Sons, Inc.
257. Cadogan, D. F. and Howick, C. J., *Plasticizers*, in *Kirk-Othmer Encyclopedia of Chemical Technology* **2000**, John Wiley & Sons, Inc.
258. Titow, M. V., *PVC Technology*, **1984**, New York: Elsevier Applied Science Publisher.
259. Coelho, J. F. J., Carreira, M., Gonçalves, P. M., Popov, A. V., and Gil, M. H., *Processability and characterization of poly(vinyl chloride)-b-poly(n-butyl acrylate)-b-poly(vinyl chloride) prepared by living radical polymerization of vinyl chloride. Comparison with a flexible commercial resin formulation prepared with PVC and dioctyl phthalate*. *Journal of Vinyl & Additive Technology*, **2006**, *12*, 156-165.
260. Braun, D., *Poly(vinyl chloride) on the way from the 19th century to the 21st century*. *Journal of Polymer Science Part a-Polymer Chemistry*, **2004**, *42*, 578-586.
261. Foley, S. R., Stockland, R. A., Shen, H., and Jordan, R. F., *Reaction of Vinyl Chloride with Late Transition Metal Olefin Polymerization Catalysts*. *Journal of the American Chemical Society*, **2003**, *125*, 4350-4361.
262. Stockland, R. A., Foley, S. R., and Jordan, R. F., *Reaction of Vinyl Chloride with Group 4 Metal Olefin Polymerization Catalysts*. *Journal of the American Chemical Society*, **2002**, *125*, 796-809.
263. Stockland, R. A. and Jordan, R. F., *Reaction of Vinyl Chloride with a Prototypical Metallocene Catalyst: Stoichiometric Insertion and β -Cl Elimination Reactions with *rac*-(EBI)ZrMe⁺ and Catalytic Dechlorination/Oligomerization to Oligopropylene by *rac*-(EBI)ZrMe₂/MAO*. *Journal of the American Chemical Society*, **2000**, *122*, 6315-6316.
264. Percec, V., Popov, A. V., Ramirez-Castillo, E., Coelho, J. F. J., and Hinojosa-Falcon, L. A., *Non-transition metal-catalyzed living radical polymerization of vinyl chloride initiated with iodoform in water at 25 degrees C*. *Journal of Polymer Science Part a-Polymer Chemistry*, **2004**, *42*, 6267-6282.
265. Percec, V., Popov, A. V., Ramirez-Castillo, E., and Weichold, O., *Living radical polymerization of vinyl chloride initiated with iodoform and catalyzed by nascent Cu-0/Tris(2-aminoethyl)amine or polyethyleneimine in water at 25 degrees C proceeds by a new competing pathways mechanism*. *Journal of Polymer Science Part a-Polymer Chemistry*, **2003**, *41*, 3283-3299.

-
266. Percec, V., Popov, A. V., Ramirez-Castillo, E., Monteiro, M., Barboiu, B., Weichold, O., Asandei, A. D., and Mitchell, C. M., *Aqueous room temperature metal-catalyzed living radical polymerization of vinyl chloride*. *Journal of the American Chemical Society*, **2002**, *124*, 4940-4941.
267. Percec, V., Popov, A. V., Ramirez-Castillo, E., and Weichold, O., *Acceleration of the single electron transfer-degenerative chain transfer mediated living radical polymerization (SET-DTLRP) of vinyl chloride in water at 25 degrees C*. *Journal of Polymer Science Part a-Polymer Chemistry*, **2004**, *42*, 6364-6374.
268. Percec, V., Ramirez-Castillo, E., Hinojosa-Falcon, L. A., and Popov, A. V., *Synthesis of ultrahigh molar mass, structural defects free poly(vinyl chloride) with high syndiotacticity and glass transition temperature by single electron transfer-degenerative chain transfer living radical polymerization (SET-DTLRP)*. *Journal of Polymer Science Part a-Polymer Chemistry*, **2005**, *43*, 2185-+.
269. Percec, V., Popov, A. V., Ramirez-Castillo, E., Coelho, J. F. J., and Hinojosa-Falcon, L. A., *Phase transfer catalyzed single electron transfer-degenerative chain transfer mediated living radical polymerization (PTC-SET-DTLRP) of vinyl chloride catalyzed by sodium dithionite and initiated with iodoform in water at 43 degrees C*. *Journal of Polymer Science Part a-Polymer Chemistry*, **2005**, *43*, 779-788.
270. Percec, V., Popov, A. V., Ramirez-Castillo, E., and Coelho, J. F. J., *Single electron transfer-degenerative chain transfer mediated living radical polymerization (SET-DTLRP) of vinyl chloride initiated with methylene iodide and catalyzed by sodium dithionite*. *Journal of Polymer Science Part a-Polymer Chemistry*, **2005**, *43*, 773-778.
271. Percec, V., Popov, A. V., and Ramirez-Castillo, E., *Single-electron-transfer/degenerative-chain-transfer mediated living radical polymerization of vinyl chloride catalyzed by thiourea dioxide/octyl viologen in water/tetrahydrofuran at 25 degrees C*. *Journal of Polymer Science Part a-Polymer Chemistry*, **2005**, *43*, 287-295.
272. Percec, V. and Popov, A. V., *Functionalization of the active chain ends of poly(vinyl chloride) obtained by single-electron-transfer degenerative-chain-transfer mediated living radical polymerization: Synthesis of telechelic alpha,omega-di(hydroxy)poly(vinyl chloride)*. *Journal of Polymer Science Part a-Polymer Chemistry*, **2005**, *43*, 1255-1260.
273. Percec, V., Guliashvili, T., Popov, A. V., Ramirez-Castillo, E., and Hinojosa-Falcon, L. A., *Ultrafast synthesis of poly(methyl methacrylate)-b-poly(vinyl chloride)-b- poly(methyl methacrylate) block copolymers by the Cu(0)/tris(2-dimethylaminoethyl)amine-catalyzed living radical block copolymerization of methyl methacrylate initiated with alpha,omega-di(iodo)poly(vinyl chloride) in the presence of dimethyl sulfoxide at 25 degrees C*. *Journal of Polymer Science Part a-Polymer Chemistry*, **2005**, *43*, 1660-1669.

274. Percec, V., Guliashvili, T., Popov, A. V., Ramirez-Castillo, E., Coelho, J. F. J., and Hinojosa-Falcon, L. A., *Accelerated synthesis of poly(methyl methacrylate)-b-poly(vinyl chloride)-b-poly(methyl methacrylate) block copolymers by the CuCl/tris(2-dimethylaminoethyl)amine-catalyzed living radical block copolymerization of methyl methacrylate initiated with alpha,omega-di(iodo)poly(vinyl chloride) in dimethyl sulfoxide at 90 degrees C*. Journal of Polymer Science Part a-Polymer Chemistry, **2005**, *43*, 1649-1659.
275. Percec, V., Guliashvili, T., Popov, A. V., and Ramirez-Castillo, E., *Synthesis of poly(methyl methacrylate)-b-poly(vinyl chloride)-b-poly(methyl methacrylate) block copolymers by CuCl/2,2'-bipyridine-catalyzed living radical block copolymerization initiated from alpha,omega-Di(iodo)poly(vinyl chloride) prepared by single-electron-transfer/degenerative-chain-transfer mediated living radical polymerization*. Journal of Polymer Science Part a-Polymer Chemistry, **2005**, *43*, 1478-1486.
276. Wannemacher, T., Braun, D., and Pfaendner, R., *Novel copolymers via nitroxide mediated controlled free radical polymerization of vinyl chloride*. Macromolecular Symposia, **2003**, *202*, 11-24.
277. Braun, D., *Controlled free-radical polymerization of vinyl chloride*. Journal of Vinyl & Additive Technology, **2005**, *11*, 86-90.
278. Sienkowska, M. J., Rosen, B. M., and Percec, V., *SET-LRP of Vinyl Chloride Initiated with CHBr₃ in DMSO at 25 degrees C*. Journal of Polymer Science Part a-Polymer Chemistry, **2009**, *47*, 4130-4140.
279. Hatano, T., Rosen, B. M., and Percec, V., *SET-LRP of Vinyl Chloride Initiated with CHBr₃ and Catalyzed by Cu(0)-Wire/TREN in DMSO at 25 degrees C*. Journal of Polymer Science Part a-Polymer Chemistry, **2010**, *48*, 164-172.
280. Mendes, J. P., Branco, F., Abreu, C. M. R., Mendonca, P. V., Serra, A. C., Popov, A. V., Guliashvili, T., and Coelho, J. F. J., *Sulfolane: an Efficient and Universal Solvent for Copper-Mediated Atom Transfer Radical (co)Polymerization of Acrylates, Methacrylates, Styrene, and Vinyl Chloride*. ACS Macro Letters, **2014**, *3*, 858-861.
281. Mendes, J. P., Mendonca, P. V., Maximiano, P., Abreu, C. M. R., Guliashvili, T., Serra, A. C., and Coelho, J. F. J., *Getting faster: low temperature copper-mediated SARA ATRP of methacrylates, acrylates, styrene and vinyl chloride in polar media using sulfolane/water mixtures*. RSC Advances, **2016**, *6*, 9598-9603.
282. Maximiano, P., Mendes, J. P., Mendonca, P. V., Abreu, C. M. R., Guliashvili, T., Serra, A. C., and Coelho, J. F. J., *Cyclopentyl methyl ether: A new green co-solvent for supplemental activator and reducing agent atom transfer radical polymerization*. Journal of Polymer Science Part a-Polymer Chemistry, **2015**, *53*, 2722-2729.
283. Mendes, J. P., Góis, J. R., Costa, J. R. C., Maximiano, P., Serra, A. C., Guliashvili, T., and Coelho, J. F. J., *Ambient temperature SARAATRP for*

- meth(acrylates), styrene, and vinyl chloride using sulfolane/1-butyl-3-methylimidazolium hexafluorophosphate-based mixtures.* Journal of Polymer Science Part A: Polymer Chemistry, **2017**, *55*, 1322-1328.
284. Abreu, C. M. R., Mendonça, P. V., Serra, A. C., Coelho, J. F. J., Popov, A. V., Gryn'ova, G., Coote, M. L., and Guliashvili, T., *Reversible Addition-Fragmentation Chain Transfer Polymerization of Vinyl Chloride.* Macromolecules, **2012**, *45*, 2200-2208.
285. Abreu, C. M. R., Maximiano, P., Guliashvili, T., Nicolas, J., Serra, A. C., and Coelho, J. F. J., *Cyclopentyl methyl ether as a green solvent for reversible-addition fragmentation chain transfer and nitroxide-mediated polymerizations.* RSC Advances, **2016**, *6*, 7495-7503.
286. Abreu, C. M. R., Mendonça, P. V., Serra, A. C., Noble, B. B., Guliashvili, T., Nicolas, J., Coote, M. L., and Coelho, J. F. J., *Nitroxide-Mediated Polymerization of Vinyl Chloride at Low Temperature: Kinetic and Computational Studies.* Macromolecules, **2016**, *49*, 490-498.
287. Barboiu, B. and Percec, V., *Metal catalyzed living radical polymerization of acrylonitrile initiated with sulfonyl chlorides.* Macromolecules, **2001**, *34*, 8626-8636.
288. Percec, V., Asandei, A. D., Asgarzadeh, F., Barboiu, B., Holerca, M. N., and Grigoras, C., *Organocopper-Catalyzed Living Radical Polymerization Initiated with Aromatic Sulfonyl Chlorides.* Journal of Polymer Science: Part A: Polymer Chemistry, **2000**, *38*, 4353-4361.
289. Percec, V., Asandei, A. D., Asgarzadeh, F., Bera, T. K., and Barboiu, B., *Cu-I and Cu-II salts of group VIA elements as catalysts for living radical polymerization initiated with sulfonyl chloride.* Journal of Polymer Science Part A Polymer Chemistry, **2000**, *38*, 3839-3843.
290. Percec, V. and Barboiu, B., *"Living" Radical Polymerization of Styrene Initiated by Arenesulfonyl Chlorides and $Cu^I(bpy)_nCl$.* Macromolecules, **1995**, *28*, 7970-7972.
291. Percec, V., Barboiu, B., Bera, T. K., Sluis, M. v. d., Grubbs, R. B., and Fréchet, J. M. J., *Designing Functional Aromatic Multisulfonyl Chloride Initiators for Complex Organic Synthesis by Living Radical Polymerization.* Journal of Polymer Science: Part A: Polymer Chemistry, **2000**, *38*, 4776-4791.
292. Percec, V., Barboiu, B., and Kim, H.-J., *Arenesulfonyl Halides: A Universal Class of Functional Initiators for Metal Catalyzed "Living" Radical Polymerization of Styrene(s), Methacrylates, and Acrylates.* Journal of the American Chemical Society, **1998**, *120*, 305-316.
293. Percec, V., Barboiu, B., Neuman, A., Ronda, J. C., and Zhao, M., *Metal-Catalyzed "Living" Radical Polymerization of Styene Initiated with Arenesulfonyl Chlorides.*

- From Heterogeneous to Homogeneous Catalysis*. *Macromolecules*, **1996**, *29*, 3665-3668.
294. Percec, V., Barboiu, B., and Sluis, M. V. D., *Self/Regulated Phase Transfer of Cu₂O/bpy, Cu(0), and Cu₂O/Cu(0)/bpy Catalyzed "Living" Radical Polymerization Initiated with Sulfonyl Chlorides - Supplemental Page*. *Macromolecules*, **1998**, *31*, 4053-4056.
295. Percec, V., Kim, H.-J., and Barboiu, B., *Scope and Limitations of Functional Sulfonyl Chlorides as Initiators for Metal-Catalyzed "Living" Radical Polymerization of Styrene and Methacrylates*. *Macromolecules*, **1997**, *30*, 8526-8528.
296. Percec, V., Kim, H.-J., and Barboiu, B., *Dissulfonyl Chlorides: A Universal Class of Initiators for Metal-Catalyzed "Living" Diradical Polymerization of Styrene(s), Methacrylates, and Acrylates*. *Macromolecules*, **1997**, *30*, 6702-6705.
297. Simões, P. N., Coelho, J. F. J., Gonçalves, P. M., and Gil, M. H., *Comparative non-isothermal kinetic analysis of thermal degradation of poly(vinyl chloride) prepared by living and conventional free radical polymerization methods*. *European Polymer Journal*, **2009**, *45*, 1949-1959.
298. Coelho, J. F. J., Simões, P. N., Mendonça, P. V., Fonseca, A. C., and Gil, M. H., *Thermal characterization of poly(vinyl chloride) samples prepared by living radical polymerization: Comparison with poly(vinyl chloride) prepared by free radical polymerization*. *Journal of Applied Polymer Science*, **2008**, *109*, 2729-2736.
299. Sienkowska, M. J. and Percec, V., *Synthesis of alpha,omega-Di(iodo)PVC and of Four-Arm Star PVC with Identical Active Chain Ends by SET-DTLRP of VC Initiated with Bifunctional and Tetrafunctional Initiators*. *Journal of Polymer Science Part a-Polymer Chemistry*, **2009**, *47*, 635-652.
300. Percec, V. and Sienkowska, M. J., *Synthesis of the Four-Arm Star-Block Copolymer [PVC-*b*-PBA-CH(CH₃)-CO-O-CH₂](₄)C by SET-DTLRP Initiated from a Tetrafunctional Initiator*. *Journal of Polymer Science Part a-Polymer Chemistry*, **2009**, *47*, 628-634.
301. Kim, Y., Cho, W.-J., and Ha, C.-S., *Dynamic Mechanical and Morphological Studies on the Compatibility of Plasticized PVC/Thermoplastic Polyurethane Blends*. *Journal of Applied Polymer Science*, **1999**, *71*, 415-422.
302. Jimenez, A., Lopez, J., Iannoni, A., and Kenny, J. M., *Formulation and Mechanical Characterization of PVC Plastics Based on Low-Toxicity Additives*. *Journal of Applied Polymer Science*, **2001**, *81*, 1881-1890.
303. Coelho, J. F. J., Carvalho, E. Y., Marques, D. S., Popov, A. V., Percec, V., and Gil, M. H., *Influence of the isomeric structures of butyl acrylate on its single-electron transfer-degenerative chain transfer living radical polymerization in*

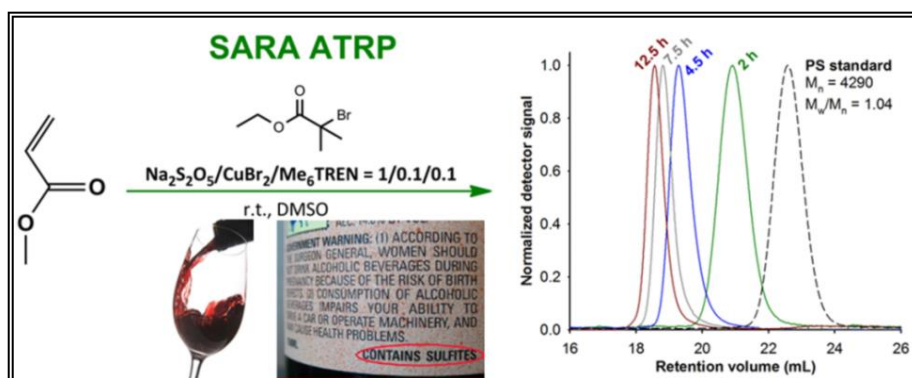
- water catalyzed by Na₂S₂O₄*. Journal of Polymer Science Part a-Polymer Chemistry, **2008**, *46*, 6542-6551.
304. Shipp, D. A., Wang, J.-L., and Matyjaszewski, K., *Synthesis of Acrylate and Methacrylate Block Copolymers Using Atom Transfer Radical Polymerization*. Macromolecules, **1998**, *31*, 8005-8008.
305. Coelho, J. F. J., Silva, A. M. F., Popov, A. V., Percec, V., Abreu, M. V., Gonçalves, P. M., and Gil, M. H., *Single electron transfer-degenerative chain transfer living radical polymerization of N-butyl acrylate catalyzed by Na₂S₂O₄ in water media*. Journal of Polymer Science Part a-Polymer Chemistry, **2006**, *44*, 2809-2825.
306. Coelho, J. F. J., Carvalho, E. Y., Marques, D. S., Popov, A. V., Percec, V., Gonçalves, P. M., and Gil, M. H., *Synthesis of poly(ethyl acrylate) by single electron transfer-degenerative chain transfer living radical polymerization in water catalyzed by Na₂S₂O₄*. Journal of Polymer Science Part a-Polymer Chemistry, **2008**, *46*, 421-432.
307. Percec, V., Ramirez-Castillo, E., Popov, A. V., Hinojosa-Falcon, L. A., and Guliashvili, T., *Ultrafast single-electron-transfer/degenerative-chain-transfer mediated living radical polymerization of acrylates initiated with iodoform in water at room temperature and catalyzed by sodium dithionite*. Journal of Polymer Science Part a-Polymer Chemistry, **2005**, *43*, 2178-2184.
308. Coelho, J. F. J., Carvalho, E. Y., Marques, D. S., Popov, A. V., Gonçalves, P. M., and Gil, M. H., *Synthesis of poly(lauryl acrylate) by single-electron transfer/degenerative chain transfer living radical polymerization catalyzed by Na₂S₂O₄ in water*. Macromolecular Chemistry and Physics, **2007**, *208*, 1218-1227.
309. Coelho, J. F. J., Góis, J., Fonseca, A. C., Carvalho, R. A., Popov, A. V., Percec, V., and Gil, M. H., *Synthesis of Poly(2-methoxyethyl acrylate) by Single Electron Transfer-Degenerative Transfer Living Radical Polymerization Catalyzed by Na₂S₂O₄ in Water*. Journal of Polymer Science Part a-Polymer Chemistry, **2009**, *47*, 4454-4463.
310. Rocha, N., Coelho, J. F. J., Barros, B., Cardoso, P. M. L., Gonçalves, P. M., Gil, M. H., and Guthrie, J. T., *Deviation from the theoretical predictions in the synthesis of amphiphilic block copolymers in a wide range of compositions based on poly(vinyl chloride) by single electron transfer: Degenerative chain living radical polymerization in suspension medium*. Journal of Applied Polymer Science, **2013**, *127*, 3407-3417.
311. Rocha, N., *Interactions in Composite Polymeric Materials - Influence on Application Properties*, in *Chemical Engineering Department* **2010**, University of Coimbra: Coimbra.
312. Percec, V., Guliashvili, T., Popov, A. V., and Ramirez-Castillo, E., *Catalytic effect of dimethyl sulfoxide in the Cu(0)/tris(2-dimethylaminoethyl)amine-*

- catalyzed living radical polymerization of methyl methacrylate at 0-90 degrees C initiated with CH₃CHCl₂ as a model compound for alpha,omega-di(iodo)poly(vinyl chloride) chain ends.* Journal of Polymer Science Part a-Polymer Chemistry, **2005**, *43*, 1935-1947.
313. Sciannamea, V., Jérôme, R., and Detrembleur, C., *In-situ nitroxide-mediated radical polymerization (NMP) processes: Their understanding and optimization.* Chemical Reviews, **2008**, *108*, 1104-1126.
314. Lligadas, G., Rosen, B. M., Bell, C. A., Monteiro, M. J., and Percec, V., *Effect of Cu(0) Particle Size on the Kinetics of SET-LRP in DMSO and Cu-Mediated Radical Polymerization in MeCN at 25 °C.* Macromolecules, **2008**, *41*, 8365-8371.
315. Nguyen, N. H., Rosen, B. M., Lligadas, G., and Percec, V., *Surface-Dependent Kinetics of Cu(0)-Wire-Catalyzed Single-Electron Transfer Living Radical Polymerization of Methyl Acrylate in DMSO at 25 °C.* Macromolecules, **2009**, *42*, 2379-2386.
316. Lligadas, G., Rosen, B. M., Monteiro, M. J., and Percec, V., *Solvent Choice Differentiates SET-LRP and Cu-Mediated Radical Polymerization with Non-First-Order Kinetics.* Macromolecules, **2008**, *41*, 8360-8364.
317. Wright, P. M., Mantovani, G., and Haddleton, D. M., *Polymerization of methyl acrylate mediated by copper(0)/Me₆-TREN in hydrophobic media enhanced by phenols; Single electron transfer-living radical polymerization.* Journal of Polymer Science Part A: Polymer Chemistry, **2008**, *46*, 7376-7385.
318. Monteiro, M. J., Guliashvili, T., and Percec, V., *Kinetic simulation of single electron transfer-living radical polymerization of methyl acrylate at 25 °C.* Journal of Polymer Science Part A: Polymer Chemistry, **2007**, *45*, 1835-1847.
319. Lligadas, G. and Percec, V., *Synthesis of perfectly bifunctional polyacrylates by single-electron-transfer living radical polymerization.* Journal of Polymer Science Part A: Polymer Chemistry, **2007**, *45*, 4684-4695.
320. Lligadas, G., Ladislaw, J. S., Guliashvili, T., and Percec, V., *Functionally terminated poly(methyl acrylate) by SET-LRP initiated with CHBr₃ and CHI₃.* Journal of Polymer Science Part A: Polymer Chemistry, **2008**, *46*, 278-288.
321. Coelho, J. F. J., Fonseca, A. C., Gonçalves, P. M. F. O., Popov, A. V., and Gil, M. H., *Particle features and morphology of poly(vinyl chloride) prepared by living radical polymerisation in aqueous media. Insight about particle formation mechanism.* Polymer, **2011**, *52*, 2998-3010.
322. Hurtgen, M., Detrembleur, C., Jerome, C., and Debuigne, A., *Insight into Organometallic-Mediated Radical Polymerization.* Polymer Reviews, **2011**, *51*, 188-213.
323. Rocha, N., Coelho, J. F. J., Cardoso, P. M. L., Barros, B., Gonçalves, P. M., Gil, M. H., and Guthrie, J. T., *Synthesis of amphiphilic PVC-b-poly(hydroxypropyl*

- acrylate) (PHPA)-b-PVC block copolymers with low PHPA contents and different molecular weights by (Single Electron Transfer)—(Degenerative Chain Transfer) living radical polymerization. Journal of Vinyl and Additive Technology, 2013, 19, 157-167.*
324. Rocha, N., Coelho, J. F. J., Góis, J. R., Gil, M. H., Gonçalves, P. M., and Guthrie, J. T., *Poly(vinyl chloride)-b-poly(hydroxypropyl acrylate)-b-Poly(vinyl chloride): Understanding the synthesis of an amphiphilic PVC block copolymer on a pilot scale. Journal of Vinyl & Additive Technology, 2013, 19, 94-104.*

Chapter 2

Inorganic Sulfites: Efficient Reducing Agents and Supplemental Activators for Atom Transfer Radical Polymerization



The contents of this chapter are published in:

Abreu, C. M. R., Mendonça, P. V., Serra, A. C., Popov, A. V., Matyjaszewski, K., Guliashvili, T., and Coelho, J. F. J., *Inorganic Sulfites: Efficient Reducing Agents and Supplemental Activators for Atom Transfer Radical Polymerization*. ACS Macro Letters, **2012**, *1*, 1308-1311;

Mendes, J. P., Branco, F., Abreu, C. M. R., Mendonça, P. V., Popov, A. V., Guliashvili, T., Serra, A. C., and Coelho, J. F. J., *Synergistic Effect of 1-Butyl-3-methylimidazolium Hexafluorophosphate and DMSO in the SARA ATRP at Room Temperature Affording Very Fast Reactions and Polymers with Very Low Dispersity*. ACS Macro Letters, **2014**, *3*, 544-547.

2.1. Abstract

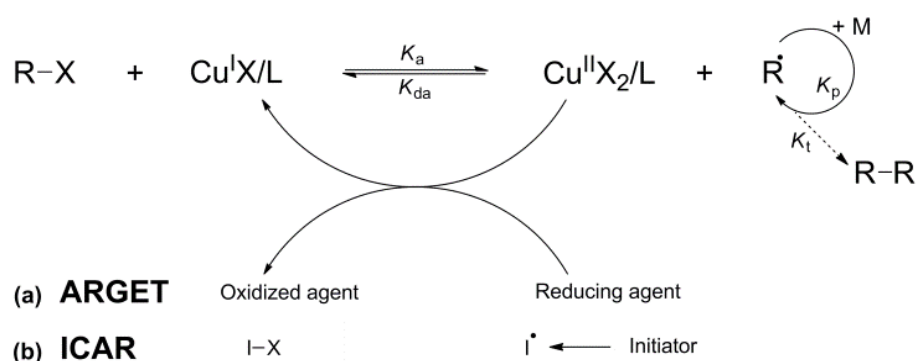
Inorganic sulfites such as sodium dithionite ($\text{Na}_2\text{S}_2\text{O}_4$), sodium metabisulfite ($\text{Na}_2\text{S}_2\text{O}_5$), and sodium bisulfite (NaHSO_3) have been studied as reducing agents for atom transfer radical polymerization (ATRP). They act not only as very efficient reducing agents but also as supplemental activators for SARA (supplemental activator and reducing agent) ATRP of methyl acrylate (MA) in dimethyl sulfoxide (DMSO) at ambient temperature. In combination with $\text{Cu(II)Br}_2/\text{Me}_6\text{TREN}$ (Me_6TREN : tris[2-(dimethylamino)ethyl]amine), they produced poly(methyl acrylate) (PMA) with controlled molecular weight, low dispersity ($D < 1.05$), and well-defined chain-end functionality. An unusual synergistic effect between an ionic liquid (IL), 1-butyl-3-methylimidazolium hexafluorophosphate (BMIM-PF_6), and DMSO mixtures is also reported. The use of ILs has never been reported for the SARA ATRP.

2.2. Introduction

Atom transfer radical polymerization (ATRP) is among the most efficient, versatile and robust reversible deactivation radical polymerization (RDRP) techniques.¹⁻⁷ It provides access to many polymeric materials with precisely controlled architecture, including stars, brushes, and nanogels, as well as block, gradient, and statistical copolymers with specific functionalities.⁸⁻¹⁵ Recently, new ATRP techniques were developed that permit reduction of transition metal complexes (typically copper with nitrogen-based ligands)⁶ used as redox active ATRP catalysts from ≥ 1000 ppm to less than 100 ppm in the presence of various reducing agents.¹⁶⁻²² The copper catalysts are responsible for forming a dynamic equilibration between tiny amounts of propagating radicals and alkyl halides as dormant species. As shown in Scheme 2.1, ATRP, as any RDRP, is accompanied by a biradical termination process, resulting in the irreversible conversion of Cu(I)/L activators to X-Cu(II)/L deactivators.

Consequently, a normal ATRP carried out with ppm amounts of Cu catalyst stops at low monomer conversion when the activator is converted to deactivator. New ATRP procedures employ various mild reducing agents that continuously regenerate the Cu(I)

species. In the ARGET^{17,22,23} (activators regenerated by electron transfer) ATRP process various organic (sugars, ascorbic acid, amines, etc.) or inorganic (e.g., tin (II) octoate) reducing agents (RA) have been used. Certain zerovalent transition metals, such as Cu, Fe, Zn, or Mg, act not only as reducing agents, but also as direct supplemental activators in SARA (supplemental activator and reducing agent) ATRP.^{16-18,24} ICAR²⁰ (initiators for continuous activator regeneration) ATRP employs conventional thermal radical initiators, such as diazo-compounds (AIBN), to react with the Cu(II) and to produce new chains. In recently reported electrochemically mediated ATRP (eATRP),²⁵ electrical current is used for the reduction process. In a similar way, light can be used in the photochemical activation/reduction process.²⁶⁻³¹



Scheme 2.1. General mechanism of (a) ARGET ATRP and (b) ICAR ATRP.

Nevertheless, the quest for efficient, inexpensive, safe, and environmentally benign reducing agents continues. Herein, it is reported the use of sulfites as a new class of efficient reducing agents (and supplemental activators) for ATRP. Sulfites are commonly used as inexpensive reducing agents in food preservation (especially wine), water treatment, leather, photography, bleach, and many other industrial chemical processes. It is tested the three most commonly used sulfites: sodium metabisulfite ($\text{Na}_2\text{S}_2\text{O}_5$), sodium dithionite ($\text{Na}_2\text{S}_2\text{O}_4$) and sodium bisulfite (NaHSO_3), as reducing agents in an ATRP of methyl acrylate (MA) carried out at ambient temperature in dimethyl sulfoxide (DMSO) solution. As will be further discussed, all sulfites performed as very efficient reducing agents. Subsequently, sodium dithionite (the most effective agent) was used in additional studies, aimed at the exploring range of effective concentrations, targeted molecular

weights and some mechanistic studies that suggest that it acted not only as a reducing agent but also as a supplemental activator, thus, following the SARA ATRP mechanism.

Ionic liquids (IL) are a class of green solvents³²⁻³⁴ that present important advantages over several conventional and harmful organic solvents. Among those, one can stress the possibility of tailoring the properties of the IL by varying the structures of both cation and anion, excellent solubility of polar substrates, low volatility, recyclability and compatibility with various organic compounds. Since the pioneer works of Haddleton,³⁵ Kubisa³⁶ and Matyjaszewski,³⁷ several reports have been published using IL as solvents for ATRP.^{32,38-41} The results revealed interesting features of these green solvents related to simplified separation of the polymer from the catalyst,^{35,37} controlled reactions in the absence of ligand, reduction of side reactions and catalytic effects.³⁸ Here, it is also reported the synergistic effect of DMSO and 1-butyl-3-methylimidazolium hexafluorophosphate (BMIM-PF₆) in the SARA ATRP of MA catalyzed by Na₂S₂O₄ and small amounts of CuBr₂/Me₆TREN deactivator complex at room temperature.

2.3. Experimental Section

2.3.1. Materials

Methyl Acrylate (MA) (Acros, 99% stabilized), was passed through a sand/alumina column before use in order to remove the radical inhibitor. Na₂S₂O₄ (Merck, >87%), Na₂S₂O₅ (Sigma–Aldrich, >99 %), NaHSO₃ (Sigma–Aldrich, >99 %), Cu(II)Br₂ (Acros, 99+% extra pure, anhydrous), deuterated chloroform (CDCl₃) (Euriso-top, +1% TMS), DMSO (Acros, 99.8+% extra pure), ethyl 2-bromoisobutyrate (EBiB) (Sigma-Aldrich, 98%), pentaerythritol tetrakis(2-bromoisobutyrate) (4f-BiB, 97 %; Sigma-Aldrich), N,N,N',N'',N'''-pentamethyldiethylenetriamine (PMDETA, 99 %; Aldrich), tetrabutylammonium hexafluorophosphate (TBAPF₆, 98 %, Sigma-Aldrich), Reichardt's dye (30) (90 %, Sigma-Aldrich), 1-butyl-3-methylimidazolium hexafluorophosphate (BMIM-PF₆, > 98 %; TCI (Tokyo Chemical Industry Co. LTD)), hexane (Fisher Chemical, 95%), polystyrene (PS) standards (Polymer Laboratories), 2-(4-hydroxyphenylazo)benzoic acid (HABA) (Sigma–Aldrich, 99.5 %) and 2,5-

dihydroxybenzoic acid (DHB) (Sigma–Aldrich, >99 %) were used as received. Tetrahydrofuran (THF) (Panreac, HPLC grade) was filtered under reduced pressure before use. Me₆TREN was synthesized according the procedure described in the literature.⁴²

2.3.2. Techniques

The chromatographic parameters of the samples were determined using high performance gel permeation chromatography HPSEC; Viscotek (ViscotekTDAmix) with a differential viscometer (DV); right-angle laser-light scattering (RALLS, Viscotek); low-angle laser-light scattering (LALLS, Viscotek) and refractive index (RI) detectors. The column set consisted of a PL 10 mm guard column (50 × 7.5 mm²) followed by one Viscotek T200 column (6 μm), one MIXED-E PLgel column (3 μm) and one MIXED-C PLgel column (5 μm). The HPLC dual piston pump was set at a flow rate of 1 mL/min. The eluent (THF) was previously filtered through a 0.2 μm filter. The system was also equipped with an on-line degasser. The tests were done at 30 °C using an Elder CH-150 heater. The samples were filtered through a polytetrafluoroethylene (PTFE) membrane with 0.2 μm pore before injection (100 μL). The system was calibrated with narrow PS standards. The dn/dc was determined as 0.063 for PMA. Molecular weight ($M_{n, GPC}$) and dispersity (\mathcal{D}) of synthesized polymers were determined by Multidetectors calibration using OmniSEC software version: 4.6.1.354.

400 MHz ¹H NMR spectra were recorded on a BrukerAvance III 400 MHz spectrometer, with a 5-mm TIX triple resonance detection probe, in CDCl₃ with tetramethylsilane (TMS) as an internal standard. Conversion of the monomer was determined by integration of monomer and polymer peaks using MestRenova software version: 6.0.2-5475.

The PMA samples were dissolved in THF at a concentration of 10 mg/mL for the MALDI-TOF-MS analysis and DHB and HABA (0.05 M in THF) were used as matrices. The dried-droplet sample preparation technique was used to obtain a 1:1 ratio (sample/matrix); an aliquot of 1 μL of each sample was directly spotted on the MTP AnchorChip TM 600/384 TF MALDI target, BrukerDaltonik (Bremen Germany) and, before the sample dried, 1 μL of matrix solution in THF was added and the mixture

allowed to dry at room temperature, to allow matrix crystallization. External mass calibration was performed with a peptide calibration standard (PSCII) for the range 700-3000 (9 mass calibration points), 0.5 μL of the calibration solution and matrix previously mixed in an eppendorf tube (1:2, v/v) were applied directly on the target and allowed to dry at room temperature. Mass spectra were recorded using an Autoflex III smartbeam1 MALDI-TOF-MS mass spectrometer BrukerDaltonik (Bremen, Germany) operating in the linear and reflectron positive ion mode. Ions were formed upon irradiation by a smartbeam laser using a frequency of 200 Hz. Each mass spectrum was produced by averaging 2500 laser shots collected across the whole sample spot surface by screening in the range m/z 500-7500. The laser irradiance was set to 35-40 % (relative scale 0-100) arbitrary units according to the corresponding threshold required for the applied matrix systems.

The UV/Vis studies were performed with a Jasco V-530 spectrophotometer. The analyses were carried out in the 200–1100 nm range at room temperature (rt).

Rheological experiments were conducted in a HAAKE™ MARS III Rotational Rheometer (Thermo Scientific, Inc.) and the data were analyzed using the HAKKE RheoWin software. The rheometer was equipped with a C35-mm cone with a 1° angle probe geometry and with a Peltier system as the temperature control unit. Rotational measurements were carried out to determine the Newtonian viscosity values of BMIM-PF₆/DMSO mixtures with different volumetric compositions (0/100, 5/95, 25/75, 50/50, 75/25, 95/5 and 100/0) at 30 °C, by performing stress sweep tests between 0.01 and 100 Pa under steady-state conditions.

2.3.3. Procedures

Typical procedure for the ATRP of MA (DP = 222) catalyzed by $[\text{Na}_2\text{S}_2\text{O}_4]/[\text{CuBr}_2]/[\text{Me}_6\text{TREN}] = 1/0.1/0.1$ in DMSO

The monomer (MA) was purified by passage through in a sand/alumina column just before addition to the reaction. A mixture of CuBr_2 (7.0 mg, 0.031 mmol), Me_6TREN (7.2 mg, 0.031 mmol) and DMSO (3.2 mL) (previously bubbled with nitrogen for

about 15 minutes) was placed in a Schlenk tube reactor that was sealed by using rubber septa. $\text{Na}_2\text{S}_2\text{O}_4$ (54.7 mg, 0.314 mmol) and a mixture of MA (6.3 mL, 69.7 mmol) and EBiB (61.2 mg, 0.314 mmol) was added to the reactor and frozen in liquid nitrogen. The Schlenk tube reactor containing the reaction mixture was deoxygenated with five freeze-vacuum-thaw cycles and purged with nitrogen. The Schlenk tube reactor was placed in an water bath at 30 °C with stirring (700 rpm). Samples of the reaction mixture were collected periodically during the polymerization by using an airtight syringe and purging the side arm of the Schlenk tube reactor with nitrogen. The samples were analyzed by ^1H NMR spectroscopy in order to determine the monomer conversion and by GPC, to determine $M_{n,\text{GPC}}$ and \bar{D} of the PMA.

Chain extension experiment: polymerization from a Br terminated PMA macroinitiator

The Br–PMA macroinitiator was obtained from a typical $\text{Na}_2\text{S}_2\text{O}_4/\text{CuBr}_2/\text{Me}_6\text{TREN}$ catalyzed ATRP reaction after precipitation in hexane. The polymer was then dissolved in THF and filtered through a sand/alumina column to remove traces of the catalyst and was reprecipitated in hexane again. The polymer was dried under vacuum until constant weight. The MA (6.3 mL, 69.7mmol) was purified in a sand/alumina column just before reaction and then added to the Br terminated PMA macroinitiator ($M_{n,\text{GPC}} = 4100$; $\bar{D} = 1.05$, 253.4 mg, 0.063mmol) in the Schlenk tube reactor. DMSO (2.0 mL previously bubbled with nitrogen for about 15 min) was added to the monomer/macroinitiator mixture in order to completely dissolve the macroinitiator. $\text{Na}_2\text{S}_2\text{O}_4$ (11.0 mg, 0.063mmol), DMSO (1.2 mL), CuBr_2 (1.4 mg, 0.006mmol) and Me_6TREN (1.5 mg, 0.006mmol) were added to the reactor. The Schlenk tube was deoxygenated by five freeze-pump thaw cycles and purged with nitrogen. Then the reactor was placed in the water bath at 30 °C with stirring (700 rpm). The reaction was stopped after 4 h and the mixture was analyzed by GPC.

UV/Vis spectroscopy of Na₂S₂O₄/CuBr₂/Me₆TREN

The solid catalyst(s) were placed in a quartz UV/Vis cell and purged with nitrogen. DMSO and Me₆TREN were mixed in a vial and bubbled with nitrogen for about 15 min to remove oxygen. This solution was then added to the UV/Vis cell, which was sealed under nitrogen. After shaking to dissolve the solids, the cell was placed in the spectrophotometer for spectra acquisition. The absorbance was measured at different times, in the 200–1100 nm range at room temperature.

Typical Procedure for the [Na₂S₂O₄]/[CuBr₂]/[Me₆TREN] = 1/0.1/0.1 catalyzed SARA ATRP of MA (DP=222) in BMIM-PF₆/DMSO = 50/50 (v/v)

In a typical SARA ATRP polymerization of MA, Na₂S₂O₄ (30.62 mg, 0.16 mmol) was placed in Schlenk reactor. A mixture of CuBr₂ (3.55 mg, 0.16 mmol), Me₆TREN (3.69 mg, 0.02 mmol) and DMSO (0.785 mL) was added to the reactor and after this a mixture of MA (3.14 mL, 34.8 mmol), EBiB (30.62 mg, 0.16 mmol) and BMIM-PF₆ (0.785 mL) was also added to the Schlenk that was sealed and frozen in liquid nitrogen. The Schlenk reactor containing the reaction mixture was deoxygenated with four freeze-vacuum-thaw cycles and purged with nitrogen. The reactor was placed in a water bath at 30 °C with stirring (700 rpm). During the polymerization, different reaction mixture samples were collected by using an airtight syringe and purging the side arm of the Schlenk reactor with nitrogen. The samples were analyzed by ¹H NMR spectroscopy to determine the monomer conversion and by GPC, to determine the $M_{n,GPC}$ and \bar{D} of the polymers.

Determination of $E_T(30)$ in BMIM-PF₆/DMSO mixtures

Different BMIM-PF₆/DMSO mixtures (5.0 mL) were prepared and small amounts of Reichardt's dye 30 (0.138 mg, 50 μM) were added. These solutions were then added to the UV/Vis cuvette and placed in the spectrophotometer for spectra acquisition. The absorbance was measured, in the 350-1100 nm range at room temperature. The $E_T(30)$ values of different BMIM-PF₆ mixtures were determined according to the expression $E_T(30) = 28591.5/\lambda_{\text{abs,máx}}(\text{nm})$.⁴³

2.4. Results and Discussion

2.4.1. SARA ATRP using Inorganic Sulfites

Preliminary experiments were conducted at ambient temperature (30 °C) in dimethylsulfoxide (DMSO) using $\text{Na}_2\text{S}_2\text{O}_4$, $\text{Na}_2\text{S}_2\text{O}_5$ and NaHSO_3 as reducing agents in an ATRP of MA. The kinetic plots are shown in Figure 2.1. The targeted number average molecular weight at full conversion was $M_n = 20000$. The catalyst was added at 10 mol % versus initiator (EBiB), and a reducing agent was added at an equimolar concentration to the initiator.

The rate of polymerization was first order in respect to monomer concentration with all three reducing agents (Figure 2.1), and the molecular weights determined by GPC were in good agreement with the theoretical values, indicating an efficient initiation and excellent control during polymerization. This is confirmed by low dispersity values of the obtained polymers (D : M_w/M_n always < 1.1) from the beginning of the polymerization to high conversion. A comparison of the kinetic data indicates that $\text{Na}_2\text{S}_2\text{O}_4$ provided the fastest polymerization of MA, indicating it is a more efficient reducing agent, allowing faster (re)generation of active Cu(I)Br/L catalyst. Reactions with sodium metabisulfite were 3.5 times slower and, with sodium bisulfite, about 2.3 times slower.

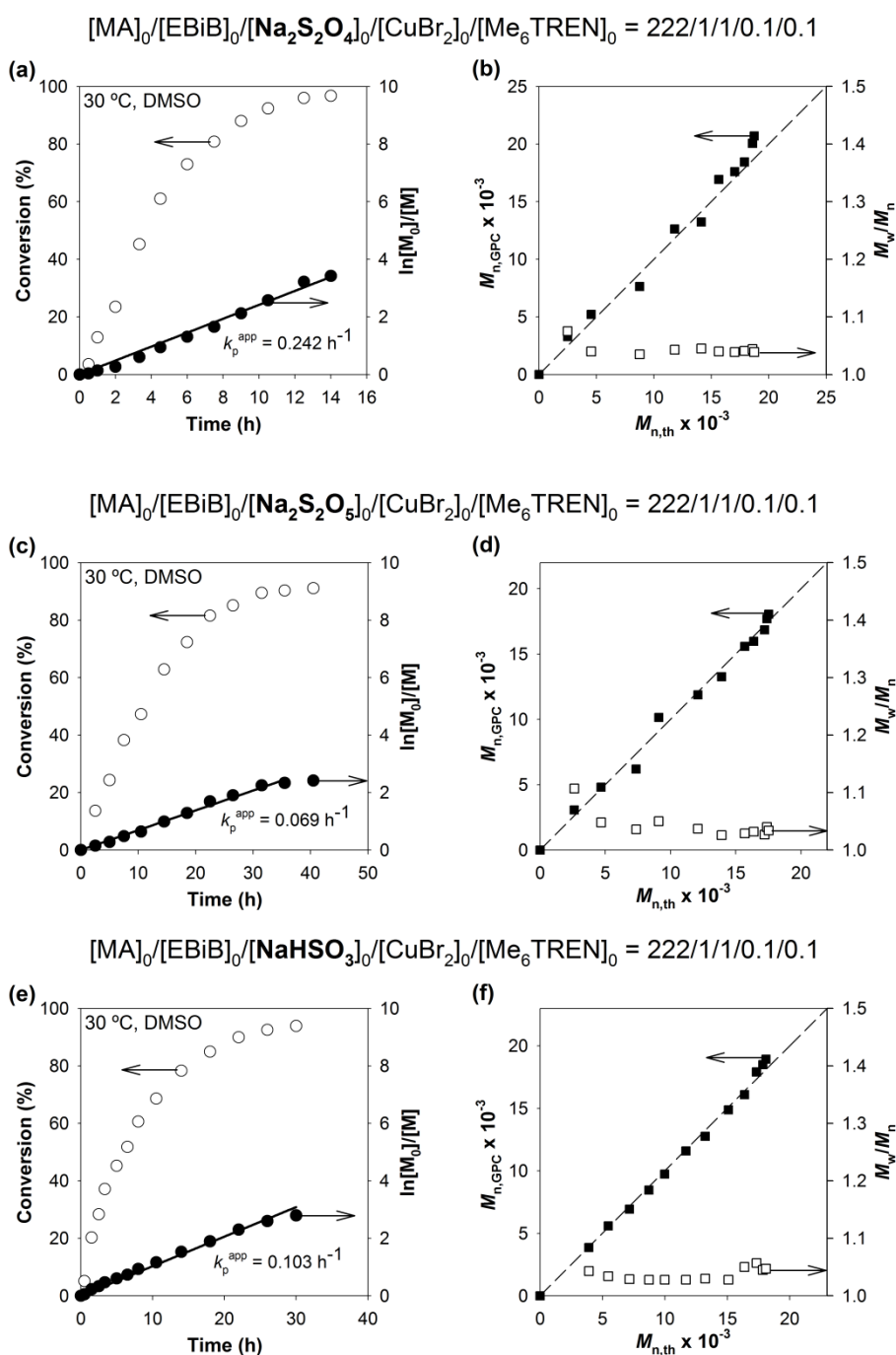


Figure 2.1. Kinetic plots of MA conversion and $\ln[M]_0/[M]$ vs. time (a, c and e) and plot of number average molecular weights ($M_{n,GPC}$) and \mathcal{D} (M_w/M_n) vs. theoretical number-average molecular weights ($M_{n,th}$) (b, d and f) for ATRP of MA in the presence of $CuBr_2/Me_6TREN$ with different reducing agents (RA = $Na_2S_2O_4$ (a and b), $Na_2S_2O_5$ (c and d) and $NaHSO_3$ (e and f). Conditions: $[MA]_0/[EBiB]_0/[RA]_0/[CuBr_2]_0/[Me_6TREN]_0 = 222/1/1/0.1/0.1$ at 30 °C in DMSO; $[MA]_0/[DMSO] = 2/1$ (v/v).

2.4.2. Model Experiments to Elucidate the SARA ATRP Mechanism

Because dithionite ($\text{Na}_2\text{S}_2\text{O}_4$) was the most efficient reducing agent, it was used in subsequent studies that are presented in Table 2.1. The ratio of $[\text{Na}_2\text{S}_2\text{O}_4]_0/[\text{CuBr}_2]_0$ was varied between 0.5/0.1 and 2/0.1 (Figure 2.2 and Table 2.1, entries 1-3). Independent of the ratio used, the control over the PMA molecular weight during polymerization was excellent. Molecular weights determined by GPC matched very well the theoretical values and low D values were obtained for the PMA. A higher $[\text{Na}_2\text{S}_2\text{O}_4]_0/[\text{CuBr}_2]_0$ ratio leads to a faster polymerization. However, the increase in the polymerization rate was relatively small, due to the limited solubility of $\text{Na}_2\text{S}_2\text{O}_4$ in the DMSO/MA mixture.

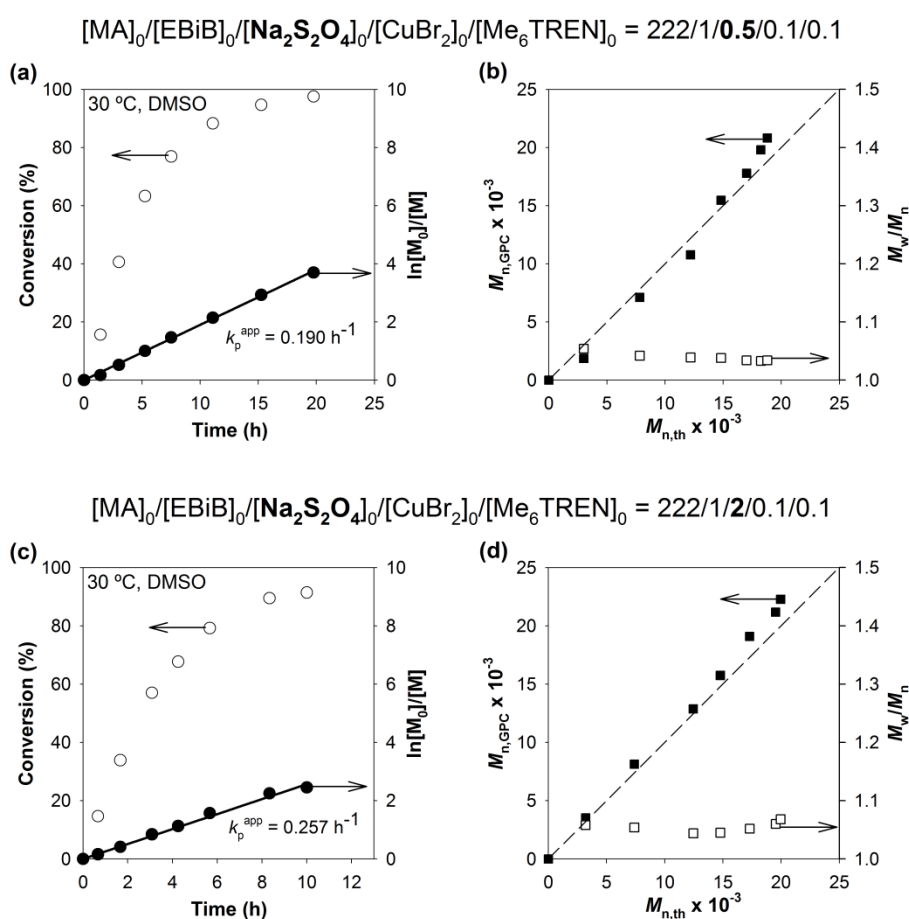


Figure 2.2. Kinetic plots of monomer conversion and $\ln[M]_0/[M]$ vs. time (a and c) and plot of $M_{n,\text{GPC}}$ and D (M_w/M_n) vs. $M_{n,\text{th}}$ (b and d) for SARA ATRP of MA catalyzed with mixed catalyst system $\text{Na}_2\text{S}_2\text{O}_4/\text{CuBr}_2/\text{Me}_6\text{TREN}$ for different $[\text{Na}_2\text{S}_2\text{O}_4]_0/[\text{CuBr}_2]_0$: 0.5/0.1 (a and b) and 2/0.1 (c and d). Conditions: $[\text{MA}]_0/[\text{EBiB}]_0/[\text{Na}_2\text{S}_2\text{O}_4]_0/[\text{CuBr}_2]_0/[\text{Me}_6\text{TREN}]_0 = 222/1/(0.5 \text{ or } 2)/0.1/0.1$ at 30 °C in DMSO; $[\text{MA}]_0/[\text{DMSO}] = 2/1$ (v/v).

The next series of experiments were carried out to elucidate the mechanism of ATRP in the presence of sulfites. No polymer was formed during the initial experiment with only MA, initiator, and Cu(II)Br₂/Me₆TREN deactivator (i.e., in absence of Na₂S₂O₄), Table 2.1, entry 4. However, polymerization of MA did occur without Cu(II)Br₂/Me₆TREN in the presence of Na₂S₂O₄, both in the absence and in the presence of the ATRP initiator (Figure 2.3 and Table 2.1, entry 5 and 6).

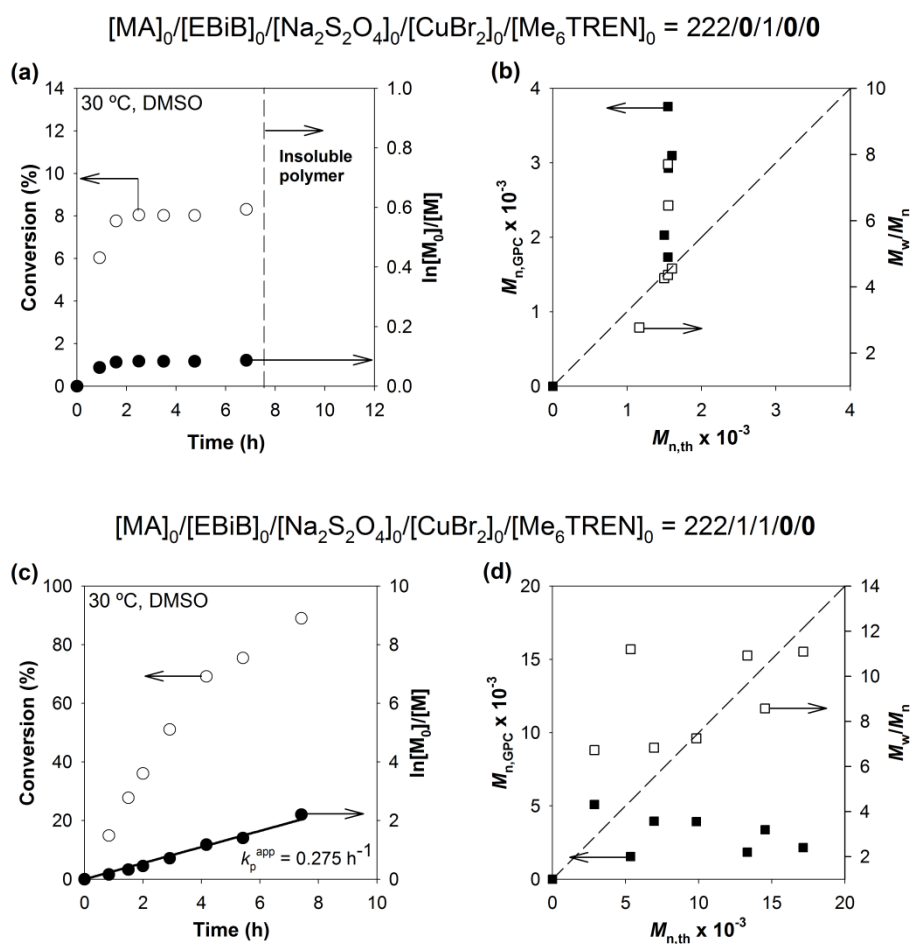


Figure 2.3. Kinetic plots of monomer conversion and $\ln[M]_0/[M]$ vs. time (a and c) and plot of $M_{n,GPC}$ and \bar{D} (M_w/M_n) vs. $M_{n,th}$ (b and d) for $[MA]_0/[Na_2S_2O_4]_0 = 222/1$ (a and b) and $[MA]_0/[EBiB]_0/[Na_2S_2O_4]_0 = 222/1/1$ (c and d) at 30 °C in DMSO; $[MA]_0/[DMSO] = 2/1$ (v/v).

In both cases the polymerization of MA occurred, but in an uncontrolled manner, as evidenced by very high dispersity values. Surprisingly, the reaction was much faster in the presence of the ATRP initiator, suggesting that sulfites can act as supplemental activators for alkyl halides.

The reduction process of $\text{Cu(II)Br}_2/\text{Me}_6\text{TREN}$ by $\text{Na}_2\text{S}_2\text{O}_4$ in pure DMSO was studied by UV-vis spectroscopy (Figure 2.4), which showed that the dithionite acted as a powerful reducing agent, converting half of Cu(II) species into Cu(I) activators within about 20 min. This indicates that the sulfites act both as supplemental activators and reducing agents, following the SARA ATRP mechanism. The very slow polymerization initiated solely by $\text{Na}_2\text{S}_2\text{O}_4$ could be due to a very small contribution from dissociation of dithionite anions to $\text{SO}_2^{\cdot-}$ radical anions that can directly initiate polymerization.

The conditions used in SARA ATRP with sulfites are similar to the so called SET-LRP⁴⁴ process in the presence of zerovalent copper. However, mechanistically SET-LRP follows SARA ATRP with copper acting as supplemental activator and reducing agent.⁴⁵⁻⁴⁸

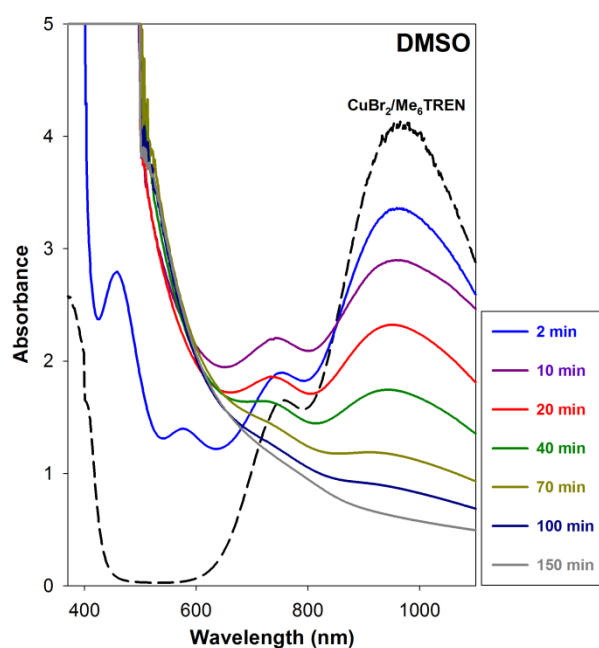


Figure 2.4. The UV-vis spectra of reduction of $\text{Cu(II)Br}_2/\text{Me}_6\text{TREN}$ by $\text{Na}_2\text{S}_2\text{O}_4$ in DMSO recorded at different reaction times (30 °C), $[\text{Na}_2\text{S}_2\text{O}_4]_0/[\text{CuBr}_2]_0/[\text{Me}_6\text{TREN}]_0 = 0.1/0.01/0.01$ mmol/mL.

Table 2.1. SARA ATRP of MA in the Presence of CuBr₂/Me₆TREN and Na₂S₂O₄ at 30 °C in DMSO (33 vol% DMSO).

Entry	[MA] ₀ /[EBiB] ₀ /[Na ₂ S ₂ O ₄] ₀ /[CuBr ₂] ₀ /[Me ₆ TREN] ₀	k _p ^{app} (h ⁻¹)	Time (h) ^a	Conv. (%) ^a	M _{n,th} x 10 ^{-3a}	M _{n,GPC} x 10 ^{-3a}	M _w /M _n ^a
1	222/1/1/0.1/0.1	0.242	14.0	96.7	18.7	20.7	1.04
2	222/1/0.5/0.1/0.1	0.190	19.8	97.5	18.8	20.8	1.03
3	222/1/2/0.1/0.1	0.257	10.0	91.4	19.5	21.2	1.06
4	222/1/0/0.1/0.1	-	50.0	0	-	-	-
5	222/0/1/0/0	0.018	6.8 ^b	8.3 ^b	1.60 ^b	3.10 ^b	4.55 ^b
6	222/1/1/0/0	0.275	7.4	89.0	17.2	2.10	11.09
7	70/1/1/0.1/0.1	0.366	8.8	95.6	5.90	6.40	1.07
8	1100/1/1/0.1/0.1	0.115	30.5	96.5	88.6	91.8	1.05
[MMA]₀/[EBiB]₀/[Na₂S₂O₄]₀/[CuBr₂]₀/[Me₆TREN]₀							
9	222/1/1/0.1/0.1	-	20.0	97.6	22.8	26.4	1.12
[S]₀/[EBiB]₀/[Na₂S₂O₄]₀/[CuBr₂]₀/[Me₆TREN]₀							
10	222/1/1/0.1/0.1 ^c	-	150.0	16.4	3.80	4.70	1.06
11	222/1/1/0.1/0.1 ^{c,d}	-	100.0	87.3	20.4	28.7	1.15

^aValues obtained from the last sample from the kinetic studies.

^bAfter 7 hours an insoluble polymer was formed.

^cDMF was used as solvent.

^dReaction temperature T = 60° C.

2.4.3. Variation of Targeted Degree of Polymerization and Monomer

The effect of the target molecular weight on the control over the polymerization is a critical parameter that should be evaluated, since it could lead to possible solubility issues of the polymer in the reaction mixture. Therefore, different targeted degrees of polymerization (DP) were investigated for the SARA ATRP of MA (Figure 2.5 and Table 2.1, entries 1, 7, 8). The polymerization rate decreased with increased targeted DP, due to the lower number of growing macroradicals. It is remarkable to note that even for the DP = 1100 the PMA dispersity values were very low ($\mathcal{D} = 1.05$) even at very high monomer conversion (96.5%), indicating minimal contribution of any side reactions with $\text{Na}_2\text{S}_2\text{O}_4$.

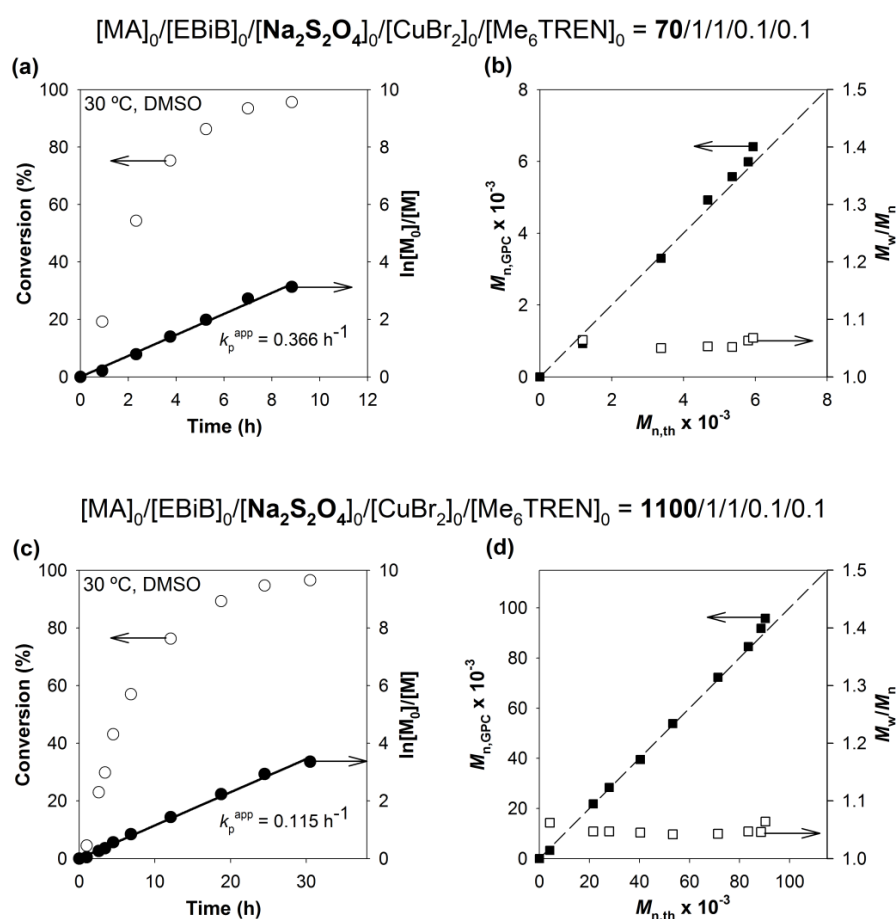


Figure 2.5. Kinetic plots of monomer conversion and $\ln[M]_0/[M]$ vs. time (a and c) and plot of $M_{n,\text{GPC}}$ and \mathcal{D} (M_w/M_n) vs. $M_{n,\text{th}}$ (b and d) for SARA ATRP of MA catalyzed with mixed catalyst system $\text{Na}_2\text{S}_2\text{O}_4/\text{CuBr}_2/\text{Me}_6\text{TREN}$ for different DP's: 70 (a and b) and 1100 (c and d). Conditions: $[\text{MA}]_0/[\text{EBiB}]_0/[\text{Na}_2\text{S}_2\text{O}_4]_0/[\text{CuBr}_2]_0/[\text{Me}_6\text{TREN}]_0 = (70 \text{ or } 1100)/1/1/0.1/0.1$ at 30°C in DMSO; $[\text{MA}]_0/[\text{DMSO}] = 2/1$ (v/v).

The new catalytic system reported in this manuscript was successfully extended to polymerization of methyl methacrylate (MMA) and styrene (S) (Table 1, entries 9-11). It is remarkable that this new catalytic system showed comparable or even better performance and control during polymerization compared to related systems with Cu(0) as an initial catalyst in DMSO or DMF respectively.

2.4.4. Solvent Mixtures of BMIM-PF₆ and DMSO in the SARA ATRP Using Inorganic Sulfites

Due to the promising results reported in the literature involving the use of ILs in radical based polymerizations,³⁵⁻³⁷ the effect of BMIM-PF₆ was evaluated in this SARA ATRP system. Preliminary experiments were performed using only BMIM-PF₆ as solvent for the MA polymerization, but no polymer was formed. This result can be justified based on the partial solubilization of the CuBr₂/Me₆TREN complex and, most importantly, to the complete insolubility of the SARA agent (Na₂S₂O₄) in the BMIM-PF₆, preventing the formation of Cu(I) activator species. With the introduction of DMSO as a cosolvent a controlled polymerization was observed. The kinetic plots of SARA ATRP carried out at room temperature in BMIM-PF₆/DMSO (ratio 5/95 and 50/50) catalyzed by Na₂S₂O₄/CuBr₂/Me₆TREN are presented in Figure 2.6 and Table 2.2 (entry 2 and 4), respectively.

The rate of polymerization (Figure 2.6) was first-order with respect to the concentration of monomer and the final conversion was close to 100%. The theoretical molecular weights were in very close agreement with $M_{n, GPC}$ for the full range of monomer conversions, which indicates a quantitative initiation and an excellent control during the entire course of the polymerization. Interesting, for a BMIM-PF₆/DMSO ratio of 50/50 (Figure 2.6 (c and d) and Table 2.2, entry 4), the kinetic data allowed us to draw the same conclusions as the ones obtained for a ratio of 5/95. However, the reaction rate was 3 times faster for the ratio 50/50 (6 times faster than the obtained for pure DMSO, Table 2.2, entry 1). In order to determine the optimal ratio BMIM-PF₆/DMSO to afford fast polymerization while maintaining the living characteristics of the system, different ratios were investigated (Figure 2.7, Figure A.1 in Appendix A, and Table 2.2, entries 1-6).

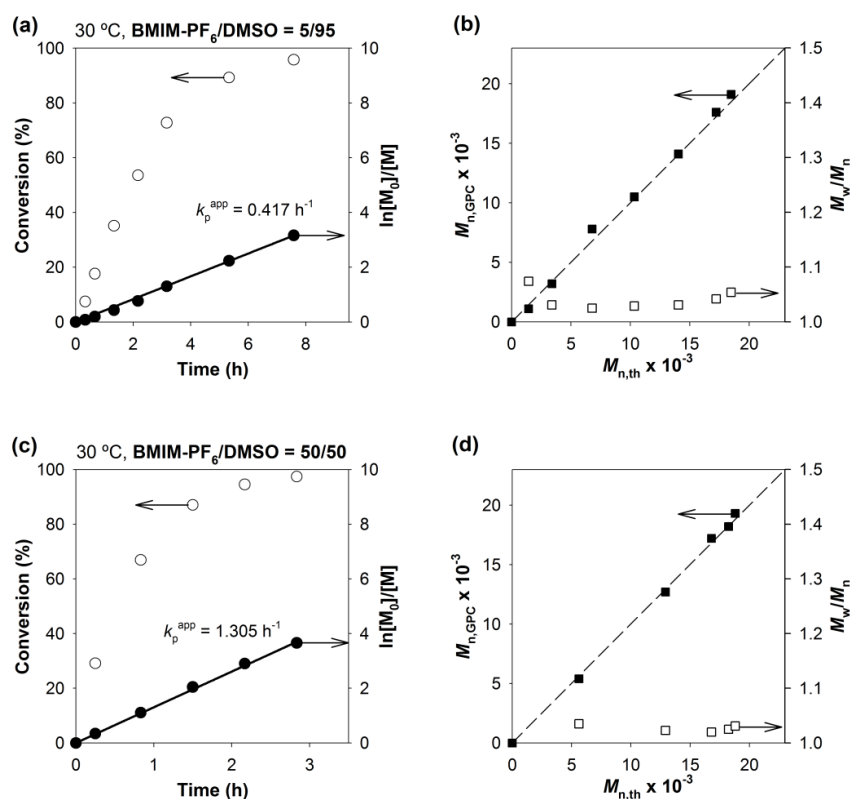


Figure 2.6. Kinetic plots of conversion and $\ln[M]_0/[M]$ vs. time (a and c) and plots of $M_{n,GPC}$ and \bar{D} (M_w/M_n) vs. $M_{n,th}$ (b and d) for the SARA ATRP of MA catalyzed by $\text{Na}_2\text{S}_2\text{O}_4/\text{CuBr}_2/\text{Me}_6\text{TREN}$ in (a and b) BMIM-PF₆/DMSO = 5/95 (v/v) and (c and d) BMIM-PF₆/DMSO = 50/50 (v/v). Conditions: $[\text{MA}]_0/[\text{solvent}] = 2/1$ (v/v); $[\text{MA}]_0/[\text{EBiB}]_0/[\text{Na}_2\text{S}_2\text{O}_4]_0/[\text{CuBr}_2]_0/[\text{Me}_6\text{TREN}]_0 = 222/1/1/0.1/0.1$ (molar); $T = 30 \text{ }^\circ\text{C}$.

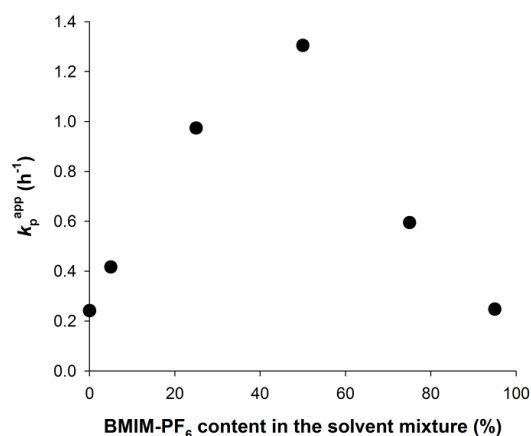


Figure 2.7. k_p^{app} values of the SARA ATRP of MA catalyzed by $\text{Na}_2\text{S}_2\text{O}_4/\text{CuBr}_2/\text{Me}_6\text{TREN}$ in BMIM-PF₆/DMSO mixtures, for different contents of BMIM-PF₆ in the reaction mixture. Conditions: $[\text{MA}]_0/[\text{solvent}] = 2/1$ (v/v); $[\text{MA}]_0/[\text{EBiB}]_0/[\text{Na}_2\text{S}_2\text{O}_4]_0/[\text{CuBr}_2]_0/[\text{Me}_6\text{TREN}]_0 = 222/1/1/0.1/0.1$ (molar); $T = 30 \text{ }^\circ\text{C}$.

Regardless the solvent ratio studied the control over the SARA ATRP of MA was perfect (\bar{D} always below 1.07) (Table 2.2). Indeed, the only observed difference was the overall polymerization rate, which as referred above was faster for the ratio DMSO/IL = 50/50. It is interesting to note that this ratio represents an optimum value for the mixture, which suggests that there is a synergistic effect between the two solvents (Figure 2.7).

Considering the perfect miscibility of the BMIM-PF₆ and DMSO for the different mixtures, it is believed that the polarity values of the mixture may play an important role in the kinetics of the polymerization. In this regard, it was reported that mixtures of BMIM-PF₆ and tetraethylene glycol (TEG) exhibit unusual synergistic solvent effect, particularly a remarkable “hyperpolarity” for the mixture. In the presence of solvatochromic probes, as $E_T(33)$, polarity of the medium is always higher in the mixtures than in pure solvents reaching a maximum value for equimolar mixtures of the two solvents.⁴³ Using this analogy, absorbance spectra of Reichardt’s dye (30) were collected in BMIM-PF₆/DMSO mixtures (Figure 2.8), showing that value of $E_T(30)$ for the different mixtures exceeds the value predicted by the simple mixture indicating that some synergistic effect occurs.

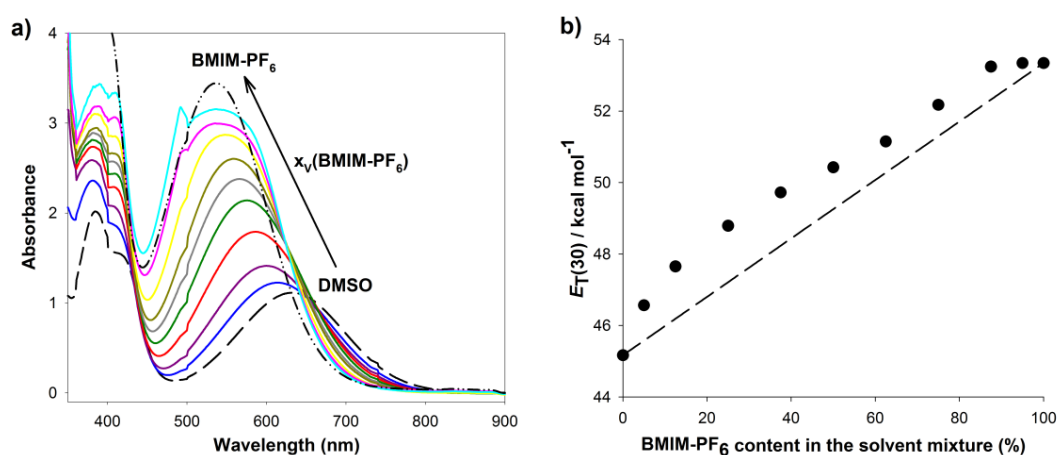


Figure 2.8. a) UV-Vis spectra in different BMIM-PF₆/DMSO mixtures with Reichardt’s dye 30 (50 μ M); b) Experimental $E_T(30)$ value in different BMIM-PF₆/DMSO mixtures (the dashed line represents the predicted $E_T(30)$).

Table 2.2. Kinetic Data for the SARA ATRP of MA in BMIM-PF₆/DMSO Mixtures.^a

Entry	BMIM-PF ₆ /DMSO ratio	Targeted DP	k_p^{app} (h ⁻¹)	Time (h) ^b	Conv. (%) ^b	$M_{n,\text{th}} \times 10^{-3b}$	$M_{n,\text{GPC}} \times 10^{-3b}$	M_w/M_n^b
1	0/100	222	0.242	14	97	18.7	20.7	1.04
2	5/95	222	0.417	7.5	96	18.5	19.1	1.05
3	25/75	222	0.974	3.6	97	18.7	20.2	1.04
4	50/50	222	1.305	2.8	98	18.8	19.3	1.03
5	75/25	222	0.595	5.9	97	18.7	19.5	1.03
6	95/5	222	0.248	10.5	93	17.9	19.1	1.07
7	50/50	100	1.588	1.7	93	8.20	8.30	1.04

^aConditions: [MA]₀/[solvent] = 2/1 (v/v); [MA]₀/[EBiB]₀/[Na₂S₂O₄]₀/[CuBr₂]₀/[Me₆TREN]₀ = DP/1/1/0.1/0.1; T = 30 °C.

^bMaximum monomer conversion obtained in the reaction.

On the other hand, the kinetic data using tetrabutylammonium hexafluorophosphate (TBAPF₆) was determined in order to evaluate if the previous results were due to the BMIM-PF₆ structure, or the speed up effect could be mainly due to the anion (PF₆). When the ratio TBAPF₆/DMSO 6/94 (Figure A.2 in Appendix A) was used, the obtained k_p^{app} was 0.295 h⁻¹, which is higher than using pure DMSO, but much lower than the value obtained for a mixture BMIM-PF₆/DMSO (5/95).

Table 2.2 summarizes the kinetic data obtained for SARA ATRP of MA in the presence of Na₂S₂O₄/CuBr₂/Me₆TREN in BMIM-PF₆/DMSO mixtures at 30 °C. Independently of the BMIM-PF₆/DMSO ratio used, the polymer architecture or the target molecular weight, the reported system allowed the synthesis of well-defined PMA at room temperature with very low dispersity ($\mathcal{D} < 1.1$) below the reported values using the same IL. The efficiency of initiation was always close 100%.

The level of control obtained under the different polymerization conditions investigated should be a direct consequence of three main aspects: high propagation rates; absence of side reactions, and fast reduction of Cu(II) species to Cu(I). On this matter, the use of IL is known to decrease the activation energy involved in the propagation steps due to high polarity.⁴⁹ The increase in the rate of polymerization was postulated based on a complex formation between the growing radicals and the IL.⁵⁰ The hypothesis was later confirmed by showing that when chiral IL were used more isotactic sequences were formed.³⁹ In contrast, the termination rate decreases³⁶ due to higher viscosity limiting the diffusion of radicals.⁴⁹

In order to evaluate the viscosity of the solvent mixture BMIM-PF₆/DMSO, rheology tests were carried out (Figure 2.9). Indeed, it was observed that there was no relevant variation of the viscosity up to a ratio 50/50. However, for higher contents of BMIM-PF₆, the increase of the viscosity was found exponential. These results show that the observed maximum rate of polymerization (k_p^{app}) at 50/50 vol % composition of BMIM-PF₆/DMSO cannot be simply explained solely based on viscosity changes and, hence, the k_p/k_t value increase. Thus, the results suggest that while IL favors k_p/k_t increase (well-known fact) the role of DMSO seems to be more complex.

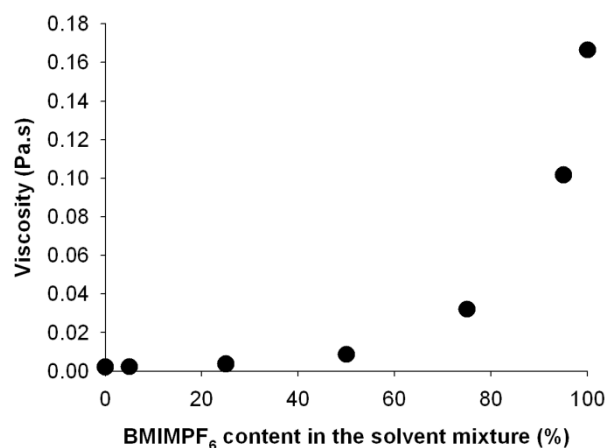


Figure 2.9. Viscosity values in different BMIM-PF₆/DMSO mixtures.

Besides the influence on the reduction rate of Cu(II) to Cu(I) (highest rate observed for ratio 50/50, see Figure A.3 in Appendix A), the DMSO may also have an important role on the mechanism involving the radical generation. The data presented in this work suggests that the ideal balance of the different factors described is observed for a ratio 50/50. The clear understanding of the full mechanism requires additional studies.

2.4.5. Analysis of the PMA Structure

The chemical structure of the PMA-Br ($M_{n, GPC} = 4.1 \times 10^3$, $D = 1.05$) synthesized by SARA ATRP using inorganic sulfites in DMSO was analyzed by ¹H NMR spectroscopy (Figure 2.10) and MALDI-TOF-MS (Figures 2.11 and 2.12).

In the ¹H NMR analysis (Figure 2.10) the protons chemical shifts were assigned according to the references: (**e**, **g**, **f**, **f'**),^{18,44} (**a**, **b**, **c**),^{18,51} (**dr**, **dm**).^{18,52} The fractions of syndiotactic and isotactic diads (**dr** and **dm** respectively) were obtained by measuring the integrals of signals **dm** and **dr**. Chain-end functionality, in percentage, was calculated as follows: % funct. = [I(**g**)/I(**c**)/6] x 100%; where I(**g**) represents the integral of PMA terminal bromo chain-end -CH₂-CH_gBr-CO₂Me at 4.2-4.3 ppm and I(**c**) the integral of initiator fragment -CH(CH₃)₂-CO₂Et at 1.15-1.05 ppm. The PMA NMR molecular weight was also calculated using the equation $M_{n, NMR} = [I(\mathbf{e}) / (I(\mathbf{c})/6) + 1] \times MW_{MA} + MW_{EBiB}$, where I(**e**) represents the integral of the C-H proton of the PMA main chain –

CH₂-CH_e-CO₂Me at 2.2-2.4 ppm and I(c) the integral of initiator fragment -CH(CH₃)₂-CO₂Et at 1.15-1.05 ppm.

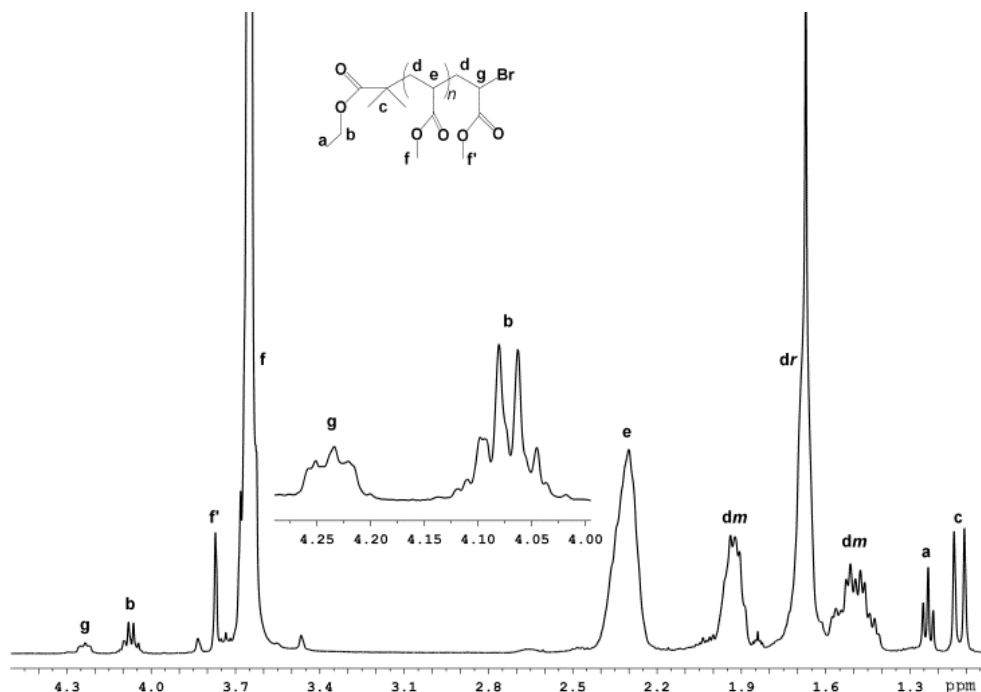


Figure 2.10. The ¹H NMR spectrum of PMA-Br ($M_{n,GPC} = 4100$; $D = 1.05$; $M_{n,NMR} = 3727$; active chain-end functionality = 90 %). The PMA is atactic: $[dr] = [dm] = 0.5$. The solvent is CDCl₃.

MALDI-TOF-MS technique was also used to determine the chemical structure of PMA synthesized by SARA ATRP. In the experiment, both HABA and DHB were tested as matrices, but only the HABA matrix gave a clearly resolved spectrum (Figures 2.11 and 2.12). The MALDI-TOF-MS of PMA-Br m/z ranging from 500 to 7500 is shown in Figure 2.11. Enlargement of the m/z 3500-4000 range is shown in Figure 2.12. Importantly, two series of main peaks are separated by an interval corresponding to a MA repeating unit (86.1 mass unit). The highest main series is attributed to a PMA-Br polymer chain showing ion forms of single alkali metal adduct $[R-(MA)_n-Br + Na^+]^+$ where R-Br is the initiator EBiB ($3489.3 = 195.1 + 38 \times 86.1 + 23.0$, where 195.1, 86.1 and 23.0 correspond to the molar mass of EBiB, MA and Na⁺ respectively). The weaker peaks are attributed to a PMA polymer chain showing ion forms of a double alkali metal adduct $[R-(MA)_n + Na^+ + K^+]^+$ ($3534.8 = 115.2 + 39 \times 86.1 + 23.0 + 39.1$, where 115.2 and 39.1 correspond to the molar mass of R and K⁺ respectively). The presence of these

peaks was ascribed by other authors⁵³⁻⁵⁷ to the occurrence of the fragmentation during ionization in the MALDI-TOF-MS analysis. Moreover, the functionality of the PMA determined by ¹H-NMR was 90 %, which confirmed that the loss of Br occurred during the MALDI-TOF-MS analysis. Therefore, the obtained PMA-Br has a well-defined structure (i.e., without any detectable structural defects). The presence of possible structural defects would cause a deviation of the distribution of *m/z* values.

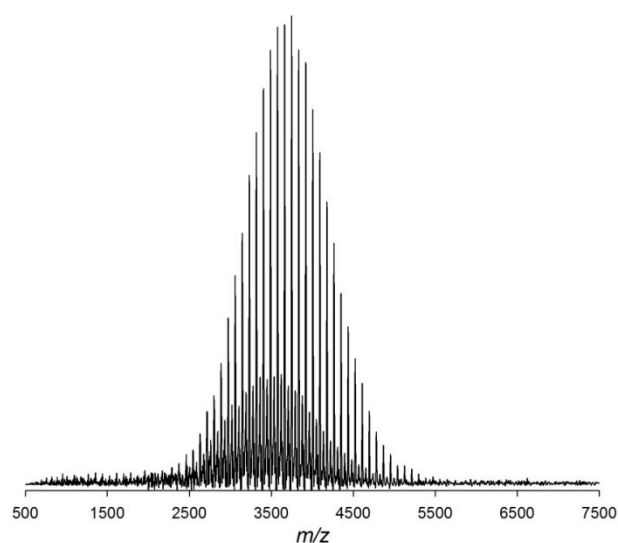


Figure 2.11. MALDI-TOF-MS in the linear mode (using HABA as matrix) of PMA-Br ($M_{n,GPC} = 4100$; $D = 1.05$) from *m/z* 500 to 7500.

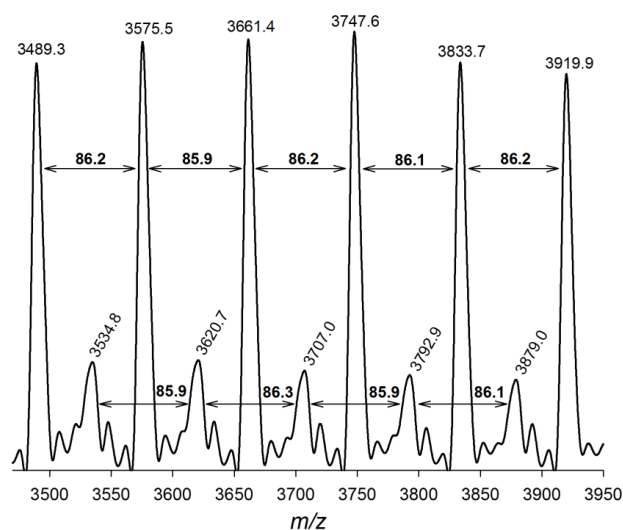


Figure 2.12. Enlargement of the MALDI-TOF-MS from *m/z* 3450 to 3950 of PMA-Br ($M_{n,GPC} = 4100$; $D = 1.05$).

Similarly, the chemical structure of the PMA-Br ($M_{n, \text{GPC}} = 6.9 \times 10^3$, $\mathcal{D} = 1.05$) synthesized by SARA ATRP in BMIM-PF₆/DMSO = 50/50 was also analyzed by ¹H NMR spectroscopy (Figure A.4 in Appendix A) and MALDI-TOF-MS (Figures A.5 and A.6 in Appendix A). The results confirmed the expected structure and a high degree of chain-end functionality (92 %).

2.4.6. Evaluation of the PMA Livingness

The “living” nature of the PMA-Br chain-ends synthesized by SARA ATRP using inorganic sulfites in DMSO was confirmed by carrying out a chain extension experiment. Figure 2.13 shows the complete shift of the entire molecular weight distribution from relatively low molecular weight PMA ($M_{n, \text{GPC}} = 4.1 \times 10^3$, $\mathcal{D} = 1.05$) to a higher molecular weight ($M_{n, \text{GPC}} = 28.4 \times 10^3$, $\mathcal{D} = 1.05$). Similarly, the “living” nature of the PMA-Br synthesized by SARA ATRP in BMIM-PF₆/DMSO = 50/50 was also confirmed (Figure A.7 in Appendix A), showing the complete movement of the macroinitiator ($M_{n, \text{GPC}} = 6.9 \times 10^3$, $\mathcal{D} = 1.05$) GPC trace towards high molecular weight fractions ($M_{n, \text{GPC}} = 21.2 \times 10^3$, $\mathcal{D} = 1.06$).

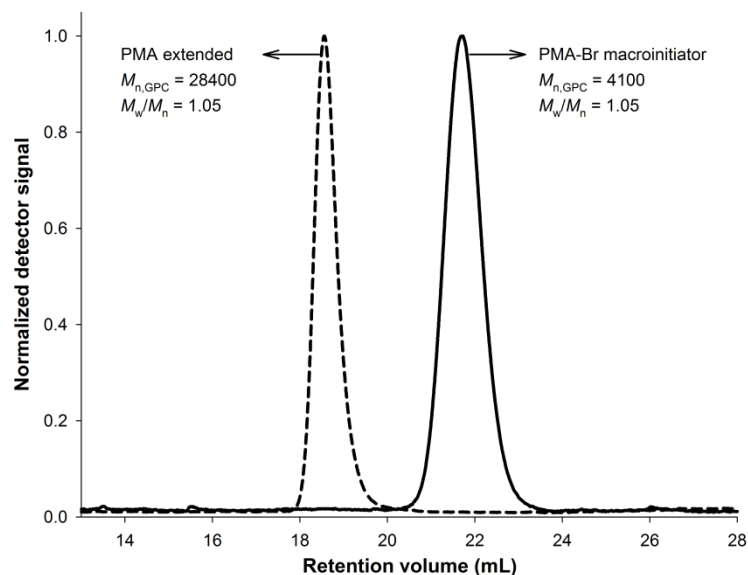


Figure 2.13. GPC traces of the PMA before (right curve) and after the chain extension (left curve) experiment.

2.5. Conclusions

To conclude, inorganic sulfites are a new class of very efficient reducing agents and supplemental activators for SARA ATRP. These new reducing agents in combination with Cu(II) species produce polymers with controlled molecular weight, low dispersity and well-defined chain-end functionality. Sulfites are eco-friendly reducing agents that are applied commercially in many industrial processes and approved by FDA as food and beverage additives. These new inorganic reducing agents should assist in more efficient ATRP and also atom transfer radical addition and cyclization processes,⁵⁸⁻⁶⁰ as well as the implementation of SARA ATRP for larger scale production of well-defined polymers. A synergistic effect of BMIM-PF₆/DMSO in the SARA ATRP using Na₂S₂O₄/CuBr₂/Me₆TREN as the catalytic system was also reported for the first time.

2.6. References

1. Matyjaszewski, K., *Atom Transfer Radical Polymerization (ATRP): Current Status and Future Perspectives*. *Macromolecules*, **2012**, *45*, 4015-4039.
2. Matyjaszewski, K. and Spanswick, J., *Copper-Mediated Atom Transfer Radical Polymerization*, in *Polymer Science: A Comprehensive Reference*, K. Matyjaszewski and M. Möller, Editors. **2012**, Elsevier: Amsterdam. p. 377-428.
3. Matyjaszewski, K. and Xia, J., *Atom Transfer Radical Polymerization*. *Chemical Reviews*, **2001**, *101*, 2921-2990.
4. Tsarevsky, N. V. and Matyjaszewski, K., "Green" *Atom Transfer Radical Polymerization: From Process Design to Preparation of Well-Defined Environmentally Friendly Polymeric Materials*. *Chemical Reviews*, **2007**, *107*, 2270-2299.
5. Kamigaito, M., Ando, T., and Sawamoto, M., *Metal-Catalyzed Living Radical Polymerization*. *Chemical Reviews*, **2001**, *101*, 3689-3746.
6. Braunecker, W. A. and Matyjaszewski, K., *Controlled/living radical polymerization: Features, developments, and perspectives*. *Progress in Polymer Science*, **2007**, *32*, 93-146.
7. Poli, R., *Relationship between One-Electron Transition-Metal Reactivity and Radical Polymerization Processes*. *Angewandte Chemie International Edition*, **2006**, *45*, 5058-5070.

8. Davis, K. A. and Matyjaszewski, K., *Statistical, gradient, block, and graft copolymers by controlled/living radical polymerizations*. *Advances in Polymer Science*, **2002**, *159*, 1-166.
9. Siegwart, D. J., Oh, J. K., and Matyjaszewski, K., *ATRP in the design of functional materials for biomedical applications*. *Progress in Polymer Science*, **2012**, *37*, 18-37.
10. Lee, H.-i., Pietrasik, J., Sheiko, S. S., and Matyjaszewski, K., *Stimuli-responsive molecular brushes*. *Progress in Polymer Science*, **2010**, *35*, 24-44.
11. Golas, P. L. and Matyjaszewski, K., *Marrying click chemistry with polymerization: expanding the scope of polymeric materials*. *Chemical Society Reviews*, **2010**, *39*, 1338-1354.
12. Gao, H. and Matyjaszewski, K., *Synthesis of functional polymers with controlled architecture by CRP of monomers in the presence of cross-linkers: From stars to gels*. *Progress in Polymer Science*, **2009**, *34*, 317-350.
13. Sheiko, S. S., Sumerlin, B. S., and Matyjaszewski, K., *Cylindrical molecular brushes: Synthesis, characterization, and properties*. *Progress in Polymer Science*, **2008**, *33*, 759-785.
14. Oh, J. K., Drumright, R., Siegwart, D. J., and Matyjaszewski, K., *The development of microgels/nanogels for drug delivery applications*. *Progress in Polymer Science*, **2008**, *33*, 448-477.
15. Coessens, V., Pintauer, T., and Matyjaszewski, K., *Functional polymers by atom transfer radical polymerization*. *Progress in Polymer Science*, **2001**, *26*, 337-377.
16. Abreu, C. M. R., Mendonça, P. V., Serra, A. C., Coelho, J. F. J., Popov, A. V., and Guliashvili, T., *Accelerated Ambient-Temperature ATRP of Methyl Acrylate in Alcohol–Water Solutions with a Mixed Transition-Metal Catalyst System*. *Macromolecular Chemistry and Physics*, **2012**, *213*, 1677-1687.
17. Zhang, Y., Wang, Y., and Matyjaszewski, K., *ATRP of Methyl Acrylate with Metallic Zinc, Magnesium, and Iron as Reducing Agents and Supplemental Activators*. *Macromolecules*, **2011**, *44*, 683-685.
18. Mendonça, P. V., Serra, A. C., Coelho, J. F. J., Popov, A. V., and Guliashvili, T., *Ambient temperature rapid ATRP of methyl acrylate, methyl methacrylate and styrene in polar solvents with mixed transition metal catalyst system*. *European Polymer Journal*, **2011**, *47*, 1460-1466.
19. Matyjaszewski, K. and Tsarevsky, N. V., *Nanostructured functional materials prepared by atom transfer radical polymerization*. *Nature Chemistry*, **2009**, *1*, 276-288.
20. Matyjaszewski, K., Jakubowski, W., Min, K., Tang, W., Huang, J., Braunecker, W. A., and Tsarevsky, N. V., *Diminishing catalyst concentration in atom transfer*

- radical polymerization with reducing agents*. Proceedings of the National Academy of Sciences, **2006**, *103*, 15309-15314.
21. Jakubowski, W. and Matyjaszewski, K., *Activators Regenerated by Electron Transfer for Atom-Transfer Radical Polymerization of (Meth)acrylates and Related Block Copolymers*. Angewandte Chemie International Edition, **2006**, *45*, 4482-4486.
 22. Jakubowski, W., Min, K., and Matyjaszewski, K., *Activators Regenerated by Electron Transfer for Atom Transfer Radical Polymerization of Styrene*. Macromolecules, **2005**, *39*, 39-45.
 23. Gnanou, Y. and Hizal, G., *Effect of phenol and derivatives on atom transfer radical polymerization in the presence of air*. Journal of Polymer Science Part A: Polymer Chemistry, **2004**, *42*, 351-359.
 24. West, A. G., Hornby, B., Tom, J., Ladmiral, V., Harrison, S., and Perrier, S., *Origin of Initial Uncontrolled Polymerization and Its Suppression in the Copper(0)-Mediated Living Radical Polymerization of Methyl Acrylate in a Nonpolar Solvent*. Macromolecules, **2011**, *44*, 8034-8041.
 25. Magenau, A. J. D., Strandwitz, N. C., Gennaro, A., and Matyjaszewski, K., *Electrochemically Mediated Atom Transfer Radical Polymerization*. Science, **2011**, *332*, 81-84.
 26. Kwak, Y. and Matyjaszewski, K., *Photoirradiated Atom Transfer Radical Polymerization with an Alkyl Dithiocarbamate at Ambient Temperature*. Macromolecules, **2010**, *43*, 5180-5183.
 27. Fors, B. P. and Hawker, C. J., *Control of a Living Radical Polymerization of Methacrylates by Light*. Angewandte Chemie International Edition, **2012**, *51*, 8850-8853.
 28. Kahveci, M. U., Acik, G., and Yagci, Y., *Synthesis of block copolymers by combination of atom transfer radical polymerization and visible light-induced free radical promoted cationic polymerization*. Macromolecular Rapid Communications, **2012**, *33*, 309-313.
 29. Konkolewicz, D., Schröder, K., Buback, J., Bernhard, S., and Matyjaszewski, K., *Visible Light and Sunlight Photoinduced ATRP with ppm of Cu Catalyst*. ACS Macro Letters, **2012**, *1*, 1219-1223.
 30. Mosnáček, J. and Ilčíková, M., *Photochemically Mediated Atom Transfer Radical Polymerization of Methyl Methacrylate Using ppm Amounts of Catalyst*. Macromolecules, **2012**, *45*, 5859-5865.
 31. Tasdelen, M. A., Ciftci, M., and Yagci, Y., *Visible light-induced atom transfer radical polymerization*. Macromolecular Chemistry and Physics, **2012**, *213*, 1391-1396.

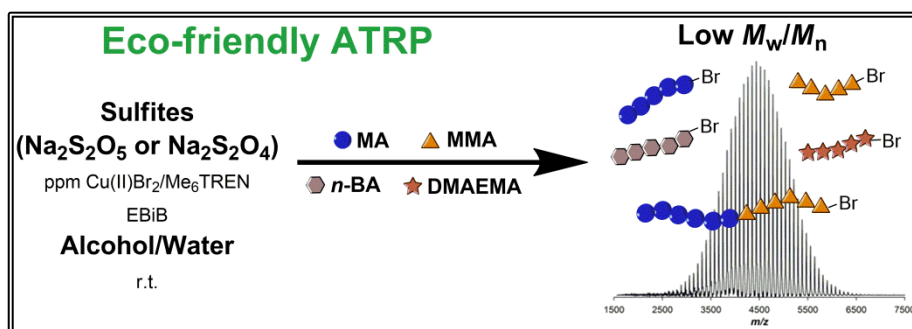
32. Erdmenger, T., Guerrero-Sanchez, C., Vitz, J., Hoogenboom, R., and Schubert, U. S., *Recent developments in the utilization of green solvents in polymer chemistry*. Chemical Society Reviews, **2010**, *39*, 3317-3333.
33. Wheeler, C., West, K. N., Liotta, C. L., and Eckert, C. A., *Ionic liquids as catalytic green solvents for nucleophilic displacement reactions*. Chemical Communications, **2001**, *10*, 887-888.
34. Huddleston, J. G., Willauer, H. D., Swatloski, R. P., Visser, A. E., and Rogers, R. D., *Room temperature ionic liquids as novel media for 'clean' liquid-liquid extraction*. Chemical Communications, **1998**, *16*, 1765-1766.
35. Carmichael, A. J., Haddleton, D. M., Bon, S. A. F., and Seddon, K. R., *Copper() mediated living radical polymerisation in an ionic liquid*. Chemical Communications, **2000**, *14*, 1237-1238.
36. Biedroń, T. and Kubisa, P., *Atom-Transfer Radical Polymerization of Acrylates in an Ionic Liquid*. Macromolecular Rapid Communications, **2001**, *22*, 1237-1242.
37. Sarbu, T. and Matyjaszewski, K., *ATRP of Methyl Methacrylate in the Presence of Ionic Liquids with Ferrous and Cuprous Anions*. Macromolecular Chemistry and Physics, **2001**, *202*, 3379-3391.
38. Percec, V. and Grigoras, C., *Catalytic effect of ionic liquids in the Cu₂O/2,2'-bipyridine catalyzed living radical polymerization of methyl methacrylate initiated with arenesulfonyl chlorides*. Journal of Polymer Science Part A: Polymer Chemistry, **2005**, *43*, 5609-5619.
39. Biedroń, T. and Kubisa, P., *Radical polymerization in a chiral ionic liquid: Atom transfer radical polymerization of acrylates*. Journal of Polymer Science Part A: Polymer Chemistry, **2005**, *43*, 3454-3459.
40. Ma, H., Wan, X., Chen, X., and Zhou, Q.-F., *Reverse atom transfer radical polymerization of methyl methacrylate in room-temperature ionic liquids*. Journal of Polymer Science Part A: Polymer Chemistry, **2003**, *41*, 143-151.
41. Biedroń, T. and Kubisa, P., *Atom transfer radical polymerization of acrylates in an ionic liquid: Synthesis of block copolymers*. Journal of Polymer Science Part A: Polymer Chemistry, **2002**, *40*, 2799-2809.
42. Ciampolini, M. and Nardi, N., *Five-Coordinated High-Spin Complexes of Bivalent Cobalt, Nickel, and Copper with Tris(2-dimethylaminoethyl)amine*. Inorganic Chemistry, **1966**, *5*, 41-44.
43. Sarkar, A., Trivedi, S., Baker, G. A., and Pandey, S., *Multiprobe Spectroscopic Evidence for "Hyperpolarity" within 1-Butyl-3-methylimidazolium Hexafluorophosphate Mixtures with Tetraethylene Glycol*. The Journal of Physical Chemistry B, **2008**, *112*, 14927-14936.
44. Percec, V., Guliashvili, T., Ladislaw, J. S., Wistrand, A., Stjerndahl, A., Sienkowska, M. J., Monteiro, M. J., and Sahoo, S., *Ultrafast Synthesis of*

- Ultrahigh Molar Mass Polymers by Metal-Catalyzed Living Radical Polymerization of Acrylates, Methacrylates, and Vinyl Chloride Mediated by SET at 25 °C.* Journal of the American Chemical Society, **2006**, *128*, 14156-14165.
45. Matyjaszewski, K., Tsarevsky, N. V., Braunecker, W. A., Dong, H., Huang, J., Jakubowski, W., Kwak, Y., Nicolay, R., Tang, W., and Yoon, J. A., *Role of Cu⁰ in Controlled/"Living" Radical Polymerization.* Macromolecules, **2007**, *40*, 7795-7806.
 46. Isse, A. A., Gennaro, A., Lin, C. Y., Hodgson, J. L., Coote, M. L., and Guliashvili, T., *Mechanism of Carbon-Halogen Bond Reductive Cleavage in Activated Alkyl Halide Initiators Relevant to Living Radical Polymerization: Theoretical and Experimental Study.* Journal of the American Chemical Society, **2011**, *133*, 6254-6264.
 47. Guliashvili, T., Mendonca, P. V., Serra, A. C., Popov, A. V., and Coelho, J. F. J., *Copper-Mediated Controlled/"Living" Radical Polymerization in Polar Solvents: Insights into Some Relevant Mechanistic Aspects.* Chemistry-a European Journal, **2012**, *18*, 4607-4612.
 48. Harrisson, S., Couvreur, P., and Nicolas, J., *Comproportionation versus Disproportionation in the Initiation Step of Cu(0)-Mediated Living Radical Polymerization.* Macromolecules, **2012**, *45*, 7388-7396.
 49. Harrisson, S., Mackenzie, S. R., and Haddleton, D. M., *Pulsed Laser Polymerization in an Ionic Liquid: Strong Solvent Effects on Propagation and Termination of Methyl Methacrylate.* Macromolecules, **2003**, *36*, 5072-5075.
 50. Harrisson, S., Mackenzie, S. R., and Haddleton, D. M., *Unprecedented solvent-induced acceleration of free-radical propagation of methyl methacrylate in ionic liquids.* Chemical Communications, **2002**, 2850-2851.
 51. Hasneen, A., Kim, S. J., and Paik, H.-j., *Synthesis and characterization of low molecular weight poly(methyl acrylate)-*b*-polystyrene by a combination of ATRP and click coupling method.* Macromolecular Research, **2007**, *15*, 541-546.
 52. Tabuchi, M., Kawauchi, T., Kitayama, T., and Hatada, K., *Living polymerization of primary alkyl acrylates with *t*-butyllithium/bulky aluminum Lewis acids.* Polymer, **2002**, *43*, 7185-7190.
 53. Beyou, E., Chaumont, P., Chauvin, F., Devaux, C., and Zydowicz, N., *Study of the Reaction between Nitroxide-Terminated Polymers and Thiuram Disulfides. Toward a Method of Functionalization of Polymers Prepared by Nitroxide Mediated Free "Living" Radical Polymerization.* Macromolecules, **1998**, *31*, 6828-6835.
 54. Coca, S., Jasieczek, C. B., Beers, K. L., and Matyjaszewski, K., *Polymerization of acrylates by atom transfer radical polymerization. Homopolymerization of 2-hydroxyethyl acrylate.* Journal of Polymer Science Part A: Polymer Chemistry, **1998**, *36*, 1417-1424.

55. Wang, J. and Sporns, P., *MALDI-TOF MS Analysis of Food Flavonol Glycosides*. *Journal of Agricultural and Food Chemistry*, **2000**, *48*, 1657-1662.
56. Schilli, C., Lanzendörfer, M. G., and Müller, A. H. E., *Benzyl and Cumyl Dithiocarbamates as Chain Transfer Agents in the RAFT Polymerization of N-Isopropylacrylamide. In Situ FT-NIR and MALDI-TOF MS Investigation*. *Macromolecules*, **2002**, *35*, 6819-6827.
57. Ayorinde, F. O., Bezabeh, D. Z., and Delves, I. G., *Preliminary investigation of the simultaneous detection of sugars, ascorbic acid, citric acid, and sodium benzoate in non-alcoholic beverages by matrix-assisted laser desorption/ionization time-of-flight mass spectrometry*. *Rapid Communications in Mass Spectrometry*, **2003**, *17*, 1735-1742.
58. Studer, A., *Tin-free radical chemistry using the persistent radical effect: alkoxyamine isomerization, addition reactions and polymerizations*. *Chem. Soc. Rev.*, **2004**, *033*, 267-273.
59. Thommes, K., Içli, B., Scopelliti, R., and Severin, K., *Atom-Transfer Radical Addition (ATRA) and Cyclization (ATRC) Reactions Catalyzed by a Mixture of [RuCl₂Cp*(PPh₃)] and Magnesium*. *Chemistry – A European Journal*, **2007**, *13*, 6899-6907.
60. Pintauer, T. and Matyjaszewski, K., *Atom transfer radical addition and polymerization reactions catalyzed by ppm amounts of copper complexes*. *Chem. Soc. Rev.*, **2008**, *37*, 1087-1097.

Chapter 3

Ambient Temperature Rapid SARA ATRP in Ecofriendly Solvents Mediated by Inorganic Sulfite/Cu(II)Br₂ Catalytic System



The contents of this chapter are published in:

Abreu, C. M. R., Serra, A. C., Popov, A. V., Matyjaszewski, K., Guliashvili, T., and Coelho, J. F. J., *Ambient Temperature Rapid SARA ATRP of Acrylates and Methacrylates in Alcohol-Water Solutions Mediated by a Mixed Sulfite/Cu(II)Br₂ Catalytic System*. *Polymer Chemistry*, **2013**, 4, 5629-5636.

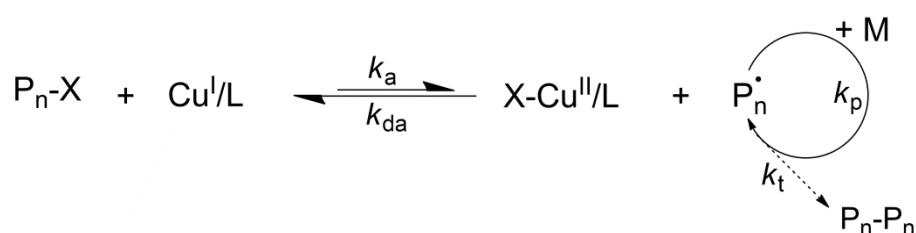
3.1. Abstract

The new generation of catalytic systems for reversible deactivation radical polymerization (RDRP) of vinyl monomers should be non-toxic, inexpensive and provide fast polymerizations in environmentally friendly media. Herein, it is reported the successful ambient temperature ATRP of several vinyl monomers (MA, *n*-BA, MMA and DMAEMA) catalyzed by inorganic sulfites (Na₂S₂O₄ and Na₂S₂O₅) and small amounts of a Cu(II)Br₂/Me₆TREN system in alcohol-water mixtures. The controlled character of ATRP of acrylates and methacrylates was confirmed by the linear increase of molecular weights with monomer conversion, narrow molecular weight distributions ($\bar{D} \sim 1.05$) and by reinitiation experiments (copolymerization and chain extension). The ¹H NMR and MALDI-TOF analyses confirmed the molecular structure and chain-end functionality of the obtained polymers. ATRP of MA using this novel catalytic system in alcohol-water mixtures with multifunctional Br-based initiators provides 4 and 6 arm star polyacrylates in a controlled manner without any observable gel formation. The data presented open up the possibility of using fast ATRP catalyzed by inorganic sulfites (approved by FDA as food and beverage additives) in solvents that are inexpensive, eco-friendly and widely used in chemical industrial processes.

3.2. Introduction

Reversible deactivation radical polymerization (RDRP) methods provide unprecedented tools for the synthesis of polymers with controlled architectures, chain-end functionalities and narrow molecular weight distributions.^{1,2} Atom Transfer Radical Polymerization (ATRP)³⁻⁸ is one of the most used methods for preparation of a wide range of polymers with specified characteristics.⁹⁻¹⁶ With the aim to develop faster, efficient and "greener" procedures without the loss of control over polymerization and chain-end functionality, a new generation of ATRP methods were developed, such as: activators regenerated by electron transfer (ARGET),¹⁷⁻²⁰ initiators for continuous activator regeneration (ICAR),^{21,22} supplementary activator and reducing agent (SARA) ATRP,²³⁻³⁵ electrochemically mediated ATRP (*e*ATRP),³⁶⁻³⁸ and photochemically mediated ATRP.³⁹⁻⁴⁵ The development of these ATRP techniques allowed the reduction of the amounts of

transition metal complexes (typically copper based complexes with nitrogen-based ligands)¹ used as redox active ATRP catalysts from ≥ 1000 ppm to less than 100 ppm in the presence of various reducing agents.^{18,19,21,24,27,29,46} As shown in Scheme 3.1, the copper catalyst complexes are responsible for a dynamic equilibrium between tiny amounts of propagating radicals and alkyl halides as dormant species. ATRP is accompanied by a unavoidable radical-radical termination process, resulting in the build-up of a small excess of an X-Cu(II)/L deactivator (persistent radical effect).⁴⁷



Scheme 3.1. General mechanism of copper catalyzed ATRP.

Recently, our research team reported²⁹ the use of sulfite salts (sodium metabisulfite - $Na_2S_2O_5$, sodium dithionite - $N_2S_2O_4$ and sodium bisulfite - $NaHSO_3$) as a new class of efficient reducing agents (and supplemental activators) for ATRP. These salts demonstrated to be efficient, inexpensive, safe, and environmentally friendly “co-catalysts” that allowed us to obtain a well-defined PMA with controlled molecular weight and low dispersity ($D \sim 1.05$) in DMSO solution. Sodium bisulfite and metabisulfite are broadly used in industrial processes as FDA approved compounds for use in food and beverage additives and also widely used in polymer making industries as part of redox pair (for example: *tert* butyl hydroperoxide / sodium metabisulfite redox pair). The use of DMSO as solvent can hamper potential industrial implementation of this technique due to its high boiling point, price and limited solubility of inorganic sulfites in DMSO/monomer mixtures. Although, reported polymerizations in pure DMSO were very well controlled and fast,²⁹ the use of more environmental friendly and less expensive solvents in the presence of limited amount of water could be a critical aspect that should be taken into consideration for a future large-scale applications. A DMSO-water system was reported to be very effective in Cu(II)-mediated hydrolysis of C-Br bonds in alkyl bromides,⁴⁸ which could eliminate the active chain ends in growing polymers. Instead of

this, alcohols and alcohol-water mixtures as polymerization solvents were reported by different research groups⁴⁹⁻⁵³ including our research team.^{28,31}

The present work intends to report the results of the successful ambient temperature SARA ATRP of activated vinyl monomers, such as MA, *n*-BA, MMA and DMAEMA, in alcohols and alcohol-water mixtures using inorganic sulfites and small amounts of Cu(II)Br₂/Me₆TREN catalytic system.

3.3. Experimental Section

3.3.1. Materials

Methyl acrylate (MA) (Acros, 99% stabilized), methyl methacrylate (MMA) (Sigma–Aldrich, 99%), *n*-butyl acrylate (*n*-BA) (Sigma–Aldrich, 99%) and 2-(dimethylamino)ethyl methacrylate (DMAEMA) (Sigma–Aldrich, 98%) were passed through a sand/alumina column before use in order to remove the radical inhibitor. Na₂S₂O₄ (Merck, >87%), Na₂S₂O₅ (Sigma–Aldrich, >99%), Cu(II)Br₂ (Acros, 99% extra pure, anhydrous), deuterated chloroform (CDCl₃) (Euriso-top, +1% TMS), ethanol (Panreac, 99.5%), ethyl 2-bromoisobutyrate (EBiB) (Sigma-Aldrich, 98%), pentaerythritol tetrakis(2-bromoisobutyrate) or tetrafunctional 2-bromoisobutyrate (4f-BiB) (Sigma-Aldrich, 97%), dipentaerythritol hexakis(2-bromoisobutyrate) or hexafunctional 2-bromoisobutyrate (6f-BiB) (Sigma-Aldrich, 97%), hexane (Fisher Chemical, 95%), polystyrene (PS) standards (Polymer Laboratories), 2-(4-hydroxyphenylazo)benzoic acid (HABA) (Sigma–Aldrich, 99.5 %) and 2,5-dihydroxybenzoic acid (DHB) (Sigma–Aldrich, >99 %) were used as received. Ultra-pure Milli Q water was used. Purified water (MilliQ®, Millipore, resistivity >18 MΩ cm) was obtained by reverse osmosis. Tetrahydrofuran (THF) (Panreac, HPLC grade) was filtered under reduced pressure before use. Me₆TREN was synthesized according a described procedure.⁵⁴

3.3.2. Techniques

The chromatographic parameters of the samples were determined using high performance gel permeation chromatography (HPGPC); Viscotek (ViscotekTDAmx) with a differential viscometer (DV); right-angle laser-light scattering (RALLS, Viscotek); low-angle laser-light scattering (LALLS, Viscotek) and refractive index (RI) detectors. The column set consisted of a PL 10 mm guard column ($50 \times 7.5 \text{ mm}^2$) followed by one Viscotek T2000 column ($6 \mu\text{m}$), one MIXED-E PLgel column ($3 \mu\text{m}$) and one MIXED-C PLgel column ($5 \mu\text{m}$). The HPLC dual piston pump was set at a flow rate of 1 mL min^{-1} . The eluent (THF) was previously filtered through a $0.2 \mu\text{m}$ filter. The system was also equipped with an on-line degasser. The tests were done at $30 \text{ }^\circ\text{C}$ using an Elder CH-150 heater. The samples were filtered through a polytetrafluoroethylene (PTFE) membrane with $0.2 \mu\text{m}$ pore before injection ($100 \mu\text{L}$). The system was calibrated with narrow PS standards. The dn/dc was determined as 0.063 for PMA. Molecular weight ($M_{n,\text{GPC}}$) and dispersity (\mathcal{D}) of synthesized polymers were determined by Multidetectors calibration using OmniSEC software version: 4.6.1.354.

400 MHz ^1H NMR spectra were recorded on a BrukerAvance III 400 MHz spectrometer, with a 5-mm TIX triple resonance detection probe, in CDCl_3 with tetramethylsilane (TMS) as an internal standard. Conversion of the monomer was determined by integration of monomer and polymer peaks using MestRenova software version: 6.0.2-5475.

The PMA samples were dissolved in THF at a concentration of 10 mg mL^{-1} for the MALDI-TOF-MS analysis. DHB and HABA (0.05 M in THF) were used as matrices. The dried-droplet sample preparation technique was used to obtain a 1:1 ratio (sample/matrix); an aliquot of $1 \mu\text{L}$ of each sample was directly spotted on the MTP AnchorChip TM 600/384 TF MALDI target, BrukerDaltonik (Bremen, Germany) and, before the sample dried, $1 \mu\text{L}$ of matrix solution in THF was added and the mixture allowed to dry at room temperature, to allow matrix crystallization. External mass calibration was performed with a peptide calibration standard (PSCII) for the range 500-9000 (9 mass calibration points), $0.5 \mu\text{L}$ of the calibration solution and matrix previously mixed in an Eppendorf tube (1:2, v/v) were applied directly on the target and allowed to dry at room temperature. Mass spectra were recorded using an Autoflex III smartbeam

MALDI-TOF-MS mass spectrometer BrukerDaltonik (Bremen, Germany) operating in the linear and reflectron positive ion mode. Ions were formed upon irradiation using a smartbeam laser with a frequency of 200 Hz. Each mass spectrum was produced by averaging 2500 laser shots collected across the whole sample spot surface by screening in the range m/z 500-9500. The laser irradiance was set to 35-40 % (relative scale 0-100) arbitrary units according to the corresponding threshold required for the applied matrix systems.

3.3.3. Procedures

Typical procedure for the SARA ATRP of MA (DP = 222) catalyzed by [Na₂S₂O₄]/[Cu(II)Br₂]/[Me₆TREN] = 1/0.1/0.1 in an ethanol-water [90/10 (v/v)] mixture

The monomer (MA) was purified by passage through in a sand/alumina column just before addition to the reaction. A mixture of Cu(II)Br₂ (7.0 mg, 0.031 mmol), Me₆TREN (7.2 mg, 0.031 mmol) and ethanol (2.8 mL), and Milli Q water (0.3 mL) (both previously bubbled with nitrogen for about 15 minutes) was placed in a Schlenk tube reactor that was sealed by using rubber septa. Na₂S₂O₄ (54.7 mg, 0.314 mmol) and a mixture of MA (6.3 mL, 69.7 mmol) and EBiB (61.2 mg, 0.314 mmol) were added to the reactor and frozen in liquid nitrogen. The Schlenk tube reactor containing the reaction mixture was deoxygenated with five freeze-vacuum-thaw cycles and purged with nitrogen. The Schlenk tube reactor was placed in a water bath at 30 °C with stirring (700 rpm). Samples of the reaction mixture were collected periodically during the polymerization by using an airtight syringe and purging the side arm of the Schlenk tube reactor with nitrogen. The samples were analyzed by ¹H NMR spectroscopy in order to determine the monomer conversion and, by GPC, to determine $M_{n, GPC}$ and \bar{D} of the PMA.

Typical procedure for the SARA ATRP of MA and MMA block copolymer catalyzed by [Na₂S₂O₄]/[Cu(II)Br₂]/[Me₆TREN] = 1/0.1/0.1 in an ethanol-water [90/10 (v/v)] mixture

The PMA-Br macroinitiator was obtained from a typical $\text{Na}_2\text{S}_2\text{O}_4/\text{Cu(II)Br}_2/\text{Me}_6\text{TREN}$ catalyzed ATRP reaction. After precipitation in hexane, the polymer was then dissolved in THF and filtered through a sand/alumina column to remove traces of the catalyst and was reprecipitated in hexane again. The polymer was dried under vacuum until constant weight was achieved. The MMA (3.5 mL, 32.9mmol) was purified in a sand/alumina column just before reaction and then added to the Br terminated PMA macroinitiator ($M_{n,\text{GPC}} = 4400$; $\bar{D} = 1.05$, 161.0 mg, 0.037mmol) in the Schlenk tube reactor. Ethanol (1.8 mL) and Milli Q water (0.2 mL) (both previously bubbled with nitrogen for about 15 min) was added to the monomer-macroinitiator mixture in order to completely dissolve the macroinitiator. $\text{Na}_2\text{S}_2\text{O}_4$ (6.4 mg, 0.037mmol), ethanol (1.35 mL), Milli Q water (0.15 mL), Cu(II)Br_2 (0.82 mg, 0.004mmol) and Me_6TREN (0.84 mg, 0.004mmol) were added to the reactor. The Schlenk tube was deoxygenated by five freeze-pump-thaw cycles and purged with nitrogen. Then the reactor was placed in the water bath at 30 °C with stirring (700 rpm). The reaction was stopped after 6 h and the mixture was analyzed by ^1H NMR spectroscopy in order to determine the MMA conversion and, by GPC, to determine $M_{n,\text{GPC}}$ and \bar{D} of the PMA-*b*-PMMA.

Chain extension experiment: polymerization from a Br terminated PMA macroinitiator

MA (3.5 mL, 38.9 mmol) was purified in a sand/alumina column just before reaction and then added to the Br terminated PMA macroinitiator ($M_{n,\text{GPC}} = 4400$; $\bar{D} = 1.05$, 190.0 mg, 0.043mmol) in the Schlenk tube reactor. Ethanol (1.8 mL) and Milli Q water (0.2 mL) (both previously bubbled with nitrogen for about 15 min) was added to the monomer-macroinitiator mixture in order to completely dissolve the macroinitiator. $\text{Na}_2\text{S}_2\text{O}_4$ (7.5 mg, 0.043mmol), ethanol (1.35 mL), Milli Q water (0.15 mL), Cu(II)Br_2 (0.96 mg, 0.004mmol) and Me_6TREN (0.99 mg, 0.004mmol) were added to the reactor. The Schlenk tube was deoxygenated by five freeze-pump thaw cycles and purged with nitrogen. Then the reactor was placed in the water bath at 30 °C with stirring (700 rpm). The reaction was stopped after 6 h and the mixture was analyzed by GPC.

3.4. Results and Discussion

3.4.1. SARA ATRP using Inorganic Sulfites in Alcohol-Water Mixtures

Our research team recently reported²⁹ the use of inorganic sulfites (Na₂S₂O₅, Na₂S₂O₄ and NaHSO₃) as reducing agents and supplemental activators in an ATRP carried out at ambient temperature in DMSO solution.

With the aim to enhance the possibilities of industrial application of this catalytic system, the replacement of DMSO as a solvent was envisaged using alcohol-water mixtures using different sulfites. Since alcohols are not good solvents for inorganic salts, the use of limited amount of water would enhance the solubility of inorganic sulfites in the polymerization mixture thus providing faster and more controlled reactions. Figure 3.1 and Table 3.1 (entries 1, 2 and 3) present the kinetic plots of ATRP of MA conducted at 30 °C in ethanol-water (EtOH/H₂O) and methanol-water (MeOH/H₂O) [90/10 (v/v)] using Na₂S₂O₄ and Na₂S₂O₅ as SARA agents. The targeted number average molecular weight at full conversion was $M_n \sim 20000$. The catalyst was added at 10 mol% *versus* initiator (EBiB), and a SARA agent was added at an equimolar concentration to the initiator.

The rate of polymerization was first order with respect to monomer concentration with the two reducing agents (Na₂S₂O₄ or Na₂S₂O₅). In two alcohol media (EtOH or MeOH)-H₂O mixtures [90/10 (v/v)] (Figure 3.1) the molecular weights determined by GPC were in good agreement with the theoretical values, indicating an efficient initiation and excellent control during polymerization. This observation is confirmed by low dispersity values of the obtained polymers (D always < 1.1) from the beginning of the polymerization to high conversions. A comparison of the kinetic data indicates that Na₂S₂O₄ provided the fastest polymerization of MA in the EtOH-H₂O [90/10 (v/v)] mixture (Table 3.1, entries 1 and 2), indicating that it is a more efficient reducing agent, allowing faster (re)generation of active Cu(I)Br/L catalyst. Reactions with Na₂S₂O₅ were 85 times slower. The same conclusion had been established in DMSO,²⁹ although the difference in polymerization rates was not as high (3.5 times slower).

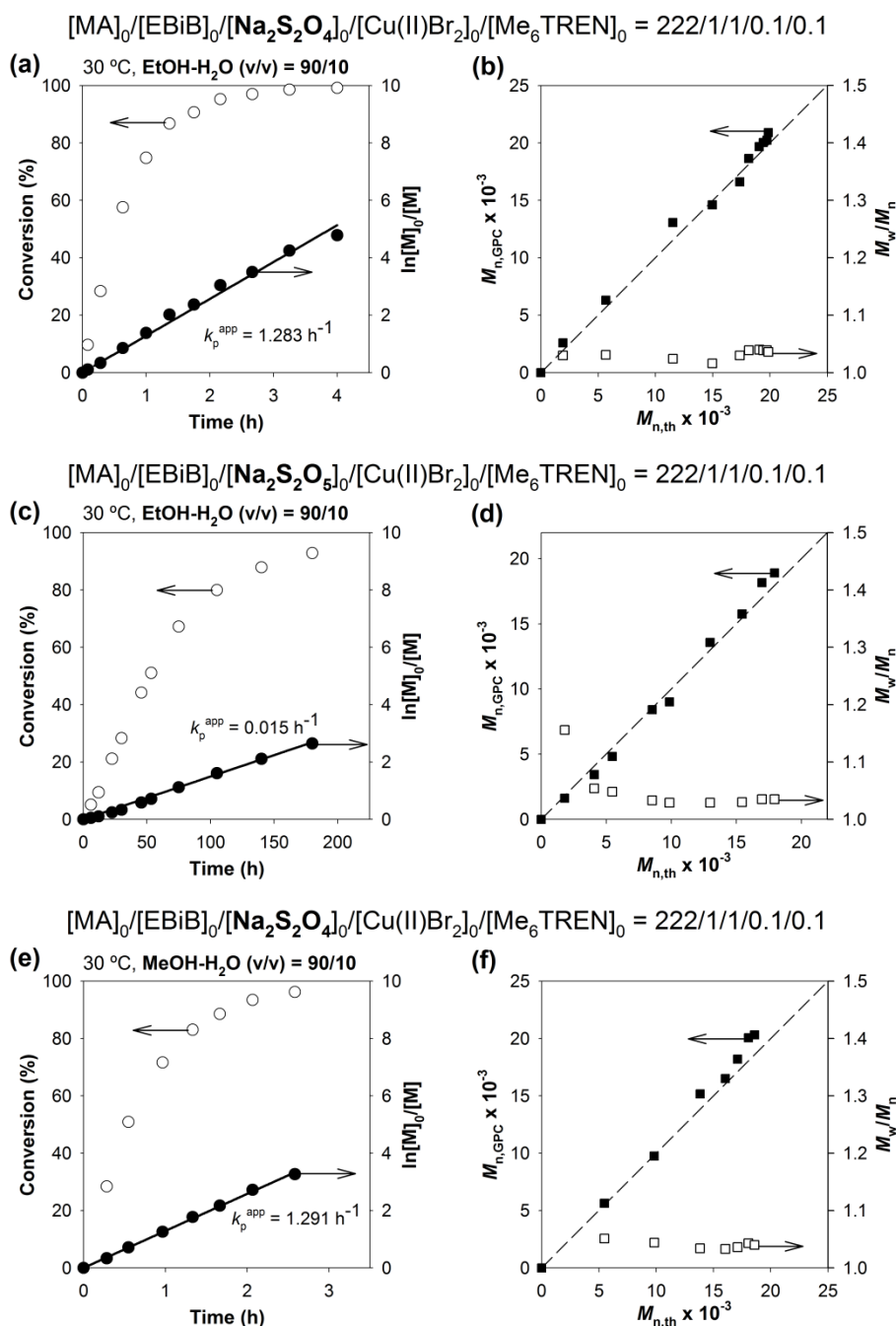


Figure 3.1. Kinetic plots of conversion and $\ln[M]_0/[M]$ vs. time (a, c, e) and plots of $M_{n,GPC}$ and \mathcal{D} (M_w/M_n) vs. $M_{n,th}$ (b, d, f) for SARA ATRP of MA catalyzed in the presence of $Cu(II)Br_2/Me_6TREN$ with different reducing agents [$Na_2S_2O_4$ (a, b, e, f) and $Na_2S_2O_5$ (c, d)] in different alcohol-water [90/10 (v/v)] mixtures [EtOH-H₂O (a, b, c, d) and MeOH-H₂O (e, f)] at 30 °C. Conditions: $[MA]_0/[solvent] = 2/1$ (v/v); $[MA]_0/[EBiB]_0/[Na_2S_2O_4$ or $Na_2S_2O_5]_0/[Cu(II)Br_2]_0/[Me_6TREN]_0 = 222/1/1/0.1/0.1$.

The use of MeOH-H₂O [90/10 (v/v)] as a solvent did not show a substantial difference compared to EtOH-H₂O (Table 3.1, entries 1 and 3). The observed slower reactions with Na₂S₂O₅ might be attributed to the limited solubility of this compound compared to Na₂S₂O₄ in organic solvent-water mixtures. Another reason for the higher reactivity of dithionite is dissociation of S₂O₄²⁻ into two SO₂^{•-} radical anions, the stronger one-electron reducing agents.⁵⁵

Because dithionite (Na₂S₂O₄) was the most efficient reducing agent, it was used in subsequent studies that are presented in Table 3.1.

3.4.2. Effect of Water Content (Solvent Mixture) on the Polymerization

In order to find the optimal ratio of EtOH-H₂O to afford faster polymerizations and maintaining the living features of the reaction, different ratios EtOH-H₂O were studied (Figure 3.2 and Table 3.1, entries 1, 4, 5 and 6).

The water content in the reaction solvent mixture was increased, starting from 10 % (v/v), until reaching a water content that hampers the polymerization with controlled/"living" features. Up to 35% (v/v) of water content, the polymerization proceeds with the first order kinetic relative to the monomer and the rate of polymerization increases with the water content (Figure 3.2). The upper limit of water content obtained for this polymerization was found to be around 35 %, which the k_p^{app} was 11.335 h⁻¹. Using 50% of water, a decrease of the rate of reaction was noticed (Figure 3.2e). Due to the reduced solubility of the produced PMA in the solvent mixture, the polymer precipitates resulting in a poor control over the molecular weight distribution (Figure 3.2f). Thus, preliminary experiments using different EtOH-H₂O ratios to dissolve a PMA sample ($M_n = 20000$, DP = 222) have shown that 35% of water is the maximum content that can be used in ethanol without polymer precipitation. The results presented in Figure 3.2 and Table 3.1 (entries 1, 4, 5 and 6) suggest that there is a maximum amount of water that can be used, which for the system described in this manuscript is around 35 % (targeted DP = 222). Apparently, this value should be closely related to the solubility of the polymer in the solvent mixture. Therefore, it could vary for other acrylates using the same experimental conditions, due to different solubility characteristic. Our research team, in a previous

publication,²⁸ had already made the same conclusion for the ATRP of MA using the catalytic system $[\text{Fe(0)}]_0/[\text{Cu(II)Br}_2]_0/[\text{Me}_6\text{TREN}]_0$ at 30 °C.

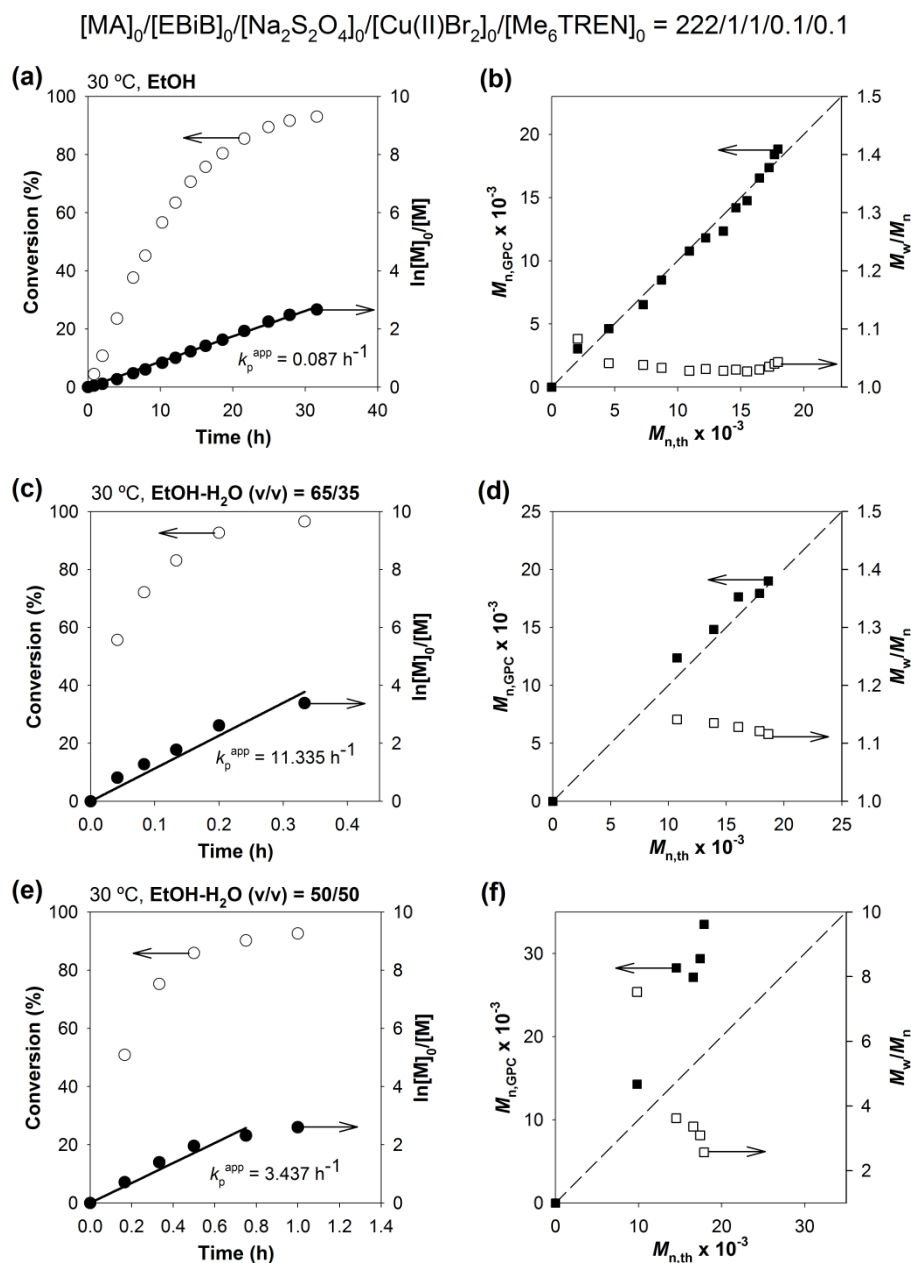


Figure 3.2. Kinetic plots of conversion and $\ln[M]_0/[M]$ vs. time (a, c, e) and plot of $M_{n,\text{GPC}}$ and D (M_w/M_n) vs. $M_{n,\text{th}}$ (b, d, f) for SARA ATRP of MA catalyzed with $\text{Na}_2\text{S}_2\text{O}_4$ in the presence of $\text{Cu(II)Br}_2/\text{Me}_6\text{TREN}$ at 30 °C in EtOH- H_2O mixtures with different contents of water. Conditions: $[\text{MA}]_0/[\text{EBiB}]_0/[\text{Na}_2\text{S}_2\text{O}_4]_0/[\text{Cu(II)Br}_2]_0/[\text{Me}_6\text{TREN}]_0 = 222/1/1/0.1/0.1$; $[\text{MA}]_0/[\text{solvent}] = 2/1$ (v/v).

3.4.3. Variation of Targeted Degree of Polymerization

The target molecular weight is a very important parameter to be considered for any catalytic system due to solubility problems associated with high molecular weight segments. The ATRP of MA was studied with different monomer/initiator ratios, *i.e.*, different targeted degrees of polymerization – DP (Figure 3.3 and Table 3.1, entries 1, 7, 8 and 9) using EtOH-H₂O [90/10 (v/v)] solvent mixture.

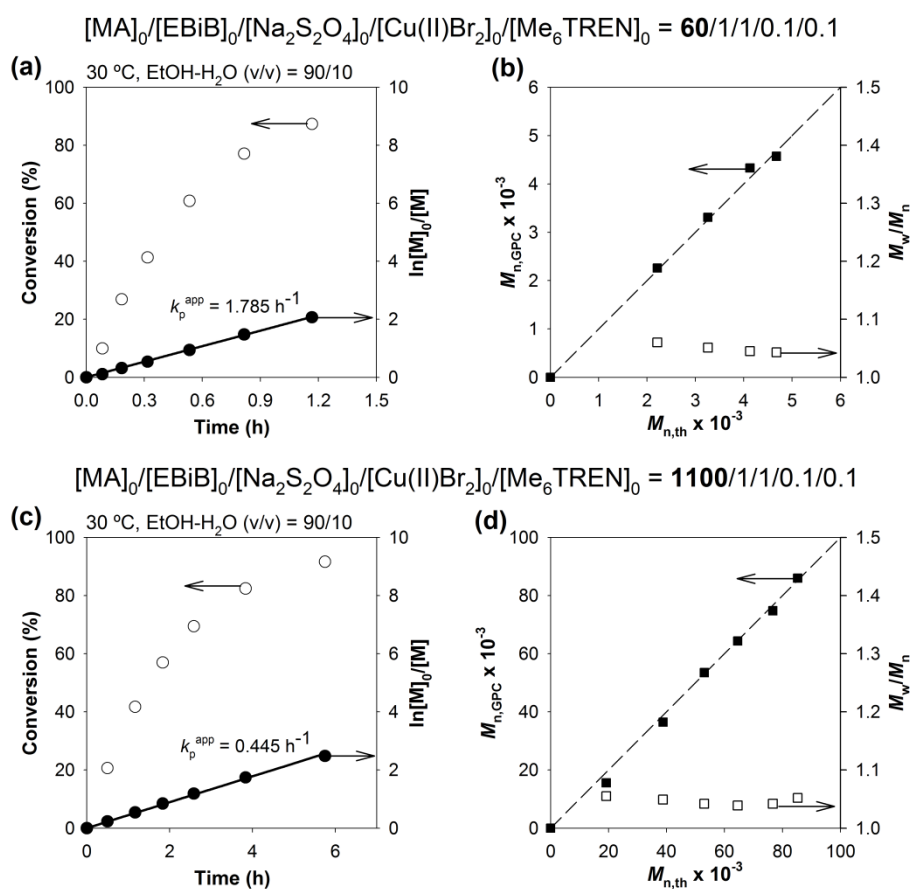


Figure 3.3. Kinetic plots of conversion and $\ln[M]_0/[M]$ vs. time (a and c) and plot of $M_{n,GPC}$ and \mathcal{D} (M_w/M_n) vs. $M_{n,th}$ (b and d) for SARA ATRP of MA catalyzed with Na₂S₂O₄ in the presence of Cu(II)Br₂/Me₆TREN at 30 °C in EtOH-H₂O (v/v) = 90/10. Conditions: [MA]₀/[solvent] = 2/1 (v/v); [MA]₀/[EBiB]₀/[Na₂S₂O₄]₀/[Cu(II)Br₂]₀/[Me₆TREN]₀ = DP/1/1/0.1/0.1, for DP = 60 (a and b) and DP = 1100 (c and d).

As expected, the polymerization rate decreased with increased targeted DP, due to the lower number of growing macroradicals. It is remarkable to note that even for the DP = 1100 the PMA dispersity values were very low ($\mathcal{D} < 1.05$) even at very high monomer

conversion (91.6%), indicating minimal contribution of any side reactions with $\text{Na}_2\text{S}_2\text{O}_4$. In a simple experiment, after 240 hours, a very high molecular weight PMA, $M_{n,\text{GPC}} = 640600$ (targeted DP = 11000, conv. = 64.2%) was obtained, in good agreement with the theoretical value, but the control over the polymerization diminishes, yielding $D = 1.35$. The loss of solubility and the very low concentration of Cu(II) (only 3 ppm) could be responsible for this.

3.4.4. Preparation of Functional Star-Shaped PMA

The utility of the SARA ATRP method reported was extended to the preparation of branched PMA, namely star-shaped. Due to their architecture, star-shaped polymers are very interesting materials showing unique properties. For instances, for high molecular weight values, a star polymer presents lower viscosity than a linear polymer of similar composition. As the star polymers synthesized by SARA ATRP present active-chain ends, it is possible to reinitiate them with further monomer supply, to prepare tailor-made star block copolymers. In addition, it is possible to modify the Br-chain-ends in order to introduce desired reactive functionalities.

The use of multifunctional initiators (4f-BiB and 6f-BiB) for the $\text{Na}_2\text{S}_2\text{O}_4/\text{Cu}(\text{II})\text{Br}_2/\text{Me}_6\text{TREN}$ catalytic system in EtOH- H_2O [90/10 (v/v)] was tested to prepare four-arm and six-arm star PMA (Figure 3.4 and Table 3.1, entries 10 and 11). The results obtained are similar to those for the monofunctional initiator. The rate of polymerization was first order with respect to monomer concentration and the molecular weights determined by GPC were in good agreement with the theoretical values. The low dispersity values of the obtained star polymers (always $D < 1.05$) from the beginning of the polymerization to high conversion proved an efficient initiation and excellent control during polymerization.

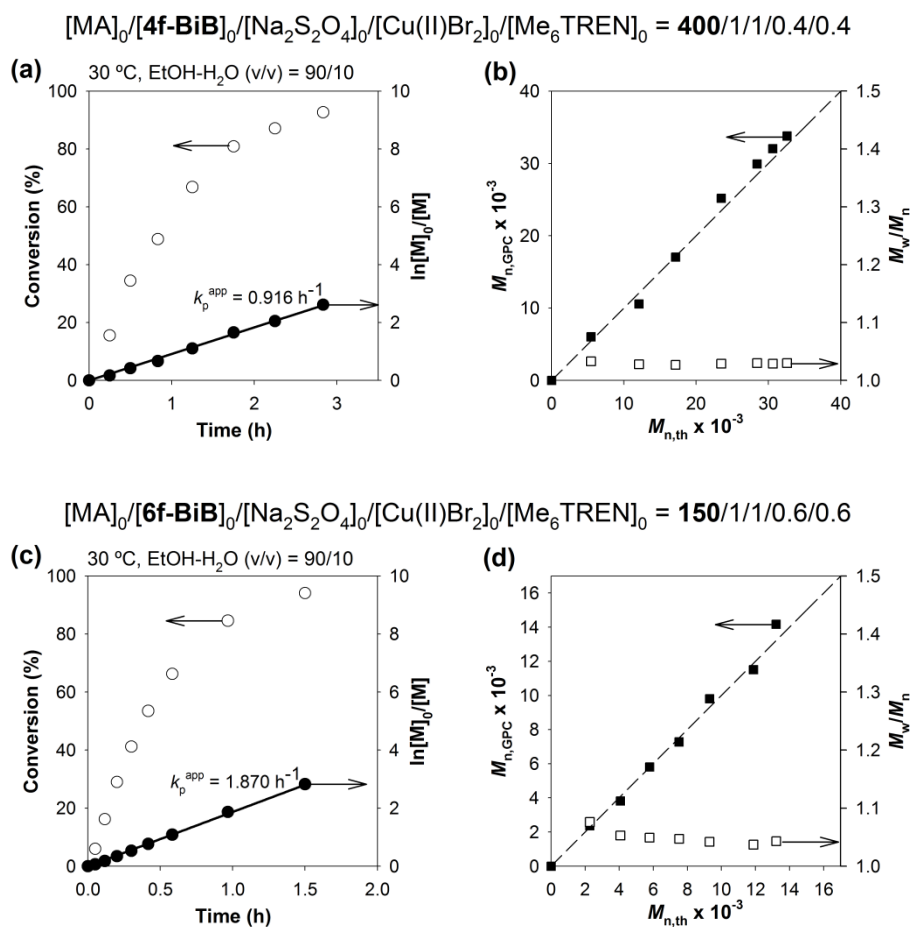


Figure 3.4. Kinetic plots of conversion and $\ln[M]_0/[M]$ vs. time (a and c) and plot of $M_{n,GPC}$ and \bar{D} (M_w/M_n) vs. $M_{n,th}$ (b and d) for SARA ATRP of MA catalyzed with $Na_2S_2O_4$ in the presence of $Cu(II)Br_2/Me_6TREN$ at 30 °C in EtOH-H₂O (v/v) = 90/10. Conditions: $[MA]_0/[solvent] = 2/1$ (v/v); $[MA]_0/[Initiator]_0/[Na_2S_2O_4]_0/[Cu(II)Br_2]_0/[Me_6TREN]_0 = (400 \text{ and } 150)/1/1/0.1/0.1$, for Initiator = 4f-BiB (a and b) and Initiator = 6f-BiB (c and d).

Table 3.1. SARA ATRP of MA in the Presence of Inorganic Sulfites ($\text{Na}_2\text{S}_2\text{O}_4$ or $\text{Na}_2\text{S}_2\text{O}_5$) and $\text{Cu(II)Br}_2/\text{Me}_6\text{TREN}$ at 30 °C in Different Alcohol-Water Mixtures (33 vol % Solvent).

Entry	$[\text{MA}]_0/[\text{EBiB}]_0/[\text{Na}_2\text{S}_2\text{O}_4]_0/[\text{CuBr}_2]_0/[\text{Me}_6\text{TREN}]_0$	EtOH-H ₂ O (v/v)	k_p^{app} (h ⁻¹)	Time (h) ^a	Conv. (%) ^f	$M_{n,\text{th}} \times 10^{-3a}$	$M_{n,\text{GPC}} \times 10^{-3a}$	M_w/M_n ^a
1	222/1/1/0.1/0.1	90/10	1.283	4.0	99.2	20.0	20.9	1.04
2	222/1/1/0.1/0.1 ($\text{Na}_2\text{S}_2\text{O}_5$) ^b	90/10	0.015	180.0	92.9	17.9	18.9	1.04
3	222/1/1/0.1/0.1	90/10(MeOH/H ₂ O) ^c	1.291	2.6	96.2	18.6	20.3	1.04
4	222/1/1/0.1/0.1	100/0	0.087	31.6	93.0	18.0	18.8	1.04
5	222/1/1/0.1/0.1	65/35	11.335	0.33	96.6	18.7	19.0	1.12
6	222/1/1/0.1/0.1	50/50	3.437	1.0	92.6	17.9	33.5	2.57
7	60/1/1/0.1/0.1	90/10	1.785	1.2	87.3	4.7	4.6	1.04
8	1100/1/1/0.1/0.1	90/10	0.445	5.8	91.6	85.2	86.0	1.05
9	11000/1/1/0.1/0.1 ^d	90/10	-	240.0	64.2	607.5	640.6	1.35
10	400/1/1/0.1/0.1 (4f-BiB) ^e	90/10	0.916	2.8	92.7	32.6	33.8	1.03
11	150/1/1/0.1/0.1 (6f-BiB) ^f	90/10	1.870	1.5	94.1	13.2	14.2	1.04

^aValues obtained from the last sample from the kinetic studies.

^b $\text{Na}_2\text{S}_2\text{O}_5$ was used as the reducing agent.

^cMeOH-H₂O [90/10 (v/v)] mixture was used as the solvent.

^d $[\text{MA}]_0/[\text{solvent}]_0 = 1/1$ (v/v) was used.

^e4f-BiB was used as the initiator.

^f6f-BiB was used as the initiator.

3.4.5. Extension to the Polymerization of Other Monomers

The Na₂S₂O₄/Cu(II)Br₂/Me₆TREN catalytic system in EtOH-H₂O [90/10 (v/v)] reported here for MA polymerization was successfully extended to the polymerization of others activated vinyl monomers as *n*-BA, DMAEMA and MMA (Figure 3.5 and Table 3.2, entries 1-3). The results are comparable to the MA case in terms of control over the polymerization and low dispersity values of the obtained methacrylate type polymers ($\mathcal{D} < 1.2$). A comparison of the kinetic data obtained for the different monomers tested with this catalytic system (Table 3.1, entry 1 and Table 3.2, entries 1-3) revealed that the polymerization of MA was the fastest and DMAEMA was the slowest. On the other hand, the polymerization of MA seems to be the best controlled ($\mathcal{D} < 1.05$) during the whole process and the polymerization of DMAEMA the least controlled ($1.17 < \mathcal{D} < 1.25$).

The effect of the solvent was analyzed by the comparison of the kinetic data obtained for MMA in DMSO (Figure B.1 in Appendix B and Table 3.2, entry 4). These results demonstrated that the polymerization of MMA using Na₂S₂O₄/Cu(II)Br₂/Me₆TREN in EtOH-H₂O [90/10 (v/v)] was faster (about 2.4 times) than in DMSO. A similar trend was observed for the polymerization of MA in EtOH-H₂O [90/10 (v/v)] (Table 3.1, entry 1) which was faster (about 5.3 times) than in DMSO (determined in our previous report²⁹). It is also remarkable that this new catalytic system showed comparable or even better performance and control during polymerization compared to related systems with Cu(0) as initial catalyst in DMSO or alcohol-water mixtures.

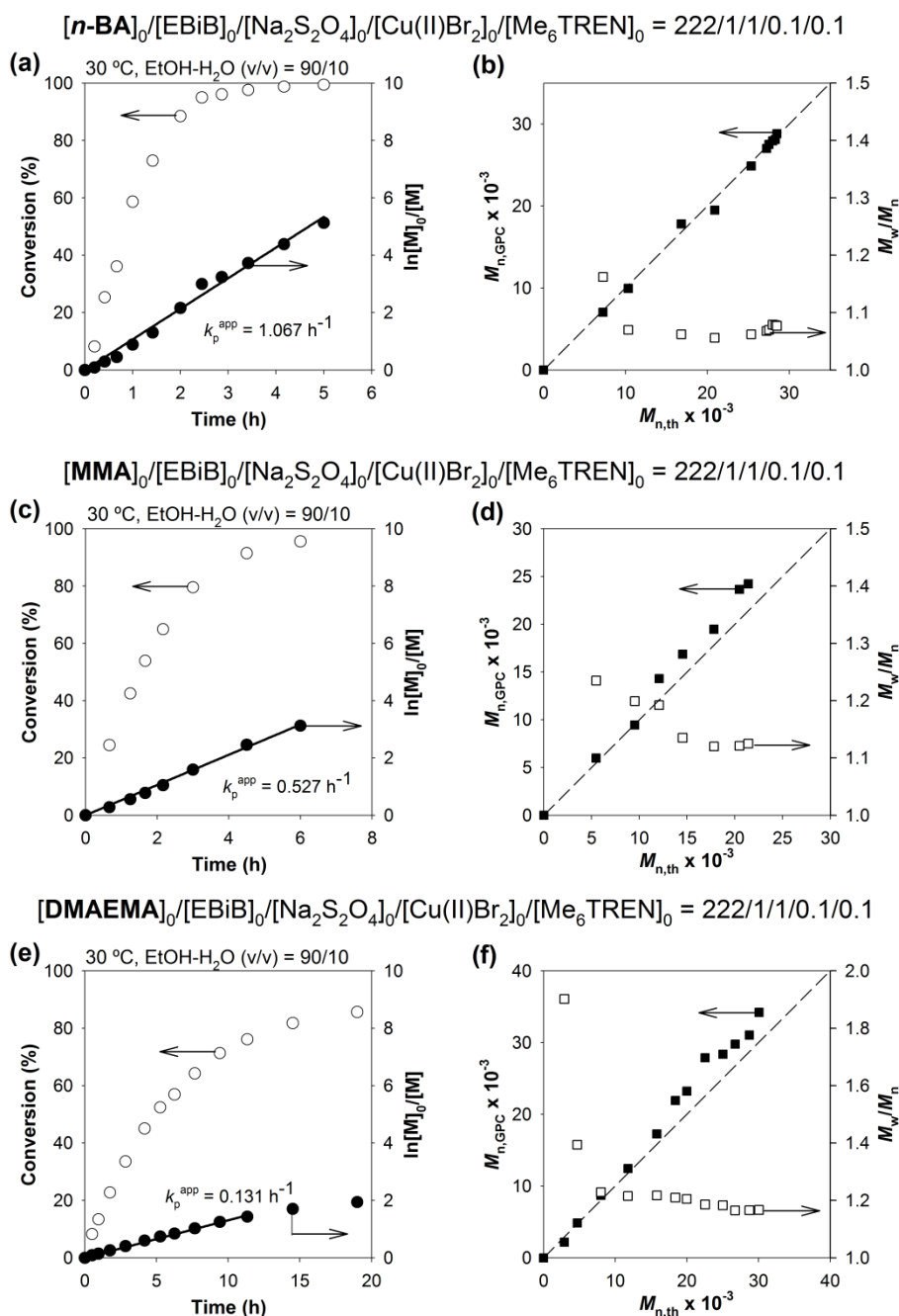


Figure 3.5. Kinetic plots of conversion and $\ln[M]_0/[M]$ vs. time (a, c, e) and plot of $M_{n,\text{GPC}}$ and \mathcal{D} (M_w/M_n) vs. $M_{n,\text{th}}$ (b, d, f) for SARA ATRP of *n*-BA (a, b), MMA (c, d) and DMAEMA (e, f) catalyzed with $\text{Na}_2\text{S}_2\text{O}_4$ in the presence of $\text{Cu(II)Br}_2/\text{Me}_6\text{TREN}$ at 30 °C in EtOH-H₂O (v/v) = 90/10. Conditions: $[\text{MA}]_0/[\text{solvent}] = 2/1$ (v/v); $[\text{Mon.}]_0/[\text{EBiB}]_0/[\text{Na}_2\text{S}_2\text{O}_4]_0/[\text{Cu(II)Br}_2]_0/[\text{Me}_6\text{TREN}]_0 = 222/1/1/0.1/0.1$.

Table 3.2. SARA ATRP of Acrylates, Methacrylates and Copolymers in the Presence of Na₂S₂O₄ and Cu(II)Br₂/Me₆TREN at 30 °C (33 vol % Solvent), [Monomer]₀/[EBIB]₀/[Na₂S₂O₄]₀/[Cu(II)Br₂]₀/[Me₆TREN]₀ = 222/1/1/0.1/0.1/0.1.

Entry	Monomer	Solvent System	k_p^{app} (h ⁻¹)	Time (h) ^a	Conv. (%) ^a	$M_{n,th} \times 10^{-3a}$	$M_{n,GPC} \times 10^{-3a}$	M_w/M_n^a
1	<i>n</i> -BA	EtOH-H ₂ O [90/10 (v/v)]	1.067	5.0	99.4	28.5	28.8	1.07
2	DMAEMA	EtOH-H ₂ O [90/10 (v/v)]	0.131	19.0	85.6	30.1	34.2	1.17
3	MMA	EtOH-H ₂ O [90/10 (v/v)]	0.527	6.0	95.6	21.4	24.2	1.12
4	MMA	DMSO	0.220	21.0	98.8	23.1	26.5	1.12
Copolymers								
5	PMA- <i>b</i> -PMA ^b	EtOH-H ₂ O [90/10 (v/v)]	-	4.0	-	-	68.2	1.10
6	PMA- <i>b</i> -PMMA ^c	EtOH-H ₂ O [90/10 (v/v)]	-	6.0	45.1	45.0	70.3	1.24

^aValues obtained from the last sample from the kinetic studies.

^bChain extension experiment were performed from PMA-Br macroinitiator ($M_{n,GPC} = 4400$, $M_w/M_n = 1.04$) and [MA]₀/[Solvent]₀ = 1/1 (v/v) was used.

^cCopolymerization experiment were performed from PMA-Br macroinitiator ($M_{n,GPC} = 4400$, $M_w/M_n = 1.04$) and [MMA]₀/[Solvent]₀ = 1/1 (v/v) was used.

3.4.6. Analysis of the PMA Structure

The structure of PMA-Br ($M_{n, \text{GPC}} = 4400$, $D = 1.04$) obtained using the catalytic system $[\text{Na}_2\text{S}_2\text{O}_4]/[\text{Cu}(\text{II})\text{Br}_2]/[\text{Me}_6\text{TREN}]$ in EtOH-H₂O [90/10 (v/v)] was studied by ¹H-NMR (Figure 3.6) and MALDI-TOF-MS (Figure 3.7).

The assignment of proton resonances have been done according to references: (**e**, **g**, **f**, **f'**),^{24,56,57} (**a**, **b**, **c**),^{24,58} (**dr**, **dm**).^{24,59-62} The signal of protons **dr** is partially overlapped with the signal of water trace in CDCl₃ at 1.6 ppm.^{24,63} The fractions of syndiotactic and isotactic diads (**dr** and **dm** respectively) were obtained by measuring the integrals of signals **dm** and **dr**.⁵⁹⁻⁶² The percentage of the chain-end functionality was calculated as follows: % functionality = $[\text{I}(\text{g})/\text{I}(\text{c})/6] \times 100\%$; where I(**g**) is the integral of the PMA terminal bromo chain-end $-\text{CH}_2-\text{CH}_g\text{Br}(\text{CO}_2\text{Me})$ at 4.24 ppm and I(**c**) is the integral of the initiator fragment $-\text{CH}(\text{CH}_{\text{c}3})_2\text{CO}_2\text{Et}$ at 1.10 and 1.15 ppm.²⁴ The PMA NMR molar mass was calculated using the equation $M_{n, \text{NMR}} = [[\text{I}(\text{e})/\text{I}(\text{g}) + 1] \times \text{MW}_{\text{MA}} + \text{MW}_{\text{EBiB}}]$; where I(**e**) is the integral of the PMA main chain C-H proton $-\text{CH}_2-\text{CH}_e(\text{CO}_2\text{Me})-$ at 2.3 ppm and I(**g**) is the integral of the active chain end $---\text{CH}_g\text{Br}$ at 4.24 ppm.

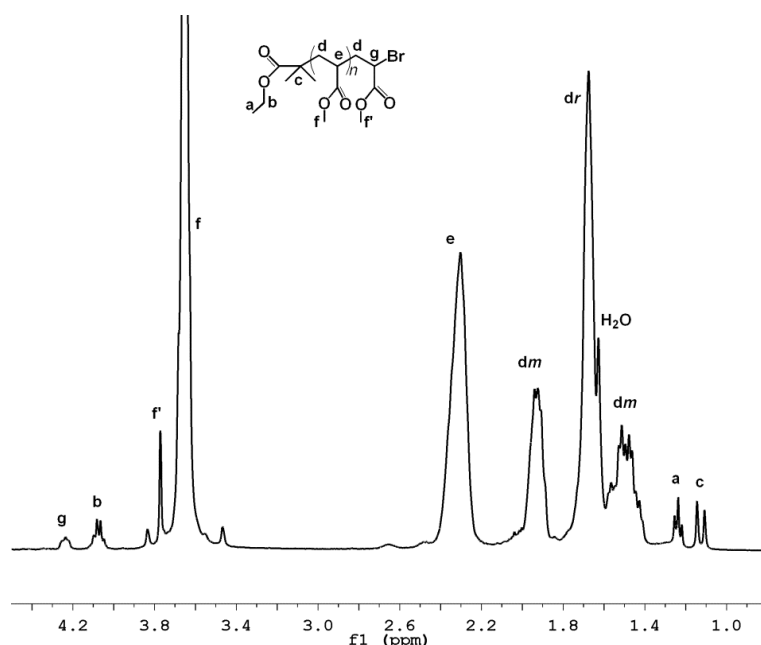


Figure 3.6. The ¹H NMR spectrum of PMA-Br obtained at high conversion ($M_{n, \text{GPC}} = 4400$; $D = 1.04$; $M_{n, \text{NMR}} = 4410$; active chain-end functionality = 99 %). The PMA is atactic: $[\text{dr}] = [\text{dm}] = 0.5$. The solvent is CDCl₃.

In MALDI-TOF-MS experiments, two types of matrices, DHB and HABA were tested, but only the former gave a clearly resolved spectrum (Figure 3.7). The MALDI-TOF-MS of PMA-Br ranging from 1500 to 7500 is shown in Figure 3.7(a). Enlargement of the 4150-4750 range is shown in Figure 3.7(b). Importantly, the series of main peaks is separated by an interval corresponding to a MA repeating unit (86.1 mass units). This main series is attributed to a polymer chain $[R-(MA)_n-Br + Na]^+$ where R-Br is the initiator EBiB ($4178.2 = 195.05 + 46 \times 86.09 + 22.99$, where 195.05, 86.09 and 22.99 correspond to the molar mass of EBiB, MA and Na⁺ respectively). Therefore, the obtained PMA-Br has a well-defined structure (i.e., without any detectable structural defects). The presence of possible structural defects would cause a deviation of m/z values of distribution. The series of less intensive peaks (Figure 3.7(b)) cannot be ascribed to any chain-end structures expected. The presence of these peaks is probably due to the occurrence of the fragmentation during ionization in the MALDI-TOF-MS analysis, as reported by other authors.⁶⁴⁻⁶⁷

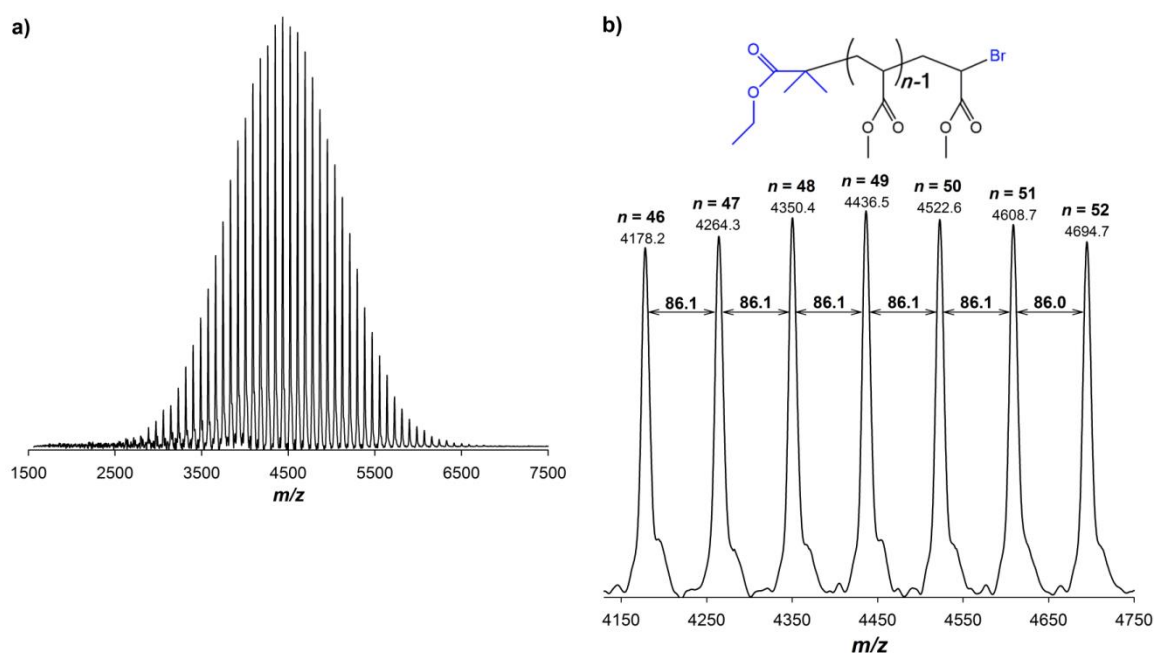


Figure 3.7. MALDI-TOF-MS (a) in the linear mode (using DHB as matrix) of PMA-Br ($M_{n,GPC} = 4400$, $D = 1.04$); (b) Enlargement of the MALDI-TOF-MS from m/z 4150 to 47500 of PMA-Br.

The structure of four arm star PMA-Br₄ ($M_{n,GPC} = 37200$, $\mathcal{D} = 1.05$) obtained using the catalytic system [Na₂S₂O₄]/[Cu(II)Br₂]/[Me₆TREN] in EtOH-H₂O [90/10 (v/v)] was studied by ¹H-NMR (Figure 3.8).

The signal of protons **dr** at 1.67 ppm is partially overlapped with the signal of water trace in CDCl₃ at 1.62 ppm.^{24,63} There are also traces of THF (resonances at 1.84 and 3.73 ppm)^{63,68} and hexanes (resonances 0.8-0.9 and 1.2-1.3 ppm),⁶⁸ which were used for PMA purification. The fractions of syndiotactic and isotactic diads (**dr** and **dm** respectively) were obtained by measuring the integrals of signals **dm** and **dr**.⁵⁹⁻⁶² The percentage of the chain-end functionality was calculated as follows: % functionality = [I(**g**)/I(**c**)/6] x 100%; where I(**g**) is the integral of the PMA terminal bromo chain-end -CH₂-CH_gBr(CO₂Me) at 4.24 ppm and I(**c**) is the integral of the initiator fragment -CH(CH₃)₂CO₂Et at 1.13 ppm.²⁴ The PMA NMR molar mass was calculated using the equation $M_{n,NMR} = [(I(e))/(I(g)/4) + 4] \times MW_{MA} + MW_{4f-BiB}$, where I(**e**) is the integral of the PMA main chain C-H proton -CH₂-CH_e(CO₂Me)- at 2.3 ppm and I(**g**) is the integral of the active chain end ---CH_gBr at 4.24 ppm).

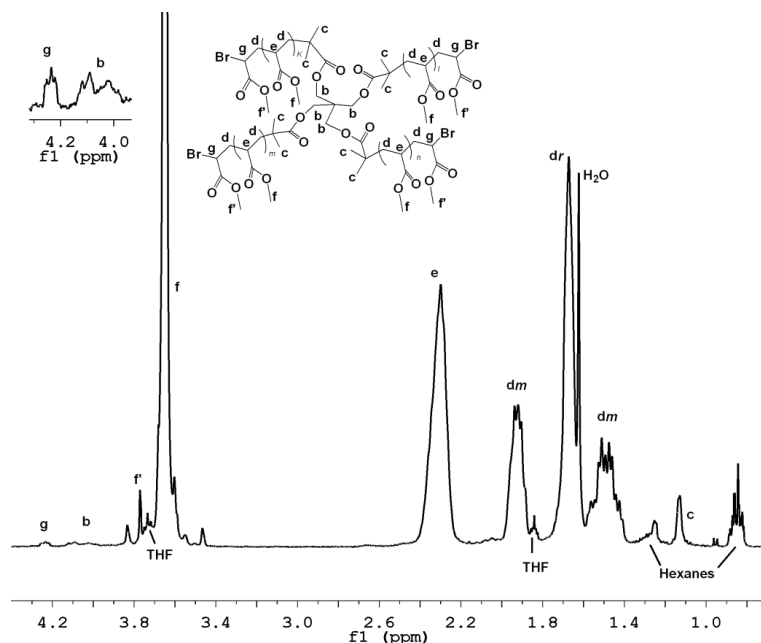


Figure 3.8. The ¹H NMR spectrum of four arm star PMA-Br₄ obtained at high conversion ($M_{n,GPC} = 37200$; $\mathcal{D} = 1.05$; $M_{n,NMR} = 43085$; active chain-end functionality = 99 %). The PMA is atactic: $[dr] = [dm] = 0.5$. The solvent is CDCl₃.

The results of ¹H NMR (Figure 3.6) and MALDI-TOF-MS (Figure 3.7) analyses for PMA-Br obtained starting from EBiB as well as ¹H NMR analysis for 4-star PMA-Br₄ (Figure 3.8) obtained from 4f-BiB confirmed the high degree of chain end functionality of the PMAs synthesized in the presence of sulfites.

3.4.7. Evaluation of the PMA Livingness

Re-initiation and copolymerization experiments were performed to evaluate the livingness of PMA chains prepared with the Na₂S₂O₄/Cu(II)Br₂/Me₆TREN in EtOH-H₂O [90/10 (v/v)] at 30 °C (Figure 3.9 and Table 3.2, entries 5 and 6). Figure 3.9 presents the GPC traces of PMA-Br macroinitiator, PMA extended and PMA-*b*-PMMA block copolymer. The results show the complete shift of the low molecular weight ($M_{n,GPC} = 4400$, $\mathcal{D} = 1.04$) GPC trace towards a very high molecular weight PMA extended ($M_{n,GPC} = 68200$, $\mathcal{D} = 1.10$) and PMA-*b*-PMMA block copolymer ($M_{n,GPC} = 70300$, $\mathcal{D} = 1.24$). These results prove the “living” character of the PMA and the possibility of using this catalytic system in the synthesis of block copolymers.

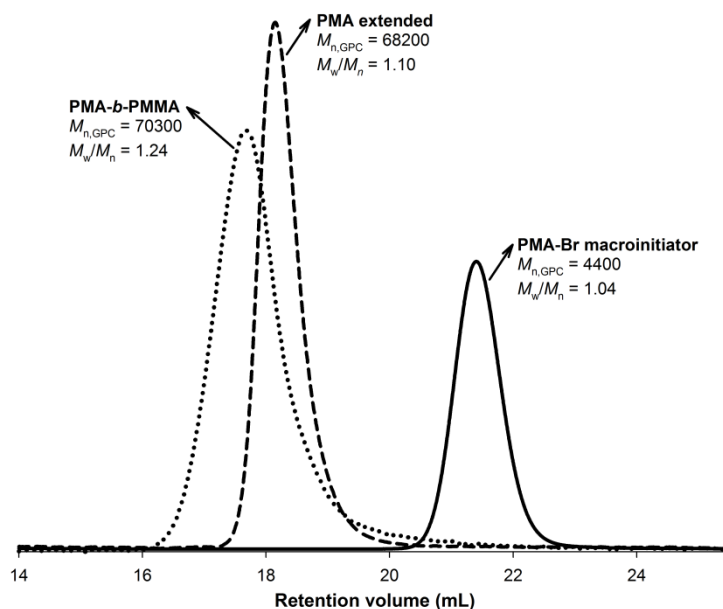


Figure 3.9. GPC traces of the PMA-Br macroinitiator before (right curve), after the chain extension experiment and PMA-*b*-PMMA block copolymer (left curves).

3.5. Conclusions

A successful eco-friendly, inexpensive and less toxic ambient temperature SARA ATRP of activated vinyl monomers (MA, *n*-BA, MMA and DMAEMA) catalyzed by inorganic sulfites (Na₂S₂O₄ and Na₂S₂O₅) and small amounts of Cu(II)Br₂/Me₆TREN system in a mixture of alcohols and water is reported. The controlled/"living" character of this catalytic system was proved by kinetic data, copolymerization and chain extension experiments. The molecular structure and chain-end functionality of the obtained polymers was confirmed by ¹H NMR and MALDI-TOF analysis. In this system, the use of inorganic sulfites (approved by FDA as food and beverage additives) and eco-friendly solvents (alcohol-water mixtures are inexpensive and have low boiling points) is a remarkable aspect for the possibility of scaling-up of the ATRP method.

3.6. References

1. Braunecker, W. A. and Matyjaszewski, K., *Controlled/living radical polymerization: Features, developments, and perspectives*. Progress in Polymer Science, **2007**, 32, 93-146.
2. Tasdelen, M. A., Kahveci, M. U., and Yagci, Y., *Telechelic polymers by living and controlled/living polymerization methods*. Progress in Polymer Science, **2011**, 36, 455-567.
3. Kamigaito, M., Ando, T., and Sawamoto, M., *Metal-Catalyzed Living Radical Polymerization*. Chemical Reviews, **2001**, 101, 3689-3746.
4. Matyjaszewski, K. and Xia, J., *Atom Transfer Radical Polymerization*. Chemical Reviews, **2001**, 101, 2921-2990.
5. Poli, R., *Relationship between One-Electron Transition-Metal Reactivity and Radical Polymerization Processes*. Angewandte Chemie International Edition, **2006**, 45, 5058-5070.
6. Tsarevsky, N. V. and Matyjaszewski, K., *"Green" Atom Transfer Radical Polymerization: From Process Design to Preparation of Well-Defined Environmentally Friendly Polymeric Materials*. Chemical Reviews, **2007**, 107, 2270-2299.
7. Matyjaszewski, K., *Atom Transfer Radical Polymerization (ATRP): Current Status and Future Perspectives*. Macromolecules, **2012**, 45, 4015-4039.

8. Matyjaszewski, K. and Spanswick, J., *Copper-Mediated Atom Transfer Radical Polymerization*, in *Polymer Science: A Comprehensive Reference*, K. Matyjaszewski and M. Martin, Editors. **2012**, Elsevier: Amsterdam. p. 377-428.
9. Coessens, V., Pintauer, T., and Matyjaszewski, K., *Functional polymers by atom transfer radical polymerization*. *Progress in Polymer Science*, **2001**, *26*, 337-377.
10. Davis, K. A. and Matyjaszewski, K., *Statistical, gradient, block, and graft copolymers by controlled/living radical polymerizations*. *Advances in Polymer Science*, **2002**, *159*, 1-166.
11. Oh, J. K., Drumright, R., Siegwart, D. J., and Matyjaszewski, K., *The development of microgels/nanogels for drug delivery applications*. *Progress in Polymer Science*, **2008**, *33*, 448-477.
12. Sheiko, S. S., Sumerlin, B. S., and Matyjaszewski, K., *Cylindrical molecular brushes: Synthesis, characterization, and properties*. *Prog. Polym. Sci.*, **2008**, *33*, 759-785.
13. Gao, H. and Matyjaszewski, K., *Synthesis of functional polymers with controlled architecture by CRP of monomers in the presence of cross-linkers: From stars to gels*. *Prog. Polym. Sci.*, **2009**, *34*, 317-350.
14. Golas, P. L. and Matyjaszewski, K., *Marrying click chemistry with polymerization: expanding the scope of polymeric materials*. *Chem. Soc. Rev.*, **2010**, *39*, 1338-1354.
15. Lee, H.-i., Pietrasik, J., Sheiko, S. S., and Matyjaszewski, K., *Stimuli-responsive molecular brushes*. *Prog. Polym. Sci.*, **2010**, *35*, 24-44.
16. Siegwart, D. J., Oh, J. K., and Matyjaszewski, K., *ATRP in the design of functional materials for biomedical applications*. *Prog. Polym. Sci.*, **2012**, *37*, 18-37.
17. Gnanou, Y. and Hizal, G., *Effect of phenol and derivatives on atom transfer radical polymerization in the presence of air*. *J. Polym. Sci., Part A: Polym. Chem.*, **2004**, *42*, 351-359.
18. Jakubowski, W., Min, K., and Matyjaszewski, K., *Activators Regenerated by Electron Transfer for Atom Transfer Radical Polymerization of Styrene*. *Macromolecules*, **2005**, *39*, 39-45.
19. Jakubowski, W. and Matyjaszewski, K., *Activators Regenerated by Electron Transfer for Atom-Transfer Radical Polymerization of (Meth)acrylates and Related Block Copolymers*. *Angewandte Chemie International Edition*, **2006**, *45*, 4482-4486.
20. Kwak, Y., Magenau, A. J. D., and Matyjaszewski, K., *ARGET ATRP of Methyl Acrylate with Inexpensive Ligands and ppm Concentrations of Catalyst*. *Macromolecules*, **2011**, *44*, 811-819.

21. Matyjaszewski, K., Jakubowski, W., Min, K., Tang, W., Huang, J., Braunecker, W. A., and Tsarevsky, N. V., *Diminishing catalyst concentration in atom transfer radical polymerization with reducing agents*. Proceedings of the National Academy of Sciences, **2006**, *103*, 15309-15314.
22. Konkolewicz, D., Magenau, A. J. D., Averick, S. E., Simakova, A., He, H., and Matyjaszewski, K., *ICAR ATRP with ppm Cu Catalyst in Water*. Macromolecules, **2012**, *45*, 4461-4468.
23. Magenau, A. J. D., Kwak, Y., and Matyjaszewski, K., *ATRP of Methacrylates Utilizing Cu(II)/L and Copper Wire*. Macromolecules, **2010**, *43*, 9682-9689.
24. Mendonça, P. V., Serra, A. C., Coelho, J. F. J., Popov, A. V., and Guliashvili, T., *Ambient temperature rapid ATRP of methyl acrylate, methyl methacrylate and styrene in polar solvents with mixed transition metal catalyst system*. European Polymer Journal, **2011**, *47*, 1460-1466.
25. Wang, Y., Zhang, Y., Parker, B., and Matyjaszewski, K., *ATRP of MMA with ppm Levels of Iron Catalyst*. Macromolecules, **2011**, *44*, 4022-4025.
26. West, A. G., Hornby, B., Tom, J., Ladmiral, V., Harrisson, S., and Perrier, S., *Origin of Initial Uncontrolled Polymerization and Its Suppression in the Copper(0)-Mediated Living Radical Polymerization of Methyl Acrylate in a Nonpolar Solvent*. Macromolecules, **2011**, *44*, 8034-8041.
27. Zhang, Y., Wang, Y., and Matyjaszewski, K., *ATRP of Methyl Acrylate with Metallic Zinc, Magnesium, and Iron as Reducing Agents and Supplemental Activators*. Macromolecules, **2011**, *44*, 683-685.
28. Abreu, C. M. R., Mendonça, P. V., Serra, A. C., Coelho, J. F. J., Popov, A. V., and Guliashvili, T., *Accelerated Ambient-Temperature ATRP of Methyl Acrylate in Alcohol-Water Solutions with a Mixed Transition-Metal Catalyst System*. Macromolecular Chemistry and Physics, **2012**, *213*, 1677-1687.
29. Abreu, C. M. R., Mendonça, P. V., Serra, A. C., Popov, A. V., Matyjaszewski, K., Guliashvili, T., and Coelho, J. F. J., *Inorganic Sulfites: Efficient Reducing Agents and Supplemental Activators for Atom Transfer Radical Polymerization*. ACS Macro Letters, **2012**, *1*, 1308-1311.
30. Guliashvili, T., Mendonca, P. V., Serra, A. C., Popov, A. V., and Coelho, J. F. J., *Copper-Mediated Controlled/"Living" Radical Polymerization in Polar Solvents: Insights into Some Relevant Mechanistic Aspects*. Chemistry-a European Journal, **2012**, *18*, 4607-4612.
31. Cordeiro, R. A., Rocha, N., Mendes, J. P., Matyjaszewski, K., Guliashvili, T., Serra, A. C., and Coelho, J. F. J., *Synthesis of well-defined poly(2-(dimethylamino)ethyl methacrylate) under mild conditions and its co-polymers with cholesterol and PEG using Fe(0)/Cu(II) based SARA ATRP*. Polymer Chemistry, **2013**, *4*, 3088-3097.

32. Peng, C.-H., Zhong, M., Wang, Y., Kwak, Y., Zhang, Y., Zhu, W., Tonge, M., Buback, J., Park, S., Krys, P., Konkolewicz, D., Gennaro, A., and Matyjaszewski, K., *Reversible-Deactivation Radical Polymerization in the Presence of Metallic Copper. Activation of Alkyl Halides by Cu⁰*. *Macromolecules*, **2013**, *46*, 3803-3815.
33. Rocha, N., Mendonça, P. V., Mendes, J. P., Simões, P. N., Popov, A. V., Guliashvili, T., Serra, A. C., and Coelho, J. F. J., *Facile Synthesis of Well-Defined Telechelic Alkyne-Terminated Polystyrene in Polar Media Using ATRP With Mixed Fe/Cu Transition Metal Catalyst*. *Macromolecular Chemistry and Physics*, **2013**, *214*, 76-84.
34. Wang, Y., Zhong, M., Zhu, W., Peng, C.-H., Zhang, Y., Konkolewicz, D., Bortolamei, N., Isse, A. A., Gennaro, A., and Matyjaszewski, K., *Reversible-Deactivation Radical Polymerization in the Presence of Metallic Copper. Comproportionation–Disproportionation Equilibria and Kinetics*. *Macromolecules*, **2013**, *46*, 3793-3802.
35. Zhong, M., Wang, Y., Krys, P., Konkolewicz, D., and Matyjaszewski, K., *Reversible-Deactivation Radical Polymerization in the Presence of Metallic Copper. Kinetic Simulation*. *Macromolecules*, **2013**, *46*, 3816-3827.
36. Bortolamei, N., Isse, A. A., Magenau, A. J. D., Gennaro, A., and Matyjaszewski, K., *Controlled Aqueous Atom Transfer Radical Polymerization with Electrochemical Generation of the Active Catalyst*. *Angewandte Chemie International Edition*, **2011**, *50*, 11391-11394.
37. Magenau, A. J. D., Strandwitz, N. C., Gennaro, A., and Matyjaszewski, K., *Electrochemically Mediated Atom Transfer Radical Polymerization*. *Science*, **2011**, *332*, 81-84.
38. Li, B., Yu, B., Huck, W. T. S., Zhou, F., and Liu, W., *Electrochemically Induced Surface-Initiated Atom-Transfer Radical Polymerization*. *Angewandte Chemie International Edition*, **2012**, *51*, 5092-5095.
39. Kwak, Y. and Matyjaszewski, K., *Photoirradiated Atom Transfer Radical Polymerization with an Alkyl Dithiocarbamate at Ambient Temperature*. *Macromolecules* (Washington, DC, U. S.), **2010**, *43*, 5180-5183.
40. Tasdelen, M. A., Uygun, M., and Yagci, Y., *Studies on Photoinduced ATRP in the Presence of Photoinitiator*. *Macromolecular Chemistry and Physics*, **2011**, *212*, 2036-2042.
41. Fors, B. P. and Hawker, C. J., *Control of a Living Radical Polymerization of Methacrylates by Light*. *Angewandte Chemie International Edition*, **2012**, *51*, 8850-8853.
42. Kahveci, M. U., Acik, G., and Yagci, Y., *Synthesis of block copolymers by combination of atom transfer radical polymerization and visible light-induced free*

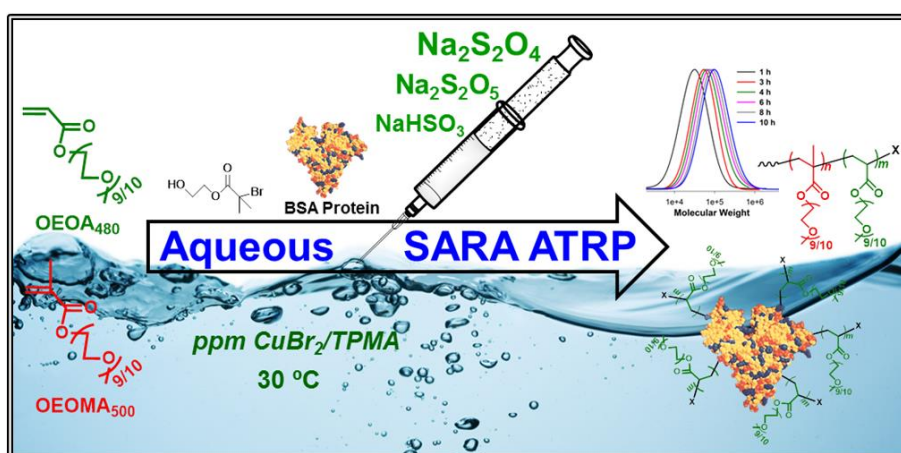
- radical promoted cationic polymerization.* Macromolecular Rapid Communications, **2012**, *33*, 309-313.
43. Konkolewicz, D., Schröder, K., Buback, J., Bernhard, S., and Matyjaszewski, K., *Visible Light and Sunlight Photoinduced ATRP with ppm of Cu Catalyst.* ACS Macro Letters, **2012**, *1*, 1219-1223.
 44. Mosnáček, J. and Ilčíková, M., *Photochemically Mediated Atom Transfer Radical Polymerization of Methyl Methacrylate Using ppm Amounts of Catalyst.* Macromolecules, **2012**, *45*, 5859-5865.
 45. Tasdelen, M. A., Ciftci, M., and Yagci, Y., *Visible light-induced atom transfer radical polymerization.* Macromolecular Chemistry and Physics, **2012**, *213*, 1391-1396.
 46. Matyjaszewski, K. and Tsarevsky, N. V., *Nanostructured functional materials prepared by atom transfer radical polymerization.* Nature Chemistry, **2009**, *1*, 276-288.
 47. Fischer, H., *The Persistent Radical Effect: A Principle for Selective Radical Reactions and Living Radical Polymerizations.* Chemical Reviews, **2001**, *101*, 3581-3610.
 48. Menchikov, L. G., Vorogushin, A. V., Korneva, O. S., and Nefedov, O. M., *An effective method for alcohol preparation by hydrolysis of organohalides in the presence of copper and its salts in aqueous DMSO.* Mendeleev Commun., **1995**, 223-4.
 49. Lobb, E. J., Ma, I., Billingham, N. C., Armes, S. P., and Lewis, A. L., *Facile Synthesis of Well-Defined, Biocompatible Phosphorylcholine-Based Methacrylate Copolymers via Atom Transfer Radical Polymerization at 20 °C.* Journal of the American Chemical Society, **2001**, *123*, 7913-7914.
 50. McDonald, S. and Rannard, S. P., *Room temperature waterborne ATRP of n-butyl methacrylate in homogeneous alcoholic media.* Macromolecules, **2001**, *34*, 8600-8602.
 51. Bontempo, D., Heredia, K. L., Fish, B. A., and Maynard, H. D., *Cysteine-Reactive Polymers Synthesized by Atom Transfer Radical Polymerization for Conjugation to Proteins.* Journal of the American Chemical Society, **2004**, *126*, 15372-15373.
 52. Kimani, S. M. and Moratti, S. C., *Ambient-temperature copper-catalyzed atom transfer radical polymerization of methacrylates in ethylene glycol solvents.* Journal of Polymer Science Part A: Polymer Chemistry, **2005**, *43*, 1588-1598.
 53. Lligadas, G. and Percec, V., *Ultrafast SET-LRP of methyl acrylate at 25 °C in alcohols.* Journal of Polymer Science Part A: Polymer Chemistry, **2008**, *46*, 2745-2754.

54. Ciampolini, M. and Nardi, N., *Five-Coordinated High-Spin Complexes of Bivalent Cobalt, Nickel, and Copper with Tris(2-dimethylaminoethyl)amine*. Inorganic Chemistry, **1966**, 5, 41-44.
55. Percec, V., Popov, A. V., Ramirez-Castillo, E., Coelho, J. F. J., and Hinojosa-Falcon, L. A., *Non-transition metal-catalyzed living radical polymerization of vinyl chloride initiated with iodoform in water at 25°C*. J. Polym. Sci., Part A: Polym. Chem., **2004**, 42, 6267-6282.
56. Percec, V., Guliashvili, T., Ladislaw, J. S., Wistrand, A., Stjerndahl, A., Sienkowska, M. J., Monteiro, M. J., and Sahoo, S., *Ultrafast Synthesis of Ultrahigh Molar Mass Polymers by Metal-Catalyzed Living Radical Polymerization of Acrylates, Methacrylates, and Vinyl Chloride Mediated by SET at 25 °C*. J. Am. Chem. Soc., **2006**, 128, 14156-14165.
57. Lligadas, G., Ladislaw, J. S., Guliashvili, T., and Percec, V., *Functionally terminated poly(methyl acrylate) by SET-LRP initiated with CHBr₃ and CHI₃*. J. Polym. Sci., Part A: Polym. Chem., **2008**, 46, 278-288.
58. Hasneen, A., Kim, S. J., and Paik, H.-j., *Synthesis and characterization of low molecular weight poly(methyl acrylate)-*b*-polystyrene by a combination of ATRP and click coupling method*. Macromol. Res., **2007**, 15, 541-546.
59. Tabuchi, M., Kawauchi, T., Kitayama, T., and Hatada, K., *Living polymerization of primary alkyl acrylates with *t*-butyllithium/bulky aluminum Lewis acids*. Polymer, **2002**, 43, 7185-7190.
60. Coelho, J. F. J., Carvalho, E. Y., Marques, D. S., Popov, A. V., Goncalves, P. M., and Gil, M. H., *Synthesis of poly(lauryl acrylate) by single-electron transfer/degenerative chain transfer living radical polymerization catalyzed by Na₂S₂O₄ in water*. Macromol. Chem. Phys., **2007**, 208, 1218-1227.
61. Coelho, J. F. J., Carvalho, E. Y., Marques, D. S., Popov, A. V., Percec, V., Goncalves, P. M. F. O., and Gil, M. H., *Synthesis of poly(ethyl acrylate) by single electron transfer-degenerative chain transfer living radical polymerization in water catalyzed by Na₂S₂O₄*. J. Polym. Sci., Part A: Polym. Chem., **2007**, 46, 421-432.
62. Coelho, J. F. J., Gois, J., Fonseca, A. C., Carvalho, R. A., Popov, A. V., Percec, V., and Gil, M. H., *Synthesis of poly(2-methoxyethyl acrylate) by single electron transfer-Degenerative transfer living radical polymerization catalyzed by Na₂S₂O₄ in water*. J. Polym. Sci., Part A: Polym. Chem., **2009**, 47, 4454-4463.
63. Gottlieb, H. E., Kotlyar, V., and Nudelman, A., *NMR Chemical Shifts of Common Laboratory Solvents as Trace Impurities*. J. Org. Chem., **1997**, 62, 7512-7515.
64. Beyou, E., Chaumont, P., Chauvin, F., Devaux, C., and Zydowicz, N., *Study of the Reaction between Nitroxide-Terminated Polymers and Thiuram Disulfides. Toward a Method of Functionalization of Polymers Prepared by Nitroxide*

- Mediated Free “Living” Radical Polymerization*. *Macromolecules*, **1998**, *31*, 6828-6835.
65. Coca, S., Jasieczek, C. B., Beers, K. L., and Matyjaszewski, K., *Polymerization of acrylates by atom transfer radical polymerization. Homopolymerization of 2-hydroxyethyl acrylate*. *Journal of Polymer Science Part A: Polymer Chemistry*, **1998**, *36*, 1417-1424.
66. Schilli, C., Lanzendörfer, M. G., and Müller, A. H. E., *Benzyl and Cumyl Dithiocarbamates as Chain Transfer Agents in the RAFT Polymerization of N-Isopropylacrylamide. In Situ FT-NIR and MALDI-TOF MS Investigation*. *Macromolecules*, **2002**, *35*, 6819-6827.
67. Abreu, C. M. R., Mendonça, P. V., Serra, A. C., Coelho, J. F. J., Popov, A. V., Gryn'ova, G., Coote, M. L., and Guliashvili, T., *Reversible Addition-Fragmentation Chain Transfer Polymerization of Vinyl Chloride*. *Macromolecules*, **2012**, *45*, 2200-2208.
68. Fulmer, G. R., Miller, A. J. M., Sherden, N. H., Gottlieb, H. E., Nudelman, A., Stoltz, B. M., Bercaw, J. E., and Goldberg, K. I., *NMR Chemical Shifts of Trace Impurities: Common Laboratory Solvents, Organics, and Gases in Deuterated Solvents Relevant to the Organometallic Chemist*. *Organometallics*, **2010**, *29*, 2176-2179.

Chapter 4

Aqueous Supplemental Activator and Reducing Agent Atom Transfer Radical Polymerization Using Inorganic Sulfites

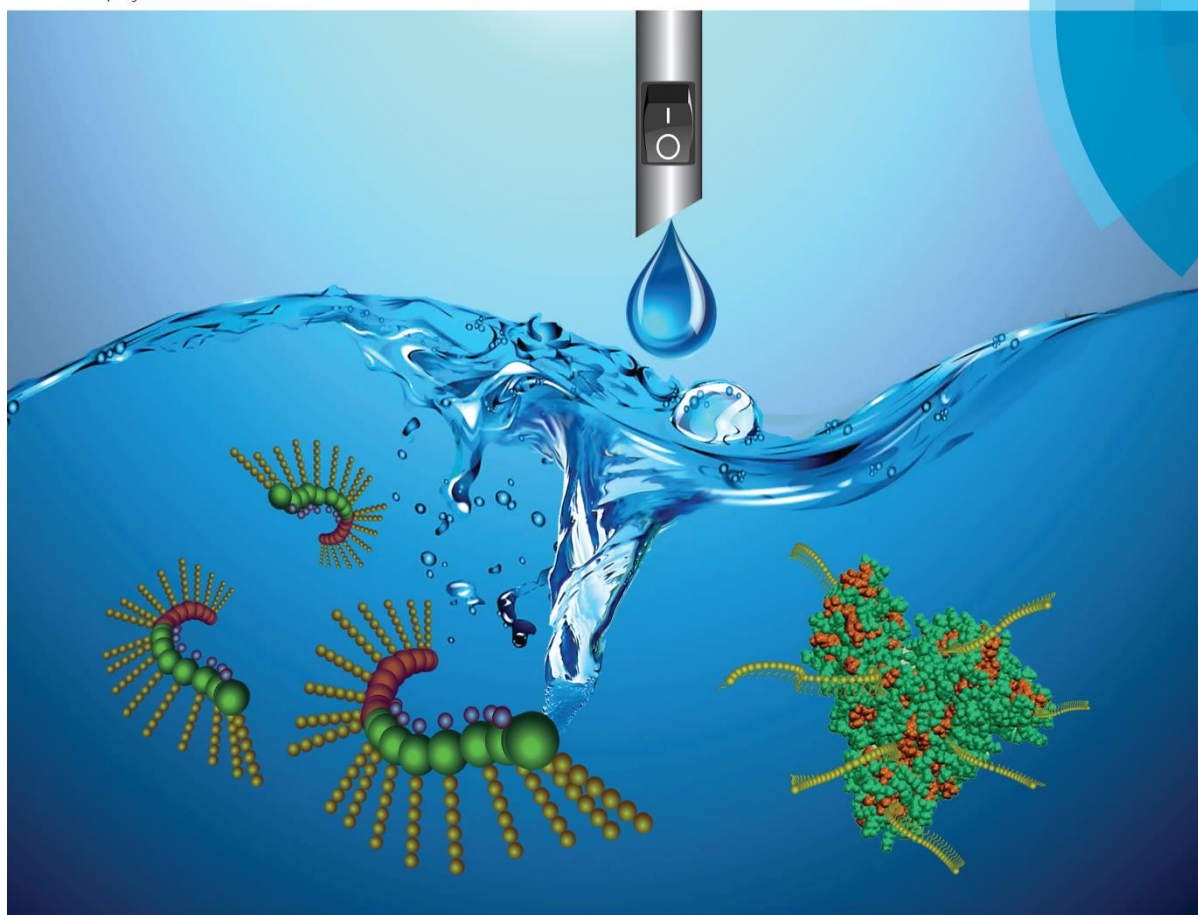


The contents of this chapter are published in:

Abreu, C. M. R., Fu, L., Carmali, S., Serra, A. C., Matyjaszewski, K., and Coelho, J. F. J., *Aqueous SARA ATRP Using Inorganic Sulfites*. *Polymer Chemistry*, **2017**, 8, 375-387.

Polymer Chemistry

rsc.li/polymers



ISSN 1759-9962



PAPER
Krzysztof Matyjaszewski, Jorge F. J. Coelho *et al.*
Aqueous SARA ATRP using inorganic sulfites

4.1. Abstract

Aqueous supplemental activator and reducing agent atom transfer radical polymerization (SARA ATRP) using inorganic sulfites was successfully carried out for the first time. Under optimized conditions, a well-controlled poly[oligo(ethylene oxide) methyl ether acrylate] (POEOA) was obtained with <30 ppm of a soluble copper catalyst using a tris(2-pyridylmethyl)amine (TPMA) ligand in the presence of an excess of halide salts (*e.g.* NaCl). Inorganic sulfites (*e.g.* Na₂S₂O₄) were continuously fed into the reaction mixture. The mechanistic studies proved that these salts can activate alkyl halides directly and regenerate the activator complex. The effects of the feeding rate of the SARA agent (inorganic sulfites), the ligand and its concentration, halide salt and its concentration, sulfite used, and copper concentration, were systematically studied to afford fast polymerizations rates while maintaining the control over polymerization. The kinetic data showed linear first-order kinetics, linear evolution of molecular weights with conversion, and polymers with narrow molecular weight distributions ($\mathcal{D} \sim 1.2$) during polymerization even at relatively high monomer conversions ($\sim 80\%$). “One-pot” chain extension and “one-pot” block copolymerization experiments proved the high chain-end functionality. The polymerization could be directly regulated by starting or stopping the continuous feeding of the SARA agent. Under biologically relevant conditions, the aqueous SARA ATRP using inorganic sulfites was used to synthesize a well-defined protein-polymer hybrid by grafting of P(OEOA₄₈₀) from BSA-O-[iBBr]₃₀.

4.2. Introduction

Reversible deactivation radical polymerization (RDRP) techniques offer control over structure that is similar to ionic living polymerizations,¹ but with all the advantages associated with radical based polymerizations.^{2,3} Nitroxide-mediated polymerization (NMP),⁴⁻⁶ atom transfer radical polymerization (ATRP),⁷⁻¹² and reversible addition-fragmentation chain transfer polymerization (RAFT)¹³⁻¹⁵ are the preferred RDRP methods in the scientific community. ATRP is among the most efficient and versatile RDRP processes. It provides access to a myriad of (co)polymers with precisely controlled

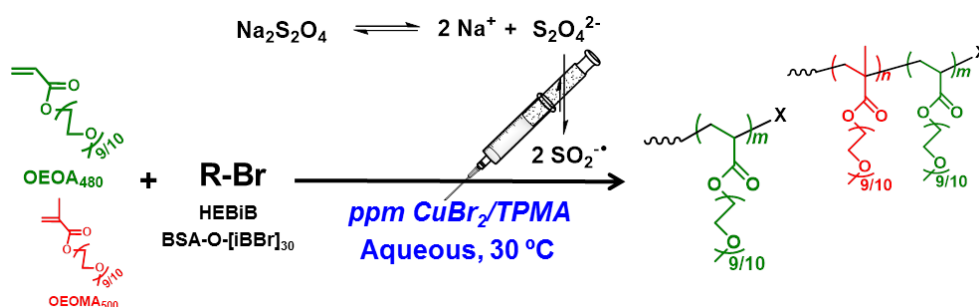
architecture, including stars, brushes, and nanogels, as well as block, gradient, and statistical copolymers with specific functionalities.^{9,16-20} Several variations of the normal ATRP method have been developed aiming to reduce the catalyst levels, such as: activators regenerated by electron transfer (ARGET) ATRP,²¹⁻²⁴ initiator for continuous activator regeneration (ICAR) ATRP,^{25,26} supplemental activator and reducing agent (SARA) ATRP,²⁷⁻³⁴ electrochemically mediated ATRP (eATRP),³⁵⁻³⁸ and photochemically mediated ATRP.³⁹⁻⁴⁴

Recently our research team has discovered a new class of efficient SARA agents for ATRP, sulfite salts: sodium metabisulfite ($\text{Na}_2\text{S}_2\text{O}_5$), sodium dithionite ($\text{N}_2\text{S}_2\text{O}_4$) and sodium bisulfite (NaHSO_3).⁴⁵ These salts can directly activate alkyl halides and also reduce *in situ* Cu(II) to Cu(I) species.⁴⁵⁻⁴⁹ In general, sulfites are efficient, inexpensive, safe, and environmentally friendly “co-catalysts” for the synthesis of well-defined polymers both in organic solvents (*e.g.* DMSO)⁴⁵ and in more eco-friendly solvents like ionic liquids,⁴⁹ alcohols and alcohols/water mixtures.⁴⁶⁻⁴⁸

One limitation associated with traditional ATRP methods is the use of organic solvents to afford homogenous reaction conditions.^{7,50} Over the years, different systems have been developed to replace these volatile and potentially hazardous organic solvents by “green” solvents^{10,51} like supercritical carbon dioxide,^{52,53} ionic liquids^{49,54-56} or water.^{24,26,30,57} Aqueous ATRP usually results in polymers with relatively high dispersity (\bar{D}) indicating either poor control or the loss of chain-end functionality.⁵⁷ This fact is due to several reasons: the large ATRP equilibrium constant in aqueous media,^{24,35} which generates high radical concentrations and consequently an increased rate of irreversible termination reactions;⁵⁸ the partial dissociation of the halide anion from a deactivator complex, leading to an inefficient deactivation of the propagating radicals;⁵⁸ some Cu(I)/ligand (L) complexes can be disproportionate or undergo partial dissociation;⁵⁸ and lastly, hydrolysis of the carbon-halogen bond that diminishes the chain-end functionality.^{24,57,58} To suppress these problems, aqueous ATRP was traditionally performed with high copper concentrations that could mitigate the deactivator dissociation, and low ratios of Cu(I)/L:Cu(II)/L to reduce the radical concentration.^{24,57,59} Aqueous ICAR²⁶ and ARGET²⁴ ATRP methods were developed aiming to control the polymerization at low Cu concentrations. In the presence of a large excess of halide salts (*e.g.* NaCl or NaBr), well-

controlled polymers of oligo(ethylene oxide) methyl ether (meth)acrylate (OEOMA) were obtained using catalyst concentration lower than 100 ppm.^{24,26} After the optimization of reaction conditions, ICAR and ARGET ATRP presented linear first-order kinetics, linear evolution of molecular weights with conversion, and final \bar{D} below 1.3. Thermoresponsive block copolymers and protein-polymer hybrids were synthesized using these techniques.^{24,26}

This study methodically investigated the different parameters of SARA ATRP of oligo(ethylene oxide) methyl ether acrylate (OEOMA) in aqueous media catalyzed by $\text{Cu(II)Br}_2/\text{TPMA}$ using a slow feeding of inorganic sulfites (*e.g.* $\text{Na}_2\text{S}_2\text{O}_4$) at room temperature (30 °C) (Scheme 4.1). This manuscript reports the optimization of reaction conditions in aqueous media for the synthesis of well-defined water-soluble polymers using low Cu concentrations. The reported system is also extended to the synthesis of block copolymers using a “one-pot” method and the preparation of a protein-polymer hybrid.



Scheme 4.1. Aqueous SARA ATRP of OEOMA₄₈₀ and OEOMA₅₀₀ by Feeding Inorganic Sulfites.

4.3. Experimental Section

4.3.1. Materials

Oligo(ethylene oxide) methyl ether acrylate (OEOMA₄₈₀, 99%, average molecular weight 480, Sigma-Aldrich) and oligo(ethylene oxide) methyl ether methacrylate (OEOMA₅₀₀,

99%, average molecular weight 500, Aldrich) were passed over a column of basic alumina (Fisher Scientific) prior to use. $\text{Na}_2\text{S}_2\text{O}_4$ (Sigma–Aldrich, 85 %), $\text{Na}_2\text{S}_2\text{O}_5$ (Sigma–Aldrich, >99 %), NaHSO_3 (Sigma–Aldrich, >99 %), 2-hydroxyethyl 2-bromoisobutyrate (HEBiB, 95%, Sigma-Aldrich), copper(II) bromide (99.99%, Sigma-Aldrich), sodium chloride (NaCl, 99.5%, Fisher Scientific), tetraethylammonium chloride (TEACl, 98%, Sigma-Aldrich), sodium bromide (NaBr, 99.5%, Fisher Scientific), bovine serum albumin (BSA, $\geq 98\%$, Sigma-Aldrich), water (H_2O , HPLC grade, Fisher Scientific), N,N-dimethylformamide (DMF, ACS grade, Fisher Scientific), deuterium oxide (D_2O , 99.9%, Cambridge Isotope Laboratories), and anhydrous magnesium sulfate (99%, Aldrich) were used as received. 1X PBS solution was prepared from 10X PBS (Thermo Fisher Scientific) and HPLC grade water. Tris(pyridin-2-ylmethyl)amine (TPMA),⁶⁰ tris[2-(dimethylamino)ethyl]amine (Me_6TREN)⁶¹ and BSA protein initiator (BSA-O-[iBBr]_{30})⁵⁹ were prepared as previously reported in the literature.

4.3.2. Techniques

A syringe pump (KDS Scientific, Legato 101) was used for the continuous feeding of the sulfites at the rate 1 $\mu\text{L}/\text{min}$ (different sulfite aqueous solutions were prepared to obtain different FR_S).

^1H nuclear magnetic resonance (NMR) spectroscopy measurements were performed on a Bruker Avance 500 MHz spectrometer and used to determine the monomer conversion in D_2O .

The chromatographic parameters of the samples were determined using a gel permeation chromatography (GPC) system equipped with a Waters 515 HPLC pump and a Waters 2414 refractive index detector using PSS columns (Styrogel 10^2 , 10^3 , 10^5 Å) with DMF containing 10 mM LiBr as the eluent at a flow rate of 1 mL/min at 50 °C. The system was calibrated with low dispersity PMMA ($M_n = 800 - 1\,820\,000$) standards. Before the injection (50 μL) the samples were filtered through a polytetrafluoroethylene (PTFE) membrane with 0.22 μm pore.

The UV-Visible studies were performed using an Agilent 8453 UV-Vis Spectrometer.

Dynamic light scattering (DLS) measurements were performed on a Malvern Zetasizer Nano ZS at 25 °C.

Sodium dodecyl sulfate-polyacrylamide gel electrophoresis (SDS-PAGE) was performed with a Bio-Rad Laboratories Mini-Protean TGX™ Precast Gels (7.5%). Staining was accomplished with Coomassie blue and washed in DI water overnight.

4.3.3. Procedures

General Procedure for Aqueous SARA ATRP of OEOA

A series of aqueous SARA ATRP using OEOA as monomer were carried out with systematically different conditions to establish the optimal reactions conditions. The conditions used for polymerization of OEOA₄₈₀ generally followed this procedure: NaCl (58.4 mg, 1.0 mmol), OEOA₄₈₀ (2.40 g, 5 mmol), 100 mM stock solution HEBiB (0.2 mL, 0.02 mmol), stock solution of 25 mM CuBr₂ and 200 mM TPMA (40 μL, 1.0 μmol of CuBr₂ and 8 μmol of TPMA) were dissolved in H₂O (7.7 mL). DMF (0.1 mL) was added as internal standard for ¹H NMR analysis. This mixture was added to a 25 mL Schlenk flask and purged with nitrogen for 30 min, and then the flask was placed in an oil bath at 30 °C. A Na₂S₂O₄ aqueous solution (64 mM) was purged with nitrogen, and the solution was continuously injected into the reaction medium using a syringe pump at the rate 1 μL/min. Samples were taken throughout the reaction for GPC and NMR analysis.

Synthesis of “One-pot” POEOMA-*b*-POEOA Block Copolymer

NaCl (58.4 mg, 1.0 mmol), OEOMA₅₀₀ (2.50 g, 5 mmol), 100 mM stock solution HEBiB (1.0 mL, 0.10 mmol), stock solution of 25 mM CuBr₂ and 200 mM TPMA (200 μL, 5.0 μmol of CuBr₂ and 40 μmol of TPMA) were dissolved in H₂O (7.7 mL). DMF (0.1 mL) was added as internal standard for ¹H NMR analysis. This mixture was added to a 25 mL Schlenk flask, purged with nitrogen for 30 min, and the flask was placed in an oil bath at 30 °C. A Na₂S₂O₄ aqueous solution (64 mM) was purged with nitrogen, and the solution

was continuously injected into the reaction medium using a syringe pump at the rate 1 $\mu\text{L}/\text{min}$. Samples were taken throughout the reaction for GPC and NMR analysis. The polymerization proceeded for 18 h (98% conversion, $M_n^{\text{th}} = 24600$, $M_n^{\text{GPC}} = 26200$, $M_w/M_n = 1.22$). After that, under continuous flow of nitrogen the excess of polymerization mixture was removed from Schlenk flask until reach a volume of 0.5 mL (POEOMA: 125 mg, 5 μmol ; CuBr_2 : 2.8 μg , 0.0125 μmol ; TPMA: 29 μg , 0.10 μmol). The OEOA₄₈₀ (2.40 g, 5 mmol) and H₂O (7.7 mL) previously bubbled with nitrogen for about 15 minutes were added. An additional Na₂S₂O₄ solution (8 mM) was purged with nitrogen, and the solution was continuously injected into the reaction medium using a syringe pump at the rate 1 $\mu\text{L}/\text{min}$ allowed to copolymerize for 20 h.

Grafting from the Protein Initiator BSA-O-[iBBr]₃₀

BSA-O-[iBBr]₃₀ (25.0 mg (protein), 0.01 mmol (initiator)), OEOA₄₈₀ (1.20 g, 2.5 mmol), stock solution of 25 mM CuBr₂ and 200 mM TPMA (20 μL , 0.50 μmol CuBr₂ and 4.0 μmol TPMA) were dissolved in 0.1 M PBS (7.7 mL). DMF (0.1 mL) was added as internal standard for ¹H NMR analysis. This mixture was added to a 25 mL Schlenk flask, purged with nitrogen for 30 min, and then placed in an oil bath at 30 °C. A Na₂S₂O₄ aqueous solution (16 mM) was purged with nitrogen, and the solution was continuously injected into the reaction medium using a syringe pump at the rate 1 $\mu\text{L}/\text{min}$. The grafted polymers were cleaved from the protein by adding 200 μL of the reaction mixture to 200 μL of 5% KOH solution. The resulting solution was allowed to react for 2 h at room temperature, followed by GPC analysis, as described elsewhere.⁵⁹

4.4. Results and Discussion

4.4.1. Aqueous SARA ATRP Using Inorganic Sulfites

Inorganic sulfites, such as Na₂S₂O₅, Na₂S₂O₄ and NaHSO₃, have recently been reported by our research team as supplemental activators and reducing agents in ATRP of (meth)acrylates.⁴⁵⁻⁴⁸ The possibility to control these polymerizations in aqueous media using only low ppm level of catalyst/L makes these systems very promising for the

preparation of (co)polymers or more complex macromolecular structures to be used in biomedical applications.

In aqueous ATRP, one of the biggest concerns is the partial dissociation of the halide anion from deactivator complex, leading to an inefficient deactivation of the propagating radicals, which affects the \bar{D} of the polymer.⁶² This issue can be mitigated by adding halide salts to increase the concentration of the XCu(II)/L species that means promote an efficient deactivation.^{24,62} For that reason, the set of experiments were planned considering the addition of an excess of halide salt (NaCl).

In our previous studies $\text{Na}_2\text{S}_2\text{O}_4$ has proven to be an extremely efficient reducing agent that quickly converts Cu(II)X_2 to Cu(I)X species.⁴⁵ Due to its poor solubility in organic solvents,⁶³ the concentrations of $\text{S}_2\text{O}_4^{2-}$ anion and consequently the concentrations of $\text{SO}_2^{\cdot-}$ resulting from dithionite anion dissociation are very small. In these solvents, an excess of $\text{Na}_2\text{S}_2\text{O}_4$, was employed,^{45,46} and the concentration of $\text{SO}_2^{\cdot-}$ species was maintained low and constant during the course of the polymerization. In aqueous media (more than 75% of water content) the $\text{Na}_2\text{S}_2\text{O}_4$ is fully soluble, and can consequently generate a very high concentration of $\text{SO}_2^{\cdot-}$ species. In the first approach, an initial experiment was carried out by adding the total amount of $\text{Na}_2\text{S}_2\text{O}_4$ at the beginning of the polymerization using the following conditions: $\text{OEOA}_{480}/\text{HEBiB}/\text{Na}_2\text{S}_2\text{O}_4/\text{CuBr}_2/\text{TPMA} = 250/1/1/0.05/0.4$ (Figure 4.1 and Table 4.1, entry 1).

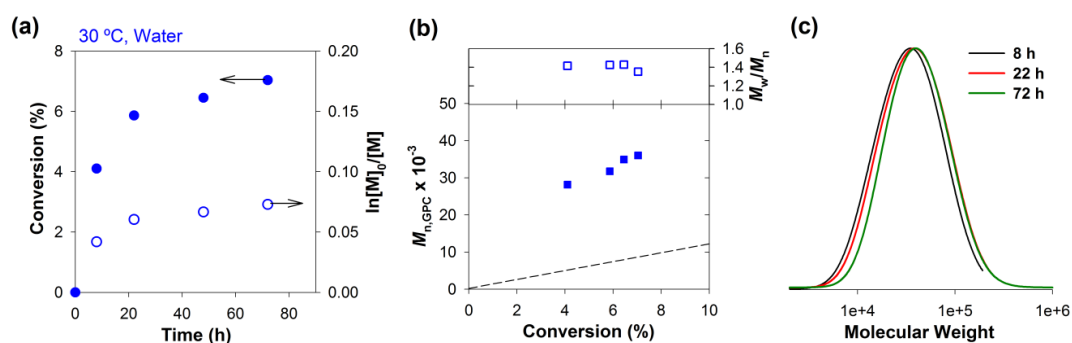


Figure 4.1. (a) Kinetic plots of conversion and $\ln[M]_0/[M]$ vs. time; (b) plot of number-average molecular weights ($M_{n, GPC}$) and \bar{D} (M_w/M_n) vs. conversion for aqueous SARA ATRP of OEOA_{480} at 30 °C; and (c) GPC traces vs. time. Conditions: $[\text{OEOA}_{480}]_0/[\text{HEBiB}]_0/[\text{Na}_2\text{S}_2\text{O}_4]_0/[\text{Cu(II)Br}_2]_0/[\text{TPMA}]_0 = 250/1/1/0.05/0.4$; $[\text{NaCl}]_0 = 100$ mM; $[\text{OEOA}_{480}]_0/[\text{Water}] = 1/3$.

The kinetic results (Figure 4.1) showed that the SARA ATRP of OEOA₄₈₀ proceeded in an uncontrolled manner. Most probably, the rapid dissolution of Na₂S₂O₄ at the beginning of the reaction led to a very high rate of Cu(I) (re)generation, depletion of [Cu(II)] and the occurrence undesired termination reactions. This effect is illustrated by the kinetic plot that does not follow linear first-order kinetics (Figure 4.1(a)). Also, the M_n^{GPC} values were much higher than M_n^{th} (Figure 4.1(b)) and a very small shift to high molecular weight fractions was observed in polymer GPC traces (Figure 4.1(c)).

Previously in aqueous based systems,²⁴ it was shown that the feeding rate (FR) of reducing agent had a major influence on the rate and the control over polymerization. Indeed, the continuous feeding of small amounts Na₂S₂O₄ over an extended period of time is essential to maintain its concentration at a relatively low level during the polymerization and achieve an efficient control over the polymerization.

4.4.2. Effect of the Feeding Rate of Sulfite (FR_S) on the Polymerization

Based on the previous results, polymerizations with varied FR_S were performed. The feeding rate of Na₂S₂O₄ (FR_S) was varied from 8 to 128 nmol/min to determine the effect of the amount of Na₂S₂O₄ on the rate of polymerizations (Figure 4.2, Figure C.1 in Appendix C and Table 4.1, entries 2-6). Indeed, higher FR_S led to higher polymerization rates. For a feeding rate of 8 nmol/min, an induction time of around 10 h was observed. A higher feeding rate of 128 nmol/min caused a significant increase of \bar{D} during the polymerization. This increase of the \bar{D} could result from either a high termination rate or inefficient deactivation steps. When feeding rates were varied from 16 to 64 nmol/min, first-order kinetic plots and good agreement between experimental and theoretical molecular weights were obtained. In addition, the \bar{D} values of the final polymer were always below 1.32. The GPC traces showed that the distributions were unimodal and moved clearly toward higher molecular weights with increasing conversions.

Figure 4.3 shows a linear dependence between k_p^{app} and $\text{FR}_S^{1/2}$ within the controlled range of FR_S values (8 – 64 nmol/min).

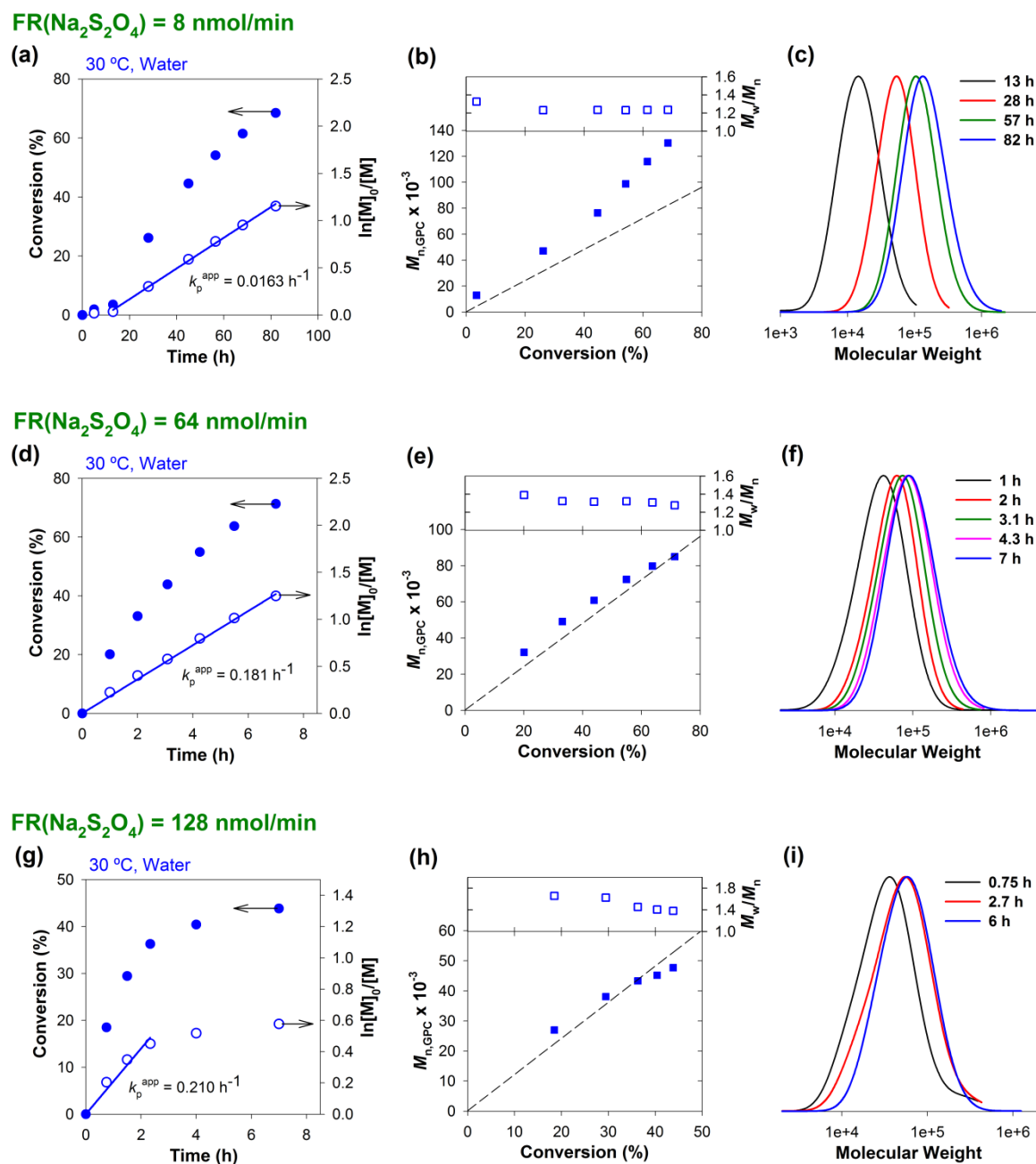


Figure 4.2. (a, d and g) Kinetic plots of conversion and $\ln[M]_0/[M]$ vs. time; (b, e and h) plot of $M_{n,GPC}$ and $D (M_w/M_n)$ vs. conversion for aqueous SARA ATRP of OEOA₄₈₀ at 30 °C; and (c, f and i) GPC traces vs. time. Conditions: $[OEOA_{480}]_0/[HEBiB]_0/[Cu(II)Br_2]_0/[TPMA]_0 = 250/1/0.05/0.4$; FR(Na₂S₂O₄) = 8 (a, b and c), 64 (d, e and f) and 128 (g, h and i) nmol/min ; $[NaCl]_0 = 100 \text{ mM}$; $[OEOA_{480}]_0/[Water] = 1/3$.

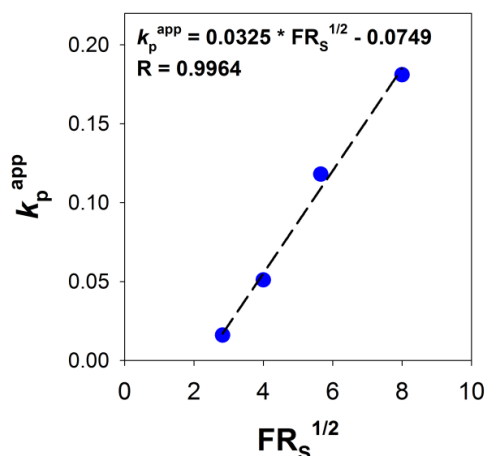


Figure 4.3. k_p^{app} values of the SARA ATRP of OEOA₄₈₀ catalyzed by CuBr₂/TPMA in water at 30 °C vs. $\text{FR}(\text{Na}_2\text{S}_2\text{O}_4)^{1/2}$. Conditions: $[\text{OEOA}_{480}]_0/[\text{HEBiB}]_0/[\text{Cu(II)Br}_2]_0/[\text{TPMA}]_0 = 250/1/0.05/0.4$; $[\text{OEOA}_{480}]_0/[\text{Water}] = 1/3$.

In an attempt to enhance the polymerization rate while maintaining the control over the polymerization, two different FR_S were used in the course of a same experiment (Figure 4.4 and Table 4.1, entry 7). The results obtained highlighted the role of the concentration of $\text{Na}_2\text{S}_2\text{O}_4$ in the rate of the polymerization, but no significant improvement in \mathcal{D} values was achieved when compared to the experiment carried out using a constant $\text{FR}_S = 64$ nmol/min during the entire polymerization. Therefore, this FR_S was used for all subsequent experiments targeting a faster and well-controlled aqueous SARA ATRP.

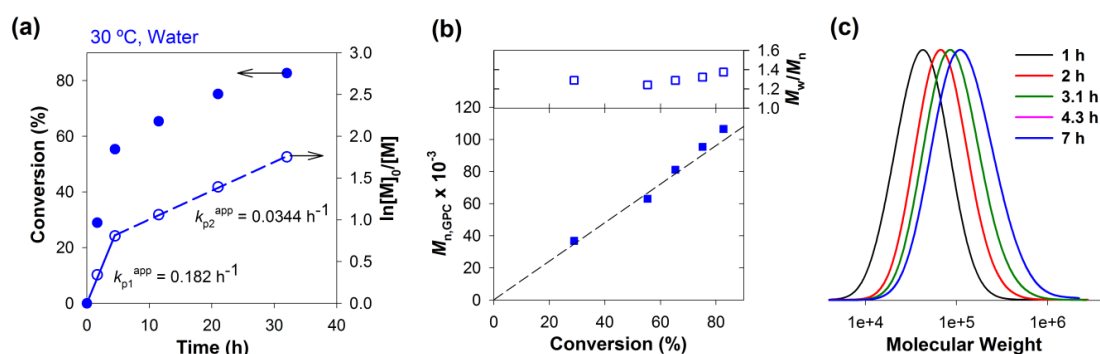


Figure 4.4. (a) Kinetic plots of conversion and $\ln[M]_0/[M]$ vs. time; (b) plot of $M_{n,\text{GPC}}$ and \mathcal{D} (M_w/M_n) vs. conversion for aqueous SARA ATRP of OEOA₄₈₀ at 30 °C; and (c) GPC traces vs. time. Conditions: $[\text{OEOA}_{480}]_0/[\text{HEBiB}]_0/[\text{Cu(II)Br}_2]_0/[\text{TPMA}]_0 = 250/1/0.05/0.4$; $\text{FR}(\text{Na}_2\text{S}_2\text{O}_4) = 64$ nmol/min (until 4.5h) and $\text{FR}(\text{Na}_2\text{S}_2\text{O}_4) = 8$ nmol/min (until 32h); $[\text{NaCl}]_0 = 100$ mM; $[\text{OEOA}_{480}]_0/[\text{Water}] = 1/3$.

Table 4.1. Aqueous SARA ATRP of OEOA₄₈₀ with Varied Feeding Rate of Na₂S₂O₄ (FR_S).

Entry ^a	[M] ₀ /[I] ₀ ^c /[Cu(II)Br ₂] ₀ /[TPMA] ₀	FR _S (nmol/min)	Cu ^b (ppm)	k _p ^{app} (h ⁻¹)	Time (h)	Conv. (%)	M _n th × 10 ⁻³	M _n ^{GPC} × 10 ⁻³	D
1	250/1/0.05/0.4	0	26	---	72	7	8.7	36.0	1.35
2	250/1/0.05/0.4	8	26	0.016	82	68	82.4	130.3	1.24
3	250/1/0.05/0.4	16	26	0.051	30	78	93.9	117.2	1.29
4	250/1/0.05/0.4	32	26	0.118	10	67	80.5	92.2	1.32
5	250/1/0.05/0.4	64	26	0.181	7	71	85.8	85.0	1.28
6	250/1/0.05/0.4	128	26	0.210	7	44	52.8	47.7	1.38
7 ^c	250/1/0.05/0.4	64 8	26	0.182 0.034	4.5 32	55 83	66.6 99.4	63.1 106.5	1.24 1.37

^aAll polymerizations were conducted with [M]₀ = 0.5 M, [I]₀ = 2 mM, and [NaCl]₀ = 100 mM.

^bCalculated by the initial weight ratio of Cu to the monomer.

^cFR_S = 64 nmol/min during 4.5h and FR_S = 8 nmol/min until 32h.

4.4.3. Model Experiments to Elucidate the SARA ATRP Mechanism

The next set of experiments was envisaged to clarify the mechanism of aqueous ATRP using $\text{Na}_2\text{S}_2\text{O}_4$. The initial experiment was carried out using only the monomer (OEOA), ATRP initiator (HEBiB), and deactivator ($\text{Cu(II)Br}_2/\text{TPMA}$) in water (i.e., in absence of $\text{Na}_2\text{S}_2\text{O}_4$), and no polymerization occurred (Table 4.2, entry 2). This result indicates that the presence of $\text{Na}_2\text{S}_2\text{O}_4$ is mandatory to promote the *in situ* formation of the active Cu(I)/L species. Using $\text{Na}_2\text{S}_2\text{O}_4$ ($\text{FR}_S = 64 \text{ nmol/min}$), even without the presence of $\text{Cu(II)Br}_2/\text{TPMA}$ complex, POEOA were obtained both in the presence (Figure 4.5 and Table 4.2, entry 3) and in the absence (Figure 4.6 and Table 4.2, entry 4) of the ATRP initiator (HEBiB). As verified by the very high D values, the polymerization of OEOA was uncontrolled in both cases. The rate of polymerization was much higher in the presence of the ATRP initiator, suggesting that sulfites can act as supplemental activators of alkyl halides in aqueous media. Similar results have been obtained when sulfites were used to polymerize (meth)acrylates in organic solvents.^{45,46} In the absence of the ATRP initiator (Table 4.2, entry 4), the polymerization was much slower (~ 230 times), which indicated that only very few polymer chains were initiated directly from the $\text{SO}_2^{\cdot-}$ radical anions.

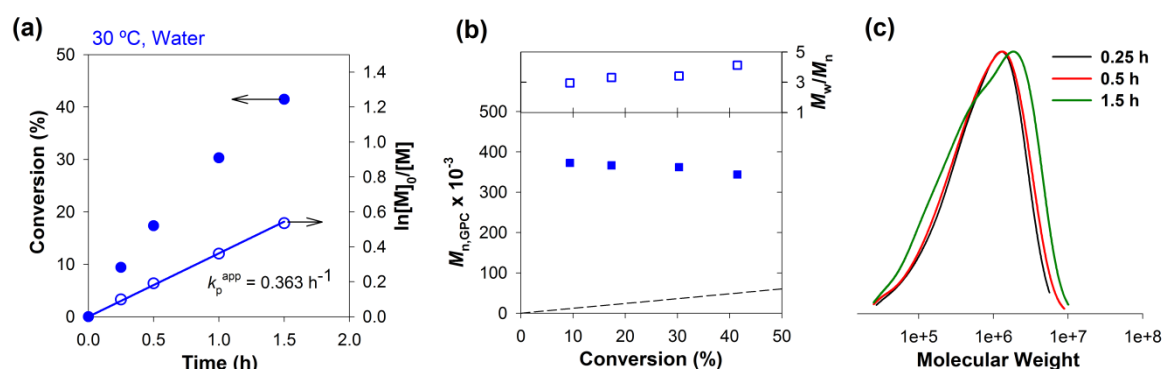


Figure 4.5. (a) Kinetic plots of conversion and $\ln[M]_0/[M]$ vs. time; (b) plot of $M_{n,\text{GPC}}$ and D (M_w/M_n) vs. conversion for aqueous SARA ATRP of OEOA₄₈₀ at 30 °C; and (c) GPC traces vs. time. Conditions: $[\text{OEOA}_{480}]_0/[\text{HEBiB}]_0/[\text{Cu(II)Br}_2]_0/[\text{TPMA}]_0 = 250/1/0/0$; $\text{FR}(\text{Na}_2\text{S}_2\text{O}_4) = 64 \text{ nmol/min}$; $[\text{NaCl}]_0 = 100 \text{ mM}$; $[\text{OEOA}_{480}]_0/[\text{Water}] = 1/3$.

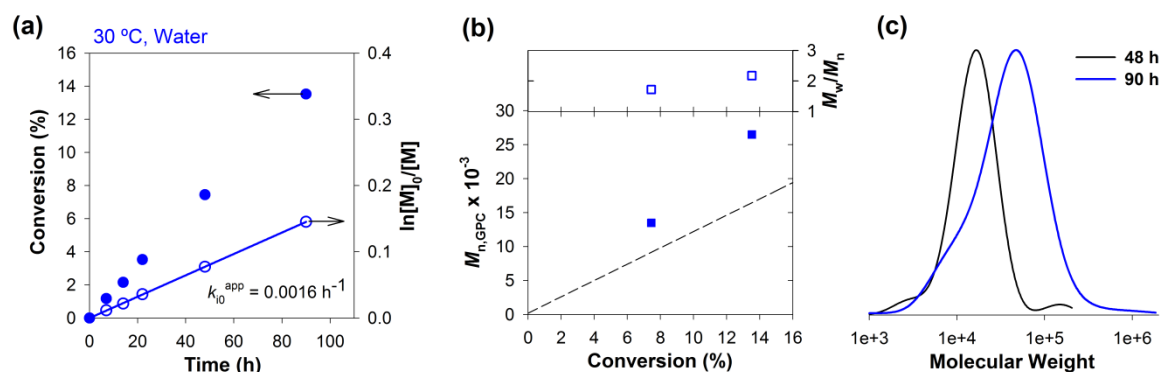


Figure 4.6. (a) Kinetic plots of conversion and $\ln[M]_0/[M]$ vs. time; (b) plot of $M_{n,GPC}$ and D (M_w/M_n) vs. conversion for aqueous SARA ATRP of OEOA₄₈₀ at 30 °C; and (c) GPC traces vs. time. Conditions: $[OEOA_{480}]_0/[HEBiB]_0/[Cu(II)Br_2]_0/[TPMA]_0 = 250/0/0/0$; $FR(Na_2S_2O_4) = 64$ nmol/min; $[NaCl]_0 = 100$ mM; $[OEOA_{480}]_0/[Water] = 1/3$.

To evaluate the role of sulfites as supplemental activators of alkyl halides in aqueous media, the supplemental activator apparent rate constant (k_{a0}^{app}) was determined for HEBiB using $Na_2S_2O_4$ (Figure 4.7 and Table 4.2, entry 5). Figure 4.7 confirms that the SO_2^- formed by dissociation of $S_2O_4^{2-}$ can activate the C-Br bond from HEBiB, as judged by 1H NMR spectrometry (Figure 4.7(a)).

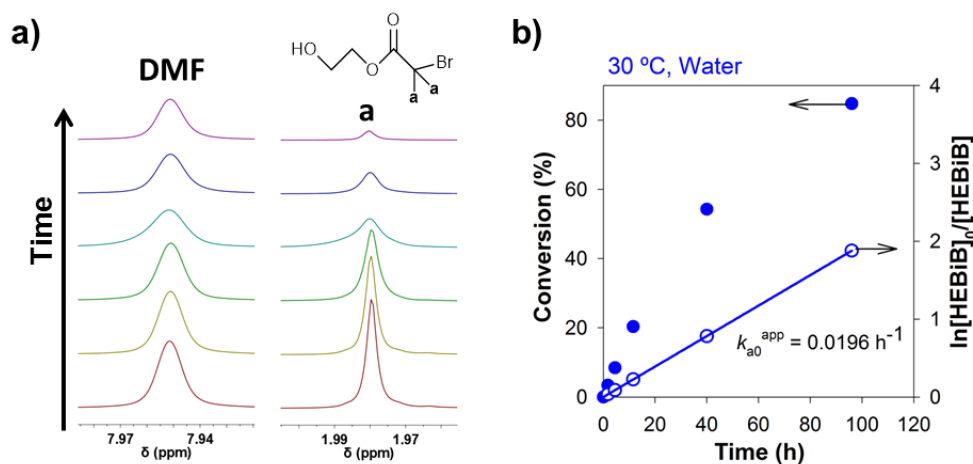


Figure 4.7. Determination of the supplemental activator apparent rate constant for HEBiB in water at 30 °C feeding $Na_2S_2O_4$. Conditions: $[HEBiB]_0 = 20$ mM; $FR(Na_2S_2O_4) = 64$ nmol/min.

UV–vis spectroscopy was used to study the reduction process of Cu(II)Br₂/TPMA by Na₂S₂O₄ in aqueous media (Figures 4.8, 4.9 and Table 4.2, entry 6). In the first experiment (Figure 4.8), a solution of [CuBr₂]₀/[TPMA]₀/[NaBr]₀ = 2.5/20/50 mM in water was used by adding all Na₂S₂O₄ ([CuBr₂]₀/[Na₂S₂O₄]₀ = 1/1) at the beginning of the experiment. The results showed that Na₂S₂O₄ acted as a powerful reducing agent in water, converting all of Cu(II) species into Cu(I) activators within about 1 second. This result corroborates the data obtained for the experiment carried out using the total amount of Na₂S₂O₄ in the beginning of the reaction (Figure 4.1). The high concentration of Cu(I)/X species led to a high concentration of radicals, which inevitably increased the termination reactions.

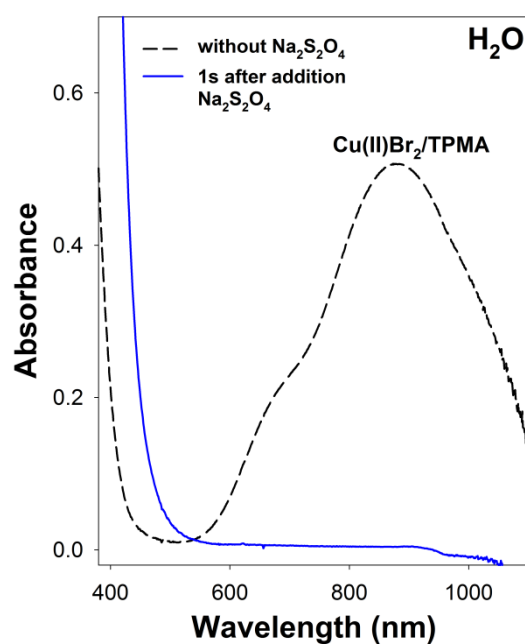


Figure 4.8. UV–vis spectra of reduction of Cu(II)Br₂/TPMA by Na₂S₂O₄ in water at 30 °C; [CuBr₂]₀/[TPMA]₀/[Na₂S₂O₄]₀/[NaBr]₀ = 2.5/20/2.5/50 mM.

In order to determine the reduction rate of [Cu(II)Br₂]₀/[TPMA]₀ in water at 30 °C, under similar conditions used for the polymerization, a solution of [CuBr₂]₀/[TPMA]₀/[NaCl]₀ = 10/80/100 mM in water was used. The feeding of Na₂S₂O₄ was set as FR_S = 64 nmol/min (Figure 4.9 and Table 4.2, entry 6). As expected, the reduction rate was much slower when compared with the total addition of Na₂S₂O₄ (Figure 4.8). For the feeding rate of

$\text{Na}_2\text{S}_2\text{O}_4$ ($\text{FR}_S = 64 \text{ nmol/min}$) approximately half of Cu(II) species were reduced to Cu(I) in about 140 min.

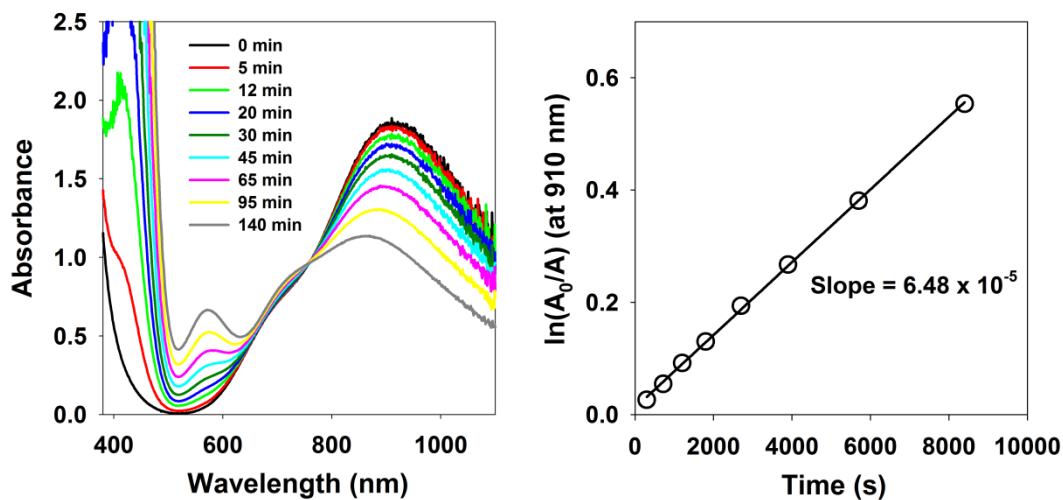


Figure 4.9. Determination of reduction rate of $[\text{Cu(II)Br}_2]_0/[\text{TPMA}]_0$ in water at $30 \text{ }^\circ\text{C}$ feeding $\text{Na}_2\text{S}_2\text{O}_4$. Conditions: $[\text{Cu(II)Br}_2]_0/[\text{TPMA}]_0/[\text{NaCl}]_0 = 10/80/100 \text{ mM}$; $\text{FR}(\text{Na}_2\text{S}_2\text{O}_4) = 64 \text{ nmol/min}$.

The results allowed us to conclude that, in aqueous systems, inorganic sulfites act both as supplemental activators and reducing agents, following the SARA ATRP mechanism. This conclusion has also been verified in the SARA ATRP of (meth)acrylates in the presence of organic solvents (*e.g.* DMSO, alcohols).^{45,46}

Table 4.2. Aqueous SARA ATRP using Inorganic Sulfites.

Entry ^a	$[M]_0/[I]_0/[Cu(II)Br_2]_0/[TPMA]_0$	FR_S (nmol/min)	Cu^b (ppm)	k_p^{app} (h ⁻¹)	Time (h)	Conv. (%)	$M_n^{th} \times 10^{-3}$	$M_n^{GPC} \times 10^{-3}$	D
1	250/1/0.05/0.4	64	26	0.181	7	71	85.8	85.0	1.28
2 ^c	250/1/0.05/0.4	0	26	---	72	0	---	---	---
3 ^d	250/1/0/0	64	0	0.363	1.5	41	50.0	344.0	4.12
4 ^e	250/0/0/0	64	0	0.0016	90	14	16.4	26.5	2.18
5 ^f	0/10/0/0	64	---	0.0196	96	85	---	---	---
6 ^g	0/0/5/40	64	---	0.233	2.3	43	---	---	---

^aAll polymerizations were conducted with $[M]_0 = 0.5$ M, $[I]_0 = 2$ mM, and $[NaCl]_0 = 100$ mM.

^bCalculated by the initial weight ratio of Cu to the monomer.

^cWithout $Na_2S_2O_4$: $[Na_2S_2O_4]_0 = 0$ mM and $FR_S = 0$ nmol/min.

^dWithout $Cu(II)Br_2/TPMA$ to prove the SARA ATRP with sulfites.

^eDetermination of k_{i0}^{app} : $[M]_0 = 0.5$ M in water feeding $Na_2S_2O_4$ ($FR_S = 64$ nmol/min).

^fDetermination of the supplemental activator constant (k_{a0}^{app}) for HEBiB ($[I]_0 = 20$ mM) in water feeding $Na_2S_2O_4$ ($FR_S = 64$ nmol/min).

^gDetermination of reduction process constant (k_{red}^{app}) by UV-vis spectroscopy of $[Cu(II)Br_2]_0/[TPMA]_0 = 10/80$ mM in water using $[NaCl]_0 = 100$ mM and feeding $Na_2S_2O_4$ ($FR_S = 64$ nmol/min).

4.4.4. Effect of the Ligand (L) and its Concentration on the Polymerization

As has been observed in aqueous ATRP, the initial presence of an excess of L compared to Cu increased the concentration of activator and consequently the polymerization rate.²⁴ In addition, this aqueous SARA ATRP requires low concentrations of the catalyst, and any partial dissociation of L from the metal complex could have a strong impact on the control over polymerization.^{24,30} This assumption was evaluated with two experiments performed using the L/Cu ratios of 2/1 and 8/1 (Figures 4.2 (d-f), 4.10 and Table 4.3, entries 1-2). As expected, the kinetic data revealed that for an 8-fold excess of L the polymerization was twice as fast. Additionally, narrow molecular weight distributions even for high monomer conversions were observed ($\mathcal{D} \leq 1.28$). The data obtained when L/Cu ratio of 2/1 was employed suggest that despite of the relatively high stability of the Cu/TPMA complex, due to low catalyst concentrations used in this aqueous SARA ATRP system, it may not be enough to stabilize catalyst complexes. Only a larger excess of L could shift equilibrium toward the Cu(I)/L species.

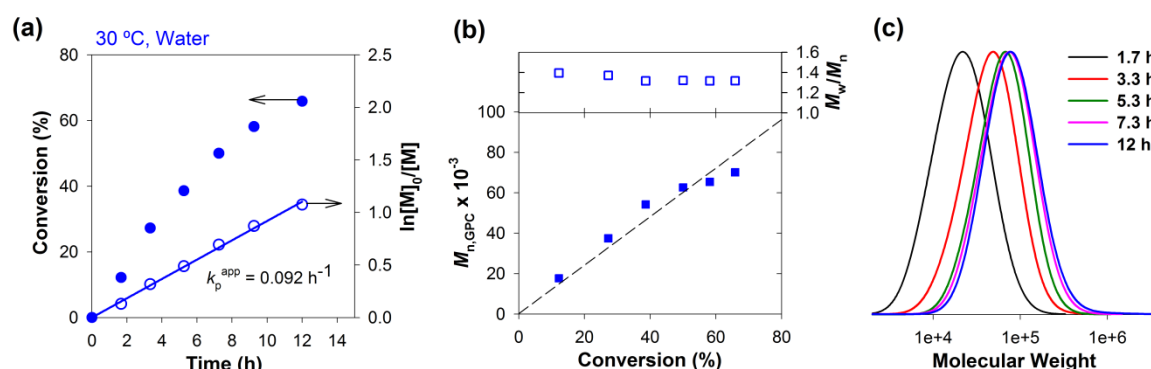


Figure 4.10. (a) Kinetic plots of conversion and $\ln[M]_0/[M]$ vs. time; (b) plot of $M_{n,GPC}$ and \mathcal{D} (M_w/M_n) vs. conversion for aqueous SARA ATRP of OEOA₄₈₀ at 30 °C; and (c) GPC traces vs. time. Conditions: $[OEOA_{480}]_0/[HEBiB]_0/[Cu(II)Br_2]_0/[TPMA]_0 = 250/1/0.05/0.1$; $FR(Na_2S_2O_4) = 64 \text{ nmol/min}$; $[NaCl]_0 = 100 \text{ mM}$; $[OEOA_{480}]_0/[Water] = 1/3$.

Another important parameter that has a decisive impact in aqueous SARA ATRP is the L used, because it defines the activity and stability of the catalyst.⁶⁴ The substitution of TPMA for Me₆TREN, an L binding stronger to Cu(II) but weaker to Cu(I),^{47,64} (Figures 4.2(d-f), 4.11 and Table 4.3, entries 1 and 3), resulted in polymerization almost 4 times

faster. However, the use of Me₆TREN resulted also in broader molecular weight distributions, which revealed an inferior control over the polymerization.

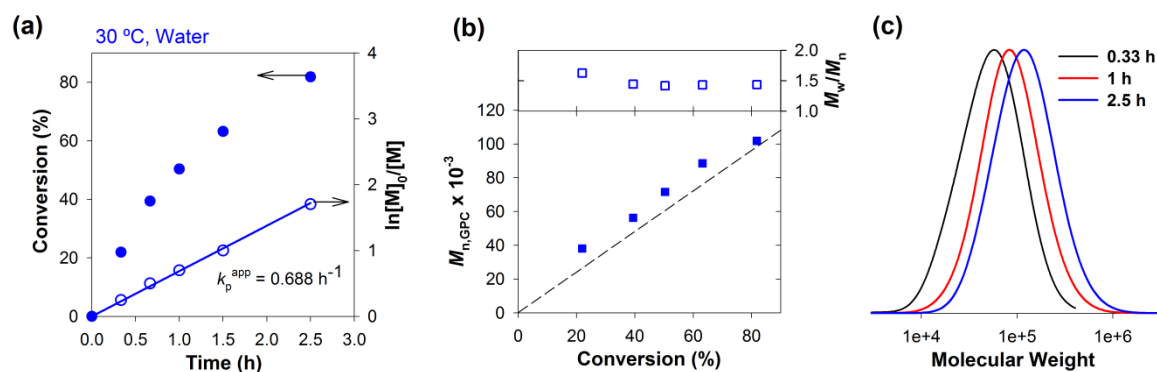


Figure 4.11. (a) Kinetic plots of conversion and $\ln[M]_0/[M]$ vs. time; (b) plot of $M_{n,GPC}$ and D (M_w/M_n) vs. conversion for aqueous SARA ATRP of OEOA₄₈₀ at 30 °C; and (c) GPC traces vs. time. Conditions: $[OEOA_{480}]_0/[HEBiB]_0/[Cu(II)Br_2]_0/[Me_6TREN]_0 = 250/1/0.05/0.4$; $FR(Na_2S_2O_4) = 64$ nmol/min; $[NaCl]_0 = 100$ mM; $[OEOA_{480}]_0/[Water] = 1/3$.

Based on the previous results, TPMA was used as L with a L/Cu ratio of 8/1 for the following experiments targeting a well-controlled aqueous SARA ATRP.

4.4.5. Effect of an Added Salt and its Concentration on the Polymerization

It is known that bromide chain ends are typically 10–100 times more ATRP active than chlorine chain ends, but carbon-chlorine bonds are more stable to hydrolysis. Based on that, the following studied parameter was the influence of the nature of halogen species on control over polymerization. The results of the experiments conducted in the presence of three different added salts (NaCl, TEACl and NaBr) are shown in (Figures 4.2(d-f), 4.12 and Table 4.4.

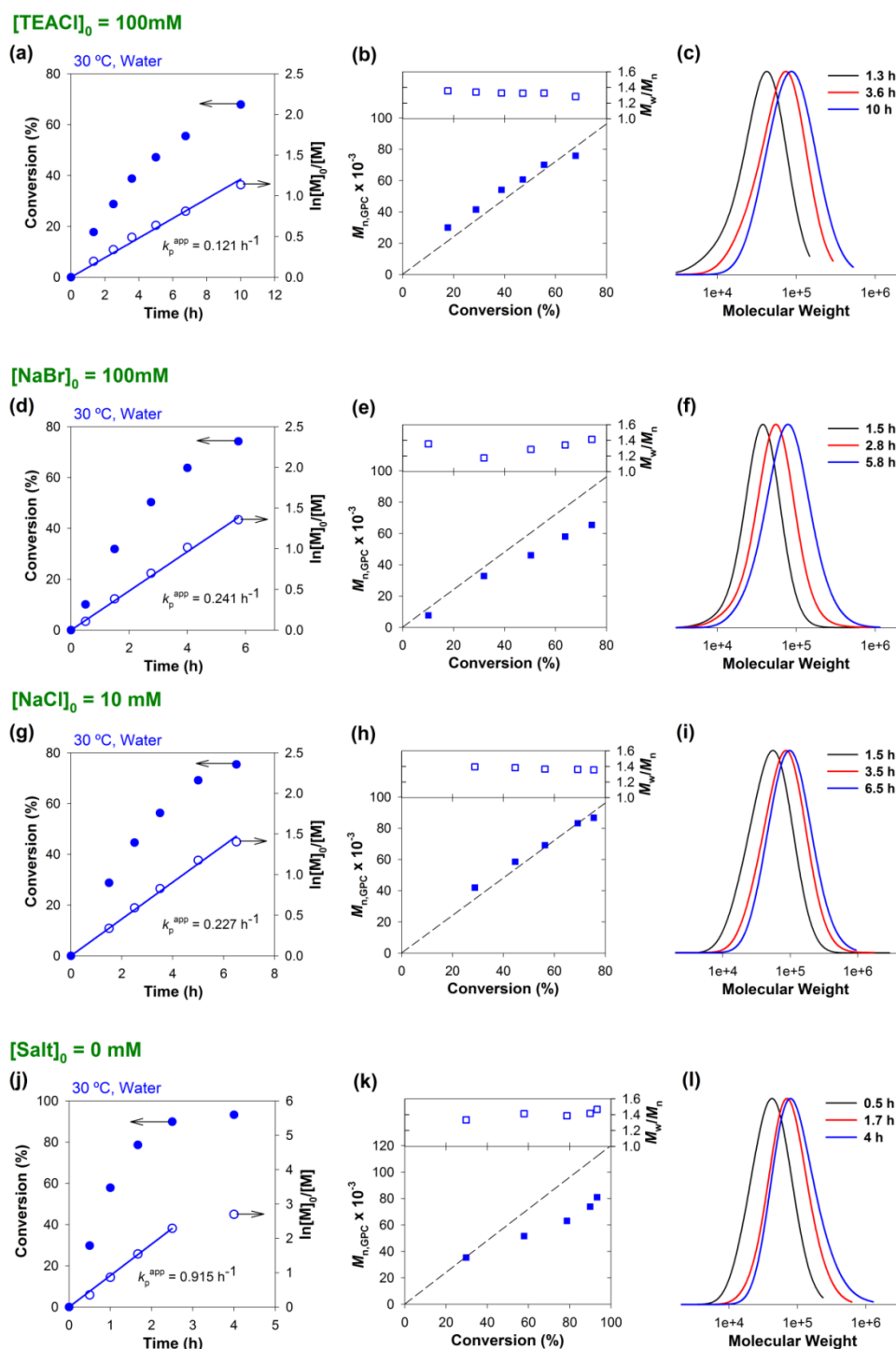


Figure 4.12. (a, d, g and j) Kinetic plots of conversion and $\ln[M]_0/[M]$ vs. time; (b, e, h and k) plot of $M_{n,GPC}$ and D (M_w/M_n) vs. conversion for aqueous SARA ATRP of OEOA₄₈₀ at 30 °C; and (c, f, i and l) GPC traces vs. time. Conditions: $[OEOA_{480}]_0/[HEBiB]_0/[Cu(II)Br_2]_0/[TPMA]_0 = 250/1/0.05/0.4$; $FR(Na_2S_2O_4) = 64 \text{ nmol/min}$; $[OEOA_{480}]_0/[Water] = 1/3$; (a, b and c) $[TEACl]_0 = 100 \text{ mM}$, (d, e and f) $[NaBr]_0 = 100 \text{ mM}$, (g, h and i) $[NaCl]_0 = 10 \text{ mM}$, and (j, k and l) $[Salt]_0 = 0 \text{ mM}$.

The polymerization in the presence of TEACl (Figure 4.12(a-c) and Table 4.4, entry 2) is similar to the polymerization with NaCl (Figure 4.2(d-f) and Table 4.4, entry 1) regarding the polymerization rate (similar k_p^{app}) and the control over polymerization (similar $\bar{D} < 1.28$ even for high monomer conversions). Additionally, both polymerizations presented linear first-order kinetics, linear evolution of molecular weight with conversion, and good correlation between the experimental and theoretical molecular weights. This indicated that probably the anion, unlike the cation, affects the polymerization. To validate this result, NaBr was also tested at the same concentration (100mM) (Figure 4.12(d-f) and Table 4.4, entry 3). The polymerization was faster compared to the ones observed for the two chloride salts, but with a poor control of the polymerization ($\bar{D} \sim 1.41$) (mainly for high monomer conversions) due to the lower hydrolytic stability of the carbon-bromide bond. The addition of halide salts shifts the ATRP equilibrium toward the formation of a stable deactivator, contributing to the improvement of the control over polymerization. The effect of the concentration of the salt on the polymerization was also studied. The influence of varying the NaCl concentration from 10 mM to 100 mM is shown in entries 1 and 4 of Table 4.4. The results showed that for higher salt concentration the slower the polymerization. This observation can be due to: a higher concentration XCu(II)/L; the formation of inactive XCu(I)/L species; or the replacement of TPMA ligands by halide anions.^{24,26,57} As is mentioned before, a NaCl concentration of 100 mM provided a perfect control over polymerization (Figure 4.2(d-f)). For lower salt concentrations, faster polymerization occurred but \bar{D} values increased to ~ 1.36 (Figure 4.12(g-i)), which suggests that a NaCl concentration of 10 mM was not enough to prevent the partial dissociation of the deactivator complex.

With no addition of any halide salts (Figure 4.12(j-l)), the polymerization was significantly faster (Table 4.4), but the control over polymerization was not so effective ($\bar{D} \sim 1.47$). The GPC traces showed that polymers synthesized in the absence of an added salt exhibited broader molecular weight distributions, which could be due to termination reactions caused by the higher radical concentration. These results confirm that, in this aqueous SARA ATRP, the addition of extra halide species is necessary to promote an efficient deactivation of growing radicals.

Table 4.3. Aqueous SARA ATRP of OEOA₄₈₀ with Varied Ligands (L) and L/Cu Ratios.

Entry ^a	[M] ₀ /[I] ₀ /[Cu(II)Br ₂] ₀ /[TPMA] ₀	L/Cu	Cu ^b (ppm)	k _p ^{app} (h ⁻¹)	Time (h)	Conv. (%)	M _n th × 10 ⁻³	M _n ^{GPC} × 10 ⁻³	D
1	250/1/0.05/0.4	8/1	26	0.181	7	71	85.8	85.0	1.28
2	250/1/0.05/0.1	2/1	26	0.092	12	66	79.2	70.1	1.32
3 ^c	250/1/0.05/0.1	8/1	26	0.688	2.5	82	98.4	101.8	1.44

^aAll polymerizations were conducted with [M]₀ = 0.5 M, [I]₀ = 2 mM, [NaCl]₀ = 100 mM and FR_S = 64 nmol/min
^bCalculated by the initial weight ratio of Cu to the monomer.
^cMe₆TREN was used as L.

Table 4.4. Aqueous SARA ATRP of OEOA₄₈₀ with Varied Salts and Salt Concentrations.

Entry ^a	[M] ₀ /[I] ₀ /[Cu(II)Br ₂] ₀ /[TPMA] ₀	Salt: mM	Cu ^b (ppm)	k _p ^{app} (h ⁻¹)	Time (h)	Conv. (%)	M _n th × 10 ⁻³	M _n ^{GPC} × 10 ⁻³	D
1	250/1/0.05/0.4	NaCl : 100	26	0.181	7	71	85.8	85.0	1.28
2	250/1/0.05/0.4	TEACl : 100	26	0.121	10	68	81.7	75.9	1.28
3	250/1/0.05/0.4	NaBr : 100	26	0.241	5.8	74	89.3	65.5	1.41
4	250/1/0.05/0.4	NaCl : 10	26	0.227	6.5	75	90.8	86.7	1.36
5	250/1/0.05/0.4	-- : --	26	0.915	4	93	112.1	81.0	1.47

^aAll polymerizations were conducted with [M]₀ = 0.5 M, [I]₀ = 2 mM, and FR_S = 64 nmol/min;
^bCalculated by the initial weight ratio of Cu to the monomer.

4.4.6. Effect of Sulfite (or SARA Agent) Used on the Polymerization

The next series of experiments were carried out to compare the efficiency of the three most commonly used inorganic sulfites ($\text{Na}_2\text{S}_2\text{O}_5$, $\text{Na}_2\text{S}_2\text{O}_4$ and NaHSO_3) in aqueous SARA ATRP ((Figures 4.2(d-f), 4.13, 4.14 and Table 4.5).

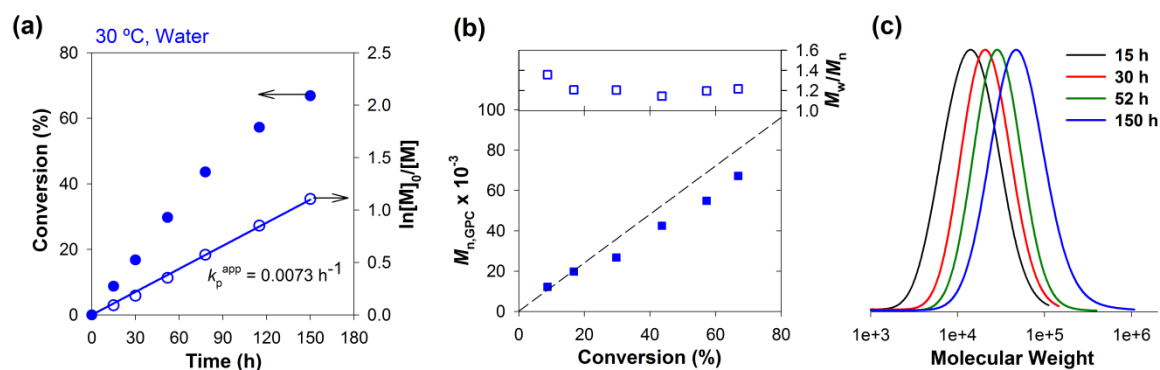


Figure 4.13. (a) Kinetic plots of conversion and $\ln[M]_0/[M]$ vs. time; (b) plot of $M_{n,\text{GPC}}$ and \mathcal{D} (M_w/M_n) vs. conversion for aqueous SARA ATRP of OEOA₄₈₀ at 30 °C; and (c) GPC traces vs. time. Conditions: $[\text{OEOA}_{480}]_0/[\text{HEBiB}]_0/[\text{Cu(II)Br}_2]_0/[\text{TPMA}]_0 = 250/1/0.05/0.4$; $[\text{OEOA}_{480}]_0/[\text{Water}] = 1/3$; $\text{FR}(\text{Na}_2\text{S}_2\text{O}_5) = 64 \text{ nmol/min}$; $[\text{NaCl}]_0 = 100 \text{ mM}$.

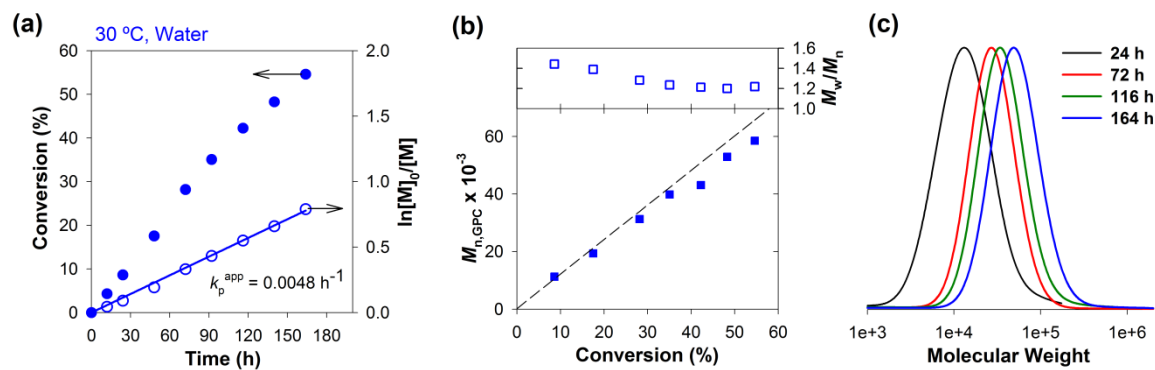


Figure 4.14. (a) Kinetic plots of conversion and $\ln[M]_0/[M]$ vs. time; (b) plot of $M_{n,\text{GPC}}$ and \mathcal{D} (M_w/M_n) vs. conversion for aqueous SARA ATRP of OEOA₄₈₀ at 30 °C; and (c) GPC traces vs. time. Conditions: $[\text{OEOA}_{480}]_0/[\text{HEBiB}]_0/[\text{Cu(II)Br}_2]_0/[\text{TPMA}]_0 = 250/1/0.05/0.4$; $[\text{OEOA}_{480}]_0/[\text{Water}] = 1/3$; $\text{FR}(\text{NaHSO}_3) = 64 \text{ nmol/min}$; $[\text{NaCl}]_0 = 100 \text{ mM}$.

The polymerization rates were first order with respect to monomer concentration, the molecular weights determined by GPC matched the theoretical values, proving the efficient initiation and excellent control during polymerizations (\mathcal{D} always < 1.28), regardless of the inorganic sulfite used. Comparing the kinetic data, $\text{Na}_2\text{S}_2\text{O}_4$ provided a

faster aqueous polymerization of OEOA (Table 4.5). Thus, $\text{Na}_2\text{S}_2\text{O}_4$ is a more efficient reducing agent, allowing a faster (re)generation of the active Cu(I)X/L catalyst. The polymerizations using $\text{Na}_2\text{S}_2\text{O}_5$ and NaHSO_3 were 25 and 38 times slower, respectively. The same conclusion was reached in the polymerization of (meth)acrylates in DMSO,⁴⁵ although the differences in polymerization rates were not as pronounced (3.5 and 2.3 times slower, respectively). Therefore, $\text{Na}_2\text{S}_2\text{O}_4$ was selected for the further set of experiments.

4.4.7. Variation of Cu Concentration, Targeted DP and Monomer

For certain applications, namely biomedical and electronics, the presence of residual Cu could be a major hurdle. For that reason, it is imperative to find balance between the optimal (minimal) Cu concentration to control the polymerization and an acceptable polymerization rate. It is known that the polymerization rate and \bar{D} of the final product in ATRP are determined by $[\text{Cu(I)}]/[\text{Cu(II)}]$ ratio and Cu(II) concentration respectively.^{3,10,65} Figures 4.2(d-f), 4.15, 4.16 and Table 4.6 (entries 1-4) show the effect of lowering the catalyst concentration (the Cu concentration was varied from 130 to 1.3 ppm) for different targeted DPs. The results suggest that lower initial Cu(II) concentrations lead to a poor control over polymerization, mainly defined by the final \bar{D} values. Also, the polymerization rate decreased with increased targeted DP, due to the lower concentration of growing radicals. It is remarkable to note that even for a very high molecular weight ($M_n^{\text{GPC}} = 267\,500$) P(OEOA₄₈₀) (targeted DP = 1 000) (Figure 4.15(a-c)), only 6.5 ppm of total copper concentration was enough to obtain acceptable values of dispersity ($\bar{D} < 1.38$). This result suggests that the effect of $\text{Na}_2\text{S}_2\text{O}_4$ on any side reactions should be small. In the attempt to reduce the initial copper concentration even more, it was tested using only 1.3 ppm (Figure 4.15(d-f)). The results indicated that 1.3 ppm of Cu concentration was too low to control the polymerization, especially above 50% of monomer conversion.

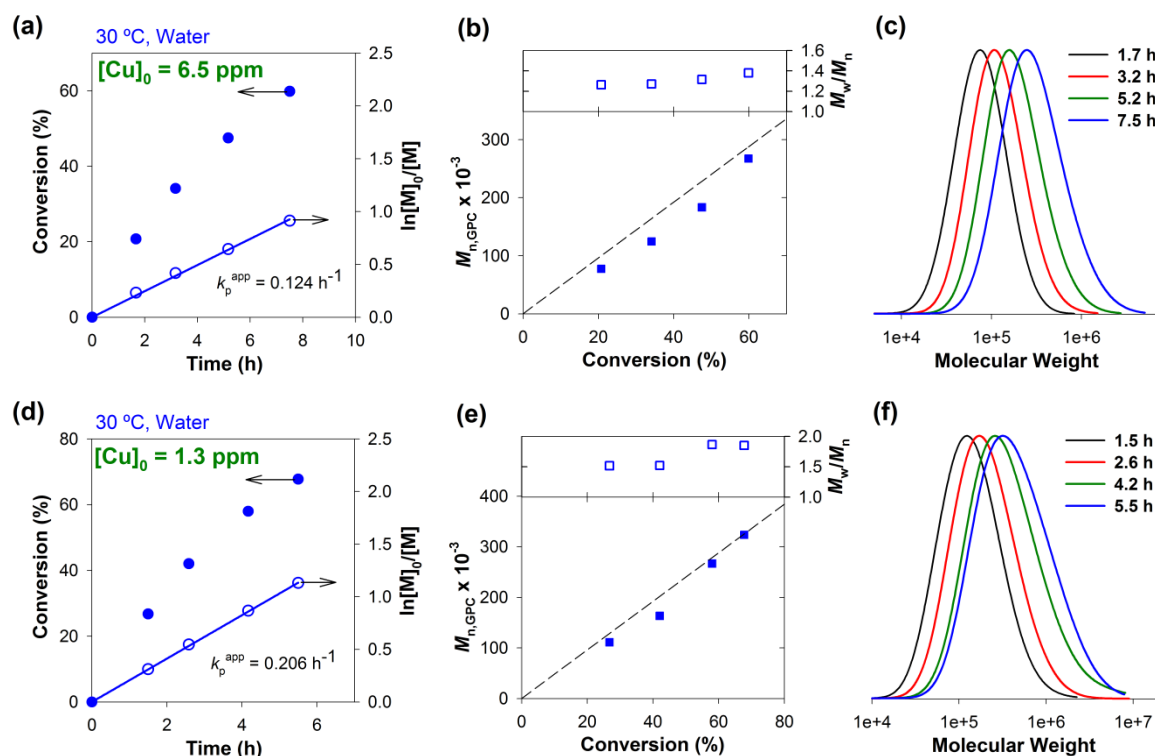


Figure 4.15. (a and d) Kinetic plots of conversion and $\ln[M]_0/[M]$ vs. time; (b and e) plot of $M_{n,GPC}$ and \bar{D} (M_w/M_n) vs. conversion for aqueous SARA ATRP of OEOA₄₈₀ at 30 °C; and (c and f) GPC traces vs. time. Conditions: (a, b and c) $[OEOA_{480}]_0/[HEBiB]_0/[Cu(II)Br_2]_0/[TPMA]_0 = 1000/1/0.05/0.4$; (d, e and f) $[OEOA_{480}]_0/[HEBiB]_0/[Cu(II)Br_2]_0/[TPMA]_0 = 1000/1/0.01/0.08$; $[OEOA_{480}]_0/[Water] = 1/3$; $FR(Na_2S_2O_4) = 16$ nmol/min; $[NaCl]_0 = 100$ mM.

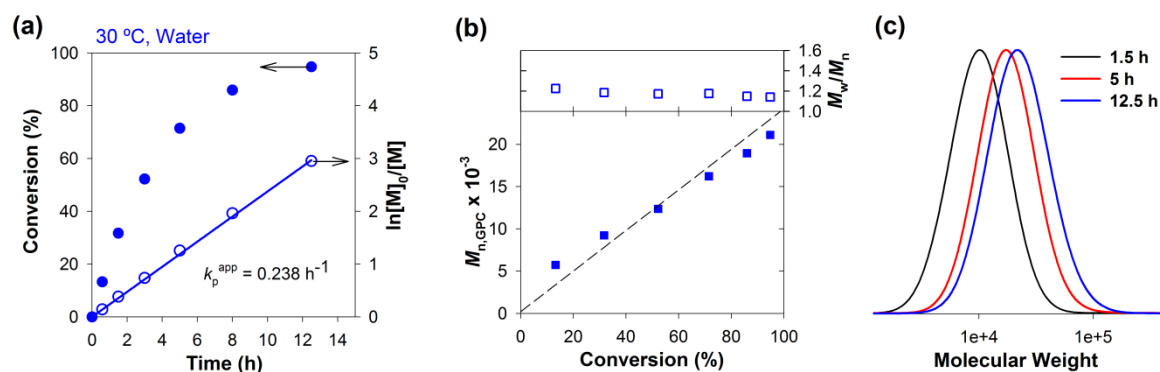


Figure 4.16. (a) Kinetic plots of conversion and $\ln[M]_0/[M]$ vs. time; (b) plot of $M_{n,GPC}$ and \bar{D} (M_w/M_n) vs. conversion for aqueous SARA ATRP of OEOA₄₈₀ at 30 °C; and (c) GPC traces vs. time. Conditions: $[OEOA_{480}]_0/[HEBiB]_0/[Cu(II)Br_2]_0/[TPMA]_0 = 50/1/0.05/0.4$; $[OEOA_{480}]_0/[Water] = 1/3$; $FR(Na_2S_2O_4) = 64$ nmol/min; $[NaCl]_0 = 100$ mM.

Table 4.5. Aqueous SARA ATRP of OEQA₄₈₀ with Various Sulfites.

Entry ^a	[M] ₀ /[I] ₀ /[Cu(II)Br ₂] ₀ /[TPMA] ₀	Sulfite	Cu ^b (ppm)	k _p ^{app} (h ⁻¹)	Time (h)	Conv. (%)	M _n th × 10 ⁻³	M _n ^{GPC} × 10 ⁻³	D
1	250/1/0.05/0.4	Na ₂ S ₂ O ₄	26	0.181	7	71	85.8	85.0	1.28
2	250/1/0.05/0.4	Na ₂ S ₂ O ₅	26	0.0073	150	67	80.5	67.3	1.22
3	250/1/0.05/0.4	NaHSO ₃	26	0.0048	164	55	65.7	58.5	1.22

^aAll polymerizations were conducted with [M]₀ = 0.5 M, [I]₀ = 2 mM, [NaCl]₀ = 100 mM and FR_S = 64 nmol/min

^bCalculated by the initial weight ratio of Cu to the monomer.

Table 4.6. Aqueous SARA ATRP of OEQA₄₈₀ and OEOMA₅₀₀ with Varied Cu Concentrations and DP.

Entry ^a	[M] ₀ /[I] ₀ /[Cu(II)Br ₂] ₀ /[TPMA] ₀	DP	Cu ^b (ppm)	k _p ^{app} (h ⁻¹)	Time (h)	Conv. (%)	M _n th × 10 ⁻³	M _n ^{GPC} × 10 ⁻³	D
1 ^c	250/1/0.05/0.4	250	26	0.181	7	71	85.8	85.0	1.28
2 ^c	1000/1/0.05/0.4	1000	6.5	0.124	7.5	60	287.6	267.5	1.38
3 ^c	1000/1/0.01/0.08	1000	1.3	0.206	5.5	68	325.4	323.6	1.85
4 ^c	50/1/0.05/0.4	50	130	0.238	12.5	95	23.0	21.1	1.14
5 ^d	50/1/0.05/0.4	50	130	0.208	18	98	24.6	26.2	1.22

^aAll polymerizations were conducted with [M]₀ = 0.5 M, [NaCl]₀ = 100 mM, and FR_S = 64 nmol/min; [I]₀ = 2 mM for entry 1, [I]₀ = 0.5 mM for entry 2 and 3, [I]₀ = 10 mM for entry 4 and 5.

^bCalculated by the initial weight ratio of Cu to the monomer.

^cM = OEQA₄₈₀.

^dM = OEOMA₅₀₀.

The optimized conditions for aqueous SARA ATRP reported in this manuscript for OEOA₄₈₀ polymerization (Figure 4.16 and Table 4.6, entry 4) were successfully extended to the polymerization of other monomer, OEOMA₅₀₀ (Figure 4.17 and Table 4.6, entry 5). The results are comparable to OEOA in terms of control over the polymerization and low dispersity values ($\mathcal{D} < 1.22$). It is worth mentioning that very high monomer conversions (>95%) were achieved in these two polymerizations (Table 4.6, entries 4 and 5) with an excellent control over molecular weights and \mathcal{D} .

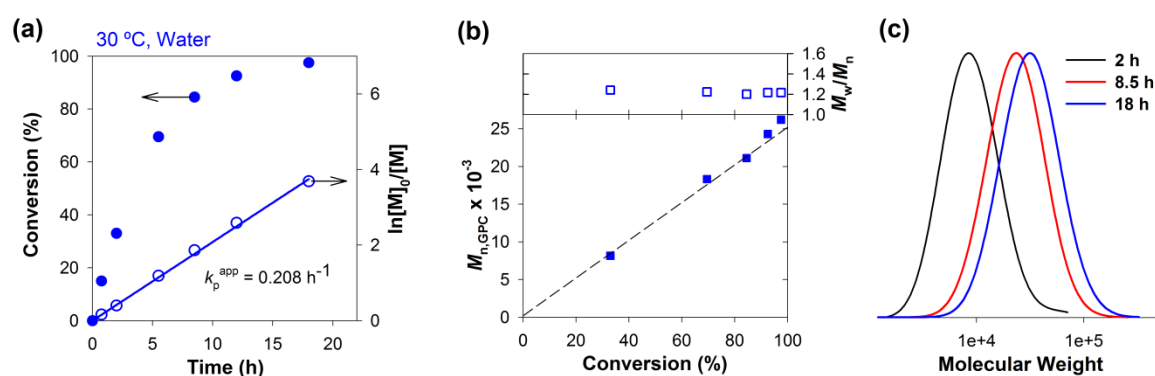


Figure 4.17. (a) Kinetic plots of conversion and $\ln[M]_0/[M]$ vs. time; (b) plot of $M_{n,GPC}$ and \mathcal{D} (M_w/M_n) vs. conversion for aqueous SARA ATRP of OEOMA₅₀₀ at 30 °C; and (c) GPC traces vs. time. Conditions: $[OEOMA_{500}]_0/[HEBiB]_0/[Cu(II)Br_2]_0/[TPMA]_0 = 50/1/0.05/0.4$; $[OEOMA_{500}]_0/[Water] = 1/3$; $FR(Na_2S_2O_4) = 64$ nmol/min; $[NaCl]_0 = 100$ mM.

4.4.8. Start/Stop Polymerizations

In this work, inorganic sulfites (*e.g.* $Na_2S_2O_4$) were fed to the reaction in order to regenerate Cu(I) species and promote controlled polymerizations. Thus, one should expect that if the feeding of the SARA agent is stopped, a significant buildup of the deactivator occurs shifting the ATRP equilibrium toward the dormant species. As has been demonstrated in aqueous photoinduced ATRP⁴³ or aqueous ARGET ATRP,²⁴ the next experiment (Figure 4.18 and Table 4.7) proved that the polymerization can be started or stopped on demand by turning on or off the feeding of $Na_2S_2O_4$. $Na_2S_2O_4$ was continuously added ($FR_S = 64$ nmol/min) to the reaction for 1 h and, under similar conditions (catalyst loading of 26 ppm), the polymerization proceeded at the same rate. It is perfectly visible in Figure 4.18, after the feeding of the $Na_2S_2O_4$ was turned off the

polymerization almost stopped. This procedure was repeated four more times until a monomer conversion of 75%. In the last cycle after the feeding was stopped (time = 9 h), the reaction was left to continue for 15 h more and no relevant differences were observed. During the course of this experiment the \bar{D} values of the obtained polymers were low and the molecular weights matched perfectly with the theoretical ones.

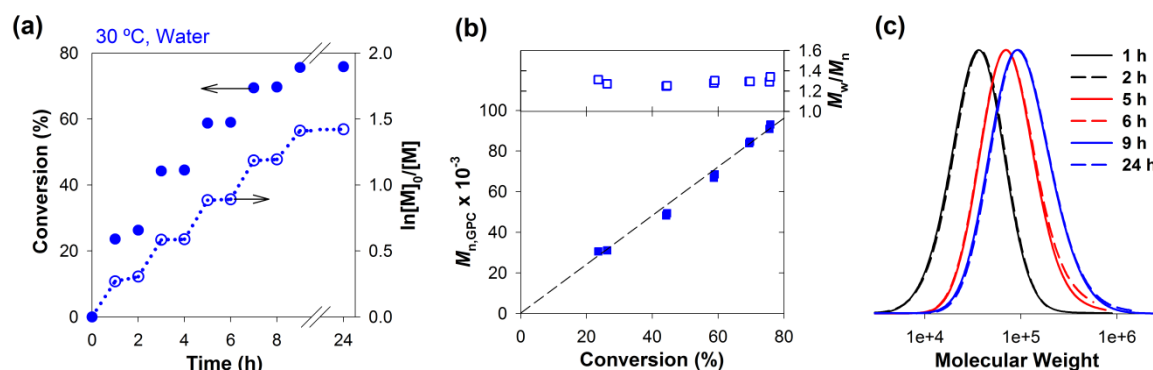


Figure 4.18. (a) Kinetic plots of conversion and $\ln[M]_0/[M]$ vs. time; (b) plot of $M_{n,GPC}$ and \bar{D} (M_w/M_n) vs. conversion for aqueous SARA ATRP of OEOA₄₈₀ at 30 °C; and (c) GPC traces vs. time. Conditions: $[OEOA_{480}]_0/[HEBiB]_0/[Cu(II)Br_2]_0/[TPMA]_0 = 250/1/0.05/0.1$; $FR(Na_2S_2O_4) = 64$ nmol/min; $[NaCl]_0 = 100$ mM; $[OEOA_{480}]_0/[Water] = 1/3$.

Table 4.7. Aqueous SARA ATRP of OEOA₄₈₀ with Start/Stop Cycles.

Entry ^a	$[M]_0/[I]_0/[Cu(II)Br_2]_0/[TPMA]_0$	Time (h)	Conv. (%)	$M_n^{th} \times 10^{-3}$	$M_n^{GPC} \times 10^{-3}$	\bar{D}
1	250/1/0.05/0.4	1 (1 h OFF)	24	28.5	30.6	1.31
		3 (1 h OFF)	44	53.3	48.3	1.25
		5 (1 h OFF)	59	70.7	66.9	1.28
		7 (1 h OFF)	69	83.5	83.9	1.29
		9 (15 h OFF)	76	90.9	90.9	1.29

^aAll polymerizations were conducted with $[M]_0 = 0.5$ M, $[I]_0 = 2$ mM, $[NaCl]_0 = 100$ mM and $FR_S = 64$ nmol/min;

4.4.9. Chain Extension Experiments

The possibility to synthesize polymers with active chain-ends, which can be functionalized or reinitiated to afford complex macromolecular structures, is one of the crucial advantages of RDRP techniques over conventional radical polymerizations. “One-

pot” re-initiation and copolymerization experiments were performed to evaluate the livingness of P(OEOA₄₈₀) (Table 4.6, entry 4) and P(OEOMA₅₀₀) (Table 4.6, entry 5) chains synthesized using aqueous SARA ATRP. As shown in Figure 4.19(a) and Table 4.8 (entry 1), a complete shift of the GPC traces during the “one-pot” chain extension experiment was achieved. The molecular weight of the starting P(OEOA₄₈₀)-Cl (95% of monomer conversion, $M_n^{\text{th}} = 23\,000$, $M_n^{\text{GPC}} = 21\,100$, $\mathcal{D} = 1.14$) shifted toward a very high molecular weight when a fresh monomer was supplied (45% of monomer conversion, $M_n^{\text{th}} = 214\,600$, $M_n^{\text{GPC}} = 201\,200$, $\mathcal{D} = 1.31$). Also, a “one-pot” P(OEOMA₅₀₀)-*b*-P(OEOA₄₈₀) diblock copolymer (43% of monomer conversion, $M_n^{\text{th}} = 206\,500$, $M_n^{\text{GPC}} = 222\,700$, $\mathcal{D} = 1.29$) was synthesized from a P(OEOMA₅₀₀)-Cl macroinitiator (98% of monomer conversion, $M_n^{\text{th}} = 24\,600$, $M_n^{\text{GPC}} = 26\,200$, $\mathcal{D} = 1.22$) (Figure 4.19(b) and Table 4.8, entry 2). These results demonstrate the “living” character of the obtained polymers and the possibility of using this aqueous catalytic system in the synthesis of more complex macromolecular structures.

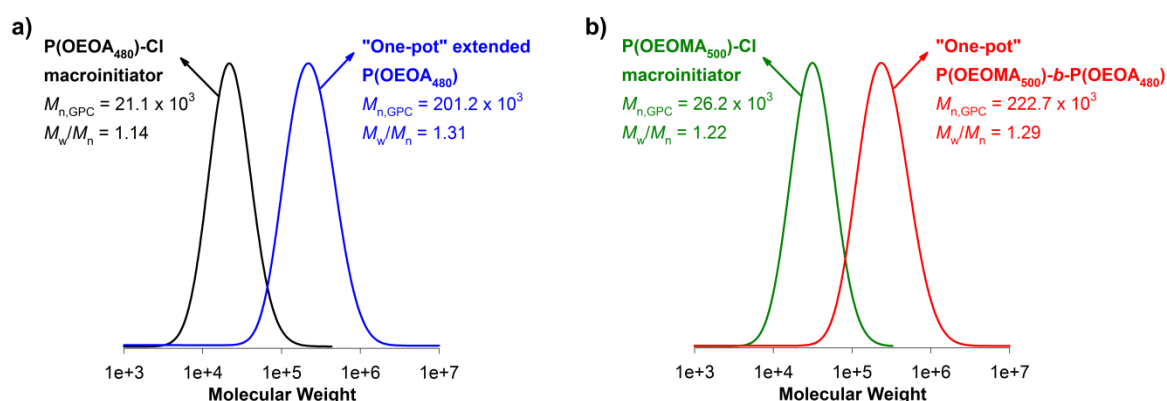


Figure 4.19. (a) GPC chromatographs of the P(OEOA₄₈₀)-Cl macroinitiator (black line) and “one-pot” extended P(OEOA₄₈₀) (blue line); (b) GPC chromatographs of the P(OEOMA₅₀₀)-Cl macroinitiator (green line) and “one-pot” P(OEOMA₅₀₀)-*b*-P(OEOA₄₈₀) block copolymer (red line).

4.4.10. Synthesis of a Protein–Polymer Hybrid

In order to explore the biologically friendly conditions of the aqueous SARA ATRP, as proof-of-concept a protein-polymer hybrid was synthesized by the “grafting from”

approach. Bovine serum albumin (BSA) was used as a model protein, which contained 30 ATRP initiating sites. The reaction was performed in phosphate buffered saline (PBS) (NaCl (137 mM – 1X) and NaH₂PO₄ (10 mM – 1X) salts) was used for protein stabilization. The grafting of P(OEOA₄₈₀) from BSA-O-[iBBr]₃₀ in PBS showed a linear first-order kinetic plot, a linear evolution of molecular weight with conversion, an excellent correlation between experimental and theoretical molecular weight values, and a relatively low dispersity values ($\mathcal{D} < 1.35$) (Figure 4.20 and Table 4.9). These results indicate that this system can be successfully used to afford protein-polymer hybrids.

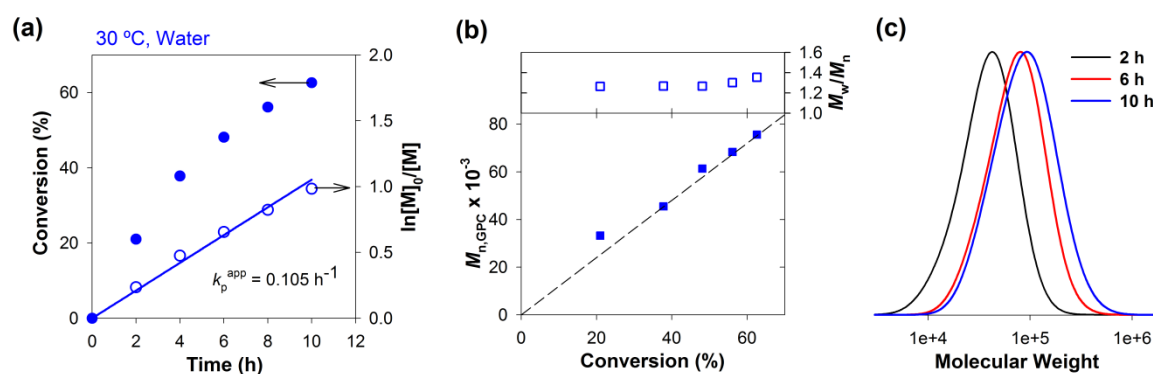


Figure 4.20. (a) Kinetic plots of conversion and $\ln[M]_0/[M]$ vs. time; (b) plot of $M_{n, GPC}$ and \mathcal{D} (M_w/M_n) vs. conversion for aqueous SARA ATRP of OEOA₄₈₀ at 30 °C; and (c) GPC traces vs. time. Conditions: $[OEOA_{480}]_0/[BSA-O-[iBBr]_{30}]_0/[Cu(II)Br_2]_0/[TPMA]_0 = 250/1/0.05/0.4$; $[OEOA_{480}]_0/[PBS] = 1/6$; $FR(Na_2S_2O_4) = 16$ nmol/min.

A sodium dodecyl sulfate-polyacrylamide gel electrophoresis (SDS-PAGE) experiment was performed to measure the changes from the native BSA to BSA modified with the ATRP initiator (BSA-O-[iBBr]₃₀), and protein-polymer hybrids (BSA-[P(OEOA₄₈₀)₃₀): 20 μL, 10 μL and 5 μL of sample mixture was added to the gel slot) (Figure 4.21). With the presence of protein markers, it is clear that the native BSA (66 kDa) was placed between 55 kDa and 72 kDa markers, and BSA-O-[iBBr]₃₀ (75 kDa) was placed slightly above 72 kDa line. As expected, the protein-polymer hybrid BSA-[P(OEOA₄₈₀)₃₀] showed broad bands above 180 kDa and complete consumption of protein initiators was observed.

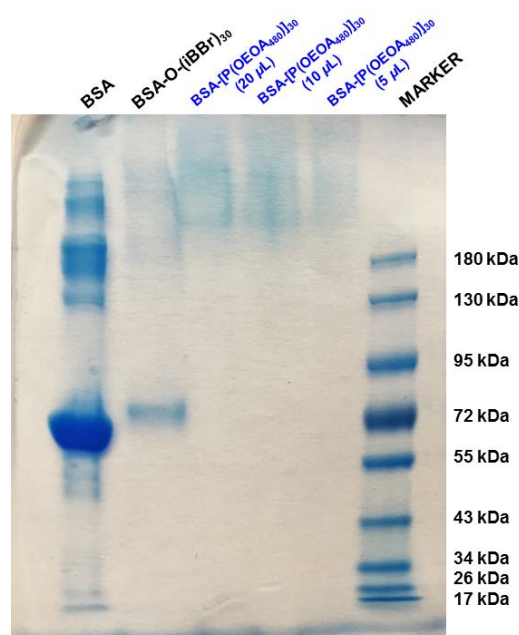


Figure 4.21. SDS-PAGE of native BSA (66 kDa), BSA-O-[iBBR]₃₀ (75 kDa), various concentrations of BSA-[P(OEOA₄₈₀)₃₀] hybrids, and protein markers.

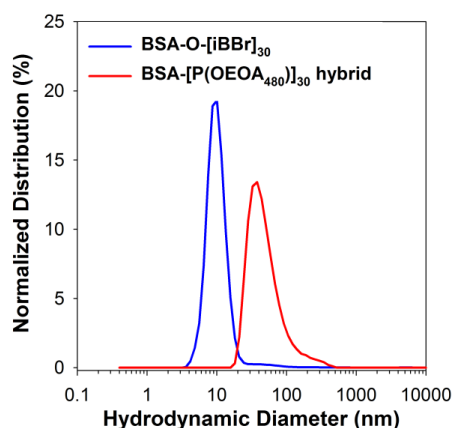


Figure 4.22. Dynamic light scattering distribution of BSA-O-[iBBR]₃₀ before polymerization (blue line) and BSA-[P(OEOA₄₈₀)₃₀] nanoparticles; Conditions: [OEOA₄₈₀]₀/[BSA-O-[iBBR]₃₀]₀/[Cu(II)Br₂]₀/ [TPMA]₀ = 250/1/0.05/0.4; [OEOA₄₈₀]₀/[Water] = 1/6; FR(Na₂S₂O₄) = 16 nmol/min.

In Figure 4.22, the results obtained by dynamic light scattering (DLS) of BSA-O-[iBBR]₃₀ nanoparticles before polymerization (diameter ($D_{\text{BSA-O-[iBBR]30}}$) = 11.35 nm; dispersity ($\text{PDI}_{\text{BSA-O-[iBBR]30}}$) = 0.387) and BSA-[P(OEOA₄₈₀)₃₀] nanoparticles ($D_{\text{BSA-[P(OEOA480)]30}}$ = 57.54 nm; $\text{PDI}_{\text{BSA-[P(OEOA480)]30}}$ = 0.256) clearly showed an increase in size and the absence of any undesirable aggregation.

Table 4.8. “One-Pot” Chain Extension Experiments from P(OEOA₄₈₀) and P(OEOMA₅₀₀).

Entry ^a	[M] ₀ /[I] ₀ /[Cu(II)Br ₂] ₀ /[TPMA] ₀	Monomer	Cu ^b (ppm)	Time (h)	Conv. (%)	M _n th × 10 ⁻³	M _n ^{GPC} × 10 ⁻³	D
1 ^c	1000/1/0/0	OEOA ₄₈₀	6.5	12	45	214.6	201.2	1.31
2 ^d	1000/1/0/0	OEOA ₄₈₀	6.5	20	43	206.5	222.7	1.29

^aAll polymerizations were conducted with [M]₀ = 0.5 M, [MI]₀ = 0.5 mM, and FR_S = 8 nmol/min;

^bCalculated by the initial weight ratio of Cu to the monomer.

^cThe P(OEOA₄₈₀)-Cl (MI) was obtained as in Table 4.6, entry 4.

^dThe P(OEOMA₅₀₀)-Cl (MI) was obtained as in Table 4.6, entry 5.

Table 4.9. SARA ATRP of OEOA₄₈₀ in PBS Initiated by BSA-O-[iBBR]₃₀.

Entry ^a	[M] ₀ /[I] ₀ /[Cu(II)Br ₂] ₀ /[TPMA] ₀	Cu ^b (ppm)	k _p ^{app} (h ⁻¹)	Time (h)	Conv. (%)	M _n th × 10 ⁻³	M _n ^{GPC} × 10 ⁻³	D
1	250/1/0.05/0.4	26	0.105	10	63	75.1	75.6	1.35

^aAll polymerizations were conducted with [M]₀ = 0.25 M, [I]₀ = 1 mM, and FR_S = 64 nmol/min;

^bCalculated by the initial weight ratio of Cu to the monomer.

4.5. Conclusions

The preparation of well-defined (co)polymers at ambient temperature (30 °C) in water using catalyst concentrations between 6 and 26 ppm was achieved by aqueous SARA ATRP of OEOA₄₈₀ and OEOMA₅₀₀ using inorganic sulfites. The critical parameters for preparation of well-controlled polymers were found to be: the slow continuous feeding of inorganic sulfites (Na₂S₂O₄) (FR_S = 16 – 64 nmol/min) to the reaction medium; the use of a large excess of halide salt (*e.g.* NaCl, [NaCl]₀ = 100 mM) and a high ratio L/Cu (8/1) to ensure the stability of the deactivator complex. Among the there different inorganic sulfites used, Na₂S₂O₄ was the most efficient SARA agent for the studied system. A start/stop polymerization proved that the reaction can be stopped and (re)started at any point simply by controlling the feed of the SARA agent. The high retention of chain-end functionality was proved by successful “one-pot” chain extension and “one-pot” block copolymerization experiments. Finally, the very low Cu catalyst concentration used, together with the inexpensive, safe, and environmentally friendly inorganic sulfites employed, suggests this aqueous SARA ATRP to be very suitable for working with biologically active molecules. As proof-of-concept, a BSA protein-polymer hybrid was successfully synthesized.

4.6. References

1. Szwarc, M., *"Living" Polymers*. Nature, **1956**, 178, 1168-1169.
2. Moad, G. and Solomon, D. H., *The chemistry of free radical polymerization*. 1st ed, **1995**, Oxford: Elsevier.
3. Braunecker, W. A. and Matyjaszewski, K., *Controlled/living radical polymerization: Features, developments, and perspectives*. Progress in Polymer Science, **2007**, 32, 93-146.
4. Georges, M. K., Veregin, R. P. N., Kazmaier, P. M., and Hamer, G. K., *Narrow Molecular Weight Resins by a Free-Radical Polymerization Process*. Macromolecules, **1993**, 26, 2987-2988.
5. Hawker, C. J., Bosman, A. W., and Harth, E., *New Polymer Synthesis by Nitroxide Mediated Living Radical Polymerizations*. Chemical Reviews, **2001**, 101, 3661-3688.

6. Nicolas, J., Guillaneuf, Y., Lefay, C., Bertin, D., Gimes, D., and Charleux, B., *Nitroxide-mediated polymerization*. *Progress in Polymer Science*, **2013**, *38*, 63-235.
7. Wang, J.-S. and Matyjaszewski, K., *Controlled/"Living" Radical Polymerization. Atom Transfer Radical Polymerization in the Presence of Transition-Metal Complexes*. *Journal of American Chemical Society*, **1995**, *117*, 5614-5615.
8. Pintauer, T. and Matyjaszewski, K., *Atom transfer radical addition and polymerization reactions catalyzed by ppm amounts of copper complexes*. *Chemical Society Reviews*, **2008**, *37*, 1087-1097.
9. Matyjaszewski, K. and Tsarevsky, N. V., *Nanostructured functional materials prepared by atom transfer radical polymerization*. *Nature Chemistry*, **2009**, *1*, 276-288.
10. Matyjaszewski, K., *Atom Transfer Radical Polymerization (ATRP): Current Status and Future Perspectives*. *Macromolecules*, **2012**, *45*, 4015-4039.
11. Matyjaszewski, K. and Tsarevsky, N. V., *Macromolecular Engineering by Atom Transfer Radical Polymerization*. *Journal of the American Chemical Society*, **2014**, *136*, 6513-6533.
12. Boyer, C., Corrigan, N. A., Jung, K., Nguyen, D., Nguyen, T.-K., Adnan, N. N. M., Oliver, S., Shanmugam, S., and Yeow, J., *Copper-Mediated Living Radical Polymerization (Atom Transfer Radical Polymerization and Copper(0) Mediated Polymerization): From Fundamentals to Bioapplications*. *Chemical Reviews*, **2016**, *116*, 1803-1949.
13. Chiefari, J., Chong, Y. K., Ercole, F., Krstina, J., Jeffery, J., Le, T. P. T., Mayadunne, R. T. A., Meijs, G. F., Moad, C. L., Moas, G., Rizzardo, E., and Thang, S. H., *Living Free-Radical Polymerization by Reversible Addition-Fragmentation Chain Transfer: The RAFT Process*. *Macromolecules*, **1998**, *31*, 5559-5562.
14. Moad, G., Rizzardo, E., and Thang, S. H., *Living Radical Polymerization by the RAFT Process – A Third Update*. *Australian Journal of Chemistry*, **2012**, *65*, 985-1076.
15. Hill, M. R., Carmean, R. N., and Sumerlin, B. S., *Expanding the Scope of RAFT Polymerization: Recent Advances and New Horizons*. *Macromolecules*, **2015**, *48*, 5459-5469.
16. Sheiko, S. S., Sumerlin, B. S., and Matyjaszewski, K., *Cylindrical molecular brushes: Synthesis, characterization, and properties*. *Progress in Polymer Science*, **2008**, *33*, 759-785.
17. Gao, H. and Matyjaszewski, K., *Synthesis of functional polymers with controlled architecture by CRP of monomers in the presence of cross-linkers: From stars to gels*. *Progress in Polymer Science*, **2009**, *34*, 317-350.

18. Golas, P. L. and Matyjaszewski, K., *Marrying click chemistry with polymerization: expanding the scope of polymeric materials*. Chemical Society Reviews, **2010**, *39*, 1338-1354.
19. Lee, H.-i., Pietrasik, J., Sheiko, S. S., and Matyjaszewski, K., *Stimuli-responsive molecular brushes*. Progress in Polymer Science, **2010**, *35*, 24-44.
20. Siegwart, D. J., Oh, J. K., and Matyjaszewski, K., *ATRP in the design of functional materials for biomedical applications*. Progress in Polymer Science, **2012**, *37*, 18-37.
21. Jakubowski, W., Min, K., and Matyjaszewski, K., *Activators Regenerated by Electron Transfer for Atom Transfer Radical Polymerization of Styrene*. Macromolecules, **2005**, *39*, 39-45.
22. Jakubowski, W. and Matyjaszewski, K., *Activators Regenerated by Electron Transfer for Atom-Transfer Radical Polymerization of (Meth)acrylates and Related Block Copolymers*. Angewandte Chemie International Edition, **2006**, *45*, 4482-4486.
23. Kwak, Y., Magenau, A. J. D., and Matyjaszewski, K., *ARGET ATRP of Methyl Acrylate with Inexpensive Ligands and ppm Concentrations of Catalyst*. Macromolecules, **2011**, *44*, 811-819.
24. Simakova, A., Averick, S. E., Konkolewicz, D., and Matyjaszewski, K., *Aqueous ARGET ATRP*. Macromolecules, **2012**, *45*, 6371-6379.
25. Matyjaszewski, K., Jakubowski, W., Min, K., Tang, W., Huang, J., Braunecker, W. A., and Tsarevsky, N. V., *Diminishing catalyst concentration in atom transfer radical polymerization with reducing agents*. Proceedings of the National Academy of Sciences, **2006**, *103*, 15309-15314.
26. Konkolewicz, D., Magenau, A. J. D., Averick, S. E., Simakova, A., He, H., and Matyjaszewski, K., *ICAR ATRP with ppm Cu Catalyst in Water*. Macromolecules, **2012**, *45*, 4461-4468.
27. Mendonça, P. V., Serra, A. C., Coelho, J. F. J., Popov, A. V., and Guliashvili, T., *Ambient temperature rapid ATRP of methyl acrylate, methyl methacrylate and styrene in polar solvents with mixed transition metal catalyst system*. European Polymer Journal, **2011**, *47*, 1460-1466.
28. Zhang, Y., Wang, Y., and Matyjaszewski, K., *ATRP of Methyl Acrylate with Metallic Zinc, Magnesium, and Iron as Reducing Agents and Supplemental Activators*. Macromolecules, **2011**, *44*, 683-685.
29. Abreu, C. M. R., Mendonça, P. V., Serra, A. C., Coelho, J. F. J., Popov, A. V., and Guliashvili, T., *Accelerated Ambient-Temperature ATRP of Methyl Acrylate in Alcohol-Water Solutions with a Mixed Transition-Metal Catalyst System*. Macromolecular Chemistry and Physics, **2012**, *213*, 1677-1687.

30. Konkolewicz, D., Kryszewski, P., Góis, J. R., Mendonça, P. V., Zhong, M., Wang, Y., Gennaro, A., Isse, A. A., Fantin, M., and Matyjaszewski, K., *Aqueous RDRP in the Presence of CuO: The Exceptional Activity of CuI Confirms the SARA ATRP Mechanism*. *Macromolecules*, **2014**, *47*, 560-570.
31. Mendes, J. P., Branco, F., Abreu, C. M. R., Mendonça, P. V., Serra, A. C., Popov, A. V., Guliashvili, T., and Coelho, J. F. J., *Sulfolane: an Efficient and Universal Solvent for Copper-Mediated Atom Transfer Radical (co)Polymerization of Acrylates, Methacrylates, Styrene, and Vinyl Chloride*. *ACS Macro Letters*, **2014**, *3*, 858-861.
32. Maximiano, P., Mendes, J. P., Mendonça, P. V., Abreu, C. M. R., Guliashvili, T., Serra, A. C., and Coelho, J. F. J., *Cyclopentyl methyl ether: A new green co-solvent for supplemental activator and reducing agent atom transfer radical polymerization*. *Journal of Polymer Science Part A: Polymer Chemistry*, **2015**, *53*, 2722-2729.
33. Nicol, E. and Nzé, R.-P., *Supplemental Activator and Reducing Agent Atom Transfer Radical Polymerization of 2-Hydroxyethyl Acrylate from High Molar Mass Poly(ethylene oxide) Macroinitiator in Dilute Solution*. *Macromolecular Chemistry and Physics*, **2015**, *216*, 1405-1414.
34. Mendes, J. P., Mendonça, P. V., Maximiano, P., Abreu, C. M. R., Guliashvili, T., Serra, A. C., and Coelho, J. F. J., *Getting faster: low temperature copper-mediated SARA ATRP of methacrylates, acrylates, styrene and vinyl chloride in polar media using sulfolane/water mixtures*. *RSC Advances*, **2016**, *6*, 9598-9603.
35. Bortolamei, N., Isse, A. A., Magenau, A. J. D., Gennaro, A., and Matyjaszewski, K., *Controlled Aqueous Atom Transfer Radical Polymerization with Electrochemical Generation of the Active Catalyst*. *Angewandte Chemie International Edition*, **2011**, *50*, 11391-11394.
36. Magenau, A. J. D., Strandwitz, N. C., Gennaro, A., and Matyjaszewski, K., *Electrochemically Mediated Atom Transfer Radical Polymerization*. *Science*, **2011**, *332*, 81-84.
37. Li, B., Yu, B., Huck, W. T. S., Zhou, F., and Liu, W., *Electrochemically Induced Surface-Initiated Atom-Transfer Radical Polymerization*. *Angewandte Chemie International Edition*, **2012**, *51*, 5092-5095.
38. Fantin, M., Isse, A. A., Venzo, A., Gennaro, A., and Matyjaszewski, K., *Atom Transfer Radical Polymerization of Methacrylic Acid: A Won Challenge*. *Journal of the American Chemical Society*, **2016**, *138*, 7216-7219.
39. Fors, B. P. and Hawker, C. J., *Control of a Living Radical Polymerization of Methacrylates by Light*. *Angewandte Chemie International Edition*, **2012**, *51*, 8850-8853.

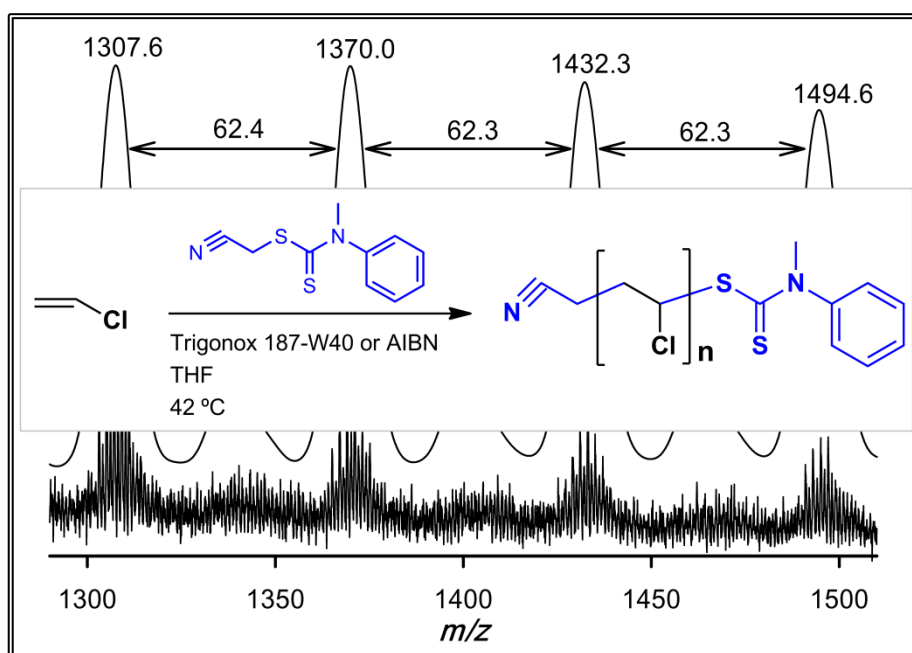
40. Konkolewicz, D., Schröder, K., Buback, J., Bernhard, S., and Matyjaszewski, K., *Visible Light and Sunlight Photoinduced ATRP with ppm of Cu Catalyst*. ACS Macro Letters, **2012**, *1*, 1219-1223.
41. Ribelli, T. G., Konkolewicz, D., Bernhard, S., and Matyjaszewski, K., *How are Radicals (Re)Generated in Photochemical ATRP?* Journal of the American Chemical Society, **2014**, *136*, 13303-13312.
42. Mosnacek, J., Eckstein-Andicsova, A., and Borska, K., *Ligand effect and oxygen tolerance studies in photochemically induced copper mediated reversible deactivation radical polymerization of methyl methacrylate in dimethyl sulfoxide*. Polymer Chemistry, **2015**, *6*, 2523-2530.
43. Pan, X., Malhotra, N., Simakova, A., Wang, Z., Konkolewicz, D., and Matyjaszewski, K., *Photoinduced Atom Transfer Radical Polymerization with ppm-Level Cu Catalyst by Visible Light in Aqueous Media*. Journal of the American Chemical Society, **2015**, *137*, 15430-15433.
44. Pan, X., Malhotra, N., Zhang, J., and Matyjaszewski, K., *Photoinduced Fe-Based Atom Transfer Radical Polymerization in the Absence of Additional Ligands, Reducing Agents, and Radical Initiators*. Macromolecules, **2015**, *48*, 6948-6954.
45. Abreu, C. M. R., Mendonça, P. V., Serra, A. C., Popov, A. V., Matyjaszewski, K., Guliashvili, T., and Coelho, J. F. J., *Inorganic Sulfites: Efficient Reducing Agents and Supplemental Activators for Atom Transfer Radical Polymerization*. ACS Macro Letters, **2012**, *1*, 1308-1311.
46. Abreu, C. M. R., Serra, A. C., Popov, A. V., Matyjaszewski, K., Guliashvili, T., and Coelho, J. F. J., *Ambient temperature rapid SARA ATRP of acrylates and methacrylates in alcohol-water solutions mediated by a mixed sulfite/Cu(II)Br₂ catalytic system*. Polymer Chemistry, **2013**, *4*, 5629-5636.
47. Gois, J. R., Konkolewicz, D., Popov, A. V., Guliashvili, T., Matyjaszewski, K., Serra, A. C., and Coelho, J. F. J., *Improvement of the control over SARA ATRP of 2-(diisopropylamino)ethyl methacrylate by slow and continuous addition of sodium dithionite*. Polymer Chemistry, **2014**, *5*, 4617-4626.
48. Gois, J. R., Rocha, N., Popov, A. V., Guliashvili, T., Matyjaszewski, K., Serra, A. C., and Coelho, J. F. J., *Synthesis of well-defined functionalized poly(2-(diisopropylamino)ethyl methacrylate) using ATRP with sodium dithionite as a SARA agent*. Polymer Chemistry, **2014**, *5*, 3919-3928.
49. Mendes, J. P., Branco, F., Abreu, C. M. R., Mendonça, P. V., Popov, A. V., Guliashvili, T., Serra, A. C., and Coelho, J. F. J., *Synergistic Effect of 1-Butyl-3-methylimidazolium Hexafluorophosphate and DMSO in the SARA ATRP at Room Temperature Affording Very Fast Reactions and Polymers with Very Low Dispersity*. ACS Macro Letters, **2014**, *3*, 544-547.

50. Qiu, J., Charleux, B., and Matyjaszewski, K., *Controlled/living radical polymerization in aqueous media: homogeneous and heterogeneous systems*. Progress in Polymer Science, **2001**, 26, 2083-2134.
51. Ouchi, M., Terashima, T., and Sawamoto, M., *Transition Metal-Catalyzed Living Radical Polymerization: Toward Perfection in Catalysis and Precision Polymer Synthesis*. Chemical Reviews, **2009**, 109, 4963-5050.
52. Xia, J., Johnson, T., Gaynor, S. G., Matyjaszewski, K., and DeSimone, J., *Atom Transfer Radical Polymerization in Supercritical Carbon Dioxide*. Macromolecules, **1999**, 32, 4802-4805.
53. Duxbury, C. J., Wang, W., de Geus, M., Heise, A., and Howdle, S. M., *Can Block Copolymers Be Synthesized by a Single-Step Chemoenzymatic Route in Supercritical Carbon Dioxide?* Journal of the American Chemical Society, **2005**, 127, 2384-2385.
54. Erdmenger, T., Guerrero-Sanchez, C., Vitz, J., Hoogenboom, R., and Schubert, U. S., *Recent developments in the utilization of green solvents in polymer chemistry*. Chemical Society Reviews, **2010**, 39, 3317-3333.
55. Anastasaki, A., Nikolaou, V., Nurumbetov, G., Truong, N. P., Pappas, G. S., Engelis, N. G., Quinn, J. F., Whittaker, M. R., Davis, T. P., and Haddleton, D. M., *Synthesis of Well-Defined Poly(acrylates) in Ionic Liquids via Copper(II)-Mediated Photoinduced Living Radical Polymerization*. Macromolecules, **2015**, 48, 5140-5147.
56. Costa, J. R. C., Mendonça, P. V., Maximiano, P., Serra, A. C., Guliashvili, T., and Coelho, J. F. J., *Ambient Temperature "Flash" SARA ATRP of Methyl Acrylate in Water/Ionic Liquid/Glycol Mixtures*. Macromolecules, **2015**, 48, 6810-6815.
57. Visnevskij, C. and Makuska, R., *SARA ATRP in Aqueous Solutions Containing Supplemental Redox Intermediate: Controlled Polymerization of [2-(Methacryloyloxy)ethyl] trimethylammonium Chloride*. Macromolecules, **2013**, 46, 4764-4771.
58. Braunecker, W. A., Tsarevsky, N. V., Gennaro, A., and Matyjaszewski, K., *Thermodynamic Components of the Atom Transfer Radical Polymerization Equilibrium: Quantifying Solvent Effects*. Macromolecules, **2009**, 42, 6348-6360.
59. Averick, S., Simakova, A., Park, S., Konkolewicz, D., Magenau, A. J. D., Mehl, R. A., and Matyjaszewski, K., *ATRP under Biologically Relevant Conditions: Grafting from a Protein*. ACS Macro Letters, **2012**, 1, 6-10.
60. Tyeklar, Z., Jacobson, R. R., Wei, N., Murthy, N. N., Zubieta, J., and Karlin, K. D., *Reversible reaction of dioxygen (and carbon monoxide) with a copper(I) complex. X-ray structures of relevant mononuclear Cu(I) precursor adducts and the trans-(μ -1,2-peroxo)dicopper(II) product*. Journal of the American Chemical Society, **1993**, 115, 2677-2689.

61. Ciampolini, M. and Nardi, N., *Five-Coordinated High-Spin Complexes of Bivalent Cobalt, Nickel, and Copper with Tris(2-dimethylaminoethyl)amine*. Inorganic Chemistry, **1966**, 5, 41-44.
62. Tsarevsky, N. V., Pintauer, T., and Matyjaszewski, K., *Deactivation Efficiency and Degree of Control over Polymerization in ATRP in Protic Solvents*. Macromolecules, **2004**, 37, 9768-9778.
63. Lough, S. M. and McDonald, J. W., *Synthesis of tetraethylammonium dithionite and its dissociation to the sulfur dioxide radical anion in organic solvents*. Inorganic Chemistry, **1987**, 26, 2024-2027.
64. Tang, W., Kwak, Y., Braunecker, W., Tsarevsky, N. V., Coote, M. L., and Matyjaszewski, K., *Understanding Atom Transfer Radical Polymerization: Effect of Ligand and Initiator Structures on the Equilibrium Constants*. Journal of the American Chemical Society, **2008**, 130, 10702-10713.
65. di Lena, F. and Matyjaszewski, K., *Transition metal catalysts for controlled radical polymerization*. Progress in Polymer Science, **2010**, 35, 959-1021.

Chapter 5

Reversible Addition-Fragmentation Chain Transfer (co)Polymerization of Vinyl Chloride



The contents of this chapter are published in:

Abreu, C. M. R., Mendonça, P. V., Serra, A. C., Coelho, J. F. J., Popov, A. V., Gryn'ova, G., Coote, M. L., and Guliashvili, T., *Reversible Addition-Fragmentation Chain Transfer Polymerization of Vinyl Chloride*. *Macromolecules*, **2012**, *45*, 2200-2208.

5.1. Abstract

Reversible deactivation radical polymerization (RDRP) of vinyl chloride (VC) via reversible addition-fragmentation chain transfer (RAFT) process is reported for the first time. The cyanomethyl methyl(phenyl)carbamodithioate (CMPCD) was found to be an efficient RAFT agent enabling the RDRP polymerization of VC monomer under certain experimental conditions. Two different radical initiators, having very distinct half-life times at room temperature, were employed in this study. The kinetic studies of RAFT polymerization of VC show a linear increase of the molecular weight with the monomer conversion and the lowest dispersity (\bar{D}) ever reported for poly(vinyl chloride) (PVC) synthesized with RDRP method ($\bar{D} \sim 1.4$). The resulting PVC was fully characterized using the matrix-assisted laser desorption ionization time-of-flight mass spectrometry (MALDI-TOF-MS), ^1H nuclear magnetic resonance spectrometry ($^1\text{H-NMR}$) and gel permeation chromatography (GPC) techniques. The $^1\text{H-NMR}$ and MALDI-TOF-MS analysis of PVC prepared via RAFT polymerization method have shown the absence of structural defects and the presence of chain-end functional groups. The “livingness” of the PVC was also confirmed by successful reinitiation and PVC-based block copolymerization experiments. The suitability of the RAFT agent was also confirmed via high-level *ab initio* molecular orbital calculations.

5.2. Introduction

Reversible deactivation radical polymerization (RDRP) methods provide unprecedented tools for the synthesis of polymers with controlled structures, architectures, chain-end fidelity and narrow molecular weight distributions. The most widely used RDRP methods are: atom transfer radical polymerization (ATRP),^{1,2} nitroxide mediated polymerization (NMP)³ and reversible addition fragmentation chain transfer (RAFT) polymerization.^{4,5} The development of the next generation of RDRP methods for control of non-activated vinyl monomers (such as vinyl acetate, *N*-vinylpyrrolidone, vinyl chloride, etc.) remains an important challenge. RDRP of vinyl chloride (VC) is of particular interest because poly(vinyl chloride) (PVC) is one of the most widely consumed polymers worldwide. Conventional free radical polymerization (FRP) of VC is the only available industrial

process to produce the polymer in large scale. PVC made via conventional FRP process lacks the thermal stability due to the presence of structural defects (allyl and tertiary chloride groups), which are the result of different unavoidable side reactions.⁶⁻¹⁰

Until 2012, the most successful RDRP of VC had been achieved by single electron transfer living radical polymerizations (SET-LRP)¹¹⁻¹³ or single electron transfer degenerative chain transfer living radical polymerizations (SET-DTLRP).^{8,14-23} Since the development of these RDRP strategies for VC polymerization, several studies involving the homopolymerization, copolymerization, functionalization and scaling-up have been published and this topic summarized in a review paper by Rosen and Percec.²⁴

Despite these advances, it remains desirable to adapt other RDRP techniques to VC so as to broaden the scope of compatible monomers for block copolymer synthesis. To this end, in the present work we investigate the RAFT polymerization of VC in the presence of cyanomethyl methyl(phenyl)carbamdithioate (CMPCD), using 2,2'-azobis(isobutyronitrile) (AIBN) or a very fast peroxide initiator (Trigonox 187-W40) (see Figure 5.1 for structures).

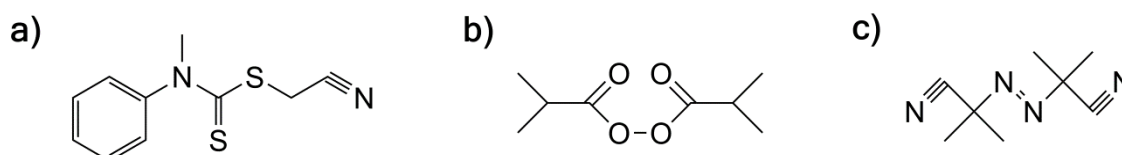


Figure 5.1. Structures of a) cyanomethyl methyl(phenyl)carbamdithioate (CMPCD), b) Trigonox 187-W40 (diisobutyryl peroxide or DIBPO) and c) 2,2'-azobisisobutyronitrile (AIBN).

5.3. Experimental Section

5.3.1. Materials

VC (99 %) was kindly supplied by CIRES Lda, Portugal. CMPCD (Sigma–Aldrich, 98 %) and Trigonox 187-W40 (40 % water and methanol emulsion of diisobutyryl peroxide

(DIBPO), AkzoNobel), deuterated tetrahydrofuran (d_8 -THF) (Euriso-top, 99.5 %), 2-(4-hydroxyphenylazo)benzoic acid (HABA) (Sigma–Aldrich, 99.5 %), α -cyano-4-hydroxycinnamic acid (CHCA) (Sigma–Aldrich, 99.5 %), and methanol (Labsolve, 99.5 %) were used as received. AIBN (Fluka, 98 %) was recrystallized three times from ethanol before use. THF (Panreac, HPLC grade) was filtered (0.2 μm filter) under reduced pressure before use. Cyclohexanone (Sigma–Aldrich, 99.8 %) and dichloromethane (Fluka, 99.9 %) were dried before use.

5.3.2. Techniques

The ^1H NMR spectra of samples were recorded with a Varian VNMRS 600 MHz spectrometer, with a warm 3-mm PFG triple resonance indirect detection probe, in THF- d_8 with tetramethylsilane (TMS) as an internal standard.

The chromatographic parameters of the samples were determined using high performance gel permeation chromatography HPSEC; Viscotek (Viscotek TDAmix) with a differential viscometer (DV); right-angle laser-light scattering (RALLS, Viscotek); low-angle laser-light scattering (LALLS, Viscotek) and refractive index (RI) detectors. The column set consisted of a PL 10 mm guard column ($50 \times 7.5 \text{ mm}^2$) followed by one Viscotek T2000 column (6 μm), one MIXED-E PLgel column (3 μm) and one MIXED-C PLgel column (5 μm). HPLC dual piston pump was set with a flow rate of 1 mL/min. The eluent (THF) was previously filtered through a 0.2 μm filter. The system was also equipped with an on-line degasser. The tests were done at 30 °C using an Elder CH-150 heater. Before the injection (100 μL), the samples were filtered through a polytetrafluoroethylene (PTFE) membrane with 0.2 μm pore. The system was calibrated with narrow polystyrene (PS) standards. The dn/dc was determined as 0.105 for PVC. Molecular weight (M_n^{GPC}) and dispersity (\mathcal{D}) of synthesized polymers were determined by Universal Calibration (the viscosity was measured directly by the viscometer detector) using OmniSEC software version: 4.6.1.354.

For the MALDI-TOF-MS analysis, the PVC samples were dissolved in THF at a concentration of 10 mg/mL. HABA and CHCA (0.05 M in THF) were used as matrix. The dried-droplet sample preparation technique was used to obtain 1:1 ratio

(sample/matrix); an aliquot of 1 μL of each sample was directly spotted on the MTP AnchorChip TM 600/384 TF MALDI target, Bruker Daltonik (Bremen, Germany), and before the sample dry, 1 μL of matrix solution in THF was added and allowed to dry at room temperature, to allow matrix crystallization. External mass calibration was performed with a peptide calibration standard (PSCII) for the range 700-3000 (9 mass calibration points), 0.5 μL of the calibration solution and matrix previously mixed in an Eppendorf tube (1:2, v/v) were applied directly on the target and allowed to dry at room temperature. Mass spectra were recorded using an Autoflex III smartbeam1 MALDI-TOF-MS mass spectrometer Bruker Daltonik (Bremen, Germany) operating in the linear and reflectron positive ion mode. Ions were formed upon irradiation by a smartbeam1 laser using a frequency of 200 Hz. Each mass spectrum was produced by averaging 2500 laser shots collected across the whole sample spot surface by screening in the range m/z 400-8000. The laser irradiance was set to 35-40 % (relative scale 0-100) arbitrary units according to the corresponding threshold required for the applied matrix systems. The theoretical isotope distribution was obtained using the *Isotope Distribution Calculator* software.²⁵

5.3.3. Procedures

RAFT polymerization of VC was carried out in a 50 mL glass high-pressure tube equipped with a magnetic stir bar. In the kinetic studies each point represents a single experiment.

Typical procedure for the RAFT polymerization of VC in THF at 42 °C with $[\text{VC}]_0/[\text{CMPCD}]_0/[\text{Trigonox}]_0 = 250/1/0.2$

A 50 mL Ace Glass 8645#15 pressure tube, equipped with bushing and plunger valve, was charged with a mixture of CMPCD (64.8 mg, 0.291 mmol), Trigonox 187 W40 (25.4 mg) and THF (5.0 mL) (previously bubbled with nitrogen for about 5 min). The precondensed VC (5 mL, 73 mmol) was added to the tube. The exact amount of VC was determined gravimetrically. The tube was closed and degassed through the plunger valve by applying reduced pressure and filling the tube with N_2 about 20 times, submerged in liquid nitrogen. The valve was closed, and the tube reactor was

placed in a water bath at 42 ± 0.5 °C with stirring (700 rpm). After 24 h, the reaction was stopped by plunging the tube into ice water. The tube was slowly opened, the excess VC was evaporated inside a fume hood, and the mixture was precipitated into 250 mL of methanol. The polymer was separated by filtration and dried in a vacuum oven until constant weight to produce 2.514 g (49.7 %) of PVC, $M_n^{\text{GPC}} = 6000$, $\mathcal{D} = 1.43$.

Typical procedure for the chain extension experiment from CTA-terminated PVC

The PVC-CTA macroCTA (conv = 47%, $M_n^{\text{th}} = 3100$, $M_n^{\text{SEC}} = 3000$, $\mathcal{D} = 1.50$) was obtained following the previously described procedure. After precipitation in methanol, the polymer was dissolved in THF and reprecipitated in methanol. The polymer was dried under vacuum until constant weight. A 50 mL Ace Glass 8645#15 pressure tube, equipped with bushing and plunger valve, was charged with a mixture of purified PVC-CTA macroCTA (655.6 mg, 0.219 mmol), Trigonox 187 W40 (19.0 mg) and THF (7.5 mL) (previously bubbled with nitrogen for about 5 min). The precondensed VC (7.5 mL, 109 mmol) was added to the tube. The exact amount of VC was determined gravimetrically. The tube was closed and degassed through the plunger valve by applying reduced pressure and filling the tube with N₂ about 20 times, submerged in liquid nitrogen. The valve was closed, and the tube reactor was placed in a water bath at 42 ± 0.5 °C with stirring (700 rpm). After 24 h, the reaction was stopped by plunging the tube into ice water. The tube was slowly opened, the excess VC was evaporated inside a fume hood, and the mixture was precipitated into 250 mL of methanol. The polymer was separated by filtration and dried in a vacuum oven until constant weight to produce 4.220 g (47.5 %) of extended PVC, $M_n^{\text{GPC}} = 10700$, $\mathcal{D} = 1.42$.

Typical procedure for the synthesis of PVC-*b*-PVAc diblock copolymer by RAFT

The PVC-CTA macroCTA (conv = 47%, $M_n^{\text{th}} = 3100$, $M_n^{\text{SEC}} = 3000$, $\mathcal{D} = 1.50$) was obtained following the previously described procedure. After precipitation in methanol, the polymer was dissolved in THF and reprecipitated in methanol. The polymer was dried under vacuum until constant weight. A mixture of VAc (7.5 mL, 81.4 mmol), Trigonox 187 W40 (14.2 mg) and PVC-CTA macroCTA (508.6 mg, 0.163 mmol), previously

dissolved in THF (7.5 mL), was added to the Schlenk reactor. The reactor was deoxygenated by five freeze-pump-thaw cycles and filled with nitrogen. Then the reactor was placed in the oil bath at 42 °C under stirring (600 rpm). The reaction was stopped after 48h, and the mixture was analyzed by ¹H NMR spectroscopy to determine the VAc conversion (46.2%) and by GPC to determine the macromolecular characteristics of the resulting PVC-*b*-PVAc diblock copolymer ($M_n^{\text{GPC}} = 16600$ and $\mathcal{D} = 1.64$).

5.3.4. Computational Procedures

To assist in the selection of a suitable RAFT agent, standard *ab initio* molecular orbital theory and density functional theory calculations were carried out using Gaussian 09²⁶ and Molpro 2012.1.²⁷

This part of the work was developed in collaboration with Michelle L. Coote research group (Australian National University). Therefore, the complete computational procedures and results are presented in Appendix D.

5.4. Results and Discussion

5.4.1. RAFT Polymerizations of VC under Different Conditions

Having selected CMPCD as our RAFT agent, we then tested it experimentally. Since PVC is not soluble in its monomer, the RAFT polymerization was conducted in the presence of different solvents that dissolve both VC and PVC (THF, cyclohexanone and dichloromethane). Results of the RAFT polymerization of VC under different conditions, summarized in Table 5.1, suggest that the combination of Trigonox 187-W40 and THF is the most successful in providing fast, yet well-controlled RAFT polymerization of VC. No polymerization occurs in dichloromethane, while a polymer with high \mathcal{D} is formed in cyclohexanone (entries 1 and 2, Table 8.1).

Table 5.1. RAFT Polymerizations of VC with CMPCD as a RAFT Agent under Different Conditions.

Entry	$[VC]_0/[CMPCD]_0/[Trigonox]_0$	$[VC]_0/[Solvent]$ (v/v)	Temp. (°C)	Time (h) ^a	Conv. (%)	$M_{n,th} \times 10^{-3}$	$M_{n,GPC} \times 10^{-3}$	M_w/M_n
1	250/1/0.2	1/1 (dichloromethane)	42	24	0	-	-	-
2	250/1/0.2	1/1 (cyclohexanone)	42	24	36	6.0	3.5	1.88
	$[VC]_0/[CMPCD]_0/[Trigonox]_0$	$[VC]_0/[THF]$ (v/v)						
3	250/1/0.2	1/1	42	24	50	8.5	6.0	1.43
4	250/1/0.2	1/1	30	24	34	7.0	4.2	1.68
5	250/1/0.2	1/1	60	24	30	6.0	3.4	1.76
6	250/1/0.1	1/1	42	24	42	9.0	5.8	1.68
7	250/1/0.5	1/1	42	24	49	9.9	6.0	1.55
8	100/1/0.2	1/1	42	24	47	3.1	3.0	1.50
9	500/1/0.2	1/1	42	24	39	14.6	7.4	1.50
10	250/1/0.2	1/1	42	48	54	9.4	7.3	1.43
11	250/1/0.2	1/3	42	48	86	15.2	4.4	1.78
12	250/1/0.2	1/5	42	48	91	18.7	3.2	1.84
	$[VC]_0/[CMPCD]_0/[AIBN]_0$							
13	250/1/0.2	1/1	42	24	38	7.1	4.2	1.70
14	250/1/0.1	1/1	42	24	36	6.8	3.7	1.67
15	250/1/0.5	1/1	42	24	44	8.2	4.5	1.76

In order to find optimal conditions for a successful RAFT polymerization of VC, mediated by CMPCD as a chain transfer agent in THF solution, we have evaluated the effect of temperature, and VC/THF and VC/CMPCD ratios on the polymerization process (Table 5.1). Reactions at different temperatures (entries 3, 4 and 5, Table 5.1) were conducted under the following conditions: $[VC]_0/[CMPCD]_0/[Trigonox]_0 = 250/1/0.2$ and $[VC]_0/[THF] \text{ (v/v)} = 1/1$. Previous studies of SET-DTLRP of VC had shown that 42-43 °C is the maximum temperature of polymerization yielding PVC with minimized structural defects and well-defined chain-end functionalities.^{8,17} Under the conditions of the present study, the optimum temperature of RAFT polymerization of VC was found to be equal to 42 °C (50 % monomer conversion in 24 h). Only a limited monomer conversion was observed at 30 and 60 °C (34 % and 30 %, respectively); moreover, the obtained PVC exhibited a broad molecular weight distribution indicating possible loss of control over the polymerization. At lower temperatures radical initiation is expected to be significantly slower, while at higher temperatures the chain transfer to VC competes with a chain transfer via RAFT mechanism.

The molar ratio $[initiator]/[CTA]$ also has an important role in the control of the PVC molecular weight during the RAFT polymerization of VC. Results at 42 °C with different $[initiator]/[CTA]$ ratios given in Table 5.1 (entries 3, 6 and 7) indicate that the lowest \bar{D} could be achieved when $[initiator]/[CTA]$ is equal to 0.2/1.

The entries 3, 8 and 9 in Table 5.1 correspond to the results of RAFT polymerizations conducted at 42 °C with different $[monomer]_0/[CTA]_0$ ratios and constant $[initiator]/[CTA]$ ratio (equal to 0.2). As expected for RDRP systems, the molecular weight of the polymers increases with the $[monomer]_0/[CTA]_0$ value. Entries 10-12 in Table 5.1 reflect the effect of the $[VC]_0/[THF]$ ratio on the RAFT polymerization of VC. Obtained results show that the conversion increases with the increase in the amount of solvent used. At the same time, however, control over the polymerization diminishes, since the obtained molecular weights of PVC decrease (rather than increase as expected) and the \bar{D} values increase. Side reactions involving chain transfer from the growing macroradicals to the solvent are assumed to be responsible for this.

Finally, performance of two different initiators – AIBN (with $t_{1/2} = 1$ h at 82 °C)²⁸ and Trigonox 187-W40 (with $t_{1/2} = 1$ h at 39 °C)²⁸ – was evaluated as a free radical source during the VC polymerization (entries 3, 6, 7, 13, 14 and 15 in Table 5.1). According to our results, Trigonox 187-W40 provides slightly higher monomer conversion and better control (lower D values and M_n^{th} are closer to M_n^{GPC} in case of Trigonox). These results may be explained by the fact that cyanoisopropyl radicals (formed by AIBN thermal decomposition) add slower to the VC monomers and RAFT agents when compared to the isopropyl radicals resulting from Trigonox. Also, addition of cyanoisopropyl radicals to RAFT agent is a reversible process. On the other hand, isopropyl radical (formed from $(\text{CH}_3)_2\text{CH-C(O)-O-O-C(O)-CH}(\text{CH}_3)_2$) should add much faster to both RAFT agent and VC monomer. Addition of isopropyl radical to RAFT agent is irreversible. Thus, in case of Trigonox any induction period should be eliminated, polymerization is expected to be faster (higher M_n at given monomer conversion) and the initiation efficiency is higher.

5.4.2. Kinetic Study and Mechanistic Aspects of RAFT Polymerization of VC

Figures 5.2-5.4 show typical kinetic experiments for the RAFT polymerization of VC in solution. Remarkably, in all cases the $\ln([M]_0/[M])$ exhibit two linear dependencies on the polymerization time. Similar behavior was observed during SET-DTLRP of VC in water/THF mixtures.^{14,15,29} The linear dependencies of $\ln([M]_0/[M])$ vs time indicate constant concentration of growing radicals throughout the polymerization. The presence of two different linear regions, a phenomenon known as hybrid behavior, is most likely caused by the differences in the initiation and reinitiation rates (by the leaving $\bullet\text{CH}_2\text{CN}$ radical in the pre-equilibrium). In all experiments M_n^{GPC} agrees with M_n^{th} and D is decreasing with the monomer conversion.

RAFT polymerizations of VC for different targeted molecular weights or targeted number-average degree of polymerization (DP_n) of 100 (Figure 5.2) and 250 (Figure 5.3) were conducted. The results presented demonstrate that it is possible to prepare well-defined PVC with a range of molecular weights, suggesting that the RAFT polymerization of VC using CMPCD is quite robust. The comparison of the results present in Figure 5.3 and 5.4 confirm that the use of Trigonox 187-W40 as initiator

provides slightly higher monomer conversion and better control (lower D values and M_n^{th} are closer to M_n^{GPC}) than AIBN.

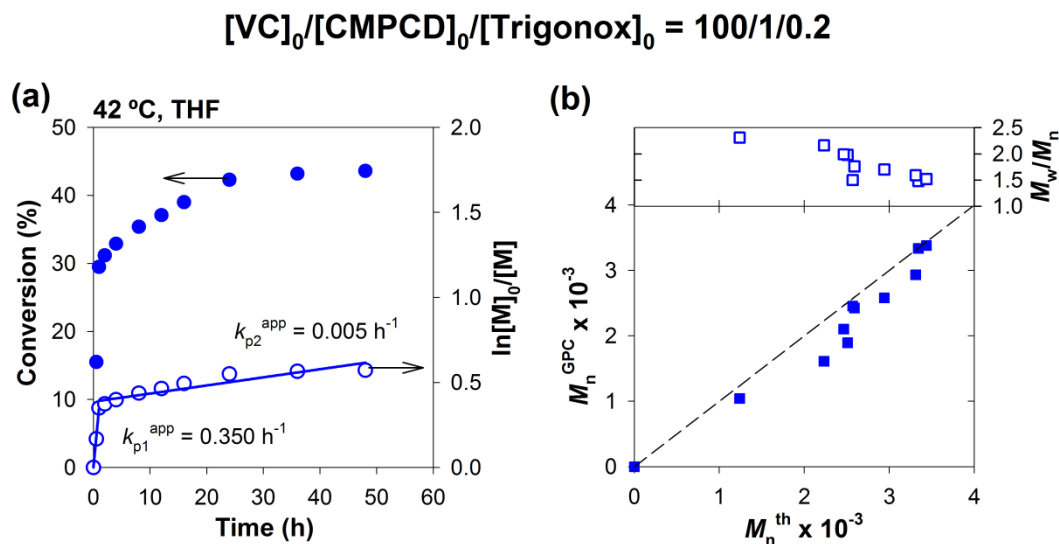


Figure 5.2. RAFT polymerization of VC in THF at 42 °C mediated by CMPCD using Trigonox 187-W40 as conventional initiator. (a) Conversion and $\ln[M]_0/[M]$ vs. time. (b) M_n^{GPC} and M_w/M_n vs. M_n^{th} . Reaction conditions: $[\text{VC}]_0/[\text{CMPCD}]_0/[\text{Trigonox}]_0 = 100/1/0.2$; $[\text{VC}]_0/[\text{THF}] = 1/1$ (v/v).

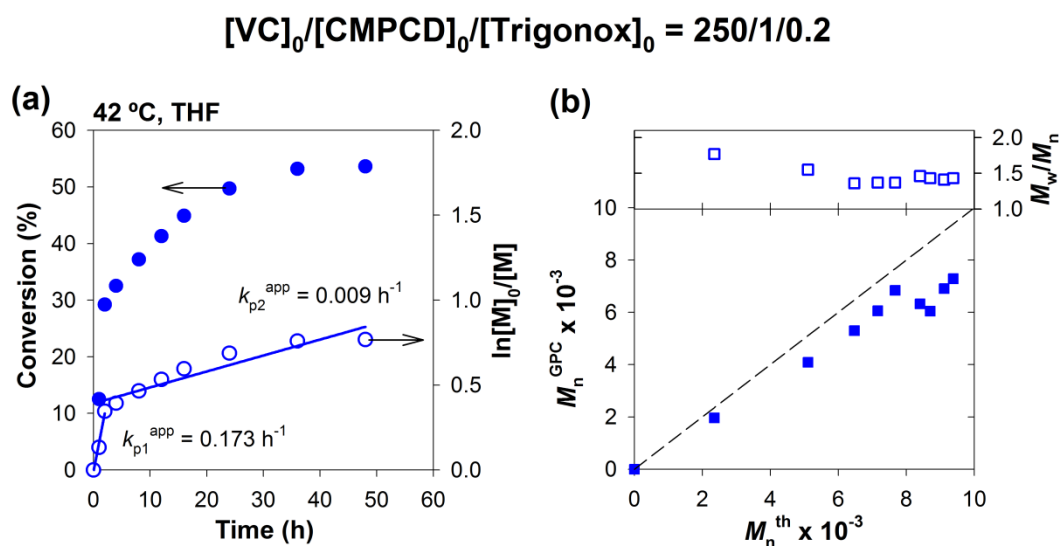


Figure 5.3. RAFT polymerization of VC in THF at 42 °C mediated by CMPCD using Trigonox 187-W40 as conventional initiator. (a) Conversion and $\ln[M]_0/[M]$ vs. time. (b) M_n^{GPC} and M_w/M_n vs. M_n^{th} . Reaction conditions: $[\text{VC}]_0/[\text{CMPCD}]_0/[\text{Trigonox}]_0 = 250/1/0.2$; $[\text{VC}]_0/[\text{THF}] = 1/1$ (v/v).

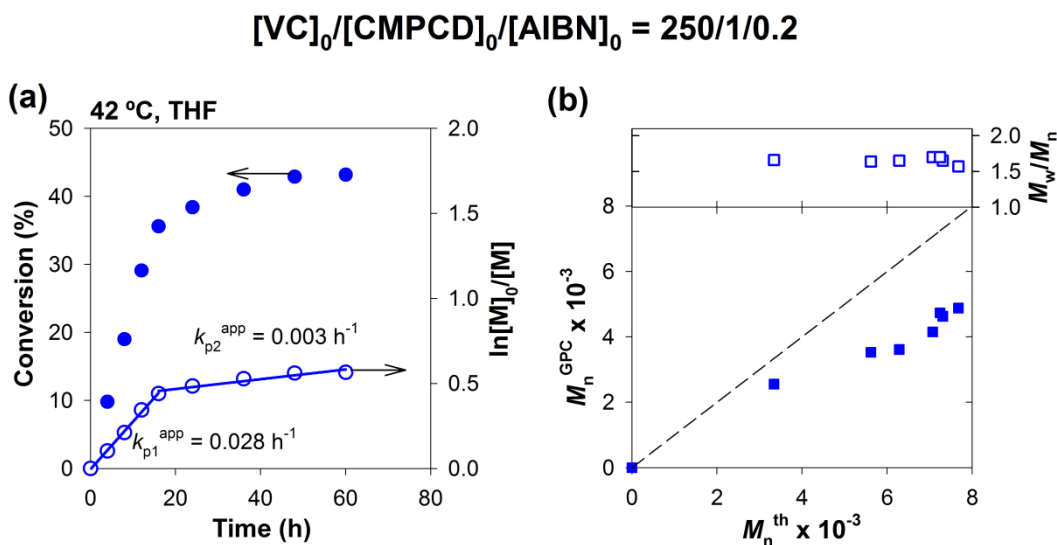
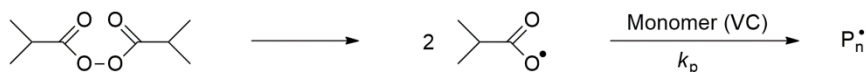


Figure 5.4. RAFT polymerization of VC in THF at 42 °C mediated by CMPCD using AIBN as conventional initiator. (a) Conversion and $\ln[M]_0/[M]$ vs. time. (b) M_n^{GPC} and M_w/M_n vs. M_n^{th} . Reaction conditions: $[\text{VC}]_0/[\text{CMPCD}]_0/[\text{AIBN}]_0 = 250/1/0.2$; $[\text{VC}]_0/[\text{THF}] = 1/1$ (v/v).

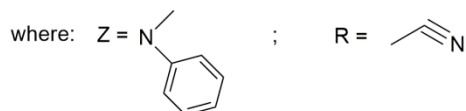
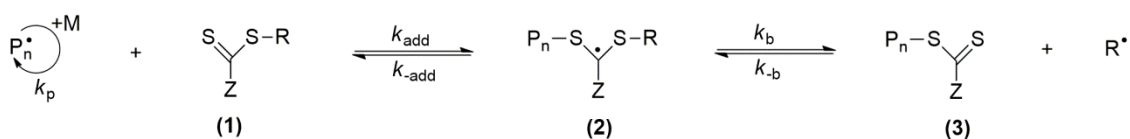
The mechanism of the RAFT polymerization of VC mediated by CMCD involves a series of reversible addition-fragmentation steps (Scheme 5.1). The adduct radical **2**, which fragments to a polymeric thiocarbonylthio compound **3** and a new radical R^\bullet is obtained by adding a propagating radical P_n^\bullet to the thiocarbonylthio compound **1**. Then the polymerization is reinitiated by the radical R^\bullet and gives a new propagating radical P_m^\bullet . Successive addition-fragmentation steps set up an equilibrium between the propagating radicals P_n^\bullet and P_m^\bullet and the dormant polymeric thiocarbonylthio compounds **3** and **5** via the intermediate radical **4**. A rising narrow molecular weight distribution (low D values) is obtained by the equilibrium of the growing chains. The majority of the polymer chains are end-functionalized throughout and till the end polymerization by a thiocarbonylthio group (dormant chains).

Scheme 5.1. Mechanism of the RAFT Polymerization of VC Mediated by CMPCD and Initiated by Trigonox 187-W40.

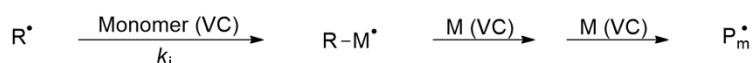
Initiation:



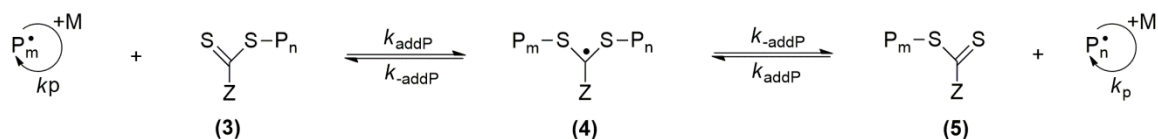
Reversible chain transfer / propagation:



Reinitiation:



Chain equilibration / propagation:



Termination:



5.4.3. Analysis of the PVC Structure

The chemical structure of the PVC synthesized by RAFT polymerization was determined with MALDI-TOF-MS and ^1H NMR techniques. In MALDI-TOF-MS experiments, two types of matrices, HABA and CHCA (Figure D.1 in Appendix D) were tested, but only the former gave a clearly resolved spectrum (Figures 5.5-5.7). The MALDI-TOF-MS of RAFT-PVC (Table 5.1, entry 8) in the linear mode with m/z ranging from 700 to 4000 is shown in Figure 5.5. Enlargement of the 1300-1500 range in the linear and reflectron

modes is shown in Figure 5.6. Importantly, two series of main peaks (for linear mode) are separated by an interval corresponding to a VC repeating unit (62.5 mass units). The highest main series is attributed to a polymer chain R-PVC-Z' (species **5**, Scheme 5.1) where R-Z' is the RAFT agent: R = -CH₂-CN and Z' = -S-C(S)-N(Me)Ph (1307.6 = 40.0 + 17 x 62.5 + 182.2 + 23, where 40.0, 62.5, 182.2 and 23 correspond to the molecular weight of R, VC, Z' and Na⁺, respectively). This particular structure was confirmed by comparing the results with a theoretical distribution shown in Figure 5.7. The enlarged spectrum (reflectron mode) from *m/z* 1300 to 1320 (*DP* = 17) shows that the isotope distribution of the polymer chain match the isotope distribution calculated for R-(PVC)₁₇-Z' + Na⁺ using *Isotope Distribution Calculator* software²⁵ (from *m/z* 925 to 945 or *DP* = 11, see Figure D.2 in Appendix D). Therefore, obtained RAFT-PVC has a well-defined structure (*i.e.*, without any detectable structural defects). The presence of possible structural defects would cause a deviation of *m/z* values and a different pattern of the isotope distribution. The series of less intensive peaks (Figure 5.6-i) cannot be ascribed to any chain-end structures expected from the RAFT polymerization. The presence of these peaks is probably due to the occurrence of the fragmentation of dithiocarbamate moieties during ionization in the MALDI-TOF-MS analysis, as reported by other authors.³⁰⁻³³

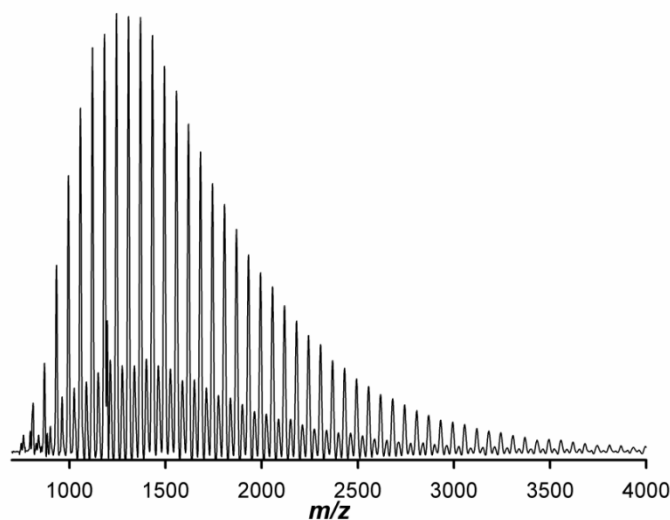


Figure 5.5. MALDI-TOF-MS in the linear mode of RAFT-PVC (Table 5.1, entry 8: $M_n^{\text{GPC}} = 3000$ g/mol, $D = 1.50$) mediated by CMPCD.

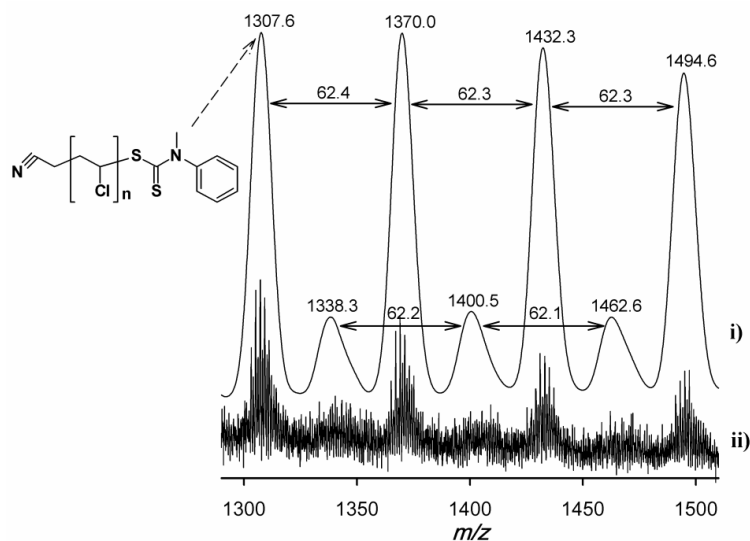


Figure 5.6. Enlargement of the MALDI-TOF-MS from m/z 1300 to 1500 of RAFT-PVC (Table 5.1, entry 8: $M_n^{\text{GPC}} = 3000$ g/mol, $D = 1.50$) mediated by CMPCD in the (i) linear and (ii) reflectron mode.

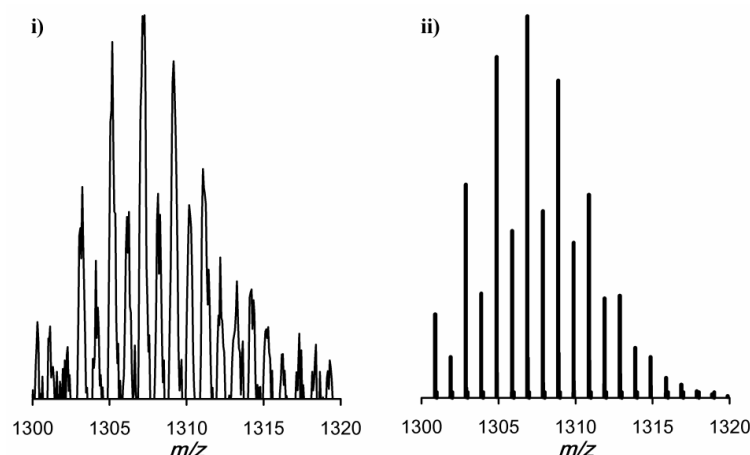


Figure 5.7. (i) Enlargement of the MALDI-TOF-MS in the reflectron mode of Figure 5.6 from m/z 1300 to 1320 and (ii) theoretical isotope distribution of the m/z 1300-1320 region ($DP = 17$, $C_{44}H_{61}Cl_{17}N_2S_2Na$) using *Isotope Distribution Calculator* software.

The ^1H NMR spectrum of the PVC sample (Table 5.1, entry 8) used in MALDI-TOF-MS analysis is shown in Figure 5.8. This spectrum confirms the main structure suggested based on the results of the MALDI-TOF-MS analysis. ^1H NMR spectra of the initiator (top) and the RAFT agent (in the middle) are also given in Figure 5.8. The spectrum of the RAFT-PVC reveals the resonances of the repeat unit $\text{CH}_2\text{-CHCl}$: **f** (1.9-2.7 ppm) and **g** (4.2-4.7 ppm), respectively. The terminal $\text{-CH}_2\text{-CHCl-S-}$ (**h** and **g'**) group resonates at

2.65 and ~ 4.7 ppm, respectively. The spectrum of the RAFT-PVC also reveals the resonances of the RAFT agent (**e**, **d**). Phenyl protons **e** resonate at 7.2-7.4 ppm and N-Me protons **d** signal at 3.75 ppm. The signal of NC-CH₂ group **c** is probably hidden in the resonance of the main chain methylene group **f** at 1.9-2.7 ppm. The initiator fragments (containing protons **a** and **b**) reveal no noticeable signals. Additionally, there is no significant amount of vinyl protons (resonances at 5.8 and 5.9 ppm are usual for free radical PVC),⁸ consistent with the vanishingly small concentrations of structural defects observed in PVC species obtained via SET-DTLRP process.^{8,17}

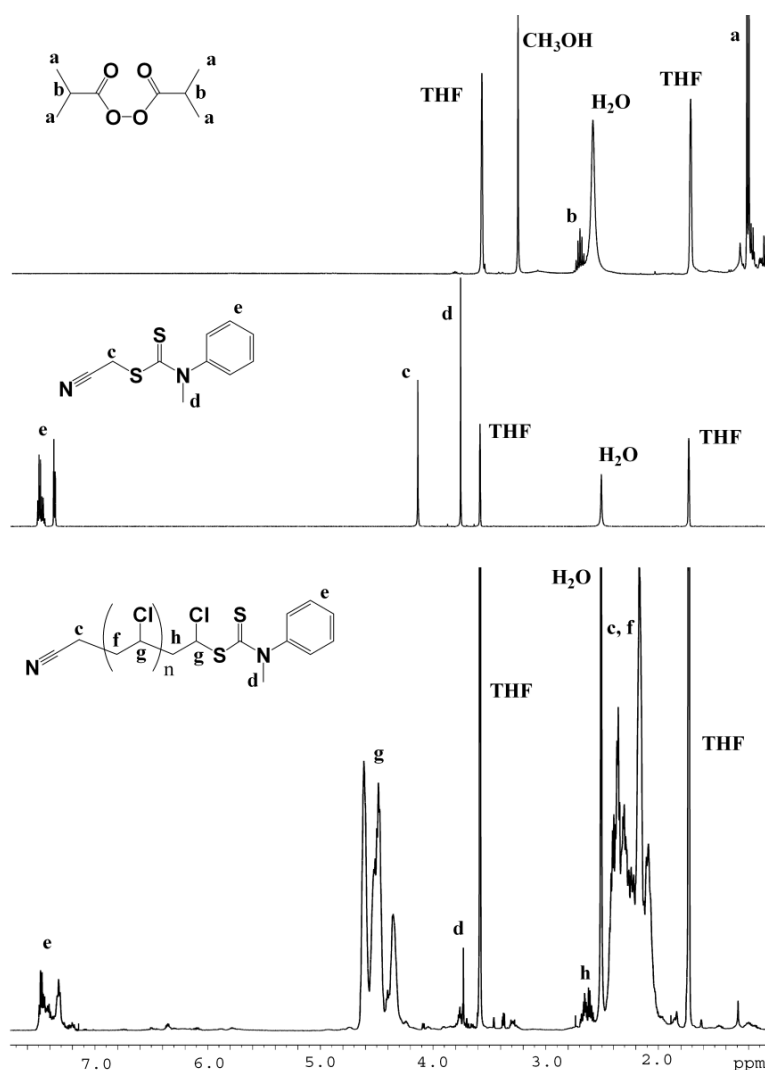


Figure 5.8. ¹H NMR spectra of Trigonox 187-W40 initiator (top), CMPCD RAFT agent (middle) and RAFT-PVC obtained (Table 5.1, entry 8: $M_n^{\text{GPC}} = 3000$ g/mol, $D = 1.50$) in *d*₈-THF.

5.4.4. Evaluation of the PVC Livingness

To prove the “living” nature of the RAFT-PVC, reinitiation experiments were performed. Figure 5.9 presents the GPC traces of PVC-CTA macroCTA (Table 5.1, entry 8), PVC extended and PVC-*b*-PVAc block copolymer. The results show the complete shift of the low molecular weight ($M_{n,\text{GPC}} = 3000$, $\mathcal{D} = 1.50$) GPC trace toward higher molecular weight PVC extended ($M_{n,\text{GPC}} = 10700$, $\mathcal{D} = 1.42$) and PVC-*b*-PVAc block copolymer ($M_{n,\text{GPC}} = 16600$, $\mathcal{D} = 1.64$). The structure of this block copolymer was confirmed by ^1H NMR (Figure 5.10). These results prove the “living” character of the PVC obtained via RAFT polymerization mediated by CMPCD and the possibility of using this method in the synthesis of block copolymers.

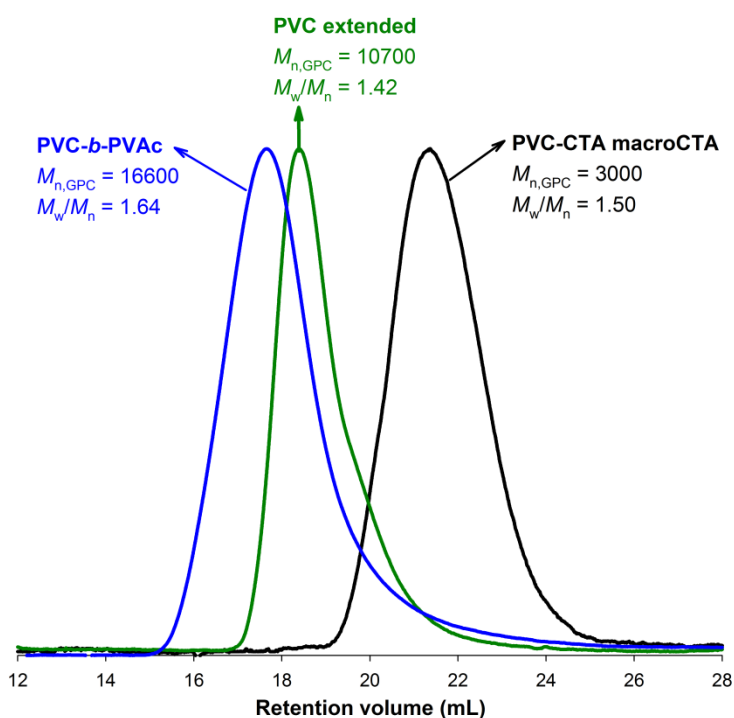


Figure 5.9. GPC traces of the PVC-CTA macroCTA before (black curve), after the chain extension experiment (green curve) and PVC-*b*-PVAc block copolymer (blue curve).

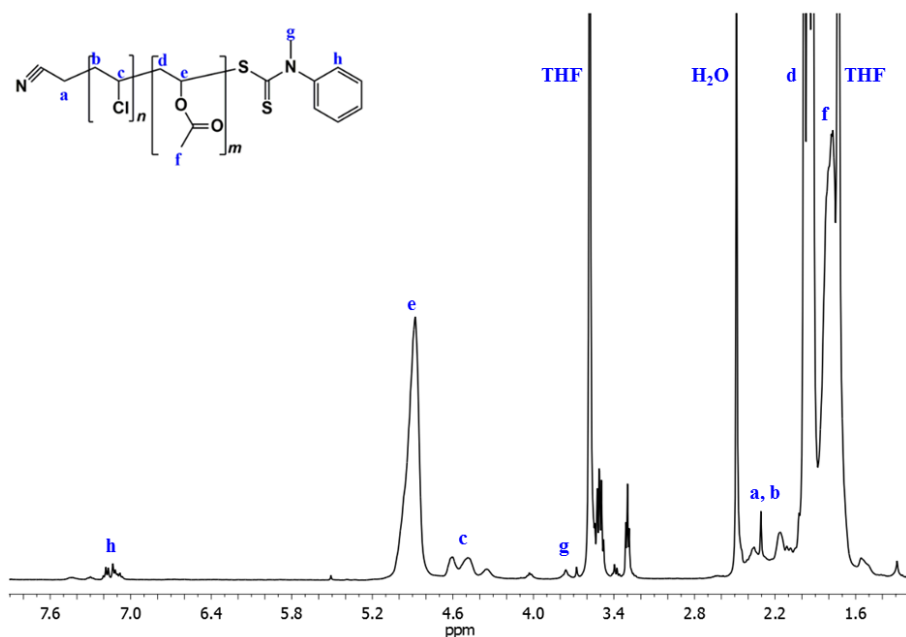


Figure 5.10. The ^1H NMR spectrum of the PVC-*b*-PVAc diblock copolymer ($M_n^{\text{GPC}} = 16600$; $\mathcal{D} = 1.64$) in $\text{THF-}d_6$.

5.5. Conclusions

To conclude, for the first time PVC with well-defined structure was successfully synthesized via RAFT polymerization using the RAFT agent cyanomethyl methyl(phenyl)carbamodithioate (CMPCD). Careful choice of reaction conditions (initiator type and concentration, solvent and concentration, temperature) is required to achieve low dispersities. The structural analysis performed via ^1H NMR and MALDI-TOF-MS experiments revealed that PVC chains had well preserved functional groups and no structural defects. The “living” nature of the PVC synthesized via RAFT polymerization method was confirmed by successful chain extension and PVC-based block copolymerization experiments. *Ab-initio* MO calculations confirmed the suitability of CMPCD as a good RAFT agent for VC polymerization. This work is of significant importance as it could open the door to various macromolecular architectures comprising PVC segments using RAFT and all its benefits compared to other RDRP methods.

5.6. References

1. Wang, J.-S. and Matyjaszewski, K., *Controlled/"living" radical polymerization. atom transfer radical polymerization in the presence of transition-metal complexes*. Journal of the American Chemical Society, **1995**, *117*, 5614-5615.
2. Matyjaszewski, K. and Xia, J., *Atom Transfer Radical Polymerization*. Chemical Reviews, **2001**, *101*, 2921-2990.
3. Georges, M. K., Veregin, R. P. N., Kazmaier, P. M., and Hamer, G. K., *Narrow molecular weight resins by a free-radical polymerization process*. Macromolecules, **1993**, *26*, 2987-2988.
4. Chiefari, J., Chong, Y. K., Ercole, F., Krstina, J., Jeffery, J., Le, T. P. T., Mayadunne, R. T. A., Meijs, G. F., Moad, C. L., Moad, G., Rizzardo, E., and Thang, S. H., *Living Free-Radical Polymerization by Reversible Addition-Fragmentation Chain Transfer: The RAFT Process*. Macromolecules, **1998**, *31*, 5559-5562.
5. Moad, G., Rizzardo, E., and Thang, S. H., *Toward living radical polymerization*. Accounts of Chemical Research, **2008**, *41*, 1133-1142.
6. Starnes, W. H., Jr., Zaikov, V. G., Chung, H. T., Wojciechowski, B. J., Tran, H. V., Saylor, K., and Benedikt, G. M., *Intramolecular Hydrogen Transfers in Vinyl Chloride Polymerization: Routes to Doubly Branched Structures and Internal Double Bonds*. Macromolecules, **1998**, *31*, 1508-1517.
7. Starnes, W. H., *Structural and mechanistic aspects of the thermal degradation of poly(vinyl chloride)*. Prog. Polym. Sci., **2002**, *27*, 2133-2170.
8. Percec, V., Popov, A. V., Ramirez-Castillo, E., Coelho, J. F. J., and Hinojosa-Falcon, L. A., *Non-transition metal-catalyzed living radical polymerization of vinyl chloride initiated with iodoform in water at 25°C*. J. Polym. Sci., Part A: Polym. Chem., **2004**, *42*, 6267-6282.
9. Starnes, W. H., Jr. and Ge, X., *Mechanism of autocatalysis in the thermal dehydrochlorination of poly(vinyl chloride)*. Macromolecules, **2004**, *37*, 352-359.
10. Starnes, W. H., Jr., *Structural defects in poly(vinyl chloride)*. J. Polym. Sci., Part A: Polym. Chem., **2005**, *43*, 2451-2467.
11. Percec, V., Guliashvili, T., Ladislav, J. S., Wistrand, A., Stjerndahl, A., Sienkowska, M. J., Monteiro, M. J., and Sahoo, S., *Ultrafast Synthesis of Ultrahigh Molar Mass Polymers by Metal-Catalyzed Living Radical Polymerization of Acrylates, Methacrylates, and Vinyl Chloride Mediated by SET at 25 °C*. J. Am. Chem. Soc., **2006**, *128*, 14156-14165.
12. Sienkowska, M. J., Rosen, B. M., and Percec, V., *SET-LRP of Vinyl Chloride Initiated with CHBr₃ in DMSO at 25 degrees C*. Journal of Polymer Science Part a-Polymer Chemistry, **2009**, *47*, 4130-4140.

13. Hatano, T., Rosen, B. M., and Percec, V., *SET-LRP of Vinyl Chloride Initiated with CHBr_3 and Catalyzed by $\text{Cu}(0)$ -Wire/TREN in DMSO at 25 degrees C*. Journal of Polymer Science Part a-Polymer Chemistry, **2010**, 48, 164-172.
14. Percec, V., Popov, A. V., Ramirez-Castillo, E., Monteiro, M., Barboiu, B., Weichold, O., Asandei, A. D., and Mitchell, C. M., *Aqueous Room Temperature Metal-Catalyzed Living Radical Polymerization of Vinyl Chloride*. J. Am. Chem. Soc., **2002**, 124, 4940-4941.
15. Percec, V., Popov, A. V., Ramirez-Castillo, E., and Weichold, O., *Living radical polymerization of vinyl chloride initiated with iodoform and catalyzed by nascent CuO /tris(2-aminoethyl)amine or polyethyleneimine in water at 25 °C proceeds by a new competing pathways mechanism*. J. Polym. Sci., Part A: Polym. Chem., **2003**, 41, 3283-3299.
16. Percec, V., Guliashvili, T., and Popov, A. V., *Ultrafast synthesis of poly(methyl acrylate) and poly(methyl acrylate)-*b*-poly(vinyl chloride)-*b*-poly(methyl acrylate) by the $\text{Cu}(0)$ /tris(2-dimethylaminoethyl)amine-catalyzed living radical polymerization and block copolymerization of methyl acrylate initiated with 1,1-chloroiodoethane and alpha,omega-di(iodo)poly(vinyl chloride) in dimethyl sulfoxide*. Journal of Polymer Science Part a-Polymer Chemistry, **2005**, 43, 1948-1954.
17. Percec, V., Popov, A. V., Ramirez-Castillo, E., Coelho, J. F. J., and Hinojosa-Falcon, L. A., *Phase transfer catalyzed single electron transfer-degenerative chain transfer mediated living radical polymerization (PTC-SET-DTLRP) of vinyl chloride catalyzed by sodium dithionite and initiated with iodoform in water at 43 °C*. J. Polym. Sci., Part A: Polym. Chem., **2005**, 43, 779-788.
18. Percec, V., Ramirez-Castillo, E., Popov, A. V., Hinojosa-Falcon, L. A., and Guliashvili, T., *Ultrafast single-electron-transfer/degenerative-chain-transfer mediated living radical polymerization of acrylates initiated with iodoform in water at room temperature and catalyzed by sodium dithionite*. J. Polym. Sci., Part A: Polym. Chem., **2005**, 43, 2178-2184.
19. Coelho, J. F. J., Carreira, M., Goncalves, P. M. O. F., Popov, A. V., and Gil, M. H., *Processability and characterization of poly(vinyl chloride)-*b*-poly(*n*-butyl acrylate)-*b*-poly(vinyl chloride) prepared by living radical polymerization of vinyl chloride. Comparison with a flexible commercial resin formulation prepared with PVC and dioctyl phthalate*. J. Vinyl Addit. Technol., **2006**, 12, 156-165.
20. Coelho, J. F. J., Mendonca, P. V., Popov, A. V., Percec, V., Goncalves, P. M. O. F., and Gil, M. H., *Synthesis of high glass transition temperature copolymers based on poly(vinyl chloride) via single electron transfer-Degenerative chain transfer mediated living radical polymerization (SET-DTLRP) of vinyl chloride in water*. J. Polym. Sci., Part A: Polym. Chem., **2009**, 47, 7021-7031.
21. Coelho, J. F. J., Fonseca, A. C., Gois, J. R., Goncalves, P. M. O. F., Popov, A. V., and Gil, M. H., *Scaling-up of poly(vinyl chloride) prepared by single electron transfer degenerative chain transfer mediated living radical polymerization in*

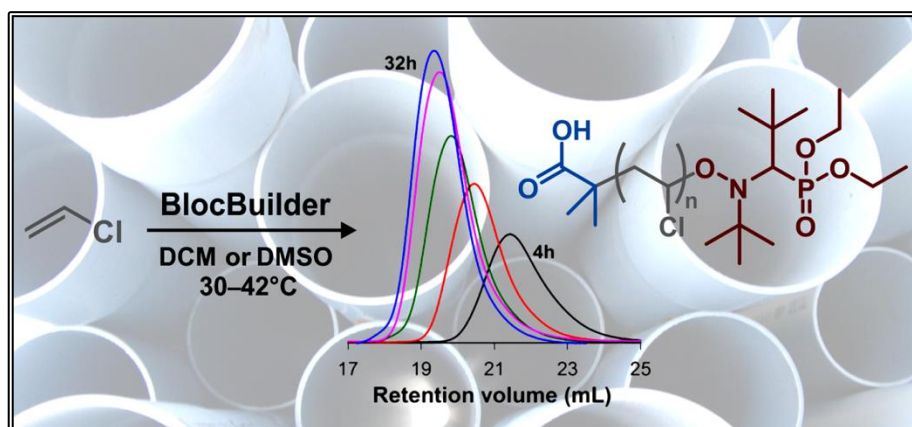
- water media: 1) *Low molecular weight. Kinetic analysis*. Chem. Eng. J., **2011**, 169, 399-413.
22. Coelho, J. F. J., Fonseca, A. C., Goncalves, P. M. F. O., Popov, A. V., and Gil, M. H., *Particle features and morphology of poly(vinyl chloride) prepared by living radical polymerisation in aqueous media. Insight about particle formation mechanism*. Polymer, **2011**, 52, 2998-3010.
 23. Coelho, J. F. J., Fonseca, A. C., Gonçalves, P. M. O. F., Popov, A. V., and Gil, M. H., *Scaling-up of poly(vinyl chloride) prepared by single electron transfer-degenerative chain transfer mediated living radical polymerization in water media—II: High molecular weight-ultra stable PVC*. Chemical Engineering Science, **2012**, 69, 122-128.
 24. Rosen, B. M. and Percec, V., *Single-Electron Transfer and Single-Electron Transfer Degenerative Chain Transfer Living Radical Polymerization*. Chem. Rev., **2009**, 109, 5069-5119.
 25. *IDCalc - Isotope Distribution Calculator*. Fev 10, 2012; Available from: <http://proteome.gs.washington.edu/software/IDCalc/>
 26. Frisch, M. J., Trucks, G. W., Schlegel, H. B., Scuseria, G. E., Robb, M. A., Cheeseman, J. R., Scalmani, G., Barone, V., Mennucci, B., Petersson, G. A., Nakatsuji, H., Caricato, M., Li, X., Hratchian, H. P., Izmaylov, A. F., Bloino, J., Zheng, G., Sonnenberg, J. L., Hada, M., Ehara, M., Toyota, K., Fukuda, R., Hasegawa, J., Ishida, M., Nakajima, T., Honda, Y., Kitao, O., Nakai, H., Vreven, T., Montgomery Jr., J. A., Peralta, J. E., Ogliaro, F., Bearpark, M., Heyd, J. J., Brothers, E., Kudin, K. N., Staroverov, V. N., Kobayashi, R., Normand, J., Raghavachari, K., Rendell, A., Burant, J. C., Iyengar, S. S., Tomasi, J., Cossi, M., Rega, N., Millam, N. J., Klene, M., Knox, J. E., Cross, J. B., Bakken, V., Adamo, C., Jaramillo, J., Gomperts, R., Stratmann, R. E., Yazyev, O., Austin, A. J., Cammi, R., Pomelli, C., Ochterski, J. W., Martin, R. L., Morokuma, K., Zakrzewski, V. G., Voth, G. A., Salvador, P., Dannenberg, J. J., Dapprich, S., Daniels, A. D., Farkas, Ö., Foresman, J. B., Ortiz, J. V., Cioslowski, J., and Fox, D. J. G., *Gaussian 09*. Gaussian 09, **2009**, Wallingford CT, USA: Gaussian, Inc.
 27. Werner, H.-J., Knowles, P. J., Knizia, G., Manby, F. R., Schütz, M., Celani, P., Korona, T., Lindh, R., Mitrushenkov, A., Rauhut, G., Shamasundar, K. R., Adler, T. B., Amos, R. D., Bernhardsson, A., Berning, A., Cooper, D. L., Deegan, M. J. O., Dobbyn, A. J., Eckert, F., Goll, E., Hampel, C., Hesselmann, A., Hetzer, G., Hrenar, T., Jansen, G., Köppl, C., Liu, Y., Lloyd, A. W., Mata, R. A., May, A. J., McNicholas, S. J., Meyer, W., Mura, M. E., Nicklass, A., O'Neill, D. P., Palmieri, P., Peng, D., Pflüger, K., Pitzer, R., Reiher, M., Shiozaki, T., Stoll, H., Stone, A. J., Tarroni, R., Thorsteinsson, T., and Wang, M., *MOLPRO, version 2012.1, a package of ab initio programs*, **2012**, see <http://www.molpro.net>.
 28. *Akzo Nobel: Initiators and Reactor Additives for Thermoplastics*. Fev 10, 2012; Available from: http://www.akzonobel.com/polymer/system/images/AkzoNobel_Initiators_and_R

factor_Additives_for_Thermoplastics_Low-res_protected_July%202010_tcm96-39468.pdf.

29. Percec, V., Popov, A. V., Ramirez-Castillo, E., and Weichold, O., *Acceleration of the single electron transfer-degenerative chain transfer mediated living radical polymerization (SET-DTLRP) of vinyl chloride in water at 25°C*. J. Polym. Sci., Part A: Polym. Chem., **2004**, 42, 6364-6374.
30. Beyou, E., Chaumont, P., Chauvin, F., Devaux, C., and Zydowicz, N., *Study of the Reaction between Nitroxide-Terminated Polymers and Thiuram Disulfides. Toward a Method of Functionalization of Polymers Prepared by Nitroxide Mediated Free "Living" Radical Polymerization*. Macromolecules, **1998**, 31, 6828-6835.
31. Schilli, C., Lanzendörfer, M. G., and Müller, A. H. E., *Benzyl and Cumyl Dithiocarbamates as Chain Transfer Agents in the RAFT Polymerization of N-Isopropylacrylamide. In Situ FT-NIR and MALDI-TOF MS Investigation*. Macromolecules, **2002**, 35, 6819-6827.
32. Pound, G., Aguesse, F., McLeary, J. B., Lange, R. F. M., and Klumperman, B., *Xanthate-Mediated Copolymerization of Vinyl Monomers for Amphiphilic and Double-Hydrophilic Block Copolymers with Poly(ethylene glycol)*. Macromolecules, **2007**, 40, 8861-8871.
33. Yan, Y. F., Zhang, W., Qiu, Y. S., Zhang, Z. B., Zhu, J. A., Cheng, Z. P., Zhang, W. D., and Zhu, X. L., *Universal Xanthate-Mediated Controlled Free Radical Polymerizations of the "Less Activated" Vinyl Monomers*. Journal of Polymer Science Part a-Polymer Chemistry, **2010**, 48, 5206-5214.

Chapter 6

Nitroxide-Mediated (co)Polymerization of Vinyl Chloride at Low Temperature



The contents of this chapter are published in:

Abreu, C. M. R., Mendonça, P. V., Serra, A. C., Noble, B. B., Guliashvili, T., Nicolas, J., Coote, M. L., and Coelho, J. F. J., *Nitroxide-Mediated Polymerization of Vinyl Chloride at Low Temperature: Kinetic and Computational Studies*. *Macromolecules*, **2016**, *49*, 490-498.

6.1. Abstract

The synthesis of poly(vinyl chloride) (PVC) by nitroxide-mediated polymerization (NMP) using the SG1-based BlocBuilder alkoxyamine at low temperature (30 and 42 °C) is reported. The reaction system was studied regarding the nature of the solvent, the monomer-to-solvent ratio, the polymerization temperature and the target molecular weight. First order kinetics and linear evolutions of the molecular weight with vinyl chloride (VC) conversion were obtained in dichloromethane (DCM) and dimethyl sulfoxide (DMSO) together with decreasing dispersities (\bar{M}_w/\bar{M}_n) down to 1.59-1.47. The resulting PVC was fully characterized by ^1H nuclear magnetic resonance spectroscopy (^1H NMR), ^{31}P NMR and size exclusion chromatography (SEC). The ^1H NMR and ^{31}P NMR revealed the existence of very small content of structural defects and the presence of chain-end functional groups (~91% SG1 chain-end functionality). Chain extension experiments were performed with VC, methyl methacrylate (MMA) and a mixture of monomers (90% of MMA and 10% of styrene (S)) and confirmed the “livingness” of the PVC-SG1 macroinitiators, giving access to different PVC-based block copolymers. High level *ab initio* molecular orbital calculations suggested that the C-O bond in the PVC-SG1 alkoxyamine is too strong to mediate the NMP of VC by simple “classic” activation-deactivation equilibrium and is possibly being mediated by a SG1-mediated dehydrochlorination mechanism. The results presented in this study established a new route to afford a wide range of new complex macrostructures based on PVC segments.

6.2. Introduction

In the past two decades, reversible deactivation radical polymerization (RDRP) methods have revolutionized the field of polymer synthesis. These approaches enable the facile design of polymers with a stringent control over their structures, their functionalities and their architectures using radical-based mechanisms.¹⁻⁶ Among the different RDRP methods, atom transfer radical polymerization (ATRP),^{1,2,7,8} reversible addition-fragmentation chain transfer (RAFT)^{3-5,9} polymerization, and nitroxide-mediated polymerization (NMP)^{6,10} remain the most popular. Nowadays, it is possible to control the polymerization of a very broad range of monomer families (e.g., styrenics, acrylates,

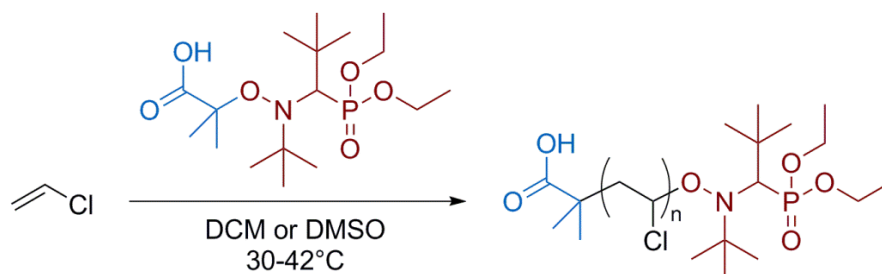
methacrylates, 1,3-dienes, etc.) using RDRP methods with certain ease and under rather mild experimental conditions. An immense part of the research effort has been focused on the development of more efficient control agents,^{5,6} more active catalysts,^{11,12} and more environmentally friendly polymerization reactions¹³ (e.g., green solvents,¹⁴⁻¹⁷ mild reaction temperatures,^{18,19} etc.). Despite all these achievements, RDRP of nonactivated monomers (e.g., vinyl acetate, VC, *N*-vinylpyrrolidone) remains enormously challenging. Poly(vinyl chloride) (PVC) is one of the highest volume polymers (~39.3 million tons in 2013)²⁰ and can only be prepared on an industrial scale by free-radical polymerization (FRP).²¹ Several features of VC make its control by RDRP methods particularly challenging, such as: (i) a very high reactivity ($k_{p,VC} = 11 \times 10^3 \text{ L mol}^{-1}\text{s}^{-1}$ (at 50 °C); $k_{p,MMA} = 0.51 \times 10^3 \text{ L mol}^{-1}\text{s}^{-1}$ (at 60 °C));²² (ii) an unusually high chain transfer constant to the monomer ($C_{M,VC} = (10.8-16) \times 10^{-4}$;²³ $C_{M,MMA} = (0.07-0.25) \times 10^{-4}$, values at 60 °C),²⁴ and (iii) the nonsolubility of PVC in its monomer as well as in most common organic solvents.²⁵

Some attempts to produce PVC by RDRP methods have been reported, namely by single electron transfer living radical polymerization (SET-LRP),²⁶⁻²⁸ single electron transfer degenerative chain transfer living radical polymerization (SET-DTLRP),^{25,29-39} cobalt-mediated radical polymerization (CMRP),^{40,41} supplemental activator and reducing agent (SARA) ATRP,^{17,19} and RAFT.²¹ However, the study of other RDRP techniques facilitates a deeper understanding of VC polymerization and broadening the number of PVC-based macromolecular structures could have valuable synthetic utility. NMP is particularly appealing for VC polymerization because of the simplicity of this protocol (an alkoxyamine, a 2-in-1 molecule, releases both the initiator and the control agent upon heating), the robustness of the process, the broad range of monomers that can be polymerized by this method, and the absence of residual catalysts, color, or toxic moieties.⁶

Braun and co-workers^{42,43} investigated the nitroxide-mediated suspension polymerization of VC at 70 °C using various nitroxides including 2,2,6,6-tetramethylpiperidin-1-yloxy (TEMPO) and di-*tert*-butyl nitroxide (DBN), and reported low polymerization rates and high D values ~ 2 . Additionally, no information regarding the structural characteristics of the resulting PVC was provided. This information would be of particular relevance

regarding the impact of temperature on the formation of structural defects that result from various unavoidable side reactions.^{25,44,45} Importantly, the presence of these unwanted structures has been shown to be the major cause for the low thermal stability of PVC.⁴⁶

In this context, here it is reported for the first time the NMP of VC using the commercially available SG1-based alkoxyamine, BlocBuilder, earlier termed MAMA-SG1 (Scheme 6.1).^{6,47,48} BlocBuilder has one of the highest dissociation rate constants ($k_d = 0.34 \text{ s}^{-1}$ at $120 \text{ }^\circ\text{C}$)⁴⁹ among commercially available alkoxyamines making it attractive for the polymerization of monomers such as VC with less stabilized propagating radicals. Moreover, considering the high occurrence of side reactions (e.g., chain transfer to monomer) at elevated temperatures ($> 60 \text{ }^\circ\text{C}$) for the polymerization of VC, here it has been chosen to conduct NMP of VC at $42 \text{ }^\circ\text{C}$, as a known standard temperature for VC RDRP.^{21,25} Another advantage of using the BlocBuilder alkoxyamine relies on the presence of a carboxylic acid group attached to the initiating moiety, which provides a convenient route for further PVC modifications to afford complex macrostructures using well-known coupling protocols.^{6,50}



Scheme 6.1. General Scheme and Conditions for the NMP of VC Initiated by the SG1-based BlocBuilder Alkoxyamine.

6.3. Experimental Section

6.3.1. Materials

VC (99.9%) was kindly supplied by CIRES Lda, Portugal. MMA (99% stabilized; Acros) and S (99%; Sigma-Aldrich) were passed over a basic alumina column before use to

remove the radical inhibitors. The BlocBuilder alkoxyamine (99%, recrystallized before use) and the SG1 nitroxide (85%) were kindly supplied by Arkema. Dichloromethane (DCM) (Fluka, HPLC grade), DMF (Sigma-Aldrich, 99.8%), DMSO (Acros, 99.8% extra pure), THF (Panreac, HPLC grade), cyclohexanone (Sigma-Aldrich, 99.8%), were distilled before use. Deuterated tetrahydrofuran (d_8 -THF) (Euriso-top, 99.5%), sulfolane (99%; Acros), 1-butyl-3-methylimidazolium hexafluorophosphate (BMIM-PF₆, > 98%; TCI - Tokyo Chemical Industry Co. LTD), methanol (Labsolve, 99.5%), and polystyrene (PS) standards (Polymer Laboratories) were used as received.

6.3.2. Techniques

The 600 MHz ¹H-NMR spectra of samples were recorded on a Varian VNMRS 600 MHz spectrometer, with a 3 mm PFG triple resonance indirect detection probe, in d_8 -THF with tetramethylsilane (TMS) as an internal standard.

³¹P-NMR spectra of samples were recorded on a Bruker Avance III 400 MHz spectrometer, with a 5 mm TIX triple resonance detection probe, in d_8 -THF with diethylphosphite (DEP) as an internal standard.

The chromatographic parameters of the samples were determined using a size exclusion chromatography set-up from Viscotek (Viscotek TDAmix) equipped with a differential viscometer (DV) and right-angle laser-light scattering (RALLS, Viscotek), low-angle laser-light scattering (LALLS, Viscotek) and refractive index (RI) detectors. The column set consisted of a PL 10 mm guard column (50 × 7.5 mm²) followed by one Viscotek T2000 column (6 μm), one MIXED-E PLgel column (3 μm) and one MIXED-C PLgel column (5 μm). A dual piston pump was set with a flow rate of 1 mL/min. The eluent (THF) was previously filtered through a 0.2 μm filter. The system was also equipped with an online degasser. The tests were done at 30 °C using an Elder CH-150 heater. Before the injection (100 μL), the samples were filtered through a polytetrafluoroethylene (PTFE) membrane with 0.2 μm pore. The system was calibrated with narrow PS standards. The dn/dc value was determined as 0.105 for PVC. Molecular weight (M_n^{SEC}) and dispersity ($\mathcal{D} = M_w/M_n$) of synthesized polymers were determined by triple detection calibration using the OmniSEC software version: 4.6.1.354.

6.3.3. Procedures

NMP of VC was carried out in a 50 mL glass high-pressure tube equipped with a magnetic stir bar. In the kinetic studies each point represents a single experiment.

Typical procedure for the NMP of VC in DCM at 42 °C with [VC]₀/[BlocBuilder]₀= 250/1

A 50 mL Ace Glass 8645#15 pressure tube, equipped with a bushing and a plunger valve, was charged with a mixture of BlocBuilder alkoxyamine (111 mg, 0.29 mmol) and DCM (5.0 mL) (previously bubbled with nitrogen for 5 min). The precondensed VC (5 mL, 73 mmol) was added to the tube. The exact amount of VC was determined gravimetrically. The tube was sealed, submerged in liquid nitrogen, and degassed through the plunger valve by applying reduced pressure and filling the tube with nitrogen about 20 times. The valve was closed, and the tube reactor was placed in a water bath at 42 ± 0.5 °C under stirring (700 rpm). After 24 h, the reaction was stopped by plunging the tube into ice water. The tube was slowly opened, the excess VC was evaporated inside a fume hood, and the mixture was precipitated into 250 mL of methanol. The polymer was separated by filtration and dried in a vacuum oven until constant weight, yielding 2.58 g (56.6%) of PVC ($M_n^{SEC} = 10800$, $D = 1.49$).

Typical procedure for the “one-pot” chain extension experiment from SG1-terminated PVC

A 50-mL Ace Glass 8645#15 pressure tube, equipped with a bushing and a plunger valve, was charged with a mixture of BlocBuilder alkoxyamine (167 mg; 0.44 mmol) and DCM (3.0 mL) (previously bubbled with nitrogen for 5 min). The precondensed VC (3.0 mL, 43.7 mmol) was added to the tube. The exact amount of VC was determined gravimetrically. The tube was sealed, submerged in liquid nitrogen, and degassed through the plunger valve by applying reduced pressure and filling the tube with nitrogen about 20 times. The valve was closed, and the tube reactor was placed in a water bath at 42 °C under stirring (700 rpm). After 7 h, the reaction was stopped by plunging the tube into ice water. The tube was slowly opened, and the excess VC was evaporated inside a fume hood. The monomer conversion (conv) were determined gravimetrically (49.1%), and the

$M_n^{\text{SEC}} = 6000$ and $\mathcal{D} = 1.60$ were determined by SEC. DCM (14.0 mL) (previously bubbled with nitrogen for 5 min) and the precondensed VC (14.0 mL, 204 mmol) were added in the medium without any purification of the previously obtained PVC-SG1 macroinitiator. The tube was sealed, submerged in liquid nitrogen, and degassed through the plunger valve by applying reduced pressure and filling the tube with nitrogen about 20 times. The valve was closed, and the tube reactor was placed in a water bath at 42 °C under stirring (700 rpm). The reaction was stopped after 48 h by plunging the tube into ice water. The tube was slowly opened, and the excess VC was evaporated inside a fume hood. The monomer conversion were determined gravimetrically (44.1%), and the $M_n^{\text{SEC}} = 20600$ and $\mathcal{D} = 1.59$ of the resulting PVC-*b*-PVC diblock copolymer were determined by SEC.

Typical procedure for the synthesis of PVC-*b*-PMMA diblock copolymer by NMP

The PVC-SG1 macroinitiator (conv = 66%, $M_n^{\text{th}} = 5000$, $M_n^{\text{SEC}} = 6600$, $\mathcal{D} = 1.56$) was obtained following the previously described procedure. After precipitation in methanol, the polymer was dissolved in THF and reprecipitated in methanol. The polymer was dried under vacuum until constant weight. A mixture of MMA (5.0 mL, 46.9 mmol) and PVC-SG1 macroinitiator ($M_n^{\text{SEC}} = 6600$, $\mathcal{D} = 1.56$, 310 mg, 0.047 mmol), previously dissolved in DMSO (5.0 mL), was added to the Schlenk reactor. The reactor was deoxygenated by five freeze-pump-thaw cycles and filled with nitrogen. Then the reactor was placed in the oil bath at 100 °C under stirring (600 rpm). The reaction was stopped after 54h, and the mixture was analyzed by ^1H NMR spectroscopy to determine the MMA conversion (45.5%) and by SEC to determine the macromolecular characteristics of the resulting PVC-*b*-PMMA diblock copolymer ($M_n^{\text{SEC}} = 44700$ and $\mathcal{D} = 1.89$).

Typical procedure for the synthesis of PVC-*b*-P(MMA-*co*-S) copolymer by NMP

The PVC-SG1 macroinitiator (conv = 66%, $M_n^{\text{th}} = 5000$, $M_n^{\text{SEC}} = 6600$, $\mathcal{D} = 1.56$) was obtained following the previously described procedure. After precipitation in methanol, the polymer was dissolved in THF and reprecipitated in methanol. The polymer was dried under vacuum until constant weight. A mixture of MMA (5.0 mL, 46.9 mmol), S (0.52 mL, 4.5 mmol), and PVC-SG1 macroinitiator ($M_n^{\text{SEC}} = 6000$, $\mathcal{D} = 1.60$, 451 mg, 0.075 mmol), previously dissolved in DMF (5.52 mL), was added to the Schlenk reactor. The

reactor was deoxygenated by five freeze-pump-thaw cycles and filled with nitrogen. Then the reactor was placed in the oil bath at 100 °C under stirring (600 rpm). The reaction was stopped after 44h, and the mixture was analyzed by ¹H NMR spectroscopy to determine the MMA (34.5 %) and S (36.8 %) conversions and by SEC to determine the macromolecular characteristics of the resulting PVC-*b*-P(MMA-*co*-S) copolymer ($M_n^{\text{SEC}} = 36400$ and $\bar{D} = 1.78$).

6.3.4. Computational Procedures

In this work it was used the high-level composite *ab initio* G3(MP2)-RAD method⁵¹ in conjunction with an ONIOM inspired approximation and M06-2X thermochemistry⁵² to obtain accurate gas-phase energies. The SMD continuum solvation method⁵³ was used to model implicit solvent effects, with dichloromethane, toluene and methyl propanoate used as solvents for the vinyl chloride, styrene and methyl methacrylate systems, respectively. Similar methodology has been previously shown to predict accurate values for the thermodynamics (and kinetics) of a wide range of radical reactions, including alkoxyamine bond disassociation energies.⁵⁴⁻⁵⁷ All standard *ab initio* molecular orbital theory and density functional theory calculations were performed using Gaussian 09⁵⁸ and Molpro 2012^{59,60} software packages.

This part of the work was developed in collaboration with Michelle L. Coote research group (Australian National University). Therefore, the complete computational procedures and results are presented in Appendix E.

6.4. Results and Discussion

6.4.1. Influence of the Solvent

In this work, the controlling ability of the BlocBuilder alkoxyamine was investigated for the polymerization of VC. Using an alkoxyamine avoids the use of an additional conventional radical initiator since both an initiating radical and a nitroxide are released at

elevated temperature. Additionally, this alkoxyamine exhibits a high dissociation rate constant ($k_d = 0.34 \text{ s}^{-1}$ at $120 \text{ }^\circ\text{C}$),⁴⁹ thus enabling NMP to proceed at low temperature, unlike many other alkoxyamines.

The first study was focused on the influence of the solvent over the polymerization. Different solvents and solvent mixtures were selected based on the solubility of PVC and further investigated for the NMP of VC initiated by BlocBuilder alkoxyamine at $42 \text{ }^\circ\text{C}$ (Table 6.1). Results showed that the BlocBuilder alkoxyamine was able to significantly improve the NMP of VC compared to early attempts by producing PVC with dispersities far below 2. This was effective in a wide range of solvents which demonstrates the versatility of the NMP system used. In particular, best results were obtained in cyclohexanone (Table 6.1, entry 4), DMSO (Table 6.1, entries 5 and 6) and especially in DCM for which $D = 1.49$ (Table 6.1, entry 8).

Table 6.1. Conversion and Macromolecular Characteristics Obtained for the NMP of VC Using Different Solvents at $42 \text{ }^\circ\text{C}$ after 24 h.

Entry ^a	Solvent	Conv. (%)	$M_{n,th} \times 10^{-3}$	$M_{n,SEC} \times 10^{-3}$	M_w/M_n
1	THF	30	5.5	5.9	1.72
2	DMF	22	5.3	5.9	1.73
3	Sulfolane/DMSO = 80/20 (v/v)	29	5.8	6.1	1.78
4	Cyclohexanone	39	7.4	7.7	1.59
5	DMSO	14	3.5	3.8	1.47
6 ^b	DMSO	22	5.3	5.8	1.58
7	BMIM-PF ₆ /DMSO = 50/50 (v/v)	32	7.0	8.8	1.59
8	DCM	57	10.7	10.8	1.49
9 ^c	DCM	29	5.3	9.7	1.56

^aReaction conditions: $[\text{VC}]_0/[\text{BlocBuilder}]_0 = 250$; $[\text{VC}]_0/[\text{solvent}] = 1/1$ (v/v).

^bPolymerization time (t_{rx}) = 48 h.

^cUsing additional SG1 free: $[\text{SG1}]_0/[\text{BlocBuilder}]_0 = 0.1$.

In an attempt to accelerate the VC polymerization, the use of [BMIM-PF₆]/DMSO = 50/50 (v/v) was examined. This confirmed the synergetic effect observed in SARA ATRP,⁶¹ since the final conversion (conv.) was much higher than in pure DMSO. THF, DMF and sulfolane/DMSO = 80/20 (v/v) (20% of DMSO was added to the sulfolane to allow the solubilization of BlocBuilder in the mixture) appeared less adequate solvents since D values ranged from 1.72 to 1.78 (Table 6.1, entries 1–3). Nevertheless, there was

in all cases a good agreement between the theoretical and experimental molecular weights, which suggested good control over the PVC structure. The addition of 10% of free SG1 (Table 6.1, entry 9) significantly reduced the final conversion but had no beneficial effect on the \bar{D} .

Based on these results, DCM was chosen as the optimal solvent for a comprehensive kinetic study of the NMP of VC. After about 30 h, a rather high VC conversion was obtained (~60%). This resulted in a first-order kinetics (Figure 6.1-a), suggesting a constant concentration of growing radicals during the polymerization. This is in sharp contrast to the two linear dependencies of $\ln[M]_0/[M]$ vs. time plots which were observed in the polymerization of VC by both SET-DTLRP²⁹⁻³¹ and RAFT²¹ but is in accordance with the SARA-ATRP method.¹⁹ Additionally, the SG1-mediated NMP of VC initiated by the BlocBuilder alkoxyamine in DCM enabled higher final monomer conversion (60%) to be reached than that obtained with the RAFT system (50%) previously reported.²¹ NMP of VC was also rather well-controlled as shown by the decrease of the \bar{D} values during the reaction as well as by the good agreement between experimental and theoretical molecular weight values (Figure 6.1-b). Finally, SEC chromatograms of PVC samples obtained at different times of reaction showed unimodal distributions with no visible sign of accumulation of dead polymer chains and significant shifts toward higher molecular weights (Figure 6.1-c).

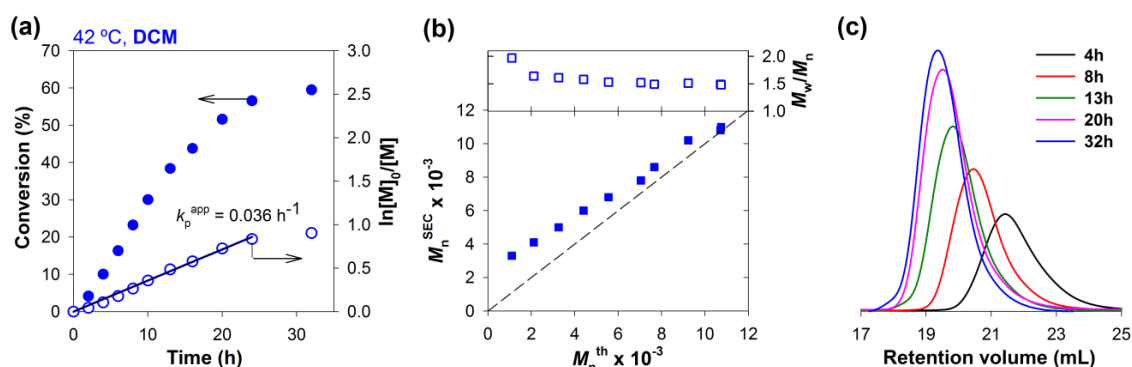


Figure 6.1. NMP of VC in DCM at 42 °C initiated by the SG1-based BlocBuilder alkoxyamine. (a) Conversion and $\ln[M]_0/[M]$ vs. time. (b) Number-average molecular weight (M_n^{SEC}) and dispersity (M_w/M_n) vs. theoretical number-average molecular weight (M_n^{th}). (c) Evolution of the SEC traces during the polymerization. Reaction conditions: $[VC]_0/[BlocBuilder]_0 = 250/1$; $[VC]_0/[solvent] = 1/1$ (v/v).

6.4.2. Influence of the Monomer Concentration

In solution NMP, the initial concentration of monomer (which also corresponds to the monomer-to-solvent ratio) may strongly influence the polymerization rate and may also sometimes impact the quality of control.^{14,62} Three different monomer-to-solvent ratios (1/2, 1/1 and 2/1) were investigated for the NMP of VC in DCM at 42 °C initiated by the BlocBuilder alkoxyamine (Table 6.2, entries 1-3).

Table 6.2. Conversion and Macromolecular Characteristics Obtained for the NMP of VC in DCM at 42 °C after 24 h.

Entry ^a	[VC] ₀ /[DCM] (v/v)	Conv. (%)	$M_{n,th} \times 10^{-3}$	$M_{n,SEC} \times 10^{-3}$	M_w/M_n
1	1/2	39	7.6	8.5	1.58
2	1/1	57	10.7	10.8	1.49
3	2/1	45	7.8	11.4	1.56

^aReaction conditions: [VC]₀/[BlocBuilder]₀ = 250/1.

Overall, the results showed no general trend regarding the influence of the initial concentration of VC. As expected, the rate of reaction increased with the initial concentration of VC (Table 6.2, entries 1–2), as higher monomer conversion was achieved for the same reaction time (i.e., 24 h). However, for the highest monomer concentration studied (i.e., [VC]₀/[DCM] = 2/1) there was an apparent decrease on the rate of polymerization, as judged by the lower monomer conversion obtained for the more diluted reaction medium (Table 6.2, entries 2–3). This might be related to the poor solubility of the VC in the growing PVC, which can cause diffusional problems during the polymerization and limit monomer conversion.

6.4.3. Influence of Polymerization Temperature

The polymerization temperature is an important parameter to consider when optimizing RDRP systems. Temperature is particularly crucial for standard NMP, as the activation/deactivation equilibrium of the initiating and propagating species are solely

governed by temperature. Also, in the case of PVC, high temperatures can contribute to the appearance of structural defects in the polymeric structure.^{25,33} NMP of VC was evaluated in the range of 30–60 °C (Table 6.3).

Table 6.3. Conversion and Macromolecular Characteristics Obtained for the NMP of VC in DCM at Different Temperatures after 24 h.

Entry ^a	T (° C)	Conv. (%)	$M_{n,th} \times 10^{-3}$	$M_{n,SEC} \times 10^{-3}$	M_w/M_n
1	30	40	7.1	7.7	1.53
2	42	57	10.7	10.8	1.49
3	60	37	6.7	6.1	1.68

^aReaction conditions: $[VC]_0/[BlocBuilder]_0 = 250/1$.

The results showed that NMP of VC can proceed successfully at near room temperature ($T = 30^\circ\text{C}$) with no detrimental effect on the control of PVC compared to the same experiment performed at 42 °C ($\bar{D} \approx 1.50$, Table 6.3, entries 1 and 2). However, when the temperature was increased up to 60 °C (Table 6.3, entry 3), a significant increase of the \bar{D} was noticed, suggesting the occurrence of side and/or irreversible termination reactions during the polymerization. This loss of control was also accompanied by a decrease in the final monomer conversion, for the same reaction time. Considering both the control over the molecular weight and the polymerization rate, a temperature of 42 °C appears to be optimal.

6.4.4. Variation of Targeted Degree of Polymerization

The robustness of a RDRP system can be evaluated by different criteria among which it is its ability to control the growth of polymer chains for different targeted molecular weights. Figure 6.2 shows the kinetics of the NMP of VC for a targeted number-average degree of polymerization (DP_n) of 100. The polymerization proceeded in a controlled manner, with a good agreement between the experimental and predicted values (and M_n^{SEC} increased linearly with VC conversion, Figure E.1 in Appendix E) as well as decreasing \bar{D} values throughout the reaction reaching ~ 1.5 (Figure 6.2-b). As with the earlier experiments performed with $DP_n = 250$ (Figure 6.1), the SEC chromatograms of

PVC samples obtained at different times intervals showed unimodal distributions with no visible sign of accumulation of dead polymer chains and constant shifts toward higher molecular weights (Figure 6.2-c).

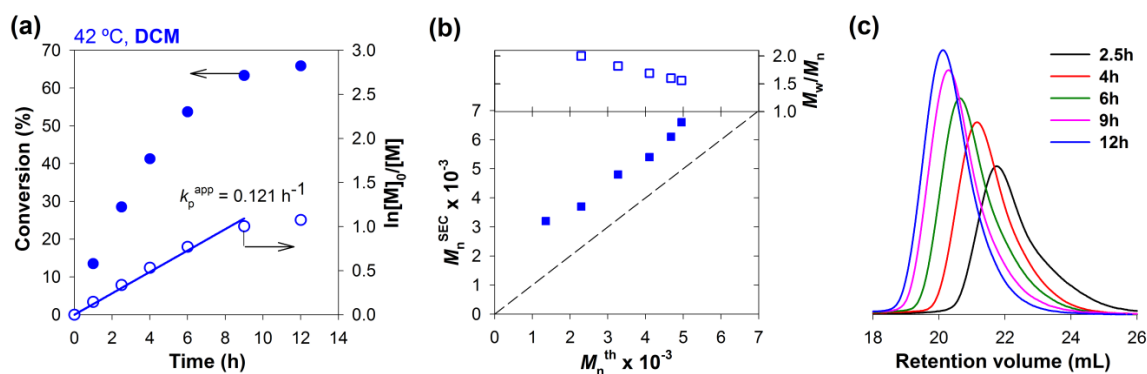


Figure 6.2. NMP of VC in DCM at 42 °C initiated by the SG1-based BlocBuilder alkoxyamine. (a) Conversion and $\ln[M]_0/[M]$ vs. time. (b) M_n^{SEC} and M_w/M_n vs. M_n^{th} . (c) Evolution of the SEC traces during the polymerization. Reaction conditions: $[VC]_0/[BlocBuilder]_0 = 100/1$; $[VC]_0/[solvent] = 1/1$ (v/v).

Additional studies were performed targeting different DP_n values of VC. The results presented on Table 6.4 demonstrate that it is possible to prepare well-defined PVC with a range of molecular weights, suggesting that the NMP of VC using BlocBuilder alkoxyamine is quite robust.

Table 6.4. Conversion and Macromolecular Characteristics Obtained for the NMP of VC in DCM at 42 °C for Different Targeted DP_n values ($[VC]_0/[BlocBuilder]_0$).

Entry	$[VC]_0/[BlocBuilder]_0$	Time (h)	Conv. (%)	$M_{n,th} \times 10^{-3}$	$M_{n,SEC} \times 10^{-3}$	M_w/M_n
1	100/1	7	49	4.3	6.0	1.60
2	100/1	12	66	5.0	6.6	1.56
3	250/1	24	57	10.7	10.8	1.49
4	500/1	24	47	15.9	16.9	1.54
5	1000/1	48	52	34.7	30.4	1.53

6.4.5. Analysis of the PVC Structure

To gain a deeper insight into the structure of the PVC obtained by SG1-mediated NMP initiated by the BlocBuilder alkoxyamine, a sample (Table 6.4, entry 1) was analyzed by ^1H NMR spectroscopy (Figure 6.3). The characteristics signals of the PVC assigned on the spectrum were in agreement with those reported in the literature.^{17,19,21} The ^1H NMR spectrum of the BlocBuilder alkoxyamine, also included in Figure 6.3, to confirm the retention of both chain-end functionalities on the polymer. The spectrum of the PVC reveals the resonances of the repeat unit $\text{CH}_2\text{-CHCl}$: **g** (1.9-2.7 ppm) and **h** (4.2-4.7 ppm), respectively. The spectrum of the PVC also reveals the resonances of the initiating and mediating BlocBuilder alkoxyamine fragments: **a** at 1.62-1.64 ppm, **b**, **c** and **f** at 1.10-1.40 ppm, **d** at 3.35-3.42 ppm, and **e** at 3.98-4.15 ppm.

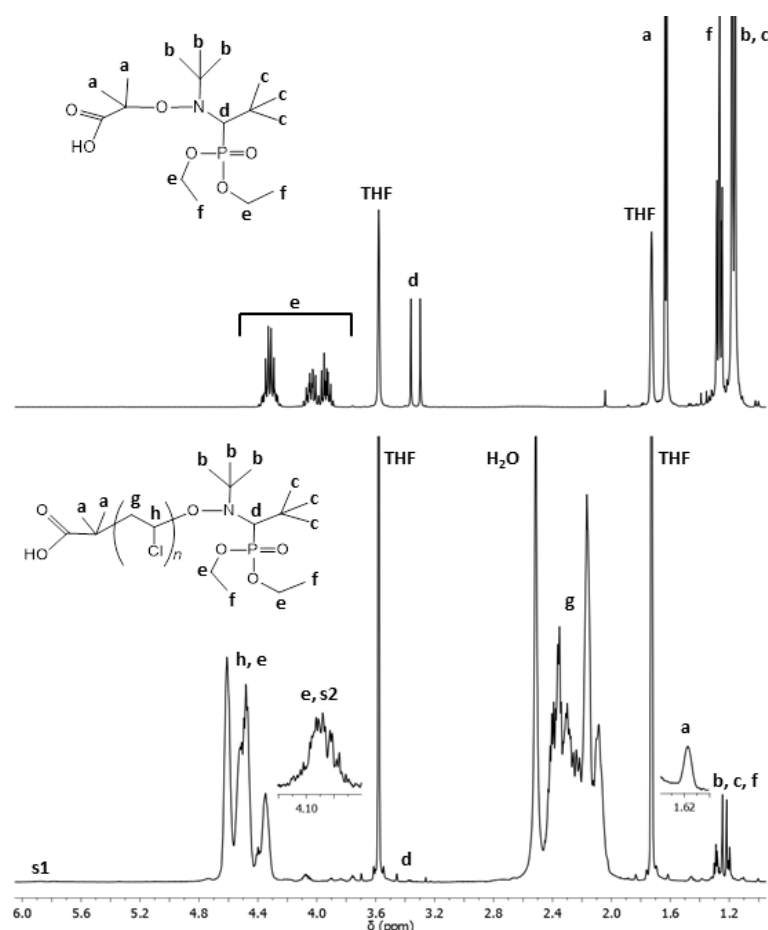


Figure 6.3. ^1H NMR spectra in d_8 -THF of (a) the BlocBuilder alkoxyamine and (b) the purified PVC ($M_n^{\text{SEC}} = 6000$; $D = 1.60$) obtained in Table 6.4, entry 1.

To evaluate the impact of the BlocBuilder alkoxyamine on the formation of structural defects, a PVC ($M_n^{\text{SEC}} = 29.3 \times 10^3$; $\bar{D} = 1.76$) was synthesized by FRP using Trigonox 187 W40 as a conventional initiator under identical conditions and compared to a PVC obtained by NMP (Table 6.4, entry 1). The most representative structural defects for transfer to monomer and easily detected is the $-\text{CH}=\text{CH}-\text{CH}_2\text{Cl}$. Comparing the signal intensities of hydrogen atoms of PVC backbone $-\text{CH}_2\text{CHCl}-$ (**h**, 4.2-4.7 ppm) and the hydrogen atoms of the $-\text{CH}=\text{CH}-\text{CH}_2\text{Cl}$ defect structure (5.8 ppm for $\text{CH}=\text{CH}$ (**s1**, Figures 6.3 and 6.4) allows quantifying the defect in PVC samples (it is not possible to do the comparison considering the 4.1 ppm for CH_2 (**s2**, Figures 6.3 and 6.4) because this signal is overlapped with **e** in the PVC-SG1). The $-\text{CH}_2\text{CHCl}-/-\text{CH}=\text{CH}-\text{CH}_2\text{Cl}$ molar ratio is 1000/0.86 for PVC-FRP while this ratio is 1000/0.42 for PVC-SG1. These results showed much less structural defects in the PVC obtained by SG1-mediated NMP, which is also in agreement with other RDRP techniques as SET-DTLRP²⁵ and RAFT.²¹

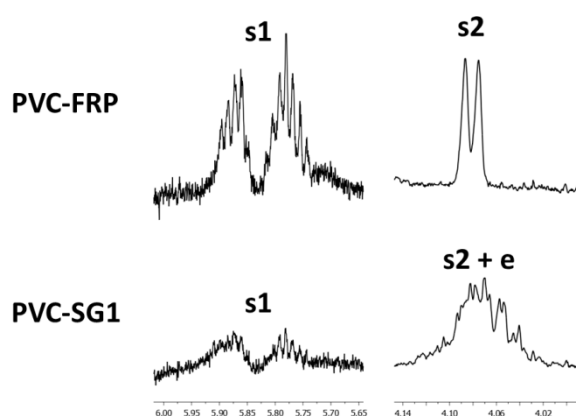


Figure 6.4. Enlargements of ^1H NMR spectra in d_8 -THF of the purified PVC ($M_n^{\text{SEC}} = 6000$; $\bar{D} = 1.60$) obtained in Table 6.4, entry 1 and a purified PVC ($M_n^{\text{SEC}} = 29.3 \times 10^3$; $\bar{D} = 1.76$) obtained by FRP using the same conditions.

To probe the end-group fidelity of the synthesized PVC, ^{31}P NMR spectroscopy was performed. This is a convenient and accurate method, which relies on the determination of the chain end functionality (CEF) by quantifying the presence of the phosphorus-containing SG1 nitroxide end group with diethyl phosphite (DEP) as an internal reference.^{23,63,64} The spectrum of PVC-SG1 is reported in Figure 6.5 and gave a CEF of ~91%, which is similar to CEF values reported for the NMP of styrenics and acrylates and clearly establishes the living nature of the PVC and retention of the SG1 fragment.

This also opens the door to chain extensions to prepare PVC-based block copolymers by NMP.

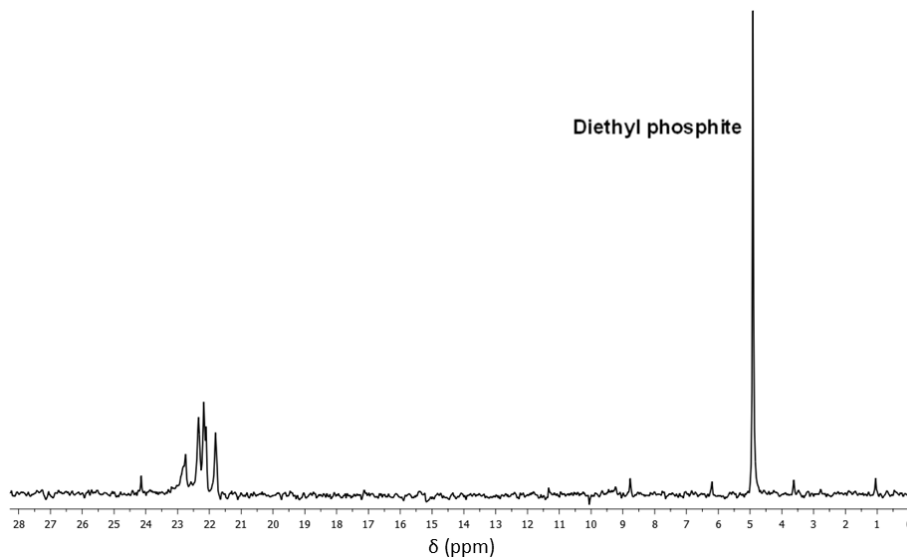


Figure 6.5. ^{31}P NMR spectrum in d_8 -THF of the purified PVC ($M_n^{\text{SEC}} = 6000$; $\mathcal{D} = 1.60$) obtained in Table 6.4, entry 1.

6.4.6. Evaluation of the PVC Livingness

The livingness of a polymer obtained by a RDRP technique is of paramount importance for block copolymer synthesis and macromolecular engineering purposes. The living character of the previously obtained PVC-SG1 (Table 6.4, entry 1) was further confirmed by a successful chain extension experiment by a “one-pot” chain extension experiment from SG1-terminated PVC of VC in DCM at 42 °C. The SEC traces presented in Figure 6.6 showed a complete shift of the low molecular weight SG1-terminated PVC macroinitiator (conv. = 49%, $M_n^{\text{th}} = 4300$, $M_n^{\text{SEC}} = 6000$, $\mathcal{D} = 1.60$) towards high molecular weight polymer (conv. = 44%, $M_n^{\text{th}} = 26500$, $M_n^{\text{SEC}} = 20600$, $\mathcal{D} = 1.59$), thus demonstrating the formation of an extended PVC-*b*-PVC.

Additionally, to diversify the range of PVC-based macromolecular architectures, a PVC-SG1 (Table 6.4, entry 2) macroinitiator ($M_n^{\text{SEC}} = 6600$, $\mathcal{D} = 1.56$) initiated the NMP of MMA to produce PVC-*b*-PMMA (conv._{MMA} = 45.5%, $M_n^{\text{th}} = 52100$, $M_n^{\text{SEC}} = 44700$, $\mathcal{D} = 1.89$) diblock copolymer and the NMP of MMA with 10% of S to produce PVC-*b*-

P(MMA-*co*-S) (conv._{MMA} = 34.5%, conv._S = 36.8%, M_n^{th} = 44800, M_n^{SEC} = 36400, \mathcal{D} = 1.78) diblock copolymer (Figure 6.7).

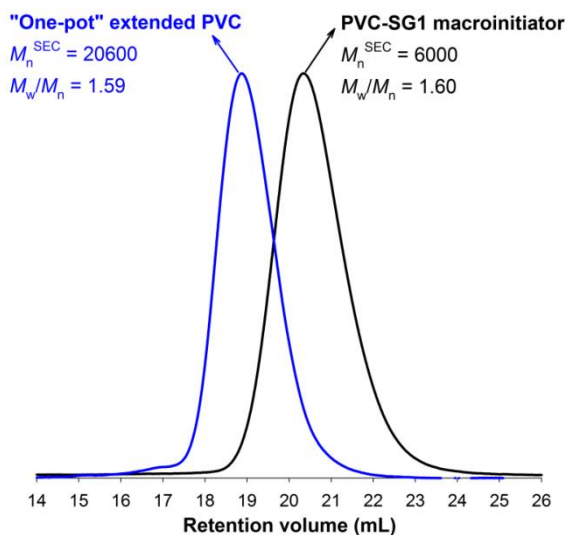


Figure 6.6. SEC chromatograms of the PVC-SG1 macroinitiator (conv. = 49%, M_n^{th} = 4300, $M_n^{\text{SEC}} = 6000$, $\mathcal{D} = 1.60$) (black line), and the extended PVC-*b*-PVC (conv. = 44%, M_n^{th} = 26500, $M_n^{\text{SEC}} = 20600$, $\mathcal{D} = 1.59$) (blue line) after "one-pot" chain extension in DCM.

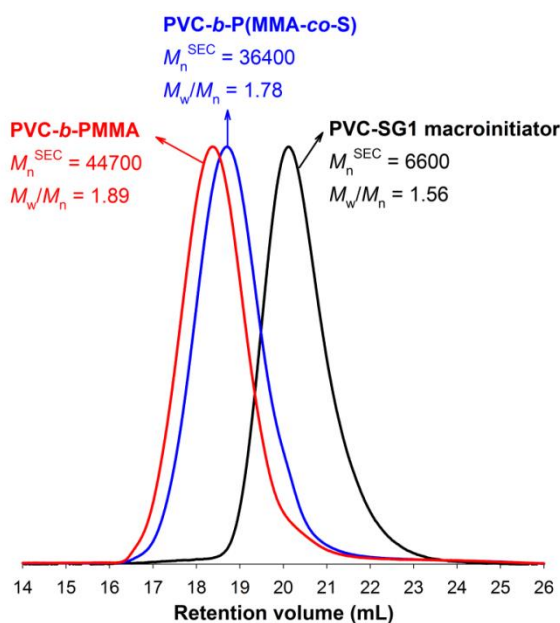


Figure 6.7. SEC chromatograms of the PVC-SG1 macroinitiator (conv. = 66%, M_n^{th} = 5000, $M_n^{\text{SEC}} = 6600$, $\mathcal{D} = 1.56$) (black line), the PVC-*b*-PMMA diblock copolymer (conv._{MMA} = 45.5%, M_n^{th} = 52100, $M_n^{\text{SEC}} = 44700$, $\mathcal{D} = 1.89$) (red line) by NMP in DMSO, and PVC-*b*-P(MMA-*co*-S) (conv._{MMA} = 34.5%, conv._S = 36.8%, M_n^{th} = 44800, $M_n^{\text{SEC}} = 36400$, $\mathcal{D} = 1.78$) (blue line) block copolymer by NMP in DMF at 100 °C for 54 and 44h, respectively.

The chemical structures of the block copolymers were confirmed by ^1H NMR spectroscopy (Figures E.2 and E.3 in Appendix E). These results demonstrated the “living” character of the PVC-SG1 macroinitiator and the possibility of using the reported system in the synthesis of unique and novel PVC-based copolymers with unprecedented properties.

6.5. Conclusions

The SG1-mediated polymerization of VC initiated by the BlocBuilder alkoxyamine was successfully performed at low temperatures (e.g., 30 and 42°C) and led to improved control on the resulting PVC compared to early results in the literature using other nitroxide structures. The structural characterizations (^1H NMR and ^{31}P NMR) suggested the existence of very small content of structural defects and the high preservation of the chain-end functionalities. PVC-SG1 macroinitiators were successfully used in chain extension experiments to produce different PVC-based diblock copolymers. This work is of significant importance as it could open the door to various macromolecular architectures comprising PVC segments using NMP and all its benefits compared to other RDRP methods.

6.6. References

1. Kamigaito, M., Ando, T., and Sawamoto, M., *Metal-Catalyzed Living Radical Polymerization*. Chemical Reviews, **2001**, *101*, 3689-3745.
2. Matyjaszewski, K. and Xia, J., *Atom Transfer Radical Polymerization*. Chemical Reviews, **2001**, *101*, 2921-2990.
3. Perrier, S., Takolpuckdee, P., and Mars, C. A., *Reversible Addition–Fragmentation Chain Transfer Polymerization: End Group Modification for Functionalized Polymers and Chain Transfer Agent Recovery*. Macromolecules, **2005**, *38*, 2033-2036.
4. Moad, G., Rizzardo, E., and Thang, S. H., *Living Radical Polymerization by the RAFT Process – A Second Update*. Australian Journal of Chemistry, **2009**, *62*, 1402-1472.

5. Moad, G., Rizzardo, E., and Thang, S. H., *Living Radical Polymerization by the RAFT Process – A Third Update*. Australian Journal of Chemistry, **2012**, *65*, 985-1076.
6. Nicolas, J., Guillaneuf, Y., Lefay, C., Bertin, D., Gimes, D., and Charleux, B., *Nitroxide-mediated polymerization*. Progress in Polymer Science, **2013**, *38*, 63-235.
7. Wang, J.-S. and Matyjaszewski, K., *Controlled/"Living" Radical Polymerization. Atom Transfer Radical Polymerization in the Presence of Transition-Metal Complexes*. Journal of American Chemical Society, **1995**, *117*, 5614-5615.
8. Matyjaszewski, K., *Atom Transfer Radical Polymerization (ATRP): Current Status and Future Perspectives*. Macromolecules, **2012**, *45*, 4015-4039.
9. Chiefari, J., Chong, Y. K., Ercole, F., Krstina, J., Jeffery, J., Le, T. P. T., Mayadunne, R. T. A., Meijs, G. F., Moad, C. L., Moas, G., Rizzardo, E., and Thang, S. H., *Living Free-Radical Polymerization by Reversible Addition-Fragmentation Chain Transfer: The RAFT Process*. Macromolecules, **1998**, *31*, 5559-5562.
10. Georges, M. K., Veregin, R. P. N., Kazmaier, P. M., and Hamer, G. K., *Narrow Molecular Weight Resins by a Free-Radical Polymerization Process*. Macromolecules, **1993**, *26*, 2987-2988.
11. Ando, T., Kamigaito, M., and Sawamoto, M., *Recent Development of Transition Metal-Catalyzed Living Radical Polymerization Design and Development of the Metal Complexes*. Kobunshi Ronbunshu, **2002**, *59*, 199-211.
12. Matyjaszewski, K. and Tsarevsky, N. V., *Macromolecular Engineering by Atom Transfer Radical Polymerization*. Journal of the American Chemical Society, **2014**, *136*, 6513-6533.
13. Tsarevsky, N. V. and Matyjaszewski, K., *"Green" Atom Transfer Radical Polymerization: From Process Design to Preparation of Well-Defined Environmentally Friendly Polymeric Materials*. Chemical Reviews, **2007**, *107*, 2270-2299.
14. Chenal, M., Mura, S., Marchal, C., Gimes, D., Charleux, B., Fattal, E., Couvreur, P., and Nicolas, J., *Facile Synthesis of Innocuous Comb-Shaped Polymethacrylates with PEG Side Chains by Nitroxide-Mediated Radical Polymerization in Hydroalcoholic Solutions*. Macromolecules, **2010**, *43*, 9291-9303.
15. Abreu, C. M. R., Mendonça, P. V., Serra, A. C., Coelho, J. F. J., Popov, A. V., and Guliashvili, T., *Accelerated Ambient-Temperature ATRP of Methyl Acrylate in Alcohol–Water Solutions with a Mixed Transition-Metal Catalyst System*. Macromolecular Chemistry and Physics, **2012**, *213*, 1677-1687.
16. Abreu, C. M. R., Serra, A. C., Popov, A., Matyjaszewski, K., Guliashvili, T., and Coelho, J. F. J., *Ambient temperature rapid SARA ATRP of acrylates and*

- methacrylates in alcohol/water solutions mediated by mixed sulfites/Cu(II)Br₂ catalytic system.* Polymer Chemistry, **2013**.
17. Maximiano, P., Mendes, J. P., Mendonça, P. V., Abreu, C. M. R., Guliashvili, T., Serra, A. C., and Coelho, J. F. J., *Cyclopentyl methyl ether: A new green co-solvent for supplemental activator and reducing agent atom transfer radical polymerization.* Journal of Polymer Science Part A: Polymer Chemistry, **2015**, DOI: 10.1002/pola.27736.
 18. Abreu, C. M. R., Mendonça, P. V., Serra, A. C., Popov, A. V., Matyjaszewski, K., Guliashvili, T., and Coelho, J. F. J., *Inorganic Sulfites: Efficient Reducing Agents and Supplemental Activators for Atom Transfer Radical Polymerization.* ACS Macro Letters, **2012**, *1*, 1308-1311.
 19. Mendes, J. P., Branco, F., Abreu, C. M. R., Mendonça, P. V., Serra, A. C., Popov, A. V., Guliashvili, T., and Coelho, J. F. J., *Sulfolane: an Efficient and Universal Solvent for Copper-Mediated Atom Transfer Radical (co)Polymerization of Acrylates, Methacrylates, Styrene, and Vinyl Chloride.* ACS Macro Letters, **2014**, *3*, 858-861.
 20. *Global demand for PVC to rise by about 3.2%/year to 2021*, ed. A.f. Polymers. Vol. 2014, **2014**, [http://dx.doi.org/10.1016/S0306-3747\(14\)70175-7](http://dx.doi.org/10.1016/S0306-3747(14)70175-7): Additives for Polymers. 10-11.
 21. Abreu, C. M. R., Mendonça, P. V., Serra, A. C., Coelho, J. F. J., Popov, A. V., Gryn'ova, G., Coote, M. L., and Guliashvili, T., *Reversible Addition-Fragmentation Chain Transfer Polymerization of Vinyl Chloride.* Macromolecules, **2012**, *45*, 2200-2208.
 22. Odian, G., *Radical Chain Polymerization*, in *Principles of Polymerization* **2004**, John Wiley & Sons, Inc. p. 198-349.
 23. Nicolas, J., Dire, C., Mueller, L., Belleney, J., Charleux, B., Marque, S. R. A., Bertin, D., Magnet, S., and Couvreur, L., *Living Character of Polymer Chains Prepared via Nitroxide-Mediated Controlled Free-Radical Polymerization of Methyl Methacrylate in the Presence of a Small Amount of Styrene at Low Temperature.* Macromolecules, **2006**, *39*, 8274-8282.
 24. Ayrey, G. and Haynes, A. C., *Chain transfer reaction of azoisobutyronitrile during polymerization of methyl methacrylate at 60°C.* Die Makromolekulare Chemie, **1974**, *175*, 1463-1470.
 25. Percec, V., Popov, A. V., Ramirez-Castillo, E., Coelho, J. F. J., and Hinojosa-Falcon, L. A., *Non-transition metal-catalyzed living radical polymerization of vinyl chloride initiated with iodoform in water at 25 degrees C.* Journal of Polymer Science Part a-Polymer Chemistry, **2004**, *42*, 6267-6282.
 26. Percec, V., Guliashvili, T., Ladislaw, J. S., Wistrand, A., Stjerndahl, A., Sienkowska, M. J., Monteiro, M. J., and Sahoo, S., *Ultrafast synthesis of ultrahigh molar mass polymers by metal-catalyzed living radical polymerization of*

- acrylates, methacrylates, and vinyl chloride mediated by SET at 25 degrees C.* Journal of the American Chemical Society, **2006**, *128*, 14156-14165.
27. Sienkowska, M. J., Rosen, B. M., and Percec, V., *SET-LRP of Vinyl Chloride Initiated with CHBr₃ in DMSO at 25 degrees C.* Journal of Polymer Science Part a-Polymer Chemistry, **2009**, *47*, 4130-4140.
 28. Hatano, T., Rosen, B. M., and Percec, V., *SET-LRP of Vinyl Chloride Initiated with CHBr₃ and Catalyzed by Cu(0)-Wire/TREN in DMSO at 25 degrees C.* Journal of Polymer Science Part a-Polymer Chemistry, **2010**, *48*, 164-172.
 29. Percec, V., Popov, A. V., Ramirez-Castillo, E., Monteiro, M., Barboiu, B., Weichold, O., Asandei, A. D., and Mitchell, C. M., *Aqueous room temperature metal-catalyzed living radical polymerization of vinyl chloride.* Journal of the American Chemical Society, **2002**, *124*, 4940-4941.
 30. Percec, V., Popov, A. V., Ramirez-Castillo, E., and Weichold, O., *Living radical polymerization of vinyl chloride initiated with iodoform and catalyzed by nascent Cu-0/Tris(2-aminoethyl)amine or polyethyleneimine in water at 25 degrees C proceeds by a new competing pathways mechanism.* Journal of Polymer Science Part a-Polymer Chemistry, **2003**, *41*, 3283-3299.
 31. Percec, V., Popov, A. V., Ramirez-Castillo, E., and Weichold, O., *Acceleration of the single electron transfer-degenerative chain transfer mediated living radical polymerization (SET-DTLRP) of vinyl chloride in water at 25 degrees C.* Journal of Polymer Science Part a-Polymer Chemistry, **2004**, *42*, 6364-6374.
 32. Percec, V., Guliashvili, T., and Popov, A. V., *Ultrafast synthesis of poly(methyl acrylate) and poly(methyl acrylate)-b-poly(vinyl chloride)-b-poly(methyl acrylate) by the Cu(0)/tris(2-dimethylaminoethyl)amine-catalyzed living radical polymerization and block copolymerization of methyl acrylate initiated with 1,1-chloroiodoethane and alpha,omega-di(iodo)poly(vinyl chloride) in dimethyl sulfoxide.* Journal of Polymer Science Part a-Polymer Chemistry, **2005**, *43*, 1948-1954.
 33. Percec, V., Popov, A. V., Ramirez-Castillo, E., Coelho, J. F. J., and Hinojosa-Falcon, L. A., *Phase transfer catalyzed single electron transfer-degenerative chain transfer mediated living radical polymerization (PTC-SET-DTLRP) of vinyl chloride catalyzed by sodium dithionite and initiated with iodoform in water at 43 degrees C.* Journal of Polymer Science Part a-Polymer Chemistry, **2005**, *43*, 779-788.
 34. Coelho, J. F. J., Carreira, M., Gonçalves, P. M., Popov, A. V., and Gil, M. H., *Processability and characterization of poly(vinyl chloride)-b-poly(n-butyl acrylate)-b-poly(vinyl chloride) prepared by living radical polymerization of vinyl chloride. Comparison with a flexible commercial resin formulation prepared with PVC and dioctyl phthalate.* Journal of Vinyl & Additive Technology, **2006**, *12*, 156-165.

35. Coelho, J. F. J., Carreira, M., Popov, A. V., Gonçalves, P. M., and Gil, M. H., *Thermal and mechanical characterization of poly(vinyl chloride)-b-poly(butyl acrylate)-b-poly(vinyl chloride) obtained by single electron transfer - degenerative chain transfer living radical polymerization in water*. *European Polymer Journal*, **2006**, *42*, 2313-2319.
36. Coelho, J. F. J., Mendonca, P. V., Popov, A. V., Percec, V., Gonçalves, P. M., and Gil, M. H., *Synthesis of High Glass Transition Temperature Copolymers Based on Poly(vinyl chloride) via Single Electron Transfer-Degenerative Chain Transfer Mediated Living Radical Polymerization (SET-DTLRP) of Vinyl Chloride in Water*. *Journal of Polymer Science Part a-Polymer Chemistry*, **2009**, *47*, 7021-7031.
37. Coelho, J. F. J., Fonseca, A. C., Góis, J. R., Gonçalves, P. M., Popov, A. V., and Gil, M. H., *Scaling-up of poly(vinyl chloride) prepared by single electron transfer degenerative chain transfer mediated living radical polymerization in water media: 1) Low molecular weight. Kinetic analysis*. *Chemical Engineering Journal*, **2011**, *169*, 399-413.
38. Coelho, J. F. J., Fonseca, A. C., Gonçalves, P. M. F. O., Popov, A. V., and Gil, M. H., *Particle features and morphology of poly(vinyl chloride) prepared by living radical polymerisation in aqueous media. Insight about particle formation mechanism*. *Polymer*, **2011**, *52*, 2998-3010.
39. Coelho, J. F. J., Fonseca, A. C., Gonçalves, P. M., Popov, A. V., and Gil, M. H., *Scaling-up of poly(vinyl chloride) prepared by single electron transfer-degenerative chain transfer mediated living radical polymerization in water media—II: High molecular weight-ultra stable PVC*. *Chemical Engineering Science*, **2012**, *69*, 122-128.
40. Piette, Y., Debuigne, A., Jerome, C., Bodart, V., Poli, R., and Detrembleur, C., *Cobalt-mediated radical (co)polymerization of vinyl chloride and vinyl acetate*. *Polymer Chemistry*, **2012**, *3*, 2880-2891.
41. Piette, Y., Debuigne, A., Bodart, V., Willet, N., Duwez, A.-S., Jerome, C., and Detrembleur, C., *Synthesis of poly(vinyl acetate)-b-poly(vinyl chloride) block copolymers by Cobalt-Mediated Radical Polymerization (CMRP)*. *Polymer Chemistry*, **2013**, *4*, 1685-1693.
42. Wannemacher, T., Braun, D., and Pfaendner, R., *Novel copolymers via nitroxide mediated controlled free radical polymerization of vinyl chloride*. *Macromolecular Symposia*, **2003**, *202*, 11-24.
43. Braun, D., *Controlled free-radical polymerization of vinyl chloride*. *Journal of Vinyl & Additive Technology*, **2005**, *11*, 86-90.
44. Starnes, W. H., Jr. and Ge, X., *Mechanism of autocatalysis in the thermal dehydrochlorination of poly(vinyl chloride)*. *Macromolecules*, **2004**, *37*, 352-359.

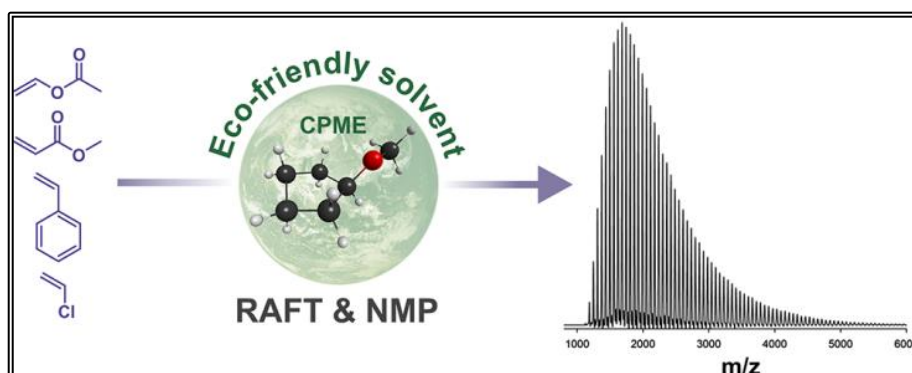
45. Starnes, W. H., Jr., *Structural defects in poly(vinyl chloride)*. J. Polym. Sci., Part A: Polym. Chem., **2005**, *43*, 2451-2467.
46. Starnes, W. H., *Structural and mechanistic aspects of the thermal degradation of poly(vinyl chloride)*. Prog. Polym. Sci., **2002**, *27*, 2133-2170.
47. Nicolas, J., Charleux, B., Guerret, O., and Magnet, S., *Novel SG1-Based Water-Soluble Alkoxyamine for Nitroxide-Mediated Controlled Free-Radical Polymerization of Styrene and n-Butyl Acrylate in Miniemulsion*. Macromolecules, **2004**, *37*, 4453-4463.
48. Chauvin, F., Dufils, P.-E., Gimes, D., Guillaneuf, Y., Marque, S. R. A., Tordo, P., and Bertin, D., *Nitroxide-Mediated Polymerization: The Pivotal Role of the k_d Value of the Initiating Alkoxyamine and the Importance of the Experimental Conditions*. Macromolecules, **2006**, *39*, 5238-5250.
49. Guégain, E., Guillaneuf, Y., and Nicolas, J., *Nitroxide-Mediated Polymerization of Methacrylic Esters: Insights and Solutions to a Long-Standing Problem*. Macromolecular Rapid Communications, **2015**, *36*, 1227-1247.
50. Bagryanskaya, E. G. and Marque, S. R. A., *Scavenging of Organic C-Centered Radicals by Nitroxides*. Chemical Reviews, **2014**, *114*, 5011-5056.
51. Henry, D. J., Sullivan, M. B., and Radom, L., *G3-RAD and G3X-RAD: Modified Gaussian-3 (G3) and Gaussian-3X (G3X) procedures for radical thermochemistry*. Journal of Chemical Physics, **2003**, *118*, 4849-4860.
52. Zhao, Y. and Truhlar, D., *The M06 suite of density functionals for main group thermochemistry, thermochemical kinetics, noncovalent interactions, excited states, and transition elements: two new functionals and systematic testing of four M06-class functionals and 12 other functionals*. Theoretical Chemistry Accounts, **2008**, *120*, 215-241.
53. Marenich, A. V., Cramer, C. J., and Truhlar, D. G., *Universal Solvation Model Based on Solute Electron Density and on a Continuum Model of the Solvent Defined by the Bulk Dielectric Constant and Atomic Surface Tensions*. The Journal of Physical Chemistry B, **2009**, *113*, 6378-6396.
54. Gryn'ova, G., Marshall, D. L., Blanksby, S. J., and Coote, M. L., *Switching radical stability by pH-induced orbital conversion*. Nat Chem, **2013**, *5*, 474-481.
55. Hodgson, J. L., Yeh Lin, C., Coote, M. L., Marque, S. R. A., and Matyjaszewski, K., *Linear Free-Energy Relationships for the Alkyl Radical Affinities of Nitroxides: A Theoretical Study*. Macromolecules, **2010**, *43*, 3728-3743.
56. Hodgson, J. L., Roskop, L. B., Gordon, M. S., Lin, C. Y., and Coote, M. L., *Side Reactions of Nitroxide-Mediated Polymerization: N–O versus O–C Cleavage of Alkoxyamines*. The Journal of Physical Chemistry A, **2010**, *114*, 10458-10466.

57. Coote, M. L., Lin, C. Y., Beckwith, A. L. J., and Zavitsas, A. A., *A comparison of methods for measuring relative radical stabilities of carbon-centred radicals*. *Physical Chemistry Chemical Physics*, **2010**, *12*, 9597-9610.
58. Frisch, M. J., Trucks, G. W., Schlegel, H. B., Scuseria, G. E., Robb, M. A., Cheeseman, J. R., Scalmani, G., Barone, V., Mennucci, B., Petersson, G. A., Nakatsuji, H., Caricato, M., Li, X., Hratchian, H. P., Izmaylov, A. F., Bloino, J., Zheng, G., Sonnenberg, J. L., Hada, M., Ehara, M., Toyota, K., Fukuda, R., Hasegawa, J., Ishida, M., Nakajima, T., Honda, Y., Kitao, O., Nakai, H., Vreven, T., Montgomery Jr., J. A., Peralta, J. E., Ogliaro, F., Bearpark, M., Heyd, J. J., Brothers, E., Kudin, K. N., Staroverov, V. N., Kobayashi, R., Normand, J., Raghavachari, K., Rendell, A., Burant, J. C., Iyengar, S. S., Tomasi, J., Cossi, M., Rega, N., Millam, N. J., Klene, M., Knox, J. E., Cross, J. B., Bakken, V., Adamo, C., Jaramillo, J., Gomperts, R., Stratmann, R. E., Yazyev, O., Austin, A. J., Cammi, R., Pomelli, C., Ochterski, J. W., Martin, R. L., Morokuma, K., Zakrzewski, V. G., Voth, G. A., Salvador, P., Dannenberg, J. J., Dapprich, S., Daniels, A. D., Farkas, Ö., Foresman, J. B., Ortiz, J. V., Cioslowski, J., and Fox, D. J. G., *Gaussian 09*. Gaussian 09, **2009**, Wallingford CT, USA: Gaussian, Inc.
59. Werner, H.-J., Knowles, P. J., Knizia, G., Manby, F. R., Schütz, M., Celani, P., Korona, T., Lindh, R., Mitrushenkov, A., Rauhut, G., Shamasundar, K. R., Adler, T. B., Amos, R. D., Bernhardsson, A., Berning, A., Cooper, D. L., Deegan, M. J. O., Dobbyn, A. J., Eckert, F., Goll, E., Hampel, C., Hesselmann, A., Hetzer, G., Hrenar, T., Jansen, G., Köppl, C., Liu, Y., Lloyd, A. W., Mata, R. A., May, A. J., McNicholas, S. J., Meyer, W., Mura, M. E., Nicklass, A., O'Neill, D. P., Palmieri, P., Peng, D., Pflüger, K., Pitzer, R., Reiher, M., Shiozaki, T., Stoll, H., Stone, A. J., Tarroni, R., Thorsteinsson, T., and Wang, M., *MOLPRO, version 2012.1, a package of ab initio programs*, **2012**, see <http://www.molpro.net>.
60. Werner, H.-J., Knowles, P. J., Knizia, G., Manby, F. R., and Schütz, M., *Molpro: a general-purpose quantum chemistry program package*. *Wiley Interdisciplinary Reviews: Computational Molecular Science*, **2012**, *2*, 242-253.
61. Mendes, J. P., Branco, F., Abreu, C. M. R., Mendonça, P. V., Popov, A. V., Guliashvili, T., Serra, A. C., and Coelho, J. F. J., *Synergistic Effect of 1-Butyl-3-methylimidazolium Hexafluorophosphate and DMSO in the SARA ATRP at Room Temperature Affording Very Fast Reactions and Polymers with Very Low Dispersity*. *ACS Macro Letters*, **2014**, *3*, 544-547.
62. Nicolas, J., Couvreur, P., and Charleux, B., *Comblike Polymethacrylates with Poly(ethylene glycol) Side Chains via Nitroxide-Mediated Controlled Free-Radical Polymerization*. *Macromolecules*, **2008**, *41*, 3758-3761.
63. Delplace, V., Harriison, S., Tardy, A., Gigmes, D., Guillauneuf, Y., and Nicolas, J., *Nitroxide-Mediated Radical Ring-Opening Copolymerization: Chain-End Investigation and Block Copolymer Synthesis*. *Macromolecular Rapid Communications*, **2014**, *35*, 484-491.

64. Delplace, V., Harrisson, S., Ho, H. T., Tardy, A., Guillaneuf, Y., Pascual, S., Fontaine, L., and Nicolas, J., *One-Step Synthesis of Azlactone-Functionalized SGI-Based Alkoxyamine for Nitroxide-Mediated Polymerization and Bioconjugation*. *Macromolecules*, **2015**, 48, 2087-2097.

Chapter 7

Cyclopentyl Methyl Ether as a Green Solvent for Reversible-Addition Fragmentation Chain Transfer and Nitroxide-Mediated Polymerizations



The contents of this chapter are published in:

Abreu, C. M. R., Maximiano, P., Guliashvili, T., Nicolas, J., Serra, A. C., and Coelho, J. F. J., *Cyclopentyl methyl ether as a green solvent for reversible-addition fragmentation chain transfer and nitroxide-mediated polymerizations*. *RSC Advances*, **2016**, *6*, 7495-7503.

7.1. Abstract

Cyclopentyl methyl ether (CPME) was successfully used as an environmentally friendly alternative to the regularly employed organic solvents (*e.g.*, tetrahydrofuran (THF), dimethyl sulfoxide (DMSO), dichloromethane (DCM) and dimethylformamide (DMF)) for the reversible-addition fragmentation chain transfer (RAFT) polymerization and nitroxide-mediated polymerization (NMP) of vinyl chloride (VC) and styrene (S). Methyl acrylate (MA) and vinyl acetate (VAc) were also successfully polymerized *via* RAFT using CPME. The kinetic data showed a linear increase of the molecular weight with the monomer conversion for both polymerization methods. The k_p^{app} data obtained in CPME were in range of the values reported for THF, DMSO, DCM and DMF, while the final conversions were higher. The polymer samples were comprehensively characterized by ^1H nuclear magnetic resonance spectroscopy (^1H NMR), ^{31}P NMR, matrix-assisted laser desorption ionization time-of-flight mass spectroscopy (MALDI-TOF-MS) and size exclusion chromatography (SEC). The “livingness” of the PVC macroinitiators prepared by RAFT and NMP were confirmed by chain-end characterization and successful reinitiation experiments. The data presented here prove that CPME is an excellent green substitute to avoid the use of toxic solvents for RAFT and NMP.

7.2. Introduction

Reversible deactivation radical polymerization (RDRP) has revolutionized the field of macromolecular synthesis. On this matter, it is now possible to synthesize tailor made (co)polymers with controlled molecular weight, topology, architecture and functionalities.¹⁻⁶ The most popular RDRP methods are: atom transfer radical polymerization (ATRP),⁵⁻⁷ nitroxide-mediated polymerization (NMP)^{2,8} and reversible addition-fragmentation transfer polymerization (RAFT).^{3,4,9-12} The intense research efforts of the scientific community during the last two decades on their mechanistic understanding^{2,11,13,14} enabled to expand the range of monomers to be controlled and the establishment of new reaction conditions that can be implemented in large scale production.

Although polymerizations in bulk and in dispersed media have been widely studied, solution polymerizations have only received a very little attention despite their numerous advantages (*e.g.*, low viscosity of the reaction medium, possibility to dilute the reaction medium and avoid the gel effect, broad variety of solvents, etc.).¹⁵⁻¹⁷ Even though water is the ideal solvent in terms of nontoxicity, very few examples of monomers/polymers are water-soluble. Therefore, alternative “green” organic solvents are highly desirable. The continuous search to find eco-friendly solvents for RDRP methods resulted in the use of water,¹⁸⁻²¹ water/alcohol mixtures,²²⁻²⁸ ionic liquids²⁹⁻³⁴ and supercritical CO₂.³⁵ CPME presents several important features that are particularly relevant. It is highly hydrophobic and presents a good stability in acidic and basic conditions.³⁶ Moreover, it leads to a low formation of peroxides as by-products, results in negative skin sensitization,³⁷ gives no genotoxicity or mutagenicity³⁸ and is approved by the Toxic Substances Control Act (TSCA) and the European List of Notified Chemical Substances (ELINCS).^{36,39} CPME is therefore very appealing to circumvent the toxicological drawbacks commonly associated with the use of DMSO, DMF, DCM and THF, which are very effective solvents for homogeneous RDRP methods of hydrophobic monomers such as VC^{15,40-43} and S.⁴⁴⁻⁴⁶

Recently, our research group introduced the use of CPME in the RDRP arena.³⁹ Here, we demonstrate that CPME is a suitable (nearly universal) solvent to perform RAFT and NMP of VC and S as well as RAFT of MA and VAc.

7.3. Experimental Section

7.3.1. Materials

VC (99.9%) was kindly supplied by CIRES Lda, Portugal. MA (Acros; 99% stabilized), S (Sigma-Aldrich; + 99%) and VAc (Sigma-Aldrich; + 99%) were passed over a basic alumina column before use to remove the radical inhibitors. The BlocBuilder alkoxyamine (99%) was kindly supplied by Arkema. Cyanomethyl methyl(phenyl)carbamodithioate (CMPCD) (Sigma-Aldrich, 98 %), 2-(dodecylthiocarbonothioylthio)-2-methylpropionic acid (DDMAT) (Sigma-Aldrich, 98

%), Trigonox 187-W40 (40 % water and methanol emulsion of diisobutyl peroxide - DIBPO), deuterated tetrahydrofuran (d_8 -THF) (Euriso-top; 99.5%), deuterated chloroform ($CDCl_3$) (Euriso-top; + 1 % tetramethylsilane (TMS)), 2-(4-hydroxyphenylazo)benzoic acid (HABA) (Sigma–Aldrich, 99.5%), CPME (Sigma-Aldrich, inhibitor-free, anhydrous, +99.9%), methanol (Labsolve, 99,5%), hexane (Fisher Chemical, 95%), and polystyrene (PS) standards (Polymer Laboratories) were used as received. Azobisisobutyronitrile (AIBN) (Fluka, 98 %) was recrystallized three times from ethanol before use. High-performance liquid chromatography (HPLC) grade THF (Panreac) was filtered (0.2 μ m filter) under reduced pressure before use.

7.3.2. Techniques

400 MHz 1H -NMR spectra and ^{31}P -NMR of samples were recorded on a Bruker Avance III 400 MHz spectrometer, with a 5 mm TIX triple resonance detection probe, in d_8 -THF and $CDCl_3$ with tetramethylsilane (TMS) and diethyl phosphite (DEP) as an internal standard respectively.

The chromatographic parameters of the samples were determined using a size exclusion chromatography set-up from Viscotek (Viscotek TDAmix) equipped with a differential viscometer (DV) and right-angle laser-light scattering (RALLS, Viscotek), low-angle laser-light scattering (LALLS, Viscotek) and refractive index (RI) detectors. The column set consisted of a PL 10 mm guard column ($50 \times 7.5 \text{ mm}^2$) followed by one Viscotek T200 column (6 μ m), one MIXED-E PLgel column (3 μ m) and one MIXED-C PLgel column (5 μ m). A dual piston pump was set with a flow rate of 1 mL/min. The eluent (THF) was previously filtered through a 0.2 μ m filter. The system was also equipped with an on-line degasser. The analyses were performed at 30 °C using an Elder CH-150 heater. Before injection (100 μ L), the samples were filtered through a polytetrafluoroethylene (PTFE) membrane with 0.2 μ m pore. The system was calibrated with narrow PS standards. The dn/dc value was determined as 0.105 for PVC and 0.185 for PS. Molecular weight (M_n^{SEC}) and dispersity ($\mathcal{D} = M_w/M_n$) of synthesized polymers were determined by triple detection calibration using the OmniSEC software version 4.6.1.354.

For the MALDI-TOF-MS analysis, the PVC samples were dissolved in THF at a concentration of 10 mg/mL. HABA (0.05 M in THF) was used as matrix. The dried-droplet sample preparation technique was used to obtain 1/1 ratio (sample/matrix); an aliquot of 1 μ L of each sample was directly spotted on the MTP AnchorChip TM 600/384 TF MALDI target, Bruker Daltonik (Bremen Germany) and, before the sample dry, 1 μ L of matrix solution in THF was added and allowed to dry at room temperature, to allow matrix crystallization. External mass calibration was performed with a peptide calibration standard (PSCII) for the range 700-3000 (9 mass calibration points), 0.5 μ L of the calibration solution and matrix previously mixed in an eppendorf tube (1/2, v/v) were applied directly on the target and allowed to dry at room temperature. Mass spectra were recorded using an Autoflex III smartbeam1 MALDI-TOF-MS mass spectrometer Bruker Daltonik (Bremen, Germany) operating in the linear and reflectron positive ion mode. Ions were formed upon irradiation by a smartbeam1 laser using a frequency of 200 Hz. Each mass spectrum was produced by averaging 2500 laser shots collected across the whole sample spot surface by screening in the range m/z 400-10000. The laser irradiance was set to 35-40% (relative scale 0-100) arbitrary units according to the corresponding threshold required for the applied matrix systems.

7.3.3. Procedures

The VC polymerizations were carried out in a 50 mL glass high-pressure tube equipped with a magnetic stir bar. In the kinetic studies each point represents a single experiment.

Typical procedure for the RAFT polymerization of VC in CPME at 42 °C with $[VC]_0/[CMPCD]_0/[Trigonox]_0 = 250/1/0.2$

A 50 mL Ace Glass 8645#15 pressure tube, equipped with a bushing and a plunge valve, was charged with a mixture of CMPCD (66 mg, 0.29 mmol), Trigonox 187 W40 (25 mg, 0.058 mmol) and CPME (5.0 mL) (previously bubbled with nitrogen for 5 min). The precondensed VC (5 mL, 73 mmol) was added to the tube. The exact amount of VC was determined gravimetrically. The tube was sealed, submerged in liquid nitrogen and degassed through the plunger valve by applying reduced pressure and filling the tube with nitrogen about 20 times. The valve was closed and the tube

reactor was placed in a water bath at $42\text{ }^{\circ}\text{C} \pm 0.5\text{ }^{\circ}\text{C}$ under stirring (700 rpm). After 24 h, the reaction was stopped by plunging the tube into ice water. The tube was slowly opened, the excess VC was distilled, and the mixture was precipitated into 250 mL of methanol. The polymer was separated by filtration and dried in a vacuum oven until constant weight, yielding 3.66 g (69.8 %) of PVC ($M_n^{\text{SEC}} = 11500$, $\mathcal{D} = 1.51$).

Typical procedure for the RAFT polymerization of S in CPME at 60 °C with $[\text{S}]_0/[\text{DDMAT}]_0/[\text{AIBN}]_0 = 222/1/0.5$

A mixture of DDMAT (59 mg, 0.16 mmol), AIBN (13 mg, 0.08 mmol) and CPME (2.0 mL) (previously bubbled with nitrogen for 5 min) was placed in a Schlenk tube reactor. S (4.0 mL, 35 mmol) was added to the reactor that was sealed, by using a glass stopper, and frozen in liquid nitrogen. The Schlenk tube reactor containing the reaction mixture was deoxygenated with four freeze-vacuum-thaw cycles and purged with nitrogen. The reactor was placed in an oil bath at $60\text{ }^{\circ}\text{C}$ with stirring (700 rpm). During the polymerization, different reaction mixture samples were collected by using an airtight syringe and purging the side arm of the Schlenk tube reactor with nitrogen. The samples were analyzed by ^1H NMR spectroscopy to determine the monomer conversion and by SEC, to determine the M_n^{SEC} and \mathcal{D} of the polymers ($t_{\text{rx}} = 49\text{ h}$, $\text{conv} = 84\%$, $M_n^{\text{SEC}} = 16000$, $\mathcal{D} = 1.09$).

Typical procedure for the “one-pot” chain extension experiment from a CTA-terminated PVC

A 50 mL Ace Glass 8645#15 pressure tube, equipped with a bushing and a plunger valve, was charged with a mixture CMPCD (99 mg, 0.44 mmol), Trigonox 187 W40 (38 mg, 0.087 mmol) and CPME (3.0 mL) (previously bubbled with nitrogen for 5 min). The precondensed VC (3.0 mL, 44 mmol) was added to the tube. The exact amount of VC was determined gravimetrically. The tube was sealed, submerged in liquid nitrogen and degassed through the plunger valve by applying reduced pressure and filling the tube with nitrogen about 20 times. The valve was closed, and the tube reactor was placed in a water bath at $42\text{ }^{\circ}\text{C}$ under stirring (700 rpm). After 5 h, the reaction was stopped by plunging the tube into ice water. The tube was slowly opened and the excess VC was distilled. The monomer conversion were determined gravimetrically (58.6 %), and the $M_n^{\text{SEC}} = 4200$ and $\mathcal{D} = 1.54$ were determined by SEC. CPME (18.0 mL) (previously bubbled with

nitrogen for 5 min), Trigonox 187 W40 (31 mg, 0.07 mmol) and the precondensed VC (18.0 mL, 262 mmol) were added in the medium without any purification of the previously obtained PVC-CTA macroCTA. The tube was sealed, submerged in liquid nitrogen and degassed through the plunger valve by applying reduced pressure and filling the tube with nitrogen about 20 times. The valve was closed, and the tube reactor was placed in a water bath at 42 °C under stirring (700 rpm). The reaction was stopped after 48 h by plunging the tube into ice water. The tube was slowly opened and the excess VC was distilled. The monomer conversion were determined gravimetrically (41.8 %), and the $M_n^{\text{SEC}} = 17300$ and $D = 1.53$ of the resulting extended PVC-*b*-PVC were determined by SEC.

Typical procedure for the NMP of VC in CPME at 42 °C with $[VC]_0/[BlocBuilder]_0 = 250/1$

A 50 mL Ace Glass 8645#15 pressure tube, equipped with a bushing and a plunge valve, was charged with a mixture of BlocBuilder alkoxyamine (111 mg, 0.29 mmol) and CPME (5.0 mL) (previously bubbled with nitrogen for 5 min). The precondensed VC (5 mL, 73 mmol) was added to the tube. The exact amount of VC was determined gravimetrically. The tube was sealed, submerged in liquid nitrogen and degassed through the plunger valve by applying reduced pressure and filling the tube with nitrogen about 20 times. The valve was closed and the tube reactor was placed in a water bath at 42 °C ± 0.5 °C under stirring (700 rpm). After 24 h, the reaction was stopped by plunging the tube into ice water. The tube was slowly opened, the excess VC was distilled, and the mixture was precipitated into 250 mL of methanol. The polymer was separated by filtration and dried in a vacuum oven until constant weight, yielding 3.30 g (63.1 %) of PVC ($M_n^{\text{SEC}} = 12000$, $D = 1.54$).

Typical procedure for the NMP of S in CPME at 80 °C with $[S]_0/[BlocBuilder]_0 = 222/1$

A mixture of BlocBuilder alkoxyamine (60 mg, 0.16 mmol) and CPME (2.0 mL) (previously bubbled with nitrogen for 5 min) was placed in a Schlenk tube reactor. S (4.0 mL, 35 mmol) was added to the reactor that was sealed, by using a glass stopper, and frozen in liquid nitrogen. The Schlenk tube reactor containing the reaction mixture was

deoxygenated with four freeze-vacuum-thaw cycles and purged with nitrogen. The reactor was placed in an oil bath at 80 °C with stirring (700 rpm). During the polymerization, different reaction mixture samples were collected by using an airtight syringe and purging the side arm of the Schlenk tube reactor with nitrogen. The samples were analyzed by ^1H NMR spectroscopy to determine the monomer conversion and by SEC, to determine the M_n^{SEC} and \mathcal{D} of the polymers ($t_{\text{rx}} = 166$ h, $\text{conv} = 71\%$, $M_n^{\text{SEC}} = 13500$, $\mathcal{D} = 1.09$).

Typical procedure for the “one-pot” chain extension experiment from SG1-terminated PVC

A 50 mL Ace Glass 8645#15 pressure tube, equipped with a bushing and a plunger valve, was charged with a mixture of BlocBuilder alkoxyamine (167 mg; 0.44 mmol) and CPME (3.0 mL) (previously bubbled with nitrogen for 5 min). The precondensed VC (3.0 mL, 43.7 mmol) was added to the tube. The exact amount of VC was determined gravimetrically. The tube was sealed, submerged in liquid nitrogen and degassed through the plunger valve by applying reduced pressure and filling the tube with nitrogen about 20 times. The valve was closed, and the tube reactor was placed in a water bath at 42 °C under stirring (700 rpm). After 10 h, the reaction was stopped by plunging the tube into ice water. The tube was slowly opened and the excess VC was distilled. The monomer conversion were determined gravimetrically (52.2 %), and the $M_n^{\text{SEC}} = 4300$ and $\mathcal{D} = 1.55$ were determined by SEC. CPME (18.0 mL) (previously bubbled with nitrogen for 5 min) and the precondensed VC (18.0 mL, 262 mmol) were added in the medium without any purification of the previously obtained PVC-SG1 macroinitiator. The tube was sealed, submerged in liquid nitrogen and degassed through the plunger valve by applying reduced pressure and filling the tube with nitrogen about 20 times. The valve was closed, and the tube reactor was placed in a water bath at 42 °C under stirring (700 rpm). The reaction was stopped after 48 h by plunging the tube into ice water. The tube was slowly opened and the excess VC was distilled. The monomer conversion were determined gravimetrically (47.2 %), and the $M_n^{\text{SEC}} = 23600$ and $\mathcal{D} = 1.61$ of the resulting extended PVC-*b*-PVC were determined by SEC.

7.4. Results and Discussion

In a previous publication from our group,³⁹ CPME was used for the first time in the SARA-ATRP using CuBr_2 /ligands (e.g., Me_6TREN , TPMA, bpy, PMDETA and TREN).³⁹ The poor solubility of metal complexes in CPME required the addition of co-solvents (e.g., H_2O and EtOH).³⁹ For RAFT and NMP, it was considered to use CMPE as the only polymerization solvent.

7.4.1. RAFT Polymerization in CPME

Preliminary RAFT polymerization experiments were conducted using MA with DDMAT as chain transfer agent (CTA) in CPME for a DP of 222. The results presented in Figure 7.1 and Table 7.1 (entry 1) show a first-order kinetics with respect to MA, a good agreement between theoretical and determined molecular weights and low D values below 1.1, indicating an excellent control of the polymerization even up to high conversions ($\sim 95\%$). These observations allowed us to conclude that CPME is a solvent compatible with RAFT systems.

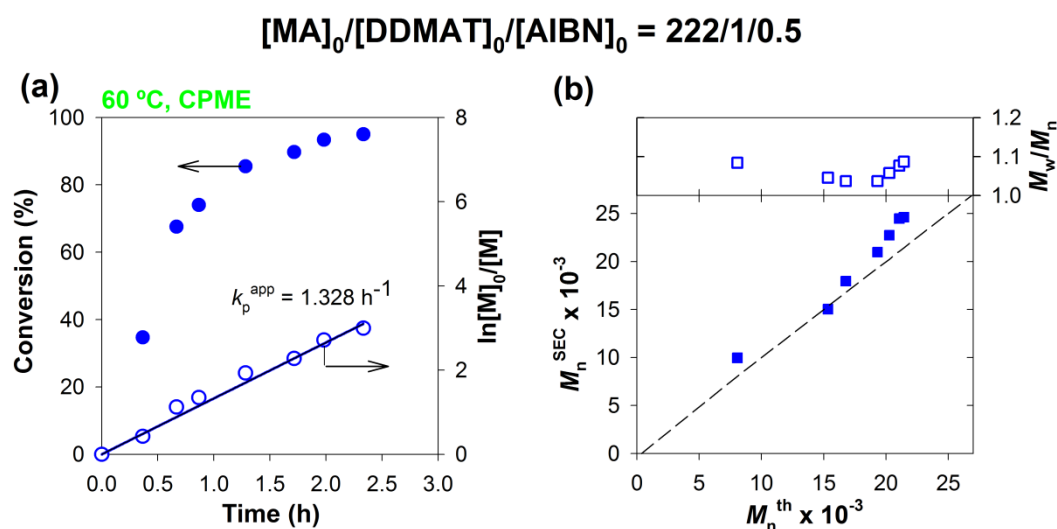


Figure 7.1. RAFT polymerization of MA in CPME at 60 °C mediated by DDMAT using AIBN as conventional initiator. (a) Conversion and $\ln[M]_0/[M]$ vs. time. (b) Number-average molecular weight (M_n^{SEC}) and dispersity (M_w/M_n) vs. theoretical number-average molecular weight (M_n^{th}). Reaction conditions: $[\text{MA}]_0/[\text{DDMAT}]_0/[\text{AIBN}]_0 = 222/1/0.5$; $[\text{MA}]_0/[\text{CPME}] = 2/1$ (v/v).

The ability to polymerize S in CPME under identical experimental conditions was then evaluated. The resulting kinetic plot (see Figure 7.2 and entry 2 in Table 7.1) reveals a linear relationship between $\ln[M]_0/[M]$ values and time, and a nearly perfect match between experimentally determined M_n values and theoretical ones together with D values of about 1.1, indicating a perfect control.

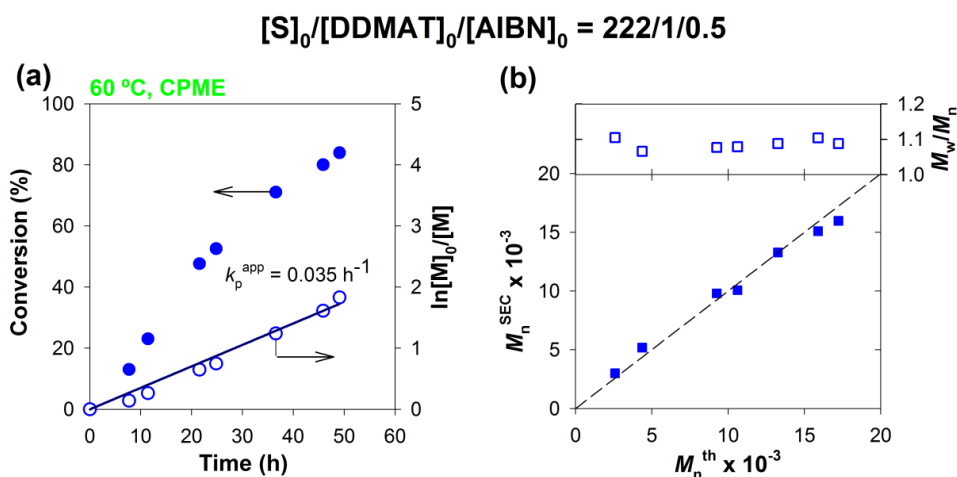


Figure 7.2. RAFT polymerization of S in CPME at 60 °C mediated by DDMAT using AIBN as conventional initiator. (a) Conversion vs. time and $\ln[M]_0/[M]$ vs. time. (b) M_n^{SEC} and M_w/M_n vs. M_n^{th} . Reaction conditions: $[S]_0/[DDMAT]_0/[AIBN]_0 = 222/1/0.5$; $[S]_0/[CPME] = 2/1$ (v/v).

In this respect, the actual RAFT system seems to approach the ideal living polymerization conditions much better than the previously-reported SARA-ATRP counterpart.^{44,46,47} Although low D values have also been obtained by SARA-ATRP, a loss of chain-end functionality at high monomer conversions has been observed, leading to a deviation of M_n^{SEC} from the theoretical ones, with an increase in D .⁴⁴ This was not observed here, thus indicating that side reactions leading to a loss of functionality were minimized. S polymerizations (in bulk or in solution) usually require high temperatures (typically in the range of 70 to 110 °C) to reach reasonably high conversions and to overcome vitrification and potential catalyst solubility issues.⁴⁴ With CPME and using RAFT, it is possible to reach high monomer conversions (>95%) at 60 °C. This feature is particularly relevant because high temperatures (especially above 60 °C) can induce S autopolymerization reactions (by thermal self-initiation) on the long term and result in a loss of molecular weight control (which also contributes for M_n^{SEC} deviation from theoretical values).⁴⁸

RAFT polymerization of S usually takes place in a DMF solution or in bulk.⁴⁴ Our results demonstrate that the use of CPME is an excellent green alternative, allowing a rate of polymerization similar to that of systems in DMF and slightly better than bulk polymerizations.^{49,50} Therefore, CPME can replace DMF for the synthesis of well-defined PS.

To demonstrate the versatility of this approach, VC polymerization in CPME was then investigated at a temperature of 42°C (based on a previous publication from our research group).¹⁵ CMPCD was used as CTA and Trigonox was selected as a conventional initiator. Conversely to S, the plot of $\ln([M]_0/[M])$ vs. time for VC (Figure 7.3) appears to have two distinct linear zones. However, this behavior has already been reported in other RAFT polymerizations of VC,¹⁵ and can be attributed to a difference in the rates of initiation by Trigonox-generated radicals, and reinitiation by the radical leaving groups $\bullet\text{CH}_2\text{CN}$ formed during the pre-equilibrium reaction of the RAFT mechanism. The apparent polymerization rate constants in CPME are slightly higher than those calculated in the previous work using THF as a solvent.¹⁵ Higher conversions were obtained at the end of the reaction, while the level of control over the molecular weight appears to remain the same (with $1.8 > D > 1.5$ and a good agreement between M_n^{SEC} and M_n^{th}).

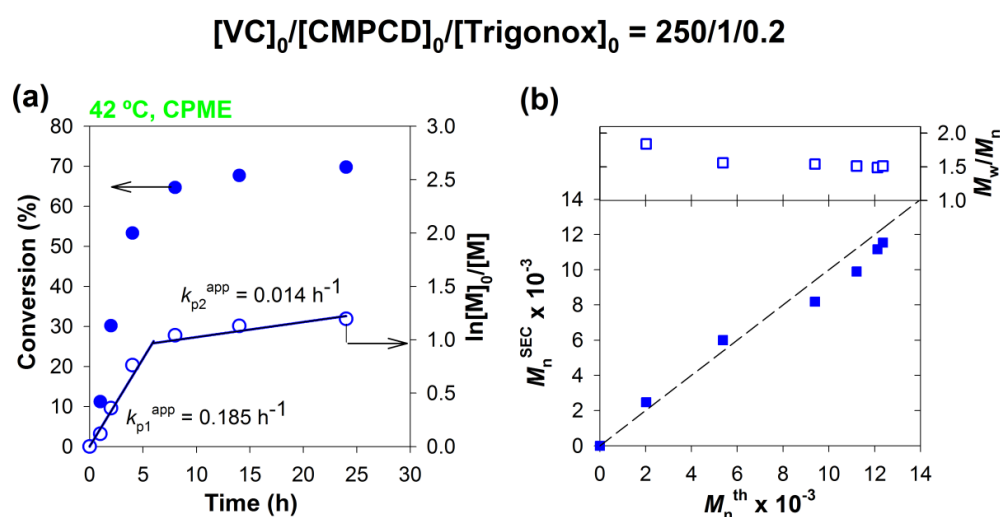


Figure 7.3. RAFT polymerization of VC in CPME at 42 °C mediated by CMPCD using Trigonox as conventional initiator. (a) Conversion and $\ln[M]_0/[M]$ vs. time. (b) M_n^{SEC} and M_w/M_n vs. M_n^{th} . Reaction conditions: $[\text{VC}]_0/[\text{CMPCD}]_0/[\text{Trigonox}]_0 = 250/1/0.2$; $[\text{VC}]_0/[\text{CPME}] = 1/1$ (v/v).

Table 7.1. Kinetic Parameters Obtained for RAFT Polymerizations in CPME with Different Monomers. Conditions: Reaction Temperature = 42 °C; [Monomer]₀/[Solvent] = 2/1 (v/v)

Entry	[M] ₀ /[CTA] ₀ /[I] ₀	k_p^{app} (h ⁻¹)	Time (h) ^d	Conv. (%) ^d	$M_{n,th} \times 10^{-3a}$	$M_{n,SEC} \times 10^{-3a}$	M_w/M_n^a
1 ^b	[MA] ₀ /[DDMAT] ₀ /[AIBN] ₀ = 222/1/0.5	1.328	2	93	21.1	24.5	1.06
2 ^b	[S] ₀ /[DDMAT] ₀ /[AIBN] ₀ = 222/1/0.5	0.035	49	84	17.2	16.0	1.08
3	[VAc] ₀ /[CMPCD] ₀ /[Trig.] ₀ = 100/1/0.5	-	2.3	99	8.7	9.0	1.18
4 ^c	[VC] ₀ /[CMPCD] ₀ /[Trig.] ₀ = 250/1/0.2	0.185	24	70	12.4	11.5	1.51
5 ^c	[VC] ₀ /[CMPCD] ₀ /[Trig.] ₀ = 100/1/0.2	-	5	59	4.5	4.2	1.54
6 ^c	[VC] ₀ /[CMPCD] ₀ /[Trig.] ₀ = 1000/1/0.2	-	48	34	22.7	17.7	1.72

^aValues obtained from the last sample from the kinetic studies.

^bReaction temperature: 60 °C.

^c[Monomer]₀/[Solvent] = 1/1.

The effect of the targeted number-average degree of polymerization (DP_n) on the reaction kinetics and the molecular weight control were then studied. Three different DP_n values were targeted: 100, 250 and 1000. As expected, the results featured in Table 7.1 (entries 4-6) show that the higher the targeted DP_n , the slower the reaction, as fewer radicals are present in the mixture at a given time. It is remarkable to note that for all the DP_n studied, better matches between the M_n^{SEC} and M_n^{th} values were obtained than those obtained in THF¹⁵ despite similar D values.

In addition to MA, S and VC, VAc was also tested using the CMPCD/Trigonox RAFT system (see Table 7.1, entry 3). An almost complete VAc conversion was achieved in less than 3 h, and the low D value obtained by SEC analysis confirmed the growth of well-defined PVAc chains.

In conclusion, the results presented in Table 7.1 confirm the robustness and the versatility of the RAFT polymerization in solution using CPME as solvent. The system allows the synthesis of different polymers in a wide range of molecular weights, while exhibiting a very high level of control that is better or at least similar to other reported solution polymerization systems.^{9,11,15}

7.4.2. Structural Analysis of the RAFT-Derived Polymers

The structure of CTA-terminated PVC chains was determined by MALDI-TOF-MS and ¹H-NMR techniques. The MALDI-TOF-MS of PVC-CTA ranging from 800 to 6000 is shown in Figure 7.4(a). Enlargement of the 1500-1900 range is shown in Figure 7.4(b). Importantly, the series of main peaks is separated by an interval corresponding to a VC repeating unit (62.45 mass units). This main series is attributed to a polymer chain $[\text{R}-(\text{VC})_n-\text{Z}' + \text{Na}]^+$ where R-Z' is the RAFT agent: R = -CH₂-CN and Z' = -S-C(S)-N(Me)Ph (1494.2 = 40.02 + 20 x 62.45 + 182.2 + 23, where 40.02, 62.45, 182.2 and 23 correspond to the molecular weight of R, VC, Z' and Na⁺ respectively). Therefore, the obtained PVC-CTA has a well-defined structure (i.e., without any detectable structural defects). The presence of possible structural defects would cause a deviation of m/z values of distribution.

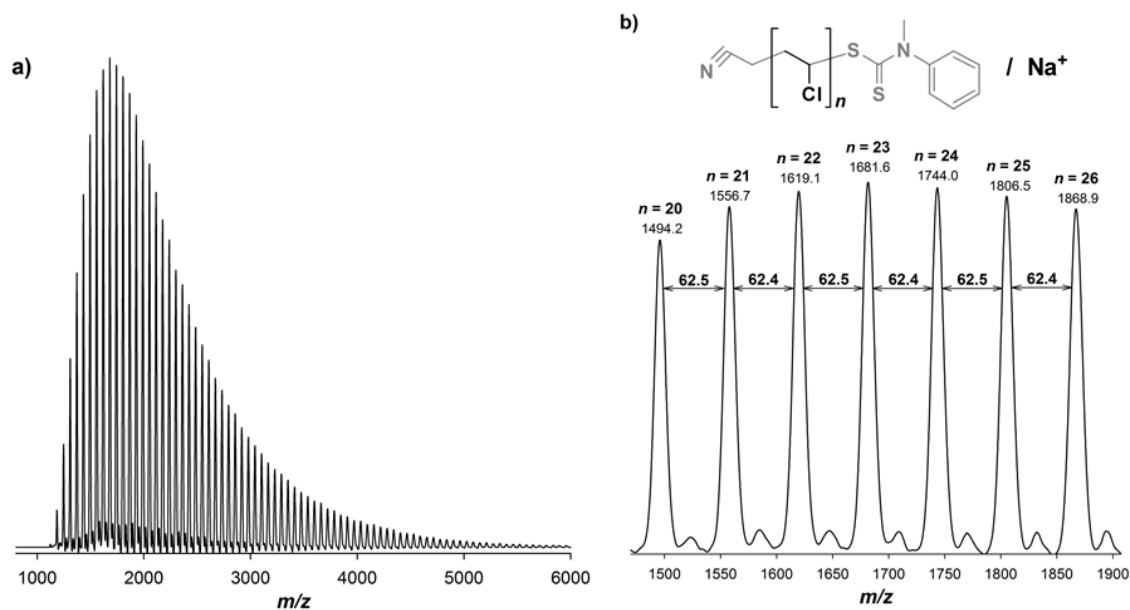


Figure 7.4. (a) MALDI-TOF-MS in the linear mode (using HABA as matrix) of PVC-CTA ($M_n^{SEC} = 4200$, $D = 1.54$) obtained in Table 7.1, entry 5; (b) Enlargement of the MALDI-TOF-MS from m/z 1500 to 1900 of PVC-CTA.

The ^1H NMR spectrum of the PVC-CTA (Figure 7.5) reveals the resonances of the repeat unit $\text{CH}_2\text{-CHCl}$: **d** (1.9-2.7 ppm) and **e** (4.2-4.7 ppm), respectively. The terminal $-\text{CH}_2\text{-CHCl-S-}$ (**f** and **e'**) group resonates at 2.65 and ~ 4.7 ppm, correspondingly. The spectrum of the PVC-CTA also reveals the resonances of the RAFT agent (**b**, **c**).¹⁵ Phenyl protons **c** resonate at 7.2-7.5 ppm, N-Me protons **b** signal at 3.75 ppm. The signal of NC- CH_2 group **a** is probably hidden in the resonance of the main chain methylene group **d** at 1.9-2.7 ppm. Additionally, there is no significant amount of vinyl protons (resonances at 5.8 and 5.9 ppm are usual for free radical PVC),⁵¹ consistent with the vanishingly small concentrations of structural defects observed in PVC species obtained via RAFT process.¹⁵

In addition, the structure of the RAFT-derived PVAc was also studied by ^1H -NMR (Figure 7.6). The signals of the PVAc main chain, **d** and **e** (at 1.9 – 2.7 ppm and 4.2 – 4.8 ppm, respectively) were identified.⁵² Furthermore, the characteristic signals of CMPCD protons (**a**, **b** and **c**), corresponding to those found previously for PVC (Figure 7.5) are also present in this spectrum, thereby confirming the presence of chain-end functionalities

(from the RAFT agent) in the PVAc chains. This conclusion is consistent with the very good control over the molecular weight that has been observed (Table 7.1, entry 3).

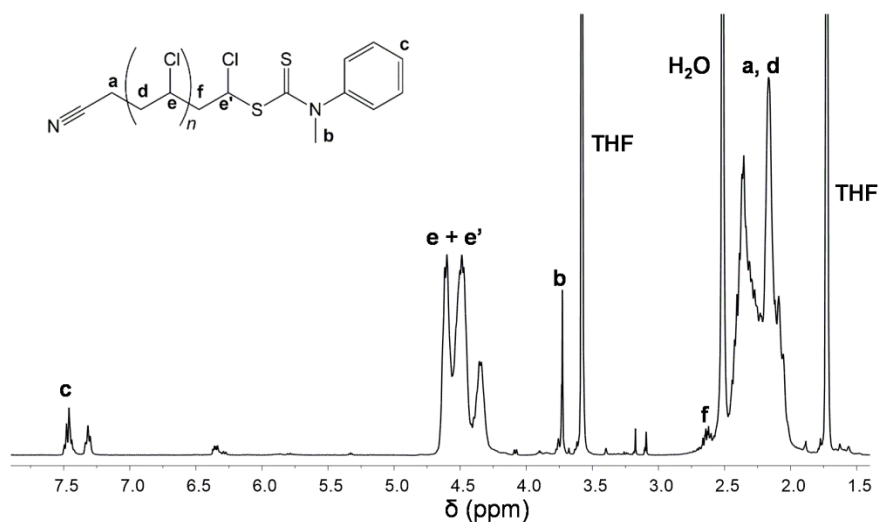


Figure 7.5. The ^1H NMR spectrum in $\text{THF-}d_8$ of PVC-CTA ($M_n^{\text{SEC}} = 4200$; $\mathcal{D} = 1.54$) obtained in Table 7.1, entry 5.

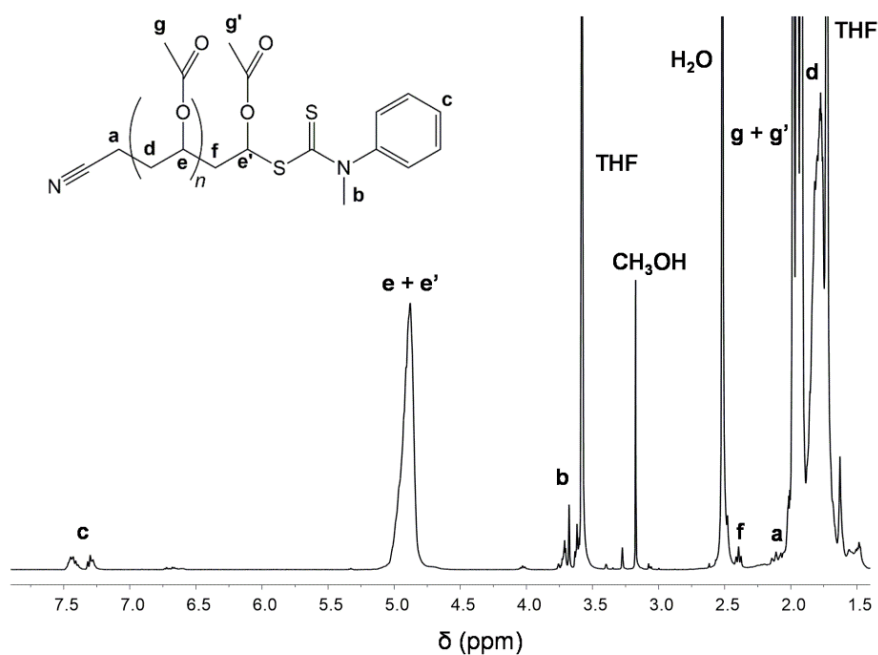


Figure 7.6. The ^1H NMR spectrum in $\text{THF-}d_8$ of PVAc-CTA ($M_n^{\text{SEC}} = 9000$; $\mathcal{D} = 1.18$) obtained in Table 7.1, entry 3.

7.4.3. Evaluation of the RAFT-Derived Polymer Livingness

The living nature of the polymers was confirmed by carrying out successful chain extension experiments using PVC (Table 7.1, entry 5) and PVAc (Table 7.1, entry 3) as macro-CTA (Figure 7.7). As shown in Figure 7.7(a), a complete shift of the SEC trace during the “one-pot” chain extension experiment was achieved. Molecular weight of the starting PVC-CTA ($\text{conv}_{\text{VC}} = 59\%$, $M_n^{\text{th}} = 4500$, $M_n^{\text{SEC}} = 4200$, $\mathcal{D} = 1.54$) has shifted toward higher molecular weight ($\text{conv}_{\text{VC}} = 42\%$, $M_n^{\text{th}} = 23800$, $M_n^{\text{SEC}} = 17300$, $\mathcal{D} = 1.53$). Also, a PVAc-*b*-PVC diblock copolymer ($\text{conv}_{\text{VC}} = 51\%$, $M_n^{\text{th}} = 41100$, $M_n^{\text{SEC}} = 30200$, $\mathcal{D} = 1.59$) was synthesized from a PVAc-CTA ($\text{conv}_{\text{VAc}} = 99\%$, $M_n^{\text{th}} = 8700$, $M_n^{\text{SEC}} = 9000$, $\mathcal{D} = 1.18$) was synthesized (Figure 7.7(b)). The structure of this block copolymer was confirmed by ^1H NMR (Figure 7.8).

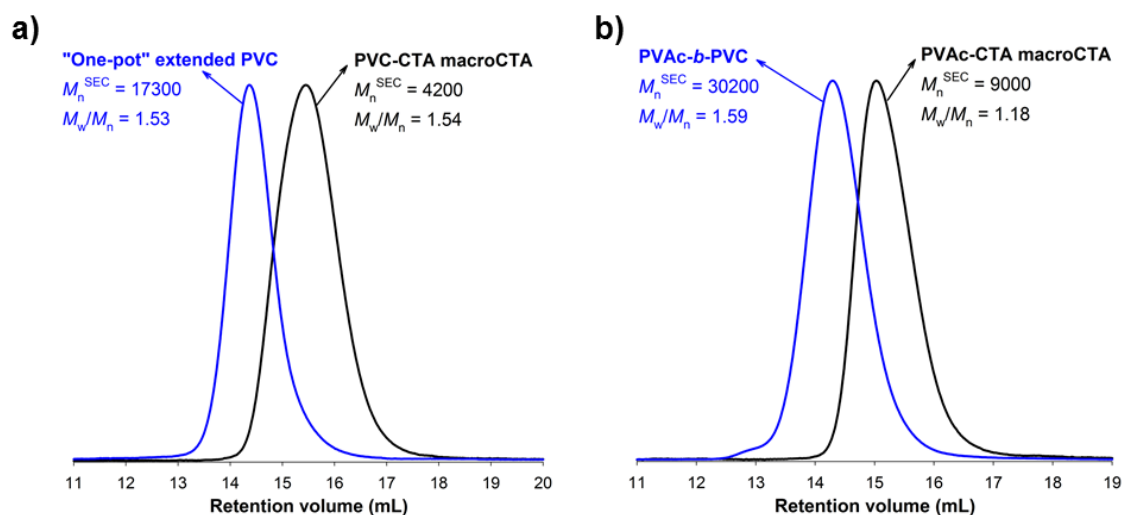


Figure 7.7. (a) SEC traces of the PVC-CTA ($\text{conv}_{\text{VC}} = 59\%$, $M_n^{\text{th}} = 4500$, $M_n^{\text{SEC}} = 4200$, $\mathcal{D} = 1.54$) macro-CTA (right curve), and the “one-pot” extended PVC ($\text{conv}_{\text{VC}} = 42\%$, $M_n^{\text{th}} = 23800$, $M_n^{\text{SEC}} = 17300$, $\mathcal{D} = 1.53$) (left curve). (b) SEC traces of the PVAc-CTA ($\text{conv}_{\text{VAc}} = 99\%$, $M_n^{\text{th}} = 8700$, $M_n^{\text{SEC}} = 9000$, $\mathcal{D} = 1.18$) macro-CTA (right curve), and the PVAc-*b*-PVC ($\text{conv}_{\text{VC}} = 51\%$, $M_n^{\text{th}} = 41100$, $M_n^{\text{SEC}} = 30200$, $\mathcal{D} = 1.59$) block copolymer (left curve).

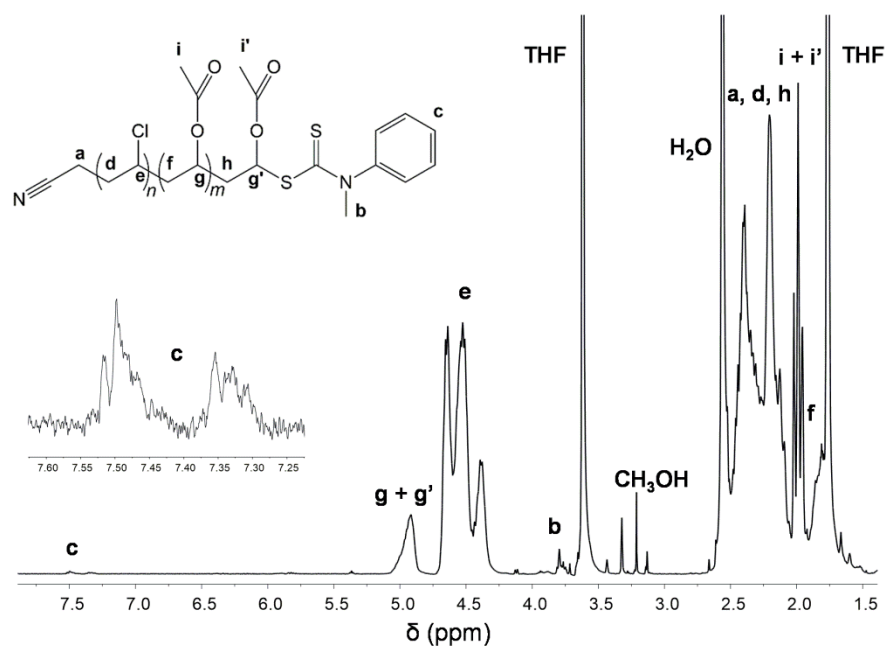


Figure 7.8. The ^1H NMR spectrum of the PVAc-*b*-PVC diblock copolymer ($M_n^{\text{SEC}} = 30200$; $D = 1.59$) in THF- d_8 .

7.4.4. NMP in CPME

For the NMP of S and VC, the BlocBuilder alkoxyamine, based on the nitroxide SG1, was selected. It is one of the most potent alkoxyamines developed so far and its use has conducted to significant advances in the control of bulk/solution and emulsion polymerizations, and the preparation of complex and functionalized polymer architectures.²

The NMP of S using this alkoxyamine is usually performed in bulk at high temperatures; between 90 and 120 °C,^{2,53-55} to enable reasonable polymerization rates. However, this range of temperatures is not fully compatible with the use of CPME (boiling point is 106 °C), unless a high pressure glassware is employed. In this context, a preliminary experiment of S polymerization was carried out at 60 °C. However, as expected, the polymerization was extremely slow as no polymer was formed even after 94 h. The temperature was then increased to 80 °C but the reaction proceeded rather slowly (Figure 7.9). Nevertheless, all the expected features of a RDRP system (e.g., first-order kinetic

with respect to monomer conversion, linear increase of M_n with monomer conversion, good match between M_n^{SEC} and M_n^{th} values and low D values decreasing with monomer conversion) were obtained with a level of control comparable to that reported for NMP of S using BlocBuilder at higher temperatures.⁵⁴⁻⁵⁶ The use of a temperature lower than those reported in the literature may also contribute to a good control over the polymerization due to a lower rate of S autopolymerization, similarly to what was earlier discussed with RAFT. Therefore, despite temperature limitations resulting in slow reactions, the very good control achieved over the polymerization of S validates the use of CPME as a solvent in the field of NMP.

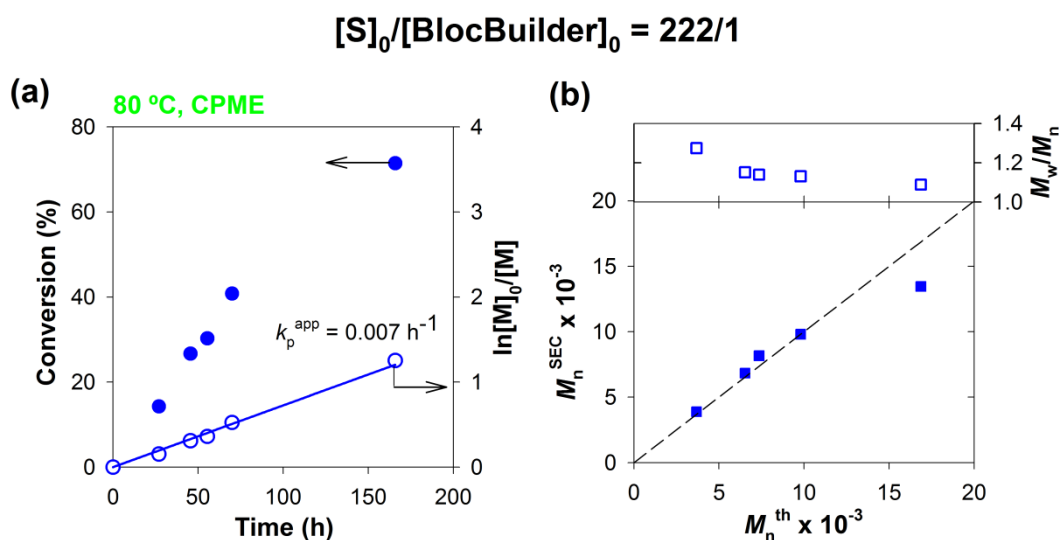


Figure 7.9. NMP of S in CPME at 80 °C initiated by SG1-based BlocBuilder alkoxyamine. (a) Conversion and $\ln[M]_0/[M]$ vs. time. (b) M_n^{SEC} and M_w/M_n vs. M_n^{th} . Reaction conditions: $[S]_0/[BlocBuilder]_0 = 222/1$; $[S]_0/[CPME] = 2/1$ (v/v).

The NMP of VC initiated by the BlocBuilder alkoxyamine in DCM or DMSO was recently proposed, and the results pointed out that a temperature of 42 °C provided the best compromise between a descent polymerization rate and a good control.⁴⁰ Based on this work, the NMP of VC was investigated with CPME as the solvent. The kinetic data show a first-order kinetic (Figure 7.10(a)) and a good agreement between M_n^{SEC} and M_n^{th} values (Figure 7.10(b)). The D follow those obtained in DCM under identical experimental conditions,⁴⁰ approaching 1.5 at the end of the reaction, which suggests a similar level of control. However, the rate of polymerization in CPME ($k_p^{\text{app}} = 0.042$) was

~20% higher than that reported using DCM ($k_p^{\text{app}} = 0.036$),⁴⁰ which stresses another advantage of replacing DCM and DMSO by CPME.

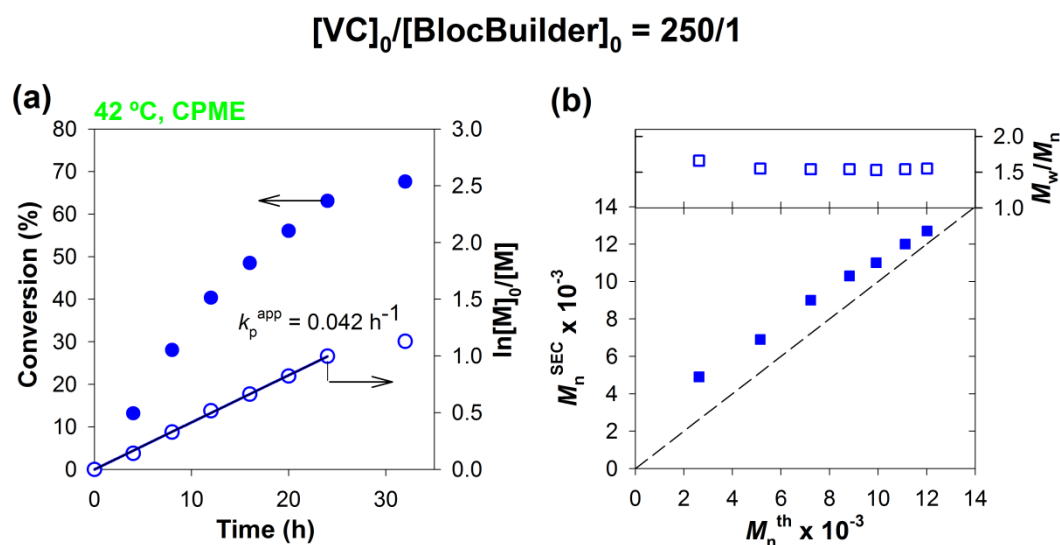


Figure 7.10. NMP of VC in CPME at 42 °C initiated by SG1-based BlocBuilder alkoxyamine. (a) Conversion and $\ln[M]_0/[M]$ vs. time. (b) M_n^{SEC} and M_w/M_n vs. M_n^{th} . Reaction conditions: $[\text{VC}]_0/[\text{BlocBuilder}]_0 = 250/1$; $[\text{VC}]_0/[\text{CPME}] = 1/1$ (v/v).

The influence of the monomer concentration in the reaction medium was then investigated for VC, by adjusting the monomer/solvent ratio and stopping the reaction after 24 h (Table 7.2, entries 1–3). It appears that a decrease in the $[\text{VC}]_0/[\text{CPME}]$ ratio from 1/1 (entry 1) to 1/2 (entry 3) has a deleterious effect on the final monomer conversion, which is caused by a change of the reaction medium (polarity and/or viscosity) upon dilution, as previously observed for different NMP systems.^{16,57} Conversely, when the $[\text{VC}]_0/[\text{CPME}]$ ratio increases from 1/1 (entry 1) to 2/1 (entry 2), dispersity increased slightly (1.54 vs. 1.69), similarly to solution NMP of oligo(ethylene glycol) methyl ether methacrylate (OEGMA) in ethanol.⁵⁷ With VC, the same observations were made in DCM system.⁴⁰

Finally the NMP system proposed here was further tested for different target DP_n . Once again DP_n values of 100 and 1000 were tested and compared with a DP_n of 250 (Table 7.2, entries 1, 4 and 5). The results not only confirm the reduction of polymerization rate as DP_n increases but also the excellent control all across the DP_n range tested.

Table 7.2. NMP of VC Initiated by the BlocBuilder Alkoxyamine at 42 °C, using CPME as a Solvent under Different Experimental Conditions.

Entry	[VC] ₀ /[BlocBuilder] ₀	[VC] ₀ /[CPME] (v/v)	Time (h)	Conv. (%)	$M_{n,th} \times 10^{-3}$	$M_{n,th} \times 10^{-3}$	M_w/M_n
1	250/1	1/1	24	63.1	11.1	12.0	1.54
2	250/1	2/1	24	58.1	10.3	11.1	1.69
3	250/1	1/2	24	42.3	7.8	8.5	1.59
4	100/1	1/1	10	52.2	3.8	4.3	1.55
5	1000/1	1/1	48	54.0	36.3	32.3	1.53

7.4.5. Structural Analysis of the NMP-Derived Polymers

The evidences of the well-defined structure of the PVC (Table 7.2, entry 4) were obtained by ¹H NMR spectroscopy (Figure 7.11). The spectrum of the PVC reveals the resonances of the repeat unit CH₂-CHCl: **g** (1.9-2.7 ppm) and **h** (4.2-4.7 ppm), respectively. It also reveals the resonances of the initiating and mediating BlocBuilder alkoxyamine fragments: **a** at 1.62-1.64 ppm, **b**, **c** and **f** at 1.10-1.40 ppm, **d** at 3.35-3.42 ppm, and **e** at 3.98-4.15 ppm. The spectrum shows the expected peaks and in particular those from the starting alkoxyamine, thus proving the chain-end functionalization, in agreement with those reported in the literature for NMP-derived PVC prepared in other organic solvents.⁴⁰

The end-group fidelity of the synthesized PVC was probed by performing ³¹P NMR spectroscopy, which is a convenient and pretty accurate method for determination of the chain end functionality (CEF) by quantifying the presence of the phosphorus-containing SG1 nitroxide end-group using diethyl phosphite (DEP) as an internal reference.^{58,59} The PVC-SG1 spectrum reported in Figure 7.12 gave a CEF of ~87%, which is similar to CEF values reported for the NMP of styrenics and acrylates. This clearly demonstrates the living nature of the PVC obtained in CPME. It also enables the design of block copolymers by NMP containing PVC segments by chain extensions.

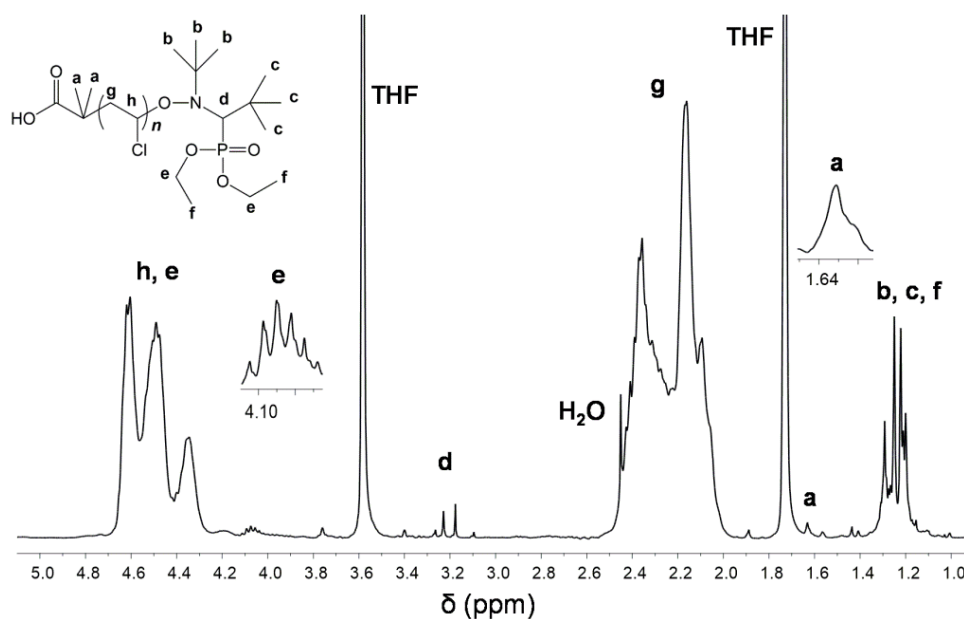


Figure 7.11. The ^1H NMR spectrum in d_8 -THF of a purified PVC ($M_n^{\text{SEC}} = 4300$; $D = 1.55$) obtained in Table 7.2, entry 4.

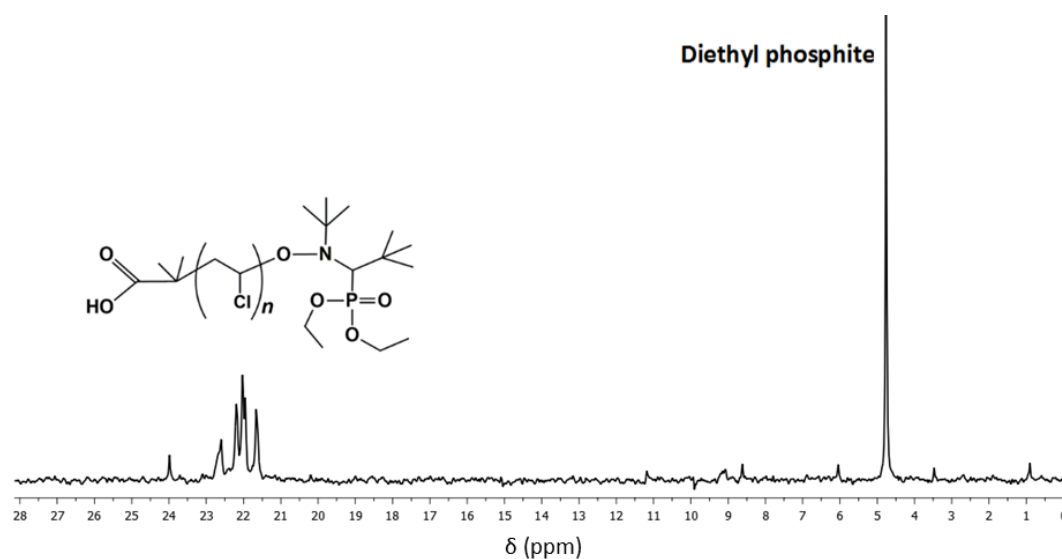


Figure 7.12. ^{31}P NMR spectrum in d_8 -THF of the purified PVC ($M_n^{\text{SEC}} = 4300$; $D = 1.55$) obtained in Table 7.2, entry 4.

7.4.6. Evaluation of the NMP-Derived Polymer Livingness

The living character of the PVC-SG1 obtained by NMP was confirmed by a successful “one-pot” chain extension experiment of VC from the SG1-terminated PVC (Table 7.2,

entry 4) in CPME at 42 °C. The SEC traces presented in Figure 7.13 showed the complete shift of the low molecular weight SG1-terminated PVC macroinitiator ($\text{conv}_{\text{VC}} = 52\%$, $M_n^{\text{th}} = 3800$, $M_n^{\text{SEC}} = 4300$, $\mathcal{D} = 1.55$) towards a higher molecular weight polymer ($\text{conv}_{\text{VC}} = 47\%$, $M_n^{\text{th}} = 29800$, $M_n^{\text{SEC}} = 23600$, $\mathcal{D} = 1.61$), thus assessing the formation of a PVC-*b*-PVC diblock copolymer.

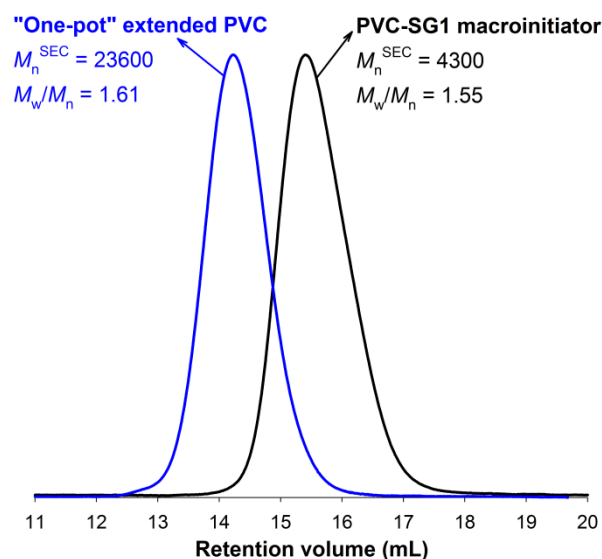


Figure 7.13. SEC chromatograms of the PVC-SG1 macroinitiator ($\text{conv}_{\text{VC}} = 52.2\%$, $M_n^{\text{th}} = 3800$, $M_n^{\text{SEC}} = 4300$, $\mathcal{D} = 1.55$) (black line) and the PVC-*b*-PVC diblock copolymer ($\text{conv}_{\text{VC}} = 47.2\%$, $M_n^{\text{th}} = 29800$, $M_n^{\text{SEC}} = 23600$, $\mathcal{D} = 1.61$) (blue line) after “one-pot” chain extension in CPME.

7.5. Conclusions

In conclusion this work reports the use of CPME for the NMP and RAFT polymerizations of VC and S as alternative to THF, DCM, DMSO and DMF. This eco-friendly solvent allowed also the RAFT polymerization of VAc and MA. The structures of the obtained polymers were confirmed by $^1\text{H-NMR}$, $^{31}\text{P-NMR}$, MALDI-TOF-MS and the living character was confirmed by successful chain extension experiments. The results proved that CPME is a suitable green solvent to be employed in two of the most popular RDRP methods.

7.6. References

1. Matyjaszewski, K. and Tsarevsky, N. V., *Macromolecular Engineering by Atom Transfer Radical Polymerization*. Journal of the American Chemical Society, 2014, *136*, 6513-6533.
2. Nicolas, J., Guillaneuf, Y., Lefay, C., Bertin, D., Gimes, D., and Charleux, B., *Nitroxide-mediated polymerization*. Progress in Polymer Science, 2013, *38*, 63-235.
3. Moad, G., Rizzardo, E., and Thang, S. H., *Living Radical Polymerization by the RAFT Process – A Third Update*. Australian Journal of Chemistry, 2012, *65*, 985-1076.
4. Moad, G., Rizzardo, E., and Thang, S. H., *Living Radical Polymerization by the RAFT Process – A Second Update*. Australian Journal of Chemistry, 2009, *62*, 1402-1472.
5. Matyjaszewski, K. and Xia, J. H., *Atom transfer radical polymerization*. Chemical Reviews, 2001, *101*, 2921-2990.
6. Kamigaito, M., Ando, T., and Sawamoto, M., *Metal-catalyzed living radical polymerization*. Chemical Reviews, 2001, *101*, 3689-3745.
7. Wang, J.-S. and Matyjaszewski, K., *Controlled/"living" radical polymerization. atom transfer radical polymerization in the presence of transition-metal complexes*. Journal of the American Chemical Society, 1995, *117*, 5614-5615.
8. Georges, M. K., Veregin, R. P. N., Kazmaier, P. M., and Hamer, G. K., *Narrow molecular weight resins by a free radical polymerization process*. Macromolecules, 1993, *26*, 2987-2988.
9. Moad, G., Rizzardo, E., and Thang, S. H., *Toward living radical polymerization*. Accounts of Chemical Research, 2008, *41*, 1133-1142.
10. Perrier, S. and Takolpuckdee, P., *Macromolecular design via reversible addition-fragmentation chain transfer (RAFT)/Xanthates (MADIX) polymerization*. Journal of Polymer Science Part a-Polymer Chemistry, 2005, *43*, 5347-5393.
11. Moad, G., Rizzardo, E., and Thang, S. H., *Living Radical Polymerization by the RAFT Process*. Australian Journal of Chemistry, 2005, *58*, 379-410.
12. Chiefari, J., Chong, Y. K., Ercole, F., Krstina, J., Jeffery, J., Le, T. P. T., Mayadunne, R. T. A., Meijs, G. F., Moad, C. L., Moad, G., Rizzardo, E., and Thang, S. H., *Living free-radical polymerization by reversible addition-*

- fragmentation chain transfer: The RAFT process.* *Macromolecules*, 1998, *31*, 5559-5562.
13. Konkolewicz, D., Wang, Y., Krys, P., Zhong, M., Isse, A. A., Gennaro, A., and Matyjaszewski, K., *SARA ATRP or SET-LRP. End of controversy?* *Polymer Chemistry*, 2014, *5*, 4396-4417.
 14. Guliashvili, T., Mendonca, P. V., Serra, A. C., Popov, A. V., and Coelho, J. F. J., *Copper-Mediated Controlled/"Living" Radical Polymerization in Polar Solvents: Insights into Some Relevant Mechanistic Aspects.* *Chemistry-a European Journal*, 2012, *18*, 4607-4612.
 15. Abreu, C. M. R., Mendonca, P. V., Serra, A. C., Coelho, J. F. J., Popov, A. V., Gryn'ova, G., Coote, M. L., and Guliashvili, T., *Reversible Addition-Fragmentation Chain Transfer Polymerization of Vinyl Chloride.* *Macromolecules*, 2012, *45*, 2200-2208.
 16. Chenal, M., Mura, S., Marchal, C., Gignes, D., Charleux, B., Fattal, E., Couvreur, P., and Nicolas, J., *Facile Synthesis of Innocuous Comb-Shaped Polymethacrylates with PEG Side Chains by Nitroxide-Mediated Radical Polymerization in Hydroalcoholic Solutions.* *Macromolecules*, 2010, *43*, 9291-9303.
 17. Kuo, K.-H., Chiu, W.-Y., and Cheng, K.-C., *Influence of DMF on the polymerization of tert-butyl acrylate initiated by 4-oxo-TEMPO-capped polystyrene macroinitiator.* *Polymer International*, 2008, *57*, 730-737.
 18. Mendonça, P. V., Averick, S. E., Konkolewicz, D., Serra, A. C., Popov, A. V., Guliashvili, T., Matyjaszewski, K., and Coelho, J. F. J., *Straightforward ARGET ATRP for the Synthesis of Primary Amine Polymethacrylate with Improved Chain-End Functionality under Mild Reaction Conditions.* *Macromolecules*, 2014, *47*, 4615-4621.
 19. Konkolewicz, D., Krys, P., Góis, J. R., Mendonça, P. V., Zhong, M., Wang, Y., Gennaro, A., Isse, A. A., Fantin, M., and Matyjaszewski, K., *Aqueous RDRP in the Presence of Cu₂O: The Exceptional Activity of CuI Confirms the SARA ATRP Mechanism.* *Macromolecules*, 2014, *47*, 560-570.
 20. Simakova, A., Averick, S. E., Konkolewicz, D., and Matyjaszewski, K., *Aqueous ARGET ATRP.* *Macromolecules*, 2012, *45*, 6371-6379.
 21. Konkolewicz, D., Magenau, A. J. D., Averick, S. E., Simakova, A., He, H., and Matyjaszewski, K., *ICAR ATRP with ppm Cu Catalyst in Water.* *Macromolecules*, 2012, *45*, 4461-4468.

22. Mendonca, P. V., Konkolewicz, D., Averick, S. E., Serra, A. C., Popov, A. V., Guliashvili, T., Matyjaszewski, K., and Coelho, J. F. J., *Synthesis of cationic poly((3-acrylamidopropyl)-trimethylammonium chloride) by SARA ATRP in ecofriendly solvent mixtures*. *Polymer Chemistry*, 2014, 5, 5829-5836.
23. Gois, J. R., Rocha, N., Popov, A. V., Guliashvili, T., Matyjaszewski, K., Serra, A. C., and Coelho, J. F. J., *Synthesis of well-defined functionalized poly(2-(diisopropylamino)ethyl methacrylate) using ATRP with sodium dithionite as a SARA agent*. *Polymer Chemistry*, 2014, 5, 3919-3928.
24. Gois, J. R., Konkolewicz, D., Popov, A. V., Guliashvili, T., Matyjaszewski, K., Serra, A. C., and Coelho, J. F. J., *Improvement of the control over SARA ATRP of 2-(diisopropylamino)ethyl methacrylate by slow and continuous addition of sodium dithionite*. *Polymer Chemistry*, 2014, 5, 4617-4626.
25. Huo, F., Wang, X., Zhang, Y., Zhang, X., Xu, J., and Zhang, W., *RAFT Dispersion Polymerization of Styrene in Water/Alcohol: The Solvent Effect on Polymer Particle Growth during Polymer Chain Propagation*. *Macromolecular Chemistry and Physics*, 2013, 214, 902-911.
26. Cordeiro, R. A., Rocha, N., Mendes, J. P., Matyjaszewski, K., Guliashvili, T., Serra, A. C., and Coelho, J. F. J., *Synthesis of well-defined poly(2-(dimethylamino)ethyl methacrylate) under mild conditions and its co-polymers with cholesterol and PEG using Fe(0)/Cu(ii) based SARA ATRP*. *Polymer Chemistry*, 2013, 4, 3088-3097.
27. Abreu, C. M. R., Serra, A. C., Popov, A. V., Matyjaszewski, K., Guliashvili, T., and Coelho, J. F. J., *Ambient temperature rapid SARA ATRP of acrylates and methacrylates in alcohol-water solutions mediated by a mixed sulfite/Cu(ii)Br₂ catalytic system*. *Polymer Chemistry*, 2013, 4, 5629-5636.
28. Abreu, C. M. R., Mendonça, P. V., Serra, A. C., Coelho, J. F. J., Popov, A. V., and Guliashvili, T., *Accelerated Ambient-Temperature ATRP of Methyl Acrylate in Alcohol–Water Solutions with a Mixed Transition-Metal Catalyst System*. *Macromolecular Chemistry and Physics*, 2012, 213, 1677-1687.
29. Costa, J. R. C., Mendonça, P. V., Maximiano, P., Serra, A. C., Guliashvili, T., and Coelho, J. F. J., *Ambient Temperature “Flash” SARA ATRP of Methyl Acrylate in Water/Ionic Liquid/Glycol Mixtures*. *Macromolecules*, 2015.
30. Anastasaki, A., Nikolaou, V., Nurumbetov, G., Truong, N. P., Pappas, G. S., Engelis, N. G., Quinn, J. F., Whittaker, M. R., Davis, T. P., and Haddleton, D. M., *Synthesis of Well-Defined Poly(acrylates) in Ionic Liquids via Copper(II)-*

- Mediated Photoinduced Living Radical Polymerization.* *Macromolecules*, 2015, 48, 5140-5147.
31. Mendes, J. P., Branco, F., Abreu, C. M. R., Mendonca, P. V., Popov, A. V., Guliashvili, T., Serra, A. C., and Coelho, J. F. J., *Synergistic Effect of 1-Butyl-3-methylimidazolium Hexafluorophosphate and DMSO in the SARA ATRP at Room Temperature Affording Very Fast Reactions and Polymers with Very Low Dispersity.* *ACS Macro Letters*, 2014, 3, 544-547.
 32. Erdmenger, T., Guerrero-Sanchez, C., Vitz, J., Hoogenboom, R., and Schubert, U. S., *Recent developments in the utilization of green solvents in polymer chemistry.* *Chemical Society Reviews*, 2010, 39, 3317-3333.
 33. Biedroń, T. and Kubisa, P., *Atom transfer radical polymerization of acrylates in an ionic liquid: Synthesis of block copolymers.* *Journal of Polymer Science Part A: Polymer Chemistry*, 2002, 40, 2799-2809.
 34. Carmichael, A. J., Haddleton, D. M., Bon, S. A. F., and Seddon, K. R., *Copper(I) mediated living radical polymerisation in an ionic liquid.* *Chemical Communications*, 2000, 1237-1238.
 35. Magee, C., Earla, A., Petraitis, J., Higa, C., Braslau, R., Zetterlund, P. B., and Aldabbagh, F., *Synthesis of fluorinated alkoxyamines and alkoxyamine-initiated nitroxide-mediated precipitation polymerizations of styrene in supercritical carbon dioxide.* *Polymer Chemistry*, 2014, 5, 5725-5733.
 36. Watanabe, K., Yamagiwa, N., and Torisawa, Y., *Cyclopentyl Methyl Ether as a New and Alternative Process Solvent.* *Organic Process Research & Development*, 2007, 11, 251-258.
 37. Watanabe, K., *The Toxicological Assessment of Cyclopentyl Methyl Ether (CPME) as a Green Solvent.* *Molecules*, 2013, 18, 3183.
 38. Antonucci, V., Coleman, J., Ferry, J. B., Johnson, N., Mathe, M., Scott, J. P., and Xu, J., *Toxicological Assessment of 2-Methyltetrahydrofuran and Cyclopentyl Methyl Ether in Support of Their Use in Pharmaceutical Chemical Process Development.* *Organic Process Research & Development*, 2011, 15, 939-941.
 39. Maximiano, P., Mendes, J. P., Mendonça, P. V., Abreu, C. M. R., Guliashvili, T., Serra, A. C., and Coelho, J. F. J., *Cyclopentyl methyl ether: A new green co-solvent for supplemental activator and reducing agent atom transfer radical polymerization.* *Journal of Polymer Science Part A: Polymer Chemistry*, 2015, DOI: 10.1002/pola.27736.

40. Abreu, C. M. R., Mendonça, P. V., Serra, A. C., Noble, B. B., Guliashvili, T., Nicolas, J., Coote, M. L., and Coelho, J. F. J., *Nitroxide-Mediated Polymerization of Vinyl Chloride at Low Temperature: Kinetic and Computational Studies*. *Macromolecules*, 2016, *49*, 490-498.
41. Hatano, T., Rosen, B. M., and Percec, V., *SET-LRP of Vinyl Chloride Initiated with CHBr₃ and Catalyzed by Cu(0)-Wire/TREN in DMSO at 25 degrees C*. *Journal of Polymer Science Part a-Polymer Chemistry*, 2010, *48*, 164-172.
42. Sienkowska, M. J., Rosen, B. M., and Percec, V., *SET-LRP of Vinyl Chloride Initiated with CHBr₃ in DMSO at 25 degrees C*. *Journal of Polymer Science Part a-Polymer Chemistry*, 2009, *47*, 4130-4140.
43. Percec, V., Guliashvili, T., Ladislaw, J. S., Wistrand, A., Stjerndahl, A., Sienkowska, M. J., Monteiro, M. J., and Sahoo, S., *Ultrafast Synthesis of Ultrahigh Molar Mass Polymers by Metal-Catalyzed Living Radical Polymerization of Acrylates, Methacrylates, and Vinyl Chloride Mediated by SET at 25 °C*. *Journal of the American Chemical Society*, 2006, *128*, 14156-14165.
44. Rocha, N., Mendonça, P. V., Mendes, J. P., Simões, P. N., Popov, A. V., Guliashvili, T., Serra, A. C., and Coelho, J. F. J., *Facile Synthesis of Well-Defined Telechelic Alkyne-Terminated Polystyrene in Polar Media Using ATRP With Mixed Fe/Cu Transition Metal Catalyst*. *Macromolecular Chemistry and Physics*, 2013, *214*, 76-84.
45. Abreu, C. M. R., Mendonca, P. V., Serra, A. C., Popov, A. V., Matyjaszewski, K., Guliashvili, T., and Coelho, J. F. J., *Inorganic Sulfites: Efficient Reducing Agents and Supplemental Activators for Atom Transfer Radical Polymerization*. *Acs Macro Letters*, 2012, *1*, 1308-1311.
46. Mendonca, P. V., Serra, A. C., Coelho, J. F. J., Popov, A. V., and Guliashvili, T., *Ambient temperature rapid ATRP of methyl acrylate, methyl methacrylate and styrene in polar solvents with mixed transition metal catalyst system*. *European Polymer Journal*, 2011, *47*, 1460-1466.
47. Mendes, J. P., Branco, F., Abreu, C. M. R., Mendonca, P. V., Serra, A. C., Popov, A. V., Guliashvili, T., and Coelho, J. F. J., *Sulfolane: an Efficient and Universal Solvent for Copper-Mediated Atom Transfer Radical (co)Polymerization of Acrylates, Methacrylates, Styrene, and Vinyl Chloride*. *Acs Macro Letters*, 2014, *3*, 858-861.
48. Mayo, F. R., *The dimerization of styrene*. *Journal of the American Chemical Society*, 1968, *90*, 1289-1295.

49. Wu, Y., Zhang, W., Zhang, Z., Pan, X., Cheng, Z., Zhu, J., and Zhu, X., *Initiator-chain transfer agent combo in the RAFT polymerization of styrene*. *Chemical Communications*, 2014, 50, 9722-9724.
50. Goto, A., Sato, K., Tsujii, Y., Fukuda, T., Moad, G., Rizzardo, E., and Thang, S. H., *Mechanism and kinetics of RAFT-based living radical polymerizations of styrene and methyl methacrylate*. *Macromolecules*, 2001, 34, 402-408.
51. Percec, V., Popov, A. V., Ramirez-Castillo, E., Coelho, J. F. J., and Hinojosa-Falcon, L. A., *Non-transition metal-catalyzed living radical polymerization of vinyl chloride initiated with iodoform in water at 25 degrees C*. *Journal of Polymer Science Part a-Polymer Chemistry*, 2004, 42, 6267-6282.
52. Piette, Y., Debuigne, A., Bodart, V., Willet, N., Duwez, A.-S., Jerome, C., and Detrembleur, C., *Synthesis of poly(vinyl acetate)-b-poly(vinyl chloride) block copolymers by Cobalt-Mediated Radical Polymerization (CMRP)*. *Polymer Chemistry*, 2013, 4, 1685-1693.
53. Charleux, B. and Nicolas, J., *Water-soluble SGI-based alkoxyamines: A breakthrough in controlled/living free-radical polymerization in aqueous dispersed media*. *Polymer*, 2007, 48, 5813-5833.
54. Grimaldi, S., Finet, J.-P., Le Moigne, F., Zeghdaoui, A., Tordo, P., Benoit, D., Fontanille, M., and Gnanou, Y., *Acyclic β -Phosphonylated Nitroxides: A New Series of Counter-Radicals for "Living"/Controlled Free Radical Polymerization*. *Macromolecules*, 2000, 33, 1141-1147.
55. Benoit, D., Grimaldi, S., Robin, S., Finet, J.-P., Tordo, P., and Gnanou, Y., *Kinetics and Mechanism of Controlled Free-Radical Polymerization of Styrene and n-Butyl Acrylate in the Presence of an Acyclic β -Phosphonylated Nitroxide \ddagger* . *Journal of the American Chemical Society*, 2000, 122, 5929-5939.
56. Nicolas, J., Charleux, B., Guerret, O., and Magnet, S., *Novel SGI-Based Water-Soluble Alkoxyamine for Nitroxide-Mediated Controlled Free-Radical Polymerization of Styrene and n-Butyl Acrylate in Miniemulsion*. *Macromolecules*, 2004, 37, 4453-4463.
57. Nicolas, J., Couvreur, P., and Charleux, B., *Comblike Polymethacrylates with Poly(ethylene glycol) Side Chains via Nitroxide-Mediated Controlled Free-Radical Polymerization*. *Macromolecules*, 2008, 41, 3758-3761.
58. Delplace, V., Harrisson, S., Ho, H. T., Tardy, A., Guillaneuf, Y., Pascual, S., Fontaine, L., and Nicolas, J., *One-Step Synthesis of Azlactone-Functionalized SGI-Based Alkoxyamine for Nitroxide-Mediated Polymerization and Bioconjugation*. *Macromolecules*, 2015, 48, 2087-2097.

59. Nicolas, J., Dire, C., Mueller, L., Belleney, J., Charleux, B., Marque, S. R. A., Bertin, D., Magnet, S., and Couvreur, L., *Living Character of Polymer Chains Prepared via Nitroxide-Mediated Controlled Free-Radical Polymerization of Methyl Methacrylate in the Presence of a Small Amount of Styrene at Low Temperature*. *Macromolecules*, 2006, 39, 8274-8282.

Chapter 8

Conclusions & Future Work



8.1. Overall Conclusions

Reversible deactivation radical polymerization (RDRP) methods have brought about an indisputable advance in the polymer synthesis possibilities with respect to its ultimate goal, the design and synthesis of materials that is only limited by the human imagination. One of the most extensively investigated RDRP techniques is the atom transfer radical polymerization (ATRP), due to the range of polymerizable monomers, versatility, robustness and relatively mild reaction conditions required for polymerizations. The major limitations associated with the ATRP method are the use of metal catalysts, which can contaminate the final product, and sometimes the inevitable use of harmful organic solvents.

To overcome these issues, the first main aim of this PhD work was the development of new ecofriendly catalytic systems. Thus, in Chapter 2 was introduced Food and Drug Administration (FDA) approved inorganic sulfites such as sodium dithionite ($\text{Na}_2\text{S}_2\text{O}_4$), sodium metabisulfite ($\text{Na}_2\text{S}_2\text{O}_5$), and sodium bisulfite (NaHSO_3) as a new class of very efficient reducing agents and supplemental activators (SARA) for ATRP. These compounds allow effective reduction of soluble metal catalysts due to the continues of regeneration *in situ* of Cu(I)X species. This SARA ATRP provided the opportunity to synthesize poly(methyl acrylate) (PMA) with controlled molecular weight, low dispersity ($\mathcal{D} < 1.05$), and well-defined chain-end functionality in combination with catalytic amounts of Cu(II)Br₂/Me₆TREN (Me₆TREN: tris[2-(dimethylamino)ethyl]amine) in dimethyl sulfoxide (DMSO) at ambient temperature (30 °C). It was also found an unusual synergistic effect between an ionic liquid, 1-butyl-3-methylimidazolium hexafluorophosphate (BMIM-PF₆), and DMSO mixtures for this ecofriendly SARA ATRP, presented in Chapter 2.

In order to create conditions for the future industrial implementation of the novel developed inorganic sulfites catalyzed ATRP, new eco-friendly solvents were studied to replace commonly used harmful organic solvents. Thus, in Chapter 3 was presented very successful (co)polymerizations of methyl acrylate (MA), *n*-butyl acrylate (*n*-BA), methyl methacrylate (MMA) and 2-(dimethylamino)ethyl methacrylate (DMAEMA), in green solvents (alcohols and alcohol-water mixtures) at ambient temperature. An important

progress regarding the state-of-art of this area was achieved regarding the establishment of reaction conditions suitable for future scale-up of this technology.

In the same line, in Chapter 4 was introduced the aqueous SARA ATRP using inorganic sulfites. After a careful optimization the reaction parameters, the successful synthesis of well-defined water-soluble polymers (*e.g.*, poly[oligo(ethylene oxide) methyl ether acrylate] (POEOA)) was achieved in aqueous media catalyzed by <30 ppm of Cu(II)Br₂/tris(2-pyridylmethyl)amine (TPMA) using a slow feeding of inorganic sulfites at ambient temperature. The results obtained in Chapter 4 demonstrated that under biologically relevant conditions, aqueous SARA ATRP using inorganic sulfites is very useful for the preparation of well-defined bovine serum albumin protein-polymer hybrids (*e.g.*, BSA-[P(OEOA₄₈₀)₃₀]).

The most successful RDRP of VC, until 2012, had been achieved by single electron transfer degenerative chain transfer living radical polymerization (SET-DTLRP) or Metal Catalyzed RDRP. In order to develop new (co)polymerization RDRP methods of VC, in Chapter 5 was presented reversible addition-fragmentation chain transfer (RAFT) polymerization of VC for the first time. The cyanomethyl methyl(phenyl)carbamodithioate (CMPCD) was found to be an efficient RAFT agent enabling the RDRP polymerization of VC under certain reaction conditions. Thus, PVC products with controlled features (the lowest dispersity ever reported for PVC obtained by any RDRP method, $D \sim 1.4$) and having well preserved functional groups and no structural defects (proved via ¹H NMR and MALDI-TOF-MS experiments) were obtained. The “living” nature of the PVC synthesized via RAFT polymerization method was confirmed by successful chain extension and PVC-based block copolymerization experiments. The work presented in Chapter 5 is of significant importance as opened the door to various macromolecular architectures comprising PVC segments using the advantages associated to the RAFT technique.

In Chapter 6, the SG1-mediated polymerization of VC initiated by the BlocBuilder alkoxyamine was successfully performed at low temperatures (*e.g.*, 30 and 42 °C) and led to improve the control of the resulting PVC compared to early results reported in the literature using other nitroxide structures. It was proved by structural characterizations

(^1H NMR and ^{31}P NMR) the existence of very small content of structural defects and the high preservation (~91%) of the PVC-SG1 chain-end functionalities. PVC-SG1 macroinitiators were successfully used in chain extension experiments to produce different PVC-based copolymers (*e.g.*, PVC-*b*-PMMA and PVC-*b*-P(MMA-*co*-S)) proving the feasibility of NMP to afford different macrostructures based on PVC.

Considering the very promising results that were obtained in Chapters 5 and 6, and in the search of green alternative to the use of toxic solvents (THF, DCM, DMSO and DMF), in the Chapter 7 was demonstrated that cyclopentyl methyl ether (CPME) is suitable (nearly universal) to perform RAFT and NMP of VC and S as well as RAFT of MA and VAc. The structures of the obtained polymers were confirmed by ^1H -NMR, ^{31}P -NMR, MALDI-TOF-MS and the living character was confirmed by successful chain extension and block copolymerization experiments.

To sum up, this PhD work allowed the development of new ATRP systems for vinyl monomers using non-toxic and inexpensive compounds that could provide fast polymerizations in environmentally friendly media. This research also contributed for the development of new VC (co)polymerizations systems using RDRP methods, representing a considerable improvement of RDRP available in the literature.

8.2. Recommendations for Future Work

This work has contributed for the development of new ATRP systems for vinyl monomers using ecofriendly reaction conditions (*e.g.*, non-toxic compounds, environmentally friendly solvents, ambient temperature) that could provide fast and controlled polymerizations. These created conditions are a remarkable advantage for the possibility of scaling-up of the ATRP method. However, there is certainly still room for the improvement especially on:

- ‡ Detailed mechanistic investigations to evaluate the relative contribution of participating elementary reactions during SARA ATRP using inorganic sulfites

should be consider. The developed kinetic model will be a valuable tool, which can be used to further explore and improve the reported SARA ATRP system.

- ‡ The creation of new inexpensive and active ligands, since some of the commercial ligands available for ATRP are relatively expensive (*e.g.*, Me₆TREN, TPMA).

This project has also contributed for the development of new VC (co)polymerizations systems using RDRP methods (*e.g.*, RAFT, NMP). The development of effective RDRP methods for nonactivated monomers, as VC, has also been of outmost importance for a deeper mechanistic understanding of these processes. However, for the future perspective of industrial implementation, the future work should include:

- ‡ The creation specific conditions such as, the use of aqueous media (heterogeneous system), mild reaction conditions and use of compounds available on large scale production.
- ‡ The development of new macromolecules based on PVC. These products will be used to explore the intrinsic characteristics of PVC namely its high versatility.

At this stage, the most important constraint that is associated with the RDRP methods is the high cost compared to the FRP process. Nevertheless, the superior performance of the new RDRP products will certainly justify higher prices and more investment.

Appendices

Appendix A

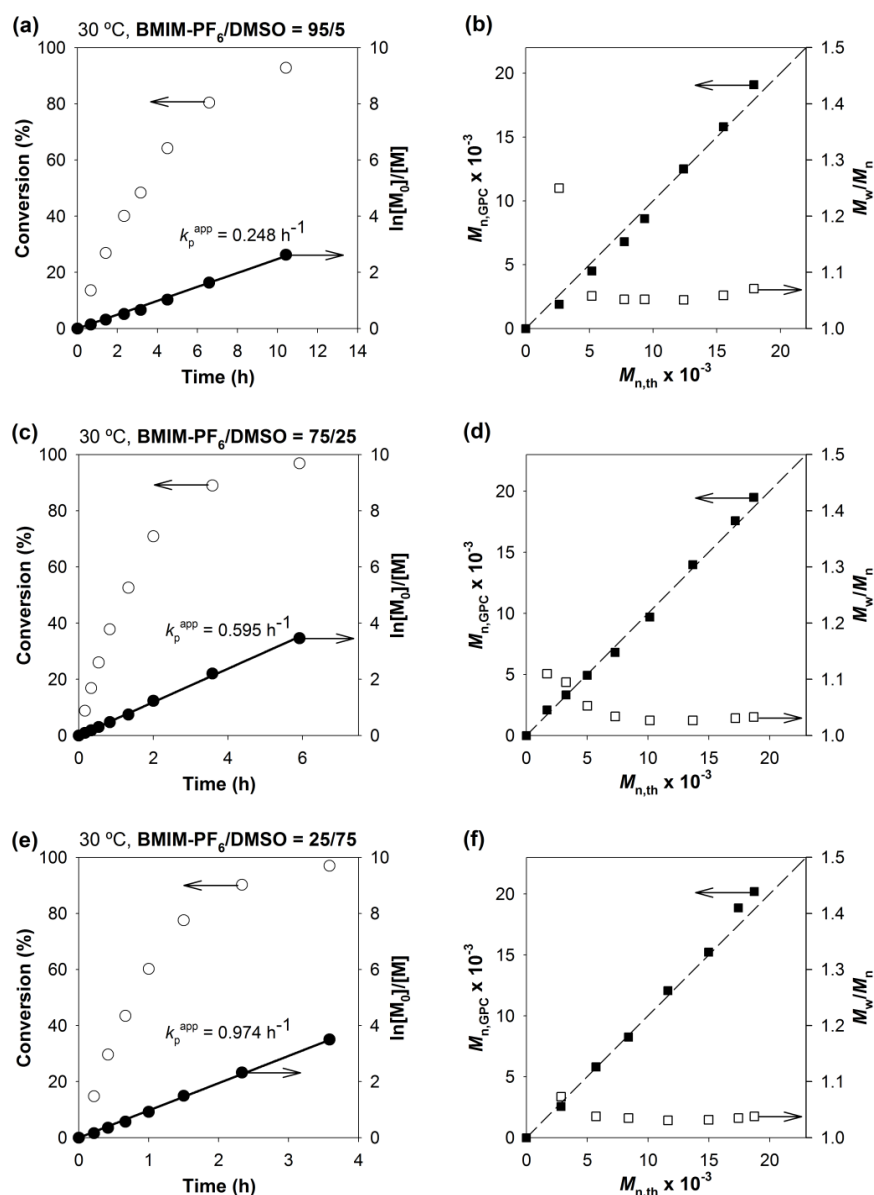
Supporting Information for Chapter 2: *Inorganic Sulfites: Efficient Reducing Agents and Supplemental Activators for Atom Transfer Radical Polymerization*

Figure A.1. (a, c and e) Kinetic plots of conversion and $\ln[M]_0/[M]$ vs. time and (b, d and f) plots of $M_{n, \text{GPC}}$ and \bar{D} (M_w/M_n) vs. $M_{n, \text{th}}$ for the SARA ATRP of MA catalyzed by $\text{Na}_2\text{S}_2\text{O}_4/\text{CuBr}_2/\text{Me}_6\text{TREN}$ in (a and b) BMIM-PF₆/DMSO = 95/5, (c and e) BMIM-

PF₆/DMSO = 75/25 and (e and f) BMIM-PF₆/DMSO = 25/75. Conditions: [MA]₀/[solvent] = 2/1 (v/v); [MA]₀/[EBiB]₀/[Na₂S₂O₄]₀/[CuBr₂]₀/[Me₆TREN]₀ = 222/1/1/0.1/0.1 (molar); T = 30 °C.

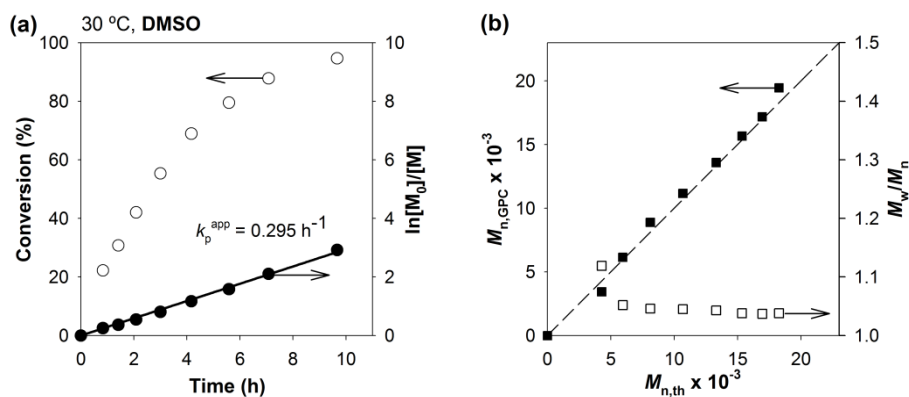


Figure A.2. Kinetic plots of conversion and $\ln[M]_0/[M]$ vs. time (a) and plots of $M_{n,\text{GPC}}$ and \bar{D} (M_w/M_n) vs. $M_{n,\text{th}}$ (b) for the SARA ATRP of MA catalyzed by Na₂S₂O₄/TBA-PF₆/CuBr₂/Me₆TREN in DMSO. Conditions: [MA]₀/[solvent] = 2/1 (v/v); [MA]₀/[EBiB]₀/[Na₂S₂O₄]₀/[TBAPF₆]₀/[CuBr₂]₀/[Me₆TREN]₀ = 222/1/1/3/0.1/0.1 (molar); T = 30 °C.

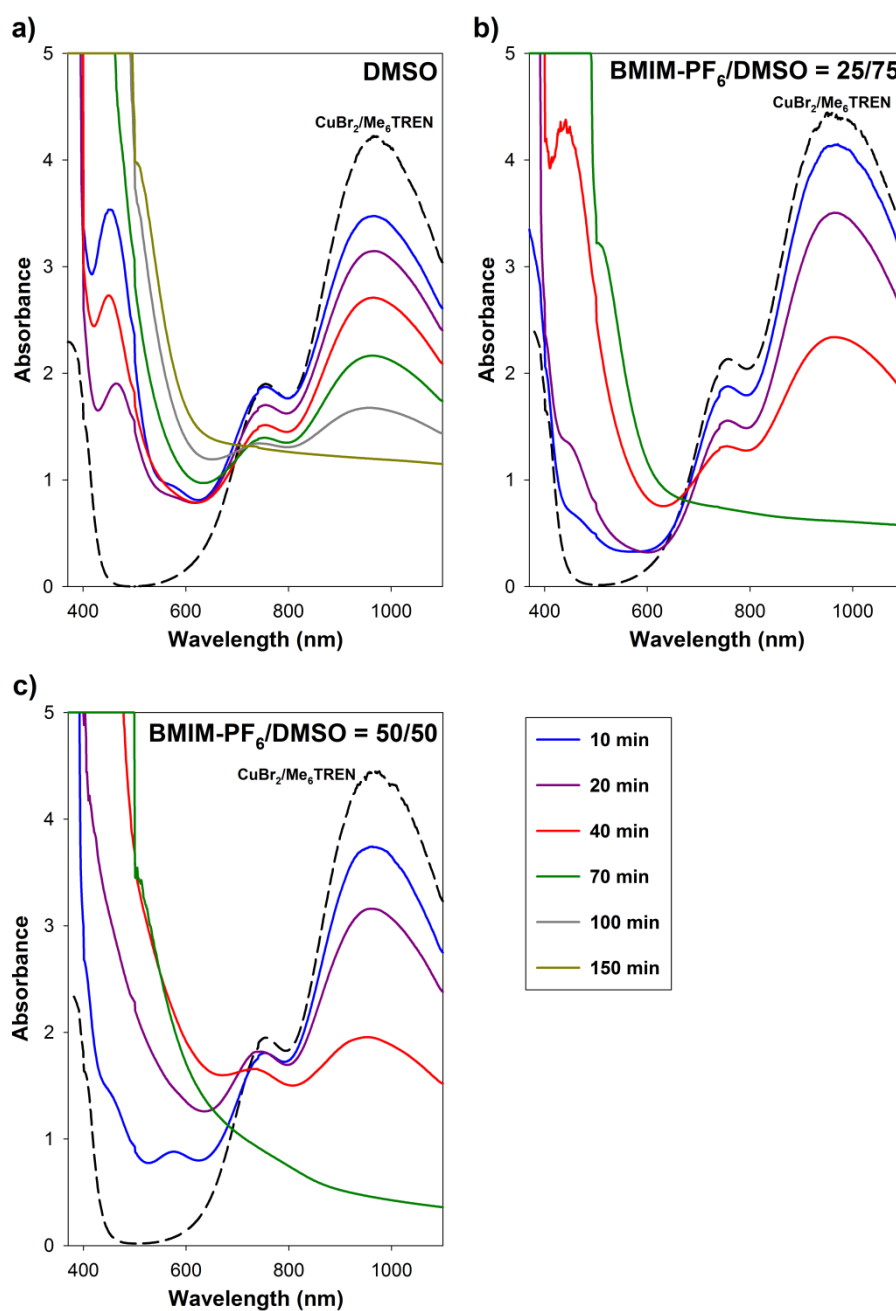


Figure A.3. UV-Vis spectra of reduction of $\text{CuBr}_2/\text{Me}_6\text{TREN}$ by $\text{Na}_2\text{S}_2\text{O}_4$ in (a) pure DMSO, (b) BMIM-PF₆/DMSO (25/75) and (c) BMIM-PF₆/DMSO (50/50) at 30°C .

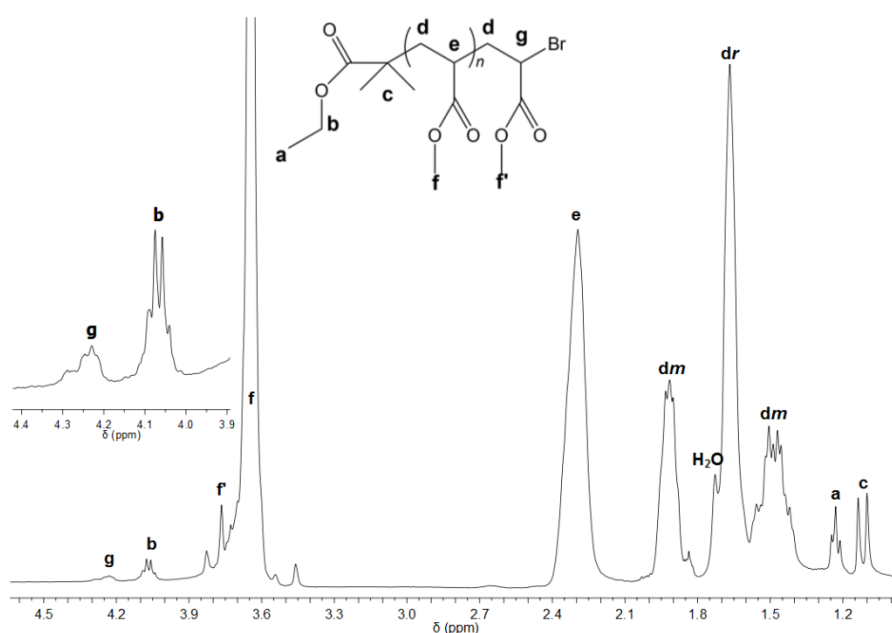


Figure A.4. ^1H NMR spectrum, in CDCl_3 , of PMA-Br obtained by SARA ATRP of MA catalyzed by $\text{Na}_2\text{S}_2\text{O}_4/\text{CuBr}_2/\text{Me}_6\text{TREN}$, in $\text{BMIM-PF}_6/\text{DMSO} = 50/50$ (v/v) at high conversion ($M_{n,\text{GPC}} = 6900$, $\mathcal{D} = 1.05$, $M_{n,\text{NMR}} = 6600$; active chain-end functionality = 92%). Conditions: $[\text{MA}]_0/[\text{solvent}] = 2/1$ (v/v); $[\text{MA}]_0/[\text{EBiB}]_0/[\text{Na}_2\text{S}_2\text{O}_4]_0/[\text{CuBr}_2]_0/[\text{Me}_6\text{TREN}]_0 = 222/1/1/0.1/0.1$ (molar); $T = 30$ °C. The PMA is atactic: $[\text{dr}] = [\text{dm}] = 0.5$.

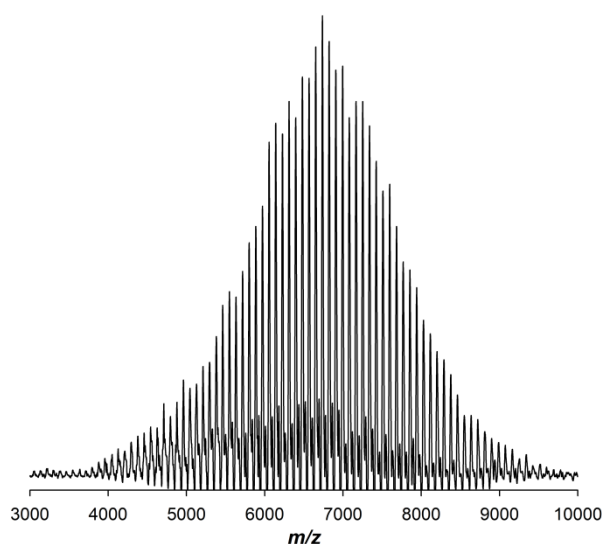


Figure A.5. MALDI-TOF-MS in the linear mode (using HABA as matrix) of PMA-Br ($M_{n,\text{GPC}} = 6.9 \times 10^3$, $\mathcal{D} = 1.05$) obtained by SARA ATRP of MA catalyzed by $\text{Na}_2\text{S}_2\text{O}_4/\text{CuBr}_2/\text{Me}_6\text{TREN}$, in $\text{BMIM-PF}_6/\text{DMSO} = 50/50$ (v/v). Conditions: $[\text{MA}]_0/[\text{solvent}] = 2/1$ (v/v); $[\text{MA}]_0/[\text{EBiB}]_0/[\text{Na}_2\text{S}_2\text{O}_4]_0/[\text{CuBr}_2]_0/[\text{Me}_6\text{TREN}]_0 = 222/1/1/0.1/0.1$ (molar); $T = 30$ °C.

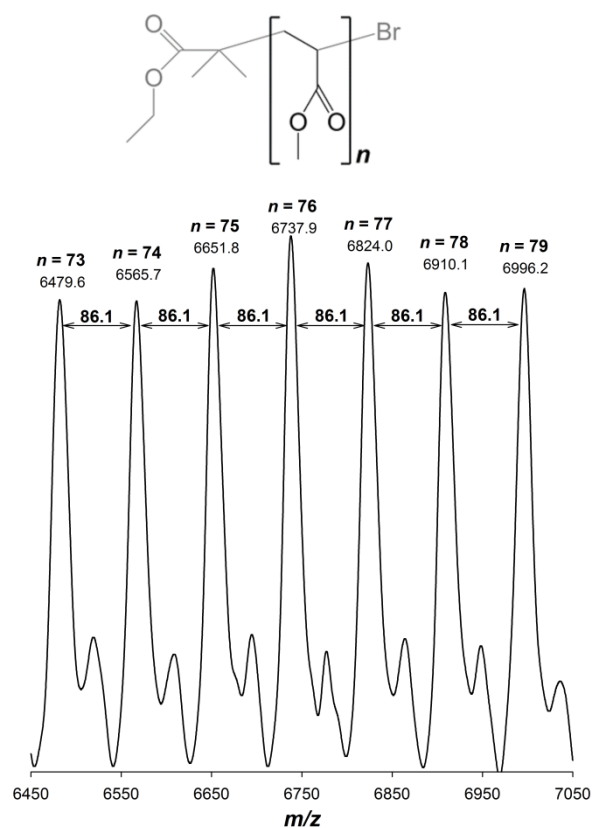


Figure A.6. Enlargement of the MALDI-TOF-MS from m/z 6450 to 7050 of PMA-Br ($M_{n,GPC} = 6.9 \times 10^3$, $\mathcal{D} = 1.05$) obtained by SARA ATRP of MA catalyzed by $\text{Na}_2\text{S}_2\text{O}_4/\text{CuBr}_2/\text{Me}_6\text{TREN}$, in $\text{BMIM-PF}_6/\text{DMSO} = 50/50$ (v/v). Conditions: $[\text{MA}]_0/[\text{solvent}] = 2/1$ (v/v); $[\text{MA}]_0/[\text{EBiB}]_0/[\text{Na}_2\text{S}_2\text{O}_4]_0/[\text{CuBr}_2]_0/[\text{Me}_6\text{TREN}]_0 = 222/1/1/0.1/0.1$ (molar); $T = 30^\circ\text{C}$.

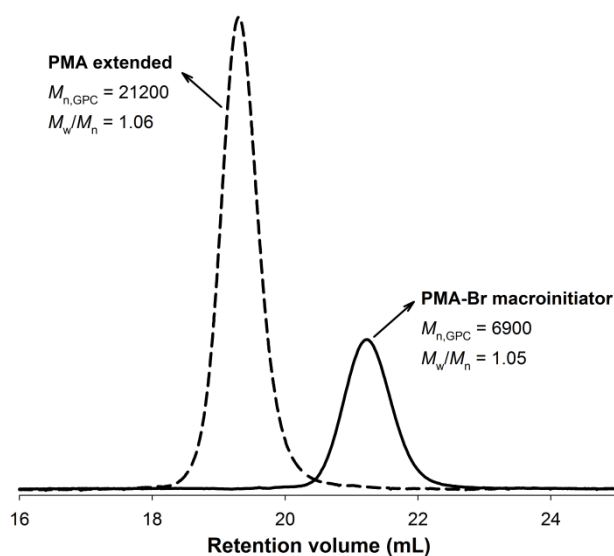


Figure A.7. GPC traces of the PMA before (right curve) and after the chain extension (left curve) experiment.

Appendix B

Supporting Information for Chapter 3: *Ambient Temperature Rapid SARA ATRP in Ecofriendly Solvents Mediated by Inorganic Sulfite/Cu(II)Br₂ Catalytic System*

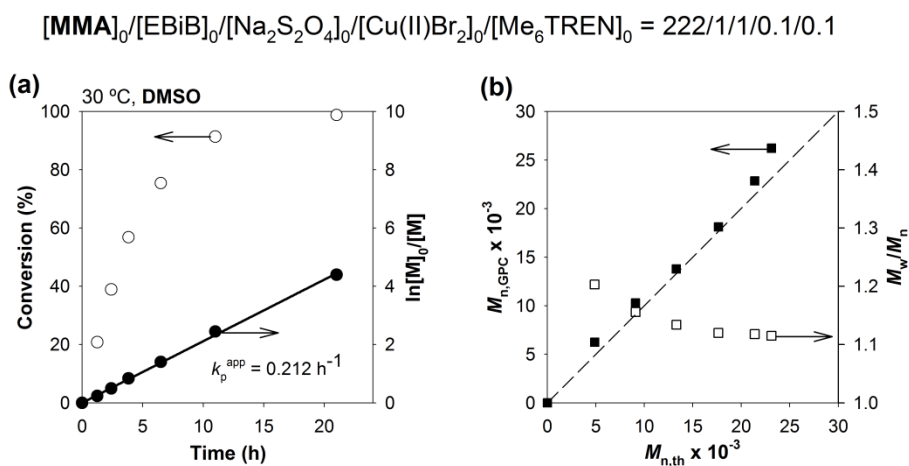


Figure B.1. Kinetic plot of conversion and $\ln[M]_0/[M]$ vs. time (a) and plot of $M_{n,\text{GPC}}$ and \bar{D} (M_w/M_n) vs. $M_{n,\text{th}}$ (b) for ATRP of MMA catalyzed with $\text{Na}_2\text{S}_2\text{O}_4$ in the presence of $\text{Cu(II)Br}_2/\text{Me}_6\text{TREN}$ at 30 °C in DMSO. Conditions: $[\text{MMA}]_0/[\text{DMSO}] = 2/1$ (v/v); $[\text{MMA}]_0/[\text{EBiB}]_0/[\text{Na}_2\text{S}_2\text{O}_4]_0/[\text{Cu(II)Br}_2]_0/[\text{Me}_6\text{TREN}]_0 = 222/1/1/0.1/0.1$.

Appendix C

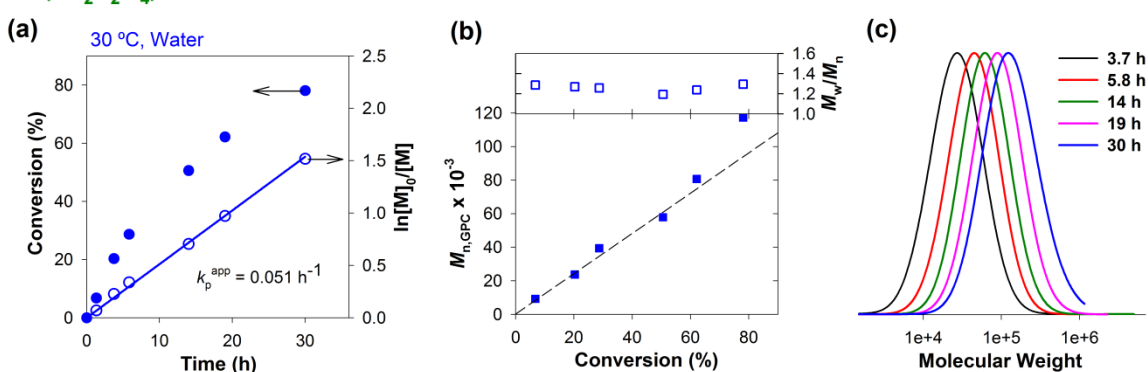
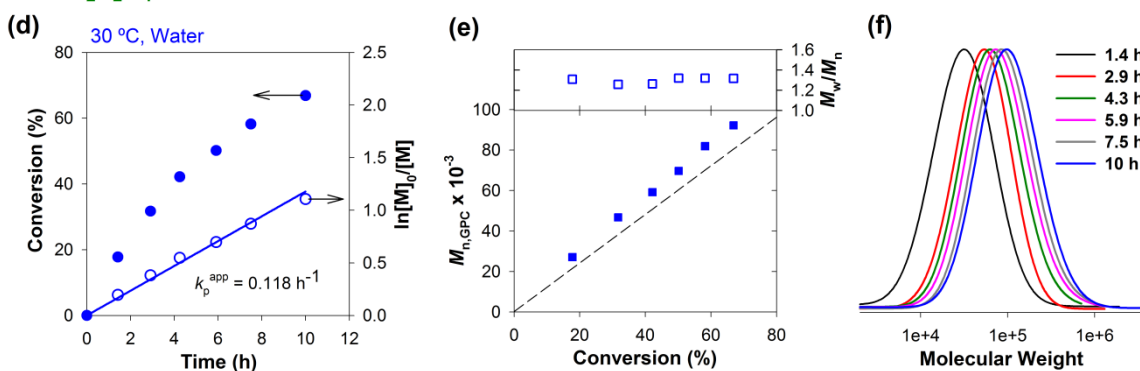
Supporting Information for Chapter 4: *Aqueous Supplemental Activator and Reducing Agent Atom Transfer Radical Polymerization Using Inorganic Sulfites*FR(Na₂S₂O₄) = 16 nmol/minFR(Na₂S₂O₄) = 32 nmol/min

Figure C.1. (a and d) Kinetic plots of conversion and $\ln[M]_0/[M]$ vs. time; (b and e) plot of $M_{n,GPC}$ and $D (M_w/M_n)$ vs. conversion for aqueous SARA ATRP of OEOA₄₈₀ at 30 °C; and (c and f) GPC traces vs. time. Conditions: $[OEOA_{480}]_0/[HEBiB]_0/[Cu(II)Br_2]_0/[TPMA]_0 = 250/1/0.05/0.4$; FR(Na₂S₂O₄) = 16 (a, b and c) and 32 (d, e and f) nmol/min ; $[NaCl]_0 = 100$ mM; $[OEOA_{480}]_0/[Water] = 1/3$.

Appendix D

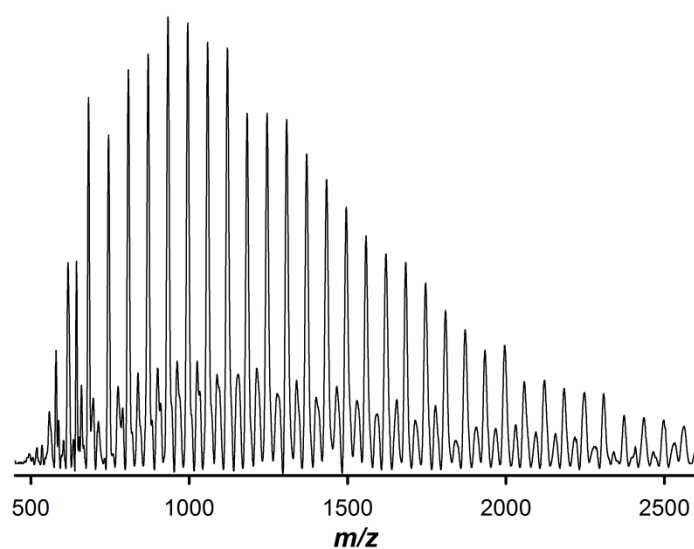
Supporting Information for Chapter 5: *Reversible Addition-Fragmentation Chain Transfer (co)Polymerization of Vinyl Chloride*

Figure D.1. MALDI-TOF-MS in the linear mode (using α -cyano-4-hydroxycinnamic acid (CHCA) as matrix) of RAFT-PVC ($M_n^{\text{GPC}} = 3300$; $D = 1.48$) mediated by CMPCD.

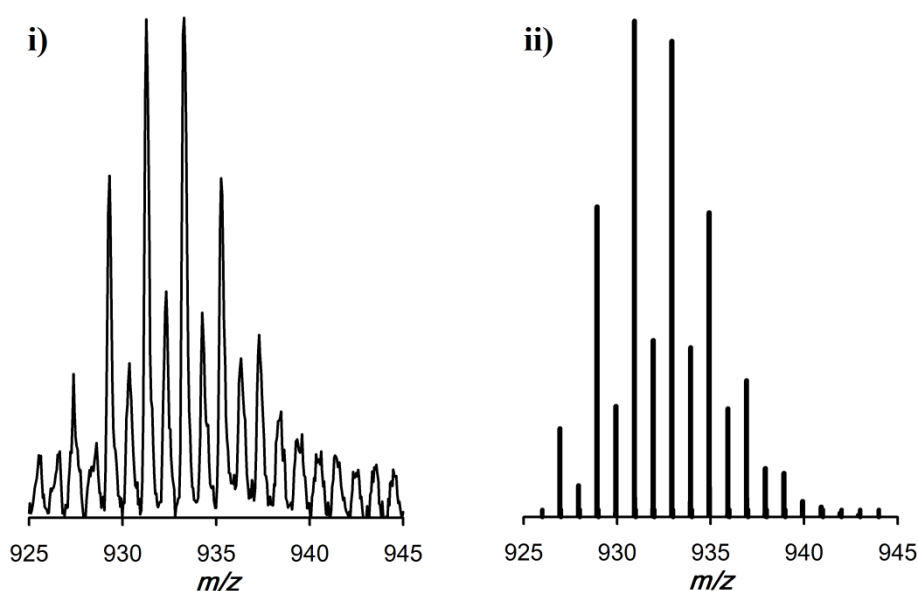


Figure D.2. (i) Enlargement of the MALDI-TOF-MS in the reflectron mode from m/z 925 to 945 and (ii) theoretical isotope distribution of the m/z 925-945 region ($DP = 11$, $C_{32}H_{43}Cl_{11}N_2S_2Na$) using *Isotope Distribution Calculator* software.

Computational Procedures

To assist in the selection of a suitable RAFT agent, standard *ab initio* molecular orbital theory and density functional theory calculations were carried out using Gaussian 09¹ and Molpro 2009.1.² Calculations were performed at a high level of theory that was based on our previous assessment studies for RAFT reactions,³ and recently shown to reproduce experimental equilibrium constants to within chemical accuracy.^{4,5} For all species, either full systematic conformational searches (at a resolution of 120⁰) or, for more complex systems, energy-directed tree searches⁶ were carried out to ensure global, and not merely local minima were located. These were performed at the B3LYP/6-31G(d) level of theory in a THF solution at 25 °C to mimic experimental conditions. The PCM⁷ solvent model was used in conjunction with UAKS model of spheres radii, and an electrostatic scaling factor was set equal to the recommended value of 1.2.⁸ Geometries of the solution-phase lowest energy conformers of all species were then relaxed in the gas phase at the B3LYP/6-31G(d) level, and frequencies were also calculated at the same level and scaled by recommended scale factors.⁹ Accurate gas-phase electronic energies were calculated using a three-layer ONIOM approach described previously.^{10,11} The core layer was treated using the W1 procedure,¹² the G3(MP2)-RAD¹³ method was applied to describe the effects of the primary substituents, and the full system was calculated using R(O)MP2/6-311+G(3df,2p) method. Gas-phase entropies and thermal corrections at 42 °C were calculated using standard textbook formulas¹⁴ for the statistical thermodynamics of an ideal gas under the harmonic oscillator approximation in conjunction with the optimized geometries and scaled frequencies. Free energies of solvation for all species were calculated at the UAKS-PCM/B3LYP/6-31G(d) level of theory at 25 °C and corrected for the phase change correction term $RT(\ln V)$. Equilibrium constants were determined according to the equation:

$$K(T) = (c^0)^{\Delta n} \exp\left(\frac{-\Delta G}{RT}\right)$$

where c^0 is the standard concentration unit equal to 1 mol L⁻¹ in solution.

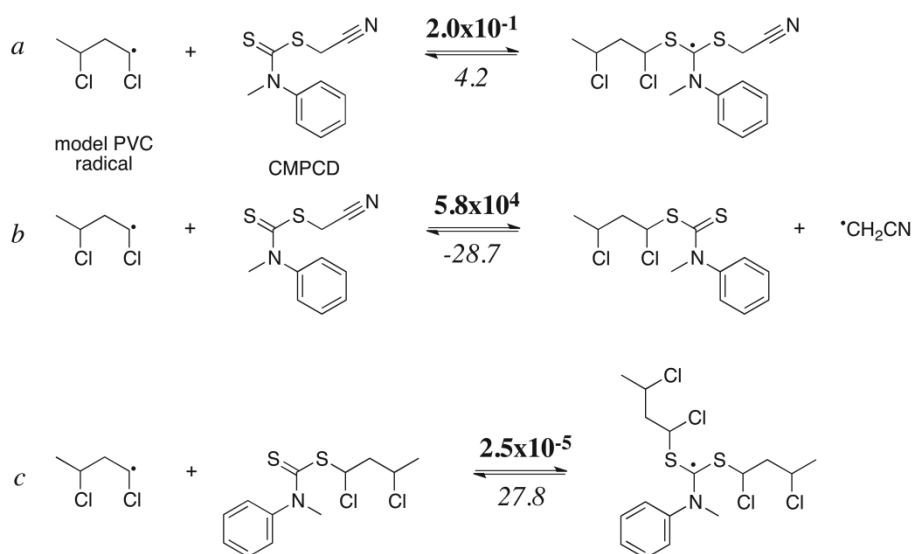
Computational Results

VC belongs to the so-called non-activated (or less activated) vinyl monomer class, which is characterized by having propagating radicals with relatively low radical stabilities. For instance, based on its calculated radical stabilization energy of 27.0 kJ mol^{-1} at the G3(MP2)-RAD level of theory, a unimeric VC propagating radical is only slightly more stabilized than the corresponding vinyl acetate derived unimeric propagating radical (24.4 kJ mol^{-1}), and considerably less than corresponding values for such activated monomers as methyl acrylate (41.3 kJ mol^{-1}), methyl methacrylate (54.9 kJ mol^{-1}) or styrene (68.0 kJ mol^{-1}).¹⁵ Less activated monomers pose two key problems when selecting an appropriate RAFT agent. First, the relatively low stabilities of their propagating radicals render them poor leaving groups from standard dithioester-type RAFT agents, leading to significant inhibition or rate retardation effects. Second, many of the typical leaving groups in initial RAFT agents do not readily reinitiate polymerization of unactivated monomers.¹⁶

To address the first problem, one typically uses RAFT agents such as xanthates or dithiocarbamates in which the “Z-group” of the RAFT agent is a lone pair donor that can undergo resonance with the thiocarbonyl group. This resonance stabilizes the RAFT agent relative to the RAFT-adduct radical, helping to promote fragmentation. In the present work we have opted for a dithiocarbamate, cyanomethyl methyl(phenyl)carbomodithioate (CMPCD, see below the model thermodynamic measures), which has already found success in the control of other unactivated monomers.¹⁶ Moreover, the $\bullet\text{CH}_2\text{CN}$ leaving group of this RAFT agent is known to be an effective initiating species for VC (e.g., Fischer and Radom report a rate coefficient of $1.2 \times 10^4 \text{ L mol}^{-1} \text{ s}^{-1}$ at $5 \text{ }^\circ\text{C}$),¹⁷ thereby simultaneously addressing the second problem. At the same time, based on previously published model calculations, this leaving group would be expected to undergo preferential fragmentation from intermediate radical.^{15,18}

To confirm that this RAFT agent would be suitable, we calculated the equilibrium constant for the addition of a dimeric VC propagating radical to CMPCD (Reaction *a* in Scheme D.1) in THF solution at $42 \text{ }^\circ\text{C}$ and also to the corresponding “polyRAFT” agent where the CH_2CN leaving group is replaced by the VC dimer radical (Reaction *c* in

Scheme D.1). In both cases, the equilibrium constants (2.0×10^{-1} and 2.5×10^{-5} L mol⁻¹ respectively) are much less than the values of 10^6 L mol⁻¹ or more typically associated with rate retardation.^{19,20} We also calculated the equilibrium constant of the chain transfer reaction in the pre-equilibrium (Reaction *b* in Scheme D.1) to confirm that fragmentation of the $\cdot\text{CH}_2\text{CN}$ leaving group is strongly favored in the pre-equilibrium, as is required for efficient chain transfer. Hence, based on these results, CMPCD is expected to be a suitable RAFT agent for control of VC polymerization.

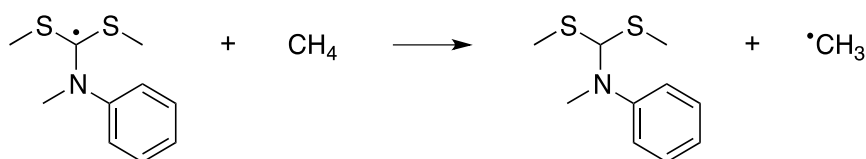


Scheme D.1. Equilibrium constants (**bold; L mol⁻¹**) and corresponding Gibbs free energies (*italics; kJ mol⁻¹*) of addition (*a* and *c*) and chain transfer (*b*) reactions in THF at 42 °C, calculated using three-layer ONIOM approximation for electronic energies and UAKS-PCM/B3LYP/6-31G(d) method for solvation free energies.

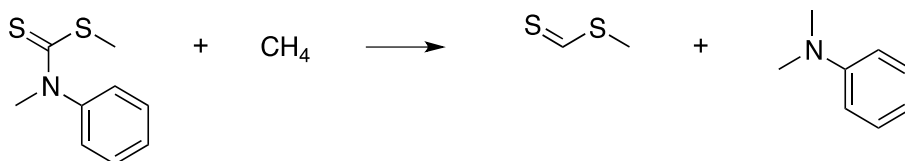
Model Thermodynamic Measures for CMPCD RAFT Agent

In all cases thermodynamic measures of the studied species are the gas-phase enthalpy changes at 0 K (ΔH^0).

1. Radical Stabilization Energy (RSE) = 77.9 kJ mol⁻¹:



2. Stability of the RAFT agent = 95.0 kJ mol⁻¹:



3. Fragmentation Efficiency = -36.7 kJ mol⁻¹:

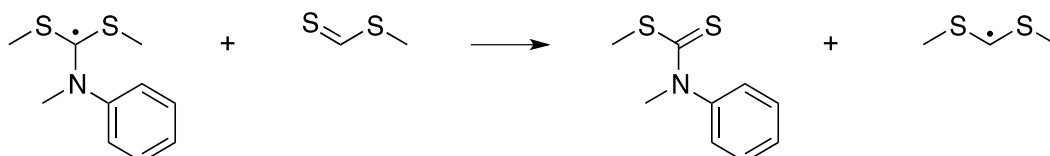


Table D.1. Gas and solution-phase energetics at 315.15 K of reactions in Scheme D.1.

Reactions	$\Delta S_{gas}, \text{J mol}^{-1} \text{K}^{-1}$	$\Delta H_{gas}, \text{J mol}^{-1}$	$\Delta G_{gas}, \text{J mol}^{-1}$	$\Delta G_{THF}, \text{J mol}^{-1}$
A	-189.223	-61.541	-1.908	1.870
B	-19.875	-30.892	-24.628	-28.729
C	-192.940	-56.370	4.435	-3.251

Table D.2. Contributions to the 0 K enthalpies of species in the model calculations.^a

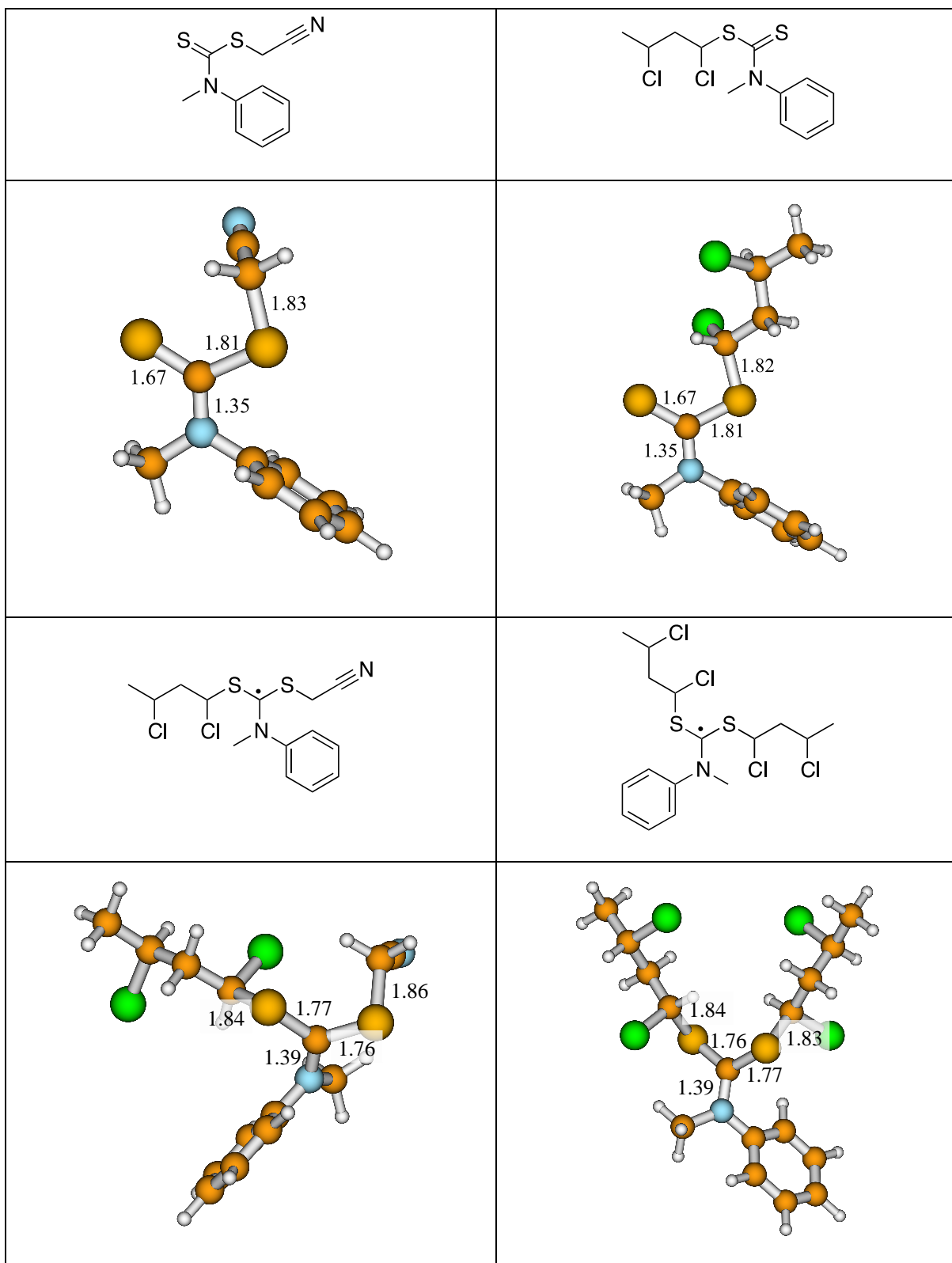
Species	E_{gas}^0 ^b	ZPVE	H_{gas}^0
CH ₄	-40.46516	0.04436	-40.42080
CH ₃ •	-39.78519	0.02926	-39.75592
S=CHSCH ₃	-874.01688	0.05495	-873.96193
•CH(SCH ₃) ₂	-913.83688	0.09078	-913.74609
CMPCD	-1199.31564	0.17893	-1199.13671
CMPCD•CH ₃	-1239.12195	0.21507	-1238.90688
CMPCD-CH ₃	-1239.76970	0.22762	-1239.54208
N(CH ₃) ₂ C ₆ H ₅	-365.73041	0.17101	-365.55940

^a All quantities are given in Hartrees; ^b Found with a G3(MP2)-RAD method.

Table D.3. Contributions to the gas and solution-phase free energies of species in this study at 315.15 K.

Layer	Species	E_{rms} , Hartrees		E_{gas}^0 , Hartrees	S_{gas} , J mol ⁻¹ K ⁻¹	T_{cs} , Hartrees	ZPVE, Hartrees	G_{gas} , Hartrees	G_{obs} , kcal mol ⁻¹
		W1	R(O)MP2 ^a						
1	CH ₃ [•]	-39.84338	-39.78519						
2	•VC (monomer)		-538.20676	-538.06690					
3	•VC (dimer)			-1075.62098	380.636	0.00934	0.09934	-1075.75624	-2.68
1	S=CHSCH ₃	-876.93905	-874.01089						
2	CMPCD		-1291.43818	-1290.95158					
3	CMPCD			-1290.95158	536.060	0.01657	0.17774	-1294.23638	-7.99
1	CH(SCH ₃) ₂	-916.82254	-913.83768						
2	CMPCD•VC (monomer)		-1829.67099	-1829.04363					
3	CMPCD•VC (dimer)			-2366.60014	727.472	0.02590	0.28044	-2369.99334	-7.73
2	•VC (monomer)		-538.20676	-538.06690					
3	•VC (dimer)			-1075.62098	380.636	0.00934	0.09934	-1075.69785	-2.68
2	CMPCD		-1291.43818	-1290.95158					
3	CMPCD			-1290.95158	536.060	0.01657	0.17774	-1291.30822	-7.99
2	•CH ₂ CN		-131.92386	-131.82433					
3	•CH ₂ CN			-131.82433	256.641	0.00490	0.03063	-131.91914	-9.63
2	CMPCD(-CH ₂ CN)-VC (monomer)		-1697.73015	-1697.20365					
3	CMPCD(-CH ₂ CN)-VC (dimer)			-2234.75957	640.180	0.02159	0.24501	-2235.09632	-2.02
1	CH ₃ [•]	-39.84338	-39.78519						
2	•VC (monomer)		-538.20676	-538.06690					
3	•VC (dimer)			-1075.62098	380.636	0.00934	0.09934	-1075.61638	-2.68
1	S=CHSCH ₃	-876.93905	-874.01089						
2	CMPCD(-CH ₂ CN)-VC (monomer)		-1697.73015	-1697.20365					
3	CMPCD(-CH ₂ CN)-VC (dimer)			-2234.75957	640.180	0.02159	0.24501	-2237.49798	-2.02
1	CH(SCH ₃) ₂	-916.82254	-913.83768						
2	CMPCD(-CH ₂ CN)•VC ₂ (monomer)			-2235.29128					
3	CMPCD(-CH ₂ CN)•VC ₂ (dimer)			-3310.40712	827.875	0.03083	0.34786	-3313.11267	-4.50

^a Found with a 6-311+G(3df,2p) basis set; ^b Value used in the determination of G_{gas} ; ^c In THF at 25 °C, calculated using UAKS-PCM/B3LYP/6-31G(d) method.

Optimized geometries of the CMPCD + VC (dimer) adducts, THF, UAKS-PCM/6-31G(d).

References

1. Frisch, M. J., Trucks, G. W., Schlegel, H. B., Scuseria, G. E., Robb, M. A., Cheeseman, J. R., Scalmani, G., Barone, V., Mennucci, B., Petersson, G. A., Nakatsuji, H., Caricato, M., Li, X., Hratchian, H. P., Izmaylov, A. F., Bloino, J., Zheng, G., Sonnenberg, J. L., Hada, M., Ehara, M., Toyota, K., Fukuda, R., Hasegawa, J., Ishida, M., Nakajima, T., Honda, Y., Kitao, O., Nakai, H., Vreven, T., Montgomery Jr., J. A., Peralta, J. E., Ogliaro, F., Bearpark, M., Heyd, J. J., Brothers, E., Kudin, K. N., Staroverov, V. N., Kobayashi, R., Normand, J., Raghavachari, K., Rendell, A., Burant, J. C., Iyengar, S. S., Tomasi, J., Cossi, M., Rega, N., Millam, N. J., Klene, M., Knox, J. E., Cross, J. B., Bakken, V., Adamo, C., Jaramillo, J., Gomperts, R., Stratmann, R. E., Yazyev, O., Austin, A. J., Cammi, R., Pomelli, C., Ochterski, J. W., Martin, R. L., Morokuma, K., Zakrzewski, V. G., Voth, G. A., Salvador, P., Dannenberg, J. J., Dapprich, S., Daniels, A. D., Farkas, Ö., Foresman, J. B., Ortiz, J. V., Cioslowski, J., and Fox, D. J. G., *Gaussian 09*. Gaussian 09, **2009**, Wallingford CT, USA: Gaussian, Inc.
2. Werner, H.-J., Knowles, P. J., Knizia, G., Manby, F. R., Schütz, M., Celani, P., Korona, T., Lindh, R., Mitrushenkov, A., Rauhut, G., Shamasundar, K. R., Adler, T. B., Amos, R. D., Bernhardsson, A., Berning, A., Cooper, D. L., Deegan, M. J. O., Dobbyn, A. J., Eckert, F., Goll, E., Hampel, C., Hesselmann, A., Hetzer, G., Hrenar, T., Jansen, G., Köppl, C., Liu, Y., Lloyd, A. W., Mata, R. A., May, A. J., McNicholas, S. J., Meyer, W., Mura, M. E., Nicklass, A., O'Neill, D. P., Palmieri, P., Peng, D., Pflüger, K., Pitzer, R., Reiher, M., Shiozaki, T., Stoll, H., Stone, A. J., Tarroni, R., Thorsteinsson, T., and Wang, M., *MOLPRO, version 2012.1, a package of ab initio programs*, **2012**, see <http://www.molpro.net>.
3. Izgorodina, E. I. and Coote, M. L., *Reliable low-cost theoretical procedures for studying addition-fragmentation in RAFT polymerization*. *Journal of Physical Chemistry A*, **2006**, *110*, 2486-2492.
4. Lin, C. Y. and Coote, M. L., *How Well Can Theory Predict Addition-Fragmentation Equilibrium Constants in RAFT Polymerization?* *Australian Journal of Chemistry*, **2009**, *62*, 1479-1483.
5. Chernikova, E., Golubev, V., Filippov, A., Lin, C. Y., and Coote, M. L., *Use of spin traps to measure the addition and fragmentation rate coefficients of small molecule RAFT-adduct radicals*. *Polymer Chemistry*, **2010**, *1*, 1437-1440.
6. Izgorodina, E. I., Lin, C. Y., and Coote, M. L., *Energy-directed tree search: an efficient systematic algorithm for finding the lowest energy conformation of molecules*. *Physical Chemistry Chemical Physics*, **2007**, *9*, 2507-2516.
7. Tomasi, J., Mennucci, B., and Cammi, R., *Quantum mechanical continuum solvation models*. *Chemical Reviews*, **2005**, *105*, 2999-3093.
8. Brinck, T., Larsen, A. G., Madsen, K. M., and Daasbjerg, K., *Solvation of carbanions in organic solvents: A test of the polarizable continuum model*. *Journal of Physical Chemistry B*, **2000**, *104*, 9887-9893.

9. Merrick, J. P., Moran, D., and Radom, L., *An evaluation of harmonic vibrational frequency scale factors*. Journal of Physical Chemistry A, **2007**, *111*, 11683-11700.
10. Izgorodina, E. I., Brittain, D. R. B., Hodgson, J. L., Krenske, E. H., Lin, C. Y., Namazian, M., and Coote, M. L., *Should contemporary density functional theory methods be used to study the thermodynamics of radical reactions?* Journal of Physical Chemistry A, **2007**, *111*, 10754-10768.
11. Lin, C. Y., Hodgson, J. L., Namazian, M., and Coote, M. L., *Comparison of G3 and G4 Theories for Radical Addition and Abstraction Reactions*. Journal of Physical Chemistry A, **2009**, *113*, 3690-3697.
12. Martin, J. M. L. and de Oliveira, G., *Towards standard methods for benchmark quality ab initio thermochemistry - W1 and W2 theory*. Journal of Chemical Physics, **1999**, *111*, 1843-1856.
13. Henry, D. J., Sullivan, M. B., and Radom, L., *G3-RAD and G3X-RAD: Modified Gaussian-3 (G3) and Gaussian-3X (G3X) procedures for radical thermochemistry*. Journal of Chemical Physics, **2003**, *118*, 4849-4860.
14. Steinfeld, J. I., Francisco, J. S., and Hase, W. L., *Chemical Kinetics and Dynamics*, **1989**, Englewood Cliffs: Prentice Hall.
15. Krenske, E. H., Izgorodina, E. I., and Coote, M. L., in *Controlled/Living Radical Polymerization: From Synthesis to Materials*, K. Matyjaszewski, Editor **2006**, American Chemical Society: Washington DC. p. 406-420.
16. Moad, G., Rizzardo, E., and Thang, S. H., *Toward living radical polymerization*. Accounts of Chemical Research, **2008**, *41*, 1133-1142.
17. Fischer, H. and Radom, L., *Factors controlling the addition of carbon-centered radicals to alkenes-an experimental and theoretical perspective*. Angewandte Chemie-International Edition, **2001**, *40*, 1340-1371.
18. , Based on the data in Table II of Reference 37, the chain transfer reaction $\bullet\text{CH}_2\text{CN} + \text{S}=\text{C}(\text{CH}_3)\text{S}-\text{CH}(\text{CH}_3)\text{Cl} \rightarrow \bullet\text{CH}(\text{CH}_3)\text{Cl} + \text{S}=\text{C}(\text{CH}_3)\text{S}-\text{CH}_2\text{CN}$ would be exothermic by 27.1 kJ mol⁻¹; it would be reasonable to assume similar qualitative results would be obtained for other RAFT-agent Z-groups.
19. Vana, P., Davis, T. P., and Barner-Kowollik, C., *Kinetic analysis of reversible addition fragmentation chain transfer (RAFT) polymerizations: Conditions for inhibition, retardation, and optimum living polymerization*. Macromolecular Theory and Simulations, **2002**, *11*, 823-835.
20. Coote, M. L., Krenske, E. H., and Izgorodina, E. I., *Computational studies of RAFT polymerization - Mechanistic insights and practical applications*. Macromolecular Rapid Communications, **2006**, *27*, 473-497.

Appendix E

Supporting Information for Chapter 6: Nitroxide-Mediated (co)Polymerization of Vinyl Chloride at Low Temperature

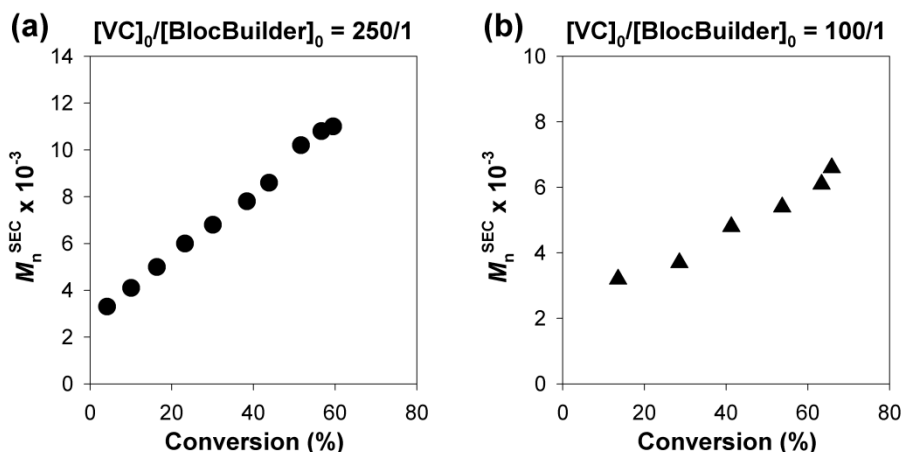


Figure E.1. NMP of VC in DCM at 42 °C initiated by the SG1-based BlocBuilder alkoxyamine. Number-average molecular weight (M_n^{SEC}) vs. conversion for different target DP_n values: (a) 250 and (b) 100. Reaction conditions: $[VC]_0/[BlocBuilder]_0 = DP_n/1$; $[VC]_0/[solvent] = 1/1$ (v/v).

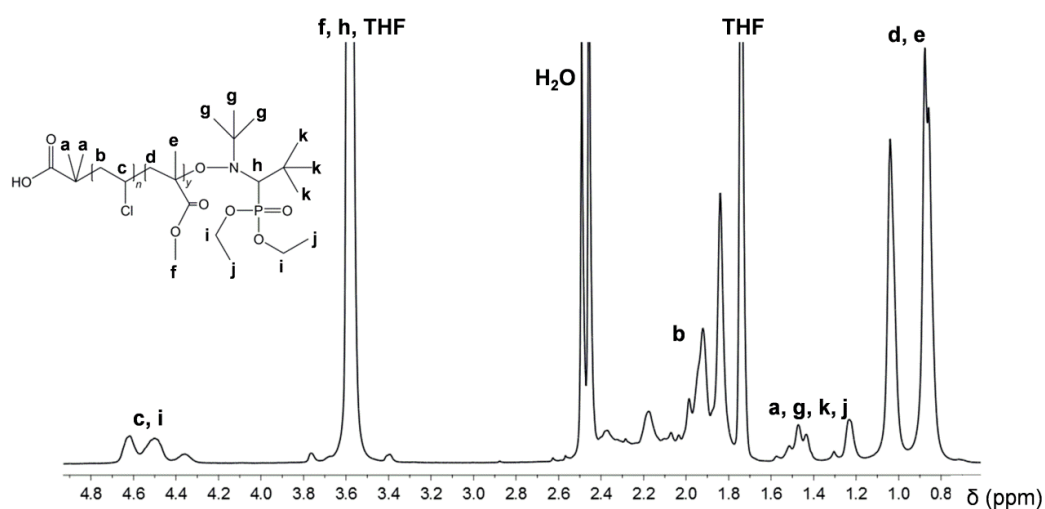


Figure E.2. ^1H NMR spectrum in d_8 -THF of the PVC-*b*-PMMA diblock copolymer (conv._{MMA} = 45.5%, $M_n^{\text{th}} = 52100$, $M_n^{\text{SEC}} = 44700$, $D = 1.89$) obtained by NMP in DMSO. Reaction conditions: $[MMA]_0/[PVC\text{-}SG1]_0 = 1000/1$; $[MMA]_0/[DMSO] = 1/1$ (v/v).

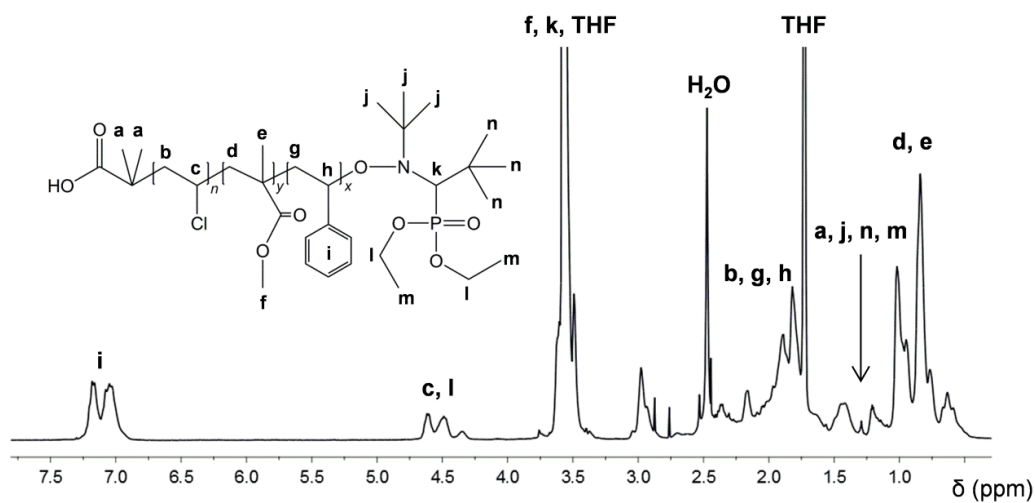


Figure E.3. ^1H NMR spectrum in d_3 -THF of the PVC-*b*-P(MMA-*co*-S) block copolymer ($\text{conv.}_{\text{MMA}} = 34.5\%$, $\text{conv.}_{\text{S}} = 36.8\%$, $M_n^{\text{th}} = 44800$, $M_n^{\text{SEC}} = 36400$, $\mathcal{D} = 1.78$) obtained by NMP in DMF. Reaction conditions: $[\text{MMA}]_0/[\text{S}]_0/[\text{PVC-SG1}]_0 = 1000/100/1$; $[\text{MMA} + \text{S}]_0/[\text{DMF}] = 1/1$ (v/v).

Details of theoretical procedures

Quantum Chemical Calculations

Standard *ab initio* molecular orbital theory and density functional theory (DFT) calculations were carried out using Gaussian 09,¹ with the exception of CCSD(T) calculations, which were performed using Molpro 2012.² Calculations on radicals were performed with an unrestricted wave function except in cases designated with an “R” prefix where a restricted open-shell wave function was used. Calculations were performed at a high-level of theory, previously shown to predict accurate values for the kinetics and thermodynamics of a wide range of radical reactions.^{3,4,5,6}

Geometries of all species were optimised at the M06-2X/6-31G(d) level of theory and frequencies were also calculated at this same level and scaled by recommended scaling factors.⁷ All geometries were verified as local minima – possessing no imaginary frequencies. Polymeric radicals and their corresponding alkoxyamines were modelled as dimers to include the penultimate unit effect. Consistent with previous work,⁸ the OEt groups of the P(=O)(OEt)₂ moiety of SG1 radicals (and their corresponding alkoxyamines) were truncated to OMe groups. Accurate energies for all species were

¹ Gaussian 09, Revision **D.01**, M. J. Frisch, G. W. Trucks, H. B. Schlegel, G. E. Scuseria, M. A. Robb, J. R. Cheeseman, G. Scalmani, V. Barone, B. Mennucci, G. A. Petersson, H. Nakatsuji, M. Caricato, X. Li, H. P. Hratchian, A. F. Izmaylov, J. Bloino, G. Zheng, J. L. Sonnenberg, M. Hada, M. Ehara, K. Toyota, R. Fukuda, J. Hasegawa, M. Ishida, T. Nakajima, Y. Honda, O. Kitao, H. Nakai, T. Vreven, J. A. Montgomery, Jr., J. E. Peralta, F. Ogliaro, M. Bearpark, J. J. Heyd, E. Brothers, K. N. Kudin, V. N. Staroverov, R. Kobayashi, J. Normand, K. Raghavachari, A. Rendell, J. C. Burant, S. S. Iyengar, J. Tomasi, M. Cossi, N. Rega, J. M. Millam, M. Klene, J. E. Knox, J. B. Cross, V. Bakken, C. Adamo, J. Jaramillo, R. Gomperts, R. E. Stratmann, O. Yazyev, A. J. Austin, R. Cammi, C. Pomelli, J. W. Ochterski, R. L. Martin, K. Morokuma, V. G. Zakrzewski, G. A. Voth, P. Salvador, J. J. Dannenberg, S. Dapprich, A. D. Daniels, Ö. Farkas, J. B. Foresman, J. V. Ortiz, J. Cioslowski, and D. J. Fox, Gaussian, Inc., Wallingford CT, 2009.

² MOLPRO 2012.1, MOLPRO, version 2012.1, a package of *ab initio* programs, H.-J. Werner, P. J. Knowles, G. Knizia, F. R. Manby, M. Schütz, P. Celani, T. Korona, R. Lindh, A. Mitrushenkov, G. Rauhut, K. R. Shamasundar, T. B. Adler, R. D. Amos, A. Bernhardsson, A. Berning, D. L. Cooper, M. J. O. Deegan, A. J. Dobbyn, F. Eckert, E. Goll, C. Hampel, A. Hesselmann, G. Hetzer, T. Hrenar, G. Jansen, C. Köppl, Y. Liu, A. W. Lloyd, R. A. Mata, A. J. May, S. J. McNicholas, W. Meyer, M. E. Mura, A. Nicklass, D. P. O'Neill, P. Palmieri, D. Peng, K. Pflüger, R. Pitzer, M. Reiher, T. Shiozaki, H. Stoll, A. J. Stone, R. Tarroni, T. Thorsteinsson, and M. Wang, , see <http://www.molpro.net>.

³ E. I. Izgorodina and M. L. Coote, *Chem Phys*, 2006, **324**, 96.

⁴ B. B. Noble and M. L. Coote, *Int Rev Phys Chem*, 2013, **32**, 467.

⁵ C. Y. Lin, E. I. Izgorodina and M. L. Coote, *Macromolecules*, 2010, **43**, 553.

⁶ J. L. Hodgson, L. B. Roskop, M. S. Gordon, C. Y. Lin and M. L. Coote, *J. Phys. Chem. A* 2010, **114**, 10458.

⁷ J. P. Merrick, D. Moran, L. Radom, *J. Phys. Chem. A* 2007, **111**, 11683

⁸ G. Gryn'ova, C. Y. Lin and M. L. Coote, *Poly Chem*, 2013, **4**, 3744

then calculated using the composite high-level *ab initio* G3(MP2)-RAD method,⁹ in conjugation with an ONIOM inspired approximation.¹⁰ The core layer was calculated using G3(MP2)-RAD method, and the full system was calculated with the R(O)MP2/GTMP2Large method. Solvation corrections were calculated using the SMD/M06-2X/6-31G(d) method, with methyl propanoate and toluene (chosen to mimic bulk methyl methacrylate and styrene, respectively), and dichloromethane as solvents.¹¹ For all species either full systematic conformational searches (at a resolution of 120°) or, for more complex systems, energy-directed tree searches,¹² were performed to ensure global, and not merely local minima were located. Lowest energy conformations were selected on the basis of their R(O)MP2/GTMP2Large solution-phase free-energies.

Free-energies of each species in solution was calculated as the sum of the corresponding gas-phase free energies and the obtained free energies of solvation and included a phase change correction term $RT \ln(RT/P)$, where R is the universal gas constant, T is the absolute temperature and P is the pressure. The entropies and thermal corrections were calculated using standard textbook formulae¹³ for the statistical thermodynamics of an ideal gas under the harmonic oscillator/ rigid rotor approximation. Free energies of solvation in methyl propanoate, toluene and dichloromethane at 25 °C were obtained using the using the popular continuum model SMD. While the use of solvation energies calibrated at 25 °C (and not 40 °C) may be the source of some minor error, it is likely to be insignificant compared with other errors arising from approximations used in these calculations. Gaussian 09¹ was used to compute SMD solvation free energies in conjunction with the relaxed solution-phase SMD/M06-2X/6-31G(d) geometries, with all parameters kept as default values for the corresponding solvent. Solvation free energies included a gas-phase to solution-phase geometry relaxation correction, estimated by the difference between the gas-phase energies of the gas and solution geometries (calculated at M06-2X/6-31G(d)).

⁹ D. J. Henry, M. B. Sullivan and L. Radom, *J. Chem. Phys.*, 2003, **118**, 4849.

¹⁰ For a review, see M. L. Coote, *Macromol. Theory Simul.*, 2009, **18**, 388.

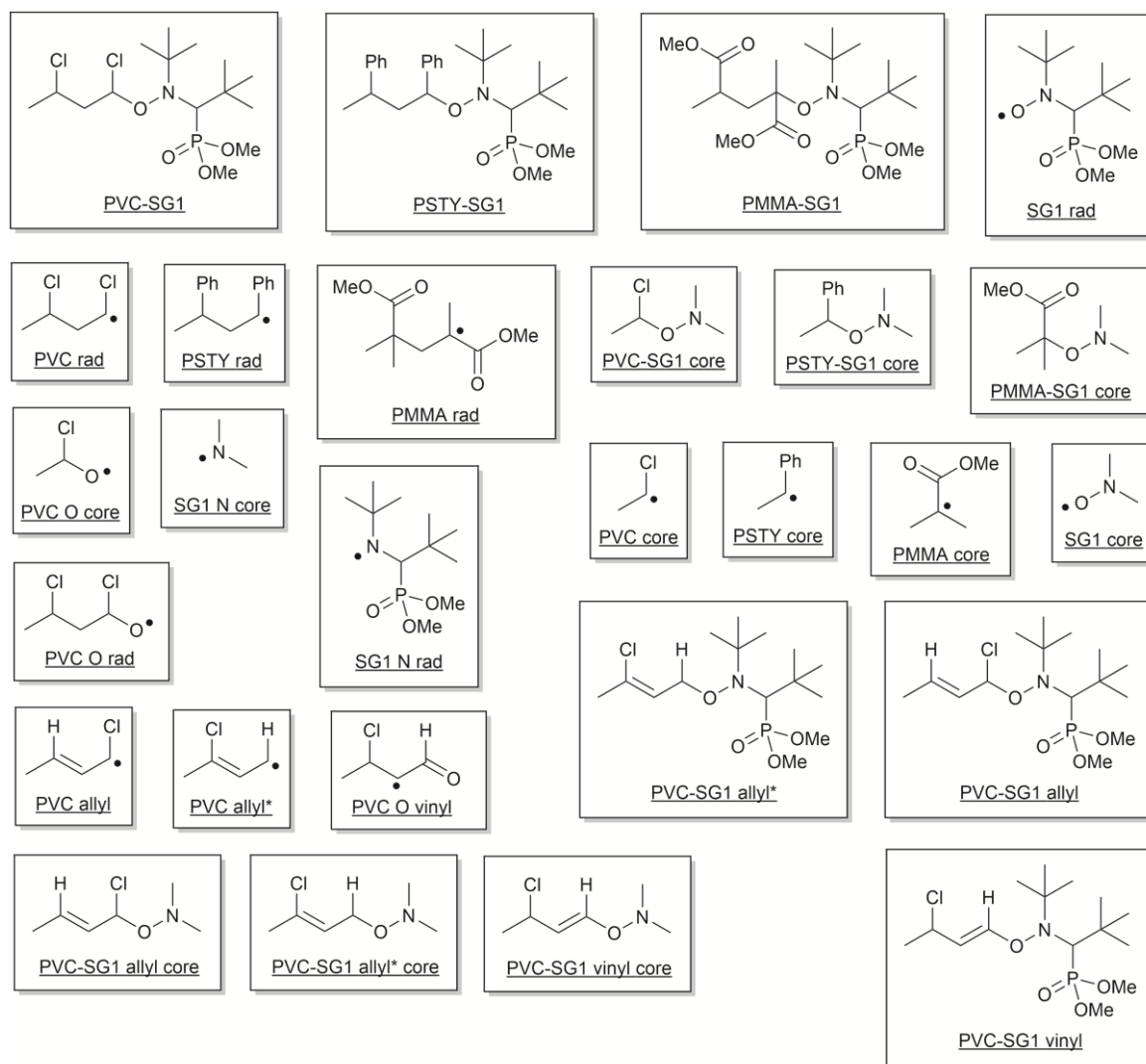
¹¹ A. V. Marenich, C. J. Cramer and D. G. Truhlar, *J Phys Chem B*, 2009, **113**, 6378-6396.

¹² E. I. Izgorodina, C. Y. Lin and M. L. Coote, *Phys. Chem. Chem. Phys.*, 2007, **9**, 2507.

¹³ J. I. Steinfeld, J. S. Francisco and W. L. Hase, *Chemical Kinetics and Dynamics*, Prentice Hall, Englewood Cliffs, 1989.

Structures examined in this work

Chemical structure of the radical fragments and alkoxyamines examined in this work and their abbreviations.



Contributions to the gas and solution-phase free energies of species

Raw electronic energies, zero-point vibrational, entropic and thermal corrections, gas-phase Gibbs free energies and enthalpies at 40 °C, as well as free energies of solvation. Unless otherwise specified, units are in Hartrees. Note that solvation corrections (ΔG_{solv}) include a change of standard state (from gas to solution) correction.

Table E.1: SG1-mediated NMP of MMA, STY and VC at 40 °C

Species	Corrections (40 °C)			Raw Energies					Thermochemistry and Solvation (40 °C)		
	S (Jmol ⁻¹ K ⁻¹)	TC	ZPVE	M062X/ 6-31G(d)	R(O)MP2/ 6-31G(d)	R(O)MP2/ GTMP2Large	URCCSD(T)/ 6-31G(d)	G3(MP2)RAD	G _{gas} (ONIOM)	ΔG_{solv}	G _{sol} (ONIOM)
PMMA core	394.05	0.009977	0.130762	-346.205885	-345.265623	-345.675548	-345.355305	-346.957459	-	-	-
SG1 core	303.07	0.006235	0.082668	-209.611937	-209.044424	-209.302224	-209.101148	-209.475874	-	-	-
PMMA-SG1 core	474.17	0.014429	0.218497	-555.903296	-554.400207	-555.067192	-554.540786	-555.518400	-	-	-
PMMA rad	573.13	0.019706	0.254976	-691.880007	-690.015756	-690.828557	-	-	-690.904145	-0.010594	-690.914739
SG1 rad	672.79	0.025543	0.354620	-1130.833450	-1128.157994	-1129.230427	-	-	-1129.10416	-0.01042	-1129.11458
PMMA-SG1	989.83	0.043720	0.615952	-1822.775896	-1818.234891	-1820.127823	-	-	-1820.03742	-0.016688	-1820.05411
PSTY core	360.65	0.008571	0.138564	-310.076996	-309.154004	-309.504453	-309.259480	-309.802158	-	-	-
PSTY-SG1 core	465.69	0.013520	0.227409	-519.773404	-518.288477	-518.894357	-518.441900	-519.358409	-	-	-
PSTY rad	529.71	0.017132	0.273048	-619.619855	-617.792040	-618.485995	-	-	-618.5567	-0.013539	-618.570239
SG1 rad	672.79	0.025543	0.354620	-1130.833450	-1128.157994	-1129.230427	-	-	-1129.10416	-0.007979	-1129.11214
PSTY-SG1	959.91	0.041493	0.634159	-1750.527869	-1746.026557	-1747.797042	-	-	-1747.69993	-0.01886	-1747.71879
PVC core	289.79	0.005758	0.050739	-538.676804	-537.871108	-538.067510	-537.921818	-538.206906	-	-	-
PVC-SG1 core	392.99	0.010703	0.140219	-748.393190	-747.020109	-747.473977	-747.121781	-747.782734	-	-	-
PVC rad	381.34	0.009363	0.098180	-1076.836681	-1075.236720	-1075.621908	-	-	-1075.69924	-0.007829	-1075.70707
SG1 rad	672.79	0.025543	0.354620	-1130.833450	-1128.157994	-1129.230427	-	-	-1129.10416	-0.01308	-1129.11724
PVC-SG1	810.63	0.033332	0.459750	-2207.760938	-2203.480387	-2204.945170	-	-	-2204.85753	-0.017818	-2204.87535
PVC O core	301.78	0.005789	0.055832	-613.864379	-612.892532	-613.167167	-612.955983	-613.347543	-	-	-
SG1 N core	283.16	0.005771	0.075353	-134.428082	-134.019620	-134.192931	-134.074387	-134.336384	-	-	-
PVC O rad	396.70	0.010123	0.102570	-1152.024548	-1150.258085	-1150.722269	-	-	-1150.83727	-0.010592	-1150.84786

SG1 N rad	651.04	0.024563	0.349000	-1055.647157	-1053.125984	-1054.115805	-	-	-1053.96335	-0.01081	-1053.97416
PVC allyl	339.22	0.007804	0.083504	-616.057375	-615.024607	-615.308333	-615.100719	-615.520197	-615.469349	-0.004542	-615.473891
PVC allyl*	336.01	0.007768	0.083295	-616.059678	-615.027145	-615.311647	-615.103259	-615.523512	-615.472526	-0.004084	-615.47661
PVC vinyl	367.05	0.008727	0.088955	-691.259938	-690.0687	-690.429128	-690.150342	-690.674761	-690.620858	-0.008803	-690.629661
PVC-SG1 allyl core	453.73	0.013498	0.172005	-825.749944	-824.149316	-824.688349	-824.278523	-825.071707	-	-	-
PVC-SG1 allyl* core	472.45	0.013641	0.171769	-825.745053	-824.143723	-824.683171	-824.272992	-825.066592	-	-	-
PVC-SG1 vinyl core	463.23	0.013469	0.172221	-825.749581	-824.148297	-824.687307	-824.276974	-825.070135	-	-	-
PVC-SG1 allyl	789.99	0.032249	0.444365	-1746.957425	-1743.243346	-1744.602777	-	-	-1744.60375	-0.016116	-1744.61986
PVC-SG1 allyl*	794.53	0.032069	0.444876	-1746.960558	-1743.246466	-1744.604464	-	-	-1744.60571	-0.014916	-1744.62062
PVC-SG1 vinyl	799.44	0.032255	0.444545	-1746.961882	-1743.249039	-1744.607342	-	-	-1744.60872	-0.018839	-1744.62756

Table E.2: SG1-mediated NMP of MMA, STY and VC at 100 °C

Species	Corrections (100 °C)			Raw Energies					Thermochemistry and Solvation (100 °C)		
	S (Jmol ⁻¹ K ⁻¹)	TC	ZPVE	M062X/ 6-31G(d)	R(O)MP2/ 6-31G(d)	R(O)MP2/ GTMP2Large	URCCSD(T)/ 6-31G(d)	G3(MP2)RAD	G _{gas} (ONIOM)	ΔG _{solv}	G _{sol} (ONIOM)
PMMA rad	624.91	0.026446	0.254976	-691.880007	-690.015756	-690.828557	-	-	-690.917862	-0.009770	-690.927632
SG1 rad	742.70	0.034641	0.354620	-1130.833450	-1128.157994	-1129.230427	-	-	-1129.120372	-0.009596	-1129.129968
PMMA-SG1	1112.23	0.059659	0.615952	-1822.775896	-1818.234891	-1820.127823	-	-	-1820.061496	-0.015864	-1820.077360
PSTY rad	581.43	0.023859	0.273048	-619.619855	-617.792040	-618.485995	-	-	-618.569429	-0.012715	-618.582144
SG1 rad	742.70	0.034641	0.354620	-1130.833450	-1128.157994	-1129.230427	-	-	-1129.120372	-0.007155	-1129.127527
PSTY-SG1	1081.69	0.057338	0.634159	-1750.527869	-1746.026557	-1747.797042	-	-	-1747.723333	-0.018036	-1747.741369
PVC rad	404.3569	0.012359	0.098180	-1076.836681	-1075.236720	-1075.621908	-	-	-1075.708234	-0.007005	-1075.715239
SG1 rad	742.70	0.034641	0.354620	-1130.833450	-1128.157994	-1129.230427	-	-	-1129.120372	-0.012255	-1129.132627
PVC-SG1	903.6792	0.045442	0.459750	-2207.760938	-2203.480387	-2204.945170	-	-	-2204.877171	-0.016994	-2204.894165
PVC O rad	422.0839	0.013427	0.102570	-1152.024548	-1150.258085	-1150.722269	-	-	-1150.846637	-0.009768	-1150.856405
SG1 N rad	718.5417	0.033348	0.349000	-1055.647157	-1053.125984	-1054.115805	-	-	-1053.979033	-0.009986	-1053.989019

Computational Studies on the Mechanism of Low-Temperature NMP of VC

NMP is a reversible deactivation radical polymerization process that employs stable nitroxide radical as a mediating species. Achieving a NMP with ‘living’ characteristics relies on the presence of a thermally labile C–O bond in the corresponding polymeric alkoxyamine, otherwise deactivation of the propagating radicals will be irreversible. The strength of this bond is dependent on the structure of the nitroxide and polymeric radical from which the alkoxyamine is composed. For a given nitroxide, the bond dissociation free-energy (BDFE) of the C–O bond depends on both the stability of the polymeric radical and its substitution; with more stable and more bulky substituted polymeric radicals affording lower BDFEs.¹ For these reasons, one would intuitively expect that NMP polymerization of VC mediated by SG1 radicals would fail, especially at low temperatures (42 °C), because deactivation of the propagating radical should be irreversible. While SG1 radicals have mediated the successful NMPs of various monomers including, *n*-butyl acrylate (*n*-BA)² and S,² these polymerizations must be performed at elevated temperatures (90–120 °C) to maintain reasonable levels of alkoxyamine homolysis. Additionally, it should also be noted that the propagating radical species in these polymerizations are significantly *more* stable and sterically hindered than VC radicals (see radical stabilization energies (RSE) in Table E.3).³ To properly quantify the governing activation-deactivation equilibrium constant (*K*) of the PVC-SG1 system, high-level theory was used to calculate the BDFE of the C–O bond in corresponding alkoxyamine (see Table E.3). For comparative purposes, the BDFEs of the C–O bonds in both PS-SG1 and PMMA-SG1 alkoxyamines were also calculated using the same computational methodology. As electron donating substituents can destabilize the O–N bond of the nitroxide,⁴ O–N breakage was also examined for VC.

Table E.3. Radical Stabilization Energies (RSE), Bond Dissociation Free-Energies (BDFE) and K for SG1-Mediated NMP of VC, S and MMA.

Monomer System (Bond Homolysis)	RSE of unimeric radical ^a	40 °C		100 °C	
		BDFE ^a	K	BDFE ^a	K
VC (C–ON)	13.2	134.0	4.5×10^{-23}	121.5	9.7×10^{-18}
VC (CO–N)	-	140.0	4.4×10^{-24}	128.0	1.2×10^{-18}
S (C–ON)	54.8	95.6	1.1×10^{-16}	83.2	2.2×10^{-12}
MMA (C–ON)	41.1	65.1	1.4×10^{-11}	51.9	5.4×10^{-8}

^aRSE and BDFE values given in kJ mol⁻¹. Dichloromethane, toluene and methyl propanoate were used as solvents for VC, S and MMA, respectively. The VC, S and MMA radicals were modeled as dimers. RSE values were taken from reference³.

At 40 °C, the C–O bond BDFE of the PVC-SG1alkoxyamine is calculated to be 134.0 kJ mol⁻¹, while the corresponding K value is 4.5×10^{-23} . Even assuming a very fast diffusion limited $k_{\text{deactivation}}$ of $\sim 10^9$ Lmol⁻¹s⁻¹, $k_{\text{activation}}$ would be 4.5×10^{-14} s⁻¹; which is approximately **10 orders of magnitude** too slow to mediate a successful NMP. In other words, the C–O bond of the PVC-SG1 alkoxyamine is around 40-50 kJ mol⁻¹ too strong to facilitate a viable NMP activation-deactivation equilibrium. Even at the elevated temperatures (100 °C) used for the MMA and MMA/S chain-extension experiments, K is still **over 5 orders of magnitude** too low to facilitate sufficient levels of PVC-SG1 macro-initiator homolysis. Alternative O–N breakage of the PVC-SG1 alkoxyamine, which would decompose the SG1 nitroxide (irreversibly) into an aminyl radical, is also thermodynamically disfavored at both 40 °C and 100 °C.

In contrast, to the unfavorable K value for the PVC-SG1 system, the C–O bond of the PS-SG1 alkoxyamine is predicted to be sufficiently labile at 100 °C (but not 40 °C) to facilitate a successful NMP. This theoretical prediction is consistent with previous experimental results, as it is well known that the NMP of S must be performed at elevated temperatures (usually ≥ 90 °C) to yield polymeric products within practical time-frames.⁵ In contrast to the other two alkoxyamines, the K value for the PMMA-SG1 system is predicted to be too large and so irreversible combination/disproportionation of propagating chains would severely compromise this NMP.⁶ Indeed, the addition of S monomer to MMA-SG1 polymerizations improves the livingness, as the intermediate styryl radicals are more susceptible deactivation by SG1 radicals.⁶ In summary, the

theoretically predicted K values are not only consistent with intuitive expectations based on a semi-quantitative analysis of the size and stability of the corresponding radical species, but also with previous experimental results in S-SG1 and MMA-SG1 systems.^{2,7} Moreover, we should emphasize that the theoretical methodology used to estimate these BDFEs has been extensively benchmarked (including against experiment) in previous studies.^{3,4,8,9}

Could dehydrochlorination facilitate reactivation?

As high-level calculations suggest that the high BDFE of the C–O bond in the PVC-SG1 alkoxyamine should completely prohibit reactivation, the presently reported experimental success is both highly surprising and intriguing. Perhaps the most straightforward explanation for the experimental success of the NMP of VC is that the SG1 radical and/or PVC-SG1 alkoxyamine participate in side-reactions, which form a more reactive intermediate alkoxyamine that is more susceptible to homolysis. If the PVC-SG1 alkoxyamine undergoes dehydrochlorination in the vicinity of the chain-ends, then the resultant allylic defect could facilitate the decomposition of the parent alkoxyamine by allowing for the elimination of a stable allylic PVC radical. Indeed, theoretical calculations indicate that two possible dehydrochlorinated PVC-SG1 structures possess much lower C–O bond BDFEs and would be able to effectively (re)activate chain growth (Figure E.4), even at low temperatures (42 °C).

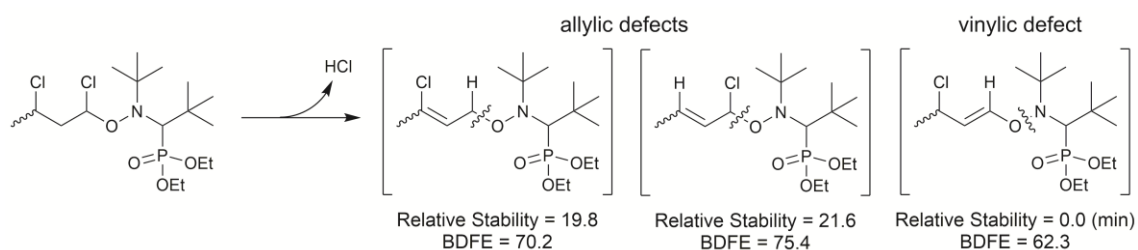


Figure E.4. Possible dehydrochlorinated PVC-SG1 structures, with relative stabilities of the alkenes. BDFEs of the marked bond and relative alkene stability calculated at 40 °C are given in kJ mol⁻¹.

Unfortunately, the exact mechanistic details of any potential dehydrochlorination reactions are currently unclear. While dehydrochlorination of unstabilized PVC is well noted at high temperatures (> 150 °C),¹⁰ the conditions used in this polymerization are

obviously much milder. However, it should be noted that amines can facilitate dehydrochlorination of PVC at lower temperatures (~ 80 °C),¹¹ and so it is possible that the SG1 is selectively mediating the dehydrochlorination mechanism in the vicinity of the chain-end. In its favour, is the absence of competing reactions in the otherwise stable PVC-SG1. Once the unsaturated defect is formed, the alkoxyamine can undergo homolysis and, given the low radical concentration, undergo several propagation steps before being trapped again by the SG1.

However, a potential problem with the mechanism is the possibility of competitively generating a vinylic PVC-SG1 structure. The O–N bond in this vinylic structure is actually less stable than the C–O bond of either allylic structure. If both defects form competitively, O–N homolysis would irreversibly decompose SG1 radicals into aminyl radicals and the resulting polymerization would be poorly controlled. While the low polydispersity of the PVC obtained in the present work ($D = 1.5$) is unprecedented, it is significantly above that of an optimized NMP for a less reactive monomer ($D < 1.2$), and formation of vinylic groups may be a possible reason for this result. The low concentration of C=C defect structures detected by ¹H-NMR in the resulting PVC may simply reflect the reversibility of the dehydrochlorination reaction under these conditions. However, we should also caution that there is limited evidence for this dehydrochlorination mechanism and so this mechanism is quite tentative. Indeed, more detailed mechanistic studies of this remarkable and surprising polymerization are currently underway.

References

1. Bagryanskaya, E. G. and Marque, S. R. A., *Scavenging of Organic C-Centered Radicals by Nitroxides*. Chemical Reviews, **2014**, *114*, 5011-5056.
2. Chauvin, F., Dufils, P.-E., Gimes, D., Guillaneuf, Y., Marque, S. R. A., Tordo, P., and Bertin, D., *Nitroxide-Mediated Polymerization: The Pivotal Role of the k_d Value of the Initiating Alkoxyamine and the Importance of the Experimental Conditions*. Macromolecules, **2006**, *39*, 5238-5250.
3. Coote, M. L., Lin, C. Y., Beckwith, A. L. J., and Zavitsas, A. A., *A comparison of methods for measuring relative radical stabilities of carbon-centred radicals*. Physical Chemistry Chemical Physics, **2010**, *12*, 9597-9610.

- Hodgson, J. L., Roskop, L. B., Gordon, M. S., Lin, C. Y., and Coote, M. L., *Side Reactions of Nitroxide-Mediated Polymerization: N–O versus O–C Cleavage of Alkoxyamines*. The Journal of Physical Chemistry A, **2010**, *114*, 10458-10466.
- Ruehl, J., Hill, N. L., Walter, E. D., Millhauser, G., and Braslau, R., *A Proximal Bisnitroxide Initiator: Studies in Low-Temperature Nitroxide-Mediated Polymerizations*. Macromolecules, **2008**, *41*, 1972-1982.
- Gryn'ova, G., Lin, C. Y., and Coote, M. L., *Which side-reactions compromise nitroxide mediated polymerization?* Polymer Chemistry, **2013**, *4*, 3744-3754.
- Nicolas, J., Dire, C., Mueller, L., Belleney, J., Charleux, B., Marque, S. R. A., Bertin, D., Magnet, S., and Couvreur, L., *Living Character of Polymer Chains Prepared via Nitroxide-Mediated Controlled Free-Radical Polymerization of Methyl Methacrylate in the Presence of a Small Amount of Styrene at Low Temperature*. Macromolecules, **2006**, *39*, 8274-8282.
- Gryn'ova, G., Marshall, D. L., Blanksby, S. J., and Coote, M. L., *Switching radical stability by pH-induced orbital conversion*. Nat Chem, **2013**, *5*, 474-481.
- Hodgson, J. L., Yeh Lin, C., Coote, M. L., Marque, S. R. A., and Matyjaszewski, K., *Linear Free-Energy Relationships for the Alkyl Radical Affinities of Nitroxides: A Theoretical Study*. Macromolecules, **2010**, *43*, 3728-3743.
- Starnes, W. H., *Structural and mechanistic aspects of the thermal degradation of poly(vinyl chloride)*. Prog. Polym. Sci., **2002**, *27*, 2133-2170.
- Bowley, H. J., Gerrard, D. L., and Biggin, I. S., *The effect of amines on the dehydrochlorination of poly(vinyl chloride)*. Journal of Vinyl Technology, **1988**, *10*, 50-52.

